NUREG-2178, Vol. 1 EPRI 3002005578

Refining And Characterizing Heat Release Rates From Electrical Enclosures During Fire (RACHELLE-FIRE)

Volume 1:
Peak Heat Release Rates and Effect of Obstructed Plume

Draft Report for Comment

U.S. Nuclear Regulatory Commission
Office of Nuclear Regulatory Research
Washington, D.C. 20555-0001

Electric Power Research Institute
3420 Hillview Avenue
Palo Alto, CA 94304-1338

AVAILABILITY OF REFERENCE MATERIALS IN NRC PUBLICATIONS

NRC Reference Material

As of November 1999, you may electronically access NUREG-series publications and other NRC records at NRC's Public Electronic Reading Room at http://www.nrc.gov/reading-rm.html. Publicly released records include, to name a few, NUREG-series publications; *Federal Register* notices; applicant, licensee, and vendor documents and correspondence; NRC correspondence and internal memoranda; bulletins and information notices; inspection and investigative reports; licensee event reports; and Commission papers and their attachments.

NRC publications in the NUREG series, NRC regulations, and Title 10, "Energy," in the *Code of Federal Regulations* may also be purchased from one of these two sources.

1. The Superintendent of Documents
   U.S. Government Printing Office
   Mail Stop SSOP
   Washington, DC 20402–0001
   Internet: bookstore.gpo.gov
   Telephone: 202-512-1800
   Fax: 202-512-2250
2. The National Technical Information Service
   Springfield, VA 22161–0002
   www.ntis.gov
   1–800–553–6847 or, locally, 703–605–6000

A single copy of each NRC draft report for comment is available free, to the extent of supply, upon written request as follows:

Address: U.S. Nuclear Regulatory Commission
Office of Administration
Publications Branch
Washington, DC 20555-0001
E-mail: DISTRIBUTION.RESOURCE@NRC.GOV
Facsimile: 301–415–2289

Some publications in the NUREG series that are posted at NRC's Web site address http://www.nrc.gov/reading-rm/doc-collections/nuregs are updated periodically and may differ from the last printed version. Although references to material found on a Web site bear the date the material was accessed, the material available on the date cited may subsequently be removed from the site.

Non-NRC Reference Material

Documents available from public and special technical libraries include all open literature items, such as books, journal articles, transactions, *Federal Register* notices, Federal and State legislation, and congressional reports. Such documents as theses, dissertations, foreign reports and translations, and non-NRC conference proceedings may be purchased from their sponsoring organization.

Copies of industry codes and standards used in a substantive manner in the NRC regulatory process are maintained at—

The NRC Technical Library
Two White Flint North
11545 Rockville Pike
Rockville, MD 20852–2738

These standards are available in the library for reference use by the public. Codes and standards are usually copyrighted and may be purchased from the originating organization or, if they are American National Standards, from—

American National Standards Institute
11 West 42nd Street
New York, NY 10036–8002
www.ansi.org
212–642–4900

Legally binding regulatory requirements are stated only in laws; NRC regulations; licenses, including technical specifications; or orders, not in NUREG-series publications. The views expressed in contractor-prepared publications in this series are not necessarily those of the NRC.

The NUREG series comprises (1) technical and administrative reports and books prepared by the staff (NUREG–XXXX) or agency contractors (NUREG/CR–XXXX), (2) proceedings of conferences (NUREG/CP–XXXX), (3) reports resulting from international agreements (NUREG/IA–XXXX), (4) brochures (NUREG/BR–XXXX), and (5) compilations of legal decisions and orders of the Commission and Atomic and Safety Licensing Boards and of Directors' decisions under Section 2.206 of NRC's regulations (NUREG–0750).

DISCLAIMER: This report was prepared as an account of work sponsored by an agency of the U.S. Government. Neither the U.S. Government nor any agency thereof, nor any employee, makes any warranty, expressed or implied, or assumes any legal liability or responsibility for any third party's use, or the results of such use, of any information, apparatus, product, or process disclosed in this publication, or represents that its use by such third party would not infringe privately owned rights.

NUREG-2178, Vol. 1 **EPRI 3002005578**

<u>R</u>efining <u>A</u>nd <u>C</u>haracterizing <u>H</u>eat Release Rates From <u>El</u>ectrica<u>l</u> <u>E</u>nclosures During <u>Fire</u> (RACHELLE-FIRE)

Volume 1:
Peak Heat Release Rates and Effect of Obstructed Plume

Draft Report for Comment

April 2015

U.S. Nuclear Regulatory Commission
Office of Nuclear Regulatory Research (RES)
Washington, D.C. 20555-0001

Electric Power Research Institute (EPRI)
3420 Hillview Avenue
Palo Alto, CA 94304-1338

U.S. NRC-RES Project Manager
M. H. Salley

EPRI Project Manager
A. Linderman

DISCLAIMER OF WARRANTIES AND LIMITATION OF LIABILITIES

THIS DOCUMENT WAS PREPARED BY THE ORGANIZATION(S) NAMED BELOW AS AN ACCOUNT OF WORK SPONSORED OR COSPONSORED BY THE ELECTRIC POWER RESEARCH INSTITUTE, INC. (EPRI). NEITHER EPRI, ANY MEMBER OF EPRI, ANY COSPONSOR, THE ORGANIZATION(S) BELOW, ANY PERSON ACTING ON BEHALF OF ANY OF THEM:

(A) MAKES ANY WARRANTY OR REPRESENTATION WHATSOEVER, EXPRESS OR IMPLIED, (I) WITH RESPECT TO THE USE OF ANY INFORMATION, APPARATUS, METHOD, PROCESS, OR SIMILAR ITEM DISCLOSED IN THIS DOCUMENT, INCLUDING MERCHANTABILITY AND FITNESS FOR A PARTICULAR PURPOSE, OR (II) THAT SUCH USE DOES NOT INFRINGE ON OR INTERFERE WITH PRIVATELY OWNED RIGHTS, INCLUDING ANY PARTY'S INTELLECTUAL PROPERTY, OR (III) THAT THIS DOCUMENT IS SUITABLE TO ANY PARTICULAR USER'S CIRCUMSTANCE; OR

(B) ASSUMES RESPONSIBILITY FOR ANY DAMAGES OR OTHER LIABILITY WHATSOEVER (INCLUDING ANY CONSEQUENTIAL DAMAGES, EVEN IF EPRI OR ANY EPRI REPRESENTATIVE HAS BEEN ADVISED OF THE POSSIBILITY OF SUCH DAMAGES) RESULTING FROM YOUR SELECTION OR USE OF THIS DOCUMENT OR ANY INFORMATION, APPARATUS, METHOD, PROCESS, OR SIMILAR ITEM DISCLOSED IN THIS DOCUMENT.

REFERENCE HEREIN TO ANY SPECIFIC COMMERCIAL PRODUCT, PROCESS, OR SERVICE BY ITS TRADE NAME, TRADEMARK, MANUFACTURER, OR OTHERWISE, DOES NOT NECESSARILY CONSTITUTE OR IMPLY ITS ENDORSEMENT, RECOMMENDATION, OR FAVORING BY EPRI.

THE FOLLOWING ORGANIZATIONS PREPARED THIS REPORT:

U.S. Nuclear Regulatory Commission, Office of Nuclear Regulatory ResearchElectric Power Research Institute

Brookhaven National Laboratory

S. Nowlen (Consultant)

Jensen Hughes, Inc.

Engineering Planning and Management

Duke Energy

THE TECHNICAL CONTENTS OF THIS DOCUMENT WERE **NOT** PREPARED IN ACCORDANCE WITH THE EPRI NUCLEAR QUALITY ASSURANCE PROGRAM MANUAL THAT FULFILLS THE REQUIREMENTS OF 10 CFR 50, APPENDIX B AND 10 CFR PART 21, ANSI N45.2-1977 AND/OR THE INTENT OF ISO-9001 (1994). USE OF THE CONTENTS OF THIS DOCUMENT IN NUCLEAR SAFETY OR NUCLEAR QUALITY APPLICATIONS REQUIRES ADDITIONAL ACTIONS BY USER PURSUANT TO THEIR INTERNAL PROCEDURES.

NOTE

For further information about EPRI, call the EPRI Customer Assistance Center at 800.313.3774 or e-mail askepri@epri.com.

Electric Power Research Institute, EPRI, and TOGETHER…SHAPING THE FUTURE OF ELECTRICITY are registered service marks of the Electric Power Research Institute, Inc.

Copyright © 2015 Electric Power Research Institute, Inc. All rights reserved.

COMMENTS ON DRAFT REPORT

Any interested party may submit comments on this report for consideration by the NRC staff. Comments may be accompanied by additional relevant information or supporting data. Please specify the report number **NUREG-2178** in your comments, and send them by the end of the comment period specified in the *Federal Register* notice announcing the availability of this report.

Addresses: You may submit comments by any one of the following methods. Please include Docket ID **NRC-2015-0059** in the subject line of your comments. Comments submitted in writing or in electronic form will be posted on the NRC website and on the Federal rulemaking website http://www.regulations.gov.

Federal Rulemaking Website: Go to http://www.regulations.gov and search for documents filed under Docket ID **NRC-2015-0059**. Address questions about NRC dockets to Carol Gallagher at 301-415-3463 or by e-mail at Carol.Gallagher@nrc.gov.

Mail comments to: Cindy Bladey, Chief, Rules, Announcements, and Directives Branch (RADB), Division of Administrative Services, Office of Administration, Mail Stop: OWFN-12-H08, U.S. Nuclear Regulatory Commission, Washington, DC 20555-0001.

For any questions about the material in this report, please contact: David W. Stroup, Senior Fire Protection Engineer, (301) 251-7609 or by e-mail at david.stroup@nrc.gov.
Please be aware that any comments that you submit to the NRC will be considered a public record and entered into the Agencywide Documents Access and Management System (ADAMS). Do not provide information you would not want to be publicly available.

ABSTRACT

The Refining And Characterizing Heat Release Rates From Electrical Enclosures During Fire (RACHELLE-FIRE) program involves a working group of experienced fire protection and fire probabilistic risk assessment researchers and practitioners focused on enhancing the methodology used to model electrical enclosure fires in nuclear power plants (NPPs). This report documents the results from the working group's efforts to develop technical information in three areas: (1) classification of electrical enclosures in terms of function, size, contents, and ventilation, (2) determination of peak heat release rate (HRR) probability distributions considering specific electrical enclosure characteristics, and (3) development of a method to account for the impact of the enclosure on the vertical thermal zone of influence (ZOI) above the enclosure during fire.

Electrical enclosures have been classified in classification groups based on their electrical function, contents, and size. Most power enclosures, such as switchgear, load centers, motor control centers, battery chargers, and power inverters, are grouped based on their function. Other electrical enclosures are classified as small, medium, and large enclosures based on their volumetric size. The classification is primarily based on the size because it can be easily assessed by visual inspection during walkdowns without opening the electrical enclosure. Distinctions based on conductor wiring insulation type (thermoplastic versus thermoset) and open versus closed door configurations have been retained for certain enclosure groupings. Peak HRR values can be refined based on visual inspection of the interior of the enclosures if fuel type, fuel quantity, and cable bundling arrangement can be expected to limit fire growth.

Peak HRR distributions for the different classification groups have been developed. These distributions are based on the results of different experimental programs intended to measure the HRR associated with fires in electrical enclosures. The working group evaluated the configuration factors in these fire tests and compared them with the actual configuration of electrical enclosures used in commercial NPPs and the available plant fire event experience. The resulting probability distributions are intended to map the configurations of the electrical enclosures in operation at the plant with the experimental factors evaluated during the test programs. As a result, HRR probability distributions are available for a wide range of electrical enclosure types and configurations.

In order to provide a comprehensive characterization of electrical enclosure fires, the working group evaluated the temperature characteristics of fire plumes associated with these events using the Fire Dynamics Simulator (FDS) program. Computer simulations of various enclosure configurations were developed for evaluating the fire burning inside electrical enclosures and the fire plume temperature characteristics that would be generated. Based on this research, new fire plume temperature profiles reflecting the obstructed nature of fire plumes generated from fires inside electrical enclosures are provided.

Finally, examples, consolidating the information described in this report, are provided. The examples have been selected and designed to illustrate how to incorporate the information documented in this report into existing approaches for modeling fires in electrical enclosures.

CONTENTS

FIGURES

TABLES

EXECUTIVE SUMMARY

During the last decade, a number of commercial nuclear power plants (NPPs) have been developing fire probabilistic risk assessments (fire PRAs) to support risk-informed applications, including a voluntary transition from a deterministic fire protection program to a risk-informed/performance-based (RI/PB) program in accordance with National Fire Protection Association (NFPA) Standard 805, 2001 Edition. Most fire PRAs are based on methods and data described in NUREG/CR-6850 (EPRI 1011989), which was developed by a joint effort of both the Nuclear Regulatory Commission's Office of Nuclear Regulatory Research (NRC-RES) and the Electric Power Research Institute (EPRI). The wide application of this methodology has identified technical areas where additional research and data could better characterize the fire risks representing as-built plant conditions.

One important element supporting fire PRAs and other performance-based approaches is the estimation of the fire hazard using mathematical fire models (i.e., "fire modeling"). Fire modeling is used to support fire PRA developments to determine the effects of fire hazards on plant risk. For most fire modeling applications, the fire's heat release rate (HRR) is the most critical and difficult-to-predict parameter in characterizing the fire hazard. Specific to commercial NPP applications, the characterization of HRRs in electrical enclosures has been identified as a key technical area requiring additional research. In order to address this need, the NRC-RES and EPRI initiated the Refining And Characterizing Heat Release Rates From Electrical Enclosures During Fire (RACHELLE-FIRE) program.

The RACHELLE-FIRE program involves a working group of experienced fire protection and fire probabilistic risk assessment researchers and practitioners focused on reaching a consensus in estimating the peak HRR distributions for electrical enclosures used in NPPs. Based on the efforts of the working group, new methods and data have been developed in three specific areas:

- Classification of electrical enclosures in terms of function, size, contents, and ventilation,
- Determination of peak HRR probability distributions considering specific electrical enclosure characteristics, and
- Development of a correction method to the vertical thermal zone of influence (ZOI) above the enclosure during fire.

Examples of fire modeling applications are included to show the differences between the current approach and the new HRR values including the effect of obstructed plume considerations.

The classification of electrical enclosures and the determination of their corresponding HRR probability distributions is currently available in Appendix G of NUREG/CR-6850 (EPRI 1011989). These distributions are applied to a given electrical enclosure based on three factors: qualified versus unqualified cable, open versus closed doors, and single versus multiple cable bundles. As suggested earlier, the methods and data documented in this report provide more refined electrical enclosure classifications and corresponding peak HRR distributions.

The new electrical enclosure classifications are based on their electrical function, size, and content. Most power enclosures such as switchgear, load centers, motor control centers, battery chargers and power inverters are grouped based on function. Other applicable electrical enclosures are classified as small, medium, or large based on their volumetric size. The classification is primarily based on the size because it can easily be assessed by visual inspection during walkdowns without the need for opening the electrical enclosure. "Large" and "medium" volumetric classifications can be refined to account for the amount of combustible fuel load, type of cable insulation material, and ventilation configuration. These refinements can result in lower HRR values based on visual inspection of the enclosure internals.

In practice, the classification described above is intended to work as follows. Electrical enclosures are first classified based on function and size. This classification should be a quick determination since it only requires external visual inspection and knowledge of the enclosure function. A "default" peak HRR distribution is assigned to this initial classification. This default distribution is intended to be conservative as no visual inspection of the enclosure internals is necessary. Based on visual inspection of the enclosure internals, the initial classification can be refined with one of two sub-groups: "low" and "very low" loading. These low and very low categories would allow analysts additional flexibility to reflect actual plant conditions identified through plant walkdowns and the examination of enclosure internals.

The revised peak HRR probability distributions (i.e., gamma distributions) for each of the new enclosure classification groups were developed based on the following factors:

- Review of experimental factors and configurations in testing programs intended to assess the HRR generated by electrical enclosure fires. Both domestic and international test programs were included within the scope of this research.
- Statistical analysis of the applicable experimental results.
- Extensive review and comparison of existing electrical enclosure configurations and operating experience in commercial NPPs and the influencing experimental factors.

Consistent with Appendices E and G of NUREG/CR-6850 (EPRI 1011989), the probability distributions are defined based on the 75th and 98th percentile values, with the 98th percentile value intended for use as the maximum (or peak) HRR to be assumed for any enclosure in a given type/function classification group. The 98th percentile value is also the value used during initial ignition source screening.

In order to provide a comprehensive characterization of electrical enclosure fires, the working group evaluated the temperature characteristics of fire plumes associated with these events using the National Institute of Standards and Technology's (NIST) Fire Dynamics Simulator (FDS), version 6.0.1. In practice, fire plume temperatures are used to define the vertical component of a zone of influence (ZOI). The vertical component of the ZOI is the region above the fire where the fire plume temperatures could damage electrical cables and/or cause damage to nearby secondary combustibles.

Current practice for determining the vertical component of the ZOI includes a relatively simple process for establishing the elevation and diameter of the fire source. Typical fire modeling also uses the closed-form correlations to predict plume temperatures given a fire located within the enclosure. This practice is conservative because the fire source is positioned assuming that the enclosure does not exist. That is, the fire plume is modeled as if the fire were out in an open location, not inside an enclosure. In reality, the enclosure itself, and especially the enclosure's top cover, disrupts the plume development as compared to open unobstructed plumes. A more realistic treatment of the fire plume calculation is provided to account for the dispersion of the plume as it interacts with the top plate of a steel enclosure. The resulting approach is intended to be used in plume temperature calculations supporting the characterization of the ZOI in the early stages of the fire (i.e., before significant room temperature increases). Finally, a method to account for obstructions when estimating fire plume temperatures and the vertical component of the ZOI is provided.

In summary, this report provides a refined approach for the characterization and modeling of fires in electrical enclosures. The report is based on recent research on electrical enclosure fires, lessons learned over the last ten years developing fire PRAs and the understanding of the corresponding risk insights, as well as new research associated with obstructed fire plumes. Examples, consolidating the information in this report, are also provided. The examples have been selected and designed to illustrate how to incorporate the research documented in this report into the existing approaches for modeling fires in electrical enclosures.

EPRI PERSPECTIVE

Since its publication in 2005, NUREG/CR-6850 (EPRI 1011989) has been extensively used as the methodology for developing fire probabilistic risk assessments (fire PRA) in support of NFPA 805 and other risk-informed applications. Initial applications of the methodology resulted in conservative estimates of risk, which generated the need for methodology revisions and refinements over the past decade. Although a number of these revisions and refinements have been finalized and implemented, several technical areas have been identified where supplementary research could better characterize the fire risks at nuclear power plants. One of the most important technical areas is the characterization of the fire hazard associated with electrical cabinets. In practice, this hazard is characterized in the form of heat release rates and the corresponding temperature profile surrounding the cabinet. In order to address this need, a working group between EPRI and NRC-RES was assembled to develop new heat release rates with consideration of new test data, operating experience, and general usage of methodology. This report documents the results of the research conducted by the working group in the form of a practical methodology. Specifically, the report provides updated technical methods and data in three areas:

- The classification of electrical cabinets in terms of function (e.g., power and control cabinets), contents, and size,
- The determination of peak heat release rate probability distributions for the corresponding electrical cabinets, and
- The development and implementation of an approach to account for obstructions when estimating fire plume temperatures generated by fires burning inside cabinets.

The original peak heat release rate values provided for use in fire PRAs are documented in NUREG/CR-6850 (EPRI 1011989) Table G-1. The five distributions are distinguished by cable qualification type, such that two or three distributions are expected to represent the peak fire intensity for all electrical cabinet fires at a particular plant. With the understanding that electrical cabinets at nuclear power plants are of many different sizes, shapes, functions, and configurations, the working group re-classified the electrical cabinets to more accurately represent the population in commercial nuclear power plants. These new classifications serve as the foundation to re-evaluate the peak heat release rate probability distributions.

The peak heat release rate probability distributions provided in this report have been developed through a consensus process, based on the results of several experimental test programs and a review of fire event experience. These peak heat release rate probability distributions can be assigned considering the cabinet function, size, and combustible content.

Existing practice models electrical cabinet fires assuming the fire is burning outside of the enclosure. In reality, the cabinet top cover disrupts the plume development as compared to fires occurring in the open. In order to understand the effects of obstructions in the temperature profile of fire plumes, Fire Dynamics Simulator was used to model fires inside electrical cabinets. Simulations were performed in which flames and fire plume flows were subjected to obstructions. The studies of the obstructed plume simulations demonstrate lower temperatures above the fire location compared to the unobstructed cases due primarily to the entrainment of fresh air above the obstructions. Based on this research, a new method is available for estimating temperatures associated with obstructed fire plumes.

With the combination of the new heat release rates and obstructed plume methodology, a more realistic representation of the fire hazard associated with electrical cabinets can be achieved.

PREFACE

This report supplements previous work on heat release rates (HRRs) and fire modeling related to the fire probabilistic risk assessment (PRA) methodology and data published in NUREG/CR-6850 (EPRI 1011989), *EPRI/NRC-RES Fire PRA Methodology for Nuclear Power Facilities*, Volumes 1 and 2, September 2005; and its Supplement 1 (EPRI 1019259), *Fire Probabilistic Risk Assessment Methods Enhancements*, September 2010.

In 2002, EPRI published *Fire Modeling Guide for Nuclear Power Plant Applications* (EPRI 1002981). In June 2014, EPRI published 3002000830, *Fire-Induced Vulnerability Evaluation (FIVE) Revision 2*, providing an updated library of fire modeling tools to predict consequences for typical hazards found in nuclear power plants. In December 2004, NRC published NUREG-1805, *Fire Dynamics Tools (FDT^s) – Quantitative Fire Hazard Analysis Methods for the U.S. Nuclear Regulatory Commission Fire Protection Inspection Program*. In July 2013, NRC published a supplement to NUREG-1805 that expanded and updated the calculation methods included in the original NUREG.

In May 2007, NRC and EPRI published NUREG-1824 (EPRI 1011999), *Verification and Validation of Selected Fire Models for Nuclear Power Plant Applications*, consisting of seven volumes on five different fire modeling tools. These reports performed a verification and validation exercise on fire modeling analysis tools for use in fire PRAs. Subsequently, NRC and EPRI published draft Supplement 1 (EPRI 3002002182) to NUREG-1824 in November 2014 for public comment. This supplement evaluates the latest versions of the models and expanded the range of validation for the models.

In November 2008, NRC published NUREG/CR-6978, *A Phenomena Identification and Ranking Table (PIRT) Exercise for Nuclear Power Plant Fire Modeling Applications.* Through the use of nuclear power plant (NPP) specific examples, the PIRT panel identified the state of knowledge and importance of key fire phenomena necessary for successful application of fire modeling to NPP scenarios.

In November 2012, NRC and EPRI published NUREG-1934 (EPRI 1023259), *Nuclear Power Plant Fire Modeling Analysis Guidelines (NPP FIRE MAG)*. This report provides fire modeling analysis guidelines for use in fire PRAs.

In an effort to facilitate use of fire modeling for NPP applications and improve understanding of the fire hazards associated with electrical cables, NRC has sponsored two major research programs. The first program examined the impact of fire on cable functionality. The results of this research were documented in the three volumes of NUREG/CR-6931, *Cable Response to Live Fire (CAROLFIRE)*, published in 2007. The second test program examined the flammability properties of cables and is documented in the NUREG/CR-7010 reports. Volume 1 of the NUREG/CR-7010 series, *Cable Heat Release, Ignition, and Spreading Tray Installations during Fire (CHRISTIFIRE)* was published in 2012 and examined cables in horizontal trays. Volume 2 was published in 2013 and provided results for cables in vertical trays and corridors. Experiments are currently underway and a third volume will explore the conditions necessary to achieve ignition of cables and effectiveness of protective measures (i.e., coatings) for cables.

In December 2014, NRC and EPRI published NUREG-2169 (EPRI 3002002936), *Nuclear Power Plant Fire Ignition Frequencies and Non-Suppression Probability Estimation Using the Updated Fire Events Database*. This report provides fire ignition frequencies and non-suppression probability estimates through the year 2009 using EPRI's updated fire events database (EPRI 1025284).

This document does not constitute regulatory requirements. NRC-RES participation in this study does not constitute or imply regulatory approval of its applications based upon this methodology.

CITATIONS

This report was prepared by the following:

U.S. Nuclear Regulatory Commission
Washington, D.C. 20555-0001
Principal Investigators:
N. Melly
D. Stroup
G. Taylor

Under contract to NRC:

Brookhaven National Laboratory
P.O. Box 5000
Upton, NY 11973
Principal Investigator:
M. Subudhi

Consultant
101 Clancy Drive, NE
Albuquerque, NM 87112
Principal Investigator:
S. Nowlen

Utility participant/preparer:

Duke Energy
410 South Wilmington St., NCRH 19
Raleigh, NC 27602
Principal Investigator:
J. DeJoseph

Electric Power Research Institute
3420 Hillview Avenue
Palo Alto, CA 94304
Principal Investigator:
A. Lindeman

Under contract to EPRI:

Jensen Hughes, Inc.
3610 Commerce Dr. Suite 817
Baltimore, MD 21227
Principal Investigators:
F. Joglar
V. Ontiveros
J. Williamson

Engineering Planning and Management
5520 Dillard Drive, Suite 250
Cary, NC 27518
Principal Investigator:
D. Miskiewicz

This report describes research sponsored jointly by the U.S. Nuclear Regulatory Commission's (NRC) Office of Nuclear Regulatory Research (RES) and the Electric Power Research Institute (EPRI).

The report is a corporate document that should be cited in the literature in the following manner:

Refining And Characterizing Heat Release Rates From Electrical Enclosures During Fire (RACHELLE-FIRE), Volume 1: Peak Heat Release Rates and Effect of Obstructed Plume, U.S. Nuclear Regulatory Commission, Office of Nuclear Regulatory Research (RES), Rockville, MD, and Electric Power Research Institute (EPRI), Palo Alto, CA: 2015. NUREG-2178, V1, and EPRI 3002005578.

ACKNOWLEDGMENTS

This report was completed using a working group, which included stakeholders from the U.S. Nuclear Regulatory Commission (NRC) and the Electric Power Research Institute (EPRI). The authors appreciate the support of their respective organizations that cooperatively shared some or all of the cost and time for participation in this study.

The working group members would like to thank Dr. Manomohan Subudhi, Brookhaven National Laboratory (BNL), for facilitating the working group discussions and developing the early drafts of this report.

Special thanks go to Dr. Justin Williamson and Dr. Victor Ontiveros of Jensen Hughes, under the guidance of Dr. Francisco Joglar, for running the National Institute of Standards and Technology (NIST) Fire Dynamics Simulator models for the obstructed plume characterization. The authors thank Dr. Kevin McGrattan of NIST for his presentation and discussions of the results from the NRC-sponsored electrical enclosure tests conducted by NIST at the Naval Research Laboratory's Chesapeake Bay Fire Test Detachment facility. The authors are grateful to Mr. Mark Schairer of EPM for his peer review of the obstructed plume study. Special thanks go to working group member Ms. Joelle DeJoseph and Duke Energy for providing a large library of electrical enclosure pictures as well as piloting the new heat release rates and obstructed plume methodology.

The technical support of Mr. Kenneth Hamburger and Mr. Philip Smith of NRC, who participated in working group meetings, provided analysis of fire test data, and supplied input to the fire size calibration exercises, is acknowledged and greatly appreciated. Timely publication of this document would not have been possible without assistance from the NRC's Office of Administration. Specifically, the authors thank Tojuana Fortune-Grasty for her efforts in publishing this report. Finally, the authors express appreciation for the editorial support provided by the EPRI staff.

ACRONYMS

AC	Alternating Current
ACRS	Advisory Committee on Reactor Safety
ADAMS	Agencywide Documents Access and Management System
ARCH_xxx	Obstruction Case with Flat Plate and Two Side Walls
BASE_xxx	Base Case with No Obstruction
BNL	Brookhaven National Laboratory
Btu	British thermal unit
CBD	Chesapeake Bay Fire Test Detachment
CCDP	Conditional Core Damage Probability
CD	Compact Disc
CDF	Core Damage Frequency
CFD	Computational Fluid Dynamics
CFR	Code of Federal Regulations
COR	Code of Record
DC	Direct Current
DUKE	Duke Energy
EPM	Engineering Planning and Management
EPRI	Electric Power Research Institute
FAQ	Frequently Asked Questions
FDS	Fire Dynamics Simulator
FEDB	Fire Events Data Base
FMC	Flexible Metal Conduit
FR	Federal Register
HAI	Hughes Associates and RJA Group
HEAF	High Energy Arcing Fault
HELEN-FIRE	Heat Release Rates of Electrical Enclosure Fires
HGL	Hot Gas Layer
HRR	Heat Release Rate
IEEE	Institute of Electrical and Electronics Engineers
IRSN	Institute de Radioprotection et de Surete Nucleaire (France)
kW	kilowatt
LFMC	Liquid-Tight Flexible Metal Conduit
MCB	Main Control Board
MCC	Motor Control Center
MW	Megawatt
NEI	Nuclear Energy Institute
NFPA	National Fire Protection Association
NIST	National Institute of Standards and Technology
NPP	Nuclear Power Plant
NRC	Nuclear Regulatory Commission
NSP	Non-Suppression Probability
OBST_xxx	Obstruction Case with Flat Plate
PAU	Plant Analysis Unit
PMMA	Poly(methyl methacrylate)
PRA	Probabilistic Risk Assessment

RACHELLE-FIRE	Refining And Characterizing Heat Release Rates From Electrical Enclosures During Fire
RES	NRC’s Office of Nuclear Regulatory Research
RI/PB	Risk-Informed/Performance-Based
SDP	Significance Determination Process
SF	Severity Factor
SIS	Switchboard Wire or XLPE-Insulated Conductor (see UL 44, TS-Insulated Wires and Cables)
SNL	Sandia National Laboratory
SR	Silicon Rubber
STD	Standard
TP	Thermoplastic
THREEWALL_xxx	Obstruction Case with Flat Plate and Three Side Walls
TS	Thermoset
UL	Underwriter Laboratory
US	United States
VAC	Voltage in AC
V&V	Verification and Validation
VTT	Valtion teknillinen tutkimuskeskus (Finland)
WG	Working Group
XLPE	Cross-Linked Polyethylene
ZOI	Zone of Influence

1

Introduction

1.1 Background

In 2001, the National Fire Protection Association (NFPA) issued the first edition of NFPA 805, *Performance-Based Standard for Fire Protection for Light-Water Reactor Electrical Generating Plants, 2001 Edition* [1][1]. On July 16, 2004, the U.S. Nuclear Regulatory Commission (NRC) amended its regulations in *Title 10, Section 50.48, of the Code of Federal Regulations (10 CFR 50.48), Fire Protection* [2], to allow U.S. utilities to adopt and maintain risk-informed, performance-based fire protection programs. Paragraph (c) of 10 CFR 50.48 endorses, with exceptions, the NFPA 805 Standard – 2001 Edition, as a voluntary alternative for demonstrating compliance with the deterministic programs given in Appendix R to 10 CFR 50 [3] in accordance with Paragraph (b) of 10 CFR 50.48 or the plant-specific fire protection license conditions.

In 2005, the Electric Power Research Institute (EPRI) and the NRC's Office of Nuclear Regulatory Research (RES) issued a joint technical report titled *EPRI/NRC-RES Fire PRA Methodology for Nuclear Power Facilities,* EPRI 1011989, NUREG/CR-6850 [4][2], presenting methods and data for conducting a fire probabilistic risk assessment (fire PRA). As utilities develop fire PRAs to support a transition to NFPA 805 or in pursuit of other risk-informed applications, the methods in NUREG/CR-6850 have been used extensively. The methodology described in NUREG/CR-6850 for modeling fires in electrical enclosures generally consisted of:

1. Identifying the electrical enclosures that should be considered ignition sources in a fire PRA (see Chapter 6 of NUREG/CR-6850 and associated fire PRA frequently asked questions (FAQs)),
2. Assigning a heat release rate probability distribution to the peak heat release rate (see Appendices E and G of NUREG/CR-6850), and
3. Determining the region nearby the electrical enclosure where the fire could generate damage to nearby equipment and cables. This region is usually referred to as the zone of influence (ZOI) (see Chapter 8 and Appendix F of NUREG/CR-6850).

Although the first and third items were not new concepts introduced by NUREG/CR-6850 (i.e., previous fire PRA methodologies provided similar or identical information), the second item was new. Earlier fire PRA methods provided the characterization of electrical enclosures using point values for the heat release rate instead of probability distributions. The reason why NUREG/CR-6850 provided the use of probability distributions was twofold. First, this approach allows for the uncertainty associated with the heat release rates (HRRs) to be considered in the risk quantification process. Second, it allows for an independent assessment of the severity factor term in the risk equation based on the characteristics of the electrical enclosure (i.e., the ignition source) and the geometry/configuration of the fire scenario that could be generated by the postulated fire.

---

[1] Ref. 1, NFPA 805, 2001 Edition is hereafter referred to as "NFPA 805", and all references to this standard refer to the 2001 edition of this standard, which is the code of record (COR) as required by NRC regulations.

[2] Ref. 4, NUREG/CR-6850 (EPRI 1011989) is hereafter referred to as "NUREG/CR-6850".

Fire modeling is used to support fire PRAs to determine the effects of fire hazards on plant cables and equipment. For most fire model applications, the HRR of the fire is the most important parameter to specify. The HRR, measured in kilowatts (kW)[3], is the rate at which the combustion reaction produces heat. Appendix G of NUREG/CR-6850 provides peak HRR distributions for fixed ignition sources, such as electrical enclosures. For electrical enclosures, five heat release distributions are specified, which are dependent on 1) the number of cable bundles, 2) the type of internal combustibles (e.g., cable insulation material), and 3) the ventilation conditions (open/closed doors).

The wide application of the methods and data summarized above over the last ten years, together with fire research conducted after NUREG/CR-6850 was published, has led to the identification of key areas in the fire modeling of electrical enclosures where refinements can be developed. Specifically:

- A number of testing programs for evaluating heat release rates in electrical enclosures have recently been completed. For example, in 2013 a series of experiments were sponsored by NRC-RES and conducted by the National Institute of Standards and Technology (NIST) at the Chesapeake Bay Fire Test Detachment (CBD) of the Naval Research Laboratory to obtain additional data to support re-quantification of HRR estimates for electrical enclosures. This testing effort used electrical enclosures removed from a nuclear facility, and electrical cables and panel wiring representative of those commonly found in U.S. nuclear power plants. In total, 112 individual fire tests were conducted, and the result of this effort is documented in a draft report, “Heat Release Rates of Electrical Enclosure Fires (HELEN-FIRE)” [7].

- An extensive collection and review of recent fire events records throughout the entire U.S. nuclear industry was conducted.

- Numerous fire PRAs have been developed providing specific information (e.g., numerous pictures of cabinet internals, detailed enclosure construction specifications, etc.) associated with potential influencing factors in electrical enclosure fires.

Refinements are necessary because a comparison of the fire modeling results and resulting risk contribution of electrical enclosure fires compared with the fire experience in the U.S. commercial nuclear industry suggests that current information may be conservative for fire scenarios presenting specific characteristics.

1.2 Approach

The characterization of fires inside electrical enclosures has been identified as a technical area where existing methods and data could be refined. In an effort to obtain more realistic data for analysis of electrical enclosure fires and associated peak heat release rates, the Nuclear Regulatory Commission’s Office of Nuclear Regulatory Research sponsored a program with the National Institute of Standards and Technology. Subsequent to the completion of that test program, RES together with the Electric Power Research Institute established a working group composed of technical experts in experimental test programs, fire PRA, operating experience, fire modeling, and circuit analysis to review the new data, other available test data, and industry experience in an effort to develop refinements in the information.

---

[3] 1 Btu/s is equal to 1.055 kW.

During the project planning phase, the project sponsors evaluated the potential approaches to achieve the specific objectives of this report. Options included the use of formal expert elicitation panels, methods development panels, and facilitated working groups. It was decided not to pursue a formal expert elicitation type process due to the availability of test data, operating experience, an established and acceptable methodology for implementation, and the understanding of influencing factors affecting the diffusion flame combustion process. The methods development panel approach was not explored because the overall method presented in NUREG/CR-6850 is considered to be reasonable and development of a different method was determined to be unnecessary. Instead, the use of a facilitated working group (WG) represented by members with the collective professional experience to reach a consensus in estimating the peak HRR distributions for electrical enclosures in typical NPP configurations and to address some of the challenging fire modeling issues was chosen. The decision to use the facilitated WG approach was based on the nature of the planned work, the urgency of the needed information to support fire PRA application reviews, increased efficiency (provided a consensus opinion could be reached quickly), and the availability of test data to support the planned efforts. Where expertise beyond the collective knowledge of the WG was needed, individual experts were consulted. At this time, consultation with non-WG experts was primarily in the fire modeling area although experts were also asked to comment on the proposed enclosure classification groups.

The WG representation was balanced between the regulator (i.e., four members from the NRC/National Laboratories) and the nuclear power industry (i.e., four members from EPRI/nuclear power industry). The WG members are listed below, along with their affiliations. Brief resumes are included in Appendix A.

Joelle DeJoseph, Duke Energy (DUKE)
Francisco Joglar, Jensen Hughes (HAI)
Ashley Lindeman, Electric Power Research Institute (EPRI)
Nicholas Melly, U.S. Nuclear Regulatory Commission (NRC-RES)
David Miskiewicz, Engineering Planning and Management (EPM)
Steven Nowlen, Consultant[4]
David Stroup, U.S. Nuclear Regulatory Commission (NRC-RES)
Gabriel Taylor, U.S. Nuclear Regulatory Commission (NRC-RES)

A number of additional subject matter experts also participated in WG meetings. Mr. Mark Henry Salley of NRC-RES provided general assistance and oversight. Dr. Kevin McGrattan of NIST provided technical assistance associated with the Fire Dynamics Simulator (FDS) software and fire test results conducted at the CBD facility. Dr. Justin Williamson and Dr. Victor Ontiveros of Jensen Hughes performed the computer simulations of obstructed plumes. Finally, Dr. Manomohan Subudhi of Brookhaven National Laboratories (BNL) served as the moderator/facilitator of the meetings and discussions.

In developing the information documented in this report, the facilitated WG held four multi-day meetings between April and September 2014. A summary of the working group's interactions is included in Appendix B. These meetings allowed the WG to effectively communicate opinions and receive constructive feedback on possible approaches for addressing the project objectives. The early meetings allowed the WG to formulate a project outline and actions to be completed,

---

[4] Steven Nowlen (retired) was a Distinguished Member of the Technical Staff at Sandia National Laboratories.

while the later meetings allowed the WG's progress to be reviewed and formalized. In the latter half of this process, weekly conference calls were also held to update WG members on the status of current and planned activities. Ultimately, the results and approaches presented in this report represent the WG's consensus opinion.

1.3 Scope and Terminology

The RACHELLE-FIRE program deals with the analysis of fires that originate in electrical or electronic equipment housed within a support structure, generally metal, that is either enclosed or made up of open rack-type panels or supports. In this report, these housings are referred to as "electrical enclosures." The term "electrical enclosure" is meant to be broadly inclusive of essentially any box or structure, with the exception of cable trays and conduits, whose primary purpose is to house electrical and/or electronic components. "Electrical enclosure" as used in this report does encompass the open rack panels used in some NPP applications even though, strictly speaking, these are not enclosures (e.g., a relay rack or an open support structure used to house instrument and/or control components).

In past practice, a variety of terms have been used to identify these same items. For example, NUREG/CR-6850 used the terms "panel" and "cabinet" extensively. The terms "relay rack," "control or circuit boards," and "junction box" are also used. In general, "electrical enclosure" is a more widely recognized and generic term used among electrical equipment manufacturers and electrical engineers (e.g., see the various standards published by the National Electrical Manufacturers Association). The term "electrical enclosure" as used in this report is inclusive of cabinets, panels, and relay racks as those terms are used in NUREG/CR-6850 and other related fire PRA documents and standards.

In NUREG/CR-6850 the term "enclosure" is used in two other contexts—namely, the regulatory issue of cables and components that share a "common enclosure" (e.g., cables routed in the same cable tray), and the modeling of "enclosure fires" (i.e., fires that occur within a room as opposed to fires that occur in an open unconfined space). The reader is cautioned not to confuse these unrelated uses of the word "enclosure."

The facilitated WG developed fire source burning behaviors characterized by a distribution on peak HRR reflecting the aleatory uncertainty associated with fire development. The WG used the same approach that was used when developing the distributions found in Appendix G of NUREG/CR-6850 and did not attempt to explicitly characterize the uncertainty of these peak HRR distributions or the appropriateness of using a two-parameter distribution profile whose parameters were derived from the 75th and 98th percentile WG consensus estimates.

The fundamental scope of this report is the characterization and analysis of those plant fire ignition sources that, under NUREG/CR-6850 - Task 6, have been counted as members of fire ignition source: Bin 4 - main control board, Bin 10 - battery chargers, and Bin 15 - electrical cabinets. The methods of this report are *not* applicable to any other fire ignition source and, in particular, are not applicable to electrical enclosures that are either not counted as fire ignition sources (per the counting information) or that are counted as junction boxes (fire ignition source Bin 18). This report also does not deal with high energy arcing fault initiated fires in any electrical enclosure (fire ignition source Bin 16).

NUREG/CR-6850 also refers to "qualified thermoplastic cables" when setting the fire characteristics of electrical enclosure fires. In this context, the designation "qualified" is a reference to the IEEE-383 cable qualification standard which originally included a vertical flame spread test[5]. The IEEE-383 flame spread test has been a common historical flammability benchmark used in the U.S. nuclear power industry, and cables that pass that test are considered "qualified" as low flame spread. Since publication of the IEEE-383 standard in 1975 it has been common practice for plants to specify low flame spread cables per that test in procurement actions. In some cases cables have also been "back-qualified" through testing done some time after procurement and/or installation. Note that the flame spread test is only a minor aspect of the overall IEEE-383 standard which focuses mainly on severe accident equipment qualification testing. Cables that pass the flame spread test may not comply with other portions of the standard but would still be considered low flammability.

The intended practice under the methods presented here is to treat qualified TP cables (i.e., cables shown to pass the IEEE-383 flame spread test) consistently with the treatment outlined in NUREG/CR-6850; namely, qualified TP cables are given equivalent status relative to fire characterization as are TS cables. That is, if the application involves TP cables but those cables were tested and passed the IEEE-383 flame spread test, then the analyst may treat those cables as equivalent to TS cables when selecting the appropriate peak HRR distribution (e.g., when applying Tables 4-1 and 4-2 from this report).

1.4 Objectives

This report documents the working group's efforts and consensus in three technical areas:

1. The classification of electrical enclosures typically selected as ignition sources in probabilistic studies (i.e., fire modeling or fire PRAs) in the commercial nuclear power industry,
2. The characterization of peak HRRs associated with the different electrical enclosures, and
3. The characterization of fire plume temperatures generated by fires inside electrical enclosures.

The research results in these three areas were consolidated in the form of technical information that can be applied in fire modeling studies supporting fire PRAs. This technical information includes:

1. The classification of electrical enclosures in terms of function, size, contents, and ventilation conditions,
2. The determination of peak HRR probability distributions considering specific electrical enclosure characteristics such as function, size, ventilation conditions, and combustible content, and
3. The characterization of fire plumes associated with fires in electrical enclosures.

It should be noted that the methods and data described in this report are a supplement to existing methods and data, primarily documented in NUREG/CR-6850, its corresponding supplement, and fire PRA FAQs. Analyses already completed with the existing methods and data can be considered bounding and may not need to be supplemented with the information provided in this document. Specifically:

---

[5] Note that since its original publication under IEEE-383, the flame spread test portion of the standard has been removed from IEEE-383 and published instead under IEEE-1202. The two tests are the same.

- The classification of electrical enclosures is consistent and does not affect the existing ignition source counting information available in Chapter 6 of NUREG/CR-6850 and applicable fire PRA FAQs.
- The probability distributions for peak HRRs can replace the ones currently available in Appendix E and G of NUREG/CR-6850. However, the existing distributions in NUREG/CR-6850 are considered bounding when compared with their corresponding counterparts described in this document.

The characterization of fire plumes generated by fires in electrical enclosures, when applicable to a given scenario, is expected to produce lower plume temperatures than the ones obtained using existing information. Consequently, the existing information is bounding, as the use of “unobstructed” fire plume temperature models produces higher gas temperatures.

The revised peak heat release rate distributions and the obstructed plume study may affect the size of the fire zone of influence (ZOI). The ZOI is a crucial element of the fire PRA development as it has a direct impact on damaged equipment postulated in the fire PRA response model.

1.5 Report Organization

This report is organized as follows:

- Chapter 2 describes the activities and process used by the working group to develop the new heat release rate distributions and the obstructed plume methodology.

- Chapters 3 and 4 discuss the classification of electrical enclosures. Chapter 3 describes the new electrical enclosure classification groups. This chapter also describes the effect of the enclosure internal fuel load configuration on the peak HRR. Chapter 4 documents the consensus peak HRR probability distributions for the different electrical enclosure classification groups.

- Chapters 5 and 6 describe the research associated with obstructed fire plume temperatures. Specifically, Chapter 5 describes the technical basis for the methodology provided in this report. The methodology and example applications are provided in Chapter 6.

- Chapter 7 provides the summary of results and conclusions of this study. In addition, areas for future research as discussed during the working group meetings are identified in this chapter.

- Appendix A includes the resumes of WG members, technical contributors, and working group moderator.

- Appendix B provides an overview of the deliberation activities of the WG members on estimating the HRR distributions for various enclosure types. This includes the process used by the WG, and defined issues that were considered by the WG in this project.

- Appendix C presents a library of pictures and descriptions for the electrical enclosure types described in Chapter 3. These pictures serve as information for the classification of electrical enclosures in specific applications.

- Appendix D summarizes the statistical analysis in support of the peak HRR probability distributions described in Chapter 4. The statistical analysis is based on available fire test results for the different enclosure classifications.

- Appendix E lists the obstructed plume temperature numerical results obtained using FDS.

- Appendix F describes several examples illustrating the application of the revised peak HRR probability distributions and the implementation of the information associated with obstructed fire plume temperatures for determining the vertical component of the ZOI.

- Appendix G is a compact disc (CD) containing the fire modeling software, input files, and other information used to develop the results in this report.

2
Overview of the Process

This chapter describes activities by the working group (WG) members and the process followed to: (1) classify electrical enclosures, (2) develop revised heat release rate (HRR) distributions for each classification, and (3) investigate the fire plume characterization generated by electrical enclosure fires. The following sections describe each of these topics in detail. Although the process for each of these three activities is described separately, there was overlap, especially between the electrical enclosure classification and the development of the updated peak HRR values.

2.1 Classification of Electrical Enclosures

The classification of electrical enclosures is based on the following process:

- Review existing enclosure classification guidance documented in Appendix G of NUREG/CR-6850. The review supported an understanding of:
    - Existing guidance for classifying electrical enclosures
    - Application/experience using the existing approach
    - Limitations and areas for enhancement/realism
- Review the fire hazards associated with electrical enclosures, including:
    - Extensive review of photographs depicting electrical enclosure internals to assess variability in fuel load and configuration
    - Equipment functional differences
    - Discussion of ignition source strength/types among the different electrical enclosures
    - Collection and review of available experimental test series
    - Review of U.S. operating experience using the Updated Fire Events Database (EPRI 1025284)
    - Focus on implementation and practical application

2.1.1 *Review of Existing Guidance*

The WG reviewed Appendix G of NUREG/CR-6850, specifically Table G-1, which lists the recommended heat release rate (HRR) probability distributions for five different types of enclosures. The classification of all electrical enclosures into five ignition source groups is based primarily on:

- Number of cable bundles, i.e., one cable bundle or more than one bundle
- Qualified or unqualified cables
- Open or closed electrical enclosure (for more than one bundle and unqualified cable)

The existing guidance uses cable bundle parameter characterization to correlate the recommended HRR values to fire test data configurations from the NRC/SNL [8] and VTT [9, 10, 11] control electrical enclosure test programs. Similarly, the ventilation configuration of the enclosure (i.e., open or closed electrical enclosure) and the qualification of the cables involved in the tests also correlated to the experimental programs.

A key limitation of the original Appendix G electrical enclosure classification approach is in its practical application. For example, the original authors have stated that their intent was that the single bundle cases would cover most of the higher voltage power switching equipment (e.g., switchgear and load centers) and most other enclosures would likely fall into the “more than one bundle” cases including those with significant fuel loads other than cables (e.g., control components). It was also intended that the “single bundle” cases would include cases where an enclosure contained more than one bundle but due to the internal configuration, fire was likely to impact only a single bundle at a time (e.g., internal separation of the bundles with no significant inter-bundle fuel available). However, unless internal inspection was possible, analysts appear to default to the higher “more than one bundle” cases and, in practice, the latter argument, fire will remain confined to one bundle, has been difficult to justify.

The WG also noted that based on Table G-1 of NUREG/CR-6850, PRA analysts had, in some cases, assigned unreasonably high peak HRR values to certain small and medium size enclosures. This is a result of the relatively low number of electrical enclosure peak HRR estimates available for selection.

The working group agreed that a classification based on size and functionality of the electrical enclosure would provide a more practical implementation of the methodology. The WG determined that these are factors that can be easily determined by visual inspection during a walkdown without the need to open the electrical enclosure. At the same time, a classification based on enclosure size and functionality generated the need for understanding the fire hazards associated with the different functions and sizes.

2.1.2 *Understanding the Fire Hazards Associated with Different Electrical Enclosures*

In order to understand the effects enclosure function, size, and combustible loading characteristics have on peak fire vulnerability, the WG reviewed hundreds of electrical enclosure photographs of closed and open door configurations currently installed in commercial nuclear power plants (NPPs). During the review process, the WG discussed in detail the typical configurations for specific types of electrical enclosures to support a common understanding among the WG members of the similarities and differences among the types of electrical enclosures found in commercial NPPs. Additionally, the WG collected and studied experimental data and operating experience associated with electrical enclosure fires. Based on these activities, the WG considered the following attributes for electrical enclosure fires in classifying all relevant ignition sources:

- An enclosure’s internal volume and the amount of combustible materials (mostly cable insulations and electronic cards) have a significant effect on the maximum fire size if the ignition remains undetected and unsuppressed.

- Experience has shown that voltage and current ratings can have a significant effect on the ignition size and duration of the pre-growth phase of a fire. However, there is essentially no evidence to show how these factors would impact the peak HRR. The presumption of the working group is that once ignited, higher ignition energies available would tend to increase the likelihood of larger fires, but ignition energy has very limited effect on the worst-case peak HRR values.

- Switchgear, load centers, motor control centers (MCCs), power inverters, and battery chargers are normally housed in closed, vented enclosures and have very small amounts of cables, limiting the size of the expected fires. Variations among the equipment manufacturers and from plant to plant installations are not significant enough to affect the fire characteristics among enclosures within each of these functional types.

- Neatly organized internals (e.g., jacket-stripped cable with conductor bundles neatly zip-tied and run in an orderly fashion along the walls of the enclosure, wires leading to enclosure internals neatly arranged and run in tight bundles between the mounted electrical and electronic devices, high levels of internal partitioning with some components housed in internal metal enclosures within a larger enclosure) are more difficult to ignite and take a longer time for initial ignition and fire growth than disorderly contents (e.g., loose or no bundling of cables, large quantities or small conductor wires routed throughout, quantities of excess or spare cable often left inside an enclosure, wide dispersal of fuels over the enclosure interior). Even given well organized contents, once the conductor bundle ties melt, tests have shown that the fire size could grow rapidly, but in general, a larger initial fire is needed and a relatively lower peak HRR value will still be expected than that given an enclosure with disorderly internals.

- Enclosure venting conditions range from fully open equipment racks to fully enclosed and tightly sealed conditions. Larger enclosures usually have some degree of venting, typically top and bottom louvers on the horizontal face of the enclosure, that provide for adequate ventilation and cooling of devices when in operation. Fire tests have shown that ventilation characteristics have a major effect on the fire growth inside an enclosure [7, 8]. A fire under an open configuration can grow to a larger size than one inside a closed enclosure, due to the ventilation effect.

- Tests have shown that cables with thermoplastic (TP) conductor insulation ignite and spread fire far more easily than those with thermoset (TS) insulation. Tests have also shown that TP cables qualified as low flame spread per the IEEE-383 standard vertical flame spread test will show substantially reduced flammability compared to an unqualified cable. Finally, switchboard (SIS) wire, which is widely used in manufacturer pre-wired installations, is also subject to rigid flammability testing and is considered at least equivalent to TS cable in terms of flammability.

- Fires more readily spread vertically upward inside an enclosure than horizontally across the enclosure width. Given enough time, conditions conducive to flame spread may result in the involvement of all combustibles inside an enclosure.

After deliberation, the WG proposed an initial set of enclosure classification groups based on enclosure type/function rather than number of cable bundles. The final classification groups evolved slightly through the rest of the process but remained largely as defined originally. Chapter 3, “Classification of Electrical Enclosures,” describes the four classification groups and associated sub-groupings in detail, along with the factors considered to support this classification. The first three groups are based on the equipment functional classification, while the last group is based on the size and is intended to represent “all other” electrical enclosures not covered by the first three classes. The classification of electrical enclosures as fire ignition sources (Bins 4, 10, and 15) in accordance with Task 6 of NUREG/CR-6850 is based on assignment of each enclosure to one of the following classification groups[1]:

- Group 1: Switchgear and Load Centers

- Group 2: MCCs and Battery Chargers

- Group 3: Power Inverters

- Group 4: All Other Electrical Enclosures

    - Group 4a: Large Enclosures
    - Group 4b: Medium Enclosures
    - Group 4c: Small Enclosures

2.2 Process Used in Developing the HRR Distributions

The WG developed the HRR distributions, as presented in Chapter 4, for each classification group by conducting the following activities.

- A literature survey that consisted of reviewing:
    - Experimental test series conducted in the U.S. and internationally over the last three decades
    - U.S. NPP operating experience documented in EPRI's Fire Events Database
- Identification of influencing factors. The WG identified the following influencing factors:
    - Electrical enclosure volume
    - Electrical enclosure function
    - Combustible type
    - Amount of combustible materials
    - Combustible material configuration
    - Electrical ignition size/potential
    - Ventilation conditions
- Calibration exercise
- Assessment of electrical enclosure heat release rates
- Building and achieving consensus
- Ensuring consistency and applicability
- Finalizing the consensus

2.2.1 *Literature Review*

The WG began with a review of the available information relevant to electrical enclosure fire behavior, including both experimental data and actual plant fire experience. The available information included:

- NRC/SNL control electrical enclosure fire tests [8],
- VTT tests from Finland [9, 10, 11],

---

[1] Each classification group is assigned a simple alpha-numeric identifier in order to simplify aspects of the discussions that follow and to promote a common PRA vocabulary. It is provided that these designations be used as “shorthand” identifiers when citing classification results for in-plant enclosures (e.g., in fire PRA databases).

- IRSN tests from France [12],
- recently completed set of tests by NRC/NIST [7], and
- the EPRI updated fire events database [13].

Each test program was discussed in some detail including consideration of the test results as well as the test objectives and approach. Actual fire experience was reviewed based on the recently updated EPRI fire events database [13], which covers U.S. commercial nuclear power plant (NPP) fire events. All of the fire events involving electrical enclosures were identified and reviewed, focusing especially on plant events occurring from 1990 through 2009. Insights from the event reports were discussed and factored into the consensus process as deemed appropriate by the WG members.

2.2.2 *Identification of Influencing Factors*

The WG identified factors that can influence the HRR generated by an electrical enclosure fire. These influencing factors form the basis for determining the probability distributions for the different electrical enclosure classifications. Specifically:

- **Electrical enclosure volume:** The electrical enclosure volume is a factor explicitly represented in the electrical enclosure classification for Group 4. The WG agreed that the enclosure volume provides a practical approach for classification.
- **Combustible type:** The combustible type is classified as either TP or TS cable for the final HRR distribution categories. Note that, per the discussion in Section 1.3 above, TP cables that are qualified as low flame spread per IEEE-383 flame spread test may be treated as equivalent to TS cables; that is, qualified TP cables may be mapped to the TS combustible type groups. Similar treatment is also given to SIS wire; that is, SIS wire is also mapped to the TS combustible type groups.
- **Amount of combustible materials:** The WG agreed that the amount of combustible material is similar for the types of electrical enclosures classified by their function (Groups 1-3) and for small enclosures (Group 4c). However, for the “all other” – large and medium enclosure classification groups (Groups 4a and 4b), the amount of combustible material can vary widely. For that reason, the “all other” – large and medium enclosure classifications (Groups 4a and 4b) were further divided to allow for additional resolution in assigning peak HRR probability distributions. The WG agreed that pursuit of this further refinement (low or very low combustible loading) requires internal inspection of the electrical enclosure.
- **Combustible material configuration:** Similar to the factor associated with the amount of combustible material, the WG agreed that the combustible configuration is similar for the types of electrical enclosures classified by their function (Groups 1-3) and for the small “all other” enclosure classification (Group 4c). However, for large and medium “all other” enclosure classifications (Groups 4a and 4b), the configuration can vary widely. For that reason, these two classifications were further divided to allow for additional resolution in assigning peak HRR probability distributions. The WG agreed that assignment of peak HRR distributions based on combustible configuration requires internal inspection of the electrical enclosure.
- **Electrical ignition size/potential:** The WG agreed that the electrical ignition size and potential can be a factor in the resulting HRR, although no clear conclusions can be reached with existing experimental data. However, this factor is implicitly included in the classification process by separating the enclosures by function (Groups 1-3) from the “all other” enclosure classification (Group 4). The peak HRR probability recommended for

the functional electrical enclosures (Groups 1-3) considered this in the determination of the 75th and 98th percentiles.

- **Ventilation conditions:** The WG agreed that the electrical enclosures classified by their function (Groups 1-3) are vented but closed (i.e., they have vents of some type but not open doors). Due to the inherent electrical hazards associated with these enclosures and the plant procedures governing their maintenance, the WG agreed that peak HRR probability distributions are only needed for closed electrical enclosure configurations. This is not the case for the "all other" enclosure classes, which have both open and closed configurations as evidenced by numerous enclosure pictures available to the group. Therefore, the WG developed probability distributions for both open and closed "all other" (Group 4) electrical enclosure configurations.

2.2.3 *Calibration Exercise*

A calibration exercise was conducted to ensure a common understanding of what a particular HRR value in kilowatts (kW) implies with respect to an electrical enclosure fire. This exercise involved the collection, by the NRC staff, of still photos and videos taken mainly from the most recent NRC/NIST test set [7]. The examples were chosen to illustrate a range of fire intensities and burning behaviors. During a webinar/conference call the NRC staff explained the attributes (i.e., amount of combustibles, ventilation condition, and cable insulation material type) of each example case and then showed the still photos and/or videos. Each WG member was then asked to predict the peak HRR value being illustrated. Time lapse videos were then shown of the tests, and the actual peak HRR measurement was provided to the WG. Initially, individual estimates showed wide variation, but by the end of the exercise, all members showed a good ability to estimate the peak HRR values for a particular fire size, specifically, accounting for the amount of combustibles.

Figure 2-1 and Figure 2-2 illustrate the fire sizes and the corresponding fire intensities in kilowatts for two examples used in the calibration exercise. Note that these are not cable insulation/enclosure fires. Nonetheless, they do visually illustrate relative fire intensities for common objects, a coffee maker and a Christmas tree, over the course of a fire test.

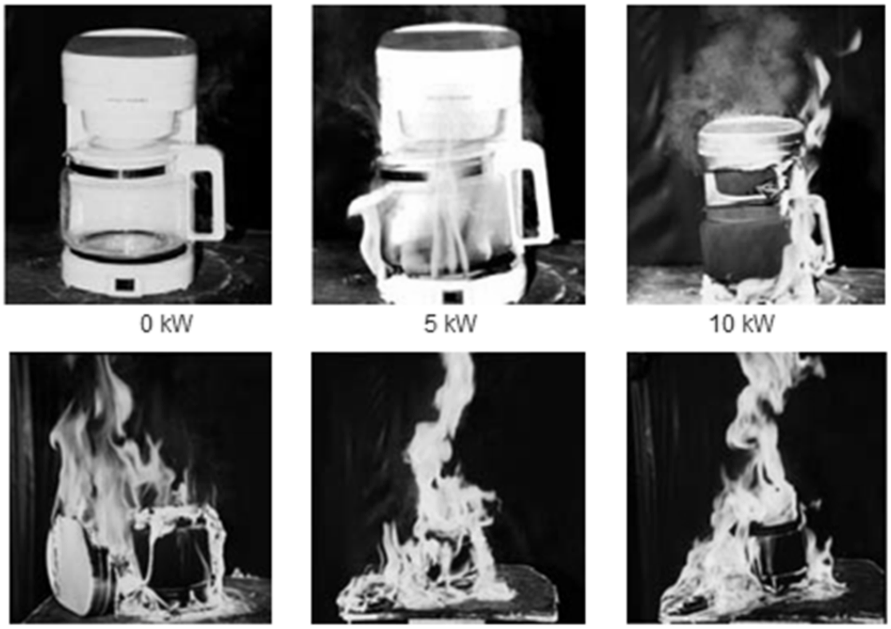

0 kW 5 kW 10 kW

25 kW 40 kW 40 kW

Figure 2-1
Fire Size/Intensity Calibration (0 to 40 kW)

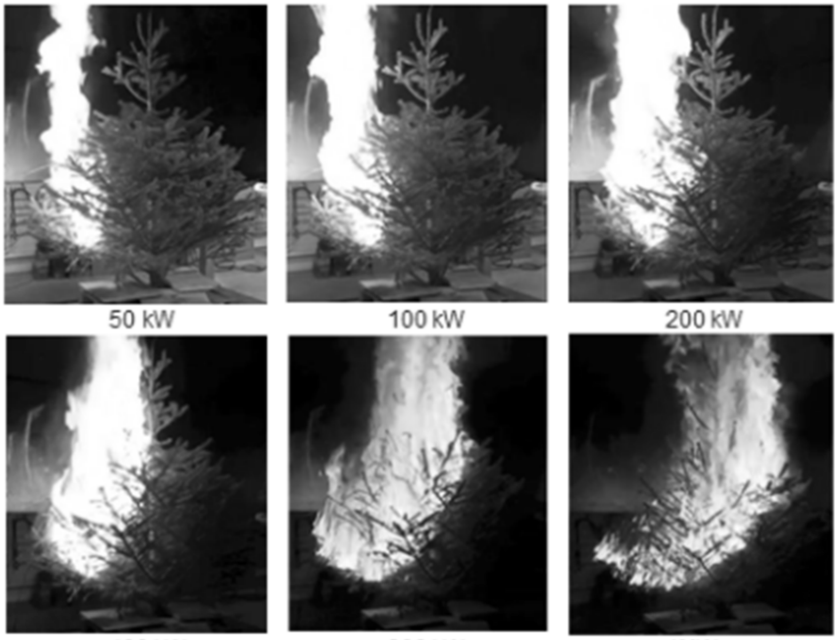

50 kW 100 kW 200 kW

400 kW 800 kW 1MW

Figure 2-2
Fire Size/Intensity Calibration (50 to 1000 kW)

2.2.4 *Assessment of Electrical Enclosure Heat Release Rates*

Each member of the WG was tasked to independently assign 75th and 98th percentile HRR values for the newly developed enclosure classification groups defined in Chapter 3. Consideration of specific experiments, operational experience, influencing factors, and so on were incorporated into the specific distributions on an individual basis.

2.2.5 *Building Consensus*

Using a consensus process the peak HRR distributions for each of the enclosure classification groups were defined. This activity took place during a WG meeting with all members present. Initially, for each enclosure type/function group, the members were polled regarding their individual estimates of the peak HRR distribution for that group (developed in the second step as noted above). A broad consensus was evident for most cases, with some outlier estimates on both the high and low sides. Each member was asked to describe their reasoning for each case and, as a more common understanding of the conditions being assumed and the applicable data set was developed, consensus values were proposed and agreement obtained. Through these discussions, preliminary consensus estimates were developed by the WG. Based on these preliminary consensus values, the WG fitted a gamma distribution based on the two HRR values corresponding to 75th and 98th percentiles for each classification group (see Appendix D.3).

2.2.6 *Ensuring Consistency and Applicability*

To ensure consistency and applicability of the consensus estimates, each of the available tests was reviewed and assigned to one or more classification groups. Certain tests were discussed and, based on one or more test-specific factors, were judged to be of questionable applicability. In some cases, tests were partly *discounted*; that is, they were considered somewhat applicable but not directly characteristic of realistic fire conditions. No attempt was made to “weigh” the discounted tests against other tests, and the discounted tests are included in the experimental data distributions, but the final recommended peak HRR distributions typically will not bound these tests. Other tests were *dismissed* entirely; that is, they were not considered applicable to actual enclosures given the nature of the fuels burned and are excluded from the data sets entirely. Appendix D presents the mapping of test data to the HRR distributions chosen by the WG members based on a consensus basis. It is emphasized that the revised peak HRR distributions are not based directly on fitting any particular set of test data. However, the available test data were used by WG members to inform their selection of representative distributions. Ultimately, the consensus distributions were compared to test data considered applicable to each enclosure classification group to ensure that any inconsistencies could either be explained (e.g., based on a sparse or otherwise poor data set) or, where possible, eliminated (see Appendix D). The EPRI fire events database was then reviewed to identify that the HRR profile for the particular enclosure encompasses all plant events.

The cases where test data were discounted or dismissed are detailed as follows (also see Appendix D.1):

- The original NRC/SNL electrical enclosure fire test series [8] included a small number of tests involving either a heptane fuel pool (Tests PCT-4A and PCT-4C) or a gas burner placed inside an otherwise empty control enclosure (Tests 21 and 22). These tests were never intended to represent an actual fire in an electrical enclosure; rather, they were intended to provide for characterization of room effects given a large, well-characterized fire within an electrical enclosure shell. These tests were not considered relevant to characterization of actual electrical enclosure fires and were *dismissed* entirely.

- One test from the original NRC/SNL test series [8] was *discounted* based on the non-representative nature of the ignition source; namely, Test 23, which involved qualified thermoset cables in a bench board electrical enclosure. For Test 23, the WG agreed that the extent of the fire growth seen in this test was likely driven largely by the intensity and duration of the ignition source, which burned at roughly 40 kW for over 30 minutes. Many test programs have shown that thermoset cables require a significant and sustained ignition source or they will likely self-extinguish. Hence, the peak heat release rate in this test, estimated at 1235 kW, would not be expected given a more realistic ignition source. In general, some form of an ignition source must be used to initiate a fire test, and the test programs considered by the WG represent a range of potential ignition sources. In the case of Test 23, the WG concluded that the ignition source used is much more intense than those to be expected for a control enclosure application and that the measured peak HRR would not have been reached had a less energetic and/or shorter duration ignition source been used. Nominally, Test 23 would be assigned to the open “all other” electrical enclosure, thermoset cable type classification group. However, the test was *dismissed* from the data set, and the corresponding peak HRR distribution was not formulated to bound this particular experiment.

- The NRC/SNL tests also included a test essentially identical to Test 23 except that unqualified thermoplastic cables were used; namely, Test 24 [8]. In this case, the test was included in the data set for open “all other” electrical enclosures with thermoplastic cables because thermoplastic cables do propagate fire more easily. However, this test was treated as an outlier case, again due to the nature of the ignition source. While this test was considered somewhat relevant, it was partially *discounted* and the corresponding peak HRR distribution does not bound this particular experiment[2]. The WG concluded that given a more realistic ignition source, full electrical enclosure involvement was still possible although the fire would have likely grown at a slower pace and reached a lower peak than that observed in the test. Test 24 is included in the test data set for the large “all other” (Group 4a), open, TP cable classification group, as shown in Appendix D.

- The majority of the IRSN tests [9, 10, 11] involved PMMA slabs burned within an electrical enclosure mock-up shell. The objective of these tests was to assess whether enclosure vent size correlated to the maximum heat release rate possible given a fire within an enclosure. The fuels in these tests are not representative of real electrical enclosures. Given the unrealistic nature of the fuels, the IRSN tests using PMMA slabs were *dismissed* from the peak HRR distribution development effort.

- The tests conducted by NIST at CBD [7] were based on a catalog of pictures obtained during walkdowns of various NPPs as well as the discretion of the test engineers. Two test scenarios in particular were chosen in order to evaluate the worst-case condition beyond that typically seen in NPPs. These tests are identified as test numbers 68, 71 (closed door), and 83 (open door, see Figure 2-3). The cabinets were filled with the maximum loading of jacket stripped cables and distributed in a manner to facilitate flame

---

[2] Similarly, the NUREG/CR-6850 HRR distribution for thermoplastic, open enclosure, multiple bundles does not bound this experiment.

spread. That is, the cables were separated to allow for the maximum burning area of the fuel and to facilitate full burnout. These cases were altered to evaluate the impact of various test conditions (e.g., ventilation, configuration, and ignition) on the fire growth within the electrical enclosures. The tests were not dismissed, but they were discounted because the cable loading arrangement was not typical of any known NPP cabinet type. However, these tests provide some indication of the absolute upper bound fire conditions that might occur given the enclosure geometry. The data was used by the working group to inform the consensus distributions. These tests along with some large fire test data from the NRC/SNL tests [8] were mapped to the large and medium size enclosure classification groups.

- The WG discounted some of the most recent NRC/NIST tests [7] based on two factors. First was the extreme ambient conditions under which the tests were conducted, and second was the fact that the smaller (1 kW and 5 kW) ignition sources used by NIST were unable to create a sustained fire under the test conditions. Most of these tests were performed with the electrical enclosures and, more importantly, the cables, at initial temperatures of 0 °C (32 °F) or less. These initial conditions likely caused some delays in, and in some cases may have prevented, cable ignition, sustained burning, and/or fire spread. Hence, while all of the NIST tests are included in at least one of the classification group test data sets, the WG chose not to include some of these tests in the experimental distributions for the other classification groups. In particular, those tests using the two smaller ignition sources (i.e., the 1 kW and 5 kW electric cartridge heaters) where the cables never ignited and no flame spread was observed were included in the small “all other” electrical enclosure (Group 4c) data set, but were excluded from the other data sets. Note that in the analysis of actual events, when estimating fire frequency, an event involving a small ignition source that self-extinguished without any substantive fire spread would be classified as non-challenging and would be excluded from the fire frequency analysis. The WG’s decisions regarding the “no ignition, no spread” tests mirror the fire frequency analysis.

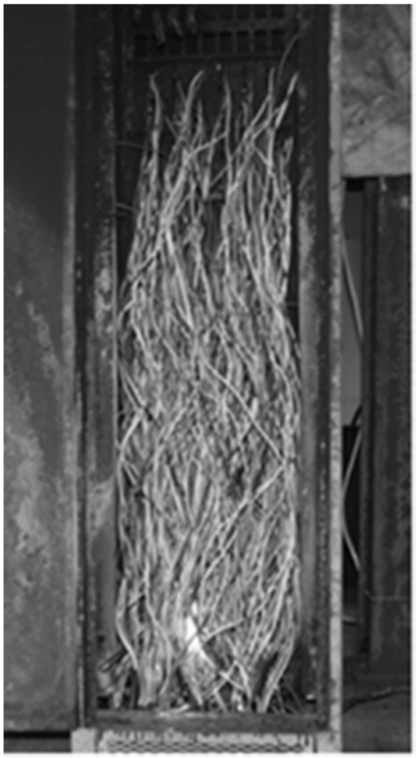

Figure 2-3
HELEN-FIRE Test No. 68

2.2.7 *Finalizing the Consensus*

As a final step, the WG had an additional opportunity to consider the consensus distributions, review again the test sets associated with each classification, and propose alternative treatment, if applicable. Based on this review, the WG found that some of the HRR profiles for the “all other” – large and medium enclosures (Groups 4a and 4b) did not address certain enclosures that have combustible loads (e.g., cables) less than what is assumed as the default condition; namely, a significant fuel load relative to enclosure volume that may be arranged in a manner conducive to fire spread. To address enclosures with limited and neatly configured combustibles, the WG added two separate sub-groups for these two enclosure classes. One sub-group (i.e., low fuel loading) represents enclosures with combustible loads relatively less than that of the default case. The second sub-group (i.e., very low fuel loading) represents enclosures with very sparse combustible loads relative to enclosure volume. In both sub-groups, it is assumed that all combustibles are neatly organized. Descriptions of these sub-groups are presented in Section 3.2.2. The WG repeated the steps discussed in Sections 2.2.2 through 2.2.7 to reach a consensus on these sub-group HRR estimates.

2.3 Method for Characterizing Electrical Enclosure Fire Plumes

The initial concept of the obstructed plume was discussed during the first meeting of the WG. The common treatment of fire plume effects for electrical enclosure fires completely ignores the effects of the enclosure surfaces, especially the top, on plume development and is therefore quite conservative. The concept involved using Fire Dynamics Simulator (FDS) as a surrogate for experimental data to support a more realistic representation of the early stage fire development and thermal insult to fire targets located within a plume. In simple terms, FDS is used as a tool to evaluate the effect an obstruction has on fire plume thermal characteristics and supports the development of an adjustment factor for the vertical zone of influence (ZOI) and plume temperature.

During the first meeting the WG identified obstruction configurations, ventilation conditions, and fire size and location, along with measurements and locations to include in the FDS simulation. During the second meeting preliminary results of the FDS simulations were presented. At this meeting, the WG decided that the approach appeared to yield encouraging results to improve the realism in modeling electrical enclosure fires, compared to existing guidance in NUREG/CR-6850. The WG suggested modifications to the electrical enclosure modeling and fire size. At the third meeting the WG determined that the work and documentation was at a level of quality to facilitate a peer review. Between the third and fourth meeting the peer review comments were received, reviewed, and incorporated into the study as appropriate. The results of this work, including the assumptions, approach, results, and correlation, are presented in Chapters 5 and 6 of this report.

3

Classification of Electrical Enclosures

This chapter describes the classification of electrical enclosures based on the enclosure's electrical function, physical size and location (e.g., free standing, wall mounted), amount and character of fuel loading, ventilation characteristics, and the cable insulation material type. Section 2.1 presents the process pursued by the working group (WG) to develop these classifications. Appendix C provides photographs of a range of electrical enclosures and their installed configuration in NPPs. This section includes some illustrative examples of those photographs.

The classification of electrical enclosures as fire ignition sources (Bins 4, 10, and 15) in accordance with Task 6 of NUREG/CR-6850 is based on assignment of each enclosure to one of the following type/function classification groups[1]:

- Group 1: Switchgear and Load Centers

- Group 2: MCCs and Battery Chargers

- Group 3: Power Inverters

- Group 4: All Other Electrical Enclosures

    - Group 4a: Large Enclosures
    - Group 4b: Medium Enclosures
    - Group 4c: Small Enclosures

The fire characterizations of these enclosure classification groups are described below. Section 3.1 describes the functionally based Groups 1-3 enclosures and Section 3.2 describes the classification and sub-grouping of Group 4 enclosures.

The discussions here are intended to highlight both similarities and differences between the various enclosure types considered. The factors highlighted in each section are those that are expected to substantially impact both the worst-case fire behaviors that might be expected (e.g., the 98th percentile peak HRR values) and the relative likelihood that, given an ignition event and in the absence of fire suppression, a large fire is likely to develop (as characterized by the 75th percentile peak HRR values). The primary factors considered in the final group classification process are as follows:

- **Physical size:** For classification Group 4, physical size is used as a general, readily obtainable characteristic that would influence fire behavior. The presumption is that a large or a medium enclosure holds the potential for higher intensity fires than a

---

[1] Each classification group is assigned a simple alpha-numeric identifier in order to simplify aspects of the discussions that follow and to promote a common PRA vocabulary. It is provided that these designations be used as "shorthand" identifiers when citing classification results for in-plant enclosures (e.g., in fire PRA databases).

comparable but much smaller enclosure simply because it has the capacity to hold more combustible fuels and more possible ignition sources. Note, however, that for classification Group 4, if visual inspection of the enclosure internals is possible, additional consideration can be given to the actual fuel load present, which may act to reduce the default fire potential of a large or a medium enclosure to, in effect, that of a smaller enclosure.

- **Cable insulation type:** The HRR distributions presented in Chapter 4 distinguish between enclosures with thermoset (TS) cable insulation (including qualified TP and SIS wire) versus unqualified thermoplastic (TP) cable insulation (including enclosures with a mix of thermoset and unqualified thermoplastic). Testing has consistently shown that unqualified TP cables ignite more easily and spread fire more readily than TS cables. However, testing also shows that if a growing fire is established in an electrical enclosure such that full burn-out of the enclosure is likely (barring suppression), the peak HRRs for TS and TP cables are quite similar. In general, the working group established the same 98th percentile peak HRR value for both cable types (with the exception of large open enclosures[2]). However, the 75th percentile peak HRR value is lower for TS cables than for TP (typically half as large). This reflects the observation that given an equivalent ignition event fire spread is less likely with TS cables than with TP cables. In other words, a larger percentage of TS cable fires are expected to remain small, even in the absence of suppression, compared to TP but, if the fire does spread, the worst-case peak HRR values are likely similar.

- **The combustible fuel load and configuration:** The total fuel load in an enclosure will influence the fire behavior, especially in cases where the fuel load is especially sparse. Equally important is the configuration of the fuels present. For example, large power cables will burn far less readily than will small instrument and control wires (the "logs versus kindling" analogy). Similarly, testing[3] has shown that cables that are tightly bound and routed in an orderly manner will burn less readily than would loosely bound cables routed in a disorderly fashion.

- **Enclosure ventilation condition:** All other factors being equal, an enclosure with very small ventilation openings will not burn as well as a very well ventilated enclosure. The approach presented does not explicitly address the ventilation conditions of a specific enclosure. However, the peak HRR distributions are expected to bound the typical ventilation conditions for the specific equipment classification group.

- **The nature of the ignition sources present:** Given the presence of higher energy ignition sources (e.g., higher power components and arc-fault sources) a higher intensity fire is more likely to develop in comparison to a similar enclosure with only low energy ignition sources present (e.g., control and instrument components).

---

[2] Based on test results, the WG concluded that a 1000 kW fire in case of the large enclosure group with TP cable insulation and open door ventilation configuration would bound all worst possible enclosure classes that may be existing in NPPs.

[3] This observation is consistent with both the original NRC's cabinet fire testing in the 1980s [8] and with the more recent NIST tests [7].

3.1 Functionally Based Enclosure Groups

All electrical enclosures in nuclear power plants (NPPs) are categorized based first on their electrical function and second on the cable insulation type (TP or TS). For some enclosures this is sufficient. In particular, switchgear, load centers, motor control centers, battery chargers, and inverters are all characterized based on function and fuel type alone. The following three functional groups have been defined to characterize the anticipated fire characteristics for these types of enclosures.

3.1.1 *Group 1: Switchgear and Load Centers*

This type/function group includes the enclosures housing higher power electrical switching and interrupting devices[4]. Switchgear and load centers are both common and readily identifiable in all plants. The term “switchgear” generally refers to medium voltage (>1000 VAC) switching equipment. The term “load center” is commonly used to describe low voltage (≤1000 VAC) switchgear.

Generally, load centers are physically smaller than the medium voltage switchgear and as many as four individual switches (typical) may be found to share a single vertical segment or cabinet as these are counted[5] under NUREG/CR-6850. For switchgear, the switch itself is generally housed in the lower section of the enclosure (due to its weight and physical size) and the associated control and monitoring equipment is housed in the upper section of the enclosure. For load centers, the actual switch and associated control and monitoring components share a common space. Switchgear and load centers have been combined into a single classification group for fire characterization purposes based on several factors.

First, these devices perform essentially the same function; namely, switching and overload protection for higher power loads associated with, most commonly, a subsidiary power distribution bus. The distinctions between switchgear and load centers are mainly associated with voltage and total power per switch.

Second, these devices have similar ignition sources and energies present; namely, those associated with failures in the primary switching unit including its input/output power leads, and those associated with the lower voltage control and monitoring components.

Third, switchgear and load center enclosures typically have limited fuel loads (i.e., in comparison to most other electrical enclosures), and the characteristics of the fuels present are similar. In both cases much of the fuel load is associated with the larger diameter input/output power cables which will not burn easily but will burn given a sufficient ignition event and/or sustained fire. The balance of fuel in both device types is associated with the control and monitoring components including smaller gauge instrument and control wiring, and this fuel will burn more easily. The presence of the control and monitoring components and wiring is one of the more significant factors considered to influence the overall fire growth potential.

---

[4] Note that switchgear and load centers are subject to high energy arcing fault (HEAF) events in addition to general thermal fires. The discussions here are limited to thermal fires only, but the working group did recognize that, consistent with the event data, some thermal fires are initiated by arc fault failures that do not reach the energy and impact levels associated with the HEAF events.

[5] In NUREG/CR-6850 Task 6, electrical cabinets are counted by vertical section. Hence, a single load center vertical section may house multiple switches. In contrast, medium voltage switchgears are typically housed individually; that is, there is typically only one switch per vertical section.

Finally, both switchgear and load centers will almost certainly be found in a closed, vented enclosure configuration due to safety standards and the need to dissipate internally generated normal heat loads[6]. Given similar enclosure conditions, fire characteristics will also tend toward similar behaviors.

Given the similarities described above, both switchgear and load centers are treated in the same manner relative to general fire characterization (again, excluding high energy arc fault treatment). Figure 3-1 provides exterior photographs of a typical bank of switchgear and load centers.

Switchgear Bank Load Centers

Figure 3-1
Switchgear and Load Center

3.1.2 *Group 2: Motor Control Centers (MCCs) and Battery Chargers*

MCCs and battery chargers are also common and readily identifiable in all plants. A typical plant will have many MCCs but typically only a handful of battery chargers. While these two device types perform markedly different functions, the two have been combined into one group for fire characterization based on similarities in size, fuel loading, and the energy available to potentially initiate a fire.

MCCs are commonly at the same voltage and powered from a load center. Typically, a single MCC will service a single end device such as a pump or motor. MCCs may also be used to supply lower level distribution buses such as house lighting and power. As with load centers, MCCs are commonly housed in stacks so that a single vertical section of MCCs (i.e., one cabinet as counted in NUREG/CR-6850) will commonly house four to five individual switches but could house as many as twelve individual switches. The fuel load for a typical MCC cabinet includes both the input/output power cables and control monitoring devices and wiring. In comparison to switchgear and load centers, the power cables will be smaller. While these smaller cables will burn more easily, they also represent a lower fuel loading than the larger

---

[6] The working group consulted a number of knowledgeable experts outside the working group regarding these enclosure configuration assumptions and none were able to cite an exception to the enclosure assumptions as cited here.

power cables associated with switchgear and load centers. The potential ignition sources also include both the power and control components.

One factor considered important by the working group is that an MCC is highly compartmented and this feature will limit the intensity of most MCC fires. Switchgear and load centers tend to be large enclosures with little internal partitioning. For MCCs, each individual switch is typically housed within its own enclosure (often referred to as a compartment or cubicle) and a vertical section, or stack, is made up of several compartments. In addition, each stack is commonly associated with a narrow vertical channel used to route field cables into and out of the compartments (see Figure 3-2). This channel is a common/shared portion of the MCC, and the possibility that fire might spread from one compartment into this vertical channel was a significant factor in the working group's assessment of the worst-case fire potential.

Figure 3-2
A Typical Vertical MCC Channel

Another factor considered important by the working group is that MCC cabinets tend to have more restrictive ventilation openings. In comparison to switchgear, for example, the heat loads associated with MCCs are much lower so that less ventilation is necessary to maintain components within operable temperatures. The limited ventilation conditions will tend to limit fire potential. However, MCCs may not be fully sealed and are subject to arc faults, albeit not at the HEAF level. An arc-fault initiated fire holds the potential to breach the MCC cabinet and the assumed fire characteristics reflect this (i.e., the arc fault may open a section of the MCC).

Figure 3-3 shows a typical bank of MCC stacks. This bank contains eight stacks and would be counted as eight vertical sections per NUREG/CR-6850. The stack on the far left contains 10 individual switches, which are near the maximum possible for a typical MCC stack configuration. By contrast, the two center stacks appear to contain just two switches each.

Figure 3-3
A Typical Bank of MCC Cabinets

The second component of this functional group is battery chargers. While less common, all plants will have a limited number of battery chargers present. Note that only those battery chargers associated with banks of large, multi-cell, emergency station batteries are included in this functional group; that is, chargers tied to the battery banks counted as Bin 1 ignition sources consistent with Task 6 of NUREG/CR-6850. This group does *not* include small battery chargers that may be associated with individual battery-powered equipment items (e.g., emergency lighting, a skid-mounted pump or motor, diesel generator start-up batteries, or a piece of portable electrical equipment).

There are typically two or three battery chargers per battery bank. Battery chargers require considerable ventilation in order to dissipate internal heat loads and should not be treated as “well-sealed” electrical enclosures under typical conditions. This was considered an important factor influencing the worst-case fire potential by the working group. Battery chargers also contain significant ignition energy sources, including the potential for internal arc faults, given connections to both a significant AC input power source and the output connections to the primary battery bank itself. On the other hand, the fuel load in a typical battery charger is limited, especially in comparison to the total volume of the enclosure. The relatively low fuel to volume ratio compared to other enclosures appears to be driven by the presence of a number of relatively large components with very little fuel contribution (e.g., transformers, rectifiers, and fuses). Like MCCs, the primary fuel loads are associated with both the input/output power cables and the control and monitoring components and wiring. Figure 3-4 shows an external view of a typical battery charger.

Figure 3-4
A Typical Battery Charger

The WG concluded that the fire characteristics for MCC and battery charger enclosures would be effectively the same despite functional differences. Both types have similar physical sizes (e.g., volume) and contain similar ignition source energy potentials. MCCs tend to have higher fuel loads but limited ventilation, whereas battery chargers tend toward lower fuel loads but more open ventilation conditions. These two off-setting factors in particular led the WG to conclude that the likely fire characteristics were similar enough that, for convenience, these two functional device types can be combined into one type/function group for fire characterization purposes.

3.1.3 *Group 3: Power Inverters*

This type/function group includes those enclosures whose primary purpose is to house a DC-to-AC power inverter. This functional group is *not* intended to include other electrical enclosures that happen to house one or more small power inverters such as those that might service individual circuits or devices. Given these constraints, inverters will be present in limited numbers at all plants.

Nominally one might anticipate that inverters and battery chargers would be quite similar given that the two devices perform complementary functions; that is, battery chargers convert AC power to DC power while inverters convert DC power to AC power. The WG found that while there are similarities, there are also important differences that are judged to significantly impact worst-case fire intensities. Like battery chargers, inverter enclosures are typically well ventilated in order to dissipate normal heat loads and should not be treated as “well-sealed” electrical enclosures under typical conditions. Further, significant electrical energy is present to act as ignition sources including both the input connections to the associated battery banks and the output connections to serviced AC distribution buses. However, the fuel loads for inverters are typically higher than those observed for battery chargers. The higher fuel load appears to be associated with the additional control and monitoring components and wiring associated with conditioning of the AC output power given that modern AC devices require reasonably “clean” input power to run reliably. In contrast, battery banks are more tolerant and require less rigorous signal conditioning of charger output. Based mainly on the higher quantity and general nature of the fuel loading, inverters are assigned to higher peak HRR levels than are battery chargers. Figure 3-5 shows a typical inverter including both an external and internal view.

Figure 3-5
A Typical Inverter Cabinet (Exterior – Left, Interior – Right)

3.2 Group 4: All Other Electrical Enclosures

If an electrical enclosure counted in fire frequency does not fit into one of the three functional groups defined in Section 3.1 above, it is treated using classification Group 4; namely, All Other Electrical Enclosures. Group 4 will also include the main control board (MCB). This group may encompass a wide range of enclosures including those associated with, for example, control components, instrumentation, low voltage breaker panels, lighting panels, communications equipment, individual or grouped switch/disconnect boxes, open rack panels, and alarm panels, among others. Group 4 is intended as a “catch-all” for all of the Bin 15 electrical cabinets not grouped based on function (i.e., per Section 3.1) plus the main control board (Bin 4).

For classification Group 4, a more complex classification basis has been defined in order to reflect differences in the fire potential for this broadly defined enclosure group. Distinctions within this group ultimately lead to seven possible classification outcomes for a given enclosure that are based on (1) the physical size and (2) the fuel loading characteristics.

3.2.1 *Assignment Based on Physical Size*

The first aspect of the characterization process is to define the enclosure as Large (4a), Medium (4b), or Small (4c). This is a simple volume-based decision using the following criteria:

- Group 4a – Large Enclosures: an enclosure with a volume greater than 1.4 m^3 (50 ft^3).

- Group 4b – Medium Enclosures: an enclosure with a volume greater than 0.34 m^3 (12 ft^3) but no more than 1.4 m^3 (50 ft^3).

- Group 4c – Small Enclosures: an enclosure with a volume of no more than 0.34 m^3 (12 ft^3).

The following paragraphs provide additional discussion regarding each of these classification group categories:

3.2.1.1 Group 4a: Large Enclosures

This type/function group is intended to cover mainly the larger control and instrumentation cabinets that are common in many areas of the plant. This group also includes low voltage power and lighting (typically 110 or 220 VAC house power) distribution panels (i.e., breaker panels) if such enclosures meeting the size criteria exist in the plant[7]. The electrical enclosures included as large enclosures may cover a wide range in terms of both physical size and function. Large enclosures would include most of the cabinets in the main control room including the main control board, but with the possible exception of some smaller computer or instrument racks if present. This group would include the typical open racks of the relay room. This group can also include a range of general electrical enclosures that may be found throughout the plant. Additional examples may include alternate shutdown panels, diesel generator control cabinets, and signal conditioning cabinets, among others. Again, the determining factor for classification as a large enclosure is the total enclosure volume, not the specific enclosure function.

Figure 3-6 and Figure 3-7 (see page 3-10) illustrate open and closed configurations of typical large enclosures.

---

[7] Note that the presence of a lighting or breaker panel meeting the large size criteria is considered unlikely and most such panels will likely fall into groups 4b and 4c.

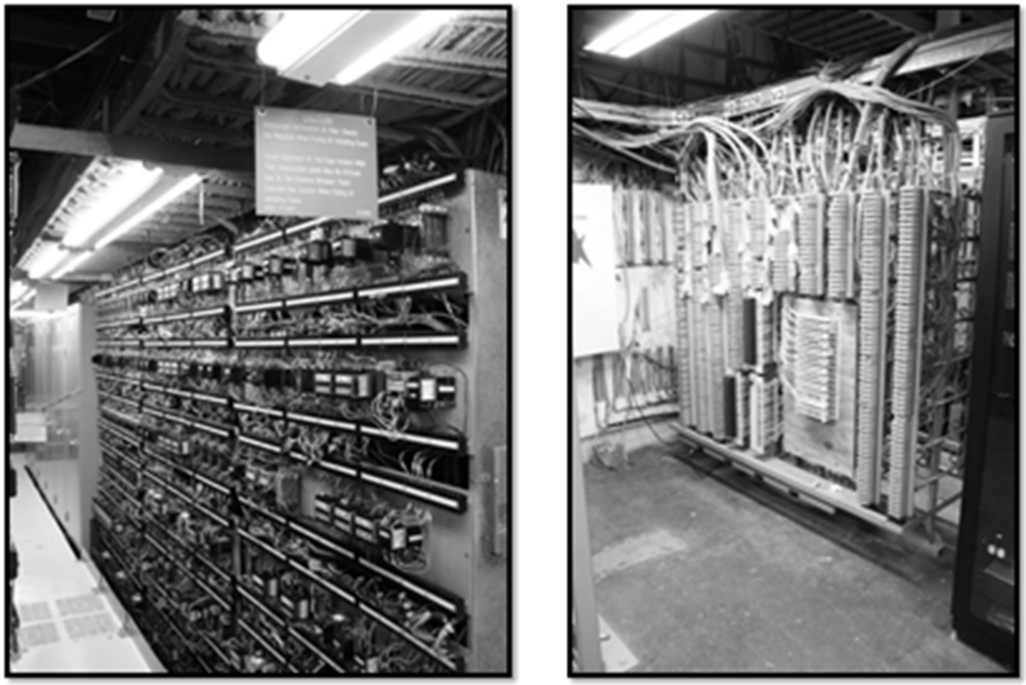

Figure 3-6
Large Enclosures (Open)

Figure 3-7
Large Enclosures (Closed)

3.2.1.2 Group 4b: Medium Enclosures

This type/function group is intended to cover enclosures that are comparatively smaller than the large enclosure group but that may still contain a substantial fuel load and significant ignition sources (see Figure 3-8). This group includes a wide range of instrument and control cabinets as well as many typical low voltage (<1000V) enclosures housing power and lighting circuit breaker panels, local control panels that may service several devices, and larger alarm panels such as a large, centralized fire protection alarm/control panel that services multiple fire protection (detection and/or suppression) systems. The group might include smaller signal conditioning cabinets. This group would also include most portable rack-mount computer and instrumentation cabinets that might, again, be found in use throughout the plant. Again, for any enclosure not meeting the functional group definitions from Section 3.1, the determining factor for categorization as a medium enclosure is the enclosure volume, not the enclosure function.

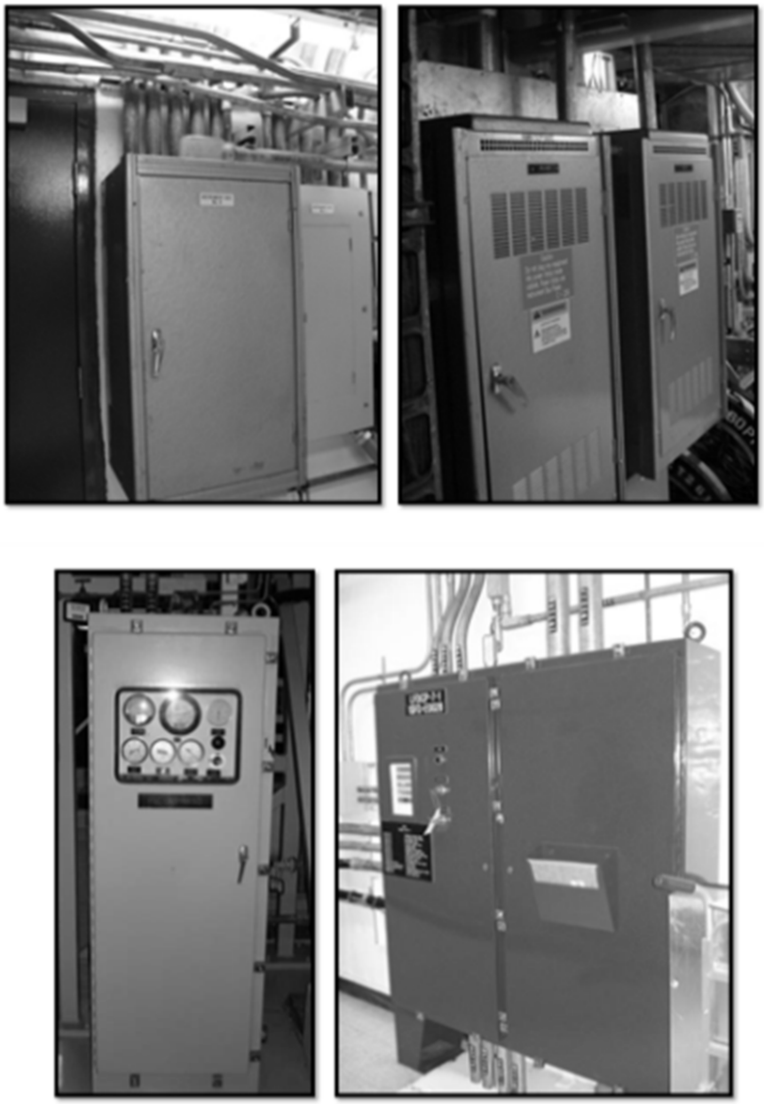

Figure 3-8
Medium Enclosures

3.2.1.3 Group 4c: Small Enclosures

This type/function group is intended to cover the range of small, often wall-mounted or pedestal-mounted, local control, alarm and switching boxes that did not meet the criteria for exclusion from the electrical enclosure ignition source counting information but that, due to their size and contents, would represent minimal fire threats. This group (see Figure 3-9) would include localized motor or pump control cabinets, small house power and lighting breaker panels, terminal block cabinets that did not meet the criteria for treatment as junction boxes, and individual switch/disconnect boxes. This group would also include localized alarm, communication, or indication panels that did not meet the fire ignition source exclusion criteria.

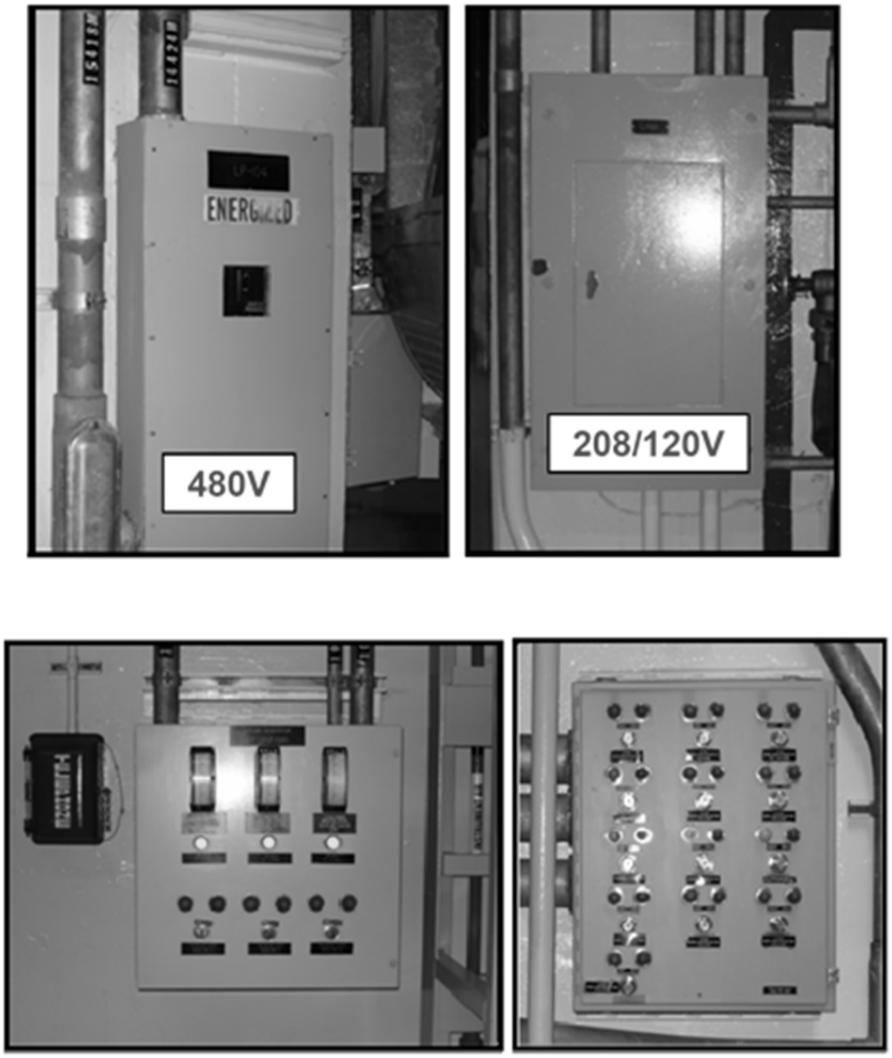

Figure 3-9
Small Enclosures (Note: top left enclosure may be well-sealed)

Note that there is no explicit voltage cutoff associated with this group and the group may include items such as 480 VAC disconnect switch boxes, fuse cabinets, and power disconnect switches that are commonly housed in individual switch cabinets. For small enclosures, the WG agreed to limit the volume to no more than 0.34 m^3 (12 ft^3). For an enclosure of this size, the amount of combustible materials present would be sharply limited, and such enclosures are normally found in a *closed* configuration. While some of these enclosures would contain significant potential ignition sources (e.g., a 480 V disconnect switch) the peak fire size would be limited by the fuel content and, for most such enclosures, the fire would be expected to remain contained inside. Even given an arc fault in a disconnect switch, which might breach the enclosure, the lack of fuel would mean that any flashover or fire would likely self-extinguish very quickly, a view supported by the event data. As a result, small enclosures are expected to present minimal threats to targets outside the box, and the provided fire characteristics reflect this assessment.

3.2.2 *Assignment Based on Fuel Loading Characteristics*

The second set of categorization criteria is limited to "Large Enclosure" and "Medium Enclosure" groups and is based on the fuel loading configuration. This second set of criteria may result in assignment of these two groups (Groups 4a and 4b) to one of three sub-groups as follows:

- Sub-Group 4a(a) or 4b(a) – Default Fuel Loading
- Sub-Group 4a(b) or 4b(b) – Low Fuel Loading
- Sub-Group 4a(c) or 4b(c) – Very Low Fuel Loading

This second categorization step is not applied to "(4c) Small Enclosures" given that the small enclosures are inherently fuel limited (as discussed above). Note also that, even for (4a) Large Enclosures and (4b) Medium Enclosures, this second categorization step is *optional*; that is, assignment of an enclosure to the Default Fuel Loading sub-group [4a(a) or 4b(a)] is acceptable without further examination of the enclosure. The assignment of an enclosure to either the Low Fuel Loading [4a(b) or 4b(b)] or Very Low Fuel Loading [4a(c) or 4b(c)] sub-group does require visual examination of the enclosure's internal content. Hence, if visual observation is not possible (e.g., the analyst is not allowed to open the enclosure) then the Default Fuel Loading is assumed.

As the names imply, the Low Fuel Loading and Very Low Fuel Loading sub-categories reflect a decreasing amount of combustibles and/or a fuel configuration less conducive to fire spread when compared with their default cases. Note that the criteria applied here are *not* based on a specific threshold fuel loading (e.g., total combustible mass). This is because it will be virtually impossible to determine the total fuel mass with any degree of confidence. Rather, the criteria are based on visual examination, analyst judgment, and comparison to sample photographs provided in this section and in Appendix C. The physical examination process will look for certain basic characteristics to determine the appropriate category for a given enclosure.

The analyst is cautioned that these considerations must include all of the fuels present within the enclosure. In particular, simply opening the access door to an enclosure does not always reveal all of the combustibles present. It is not expected that the analyst would open and examine the interior of small electrical enclosures housed within a larger enclosure (e.g., a vendor-provided electrical housing or smaller purpose-built enclosures housing a small fraction of the enclosure contents). However, in many enclosures quantities of fuels may be hidden behind intermediate partitions or component mounting panels. That is, components may be mounted onto internal partitioning panels so that they are readily accessible for service. This may be accompanied by through-wiring such that the lead cables are hidden behind the mounting panels. In some cases, opening both sides of the panel may still leave a central wire-routing space hidden. The analysis is expected to identify such spaces, if they exist, and to include any hidden fuels in the assessment.

The easiest of the three categories to identify should be the Very Low Fuel Loading configuration; hence, this sub-group is covered first.

<u>Very Low Fuel Loading</u>

Figure 3-10 illustrates two enclosures each with a very low fuel load. The enclosure on the left would be a Large Enclosure Group [4a(c)], and the enclosure on the right would be a Medium Enclosure Group [4b(c)].

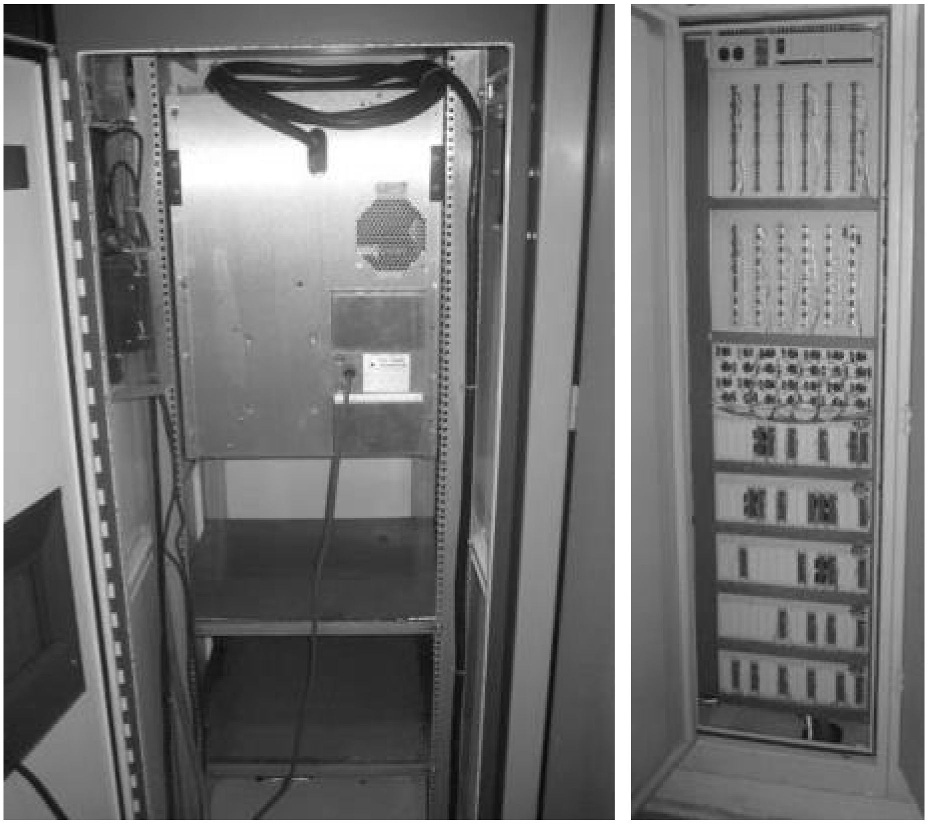

Figure 3-10
Two "Very Low Fuel Loading" Enclosures

In this sub-group, the electrical enclosure should show a very sparse fuel load including consideration of all combustible materials present. There should be only a small number of cables and components present in comparison to the total enclosure volume. The combustible contents should be both limited in quantity and widely dispersed within the enclosure. The cables that are present should be neatly arranged and restrained; for example, those cables present should be routed in an orderly fashion and tied to internal restraints. The intent here is that the combustibles present should be arranged such that if a fire were to ignite somewhere in the enclosure, it would be very unlikely to spread to nearby combustibles.

Characteristics that would *preclude* this categorization would include a significant loading of printed circuit cards, or the presence of components with a significant potential for energetic faults (i.e., arc-flash type failures with significant energy[8]).

This category would commonly apply to a range of instrument and control cabinets (or open racks) where there are relatively few components present and each instrument, indicator, or switch is serviced by only one or two small cables. The fuels should be dispersed widely over the enclosure volume such that fire spread would be difficult to achieve. Typically, the fuel load would be limited to only face-mounted components and the wires servicing those components.

Distinguishing between the Default [Sub-Groups 4a(a) or 4b(a)] and Low Fuel Loading [Subgroups 4a(b) or 4b(b)] configurations will require more judgment in application. The distinctions are based on not only the raw fuel load (e.g., total combustible mass) but also the configuration of that fuel load. That is, if the internal cable conductors are tightly bundled (no air gaps visible), and wires leading to the electrical or electronic devices are neatly organized, fire is less likely to spread. In contrast, cables in loose bundles (air gaps visible between adjacent cables) or run in Panduit (e.g., routed without ties in a vertical cable routing channel) will burn more readily and would be indicative of a default fuel load. The presence or absence of other combustible materials is also important to this assessment. In order to assess these conditions, the enclosure must be opened and an assessment must be performed. Descriptions of these two rating levels are provided below.

Default Fuel Loading

This would be the default assignment made to an enclosure unless the enclosure contents can be visually examined and dispositioned. A Default Fuel Loading would represent a relatively high density of fuels (i.e., in comparison to enclosure volume) which includes both cables and all other flammable materials present (e.g., circuit cards, switches, relays, etc.). The fuel may be distributed throughout the enclosure and may be arranged in a somewhat disorderly fashion. Some abandoned in place legacy cables may also be present. An enclosure with a high load of control components and/or circuit cards would typically imply a default fuel loading.

Low Fuel Loading

This loading implies a fuel configuration that is light and/or moderate but not conducive to fire spread. Assignment of this rating level to an enclosure implies that if a fire were to ignite, the fuel loading is such that fire development will be both slow and difficult. For example, cables in tight bundles (no air gaps visible between cables in the bundle) are more difficult to burn and are considered as one indicator of a fuel load that is not conducive to fire spread (see Figure 3-11).

---

[8] This criterion is intended to cover items with voltages in excess of 125 VDC or 220 VAC. All devices have some potential for arcing, including a light switch. The intent here is to cover only those devices with a significant arc flash potential, e.g., ones that would require personal protective equipment per appropriate IEEE standards.

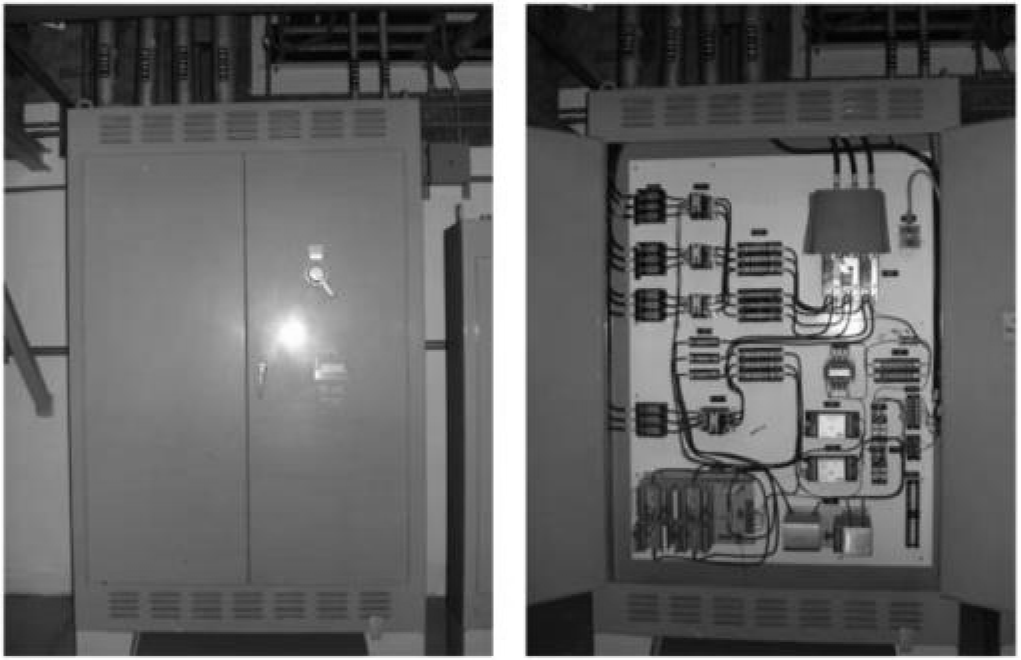

Figure 3-11
Large Enclosure (Closed and Open Configurations): Example of a "Low Fuel Loading" Subgroup

To assist in the decision making process, Table 3-1 provides information that may be used to assign the Default Fuel Loading versus Low Fuel Loading ranking to a given enclosure. Note that both sets of criteria must be met for assignment to a lower fuel loading condition. If one set of criteria is met and the other is not, the Default Fuel Load ranking would apply.

Table 3-1
Distinguishing Characteristics for Default versus Low Fuel Loading Conditions

Characteristic	Conditions Indicative of Default Fuel Loading	Conditions Indicative of Low Fuel Loading
Fuel Loading Level and Fuel Types	There is a relatively high content of fuels including both cables and other combustible materials, or there is a significant load of printed circuit cards present. Bundles of excess or spare cable may be present (e.g., loops of excess or spare cable often found in the bottom of the enclosure). There is a relatively heavy load of smaller diameter (e.g., light power, control, or instrument) cables present where the cable jackets have been stripped and individual conductors routed to teminations within the enclosure. This would include higher load termination or terminal block cabinets, breaker cabinets, fuse cabinets, switching transfer cabinets, etc.	The fuel load is at most moderate and is comprised mainly of cables. There are no, or at most a handful of, open or exposed printed circuit cards present. Or, If combustibles other than cables are present in moderate quantities (e.g., circuit cards or other components) they are housed in closed metal boxes within the larger enclosure. These internal boxes may be vented, but should not have any fully open sides (e.g., an open-back rack mount circuit card cabinet would not meet this criterion).
Cable Bundling Arrangment	Cables may or may not be bundled. If cables are bound or bundled, air gaps between cables are evident (i.e., the bundles are not tight). Cables may be routed in cable wire-ways (e.g., Panduit) but are not tightly bound within the wire-way. Cables may also hang loosely in the enclosure with little or no restraint. Cables leading into the enclosure may be tightly bundled, but the wires leading to individual components are not. For example, when the cables are stripped of their jackets, the individual conductors are routed to their terminations in a somewhat disorderly fashion (e.g., without restraint or in loose bundles).	Cables will be routed in tight bundles (no air gaps evident between cables) and in an orderly manner. Bundles will be separated from each other and will be secured to internal panel elements (e.g., structural supports or other internals). If cable wire-ways (e.g., Panduit) are used, the cables in the wire way are tightly bound within the wire-way. Wires or individual conductors leading to internal components are also tightly bundled, are arranged in an orderly manner, and are secured to supporting elements (e.g., panels or support structures).

4

Peak Heat Release Rates for Electrical Enclosures

This chapter describes the peak heat release rate (HRR) probability distributions provided by the working group (WG). The process used to develop these probability distributions is discussed in Chapter 2.

For each enclosure type as defined in Chapter 3, a gamma distribution was fitted to the 75th and 98th fire intensity values which were defined based on the consensus process described in Section 2.2. The consensus peak HRR distributions are all defined as gamma distributions, largely as a matter of convenience but also because the characteristics of the gamma distribution match desired characteristics of the peak HRR distribution. In particular, the distribution is strictly positive, and second, the likelihood of large fires becomes very small. The distributions for the three functional classification groups (Groups 1, 2, and 3) are defined in Table 4-1.

Included in the table are the shape parameter, alpha (α), and rate parameter, beta (β), characterizing each gamma distribution. Also given are the corresponding 75th and 98th percentile HRR values. The 98th percentile value is the peak HRR value provided for use in the fire ignition source screening Task 7 from NUREG/CR-6850. That is, as with the original NUREG/CR-6850 values, the 98th percentile represents the worst-case peak fire intensity for each classification group. That is, the analyst is not expected to postulate fire intensities in excess of the 98th percentile value.

Table 4-1
Peak HRR Distributions for Functionally Based Classification Groups 1, 2, and 3 Enclosures

Classification Group	Fuel Type* (TS or TP)	Alpha	Beta	75th Percentile (kW)	98th Percentile (kW)
1 – Switchgear and Load Centers	**TS**	0.32	79	30	170
	TP	0.99	44	60	170
2 – MCCs and Battery Chargers	**TS**	0.36	57	25	130
	TP	1.21	30	50	130
3 – Power Inverters	**TS**	0.23	111	25	200
	TP	0.52	73	50	200

Notes:
It is assumed that, based on electrical code and personnel safety compliance requirements, all switchgear, load centers, MCCs, battery chargers, and power inverters would be normally closed enclosures that are opened only when under service. For these electrical enclosures no open enclosure fire condition has been provided for and should not be assumed given a normally closed condition. If a normally open enclosure of these types is encountered, the closed enclosure distributions presented here would not apply.

* Per Sections 1.3 and 2.2.2, qualified TP cables (cables that have been tested and passed the IEEE-383 vertical flame spread test) and SIS wire may be mapped to the TS fuel type groups.

Also note that these revised distributions only characterize the peak HRR values. It is presumed that the analysis will include, as necessary to the analysis goals, consideration of the transient nature of the fire development process (i.e., growth to the peak HRR over time, steady burning, and fuel burnout). The new peak HRR distributions presented here are, by intent, compatible with the commonly applied methods of fire analysis in this regard.

In practice, for any given electrical enclosure, the enclosure is first categorized in accordance with Chapter 3 and placed into one of the available type/function classification Groups 1 through 4. The cable type present in the enclosure is classified in one of two groups. The first group is cable that is either thermoset (TS) or qualified thermoplastic (TP). The second group is unqualified thermoplastic (TP) cable. For classification Group 4 enclosures, the sub-categorization process based on fuel loading and configuration may also be applied (i.e., defining as Default Fuel Loading, Low Fuel Loading, or Very Low Fuel Loading). If this process is not applied, then the default categorization will apply. The distributions for classification Group 4 are defined in Table 4-2, including both the size and fuel characterization aspects of Group 4.

Table 4-2
Peak Heat Release Rate Distributions for Classification Group 4 (All Other) Electrical Enclosures

Enclosure Class/Function Group	Enclosure Ventilation (Open/ Closed Doors)	Fuel Type* (TS/TP Cables)	Gamma Distribution Characteristics											
			(a) Default				(b) Low Fuel Loading				(c) Very Low Fuel Loading			
			Alpha	Beta	75th Percentile (kW)	98th Percentile (kW)	Alpha	Beta	75th Percentile (kW)	98th Percentile (kW)	Alpha	Beta	75th Percentile (kW)	98th Percentile (kW)
4a – Large Enclosures >1.42 m^3 (>50 ft^3)	Closed	TS	0.23	223	50	400	0.23	111	25	200	0.38	32	15	75
	Closed	TP	0.52	145	100	400	0.52	73	50	200	0.88	21	25	75
	Open	TS	0.26	365	100	700	0.26	182	50	350	0.38	32	15	75
	Open	TP	0.38	428	200	1000	0.38	214	100	500	0.88	21	25	75
4b – Medium Enclosures ≤1.42 m^3 (50 ft^3) and > 0.34 m^3 (12 ft^3)	Closed	TS	0.23	111	25	200	0.27	51	15	100	0.88	12	15	45
	Closed	TP	0.52	73	50	200	0.52	36	25	100	0.88	12	15	45
	Open	TS	0.23	182	40	325	0.19	92	15	150	0.88	12	15	45
	Open	TP	0.51	119	80	325	0.30	72	25	150	0.88	12	15	45
4c – Small Enclosures ≤ 0.34 m^3 (12 ft^3)	Not Applicable	TS/TP	0.88	12	15	45	The fuel load characterization approach is not applicable to small enclosures.							

Notes:

1. Sub-categories **Column (b):** Low Fuel Loading and **Column (c):** Very Low Fuel Loading may require opening enclosure doors to assess the internal configuration consistent with the discussions in Section 3 of this report.
2. The open control cabinet condition would include open instrument racks (if they were considered potential fire ignition sources), open relay racks, open-back main control room cabinets, and cabinets that are open to a service walkway (e.g., the intermediate walkway present between the front and back sections of a main control board at some plants). Enclosures with doors made out of combustible materials (e.g., plastic, Plexiglas, cloth) should be considered open during a fire.

* Per Sections 1.3 and 2.2.2, qualified TP cables (cables that have been tested and passed the IEEE-383 vertical flame spread test) and SIS wire may be mapped to the TS fuel type groups.

4.1 Practice for Establishing Fire Diameter

Fire plume correlations, including the Heskestad plume temperature correlation, require that the user specify a fire diameter (or area) in a fire model. The selected fire diameter can significantly impact the resulting calculations. NUREG/CR-6850 does not provide any information on fire diameter, leaving the choice to analyst judgment. FAQ 08-0043, *Location of Fires within Electrical Cabinets*, provides some related guidance by recommending assumed locations for modeling electrical enclosure fires. Fire locations are specified based on the presence and configurations of the vents and potential for failure of the enclosure doors. While in some instances the area of the base of the fire might be assumed equal to the vent area, the FAQ does not directly address this issue.

Since publication of NUREG/CR-6850, a verification and validation (V&V) of fire models for use in PRA applications has also been completed and reported in NUREG-1824 (EPRI 1011999) [20]. As a part of the effort, a specific group of experimental data sets was used as the basis for model validation; hence, the parameter range represented by the applied experimental data sets defines the range over which the validation results are applicable. That information provides an opportunity to characterize a range of appropriate fire diameter values that would fall within the validation range of the V&V report.

Specific to the case of fire plume calculations, a non-dimensional group called 'Q^*_d' is defined[1] as follows:

$$Q^*_d = Q / [\rho_\infty \cdot c_{p\infty} \cdot T_\infty \cdot g^{1/2} \cdot D^{5/2}] \qquad (4\text{-}1)$$

Where:

Q = fire heat release rate (kW)
ρ_∞ = ambient air density (~1.2 kg/m^3)
$c_{p\infty}$ = specific heat ambient air (1.0 kJ/kg·°K)
T_∞ = ambient temperature (~293 °K)
g = gravitational acceleration (9.8 m/s^2)
D = fire diameter (m)

This group is related to the "Froude Number" which characterizes the ratio of momentum driven flows to buoyancy driven flows and is especially relevant to plume fire behavior. A high value of this dimensionless group implies a fire with a relatively small diameter compared to the fire intensity; that is, a largely momentum driven fire plume. In the extreme, a high value would imply a jet fire. Conversely, a low number implies a fire that is dispersed over a wide surface in comparison to fire intensity; that is, a largely buoyancy driven fire plume. As stated in the V&V report, a typical value of Q^*_d is on the order of 1.0. The validated range is 0.4-2.4 (see the second row of Table 2-5 in Volume 1 of NUREG-1824, EPRI 1011999 [20]).

Using this information, it is possible to characterize the relationship between fire intensities (i.e., HRRs) and the range of fire diameters that fall within the validation basis provided by NUREG-1824, EPRI 1011999 [20]. In practice, when given a particular fire intensity value the implied range of fire diameter values that would fall within the bounds of the NUREG-1824, EPRI 1011999 validation basis can be calculated.

---

[1] See the first row in Table 2-4 of Volume 1 of NUREG-1824, EPRI 1011999 [20].

To do this, it is easiest to re-order Equation 4-1 to solve for D as a function of Q and Q^*_d as follows:

$$D = [Q / (C_1 \cdot Q^*_d)]^{2/5} \qquad (4\text{-}2)$$

Where:

$$C_1 = \rho_\infty \cdot c_{p\infty} \cdot T_\infty \cdot g^{1/2} \qquad (4\text{-}3)$$

Using this modified relationship and the maximum and minimum values of Q^*_d represented in the V&V experimental data sets (i.e., 2.4 and 0.4), the range of diameter values is easily calculated. Note again that the minimum diameter is associated with the maximum value of Q^*_d and vice versa. The results for a range of fire intensities are shown in Table 4-3 and the same results are plotted in Figure 4-1. Also, Table 4-4 provides minimum and maximum fire diameter values specific to each of the unique 98th percentile HRR values provided by the WG in Table 4-1 and Table 4-2 for electrical enclosures.

Table 4-3
Range of Fire Diameters as a Function of Fire Intensity (HRR) That Remain Within the Validation Range for the Plume Correlations

Fire Intensity HRR Values (kW)	Minimum Fire Diameter $Q^*_d = 2.4$ (m)	Maximum Fire Diameter $Q^*_d = 0.4$ (m)
5	0.0814	0.1668
10	0.1075	0.2200
25	0.1550	0.3175
50	0.2046	0.4189
100	0.2699	0.5527
250	0.3894	0.7974
350	0.4455	0.9123
500	0.5139	1.0522
700	0.5879	1.2038
850	0.6354	1.3010
1000	0.6780	1.3884

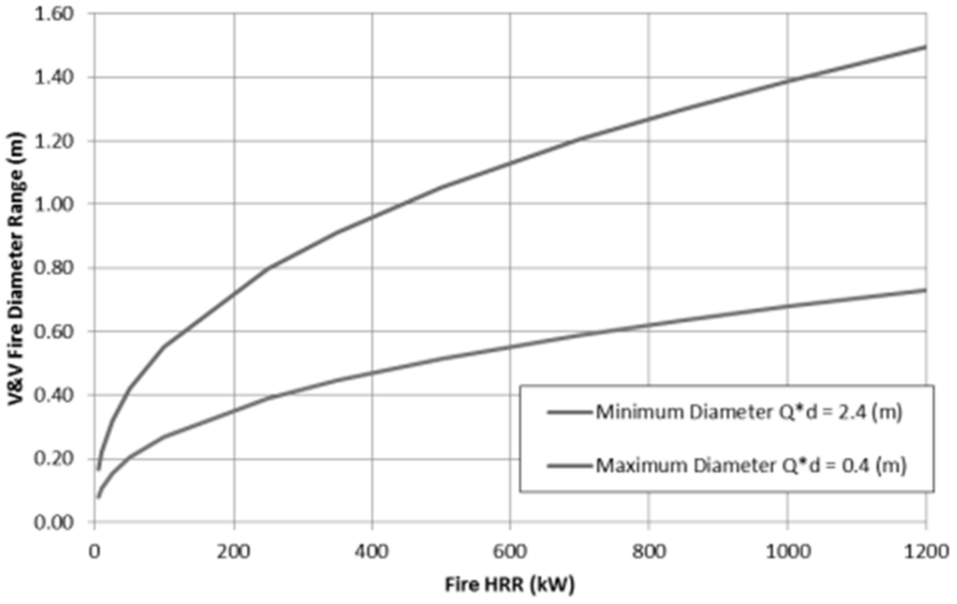

Figure 4-1
A Graphical Representation of the Data in Table 4-3

Table 4-4
Minimum and Maximum Fire Diameter Values for the 98th Percentile HRR Values Cited in Tables 4-1 and 4-2

98th Percentile HRR Values (kW)	Minimum Fire Diameter $Q^*_d = 2.4$ (m)	Maximum Fire Diameter $Q^*_d = 0.4$ (m)
45	0.1961	0.4016
75	0.2406	0.4926
100	0.2699	0.5527
130	0.2998	0.6139
150	0.3175	0.6501
170	0.3338	0.6834
200	0.3562	0.7293
325	0.4325	0.8857
350	0.4455	0.9123
400	0.4700	0.9624
500	0.5139	1.0522
700	0.5879	1.2038
1000	0.6780	1.3884

4.2 Special Fuel Loading Configurations

There are three special fuel loading configuration cases that could impact the assignment of a Group 4 electrical enclosure to the Default Fuel Loading, Low Fuel Loading, or Very Low Fuel Loading sub-group. In particular, there are certain cable routing configurations that would limit the exposure of fuels that may be present or that would eliminate potential ignition sources. These special configurations may be taken into consideration during the assignment process, as described in the follow paragraphs.

4.2.1 *Special Case 1: No Ignition Sources Present*

The first special case is an electrical enclosure that has no ignition sources present. This condition will likely not be obvious based on external examination. Hence, an enclosure counted during the initial ignition source counting process may need to be reconsidered if this special case does apply.

A limited number of electrical enclosures found in nuclear power facilities may be effectively empty on internal inspection. These may be enclosures that once housed plant equipment but at some point were emptied and abandoned, enclosures installed as spare compartments against future need, or enclosures that only contain cables routed to other electrical enclosures or floor elevations (i.e., a cable pass-through with no terminations or end devices present).

In addition, enclosures containing some level of cables and components may be found that have been fully and permanently de-energized and are no longer in use. In the case of electrical enclosures, the fire ignition source is universally electrical in nature. Hence, without electrical energy present, there is no fire potential. Note that this particular case would not be applicable to an enclosure that is de-energized during some modes of plant operation but energized during others. Current methods do not extend to special treatment for such enclosures and it is not the intent of this method to address such cases. However, an enclosure that has been fully and permanently de-energized can be considered to have no ignition sources present.

Figure 4-2 provides an example of an enclosure that only contains pass-through electrical cables and some abandoned panel wiring (no terminations, no end devices). Since no ignition sources are present in the enclosure, it should not be counted as an ignition source and hence, no heat release rate would be assigned to it. It is provided that if such an enclosure is encountered, it should be removed from the list of ignition sources (i.e., it would no longer be considered as a potential source of a fire scenario). It is also provided that removal from the analysis be documented carefully including the basis for the decisions taken.

Figure 4-2
Cropped Photo of Electrical Enclosure with Bundled Panel Wiring and Cable, Limited Combustible Loading, and No Ignition Sources

4.2.2 *Special Case 2: Cables Enclosed in Conduits*

Rigid metal conduit[2], flexible metal conduit (FMC), and liquid-tight flexible metal conduit (LFMC) are raceways of circular cross-section made from either metal tube or, in the case of flexible conduits, helically wound, formed, interlocked metal strips. Analysts may find that on internal inspection, the cables within an electrical enclosure are contained in such conduits. The use of flexible conduit within an enclosure is more likely than rigid conduit, but the use of rigid conduit cannot be precluded.

In general fire PRA practice, cables that are enclosed in metal conduit (rigid or flexible) are considered potential damage targets but are not considered to contribute to fuel loading or fire spread. Extending this concept to electrical enclosures, it is provided that in assessing the fuel

---

[2] Rigid metal conduit, as that term is used here, is intended to include a range of products including actual rigid metal conduit (RMC) which is thick-walled threaded tubing, galvanized rigid conduit (GRC), intermediate metal conduit (IMC), electrical metallic tubing (EMT), and aluminum conduit.

load, do not include cables that are routed in rigid or flexible metal conduit. That is, such cables do not need to be considered as adding to the cabinet fuel load. The other criteria for assignment to a particular fuel configuration (default, low, or very low) would apply based on any other combustibles present (e.g., cable not in conduit or other components).

LFMC differs from FMC in that the former has an outer liquid-tight, non-metallic, sunlight-resistant jacket over an inner flexible metal core. This outer jacket is typically a fire retardant polyvinyl chloride (PVC) thermoplastic that is of very low flammability. The flexible conduit provides a barrier between the energized insulated electrical conductors internal to the flexible conduit and external combustible materials within the electrical enclosure. Cables routed in LFMC will burn less intensely than would cables routed randomly within an enclosure. Hence, the LFMC is also considered a routing configuration that is less conducive to fire development (e.g., similar to tight versus loose bundles).

It is provided that while cables routed in LFMC cannot be dismissed as a contributor to fuel load entirely (because of the outer jacket), if most of the cables present are routed in LFMC this would generally allow for one step down in the fuel loading configuration assignment provided other assignment criteria are met. The presence of a small percentage of exposed cables would be permissible, but regardless, the criteria associated with the lower fuel configuration assignment must be met. That is:

- An enclosure that might otherwise be classified as a Default Fuel Loading might be reduced to a Low Fuel Loading provided the other criteria for Low Fuel Loading are also met (Table 3-1).
- An enclosure that could be assigned to the Low Fuel Loading group might be reduced to a Very Low Fuel Loading, again, provided the other criteria for Very Low Fuel Loading are also met (Table 3-1).
- An enclosure already assigned a Very Low Fuel Loading would remain a Very Low Fuel Loading enclosure.

Figure 4-3 illustrates two enclosure sections where flexible conduit is used exclusively to route panel wiring and electrical cables. The picture on the left in Figure 4-3 would likely fall into a Default Fuel Loading configuration if all the cables were exposed. Given the use of LMFC, the fuel loading assignment would be reduced to Low. The picture on the right in Figure 4-3 shows an enclosure where the cables are routed in FMC (in this case <u>not</u> LMFC). In this case, the consideration of the other fuels present would be necessary before an assignment can be made, but the cables in the FMC would not be included in the fuel load. Based on what is visible in the picture, the fuel loading assignment would likely be Low initially if all of the cables present were exposed. Excluding the cables in FMC from the fuel load may allow for a reduction to Very Low Fuel Loading depending on the nature of the fuels present in the metal enclosed wire-ways (see discussion of wire-ways below).

As always, it is provided that proper documentation be included and maintained with the fire PRA records.

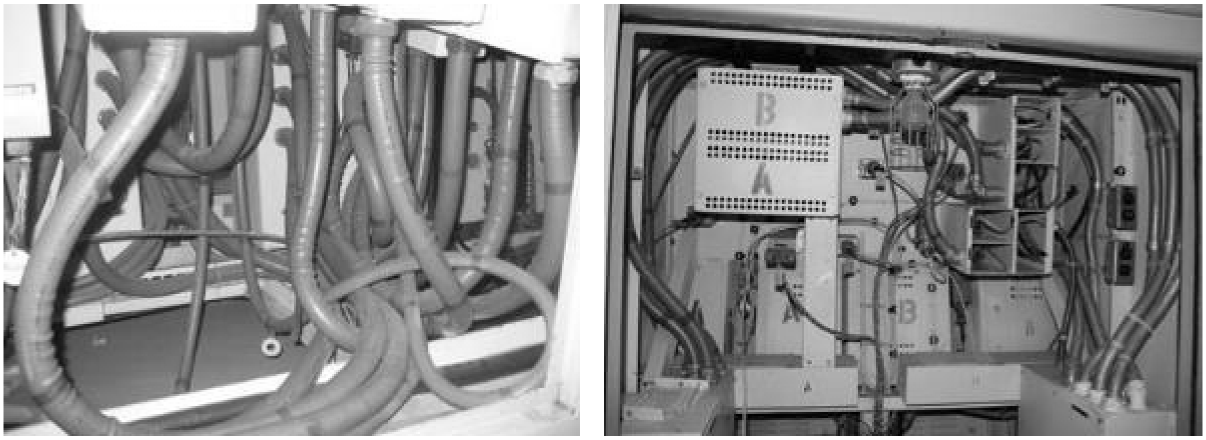

Figure 4-3
Photograph of LFMC (left) and FMT (right) Within Electrical Enclosure

4.2.3 *Special Case 3: Metal Enclosed Wire-Ways and Switch/Device Covers*

Especially in later vintage plants, the inclusion of a design philosophy of train separation within an electrical enclosure included the use of metal enclosed wire-ways, switch covers, or device covers to separate redundant trains of insulated electrical conductors and cable. Examples of metal enclosed wire-ways and switch/device covers are shown in Figure 4-4 and Figure 4-5. This configuration is similar in some ways to the use of metal conduit, although the wire-ways typically have a larger cross-section than the conduits likely to be found inside an enclosure. The wire-ways and switch/device covers are also designed with removable covers that allow for access to the enclosed wiring. Finally, the wire-ways may include a limited degree of ventilation but are enclosed such that air flow into and out of the wire-way is sharply restricted. Despite these differences, the use of enclosed metal wire-ways or switch/device covers is considered to reduce the fire potential for an electrical enclosure in much the same way that conduits do.

Figure 4-4
Photograph of Metal Enclosed Wire-Ways Within Electrical Enclosure (MCB)

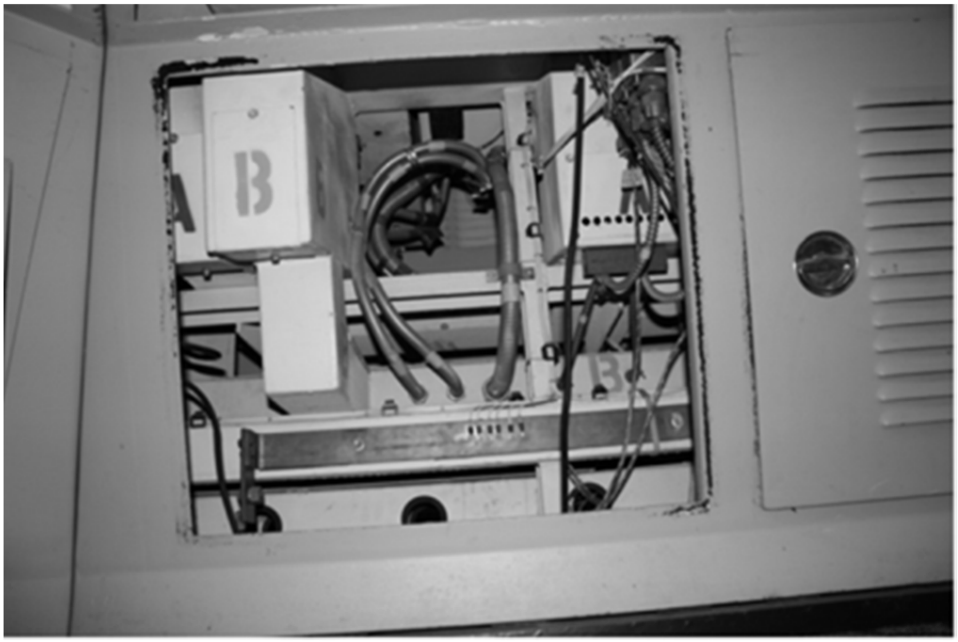

Figure 4-5
Photograph of Switch/Devices Cover (Labeled B) Within an Electrical Enclosure

In those enclosures where metal enclosed wire-ways are used to route cables, the same approach as that described above for LFMC is provided (see the three examples for LFMC cited immediately above). That is, given that most of the cables present are routed in metal enclosed wire-ways or secured in switch and/or device covers, the fuel loading configuration assignment may be reduced by one step. The presence of a small percentage of exposed cables would be permissible, but regardless, all of the other criteria for the lower fuel configuration assignment must be met. For the cases shown in Figure 4-4 and Figure 4-5, the final fuel loading assignment would likely be either Low Fuel Loading or Very Low Fuel Loading depending on the details of the other fuels present (which cannot be easily discerned from the picture).

Note that this special case does not extend to non-metallic (e.g., plastic or fiberglass) wire-ways or to metallic wire-ways that are substantially ventilated. That is, these are installed wire-ways that are not enclosed, but rather, have large and regular openings (essentially alternating between solid “fingers” and open gaps) that allow for wire/cable entry and exit. Based on both photographs and the experience of the working group members, wires are often routed within such wire-ways in a loose arrangement of individual insulated conductors rather than in tightly bound bundles. A fire within such a wire-way might spread as easily as a fire in a loose cable bundle given ready access to oxygen and a high degree of exposed fuel surface area. Further, a non-metallic wire-way itself represents combustible fuel, albeit likely of a low flammability. While the use of non-metallic and/or highly ventilated wire-ways may impact fire behavior, there is currently no experimental basis for assessing the effects, and the effects may not be positive (i.e., they may not reduce fire potential, depending on details of the Installation). Hence, the working group decided that non-metallic and/or substantially ventilated wire-way systems would not qualify for this special case. An example of a ventilated wire-way that would be excluded from this special case (i.e., the wires in the wire-ways would be counted as exposed fuel) is shown in Figure 4-6. Likewise, substantially ventilated switch and/or device covers would be excluded from this special case for the same reasons. An example of a ventilated switch and/or device covers is shown in Figure 4-7.

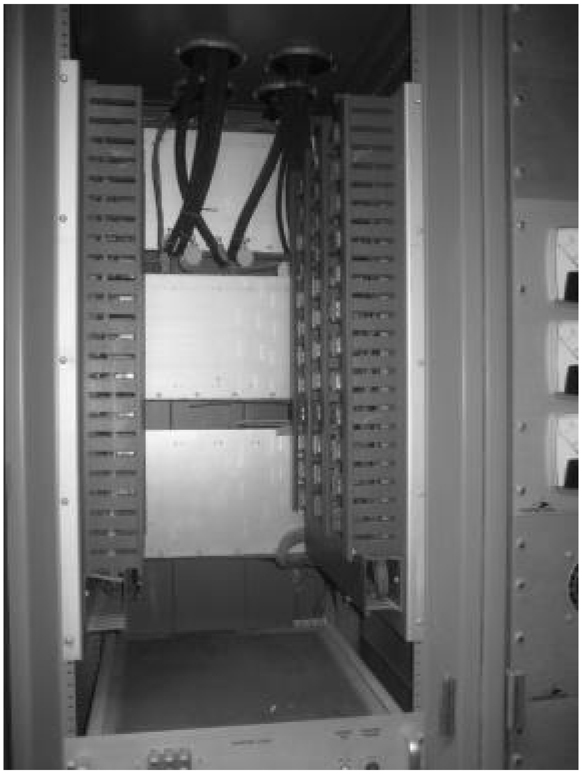

Figure 4-6
An Example of Non-Enclosed Wire-Ways That Would Not Qualify as Metal Enclosed Wire-Ways

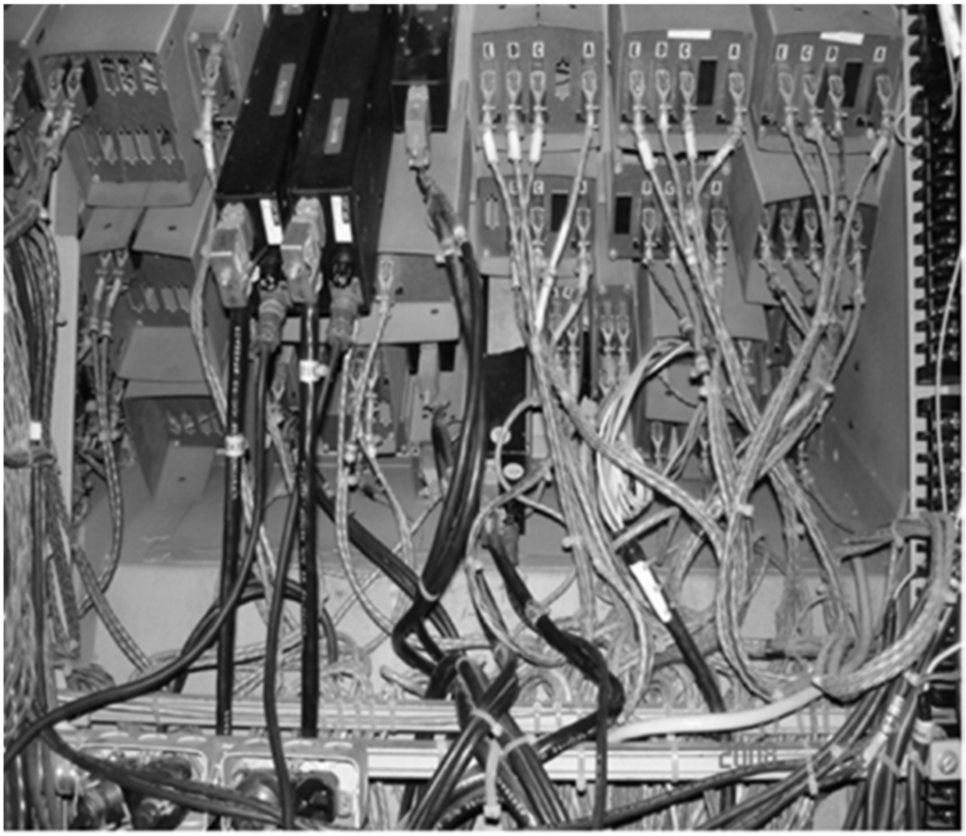

Figure 4-7
An Example of Substantially Ventilated Switch and/or Device Covers That Would Not Qualify for Reduction

As a final note, these three special configurations are not mutually exclusive. For example, the picture on the right in Figure 4-4 shows an enclosure section that actually includes both FMC and metal enclosed wire-ways. This is not unexpected, and the conditions should be evaluated consistently with the aggregate conditions as they exist.

5

Correlation of Obstructed Plume Models with Heskestad Plume Predictions

This chapter describes the methodology used in characterizing axisymmetric fire plume models for enclosure fires. The Heskestad correlation is used as a basis for comparison of the obstructed plume predictions using the Fire Dynamics Simulator (FDS) computer software. Appendix E presents all results of the computer simulation studies representing obstructed and unobstructed plume effects, bias and uncertainty evaluation, sensitivity analysis of an opening on the top obstruction plate, and the sensitivity study of vertical source configuration.

5.1 Assumptions and Limitations

The Heskestad fire plume correlation is used for characterizing axisymmetric fire plumes [22, 34] as a basis for comparison of the obstructed plume model predictions from the FDS computer simulations. The following reasons are taken into consideration:

- The Heskestad correlation is a widely used model for calculating fire plume temperatures [4, 15, 18, 20, 34];
- The Heskestad correlation has been verified and validated for commercial nuclear power plant applications [18, 20, 21];
- As an algebraic mathematical model, the Heskestad correlation can be easily evaluated and applied for the purposes of this research and for fire PRA applications; and
- A review of a multitude of thermal plume correlations by Beyler [28] concluded that several reported correlations utilize a nearly identical approach to that utilized by Heskestad.

Note that the Heskestad correlation assumes axisymmetric plumes with the source of energy concentrated at a point in space near the base of the fire (i.e., the virtual origin). Consequently, this study includes fires modeled as axisymmetric plumes compared with FDS simulations with similar fire sources impacted by obstructions.

5.1.1 *Fire Dynamics Simulator*

Although the Fire Dynamics Simulator (FDS) is routinely used for solving practical fire problems in fire protection engineering, including fire reconstruction investigations, sprinkler design, and smoke management, it is also useful as a tool to study fundamental fire dynamics and combustion [30], including low speed transport of heat and combustion products from fire. This latter purpose serves as motivation for using FDS Version 6.0.1 as the source of the fire plume simulations developed in this study.

The following reasons justify the use of FDS Version 6.0.1:

- FDS provides the flexibility to model the scenarios with the selected influencing factors required for supporting the study of obstructed plume flows.

- FDS has been verified and validated for commercial nuclear power plant applications [21]. NIST updates the FDS verification and validation (V&V) study with each new version release [33].
- There is precedent in the commercial nuclear industry in using FDS for NFPA 805 applications. For example:
    - An FDS simulation provides the technical basis in the approach described in fire PRA FAQ 13-0004 [24] dealing with “sensitive electronics” inside electrical cabinets.
    - A number of fire PRAs have used FDS in support of the fire modeling calculations for estimating time to control room abandonment due to fire generated conditions.
- In comparison to an experimental program, FDS models can be revised and reproduced at very little cost or time delay.
- FDS base case simulations for fire plumes (i.e., unobstructed plumes in the application described here) have been compared with fire plume temperature correlations as a benchmark.
    - In Section 5.2, FDS results of baseline unobstructed configurations are compared to the Heskestad correlation to demonstrate consistent predictions between the two models.
    - Also in Section 5.2, FDS results of obstructed configurations are compared to the Heskestad correlation to demonstrate that the obstruction may reduce the plume temperature significantly.
    - In Section 5.3, FDS results of obstructed configurations are compared to FDS results of the unobstructed configurations to identify systematic functional trends in the data (e.g., construction type, fire base height, fire diameter, etc.).
    - In Section 5.3.7.1, all of the results are compared using statistical analysis in order to develop appropriate guidance for the treatment of obstructed plumes using a modified Heskestad correlation.

5.1.2 *Zone of Influence Applicability*

The information developed here applies to determining the fire plume component (i.e., vertical ZOI distance and potential horizontal shift of the plume) generated in the initial stages of the fire.

The analysis does not include room heat up effects (i.e., development of a room hot gas layer). The scope of this analysis is limited to the evaluation of a fire plume that is not influenced by the presence of walls or ceiling of the surrounding compartment. This limitation prevents any direct evaluation of the potential effects of an obstructed plume on the development of a room hot gas layer. The practical implication of this is that the information is focused on the “early stages” of a fire where substantial smoke accumulation and room heat up has not yet occurred. This limitation also prevents any direct evaluation of the potential effects of an obstructed plume on the smoke visibility reduction in a compartment. Existing guidance for the evaluation of smoke visibility reduction is still applicable and should be used without modification.

This analysis also does not provide any justification to alter the treatment of the thermal radiation horizontal ZOI. The existing guidance provided in NUREG/CR-6850, and NUREG/CR-6850 Supplement 1, should be used to determine the thermal radiation horizontal ZOI.

Implications on the maximum extent of the vertical and horizontal ZOI due to an obstructed plume will be discussed in Chapter 6.

5.1.3 *Flame Height*

The effect that an obstruction may have on flame height has not been previously investigated. In many cases the flames impinge upon or encompass the obstructions. The maximum extent of the vertical ZOI includes contribution from both the flame impingement region and the plume. The outcome of this study will have no impact on damage predictions for targets exposed to direct flame impingement. More advanced techniques that utilize event tree analysis to credit the delay in damage states have to carefully consider the treatment of the flame impingement zone using the existing information in NUREG/CR-6850.

5.1.4 *Types of Obstructions*

The obstructions modeled in this investigation represent electrical enclosure surfaces, including the enclosure top and, in some cases, the side walls of the enclosures. The top obstructions are located within the flame, intermittent, and plume regions of the fire source. Ratios of mean flame height, L, as determined using the correlation provided by Heskestad (Equation 5 in Ref. 22) to the elevation of the top obstruction (H = 2.3 m (7.5 ft)) range from L/H = 0.22 to 2.06. These obstructions are considered to be in the near-flame region most appropriate for NPP applications, and are representative of a typical enclosure height evaluated in fire PRAs. Side obstructions have been implemented in a way that would demonstrate their effect on the thermal plume without appreciably limiting the supply of oxygen to the fire source. The configurations explored here emphasize the effect of the top surface, while also considering the possibility that side surfaces may produce increased thermal exposures.

The obstructions modeled in this investigation include top obstructions without any openings. A number of sensitivity simulations are performed using openings of various percentages of the obstruction top surface area. These additional simulations are used to determine applicability of information when applied to enclosures with openings at the top.

5.1.5 *Other Applicability Limitations*

- The methodology described in Chapters 5 and 6 of this report (i.e., the evaluation temperatures associated with obstructed fire plume flows) is provided for scenarios involving fires in open or closed electrical enclosures. Enclosure walls may have openings or vents. That is, for practical applications, electrical enclosures must have at least three metal walls and a solid top cover.

    - The enclosure walls may have openings or vents. Since the FDS simulations were conducted with enclosures with “no walls” (i.e., only a cabinet top), with two side walls, and with three walls to ensure the fire is not oxygen limited, this recommendation ensures a conservative application of the approach even if the enclosure walls have openings or vents.

    - Since FDS has the inherent capability to predict plume temperatures under the influence of an obstruction, FDS results should never be adjusted in post-processing calculations to account for the obstructed plume credit. The bias correction developed in this report does not apply to results obtained directly from FDS and is only intended for use with the Heskestad fire plume temperature correlation. A qualified user of FDS should develop an appropriate set of inputs to address the effects of cabinet obstructions directly, and not by adjusting the output data with a bias correction.

  - The simulations developed in FDS consist of enclosure obstructions with steel thermo-physical properties consistent with electrical enclosure tops found in NPP applications. Information is limited to metal or other similarly robust obstructions that could not fail (melt or burn away) at elevated temperatures and allow unobstructed plume flows. Note that the results show that the effect of the obstruction is not strongly sensitive to small openings in the top surface, up to 5% of the top surface area as indicated in Section 5.3.7.2. Therefore, small openings (≤ 5% of top plate) that may be generated by the heat from the fire due to warping or tearing of weld joints, etc. can be ignored provided the material is sufficient to withstand melting or burn away when directly exposed to flames. The analysis also shows that the result is not strongly sensitive to varying the thickness of the enclosure surface material in Section 5.3.7.5. Therefore, the recommendations can be applied to any electrical enclosure provided the above limitations are also met.

- Temperature predictions at specified intervals are made up to 6 m (20 ft.) above the fire source, which is the typical elevation of room heights in NPPs. The analysis is based on the highest temperature predicted in the particular plane elevation.

- Heat release rates (HRR) up to a limit of 1000 kW, which is roughly equal to the highest 98th percentile HRR value provided for ignition sources in Tables 4.1 and 4.2 of this report. This limit also corresponds to the maximum HRR specified for a 98th percentile electrical enclosure fire in NUREG/CR-6850.

- The current investigation does not consider the effects on the plume temperature after fire spread to secondary combustibles, such as cable trays or exposed cables ignited above the initiating fire source.

- The current investigation does not consider the potential effects of a fire located adjacent to a wall or corner; however, there is no evidence to suggest that this analysis will invalidate the current treatment of these configurations. Existing information on the treatment of wall and corner effects on the plume ZOI may be applied.

- The current investigation applies to defining the thermal plume exposure and extent of the ZOI, assuming relevant temperature exposures for thermoplastic (TP) and thermoset (TS) cable targets. The range of relevant temperatures includes 130 °C (266 °F) to 800 °C (1470 °F) as defined in Section 5.3.6.

5.2 Technical Approach

The Heskestad plume correlation is typically used for unobstructed plume simulations and modified to account for changes in plume temperature due to an obstruction. This modification is estimated through a comparison of the results of fire model simulations against the existing Heskestad plume correlation. The software used to simulate and estimate fire plume temperatures subject to obstructions in this study is FDS Version 6.0.1.

FDS is a computational fluid dynamics (CFD) tool, developed and maintained by the National Institute of Standards and Technology, capable of studying fundamental fire dynamics and combustion [30], including low speed transport of heat and combustion products from a fire. FDS solves numerically a form of the Navier-Stokes equations (i.e., conservation of momentum in fluid flow) appropriate for low speed, thermally driven flow with an emphasis on smoke and heat transport from fires. The formulation of the equations and the numerical algorithm are contained in the FDS Technical Reference Guide [31]. Verification and validation of the model are discussed in the FDS Verification and Validation Guides [32, 33]. FDS has also been verified and validated for commercial nuclear applications [21].

5.2.1 *Review of Past Studies*

A review of the literature was conducted to identify existing studies related to obstructed plumes. Most studies including fire plume flows subject to an obstruction focus on one of two areas: (1) exposure to objects of varying sizes and geometries in a fire plume, and (2) delayed actuation and impeding discharge patterns of sprinklers caused by obstructions. However, no specific study associated with fire plume temperatures above obstructions was noted. Information on the impact of obstructions on plume temperatures is needed in the nuclear power industry as more realism is factored into the modeling of electrical enclosure fires. Fires ignite inside electrical enclosures, and it may be overly conservative to model the plume without any consideration of the effects that the top of the enclosure may have on the plume temperature and hence, on the vertical ZOI.

5.2.2 *Plume Theory*

The point source solution of turbulent plume flow has shown a remarkable ability to correlate velocities, temperatures, and mass flow rates above the flame tip [23, 28, 34]. This solution assumes the fire to be a single point source of heat located near the base of the fire. The details of the point source become less observable as the distance from the point increase until only the total heat output of the fire becomes relevant. This investigation focuses on the near field plume behavior, where the temperatures of interest are comparable to the damage thresholds of electrical cables used in NPPs.

5.2.2.1 Plume Scaling

Significant efforts have been undertaken in the study of plume theory. Relations developed by Zukoski [29] are capable of estimating plume temperatures and velocities for fires uninfluenced by obstructions. Using these relationships, the following simplified proportionality allows for an estimation of the plume centerline temperatures at different elevations above a fire source by Beyler [28]

$$\Delta T_m \sim \dot{Q}^{2/3} z^{-5/3} \tag{5-1}$$

Where, ΔT_m is the rise in plume temperature above ambient in Kelvin, $\dot{Q}$ is the heat release rate in kW, and z is the height above the fire source in meters. Constants of proportionality have been determined by a number of investigators. The constant of proportionality, A, modified to include the virtual origin, z_0, can be estimated as:

$$A \approx \frac{\Delta T_m}{\dot{Q}^{2/3}(z-z_0)^{-5/3}} \tag{5-2}$$

When comparing these constants of proportionality determined by various investigators, values range from 21.6 to 29.7. A value of 26 is suggested for use when the convective heat release rate is known and 22 when flame radiation is significant. One of the relations that follow the above proportionality is the Heskestad fire plume correlation.

5.2.2.2 Heskestad Plume Temperature

In this investigation the correlation used to predict the changing fire plume temperature was developed by Heskestad:

$$\Delta T = 9.1\left[\frac{T_0}{(gc_p^2\rho_0^2)}\right]^{1/3}\dot{Q}_c^{\,2/3}(z-z_0)^{-5/3} \tag{5-3}$$

Where, ΔT is the change in temperature above ambient, g is the acceleration due to gravity, c_p is the specific heat of air, ρ is the density of air, $\dot{Q}_c$ is the convective heat release rate, z is the height above the top of the combustible, and z_0 is the height of the virtual origin calculated as:

$$z_0 = -1.02D + 0.083\dot{Q}^{2/5} \tag{5-4}$$

Where, D is the diameter of the fire source (m) and $\dot{Q}$ is the heat release rate (kW).

This correlation is only valid above the mean flame height, L. The mean flame height can be calculated as:

$$L = -1.02D + 0.230\dot{Q}^{2/5} \tag{5-5}$$

The Heskestad fire plume correlation is chosen for this study because it is identified as the preferred correlation for use in calculating the damage temperature in ZOI applications by NUREG/CR-6850 (Appendix F). In addition, the correlation is currently verified and validated for use in fire PRA [21].

To determine the effects on plume temperature rise caused by an obstruction on targets above the obstruction, a modification of the Heskestad fire plume correlation is made to account for changes in the fire plume temperature rise as given below:

$$\Delta T = B\left(9.1\left[\frac{T_0}{(gc_p^2\rho_0^2)}\right]^{1/3}\right)\dot{Q}_c^{\,2/3}(z-z_0)^{-5/3} \tag{5-6}$$

Where, B is a bias determined from differences between the plume temperature rise above a fire subject to an obstruction and those of the unmodified Heskestad fire plume correlation.

5.2.3 *The FDS Simulation Parameters*

Using FDS, one hundred fifty six (156) simulations, thirty nine (39) unobstructed and one hundred seventeen (117) with obstructions, were performed to develop the simulated plume temperature data for this study. Four influencing factors have been chosen to define a “test matrix,” namely, heat release rate, fire diameter, elevation of the fire source, and number of enclosure walls included with the obstruction. These factors are based on the study of fire plume flows currently available in the fire protection engineering literature and the specific needs for this study.

5.2.3.1 Heat Release Rate (HRR)

The HRR is perhaps the most important influencing factor in all fire modeling applications. In the specific case of axisymmetric fire plumes, it represents the energy released at a point in space near the base of fire generating the upward movement of flows. Heat release rate values selected for this study range from approximately 50 to 1000 kW (which is approximately the highest fire intensity) applied for electrical enclosure heat release rate scenarios.

5.2.3.2 Fire Source Diameter

The fire source diameter characterizes the size of the fire base. It has been identified as an important parameter governing fire plume temperatures, because it has a strong influence on plume velocities, entrainment, and flame heights. Consequently, it is included as an influencing factor to evaluate its impact on fire plume temperatures subject to obstructions. The range of fire diameters selected for this study are 0.3 m (1 ft.), 0.6 m (2 ft.), 0.9 m (3 ft.), and 1.2 (4 ft.). The Fire Froude Number (Q*) is used to select pairings of fire diameters and HRRs appropriate for this investigation. Q* values ranging between 0.34 and 1.87 were calculated for the parameters used in this study. These values fall mostly within the validated range, 0.4 to 2.4, of the Q* as reported in Table 2-5 in Volume 1 of NUREG-1824 [21], with a small set of configurations less than the minimum valid Fire Froude Number of 0.4. These configurations are not anticipated to invalidate the conclusions generated in this study because the substantial validation performed for FDS [33] exceeds the limits reported in NUREG-1824 [21], and the model inputs are prescribed within the existing validation range for use of the FDS.

5.2.3.3 Obstruction Configuration

Electrical enclosures represent a common ignition source in nuclear power plant fire scenarios. When developing a zone of influence, the fire within an enclosure may be subject to the enclosure top and sides as an obstruction within the plume region. The obstructions used in this investigation consist of a flat plate obstruction with a thickness of 0.0015 m (0.06 in) centered over the fire source at an elevation of 2.3 m (7.5 ft) with a varying number of walls. The dimensions of the obstructions are 8 cm (3 in) larger than the fire base on a side, and change in size with the fire source used in each simulation. Obstructions representing electrical enclosures with no walls and a top cover, two walls with a top cover, and three walls with a top cover are used in this investigation.

Three different obstructions used in the investigation are shown in Figure 5-1. The first type of obstruction is a single flat plate obstruction (circled in red). The second obstruction includes the flat plate and two walls (identified by red arrows) running from the floor surface to the flat plate obstruction, resembling an arch. The other two surfaces are open to the environment (signified by the blue line). The third obstruction is similar to the arch obstruction with an additional, third wall that allows smoke and heat to exit only on the side indicated by the blue arrow.

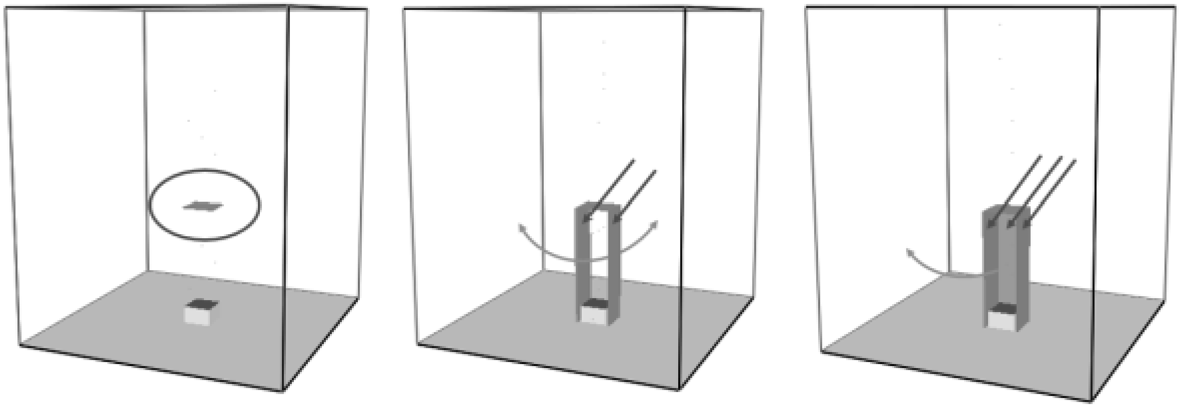

Figure 5-1
Obstruction Geometries: Flat Plate, Arch, Three Walls

In Figure 5-2, the change in elevation of the fuel source is presented. The three elevations used in this investigation are 0.3 m (1 ft) – one foot above the floor surface, 1.1 m (3.6 ft) – half the distance between the floor surface and the top of the obstruction, and 2 m (6.6 ft) – one foot below the top of the obstruction.

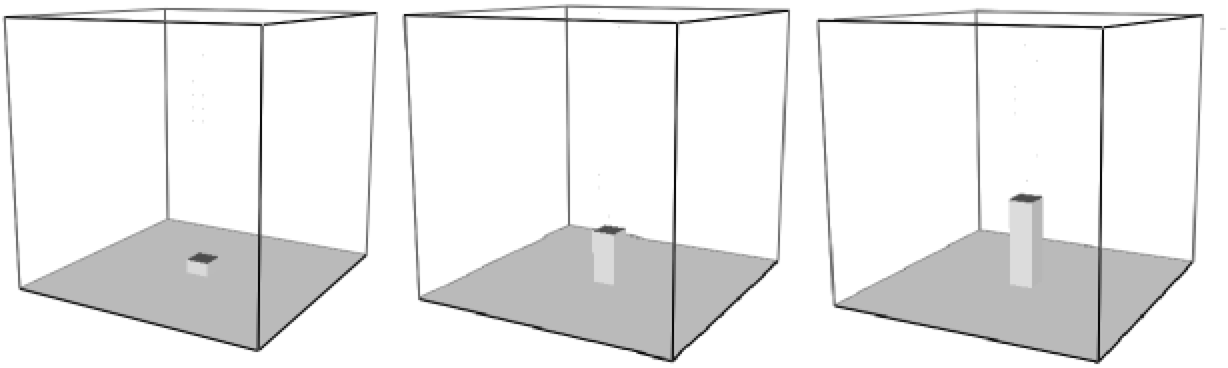

Figure 5-2
Simulation Fire Source Elevations: 0.3048 m, 1.143 m, 1.9812 m

Evidence gathered from these simulations is used to determine the effect of an obstruction on plume temperatures and subsequently determine any resulting change in the ZOI.

5.2.3.4 Enclosure Configurations

Figure 5-3 illustrates three enclosure configurations seen in NPPs where the obstructed plume effects are realized. Without considering the wall effect, the enclosure presented in Figure 5-3a is an example of the single flat plate obstruction geometry. The enclosure is vented on all four sides with a solid top (circled in red). The enclosure presented in Figure 5-3b has a solid top and two side walls, resembling arch obstruction geometry (circled in red). The remaining two top sides are vented to the environment. The enclosure presented in Figure 5-3c is an example of the three-wall obstruction geometry. The enclosure has three solid walls, a solid top, and a single door with slotted vents (circled in red).

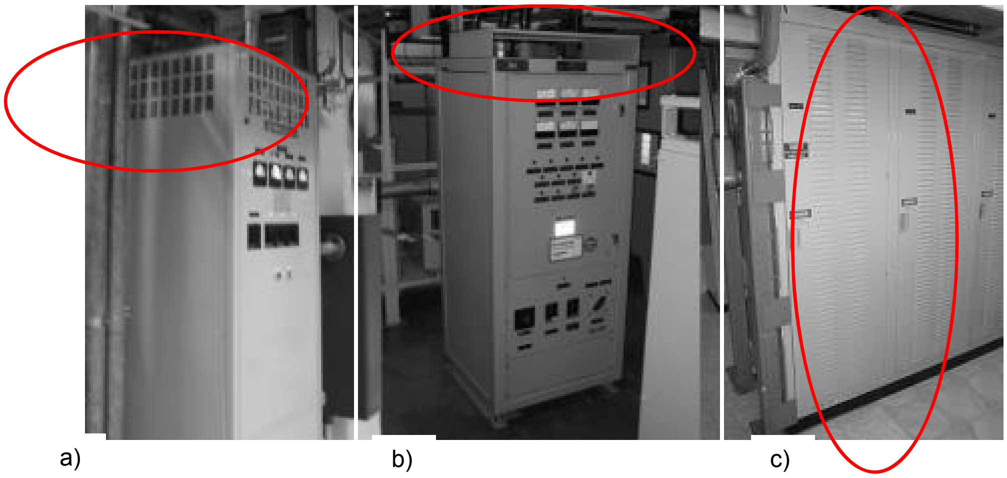

a) b) c)

Figure 5-3
Obstruction Configurations: Flat Plate, Arch, and Three Walls

5.2.3.5 FDS Simulation Matrix

A matrix of simulations performed in this investigation is presented in Table 5-1. Each case study included three obstructed cases and one unobstructed case. In Table 5-1, the different pairings of HRR, source diameter, and elevation used in this investigation are presented. Pairings of HRR and source diameter are selected using Q* as identified in Section 5.2.3.2. Each of the groupings presented in Table 5-1 is used for a simulation with each of the three obstruction geometries described in Sections 5.2.4.2 to 5.2.4.4. Additionally, a baseline, unobstructed, geometry is simulated to obtain plume temperatures to be compared with those measured in the obstructed simulations.

Table 5-1
FDS Obstructed Plume Simulation Test Matrix

	Fire Source Diameter (m)				**Fire Source Elevation (m)**		
HRR (kW)	**0.3**	**0.6**	**0.9**	**1.2**	**0.3**	**1.1**	**2**
50	X	N/A	N/A	N/A	X	X	X
100	X	N/A	N/A	N/A	X	X	X
200	N/A	X	N/A	N/A	X	X	X
300	N/A	X	X	N/A	X	X	X
400	N/A	X	X	N/A	X	X	X
500	N/A	X	X	N/A	X	X	X
600	N/A	X	X	N/A	X	X	X
1,000	N/A	N/A	X	X	X	X	X

N/A signifies no FDS simulation was performed.

Note that most of the obstructions modeled in this investigation include top obstructions without any openings or penetrations. In addition, a number of sensitivity simulations were completed using openings of various percentages of the obstruction top surface area. These additional simulations are used to determine the applicability of information presented in this study when applied to enclosures with openings or penetrations on the enclosure's top.

5.2.3.6 Simulation Compartment

The compartment (i.e., the computational space) for the simulations used in this investigation measures 5 m (16 ft) x 5 m (16 ft) x 6 m (19.7 ft) (see Figure 5-4). The compartment is open on all sides and includes a concrete floor. In this investigation room heat up effects are not included. A mesh of 125 x 125 x 150 was used for each simulation, resulting in a grid resolution of 4 cm [δx (m)].

For simulations involving buoyant plumes, a measure of how well the flow field is resolved is given by the non-dimensional expression $D^*/\delta x$, where D^* (m) is a characteristic fire diameter:

$$D^* = \left(\frac{\dot{Q}}{\rho_0 c_p T_0 \sqrt{g}}\right)^{\frac{2}{5}} \qquad (5\text{-}7)$$

All other terms have been defined for Equation 5-7. The values of $D^*/\delta x$ defined in this investigation range from 7.3 to 19.6, which falls within or exceeds the values of $D^*/\delta x$ used in the validation study of FDS [21]. A larger ratio means more fire dynamics are resolved directly by FDS and the results are considered more accurate.

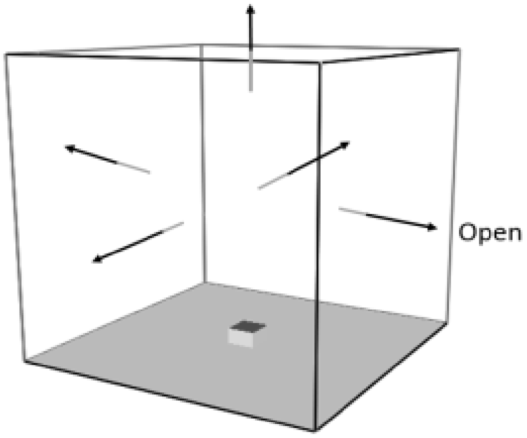

Figure 5-4
Simulation Compartment

5.2.3.7 Temperature Measurement Plane

Temperature predictions are obtained using slice files in FDS every 0.03 seconds. Slice files save horizontal planar slices of data at user specified locations (see Figure 5-5). This is the equivalent of experimentally placing thermocouple devices at 4 cm (1.6 in) spacing in the horizontal plane at each elevation. Temperatures used in this investigation are averaged over a period of 10 seconds in order to determine averaged plume centerline data in a manner similar to that used to develop the plume correlations by Heskestad. Each simulation predicts a total time of 30 seconds which, as discussed in Section 5.2.4.1, is longer than necessary to achieve steady state plume conditions. The slice files are included at elevations spaced every 0.3 m (1 ft) from the floor to the top of the 6 m tall compartment. Using the slice file to record temperature measurements ensures that the maximum plume temperature can be recorded for analysis, regardless of its location within the compartment. This is especially important as different obstruction geometries shift the plumes location away from the center of the fire source (see Figure 5-5). The maximum plume temperature at elevations above the obstruction is used to determine the effect of an obstruction on plume temperatures and develop information for any resulting change in the ZOI.

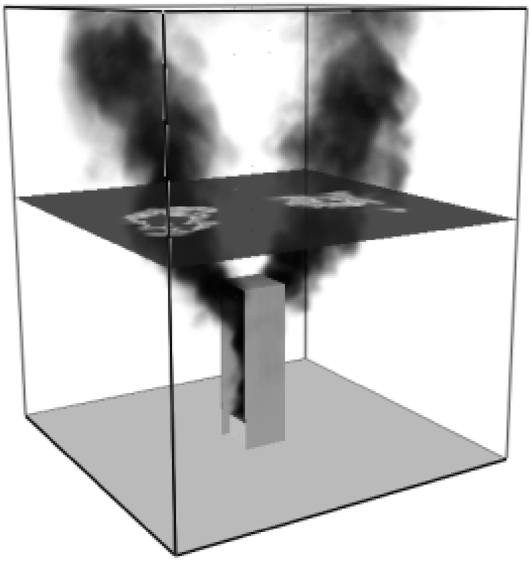

Figure 5-5
Slice File FDS Simulation Temperature Measurements

5.2.4 *Preliminary FDS Simulations*

In this section, the results for simulations with fuel sources under different obstruction configurations are reviewed and analyzed to ensure proper implementation of the analysis and to confirm that the results provide the correct data. First, the results for unobstructed fires are discussed for 200 kW and 1000 kW fires. This is then followed by six simulations consisting of 200 kW and 1000 kW fires subject to the three different obstruction configurations.

5.2.4.1 No Obstruction – Baseline

Simulations with the fire source subject to no obstructions for each of eight HRRs, three diameters, and three fire source elevations used in this investigation were performed for comparison against the obstructed cases. In Figure 5-6, unobstructed fires with HRRs of 200 kW and 1000 kW are presented. Also shown in Figure 5-6 are two of the fire source diameters and elevations used in the investigation. The 200 kW fire has an effective fire source diameter of 0.6 m (1 ft) and a source elevation of 1.1 m (3.6 ft). The 1000 kW fire has an effective fire source diameter of 0.9 m (3 ft) and a fire source elevation of 2 m (6.6 ft).

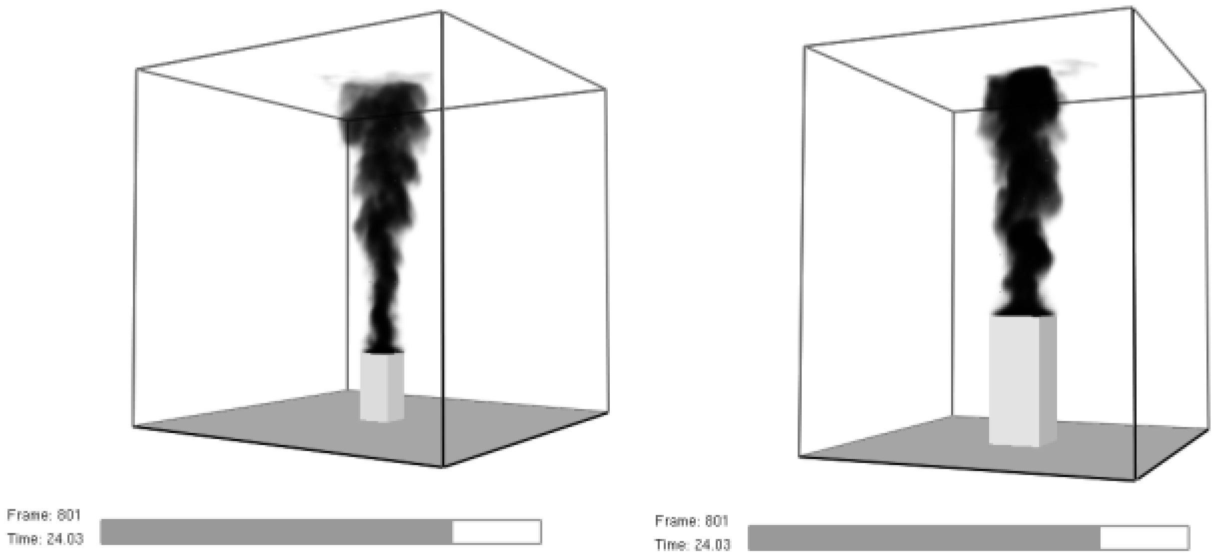

Figure 5-6
a) 200 kW, 0.6 m (diameter), 1.1 m (elevation) and b) 1000 kW, 0.9 m (diameter), 2 m (elevation) – Non-Obstructed Geometry

Figure 5-7 and Figure 5-8 show the HRR versus time for the two unobstructed simulations presented in Figure 5-6. The HRRs shown are the FDS default described by:

$$\dot{Q}(t) = \dot{Q}_0 \cdot tanh\left(\frac{t}{\tau}\right) \qquad (5\text{-}8)$$

Where, $\dot{Q}_0$ is the user-specified HRR in kW, t is elapsed time in seconds, and τ is the time for the HRR to ramp up to its prescribed value in seconds. The default value for τ in FDS, one second, was specified in this investigation. This fire growth rate is considerably faster than that provided by NUREG/CR-6850, and is applied here to achieve a fast steady state performance and limit simulation time. For this study, only the steady state behavior of the plume is of interest. The HRR for the two simulations quickly reaches the user-specified values of 200 kW and 1000 kW and varies throughout the remainder of the simulation due to turbulent fluctuations simulated by FDS. In Figure 5-7 and Figure 5-8, the one-second time-averaged HRR is presented along with the resulting HRR described by Equation 5-8 directly to verify that the HRR has been implemented correctly.

In Figure 5-9, the fire plume temperatures predicted by FDS and the Heskestad fire plume correlation (Equation 5-3) are presented. For the 200 kW and 1000 kW fires, the Heskestad fire plume correlation agrees with the FDS simulated plume temperatures. Note that the FDS and Heskestad predictions are essentially the same with only minor variations. The most significant variation is that for the larger fire, FDS predicts somewhat lower temperatures in the flame zone region very close to the fire source. This is of no major significance to this study because the predicted temperatures for both models are in the 700-900 °C range, which is well in excess of values of interest to fire PRA (e.g., typical cable or component failure temperatures).

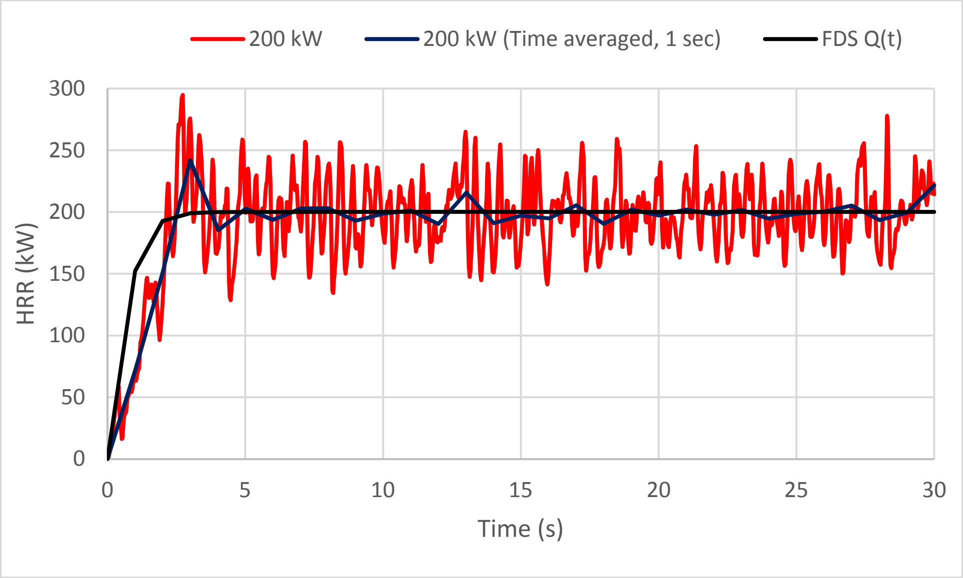

Figure 5-7
HRR vs. Time, Unobstructed Simulation – 200 kW, 0.6 m (diameter), 1.1 m (elevation)

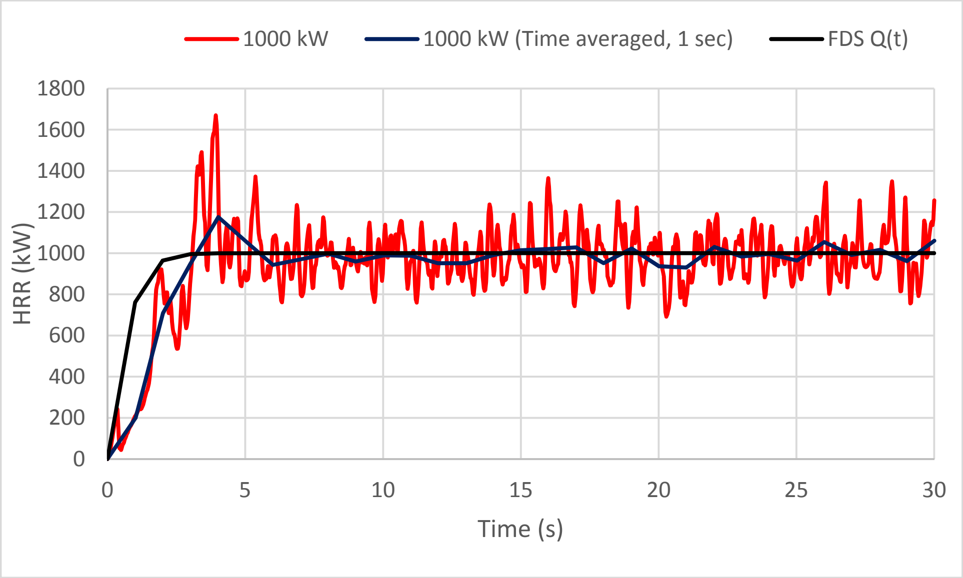

Figure 5-8
HRR vs. Time, Unobstructed Simulation – 1000 kW, 0.9 m (diameter), 2 m (elevation)

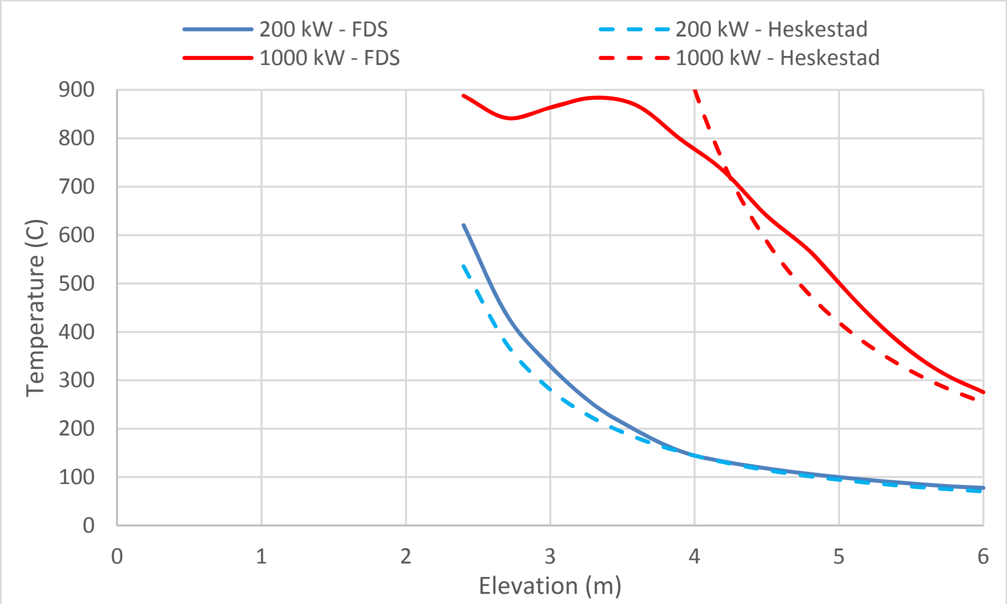

Figure 5-9
Temperature vs. Elevation Above Floor, Unobstructed Simulation – 200 kW, 0.6 m (diameter), 1.1 m (elevation) and 1000 kW, 0.9 m (diameter), 2 m (elevation)

5.2.4.2 Flat Plate Obstruction

Figure 5-10 shows fires with HRRs of 200 kW and 1000 kW subject to a flat plate obstruction. The HRRs for the simulations presented in Figure 5-10 are similar to those presented in Figure 5-7 and Figure 5-8.

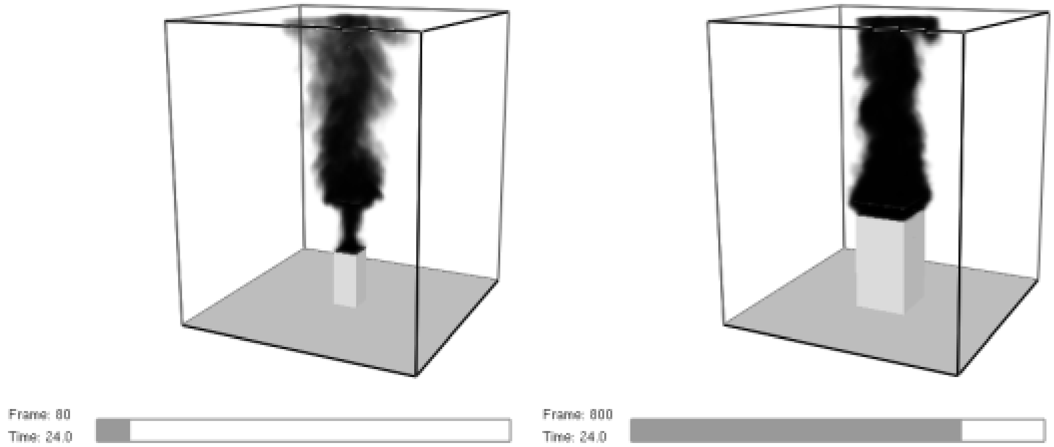

Figure 5-10
a) 200 kW, 0.6 m (diameter), 1.1 m (elevation) and b) 1000 kW, 1.2 m (diameter), 2 m (elevation) – Plate Obstruction

Figure 5-11 presents the temperature at different elevations versus time for the flat plate obstruction simulation with a 200 kW fire. These results show that the temperature becomes sufficiently steady after 15 seconds, and within the 30 second duration of the simulations used in this investigation. Several sensitivity cases were completed using both extended simulation times and the FDS input parameter ‘TIME_SHRINK_FACTOR,’ which reduces the specific heats of various materials by a user specified factor. These results, supported by the global energy balance provided with each simulation, show that the transient heating of the top surface of the enclosure plays no role in the long term trend of the simulated plume temperatures.

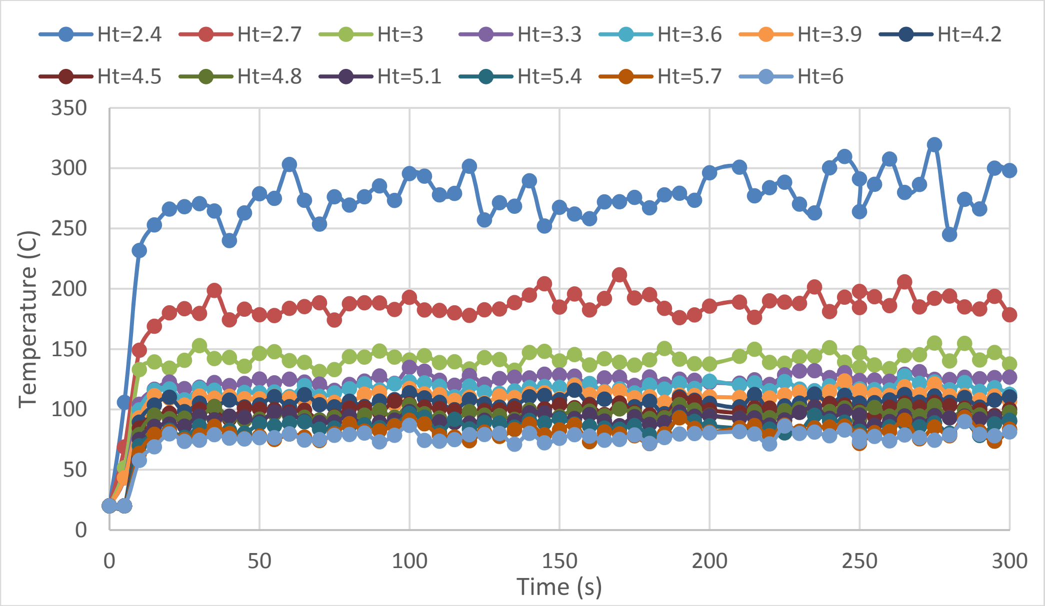

Figure 5-11
Temperature vs. Time, Flat Plate – 200 kW, 0.6 m (diameter), 2 m (elevation) – Elevations Above the Obstruction

Figure 5-12 presents the temperature profiles for the 200 kW and 1000 kW HRRs subject to a flat plate obstruction. Also included is the Heskestad (Equation 5-3) fire plume correlation temperature with identical model inputs. A comparison between the results suggests that the Heskestad plume temperature equation is over-predicting the plume temperature fires obstructed by a flat plate. This over-prediction suggests that the flat plate obstruction has reduced the plume temperature rise at elevations above the obstruction. It is likely that as the plume flows around the obstruction it is slightly broken up and results in an increased entrainment of fresh cool air. This entrainment reduces the plume temperature when compared to an unobstructed case predicted by the Heskestad fire plume correlation.

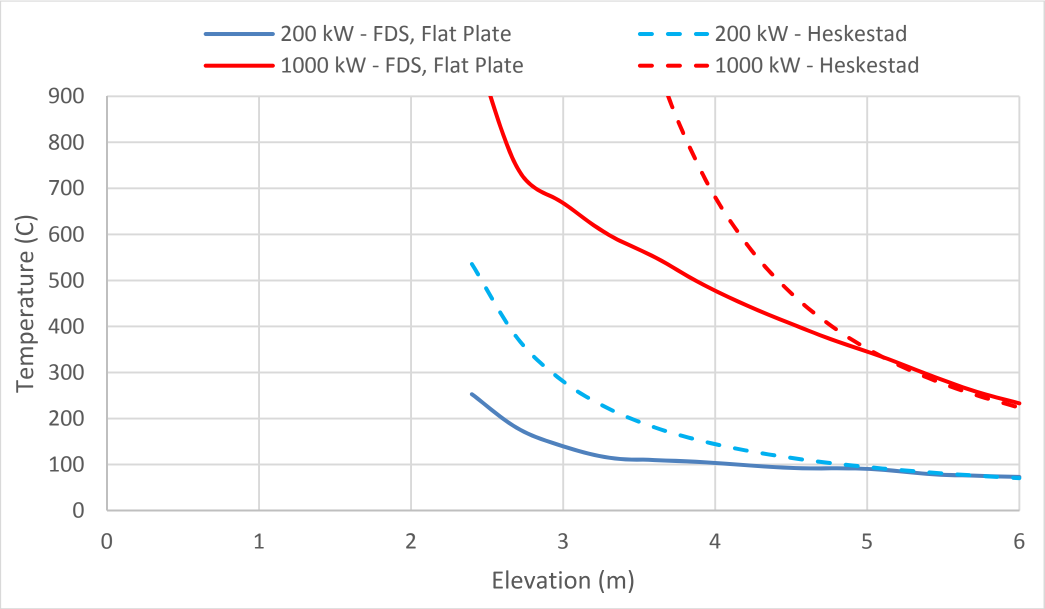

Figure 5-12
Temperature vs. Elevation Above Floor, Flat Plate Obstruction – 200 kW, 0.6 m (diameter), 1.1 m (elevation) and 1000 kW, 1.2 m (diameter), 2 m (elevation)

5.2.4.3 Arch Obstruction

Figure 5-13 shows simulations of a 200 kW fire and a 1000 kW fire subject to an arch obstruction, a flat plate ceiling located at an elevation of 2.3 m, and two walls. Plots of the HRR vs. Time for the 200 kW and 1000 kW fires are similar to those seen in Figure 5-7 and Figure 5-8.

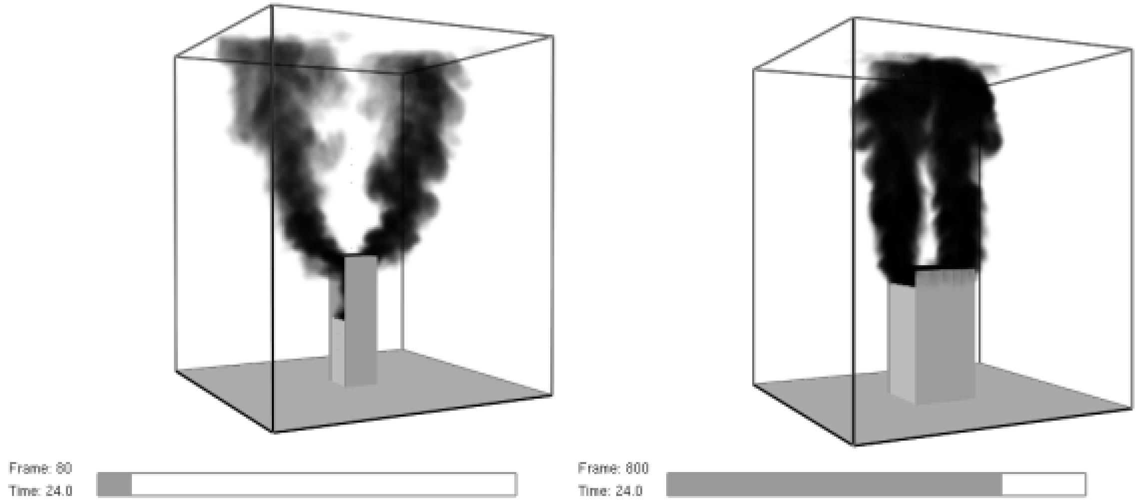

Figure 5-13
a) 200 kW, 0.6 m (diameter), 1.1 m (elevation) and b) 1000 kW, 1.2 m (diameter), 2 m (elevation) – Arch Obstruction

The temperature profiles for the 200 kW and 1000 kW simulation are presented in Figure 5-14.

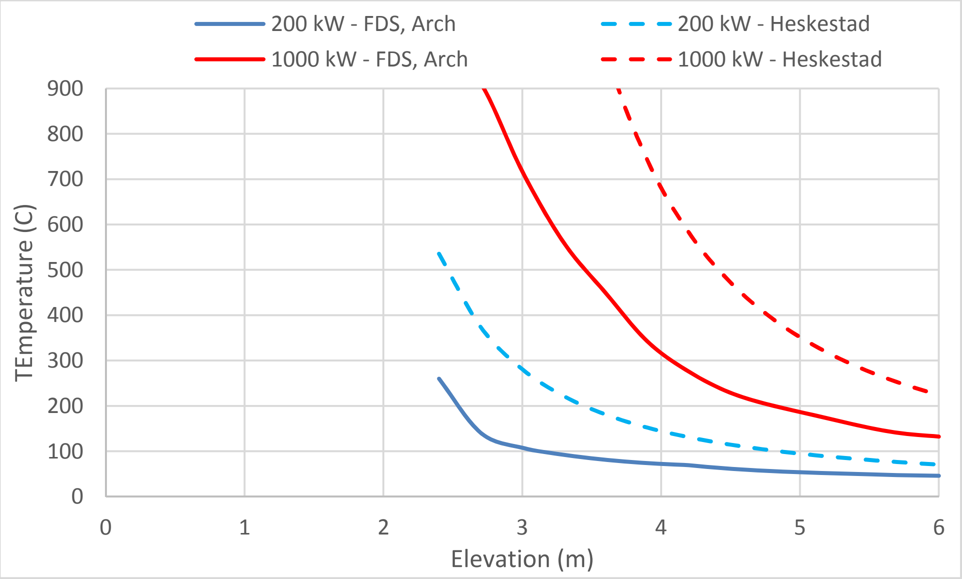

Figure 5-14
Temperature vs. Height Above Floor – Arch Obstruction – 200 kW, 0.6 m (diameter), 1.1 m (elevation) and 1000 kW, 1.2 m (diameter), 2 m (elevation)

Figure 5-14 includes the Heskestad correlation plume temperatures using identical inputs. It appears that the arch obstruction is also influential on the plume temperatures, as the simulated temperatures are lower than those predicted by the Heskestad fire plume correlation. This is likely a result of the increased entrainment resulting from the two plumes created by the arch obstruction geometry (see Figure 5-13). Being split into two separate plumes increases the surface area available for the plumes to entrain cooler fresh air which results in lower plume temperatures above the obstruction.

5.2.4.4 Three-Wall Obstruction

Figure 5-15 shows simulations of a 200 kW fire and a 1000 kW fire subject to a three-wall obstruction, a flat plate ceiling located at an elevation of 2.3 m (7.5 ft) and three walls. Plots of the HRR vs. Time for the 200 kW and 1000 kW fires are similar to those seen in Figure 5-7 and Figure 5-8.

The temperature profiles for the 200 kW and 1000 kW fires are presented in Figure 5-16.

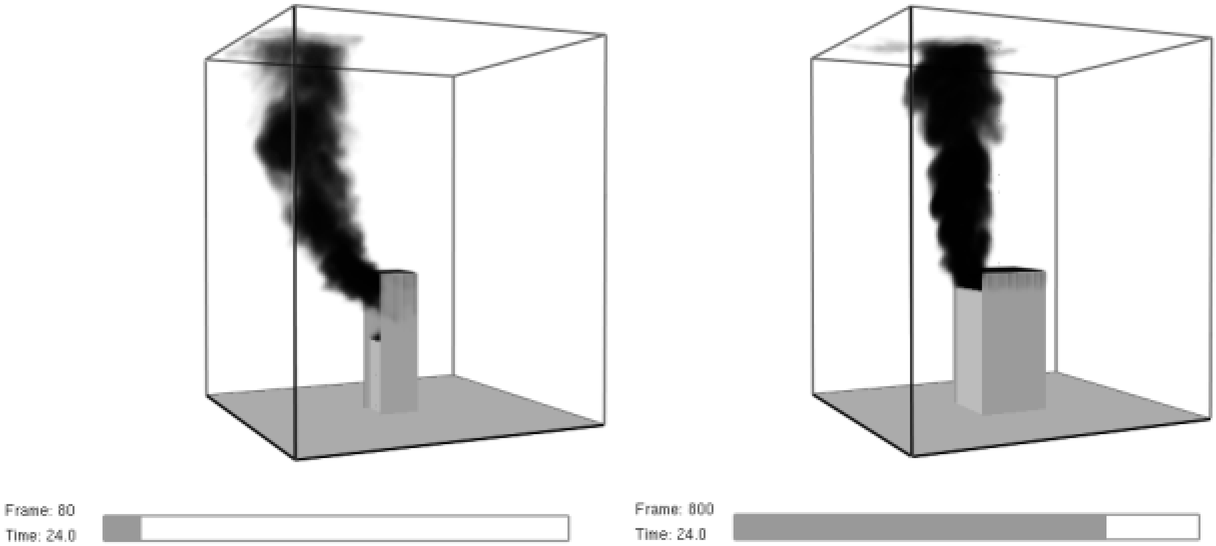

Figure 5-15
a) 200 kW, 0.6096 m (diameter), 1.1 m (elevation) and b) 1000 kW, 1.2 m (diameter), 2 m (elevation) – Three-Wall Obstruction

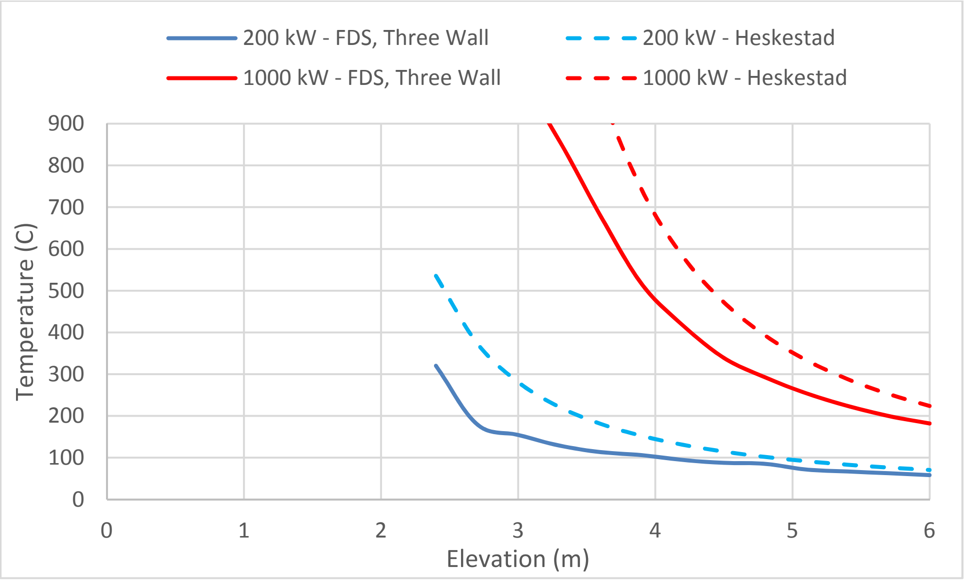

Figure 5-16
Temperature vs. Height Above Floor – Three-Wall Obstruction – 200 kW, 0.6 m (diameter), 1.1 m (elevation) and 1000 kW, 1.2 m (diameter), 2 m (elevation)

Figure 5-16 includes the Heskestad correlation plume temperatures using identical inputs. It appears that the three-wall obstruction, similar to the flat plate and arch obstruction, influences plume temperatures, as the simulated temperatures are lower than those predicted by the Heskestad fire plume correlation. Once again, this is likely a result of an increased entrainment of fresh, cool, air in the plume caused by the obstruction.

5.2.4.5 Statistical Analysis

The bias introduced by the plume obstructions is evaluated using the statistical model provided in NUREG-1934 [18]. In this study, the 'Experimental' value (*E*) may be either the unobstructed FDS prediction, or the unbiased Heskestad plume from Equation 5-3 [34]. The 'Modeled' value (*M*) will be the obstructed FDS prediction. This way, the experiment value is based on an established method to predict plume temperatures that is accepted when used within valid limits established by NUREG-1824 [21]. The model value is then the new information developed in this study that is biased by the presence of the obstruction. The following expressions are used to define the statistical analysis:

$$E|\theta \sim N(\theta, \sigma_E^2); \;\; \tilde{\sigma}_E = \sigma_E/\theta \qquad (5\text{-}9)$$

$$M|\theta \sim N(\delta\theta, \sigma_M^2); \;\; \tilde{\sigma}_M = \sigma_M/\delta\theta \qquad (5\text{-}10)$$

$$\overline{\ln\left(\frac{M}{E}\right)} = \frac{1}{n}\sum_{i=1}^{n} \ln\left(\frac{M_i}{E_i}\right) \qquad (5\text{-}11)$$

$$\tilde{\sigma}_M^2 + \tilde{\sigma}_E^2 = \frac{1}{1-n}\sum_{i=1}^{n}\left[\ln\left(\frac{M_i}{E_i}\right) - \overline{\ln\left(\frac{M}{E}\right)}\right]^2 \qquad (5\text{-}12)$$

$$\delta = \exp\left(\overline{\ln\left(\frac{M}{E}\right)} + \frac{\tilde{\sigma}_M^2}{2} - \frac{\tilde{\sigma}_E^2}{2}\right) \qquad (5\text{-}13)$$

Where, $N(\mu, \sigma^2)$ indicates a normal distribution with mean, μ, and standard deviation, σ, and the quantities θ, E, and M are the True, Experimental, and Modeled quantities of interest. In this case, E and M are defined as the plume temperature rise above ambient. The relative standard deviations, $\tilde{\sigma}_E$ and $\tilde{\sigma}_M$, are necessary in this framework and represent the fraction of the measured quantity that can be attributed to uncertainty. The quantity $\tilde{\sigma}_E$ is considered an input to the statistical model and can be estimated from prior analysis. The model bias, δ, is the primary quantity of interest for this study since it is equivalent to the term B proposed in Equation 5-6.

5.3 FDS Simulation Results

The FDS simulation results for all these cases are reported in Appendix E (Table E-1 for obstructed plume cases and Table E-2 for the unobstructed plume base case).

In Figure 5-17, the temperature increase results from all FDS simulations with obstructions are compared to unobstructed simulations with the same fire characteristics. Included in Figure 5-17 are temperature measurements made from directly above the obstructions, up to an elevation of 6 m (19.7 ft) at 0.3 m (1 ft) intervals. The x-axis is the unobstructed plume temperature rise. The y-axis is the equivalent obstructed plume temperature rise. Consequently, if the obstructed and unobstructed measurements are close to each other, all the points would fit along the diagonal (bold black line). Data points below the diagonal suggest lower obstructed plume values when compared with the corresponding unobstructed predictions.

The results in Figure 5-17 show that obstructions do indeed influence plume temperatures. Two observations can be made. In most cases, it appears the obstruction reduces the plume temperatures above the obstructions. However, in a few cases the obstructed temperatures are greater than those of the unobstructed fire. These cases can be identified by relation to the 'perfect match line,' an indication of when the obstructed and unobstructed temperatures are equal. It is likely that these instances in which the obstructed temperatures are greater than the unobstructed temperatures are a result of different entrainment behavior caused by the obstructions. Of the results where the obstructed temperatures are greater than the unobstructed case, all measurements were taken at an elevation of 3 m (9.8 ft) or lower, within 0.7 m (2.3 ft) of the top obstruction, with flames reaching consistently or intermittently above the top obstruction. Furthermore, each of the configurations that exceed the match line corresponds to a fire located 0.3 m (1 ft) above the floor. This result suggests a limit of applicability for fires that are located near the base of the enclosure, and this configuration is explored in greater detail below.

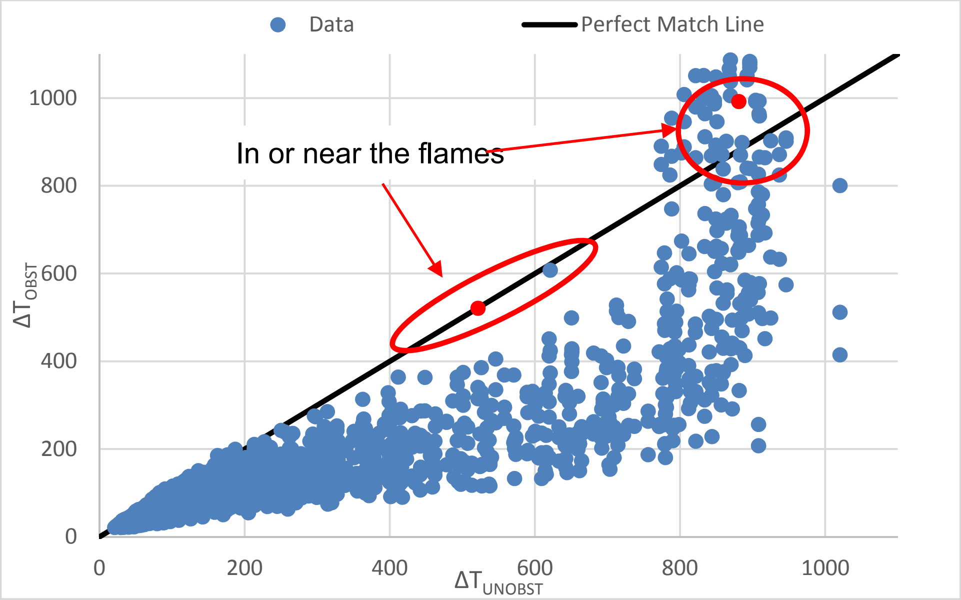

Figure 5-17
Unobstructed versus Obstructed Plume Temperatures

5.3.1 *Analysis of Non-Conservative Results*

In Figure 5-18 screen captures from one the simulations for the red dots near 500 °C (932 °F) highlighted in Figure 5-17 is shown. The data is from measurements made at an elevation of 2.4 m (7.9 ft), approximately 0.1 m (0.3 ft) above the top obstruction. In both incidents, the flames can be seen intermittently expanding above the top obstruction.

Results from the simulations presented in Figure 5-18 show the flames intermittently reaching out and above the ceiling of a three-wall obstruction. The spillover of the flames has an effect of increasing the 10 second time averaged temperature used in this analysis. The increased flame heights and resulting increased temperatures are likely a result of reduced entrainment within the obstruction. However, the remainder of the plume temperatures above the obstruction are lower than those for an unobstructed case.

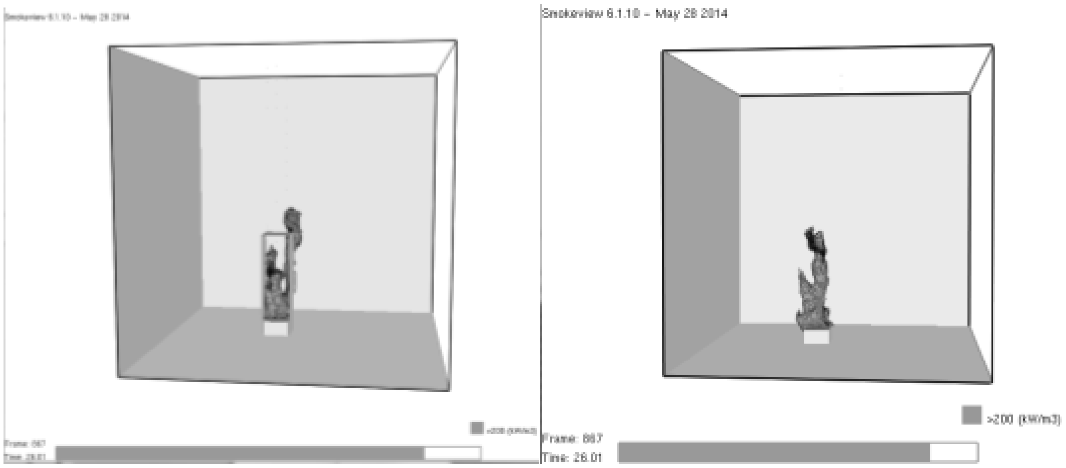

Figure 5-18
a) Three-Wall Obstruction, 500 kW, 0.3 m b) No Obstruction, 500 kW, 0.3 m

Another case where two simulations produce data above the perfect match line is examined for the red region near 900 °C (1652 °F) circled in Figure 5-17. In Figure 5-19, the comparison between a three-wall obstruction around a fire source at an elevation of 2 m (6.6 ft) and that of an unobstructed case is presented. Comparing these simulations, the flame length in the unobstructed simulation is greater than that observed in the obstructed simulation. Since both cases are within the flame region of the fire source, it is normal that they both produce temperatures near 900 °C (1652 °F), which is widely reported as the temperature within the flame by Heskestad. Since temperatures very near and inside the flame do not correlate with height as indicated in Equation 5-3, temperatures near the flame temperature should be filtered from the final analysis to determine the bias induced by the obstructions.

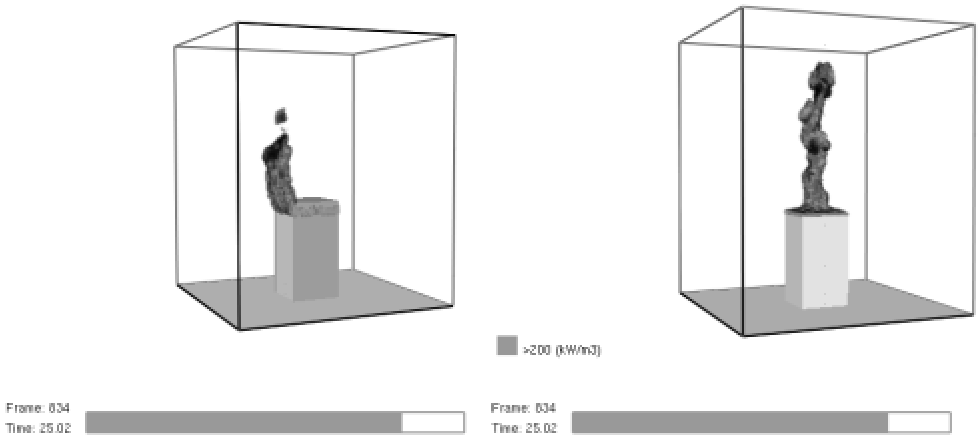

Figure 5-19
a) Three-Wall Obstruction, 1000 kW, 1.2192 m b) No Obstruction, 1000 kW, 1.2 m

5.3.2 *Obstruction Configuration*

The same results presented in Figure 5-17 are presented once again in Figure 5-20; however, they are now grouped by the configuration of the obstruction used in the simulations.

Grouping the data by obstruction geometry does not point out any significant trends. This suggests that the geometry of an obstruction is not significant in terms of how the temperature rise is affected, but that simply the presence of an obstruction is influential.

However, some observations can be made from the results presented in Figure 5-20. It appears that the plume temperatures from the fires subjected to the three-wall obstruction are slightly closer to those of the unobstructed case when compared to the arch and flat plate geometries, which appear to have larger differences on average. The different performances are not considered to be statistically significant, and the ultimate information does not distinguish between the three configurations of the obstruction.

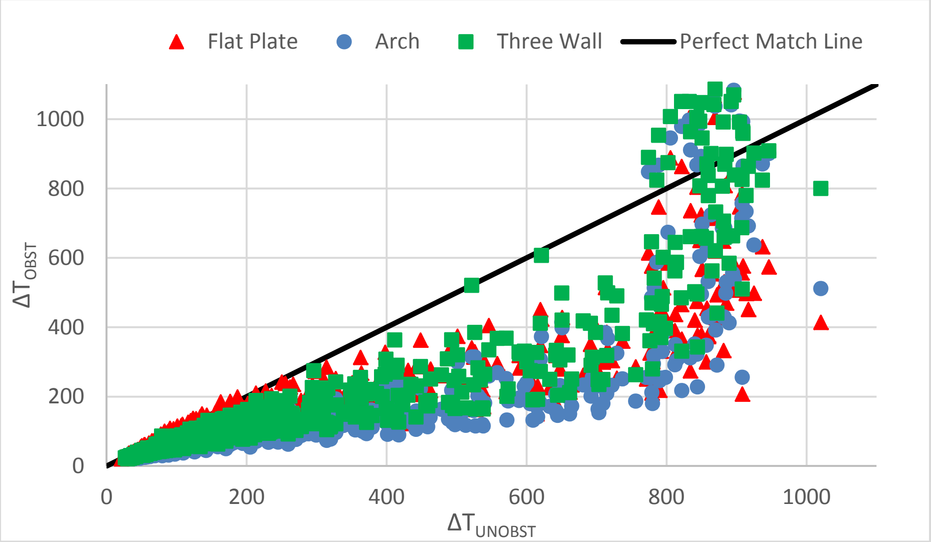

Figure 5-20
Unobstructed versus Obstructed Plume Temperatures – Different Geometries

In Figure 5-21, plume flows for the three different obstructions are presented for comparison with an unobstructed case. A comparison between Figure 5-21a and Figure 5-21d indicates that the flat plate obstruction has a tendency to increase the plume width at elevations around and above the obstruction. This causes an increased entrainment of fresh air into the plume and the observed reduced plume temperatures.

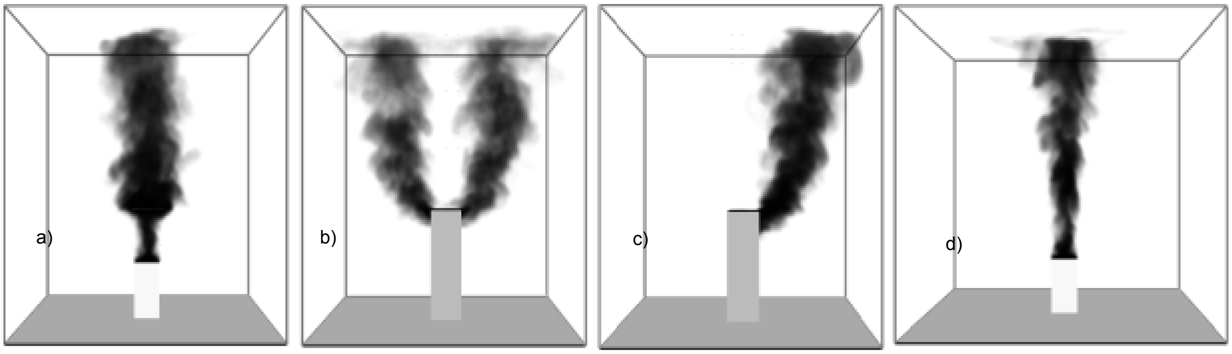

Figure 5-21
Plume Flows Subject to Different Obstruction Geometries: a) Flat Plate, b) Arch, c) Three-Wall, d) Unobstructed

As discussed in the previous section, the arch obstruction, Figure 5-21b, causes the plume to be split into two separate plumes directly above the obstruction. (It is possible for the two separate plumes to reconcile at higher elevations as shown in Figure 5-13. This split allows for an increased surface area with which fresh air can be entrained and the plume temperatures can be reduced.)

Plumes subject to the three-wall obstruction geometry (Figure 5-21c) are shifted off center when compared to the unobstructed geometry. Similar to the flows subject to the flat plate obstruction, the three-wall obstruction appears to increase the plume width around and above the obstruction. This is likely the cause of the lower plume temperatures above the three-wall obstruction. In the previous section it was suggested that the three-wall obstruction geometry limits entrainment of fresh air at elevations below the top of the obstruction and that this entrainment likely increases the temperatures around and directly above the top. The competing effects of an increased entrainment from a larger plume area above the obstruction and the reduced entrainment within the obstruction are likely a reason temperatures above this obstruction are slightly higher than those of the other obstructions observed.

5.3.3 *Fire Source Diameter*

In Figure 5-22, the unobstructed and obstructed temperature comparisons are split into groups based on the different fire source diameters.

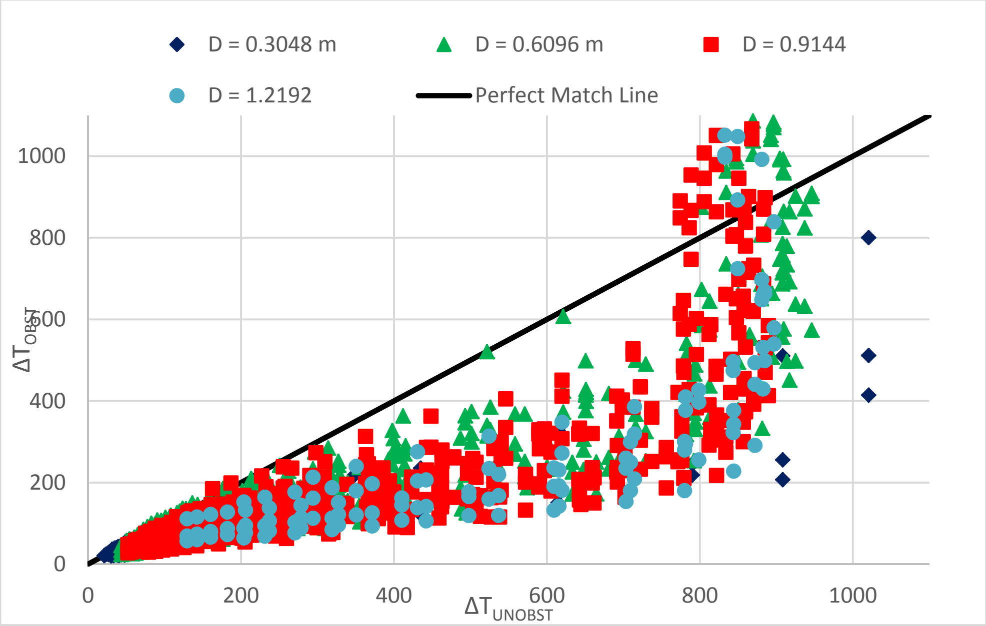

Figure 5-22
Unobstructed versus Obstructed Plume Temperatures – Different Fire Source Diameters

This grouping shows that, except at the lower ranges of plume temperature rises, only the larger diameter fires show instances of obstructed temperature rises greater than the unobstructed cases. Recalling the test matrix, the larger diameters allow for fires with larger HRRs, given the ranges on Q* for NPP scenarios [21]. This likely contributes to the limited amount of fires with diameters of 0.3 m (1 ft) that produce temperatures near the flame temperature.

5.3.4 *Heat Release Rate*

In Figure 5-23 the unobstructed and obstructed temperature comparisons are split into groups based on the different heat release rates.

Grouping the comparisons by HRR, similar to the comparison of different obstruction geometries, no clear trend is seen. There is evidence of lower obstructed plume temperatures from fires ranging from the lowest HRR used in this investigation of 50 kW to those of the largest with a HRR of 1000 kW. This shows that the presence of an obstruction and its effect on the plume temperatures is observable over a range of different HRRs. If any trend can be gleaned from the results grouped by HRR, it is that the results appear similar to those of the fire source diameter groupings presented in Figure 5-22 in which smaller fires are grouped at lower temperature and larger fires are capable of exceeding the unobstructed case in some configurations.

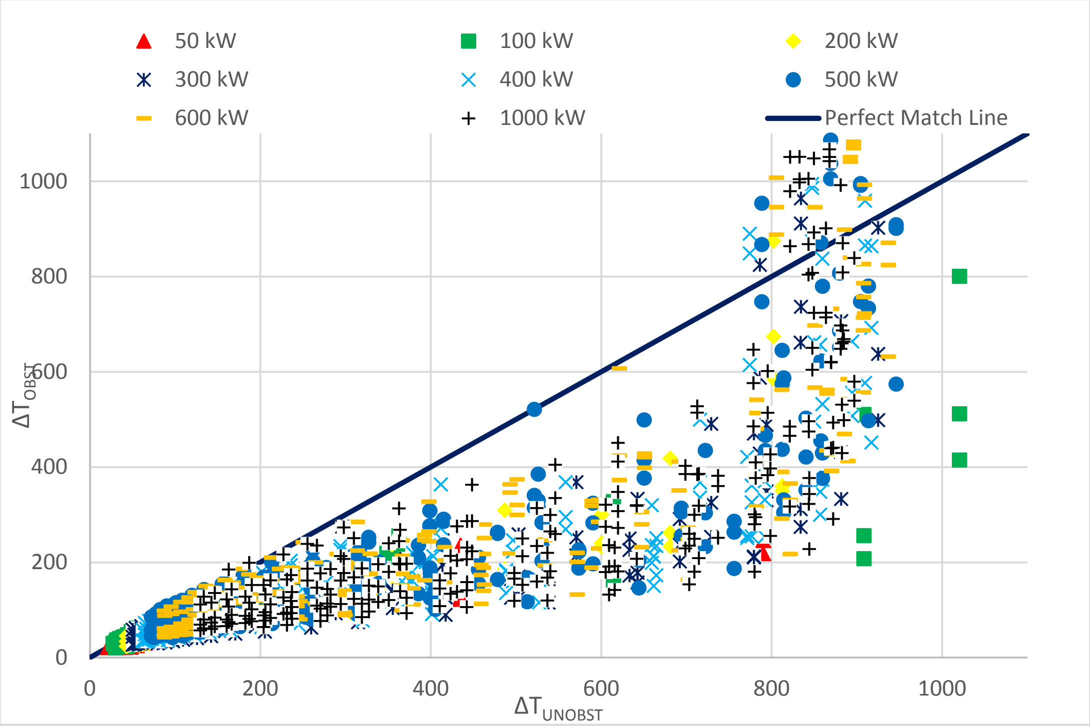

Figure 5-23
Unobstructed versus Obstructed Plume Temperatures – Different HRRs

5.3.5 *Fire Source Elevation*

In Figure 5-24 the simulations used in this investigation are grouped by the elevation of the fire source.

Grouping the data by fire source elevation brings insights as to the effect of an obstruction on plumes modeled in electrical enclosures. Following the ‘one-foot rule,’ current information [15] recommends that if an enclosure is unvented, a fire should be assumed to be located at an elevation of one foot below the top of the enclosure. In Figure 5-24, it is clear that the fires located 0.3 m (1 ft.) above the ground demonstrate different behavior than either of the elevated fuel sources. The average behavior of these cases demonstrates lower temperatures, but the variability of the case suggests that it is possible that the fire performs similarly to an unobstructed case. A number of possibilities are considered to account for these observations. As already discussed, in some cases it is likely the obstruction causes a focusing of the plume flow when compared to an unobstructed case. It is also possible that in some cases the walls at the edge of the simulation compartment cause a tilting of the plume flow such that the flow is not significantly affected by the presence of the obstruction and the natural variation in turbulent plume flow results in higher temperatures. This suggests that the information proposed in this investigation should not include fires at elevations less than half the height of the enclosure, as they behave similarly to fires in unobstructed configurations.

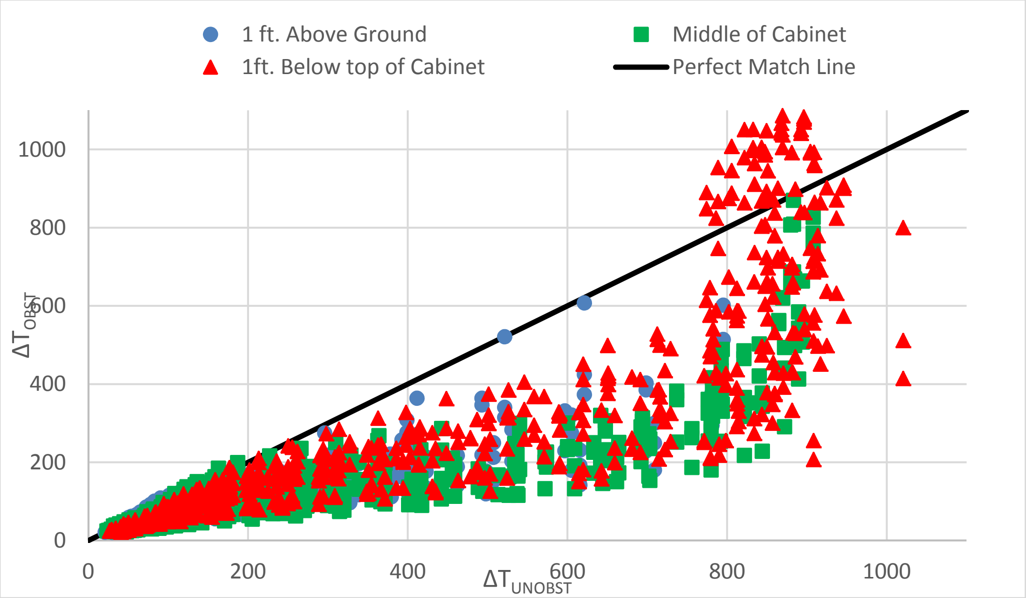

Figure 5-24
Unobstructed versus Obstructed Plume Temperatures – Different Fire Source Elevations

Additionally, current information in NUREG/CR-6850, Supplement 1 [15] states that the location of the fire be based on visual observation of the enclosure internals. However, this can be challenging if there are numerous cable bundles in different orientations or for cases in which a visual inspection of the enclosure internals is unavailable. In such cases, current information stipulates that fires are to be located 0.3 m (1 ft.) below the top of the enclosure, at the uppermost vent if the enclosure is vented, or at the highest location of any door or opening that may be expected to fail [15]. Therefore, given the observations that the fires located 0.3 m (1 ft.) above the ground are less likely to exhibit obstructed plume behavior and in keeping with current information, the results from simulations for fires located 0.3 m (1 ft.) above the ground are not included in the further analysis and information provided in this investigation.

5.3.6 *Statistical Analysis*

The results presented above indicate the necessity to define valid limits on the selection of temperature data for this analysis for determination of plume ZOI. As discussed above, temperatures within the flame region have been filtered out of the analysis. Temperatures within the flame height are typically not necessary in fire PRAs, in favor of more conservative treatments of damage (i.e., targets within the flame are damaged instantly). Since the maximum extent of the plume vertical ZOI always contains the flame height region, knowledge of the flame height is not necessary to develop a conservative treatment in the fire PRA. Furthermore, correlations such as that developed by Heskestad do not apply for temperatures very near the flames where near constant temperature rise is observed. This behavior effectively limits the data used in this analysis to temperatures less than approximately 800 °C (1472 °F).

Additionally, temperatures below 130 °C (266 °F) are below temperatures that are used for target damage in NPP applications (i.e., 205 °C (400 °F) and 330 °C (626 °F) for thermoplastic and thermoset cables, respectively, per NUREG/CR-6850, Table 8-2). This temperature was chosen because it results in a negligible probability of causing damage for the 205°C (400 °F) limit using the bias (1.18) and normalized standard deviation (0.20) calculated for FDS [33]. A simple means of assessing the probability that a given prediction exceeds a threshold value due to model uncertainty is provided in NUREG-1934/EPRI 1023259 [18]. This probability may be determined from the following equation:

$$P(x > x_c) = \frac{1}{2}\,\mathrm{erfc}\left(\frac{x_c - \mu}{\sigma\sqrt{2}}\right) \qquad (5\text{-}14)$$

Where, P is the probability, x is a parameter value, x_c is a threshold parameter value, μ is the mean ‘true’ predicted value of the parameter, σ is the standard deviation of the model prediction for the parameter of interest, and the complementary error function is denoted by ‘erfc’. The mean value is determined from the model bias as follows:

$$\mu = M/\delta \qquad (5\text{-}15)$$

Where, M is the model prediction and δ is the model bias. The standard deviation is computed from the normalized standard deviation as follows (NUREG-1934, 2012):

$$\sigma = \tilde{\sigma}_M(M/\delta) \qquad (5\text{-}16)$$

Where, $\tilde{\sigma}_M$ is the normalized standard deviation.

The model bias and normalized standard deviation for FDS, Version 6 are as follows [33]:

- Plume Temperature (model bias): 1.18
- Plume Temperature (normalized standard deviation): 0.20

Following the procedures above, a model temperature prediction of 130 °C (266 °F) would result in a 0.00006% chance of causing damage to a target with a 205 °C (400 °F) critical temperature, due to model uncertainty.

5.3.7 *Summary of Results*

Recall that in the discussion of plume scaling theory in Section 5.2.2.1, a proportionality constant (A) was defined in Equation 5-2 (shown below again) as characterizing the ratio of plume temperature rise to a functional group made up of the fire HRR, and the distance from the fire’s virtual origin:

$$A \approx \frac{\Delta T_m}{\dot{Q}^{2/3}(z - z_0)^{-5/3}} \qquad (5\text{-}17)$$

Further, Beyler [28] noted that the values reported by various investigators ranged from 21.6 to 29.7. Results from this investigation have been used to estimate modified average proportionality constants for fires subject to an obstruction. The average proportionality constants for the flat plate, arch, and three-wall obstructions are 16.6, 10.9, and 16.2, respectively. The fact that these values are lower than those reported for unobstructed plumes reflects the observation that the obstructions cause lower fire plume temperatures than would be observed for an unobstructed plume given the same fire HRR and elevation above the fire source.

The relative magnitude of these three values is also interesting. The lowest value, indicating the most significant effect relative to reducing plume temperatures, is associated with the arch configuration. This likely reflects the fact that the arch splits the plume into two parts that may not re-form over the obstruction, leading to enhanced entrainment as noted earlier. The highest value, indicating the least significant temperature reducing effect, is associated with the flat plate. In this case, the plume is disrupted, but re-forms into a single plume directly above the obstruction. As a result, the impact on temperature is reduced somewhat compared to the other cases. The three-wall configuration falls between the other two cases. With the three-wall obstruction a single plume is maintained, but that plume is diverted sharply sideways before regaining upward momentum.

In Figure 5-25 the temperature rise above an obstruction predicted using the average proportionality constants for the different obstructions plotted against the elevation ‘z’ (see Section 5.2.2.1) above the source normalized by the characteristic fire diameter, *D**, is presented. For comparison, the temperature rise predicted using the suggested proportionality constant of 26 by Beyler is included in Figure 5-25. These predictions are made using a representative case evaluated in this investigation: a HRR of 600 kW, a fire source diameter of 0.6096 m, an ambient temperature of 20 °C (68 °F), and a radiative fraction of 0.3.

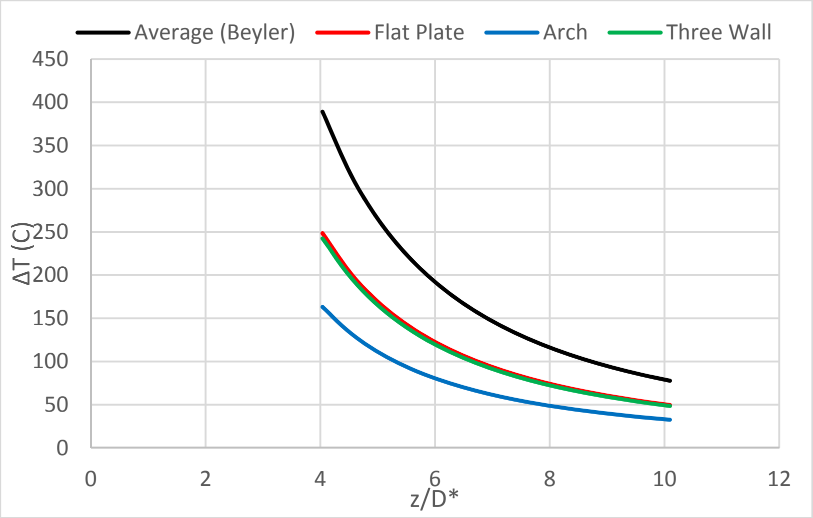

Figure 5-25
Obstruction Effect on Plume Proportionality Constant

The lower temperature rise predictions for the obstructed cases are evidence that the obstructions are reducing the plume temperatures above an obstruction. Also of note is that the temperature predictions for the three geometries are very similar, and it is not necessary to differentiate between them in the information.

Figure 5-25 demonstrates that the observed results for obstructed plumes can dramatically decrease plume temperatures and reduce the corresponding vertical ZOI for these fires using this approach.

5.3.7.1 Bias and Uncertainty

For the use of the results presented in this investigation with the Heskestad fire plume correlation in probabilistic analyses, model bias and uncertainty statistics for the plume temperature rise are provided in Table 5-2. The statistics provided were determined following the methods outlined in the FDS user's guide [30]. Table E-3 in Appendix E presents the FDS results for this evaluation.

The bias of 0.62 estimated by a comparison of the temperature rise measured above an obstruction in the simulations to those estimated by the Heskestad fire plume correlation is the bias to be used when estimating obstructed plume temperatures using Equation 5-6 and the vertical plume ZOI. Examples of how to apply this bias and determine the change in the plume temperature rise and the vertical ZOI for a fire subject to an obstruction are presented in following section.

Table 5-2
Bias and Uncertainty of Obstructed and Unobstructed Plume Temperature Rise

Comparison	Bias	Model Uncertainty	Experimental Uncertainty [33]
Obstructed versus Unobstructed	0.54	0.32*	0.20
Unobstructed versus Heskestad	1.17	0.14	0.20
Obstructed versus Heskestad	0.62	0.28*	0.20

*Note: Observing the results presented in Figure 5-26 and Figure 5-28, the actual scatter in the data supports an estimated model uncertainty closer to 20%.

In Figure 5-26, a comparison of the bias and uncertainty results is presented with the obstructed and unobstructed plume temperature comparison results. This comparison is used to demonstrate that the two configurations demonstrate different performance and that this difference is sufficient to warrant enhanced treatment. The bias shows a clear tendency of the plume temperature rise from a fire subject to an obstruction to be lower than the unobstructed case by around 46%, which is considered significant.

In Figure 5-27, results from simulations without obstructions are compared with the plume temperature rise predicted when using the Heskestad fire plume correlation. This comparison is used to demonstrate that both FDS and the Heskestad fire plume correlation produce similar results when used to predict identical configurations. The figure shows similarity between the FDS simulations and the Heskestad fire plume correlation. There is a slight tendency for the FDS simulated results to be higher than those predicted by the Heskestad fire plume correlation with a bias of 1.17; however, the difference between the two models is considered to be acceptable.

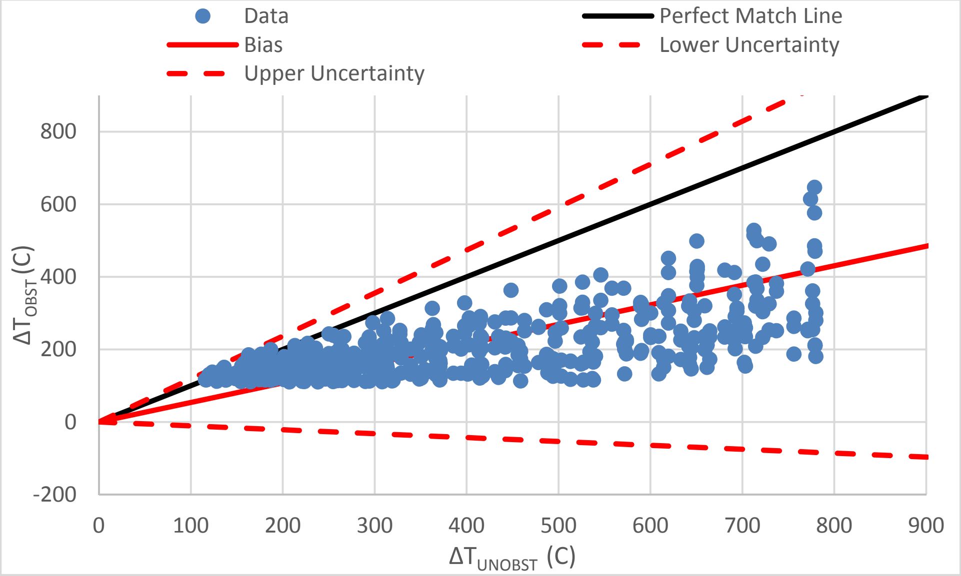

Figure 5-26
Unobstructed versus Obstructed Plume Temperatures – Bias and Uncertainty

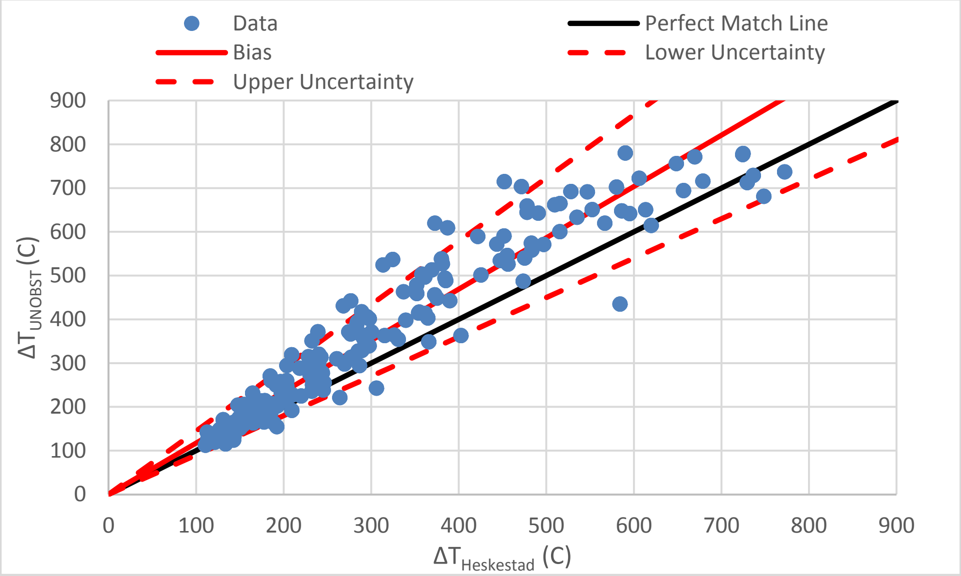

Figure 5-27
Heskestad versus Unobstructed Plume Temperatures – Bias and Uncertainty

When the plume temperature rise results for the simulations with obstructions are compared with the Heskestad fire plume correlation a difference is clear. In Figure 5-28, the obstructed fire plume temperature rise results are compared with the Heskestad fire plume correlation. The results show a clear estimation of lower temperatures for fires subject to obstructions. This suggests that in using the Heskestad fire plume correlation without accounting for obstruction cooling, fire plume temperatures are being over-estimated. The bias estimated when comparing the obstructed plume temperature rise to those estimated by the Heskestad fire plume correlation is 0.62.

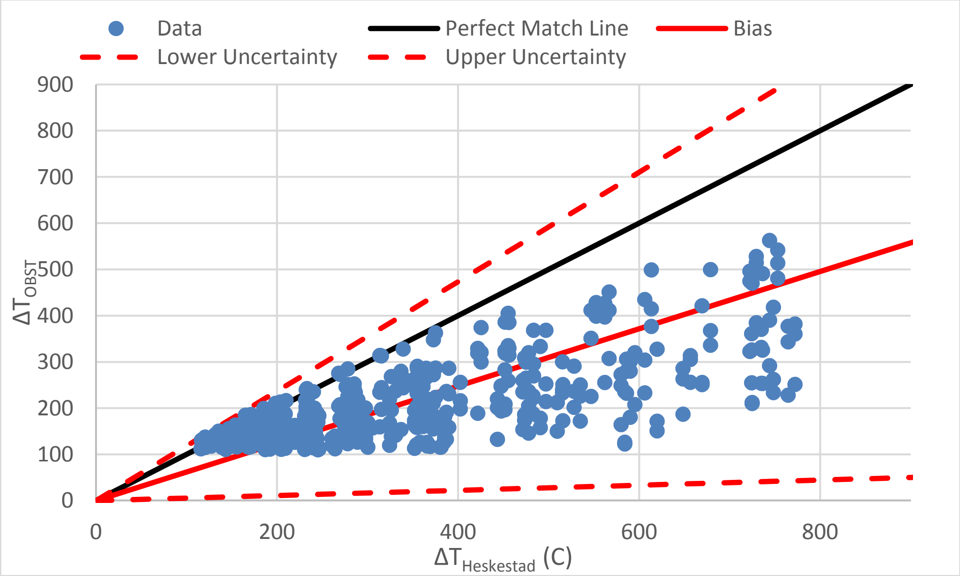

Figure 5-28. Heskestad versus Obstructed Plume Temperatures – Bias and Uncertainty

Results and evidence gathered from this investigation have potential to influence ZOI damage applications for NPP scenarios.

5.3.7.2 Sensitivity to Center Openings on the Obstruction

A number of simulations are performed with openings of varying sizes in the top of the obstruction. The opening is described as single opening in the center of the obstruction, as this is considered to be a conservative representation of distributed openings or penetrations that would be characteristic in NPPs. The sizes used in this analysis ranged from 6.5% to 14% of the total top surface area. The temperature rise above the obstruction using the different openings was compared to the temperature rise above unobstructed fires. The FDS results for this evaluation are presented in Table E-4 of Appendix E.

Opening percentages are dependent on the grid size and the source diameter of the simulations. Openings of sizes around 10% were selected to determine the effect of an opening on the plume temperatures above an obstruction. Two HRRs, 200 kW and 600 kW, were also used in these simulations to determine if changes caused by an opening were sensitive to changes in the HRR. The effect of an opening on the plume temperature above an obstruction does not appear to be sensitive to changes in the HRR.

The resulting biases presented in Table 5-3 show that openings of around 6.5% result in a fire plume temperature rise bias of 0.68, which differs from the obstructed bias of 0.54. As the cabinet open percentage increases to 12-14% of the total cabinet top area, the bias increases to 0.77, which is a noticeable departure from 0.54. These differences are considered sufficient to warrant an additional limit of applicability. Based on an interpolation of the evidence, a 5% opening would result in an approximate bias difference of less than 15% when compared to the obstructed cases with no openings. In practice, a change in the exposure of less than 15% is considered insensitive to the parameter variation relative to the uncertainty of the overall fire PRA. A 15% percent threshold is selected based on the uncertainty in the measurement of the HRR parameter [35], which reportedly ranges from 17% to 23%. Because the heat release rate is a primary input and the value is set based on information provided in Chapter 4 of this report, the output resolution is selected to be consistent with the uncertainty in the input. Therefore, the information provided in this investigation is applicable for enclosures with openings up to 5% of the total top surface area. Any enclosure with cumulative openings in the top greater than 5% should be treated as an unobstructed geometry. An enclosure top may have penetrations, but as long as those penetrations are properly sealed those penetrations do not contribute to the cumulative opening area. Properly sealed openings include cable inside steel conduit, cable trays with solid steel top and bottom covers, and other penetrations with approved non-combustible wrap materials. Any opening that may allow airflow through the top of the enclosure should be considered in the 5% cumulative opening fraction, including all penetrations which cannot be clearly observed as well sealed.

Table 5-3
Bias and Uncertainty of Obstructed (with Center Opening) and Unobstructed Plume Temperature Rise

Comparison	Bias	Model Uncertainty	Experimental Uncertainty [33]
Obstructed versus Unobstructed	0.54	0.32	0.20
Opening (6.5%) versus Unobstructed	0.68	0.14	0.20
Opening (12-14%) versus Unobstructed	0.77	0.17	0.20

5.3.7.3 Sensitivity to Fire Orientation

A number of simulations were performed with fires oriented vertically (See Figure 5-29). In these simulations the fire source originates at the floor of the simulation compartment and reaches to an elevation of 1.96 m (6.4 ft), approximately 0.3 m (1 ft.) below the top of the obstruction. In configuration a), fuel is released on all sides and across the full height of the column shaped fire source to simulate the effect of distributed combustible materials in the center of the enclosure. In configuration b), fuel is released on all interior surfaces of the electrical enclosure to simulate the effect of combustible materials mounted solely to the walls of the enclosure. The simulations using the vertical fire source are compared to the simulations with horizontal fire sources at different elevations used to develop the information presented in this report. Table E-5 of Appendix E presents the FDS results for this sensitivity evaluation.

Comparing the different simulations, the vertical fire source plume temperatures are very similar to those of a horizontal fire source with an elevation located in the center of the enclosure. Plume temperatures from simulations using horizontal fire sources located 0.3 m (1 ft.) below the top of the obstruction are found to be more conservative than those observed in the vertical fire source simulations. This suggests that assuming a horizontal fire source located 0.3 m (1 ft.) below the top of the obstruction results in a conservative analysis when compared to simulating a vertical fire source.

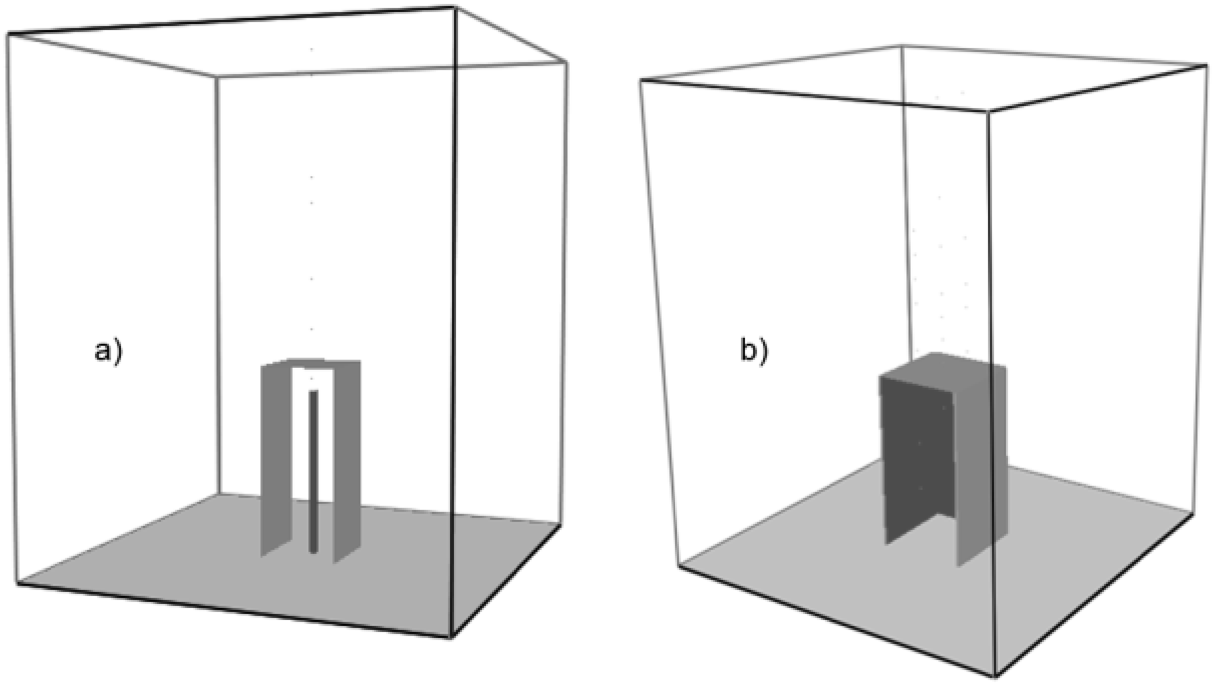

Figure 5-29
a) Vertically Oriented Fire Source, b) Fire Source Located Along the Cabinet Wall Surfaces

The opposite is found when comparing the vertical fire source plume temperatures with a horizontal fire source located 0.3 m (1 ft.) from the ground. In this comparison, the plume temperatures from the vertical fire source often exceed those of the horizontal source, resulting in a non-conservative comparison. As discussed in Section 6.4, the information following this investigation does not apply to fires located at elevations lower than the mid height of the enclosure. Therefore, a vertically oriented fire source can be conservatively represented by a horizontal fire source applied within the limits of implementation, and no additional restrictions are required.

5.3.7.4 Sensitivity to Obstructions with a Soffit

A number of simulations were performed using top obstructions equipped with a vertical soffit (see Figure 5-30). In these simulations the soffit is specified to extend 12 cm (6 in) below the top obstruction. This configuration is intended to simulate the possible effect of the soffit to change the thermal plume dynamics. Primarily, the soffit has the effect of reducing the horizontal extent of the plume observed in Figure 5-21 for some configurations.

Comparing the different simulations, the results of the top surface with a soffit are very similar to those of the flat top surface considered as the basis of this report. Plume temperature predictions of the soffit sensitivity cases are plotted with the original results in Figure 5-31. The results of the soffit obstructions fall within the existing scatter of data, or may fall below the existing data. This indicates that the existing approach for defining the bias and uncertainty will conservatively bound the effects of the soffit.

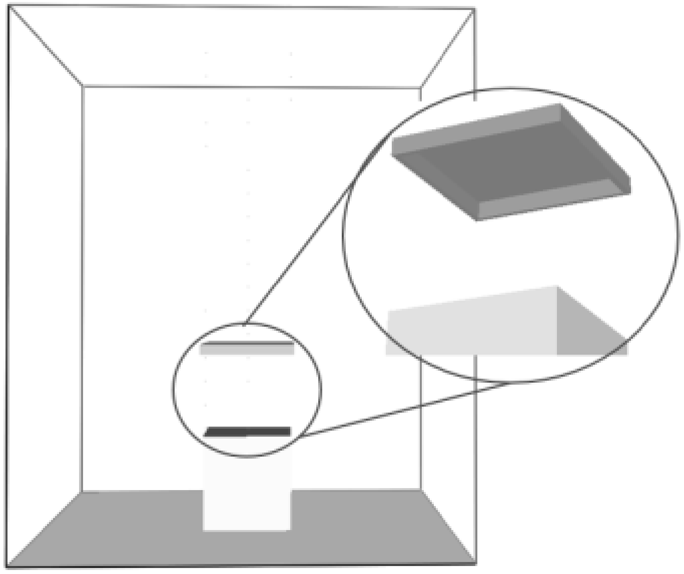

Figure 5-30
Top Obstruction with a Soffit

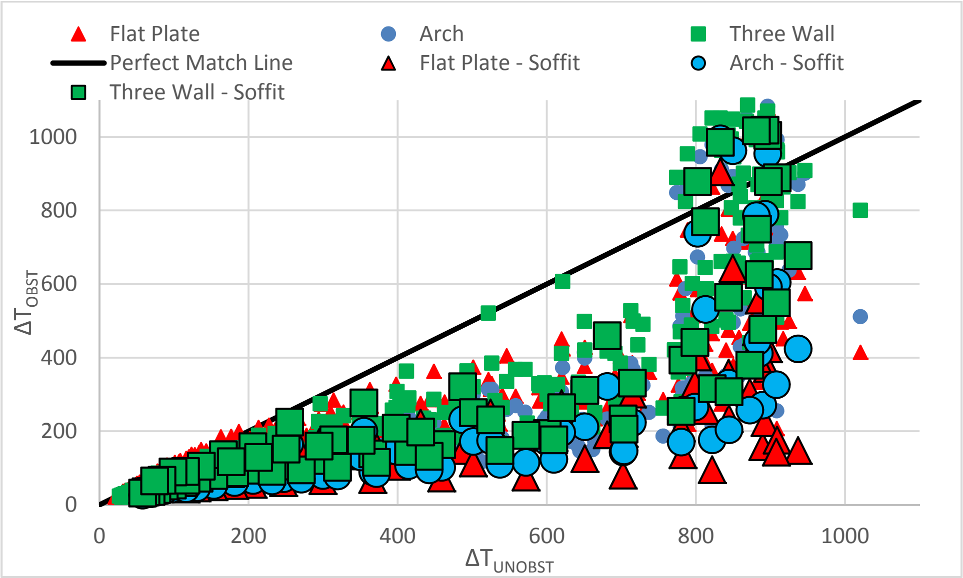

Figure 5-31
Unobstructed vs. Obstructed Plume Temperatures – Soffit Sensitivity

5.3.7.5 Sensitivity to Thickness of Steel Enclosure

A number of simulations were performed using top obstructions with various specified material thicknesses. The default material thickness used in this study is 0.0015 m, and the sensitivity cases consider effects of thicknesses of 0.001 m and 0.01 m. These configurations are intended to simulate the possible effect of the material thickness to alter the plume temperatures through surface heat transfer effects.

Comparing the different simulations, the results of varying the thickness of the top surface are very similar to those of the default thickness considered as the basis of this report. Plume temperature predictions of the sensitivity cases are plotted with the original results in Figure 5-32. The results of the sensitivity cases fall within the existing scatter of data. This indicates that the existing approach for defining the bias and uncertainty can accurately predict the effects of various top obstruction thicknesses between 0.001 m and 0.01 m.

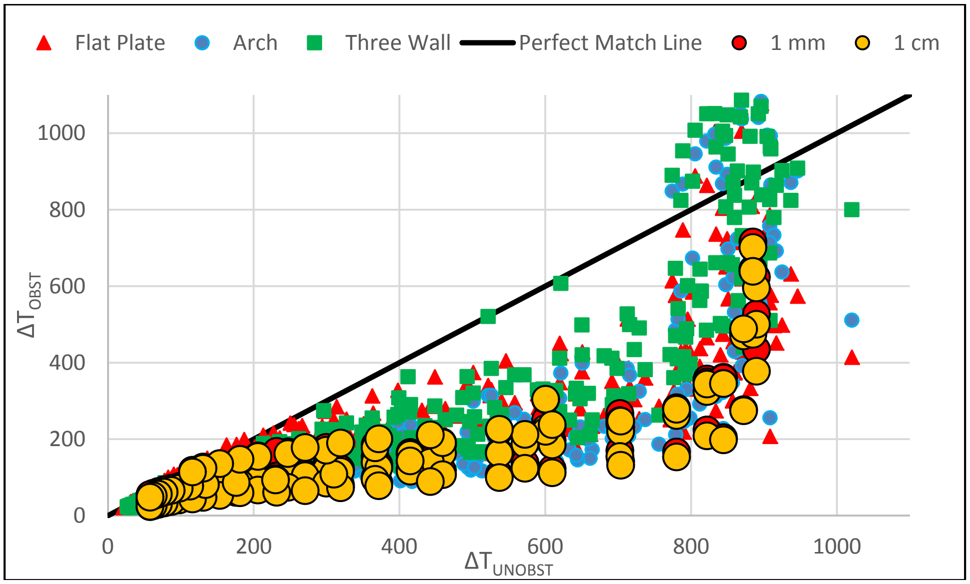

Figure 5-32
Unobstructed vs. Obstructed Plume Temperatures – Enclosure Thickness Sensitivity

5.3.8 *Horizontal Zone of Influence*

A horizontal ZOI may be defined for any ignition source defined in the fire PRA. This zone of influence is designed to determine the targets that may be damaged by thermal radiation exposure from the ignition source. While evaluating the obstructed plume temperatures, it was observed that a substantial horizontal component of the plume shift may occur. This section will quantify the observed horizontal shift of the obstructed plume, and compare the observed shift to existing methods of quantifying the extent of the horizontal ZOI.

5.3.8.1 Existing Definition of Horizontal ZOI

There are a number of existing methods to determine the horizontal zone of influence associated with an electrical enclosure fire. This section will not attempt to define all potential approaches that are validated for defining the horizontal ZOI, but will focus on the simplest and most common method in application. The Fire Protection Significance Determination Process (SDP) [19] defines the ZOI as the “ball and column” approach illustrated in Figure 5-33. Here, the radius, *R*, of the ball portion is defined as the critical radial distance that the ignition source may produce thermal radiation damage to an electrical target (e.g., cables). The height, *H*, of the column portion is defined as the critical vertical distance that the ignition source may produce thermal plume damage to an electrical target. The union of these two damage zones is typically evaluated as a cylindrical volume with a radius, *R*, and a height, *H*, inside which all electrical targets will be damaged given the occurrence of a 98th percentile fire size in the ignition source.

The height of the cylinder can be defined exactly using Equation 5-3 for the unobstructed plume or Equation 5-6 for the obstructed plume with the appropriate selection of the model bias. The radius of the cylinder can be defined in a number of ways, but the simplest is the Point Source Model (PSM, Equation 5-18) defined in NUREG-1805, Supplement 1.

$$r = \sqrt{\frac{X_r \dot{Q}}{4\pi \dot{q}''}} \qquad (5\text{-}18)$$

Where r (m) is the radial distance from the source location, X_r (-) is the radiative fraction, $\dot{Q}$ (kW) is the HRR, and $\dot{q}''$ (kW/m²) is the radiative damage heat flux. Note that the guidance in NUREG/CR-6850 Supplement 1 suggests that the source location of the fire for an electrical enclosure should be treated as the edge of the enclosure to account for burning at the vent. Tables of the dimensions of the ZOI can be calculated for many different heat release rate and target thermal property combinations, examples of which are provided in NUREG/CR-6850, Table F-2 and the Fire Protection SDP, Table 2.3.2. The distance from the center of the electrical enclosure to the edge of the ZOI is then defined as:

$$R_{Rad} = r + \frac{W}{2} = \sqrt{\frac{X_r \dot{Q}}{4\pi \dot{q}''}} + \frac{W}{2} \qquad (5\text{-}19)$$

Where R_{Rad} is an appropriate metric to compare the horizontal extent of the ZOI produced by the shifted plume associated with the obstructed plume simulations.

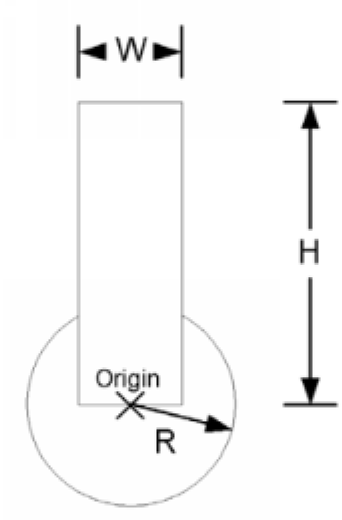

Figure 5-33
SDP Ball and Column

W: The diameter of the ignition source (m)
R: Critical the radial distance (heat flux) (m)
H: Critical distance for plume heights (m)

5.3.8.2 Horizontal Plume Shift ZOI

The obstructed plume simulation results demonstrated horizontal shifts of the plume centerline. This shift has the potential to expand the horizontal zone of influence associated with the ignition source. This effect is visualized in Figure 5-34, where the arch and three-wall obstructions produce clear horizontal shifts of the plume. The location of the plume centerline can be evaluated directly from the FDS slice file results in parallel with the determination of the peak centerline plume temperature as described in Section 5.2.3.7. This approach is visualized in Figure 5-35, and the location of the peak plume temperature relative to the center of the electrical enclosure is defined as R_{PO} (m). This metric allows for an immediate comparison of the plume shift to the thermal radiation ZOI.

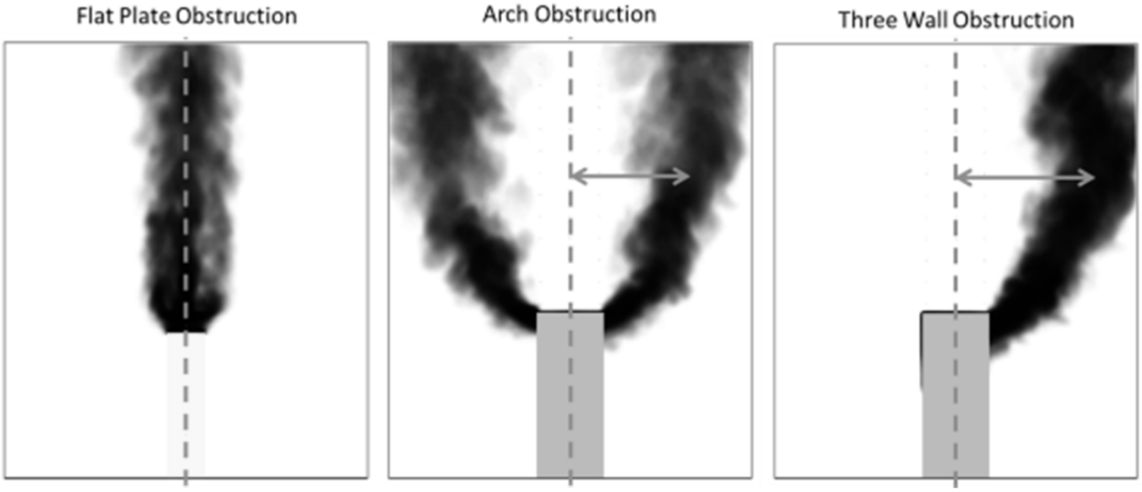

Figure 5-34
Obstruction Plume Shift

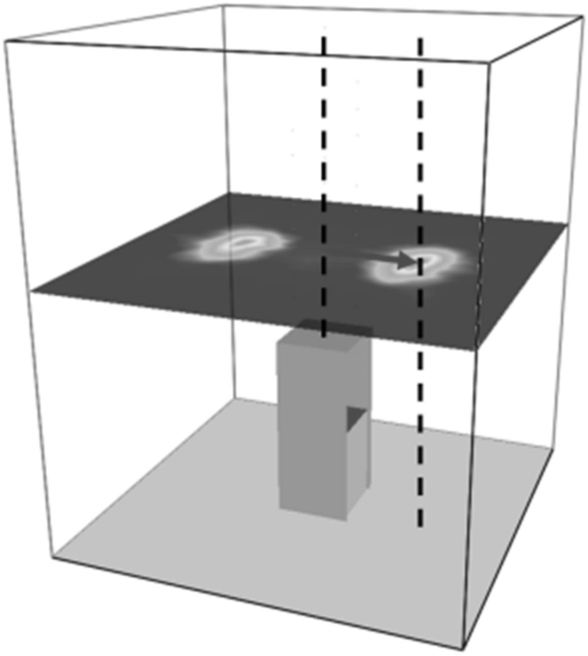

Figure 5-35
Determination of Horizontal Plume Shift

Comparison of the FDS simulation predictions of horizontal plume shift to the results determined for the PSM using Equation 5-19 are provided in Figure 5-36. The values for the distance that the plume has shifted from the centerline of the electrical enclosure are provided on the y-axis, and the values for the distance from the centerline of the thermal radiation ZOI are provided on the x-axis. The results show that for most cases, the thermal radiation ZOI extends farther than the plume will be shifted by the top obstruction. The data circled above the perfect match line in Figure 5-36 are all less than 200 °C (392 °C). These data correspond to locations that are above the plume ZOI for thermoset targets.

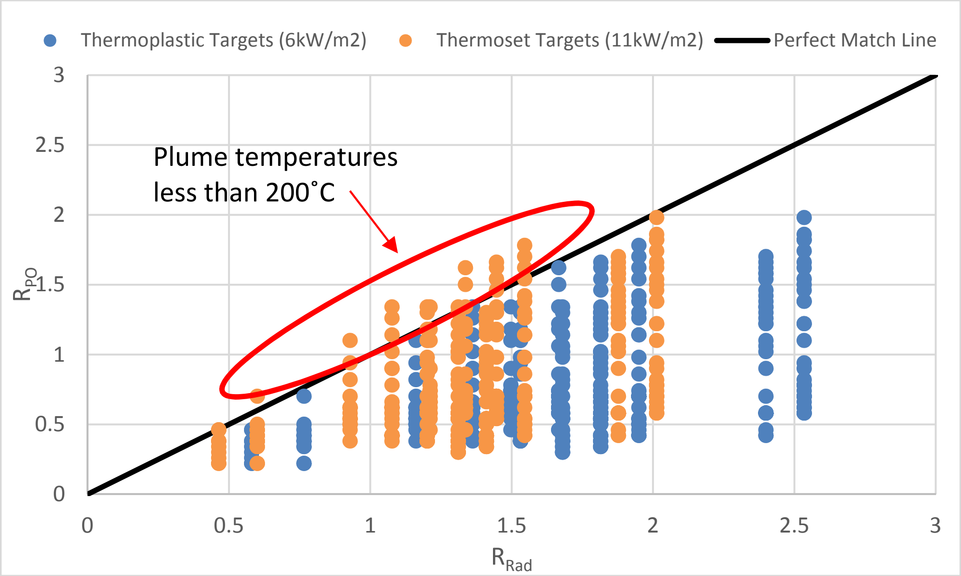

Figure 5-36
Comparison of Horizontal ZOI Resulting from Plume Shift to Thermal Radiation Exposure

A different way to quantify the plume shift is a similar approach to that taken in NUREG/CR-7010, in which the ignition of cable trays within a stack can be defined as an inverted frustum (trapezoid) with an angle of expansion of 35° with height. Here, the rate of expansion of the plume is defined in a similar way, where the base of the frustum is defined as the fire base height with dimensions equivalent to the plan dimensions of the electrical enclosure. Analyzing the data in Figure 5-36 using this approach, it can be found that the maximum angle observed from any FDS simulation of an obstructed plume is 28° from the vertical. In application, this angle can be treated as 30° for simplicity and conservatism. The illustration of the maximum extent of a thermal plume ZOI using this approach is provided in Figure 5-37.

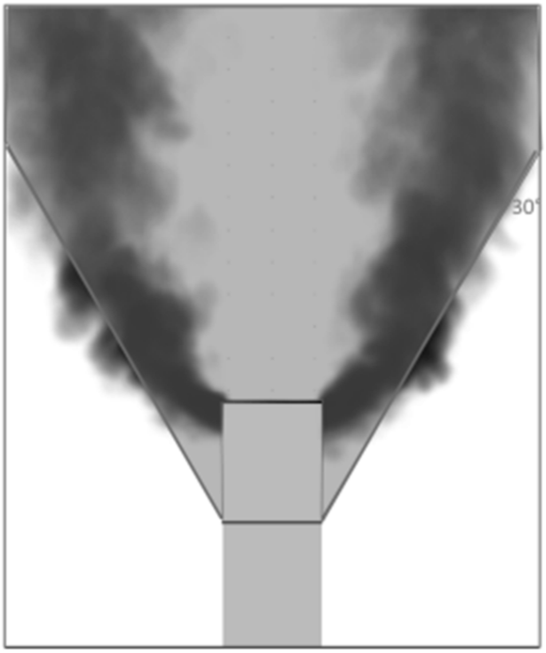

Figure 5-37
Maximum Angle from Horizontal Plume Shift

5.3.8.3 Recommendations

The findings from the FDS simulations demonstrate the following guidance can be applied to electrical enclosure fires that can be credited as having a solid top obstruction.

- The overall zone of influence should be defined using the ball and column concept introduced in the SDP [19] and described in NUREG/CR-6850, resulting in a cylindrical shape that incorporates the vertical extent of the plume and the horizontal extent of the thermal radiation from the fire source.
- The height of the column should be defined by Equation 5-6 for configurations in which the obstructed plume credit is applicable. In all other cases where the obstructed plume cannot be justified, existing methods shall be used corresponding to unobstructed plume temperature correlations.
- The width of the column should be defined using approved techniques for defining the horizontal extent of the thermal radiation from the source and the damage threshold of the most susceptible targets. The obstructed plume shall not be credited for reducing the extent of the horizontal ZOI at this time. The width defined in this manner (i.e., using flame radiation models) will always bound the expected horizontal shift of the thermal plume due to the electrical enclosure top obstruction.
- In specific applications where the location of the fire plume is of direct interest to the analysis, the plume location can be defined to fall within an inverted frustum (trapezoid). The base shall be defined at the fire base height with plan dimensions equivalent to the electrical enclosure. At elevations higher than the fire base height, the volume should expand with an angle of 30° relative to the vertical. The plume has been observed to always be located within this volume, regardless of the nature of the fuel source or electrical enclosure geometry.

The maximum extent of the ZOI is summarized in Figure 5-38 for both the unobstructed and obstructed plume cases.

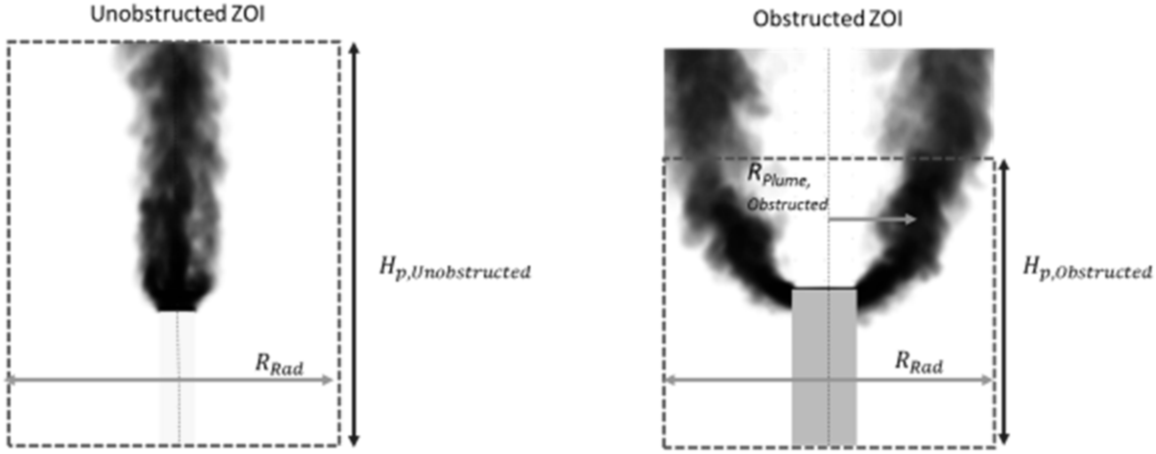

Figure 5-38
Recommended ZOI for an Electrical Enclosure Fire a) Without Top Obstruction Credit, and b) with Top Obstruction Credit

6

Correction for Zone of Influence Due to Obstructed Plume Effect

This chapter presents the methodology and the development of an adjustment for the vertical thermal zone of influence (ZOI) for enclosure fires based on the Fire Dynamics Simulator (FDS) results presented in Chapter 5.

6.1 Assessment of FDS Simulation Results

The results presented in Chapter 5 have shown that for cases in which the fire plume flow is obstructed by different geometries, plume temperatures are often reduced above the obstruction. These reduced temperatures do not appear to be limited to a specific obstruction geometry, heat release rate (HRR), or fire source diameter. The results have been shown to be sensitive to some input parameters, and limits of implementation have been provided in Section 6.4, as appropriate. As a result, the vertical ZOI may be modified using the same approach independent of specific obstruction geometry, HRR, or fire source diameter provided the analyst applies the methodology with consideration for all of the assumptions and limitations provided in Section 5.1.

The height above the fire base, z_B, with an obstruction present for which temperatures are high enough to cause damage can be determined through an algebraic modification of the Heskestad fire plume correlation shown below as:

$$z_B = \left(\frac{B \cdot 9.1 \left[\frac{T_0}{\left(g c_p^2 \rho_0^2 \right)} \right]^{1/3} \dot{Q}_c^{2/3}}{\Delta T} \right)^{3/5} + z_0 \qquad \text{(6-1)}$$

Where, *B* is the bias observed in the comparison between the plume temperature rise of flows subject to an obstruction and those predicted by the Heskestad fire plume correlation. Equation 6-1 can be used directly to determine the maximum extent of the thermal plume ZOI for fire PRA applications.

6.2 Prediction of ZOI Correction

6.2.1 *Temperature Rise (Example 1)*

Using the values presented in Figure F-3 of NUREG/CR-6850 (Appendix F, page F-6), predict the exposure temperature for a fire using the existing information for unobstructed plumes, and the updated information for obstructed plumes.

The required inputs from Figure F-3 of NUREG 6850/CR-6850 (Appendix F, page F-6) are HRR of 211 kW, fire diameter of 0.6 m, radiative fraction of 0.4, and an assumed ambient temperature of 20 °C (68 °F). Equation 5-3 (shown again below) was used to predict the plume centerline temperature for the unobstructed plume.

$$\Delta T = 9.1 \left[\frac{T_0}{(g c_p^2 \rho_0^2)} \right]^{1/3} \dot{Q}_c^{\,2/3} (z - z_0)^{-5/3} \qquad (6\text{-}2)$$

Equation 5-6 (shown again below), with a bias, *B* = 0.62, was used to predict the plume centerline temperature for a plume obstructed by the enclosure top.

$$\Delta T = B \left(9.1 \left[\frac{T_0}{(g c_p^2 \rho_0^2)} \right]^{1/3} \right) \dot{Q}_c^{\,2/3} (z - z_0)^{-5/3} \qquad (6\text{-}3)$$

The results were plotted with both temperature predictions versus the height above the fire base as illustrated in Figure 6-1, demonstrating a dramatic reduction in plume centerline temperature predictions for the obstructed plume relative to the unobstructed plume.

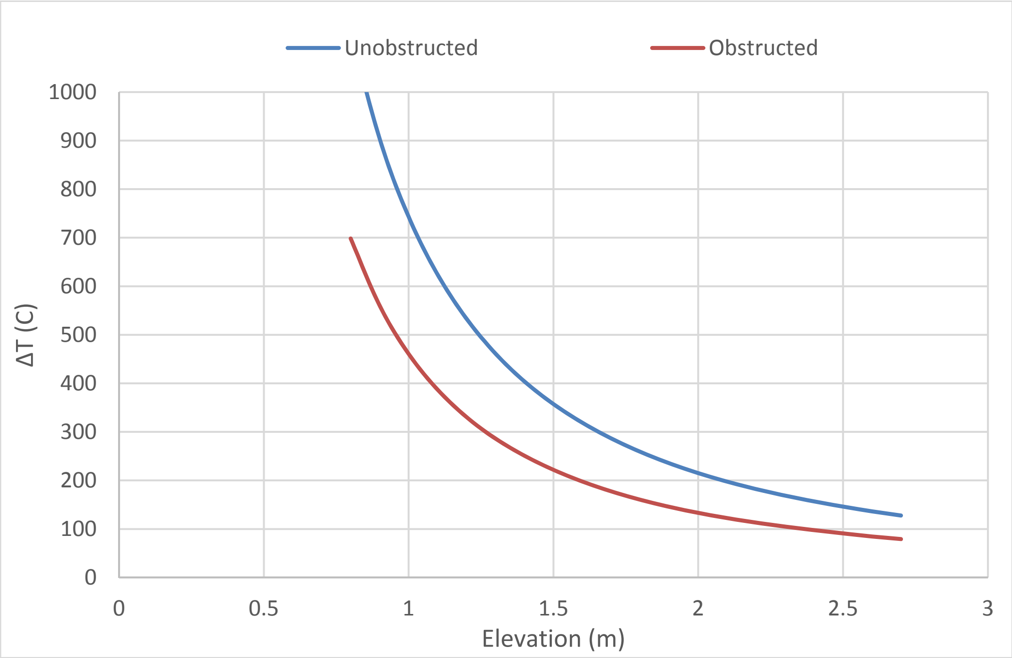

Figure 6-1
Unobstructed and Obstructed Temperature Predictions

6.2.2 *Zone of Influence (Example 2)*

Once again using the values presented in Figure F-3 of NUREG/CR-6850 (Appendix F, page F-6), predict the maximum thermal plume ZOI height for a fire using the existing information for unobstructed plumes, and the updated information for obstructed plumes.

The required inputs from Figure F-3 of NUREG/CR-6850 (Appendix F, page F-6) are HRR of 211 kW, fire diameter of 0.6 m (2 ft), radiative fraction of 0.4, and an assumed ambient temperature of 20 °C (68 °F). No information is provided for the target failure properties;

therefore, both thermoset (330 °C (626 °F)) and thermoplastic (205 °C (400 °F)) cables are evaluated.

Use Equation 6-1 with a bias, B = 1.0, for the unobstructed plume case to evaluate the vertical plume ZOI elevation. Use the same HRR, fire diameter, assumed radiative fraction, and a bias of 0.62 to evaluate the vertical plume ZOI elevation for an obstructed plume. The results of this analysis are provided in Table 6-1, demonstrating a dramatic reduction in plume centerline temperature predictions. Visual representations of the changes in the vertical ZOI for obstructed plumes are presented in Figure 6-2.

Table 6-1
Example 2 ZOI Calculations

Target Type	Configuration	Bias	Heat Release Rate (kW)	Fire Diameter (m)	Radiative Fraction	Ambient Temperature (°C)	ZOI Height (m)
Thermoplastic (205°C)	Unobstructed	1.0	211	0.6	0.4	20	2.2
	Obstructed	0.62	211	0.6	0.4	20	1.7
Thermoset (330°C)	Unobstructed	1.0	211	0.6	0.4	20	1.6
	Obstructed	0.62	211	0.6	0.4	20	1.3

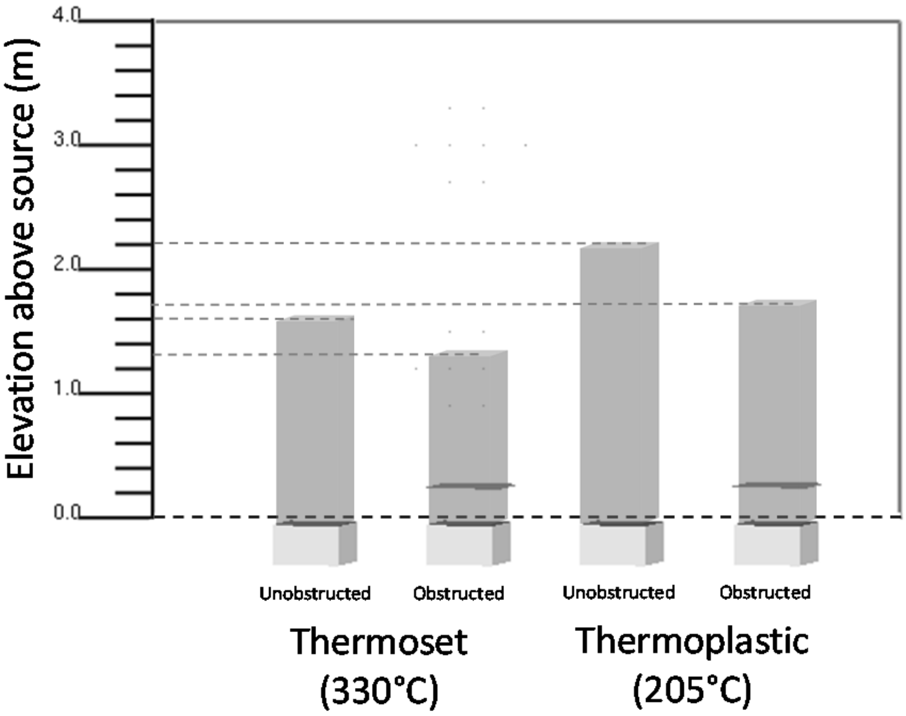

Figure 6-2
Vertical Plume ZOI

Comparing these results shows a reduction in the vertical plume ZOI elevation when crediting the obstruction for reducing the plume centerline temperature.

6.2.3 *Zone of Influence Sensitivity (Example 3)*

Evaluate the overall sensitivity of the zone of influence for an obstructed plume relative to an unobstructed plume.

Evaluate the ratio of Equation 6-1 to the Heskestad fire correlation (Equation 6-3) solved for *z*, (i.e., Equation 6-1 with *B* = 1.0). This evaluation shows the change in the ZOI elevation when a plume flow is subject to an obstruction relative to an unobstructed plume as:

$$\frac{z_B}{z} \sim B^{\frac{3}{5}} = 0.62^{\frac{3}{5}} = 0.75 \qquad (6\text{-}4)$$

The result in Equation 6-4 shows that the ZOI dimension of an obstructed plume is approximately 75% relative to the size of the initial ZOI evaluated using the Heskestad correlation.

Alternatively, it is appropriate to evaluate several specific configurations and show the difference between the two approaches graphically. The results of this analysis are obtained by solving Equation 6-1 for each of the fire configurations used in this analysis. The results of this analysis are provided in Figure 6-3, showing the difference in the vertical ZOI elevations at which fire plume temperatures are estimated to cause damage to

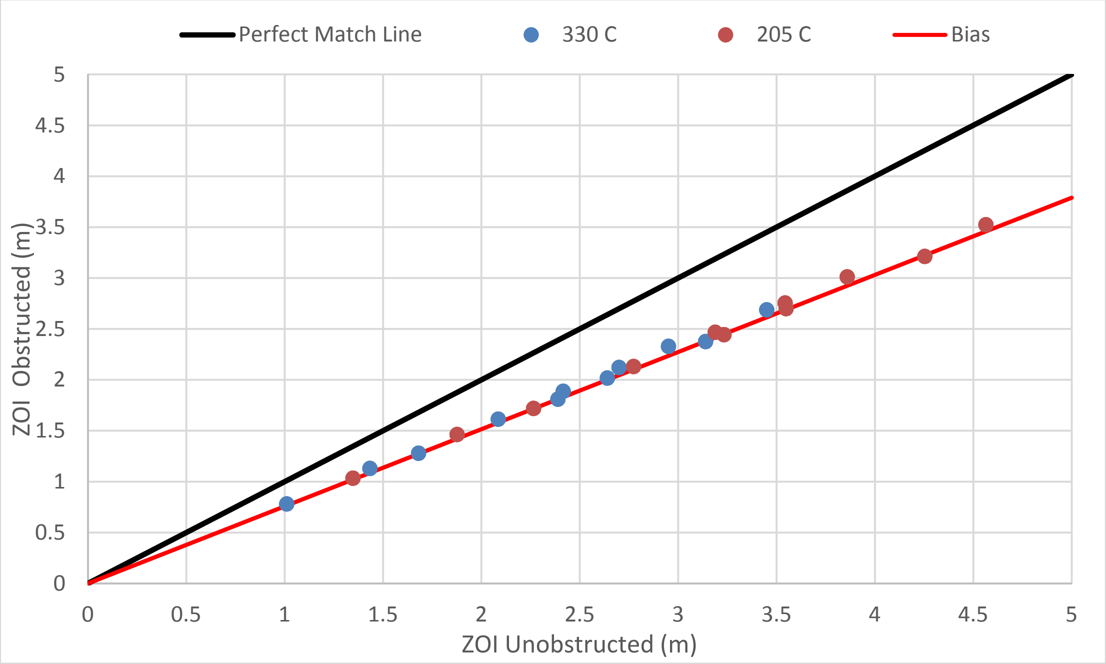

Figure 6-3
ZOI Difference for Obstructed and Unobstructed Plume Flows Using Heskestad Fire Plume Correlation

thermoset (330°C (626 °F)) and thermoplastic (205 °C (400 °F)) cables. The difference in the ZOI can be calculated as a bias following the technique outlines in the FDS manual, or in this case a linear correlation fit. The resulting bias is 0.76, showing a decrease in vertical ZOI of around 24% for fire plume flows subject to an obstruction. This closely matches the calculated change in elevation presented in Equation 6-4.

An analyst may use this information to estimate the reduction in overall risk that can be attributed to implementing the obstructed plume information provided in this report. The reduced ZOI may result in fewer risk important targets being exposed by the ignition source, and therefore reduced risk in the fire PRA.

6.2.4 *Fire Protection SDP Application (Example 4)*

During an inspection, it was noted that a section of fire wrapped cable tray was not properly maintained. This section of cable tray was noted to be within the plume ZOI of an electrical enclosure that was previously screened from the PRA analysis. The inspection finding initiated an SDP analysis of the configuration.

The electrical enclosure has a height of 2.3 m (7.5 ft) and width (diameter) of 0.9 m (3 ft), and the fire base height is specified as 2.0 m (6.6 ft) in accordance with the guidelines of NUREG/CR-6850 Supplement 1. The electrical enclosure is located in a compartment with a very high ceiling, and the development of a hot gas layer (HGL) has been screened based on detailed fire modeling of the worst configuration in the compartment. The electrical enclosure contains non-qualified, thermoplastic cables, and has been assigned an HRR of 464 kW based on NUREG/CR-6850 guidance for the 98th percentile fire size. The ambient temperature in the compartment is 20 ˚C (68 ˚F). The cable tray contains thermoplastic cables and is located at an elevation of 4.9 m (16 ft) above the floor. The separation between the fire base and the cable tray is 2.9 m (9.5 ft). The ZOI height from the table values presented in NUREG/CR-6850 Figure F-3 is 3.2 m (10.5 ft), confirming that the cable tray is within the plume ZOI for an unobstructed plume. A diagram of the configuration evaluated is provided in Figure 6-4.

However, the electrical enclosure has a solid top with no openings in the top surface. The electrical enclosure has sufficient side venting to fit the requirements to be treated as an obstructed plume configuration. The analysis is then performed using the obstructed plume credit as detailed above. Using Equation 6-1 with a bias, B=0.62, the total vertical ZOI is reduced to 2.3 m (7.5 ft) from the fire base height. Therefore, the cable tray is outside the obstructed electrical enclosure ZOI and only the enclosure itself will fail during the event analysis. A further reduction in the vertical ZOI could be credited to the analysis by using the 400 kW HRR as described in Table 4-2 of this report for large, closed enclosures with unqualified cables, but the additional analysis is unnecessary.

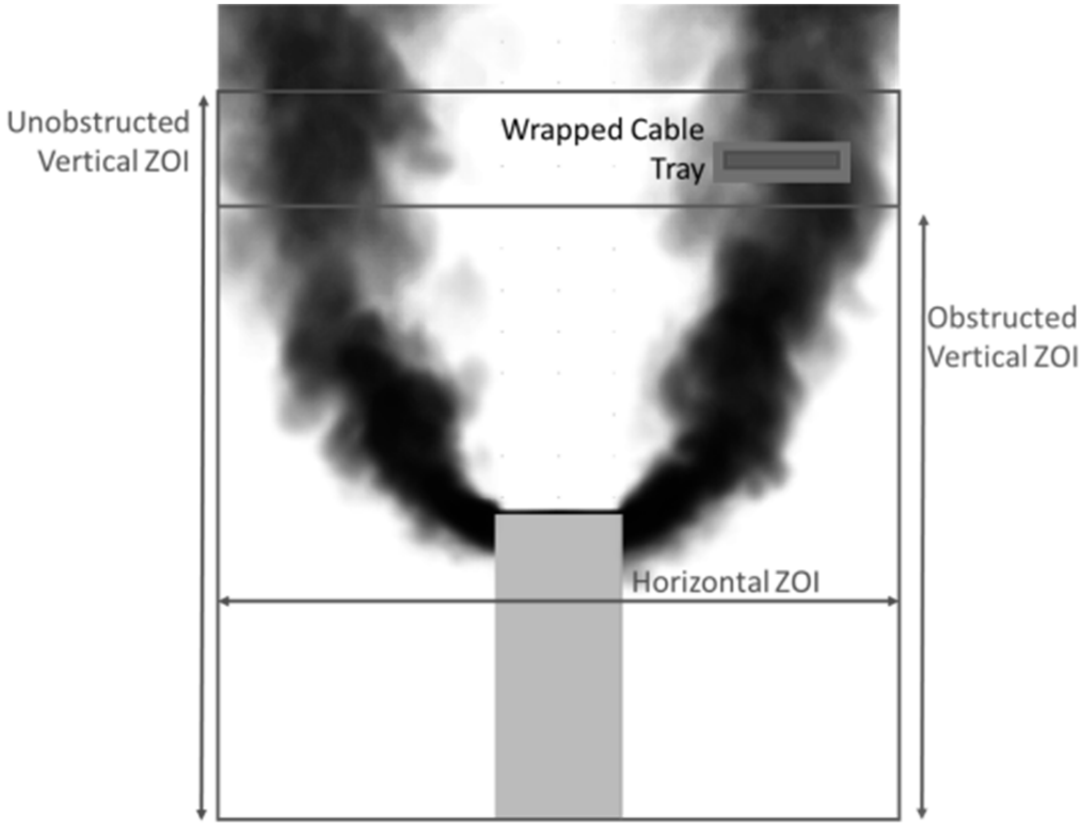

Figure 6-4
Example 4, Reduction in Vertical ZOI Due to Obstructed Plume Credit

6.2.5 *Fire PRA Application (Example 5)*

An electrical enclosure fire scenario is being considered for inclusion in the Fire PRA. The electrical enclosure is considered to contain multiple bundles of unqualified cable, with closed doors, and will be treated as a Group 4a Enclosure class fire with 400 kW peak heat release rate per Table 4-2 of this report. The enclosure has a solid top with no opening, and vents located on two of the four sides of the enclosure approximately 0.3 m (1 ft) below the top of the enclosure. The enclosure has a height of 2.3 m (7.5 ft) and assumed diameter of 0.9 m (3 ft). The enclosure is located in a compartment with a very high ceiling, and the development of an HGL has been screened based on detailed fire modeling of the worst configuration in the compartment. The ambient temperature in the compartment is 20 ˚C (68 ˚F).

Two cable trays containing unqualified thermoplastic cables are located above the electrical enclosure. One of the cable trays, cable tray 1, is located within the plume ZOI of the electrical enclosure, and is considered to ignite as a secondary combustible. The second cable tray, cable tray 2, is located outside of the ignition source ZOI; however, the combined ZOI of the electrical enclosure and the burning cable tray 1 is considered to damage tray 2. Both trays are located at an elevation of 4.7 m (15.4 ft) from the floor.

Following the guidance outlined in NUREG/CR-6850 assuming the fire is at the top of the electrical enclosure, using Equation 6-1 with a bias, B=1.0, assuming an unobstructed source, the vertical distance above the source for which a thermoplastic cable would be damaged is 2.8 m (9.2 ft). Following the guidance outlined in Supplement 1 to NUREG 6580 (EPRI

1019259) and placing the source at an elevation of 0.3 m (1 ft) below the top of the enclosure, the total vertical ZOI for this enclosure is found to be 4.8 m (15.7 ft) above the floor. This means that cable tray 1 is within the vertical plume ZOI of an unobstructed plume. As a result, cable tray 2 is damaged by the combined ZOI of the electrical enclosure and cable tray 1.

Repeating the analysis and crediting the effect of the obstruction caused by the enclosure, a different result is estimated. Returning to Equation 6-1 and using a bias, B=0.62, the total vertical ZOI becomes 4.1 m (13.5 ft) from the floor. Now, both cable trays are outside the electrical enclosure ZOI. A comparison of the change in the ZOI following the two estimates is presented graphically in Figure 6-5.

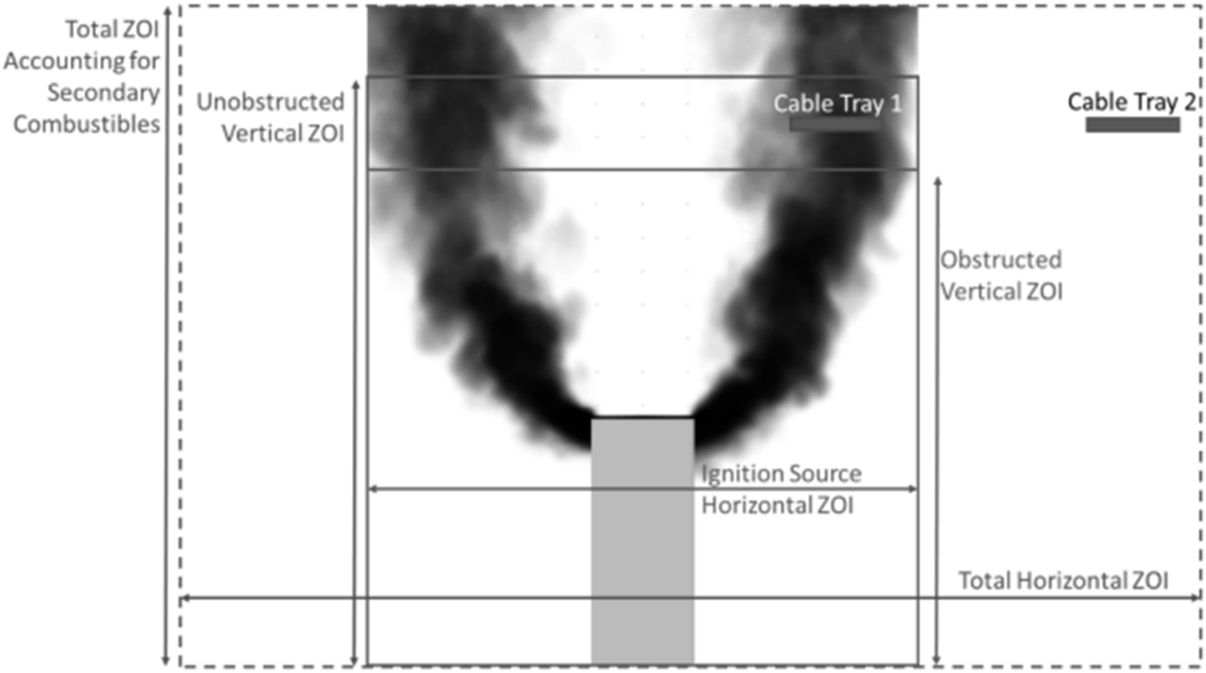

Figure 6-5
NFPA 805 Example Reduction of Vertical ZOI

In Figure 6-5, the solid red box represents the initial ZOI for the “unobstructed” electrical enclosure. The first and second damage states presented in the event tree above are reached by damage to the electrical enclosure and the cable tray 1 which fall within this ZOI. The larger box, bounded by the red dashed line, represents the increased ZOI resulting from the combined burning of the electrical enclosure and cable tray 1. Cable tray 2 is within this larger ZOI and therefore damaged (the third damage state in the event tree above).

Accounting for the obstruction of the enclosure top, the blue solid box represents the modified ZOI for the electrical enclosure. The reduction to the vertical ZOI limits the damage to the electrical enclosure itself, and all subsequent damage states are unnecessary.

6.3 Plume Temperature and ZOI Corrections

In the FDS simulations, an area of limited information for estimating the vertical damage ZOI for fire plumes subject to an obstruction such as the top surface of an electrical enclosure was explored. Data for exploration into this phenomenon was developed using FDS Version 6.0.1 to produce a series of simulations in support of this analysis. Results from these simulations were used to justify correction to the Heskestad fire plume correlation to estimate the change in the vertical damage ZOI. A number of different parameters, including the heat release rate, the fire source diameter, the fire source elevation, and the geometry of the obstruction, are varied to determine their influence on the fire plume temperature rise.

The information provided for estimating the reduced vertical damage ZOI observed is independent of, and is applicable over, varying ranges of HRR, fire source diameters, and obstruction geometries. Therefore, the provided information is appropriate for representing the hazards to cables due to fire plume temperatures for practical applications in the commercial nuclear power industry.

Results suggest that a reduction of 38% (i.e., 1-B = 1-0.62 = 0.38) is appropriate when estimating the plume temperature rise above an obstruction using the Heskestad fire plume correlation. As a result of the change in plume temperature rise, an approximate 24% reduction in the vertical damage ZOI dimension for fire plume flows above an obstruction is observed. The reduced ZOI may result in fewer risk important targets being exposed by the ignition source, and therefore reduced risk in the fire PRA.

6.4 Application of the Correction

The obstructed plume analysis was subjected to a limited peer review. Through analysis of the results and the assumptions and limitations stated in Section 5.1.5, the following limits are provided for the implementation of the obstructed plume correction:

- The obstructed plume correction does not apply to fires with a base elevation located below the half height of the enclosure. Results suggest that fires located below the half height of the enclosure may produce plume temperatures equivalent to an unobstructed plume. Therefore, in scenarios where the fire base elevation is considered below the half height of the enclosure, the plume should be treated as an unobstructed plume. This limitation may not have any impact in commercial nuclear applications, since current fire PRA information recommends fires be located near the top of electrical enclosures (see Chapter 12 of Ref. 15).

- The obstructed plume correction does not apply to electrical enclosures that have a cumulative opening on the top plate greater than 5% of its total surface area. Therefore, any enclosure with a cumulative opening greater than 5% should be treated as an unobstructed configuration. Note that an enclosure top may have penetrations, but only as long as those penetrations are properly sealed such that they do not contribute to the cumulative opening area. Properly sealed openings include cables inside steel conduit that is fitted tightly at the top plate interface, and other penetrations sealed with approved non-combustible wrap materials.

- The obstructed plume correction does not apply to configurations that include burning of secondary combustible materials. The obstructed plume correlation, however, may be used to establish the likelihood that secondary combustibles may be ignited through the definition of the primary ignition source ZOI. The obstructed plume correction is limited to the ignition source only. That is, in the case of secondary combustible ignition (i.e., cable trays), the subsequent analysis should follow existing information and modeling techniques.

- The obstructed plume correction does not apply to analysis that determines the hot gas layer (HGL) damage. The plume correction may only be used for the duration of time in which thermal plume exposure is postulated but hot gas layer temperature has not reached the damage criteria. Existing information and modeling techniques should be used to evaluate the likelihood and timing of hot gas layer damage. Modeling techniques exist that can combine the effects of a thermal plume immersed in a hot gas layer, although these techniques may only be applied to exposures within the thermal plume prior to the hot gas layer damage state.

- The obstructed plume correction does not apply to analyses that determine the visibility reduction due to smoke accumulation. Smoke accumulation has not been evaluated directly in this report, and the findings of this report do not invalidate existing guidelines for the evaluation of visibility.

- The obstructed plume correction may be applied to the evaluation of the ceiling jet damage ZOI; however, careful consideration must be observed that the correction technique considers the remaining assumptions and limitations specified in Section 5.1.5. Application to the ceiling jet ZOI is justified by the direct association of the ceiling jet temperature with the thermal plume temperature.

- The obstructed plume correction does not apply to the evaluation of the horizontal thermal flame radiation ZOI. Existing information and modeling techniques should be used to evaluate the extent of the horizontal ZOI. The overall extent of the ZOI should be evaluated following the guidance in Section 5.3.8.

- The bias due to obstructed plume is not applicable to reducing the flame temperature; however, the current information should be applied to direct flame exposures.

- The bias recommended in this report shall not be applied to FDS predictions of plume temperatures. The bias correction does not apply to FDS results and is only intended for use with the Heskestad correlation. A qualified user of FDS should develop an appropriate set of inputs to address the effects of enclosure obstructions directly, and not by adjusting the output data with a bias correction.

7

Summary, Conclusions, and Future Research

This chapter summarizes the results and conclusions described in this report with the objective of consolidating the new information for the practical application of this research. This chapter starts by listing the main objectives of this study so that they serve as the framework for the summary and conclusions. The specific objectives of this report are:

1. The classification of electrical enclosures in terms of function, size, content, and ventilation conditions,
2. The determination of peak heat release rate probability distributions considering specific electrical enclosure characteristics such as function, size, ventilation conditions, and combustible content, and
3. The characterization of fire plumes associated with fires in electrical enclosures.

The objectives listed above have been addressed through research focused in a number of technical areas. In order to address the classification of electrical enclosures and their corresponding flammability characterization, the results of a number of experimental test programs were evaluated. In addition, an extensive review of the fire events data that had been collected by EPRI was conducted in an effort to reflect the fire experience at NPPs in the provided enclosure classifications and the peak heat release rate probability distributions.

The practical implication of the provided electrical enclosure classification and peak heat release rate probability distributions is the ability to calculate severity factors that better reflect characteristics of the electrical enclosures. It should be noted that the severity factors are calculated using the methodology currently described in Chapter 8 and Appendices E and F of NUREG/CR-6850.

In order to address the characterization of plumes generated by fires in electrical enclosures, a number of fire simulations were conducted using the Fire Dynamics Simulator (FDS) program. Fire plumes generated by fires inside an electrical enclosure may be obstructed by the enclosure walls, disrupting the fire induced flows, and at the same time producing different temperature profiles within the fire plume. The temperature profiles of these obstructed fire plumes were analyzed to develop information for determining a vertical component of the zone of influence reflecting fires inside electrical enclosures. The recommendations for determining a vertical component of the zone of influence considering fires inside the electrical enclosure relax the assumption in existing fire PRA information that fires are postulated outside the enclosures.

The research described above is bounded by specific assumptions and limitations that must be accounted for when applying the methodology in practical applications. To clarify these assumptions and limitations, detailed example applications have been developed and included in this report. The examples are intended to illustrate the implementation of the provided approach within the context of a fire PRA or fire modeling analysis.

A summary of the results of this research is described in the following sections.

7.1 Classification of Electrical Enclosures

A new classification of electrical enclosures has been developed. This new classification is based on cabinet function, volumetric size, combustible content, and ventilation configuration. The new classification options are intended to more accurately represent the electrical enclosure population and simplify the process of determining which peak heat release rate probability distribution is assigned to the electrical enclosure.

Based on electrical function, the electrical enclosures are grouped as follows:

- Switchgear and load centers
- Motor control centers and battery chargers
- Power inverters

The classification above is mostly for enclosures associated with power distribution. Other electrical enclosures identified as ignition sources are classified based primarily on volumetric size as follows:

- Large enclosures, characterized by having a volume larger than 1.4 m^3 (50 ft^3),
- Medium enclosures, characterized by having volumes between 0.34 m^3 (12 ft^3) and 1.4 m^3 (50 ft^3), and
- Small enclosures, characterized by having volumes smaller than 0.34 m^3 (12 ft^3).

Examples of these electrical enclosures include relay panels, termination cabinets, the main control board, etc. The initial classification of these enclosures by volumetric size provides an easy grouping process consisting of visual examination external to the enclosure during walkdowns. Large and medium volumetric classifications can be refined to account for the amount of combustible fuel loads, type of cable insulation material, and their ventilation configuration. These refinements can result in lower heat release rate values based on visual inspection of the cabinet internals.

7.2 Peak Heat Release Rate Probability Distributions

The classification described in the previous section provides the framework for assigning probability distributions for the peak heat release rate associated with the electrical enclosures. Selected probability distributions for peak heat release rates were originally described in NUREG/CR-6850 and applied to a given enclosure based on three factors: qualified versus unqualified cable, open versus closed enclosures, and single versus multiple cable bundles that could be ignited. This report described the new probability distributions with direct correspondence to the classification described earlier. It should be noted that the probability distributions described in Appendices E and G of NUREG/CR-6850 may not need to be replaced with the ones described in this report, as they are bounding.

The revised peak HRR probability distributions (i.e., gamma distributions) for each of the new enclosure classification groups were developed based on the following factors:

- Review of experimental factors and configurations in testing programs intended to assess the heat release rate generated by electrical enclosure fires. Both domestic and international test programs were included within the scope of this research.
- Statistical analysis of the applicable experimental results.

- Extensive review and comparison of existing electrical enclosures configuration and operating experience in commercial nuclear plants and the influencing experimental factors.

The distributions are defined based on the 75th and 98th percentile values, with the 98th percentile value intended for use as the maximum HRR to be assumed for any enclosure in a given type/function classification group. The 98th percentile value is also the value provided for use during ignition source screening as currently described in Chapter 8 and Appendix G of NUREG/CR-6850.

Table 7-1 presents the electrical enclosure classifications and the provided peak HRR probability distributions.

Table 7-1
Peak Heat Release Rate Distributions for Electrical Enclosures

Enclosure Class/Function Group	Enclosure Ventilation (Open/Closed Doors)	Fuel Type* (TS/TP Cables)	Gamma Distribution Characteristics											
			(a) Default				(b) Low Fuel Loading				(c) Very Low Fuel Loading			
			Alpha	Beta	75th Percentile (kW)	98th Percentile (kW)	Alpha	Beta	75th Percentile (kW)	98th Percentile (kW)	Alpha	Beta	75th Percentile (kW)	98th Percentile (kW)
1 - Switchgear and Load Centers	Closed	TS	0.32	79	30	170	NOT APPLICABLE							
	Closed	TP	0.99	44	60	170								
2 - MCCs and Battery Chargers	Closed	TS	0.36	57	25	130								
	Closed	TP	1.21	30	50	130								
3 - Power Inverters	Closed	TS	0.23	111	25	200								
	Closed	TP	0.52	73	50	200								
4a - Large Enclosures [>1.42 m^3 (>50 ft^3)]	Closed	TS	0.23	223	50	400	0.23	111	25	200	0.38	32	15	75
	Closed	TP	0.52	145	100	400	0.52	73	50	200	0.88	21	25	75
	Open	TS	0.26	365	100	700	0.26	182	50	350	0.38	32	15	75
	Open	TP	0.38	428	200	1000	0.38	214	100	500	0.88	21	25	75
4b - Medium Enclosures [≤1.42 m^3 (50 ft^3)] and > 0.34 m^3 (12 ft^3)	Closed	TS	0.23	111	25	200	0.27	51	15	100	0.88	12	15	45
	Closed	TP	0.52	73	50	200	0.52	36	25	100	0.88	12	15	45
	Open	TS	0.23	182	40	325	0.19	92	15	150	0.88	12	15	45
	Open	TP	0.51	119	80	325	0.30	72	25	150	0.88	12	15	45
4c - Small Enclosures [≤ 0.34 m^3 (12 ft^3)]	Not Applicable	TS or TP	0.88	12	15	45	NOT APPLICABLE							

* Per Sections 1.3 and 2.2.2, qualified TP cables (cables that have been tested and passed the IEEE-383 vertical flame spread test) and SIS wire may be mapped to the TS fuel type groups.

7.3 Obstructed Plume Analysis

The investigation of fire plume temperature subject to obstructed flows was conducted using the Fire Dynamics Simulator (FDS) fire modeling program. The fire scenario configurations investigated are intended to mimic those created by fires burning inside electrical enclosures and are limited to thermal plume conditions in the early stages of the fire (i.e., before significant room temperature increases).

This study developed a characterization of fire plume temperatures subject to an obstruction so that specific information can be provided on determining the vertical component of the zone of influence. Results suggest that a reduction of 38% is appropriate when estimating the plume temperature rise above an obstruction and using the Heskestad fire plume correlation. As a result of the change in plume temperature rise, an approximate 24% reduction in the vertical damage ZOI dimension for fire plume flows above an obstruction is observed. Analysts are referred to Section 6.4 for specific information and restrictions on the application of these factors.

7.4 Example Applications

Examples consolidating the information described in this report were developed and included in Appendix F. These examples have been selected and designed to illustrate how to incorporate the provided methodology for modeling in electrical enclosures. The examples specifically address how to account for the assumptions and limitations associated with the research and information documented in this report.

7.5 Future Research

During the working group meetings, a number of topics were discussed with potential to impact the realism in modeling electrical enclosure fires and fire probabilistic risk assessments. A new classification system for electrical enclosures, revised peak heat release rate probability distributions, and an obstructed plume analysis methodology were three topics that were discussed and are presented in this report. A number of areas have been left for future research. The panel intends to reconvene and discuss if there are any remaining topics that should be pursued in the future. In addition, the U.S. Nuclear Regulatory Commission is initiating a series of fire tests to further explore the fire hazards associated with electrical cabinets.

8
References

1. NFPA 805, “Performance-Based Standard for Fire Protection for Light-Water Reactor Electric Generating Plants,” 2001 Edition, National Fire Protection Association, Quincy, MA.
2. 10 CFR 50.48 (Title 10 of the Code of Federal Regulations, Part 50, Section 50.48), “Fire Protection.”
3. Appendix R to 10 CFR 50, “Fire Protection Program for Nuclear Power Facilities Operating Prior to January 1, 1979.”
4. NUREG/CR-6850 and EPRI 1011989, “EPRI/NRC-RES Fire PRA Methodology for Nuclear Power Facilities,” Volume 1: Summary and Overview and Volume 2: Detailed Methodology. Electric Power Research Institute, Palo Alto, CA and U.S. Nuclear Regulatory Commission, Office of Nuclear Regulatory Research (RES) Rockville, MD, September 2005.
5. EPRI 1022993, “Evaluation of Peak Heat Release Rates in Electrical Cabinet Fires – Reanalysis of Table G-1 of NUREG/CR-6850 and Table G-1 of EPRI 1011989,” Electric Power Research Institute, Palo Alto, CA, February 2012.
6. NRC comments on the Recent Fire PRA Methods Review Panel Decisions and EPRI 1022993, “Evaluation of Peak Heat Release Rates in Electrical Cabinet Fires.” ML12172A406, June 20, 2012.
7. NUREG/CR-7197, “Heat Release Rates of Electrical Enclosure Fires (HELEN-FIRE),” K. McGrattan, S. Bareham, National Institute of Standards and Technology, draft, October 2014.
8. NUREG/CR-4527, “An Experimental Investigation of Internally Ignited Fires in Nuclear Power Plant Control Cabinets,” J. Chavez, SAND86-0336, Volumes 1 and 2, April 1987.
9. VTT Publications 186, “Full Scale Fire Experiments On Electronic Cabinets,” J. Mangs and O. Keski-Rahkonen, VTT Technical Research Centre of Finland, 1994.
10. VTT Publications 269, “Full Scale Fire Experiments On Electronic Cabinets II,” J. Mangs and O. Keski-Rahkonen, VTT Technical Research Centre of Finland, 1996.
11. VTT Publications 521, “On the Fire Dynamics of Vehicles and Electrical Equipment,” J. Mangs and O. Keski-Rahkonen, VTT Technical Research Centre of Finland, 2004.
12. Plumecocq, W., M. Coutin, S. Melis, L. Rigollet, Characterization of Closed-Doors Electrical Cabinet Fires in Compartments, Fire Safety Journal 46, 2011.
13. NUREG-2169 and EPRI 3002002936, “Nuclear Power Plant Fire Ignition Frequency and Non-Suppression Probability Estimation Using the Updated Fire Events Database,” Electric Power Research Institute, Palo Alto, CA and U.S. Nuclear Regulatory Commission, Office of Nuclear Regulatory Research (RES) Rockville, MD, December 2014.
14. FAQ 13-0006, “Modeling Junction Box Scenarios in a Fire PRA,” Rev. 0, F. Joglar, May 2013.
15. NUREG/CR-6850, Supplement 1, “Fire Probabilistic Risk Assessment Methods Enhancements,” EPRI 1019259, Electric Power Research Institute, Palo Alto, CA and U.S. Nuclear Regulatory Commission, Office of Nuclear Regulatory Research (RES) Rockville, MD, September 2010.

16. FAQ 14-0009, “Treatment of Well-Sealed Electrical Panels Greater than 440V,” Rev. D, NextEra Energy, July 1, 2014.

17. National Institute of Standards and Technology (NIST), Fire Dynamics Simulator (FDS) User’s Guide, Version 6.0.1, NIST Special Publication 1019, Sixth Edition, November 2013.

18. NUREG-1934 and EPRI 1023259, “Nuclear Power Plant Fire Modeling Analysis Guidelines (NPP FIRE MAG) – Final Report,” Electric Power Research Institute, Palo Alto, CA and U.S. Nuclear Regulatory Commission, Office of Nuclear Regulatory Research (RES) Rockville, MD, November 2012.

19. Technical Basis for Fire Protection Significance Determination Process (IMC 0609, Appendix F) At Power Operations, February 2005.

20. NUREG-1824, Verification and Validation of Selected Fire Models for Nuclear Power Plant Applications, Volume 1: Main Report, EPRI 1011999, Electric Power Research Institute, Palo Alto, CA and U.S. Nuclear Regulatory Commission, Office of Nuclear Regulatory Research (RES) Rockville, MD, May 2007.

21. NUREG-1824, Verification and Validation of Selected Fire Models for Nuclear Power Plant Applications, Volume 7: Fire Dynamics Simulator (FDS), EPRI 1011999, Electric Power Research Institute, Palo Alto, CA and U.S. Nuclear Regulatory Commission, Office of Nuclear Regulatory Research (RES) Rockville, MD, May 2007.

22. Heskestad, Gunnar. “Engineering Relations for Fire Plumes.” Fire Safety Journal 7.1, pp 25-32, 1984.

23. NUREG-1805, “Fire Dynamics Tools (FDTs) – Quantitative Fire Hazard Analysis Methods for the U.S. Nuclear Regulatory Commission Fire Protection Inspection Program,” Supplement 1, Volumes 1 & 2, June 2013.

24. FAQ 13-0004, “Clarifications on Treatment of Sensitive Electronics,” NextEra Energy, Rev. 1, June 26, 2013.

25. NFPA 13, National Fire Protection Association Standard for the Installation of Sprinkler Systems. National Fire Protection Association, 2010.

26. Davis, W. D., G. P. Forney, and R. W. Bukowski, "Developing Detector Siting Rules from Computational Experiments in Spaces With Complex Geometries." Fire Safety Journal 29.2, pp 129-139, 1997.

27. U.S. NRC Generic Letter No. 86-10, “Implementation of Fire Protection Requirements,” April 1986.

28. Beyler, C. L. “Fire Plumes and Ceiling Jets.” Fire Safety Journal 11.1, pp 53-75, 1986.

29. Zukoski, E. E., T. Kubota, and B. Cetegen. “Entrainment in Fire Plumes,” Fire Safety Journal 3.3, pp 107-121, 1981.

30. McGrattan, K.B., et al., “Fire Dynamics Simulator User’s Guide,” National Institute of Standards and Technology and VTT Technical Research Centre of Finland, Sixth Edition, November 2013.

31. McGrattan, K. B., et al., “Fire Dynamics Simulator, Technical Reference Guide, Volume 1: Mathematical Model,” National Institute of Standards and Technology and VTT Technical Research Centre of Finland, Sixth Edition, April 2013.

32. McGrattan, K. B., et al., “Fire Dynamics Simulator, Technical Reference Guide, Volume 2: Verification Guide,” National Institute of Standards and Technology and VTT Technical Research Centre of Finland, Sixth Edition, November 2013.

33. McGrattan, K. B., et al., “Fire Dynamics Simulator, Technical Reference Guide, Volume 3: Validation,” National Institute of Standards and Technology and VTT Technical Research Centre of Finland, Sixth Edition, November 2013.

34. Heskestad, G., “Fire Plumes, Flame Height, and Air Entrainment,” Section 2–1, SFPE Handbook of Fire Protection Engineering, 4th Edition, 2008.

35. Janssens, M., “Calorimetry,” Section 3-2, “The SFPE Handbook of Fire Protection Engineering,” 4th Edition, 2008.

36. EPRI 3002000830, “Fire-Induced Vulnerability Evaluation (FIVE) User’s Guide Revision 2,” Electric Power Research Institute, Palo Alto, CA, 2014.

Appendix A

WG Members, Non-WG Contributors, and Facilitator Resumes

This appendix presents the resumes of the working group (WG) members and the facilitator. Also, it includes the resumes of two non-WG experts who performed the obstructed plume simulations using the FDS fire modeling program.

Joelle DeJoseph, Duke Energy

EDUCATION

University of Maryland, College Park, MD; May 2004
Masters of Science; Major: Fire Protection Engineering
Stevens Institute of Technology, Hoboken, NJ; May 1999
Bachelor of Engineering; Major/Concentration: Mechanical Engineering/Manufacturing
New York University, New York, NY; May 1999
Bachelor of Science; Major/Minor: Mathematics/Computer Applications
Registrations: Professional Engineer (P.E.) – North Carolina #033827
Fundamentals of Engineering (E.I.T.) – Massachusetts #21069

EXPERIENCE

Duke Energy, Nuclear Generation Group, Raleigh, NC April 2010-present
Fire Protection Engineer, Senior Engineer

- Fire Protection engineering supporting fire Probabilistic Rick Assessment (PRA) development for Duke Energy sites, including walkdowns and fire modeling
- Lead the transition to the NFPA 805 performance based approach for fire protection at two nuclear power plants
- Fire modeling lead for fleet fire protection at Duke Energy
- Fire PRA Peer review
- NFPA 805 License Amendment Request (LAR) audit team lead
- NFPA 805 LAR Request for Additional Information (RAI) response experience
- Subject matter expert for NFPA 805 monitoring, Very Early Warning Fire Detection Systems (VEWFDS), and surveillance optimization
- Fire Protection Program Manager experience at a nuclear power plant
- Fire Protection System Engineer experience at a nuclear power plant

Kidde Aerospace and Defense, Wilson, NC September 2006-March 2010
Fire Protection Development Engineer, Ground Vehicles

- Develop fire suppression (explosion protection) extinguisher for use in military ground vehicles
- Evaluate fire extinguishing agent effects on crew, including acid gas (specifically HF) concentration, discharge force, and decibel level
- Responsible for overseeing production manufacturing, including procurement, process, welding and pressure testing, first article inspection and conformance

Hughes Associates, Inc., Warwick, RI July 2004-September 2006
Fire Protection Engineer

- Provide design, design review, and specification development of fire protection systems. Work experience includes specification of system performance criteria, composition of design drawings, review of shop drawings, inspection of compliance with applicable codes and standards, and acceptance testing of installed systems.
- Developed and evaluated performance-based design alternatives
- Provided design analysis of new and existing life safety systems
- Audited and tested existing fire protection systems

- Review of building code, fire prevention, and reference documents as they pertain to client issues

University of Maryland, College Park, MD July 2003-June 2004

Graduate Research Assistant, Yucca Mountain Project

- Development and implementation of a tunnel tenability assessment methodology
- Estimated intensity and duration of the fire source term for the postulated fire
- Calculated fire-induced conditions, including visibility, temperature, and gas concentrations, resulting from the specified fire source as a function of time and location
- Established risk and assess impact on project
- Review outside work, including methodologies and calculations

Bureau of Alcohol, Tobacco, and Firearms, Beltsville, MD July 2003-December 2003

Fire Research Laboratory, Student Intern

- Set-up and testing of research equipment
- Arrange and run test experiments for fire investigator classes
- Collect and document data for test fires

Affiliated Engineers Metro DC, Rockville, MD September 2002-July 2003
Affiliated Engineers NW, Seattle, WA April 2001-August 2002

Plumbing, Piping, and Fire Protection Design Engineer

- Design of plumbing and piping systems for major buildings: universities, hospitals, research centers, etc.
- Comprehensive analytical assessment of water, compressed air, vacuum, specialty gas systems for commercial uses
- Liaison between client, architect, and contractor concerning city building code and regulations

Jaros Baum & Bolles, New York, NY July 1999-September 2000

Plumbing and Fire Protection Design Engineer

- Design of entire plumbing and fire protection systems for major commercial buildings: office buildings, hotels, financial institutions, etc.
- Comprehensive analytical assessment of water systems for domestic and fire protection requirements; incl. detailed hydraulic and load calculations
- Liaison between client, architect, and contractor concerning city building code and regulations

PRESENTATIONS

- NRC Commission Briefing on NFPA 805, Fire Protection, June 19, 2014
- NEI Fire Protection Forum 2013: Safety and Operational Improvements at Harris Nuclear Plant
- NEI Fire Protection Forum 2013: Very Early Warning Fire Detection System (VEWFDS) Studies

Francisco Joglar, Jensen Hughes

EDUCATION

Ph.D., Reliability Engineering, University of Maryland, 2000

M.S., Fire Protection Engineering, University of Maryland, 1998

B.S., Industrial Engineering, University of Puerto Rico, 1997

Registered PE

VA, No. 038817 (2004)

Dr. Francisco Joglar, PE, is a Senior Consultant with 14 years' experience. Dr. Joglar has a strong background in fire modeling, statistics and uncertainty analysis. Since 2001, he has been researching and consulting in fire protection engineering and probabilistic risk assessment for the commercial nuclear industry. In the research area, he has been developing fire protection and fire risk technology for the Electric Power Research Institute (EPRI) and supporting joint research projects between EPRI and the US NRC Office of Research. In the consulting area, he has participated in numerous fire modeling and fire risk projects in various capacities including fire risk analyst, technical lead, project manager, and technical oversight. For the last six years, Dr. Joglar has been teaching a master degree level course in fire risk analysis at the University of Maryland, Department of Fire Protection Engineering. He also teaches a master degree level Fire Protection Engineering course every year at Cal Poly.

PROFESSIONAL HIGHLIGHTS

Senior Consultant, Hughes Associates, Baltimore, MD, 2012–present. Responsibilities include supervisory and managerial duties, project management, and consulting services to the commercial nuclear industry in the areas of safe shutdown analysis, fire modeling, probabilistic risk assessment, NFPA 805, and fire research.

Fire Protection Engineer, Science Applications International Corporation (SAIC), 2001–2012. Responsibilities included project management and consulting services to the commercial nuclear industry in the areas of safe shutdown analysis, fire modeling, probabilistic risk assessment, NFPA 805, and fire research. Technical lead for the following Fire PRA studies in the United States: San Onofre Nuclear Generating Station, Kewaunee Power Station, VC Summer Power Station, and Nine Mile Point-1. Internationally, has offered consulting services in Brazil for the ANGRA Unit 1 Fire PRA. Project manager for the Nine Mile Point-1 and Prairie Island Fire PRAs. In addition, served as technical lead and project manager for numerous projects associated with fire modeling and fire risk analysis. Participated as a peer reviewer for four Fire PRAs. Member of the writing committees for the following commercial nuclear industry milestone projects:

- NUREG/CR-6850/EPRI 1011989, "EPRI/NRC–RES Fire PRA Methodology for Nuclear Power Facilities Volume 2 Detailed Methodology," 2005.
- NUREG-1934/EPRI-1019195, "Nuclear Power Plant Fire Modeling Application Guide," 2012.
- NUREG-1824/ EPRI 1011999, "Verification and Validation of Selected Fire Models for Nuclear Power Plant Applications, Volume 1". 2007.

Member of the ASME/ANS Fire PRA Standard writing committee, ASME/ANS RA-Sa-2009 Standard for Probabilistic Risk Assessment for Nuclear Power Plant Applications.

Author of the Reliability Engineering chapter of the Society of Fire Protection Engineers (SFPE) Handbook, the most widely used technical reference in the US fire protection community. Actively participates in the development of selected Fire PRA FAQ responses which are technical supplements to documented fire risk methods. Provides Fire Modeling and Fire PRA training through EPRI to Fire Protection and Fire PRA professionals in the nuclear industry.

SELECTED PUBLICATIONS AND PRESENTATIONS:

NUREG/CR-6850/EPRI 1011989, “EPRI/NRC–RES Fire PRA Methodology for Nuclear Power Facilities Volume 2 Detailed Methodology,” 2005.

NUREG-1934/EPRI-1019195, “Nuclear Power Plant Fire Modeling Application Guide,” 2012.

NUREG-1824/ EPRI 1011999, “Verification and Validation of Selected Fire Models for Nuclear Power Plant Applications, Volume 1,” 2007.

Joglar, F., “Reliability, Maintainability & Availability,” Section/Chapter 5-3, SFPE Handbook of Fire Protection Engineering, 4th Edition, DiNenno et al. (eds.), National Fire Protection Association, Quincy, MA, 2008, pp. 5-25–5-68.

EPRI TR-1002981, “Fire Modeling Guide for Nuclear Power Plant Applications,” 2002.

Presented conference papers in Probabilistic Safety Analysis (PSA) 2009, 2011, 2013, and Probabilistic Safety Analysis and Management (PSAM) 2010.

Ashley Mossa Lindeman, EPRI

EDUCATION

Worcester Polytechnic Institute May 2007
Graduated with a Bachelor of Science in Mechanical Engineering with a concentration in thermal-fluids

Rensselaer Polytechnic Institute June 2010
Graduated with a Master of Engineering in Mechanical Engineering

WORK EXPERIENCE

Electric Power Research Institute May 2013-Present
Technical Leader / Project Manager, Risk & Safety Management (May 2013-Pres)

- Fire PRA research management: Manage projects to further advance the research within the area of fire probabilistic risk analysis for commercial nuclear power plants. Oversee projects in the area of fire events analysis, fire-induced circuit failure, fire modeling, fire damage consequences and fire model uncertainty.
- Technical contributor to FPRA research: Participated in the classification of fire events for use in the calculation of fire ignition frequencies and non-suppression probability estimation.
- Fire PRA Training Instructor: Instructed selected portions of the fire analysis module in the joint EPRI/NRC Fire PRA Training.
- Member of the ASME/ANS Fire PRA standard writing committee

Westinghouse Electric Company June 2007-May 2013
Senior Engineer, Risk Applications and Methods II (July 2010-May 2013)

- Fire PRA model development using NUREG/CR-6850: Key individual in the fire PRA development including author or co-author on the following tasks: plant partitioning, fire ignition frequencies, zone of influence, fire scenario selection/scoping fire modeling, qualitative screening, quantitative screening and quantification. Provided peer review support for the utility during the industry peer review.
- NFPA 805 Transition and Fire PRA for Fort Calhoun Station: Authored or co-authored the following tasks in support of the Fire PRA project: plant partitioning, fire ignition frequencies, main control room habitability analysis, fire scenario selection, HRA and quantification. Provided peer review support for the utility during the industry peer review. Performed fire risk evaluations, supported the on-site NRC audit of the NFPA 805 transition, and responded to requests for additional information related to probabilistic risk assessment and fire modeling.
- Technical lead for international fire PRA: Provided support from bid and proposal phase through project initiation on differences between US methodology and EdF specific methodology. Supported Fire PRA technical questions from a multi-national team located in four different time zones.
- Industry Fire PRA Peer Review Experience: Participated in three domestic Pressurized Water Reactor Owner’s Group (PWROG) fire PRA peer reviews and one international fire PRA peer review.

- Project Manager Level 1: Satisfied classroom training and on the job training requirements of the Westinghouse Project Manager Development Program
- Technical Leader Level 1: Satisfied requirements of the Technical Leader Development Program.

Engineer, Risk Applications and Methods II (June 2007-July 2010)

- Performer for international PWR safe shutdown analysis: Primary tasks involved developing component list, tracing safe shutdown flowpaths, and supported execution of safe shutdown analysis using the Risk Spectrum software. Participated in walkdowns in support of both the fire and flood portions of the project.
- Piloted draft EPRI/NRC Fire HRA Guidelines (NUREG-1921) for the PWROG: Participated in operator interviews and supported development of WCAP technical report.
- Domestic fire PRA support: Performed on-site plant walkdowns, plant partitioning and fire ignition frequencies tasks.

PUBLICATIONS

- NUREG-2169 and EPRI 3002002936, Fire Ignition Frequencies and Non-Suppression Probability Estimation Using the Updated Fire Events Database, November 2014.
- OECD International Workshop on Fire PRA– Insights and Opportunities from the EPRI Updated Fire Events Database, April 2014.

Nicholas Melly, NRC

EDUCATION

The University of Maryland – College Park, MD
Bachelor of Science in Fire Protection Engineering, 2008

EXPERIENCE

U.S. Nuclear Regulatory Commission – Rockville, MD 7/2009-Present
Fire Protection Engineer Office of Nuclear Regulatory Research

- Competed detailed circuit analysis and data processing of results for research projects which resulted in the publication of Electrical Cable Test Results and Analysis During Fire Exposure (ELECTRA-FIRE NUREG 2128)
- Managed DOE work related to the revision of NUREG/CR-6850, Integration of NFPA 805 Frequently Asked Questions, Development of generic fire PRA methods, analyses related to fire PRA methods and Level 3 PRA Evaluation
- Instructed NUREG/CR-6850 Training related to Sections 2, 4, 5, 7, 14, and 15.
- Represented the NRC at International OECD Fire-Events Database and High-Energy Arching Fault Task Group Meetings
- Presented International research plans to NRC management
- Presented papers documenting NRC fire research findings at numerous technical conferences

Jacobs Engineering Group - Conshohocken, PA1/2009-6/2009
Fire Protection Engineer

- Designed a sprinkler system to be installed on a U.S. military facility chapel in Japan
- Designed a sprinkler system for a Pharmaceutical facility
- Designed wet pipe and dry pipe systems accounting for environmental conditions and freezer room applications
- Conducted probabilistic risk assessment and heat transfer analysis
- Evaluated protection of steel structural member s under high temperature exposure conditions
- Evaluated airflow simulations over essential pharmaceutical machinery to meet safety requirements

Triad Fire Protection - Springfield, PA 6/2008-12/2008
Fire Protection Engineer

- Designed smoke detection systems and fire alarm systems
- Conducted research to identify the applicable design codes and standards for NPP applications
- Conducted hydraulic network analysis of sprinkler systems

SELECTED PUBLICATIONS

- NUREG-2169, "Nuclear Power Plant Fire Ignition Frequency and Non-Suppression Probability Estimation Using the Updated Fire Events Database: United States Fire Event Experience Through 2009"

- NUREG-2128, "Electrical Cable Test Results and Analysis During Fire Exposure (ELECTRA-FIRE), A Consolidation of Three Major Fire-Induced Circuit Cable Failure Experiments Performed Between 2001 and 2011
- Enhancements in the OECD FIRE Database - Fire Frequencies and Severity of Events, W. Werner, R. Bertrand, A. Huerta, J. S.Hyslop, N. Melly, and M. Rowekamp, Proceedings of SMiRT 21, 12th International Seminar on Fire Safety in Nuclear Power Plants and Installations, München, Germany
- Incorporation of NFPA-805 Internal Fire Scenarios into SPAR all Hazard Models S. Sancaktar, F. Ferrante, N. Melly U.S. Nuclear Regulatory Commission, Washington DC, USA 20555-0001, 2011
- OECD FIRE Database Applications and Challenges -A Recent Perspective, Marina Roewekamp, Matti Lehto, Heinz-Peter Berg, Nicholas Melly, Wolfgang Werner Paper presented at OECD/NEA/CSNI/WGRISK International Workshop on Fire PRA, Garching, Germany
- Expert Judgment: An Application in Fire-Induced Circuit Analysis, Gabriel Taylor P.E., Nicholas Melly, Tammie Pennywell, Paper presented at OECD/NEA/CSNI/WGRISK International Workshop on Fire PRA, Garching, Germany

David Miskiewicz, Engineering Planning & Management, Inc.

EDUCATION

1975–1979 B.S., Nuclear Engineering, Pennsylvania State University, State College, PA

Summary

Nuclear engineer with over 30 years of experience working in the nuclear power industry. Currently Mr. Miskiewicz is managing the Risk Services Division for EPM. David has been a practicing PRA engineer for more than 20 years with extensive industry involvement including leading, presenting and instructional roles, and is a recognized expert in PRA. He has additional experience with software development and systems and design engineering activities including work related to reactor internals and reactor vessel integrity.

EXPERIENCE

2012–Present EPM, Inc., Raleigh, NC

- Manage operations and personnel within the Risk Services Division of EPM.
- Project manager and technical lead for development of Robinson Fire PRA to support NFPA-805.
- Project oversight and consulting support for completion of Point Beach Fire PRA and LAR preparation to support NFPA-805 transition.
- Member NEI 805 Task Force and Fire PRA Task Force
- Member of ASME CNRM Subcommittee on Model Maintenance, Special Committee on Inquiries, and the Part 4 (Fire PRA Standards) writing team
- Participant in various EPRI/NRC MOU projects

2005–2012 Progress Energy, Raleigh, NC

- Support the Progress Energy Fleet of Nuclear Plants. Responsibilities include maintaining PSA models, performing PSA applications, and responding to emergent plant issues.
- Project management and technical lead for development of fire PRAs to support transition of the Progress Energy fleet to NFPA-805.
- Software owner for PSA software used at Progress Energy. Upgraded and completed in-house SQA for the latest versions of EPRI R&R software in 2006.
- Participated in Limerick Peer Review against the ASME Standard
- Member NEI 805 Task Force and Fire PRA Task Force
- Member of ASME CNRM Subcommittee on Technology, Special Committee on Inquiries, and the Fire PRA Standards writing team
- Participant in various EPRI/NRC MOU projects

2001–2005 Progress Energy, Crystal River, FL

- Support the Progress Energy Fleet of Nuclear Plants
- Primary responsible individual for CR3 PRA models and applications. Extensive interface experience with plant engineering, operations, work controls, and licensing groups.

- Applications performed include 14day Emergency Diesel AOT extension, One time AOT extensions for Service water, Chilled water, Emergency Diesels, Emergency Feedwater, and ILRT extensions for several plants.
- Experienced with product development and regulatory interface related to the Significance Determination Process [19].
- Chairman of B&W Owners Group Risk Applications Committee
- Member NEI Risk Applications Task Force
- Member ASME PSA Standard Addendum B writing team
- Participated in 3 external NEI PSA Peer Certification Teams.
- Developed Tool and database for reviewing PRAs against the ASME Standard which was a prototype for the ePSA module offered by EPRI.

1987–2001 Florida Power Corporation, Crystal River, FL

- Responsible for the CR3 PRA model and applications
- Completed extensive models updates resulting from CR3 1.5 year design outage.
- Temporarily served as the Maintenance Rule Supervisor responsible for setting up CR3 expert panel and preparing for baseline 10CFR50.65 inspection. Also, served as Chairman of Maintenance Rule Expert Panel for several years.
- Member of B&W Owners Group Risk Applications Committee
- Involved in the preparation and submittal of IPE and IPEEE for Crystal River unit 3.
- Developed various in-house software applications which significantly increased the efficiency of certain aspect of PSA analysis. These included and online risk monitoring at CR3 (pre-EOOS), a plant specific data management tool, a fire scenario evaluation tool, HRA and maintenance unavailability calculators, a level 2 bridge tree tool, and a component risk ranking tool.

1983–1998 Florida Power Corporation, Crystal River, FL & St. Petersburg, FL

- Chairman and/or member of B&W Owners Group Materials Committee and Reactor Vessel Working Group respectively from 1986-1998.
- Technical lead for development of LTOP technical specifications for CR3. Also responsible for implementation of PLTR and management of the reactor vessel surveillance program at CR3.
- Engineer in Mechanical Design group responsible for plant modifications including replacement of reactor vessel internals bolting and HPI nozzle safe ends.

1979–1983 Gilbert/Commonwealth, Inc., Reading, PA

- Field engineer working as consultant/contractor for nuclear utilities. Primary field was radioactive waste system upgrades.
- Design engineer in the radwaste management section. Participated in radwaste reduction, spent fuel storage and decommissioning projects.

Steven Nowlen, Consultant

Retired from SNL in June 2014

EDUCATION AND HONORS

Appointed to the rank of Distinguished Member of the Technical Staff at Sandia National Laboratories, October 2001, an honor reserved for no more than 10% of the SNL engineering/science staff.

Master of Science, Mechanical Engineering, Michigan State University, East Lansing Michigan, March 1984.

DuPont Research Fellow, Department of Mechanical Engineering, Michigan State University, 1981-1983

Bachelor of Science with High Honor, Mechanical Engineering, Michigan State University, East Lansing Michigan, December 1980, Graduated Phi Beta Kappa

PROFESSIONAL EXPERIENCE

Since joining Sandia in 1983, I have been active in both experimental and analytical research in the fields of nuclear power plant safety with a focus on fire safety and quantitative fire risk analysis. I have been Sandia's technical and programmatic lead for the nuclear power fire research programs since 1987. My responsibilities include direct technical contributions, technical team leadership, sponsor interactions, program planning and program management. The most important application of my research has been in the development and application of probabilistic risk assessment (PRA) methods for fires in nuclear power plants; that is, quantitative assessments of the impact of fires on nuclear power plant safety and operations. I also have experience in harsh environment equipment qualification testing and accelerated thermal and radiation aging of materials.

My experimental work has included the planning, execution, evaluation, and reporting of fire safety experiments, as well as the interpretation, evaluation, and application of experimental results generated by other researchers. Specifically, I have experience in the testing of fire growth behavior, large-scale room fires, enclosure ventilation and smoke purging, cable and electrical equipment fire-induced damage, smoke particulate characterization, fire barriers, smoke damage effects on digital equipment, and cable ampacity and ampacity derating.

As a secondary aspect of my experimental experience, I have also participated in Equipment Qualification tests assessing the performance of electrical equipment in the harsh steam and radiation environments associated with nuclear power plant severe accidents. This work has included both accelerated thermal and radiation aging of electrical cables and the evaluation of equipment performance during harsh environmental exposures such as loss of coolant accidents.

Related analytical efforts in the area of fire safety have included the evaluation and validation of computer fire simulation models, the review and analysis of actual fire events in nuclear power plants, fire risk assessment analytical support work, the development and evaluation of fire risk assessment methods, and the development and evaluation of analytical methods for cable ampacity and fire barrier ampacity derating assessments. I have also participated as an expert consultant in various inspection activities for U.S. Nuclear Regulatory Commission (NRC).

I have performed training for the NRC staff in the application of the NRC Significance Determination Process (SDP) for fire protection inspection findings. I am currently participating in an effort to develop and deploy inspector training for application to those NRC licensees transitioning to the new risk-informed, performance-based fire protection requirements. I also act as technical coordinator and classroom instructor for the annual Fire PRA training course offered as a part the NRC Office of Nuclear Reactor Research (RES) and Electric Power Research Institute (EPRI) collaboration on fire research. This training course has been conducted annually since 2005 and routinely attracts well over 100 participants per year.

I was a member of the U.S. NRC Senior Review Board for the review of Individual Plant Examination for External Events (IPEEE). I am currently a member of the ASME/ANS Joint Committee on Nuclear Risk Management Subcommittee on Standard Maintenance. I also co-chair the associated working group on fire risk.

My publication list is available on request and includes 10 journal articles, approximately 30 formal SNL technical reports, five invited conference papers and over 20 other general conference papers. I also co-authored a section of the SFPE *Handbook of Fire Protection Engineering* entitled “Risk Assessment for Nuclear Power Plants.”

Notable Roles and Accomplishments

SNL technical area lead and program manager for nuclear power plant related fire research (1987-present)

Voting member of the American Society of Mechanical Engineers (ASME) American Nuclear Society (ANS) Joint Committee for Nuclear Risk Management (JCNRM) Subcommittee on Standards Maintenance

Co-Chair of the ASME/JCNRM *Standard for Level 1 / Large Early Release Frequency Probabilistic Risk Assessment for Nuclear Power Plant Applications* Fire Working Group (RA-Sa-2009)

Leading member of the core writing team for the American Nuclear Society (ANS) Standard on Fire PRA methodology (ANSI/ANS-58.23-2007)

Lead author and NRC technical team lead for the consensus Fire PRA methodology NUREG/CR-6850 which was developed as a collaboration between the NRC and the Electric Power Research Institute (EPRI))

Technical Coordinator for development of the U.S. NRC Significance Determination Process (SDP) for risk-informed fire inspections (2003-2004)

Technical coordinator and instructor for the annual NRC/EPRI Fire PRA methodology training sessions (2004-present)

Member of the Nuclear Regulatory Commission (NRC’s) Senior Review Board for the review and evaluation of licensee submittals under the Individual Plant Evaluation of External Events Program (1995-2001)

Technical advisor to the U.S. NRC staff during development of the National Fire Protection Association (NFPA) *Performance-Standard for Fire Protection for Light Water Nuclear Reactor Electric Generating Plants* (NFPA 805) (1995-2001)

Qualified as an expert witness in nuclear power plant fire safety in U.S. Federal Criminal District Court (1995)

Victor Ontiveros[1], Jensen Hughes

EDUCATION

Ph.D., Reliability Engineering, University of Maryland, 2013
M.S., Fire Protection Engineering, University of Maryland, 2010
B.S., Fire Protection Engineering, University of Maryland, 2007
A.A., General Studies, Montgomery College, 2004

Victor Ontiveros, PhD, is a recent graduate from the University of Maryland with degrees in Fire Protection and Reliability Engineering. During his studies, Dr. Ontiveros spent considerable time working on model development and uncertainty quantification. Dr. Ontiveros has extensive laboratory experience including material fatigue testing and laboratory setup and organization. He has experience performing Occupational Safety and Health inspections in spaces ranging from office space to machine shops and outdoor spaces. He has provided support in fire PRA projects at Prairie Island and Monticello Nuclear Generating Plants.

PROFESSIONAL HIGHLIGHTS

Engineer II, Hughes Associates, Baltimore, MD, present. Responsibilities include fire analysis scenario analysis, fire modeling, plant walkdowns, and fire probabilistic risk assessment.

Graduate Research Intern, Dept. of Mechanical Engineering, University of Maryland, College Park, MD, 2008–2014. Organized and set up Department of Mechanical Engineering Mechanics and Reliability Lab. Worked with Campus Facilities to ensure requirements for laboratory space were met. Administered retrofitting of load frames. Instructed and assisted fellow students in laboratory capabilities and experimental testing. Planned and researched for Ph.D. dissertation: developed and implemented accelerated fatigue experiments of aluminum alloys; and developed strain energy expended and thermodynamic entropy based models for determination of life expended. For master's thesis: accounted for uncertainty for sub-models used within fire simulation codes; updated state of knowledge using Bayesian methodology; and determined 'real' parameter values given uncertain model predictions and experimental measurements.

AWARDS

Recipient, Montgomery Scholar at Montgomery College Rockville, two-year tuition and summer study at Cambridge University, England, Summer 2003; Beacon Conference finalist in Technology and Technological Studies, 2004
Recipient, Alfred P. Sloan Foundation Minority Ph.D. Program in Mathematics, 2011–2012
Recipient, Willie M. Webb Reliability Engineering Fellowship, 2012–2013

PUBLICATIONS AND PRESENTATIONS

Ontiveros, V., "Strain Energy and Thermodynamic Entropy as Prognostic Measures of Crack Initiation in Aluminum Alloys," Ph.D. Dissertation, University of Maryland, College Park, MD, January 2014.

---

[1] Not a working group member.

Zhu, S.P., Huang, H.Z., Ontiveros, V., He, L.P., and Modarres, M., “Probabilistic Low Cycle Fatigue Prediction Using Energy-based Damage Parameter and Accounting for Model Uncertainty,” *Int. J. Damg, Mech.,* **21**, December 2011, pp. 1128–1153.

Zhu, S.P., Huang, H.Z., Ontiveros, V., He, L.P., and Modarres, M., “Probabilistic Life Prediction for High Temperature Low Cycle Fatigue Using Energy-Based Damage Parameter and Accounting for Model Uncertainty,” IDETC/CIE2001, Washington DC, August 28–31, 2011, pp. 435–443.

Smith, R., Ontiveros, V., Paradee, G., Modarres, M., and Hoffman, P., “Probabilistic Strain Energy Life Assessment Model,” ICM11, Milano, Italy, June 5–9, 2011.

Ontiveros, V. and Modarres, M., “An Integrated Methodology for Assessing Model Uncertainty in Fire Simulation Codes,” *PSA,* Wilmington, NC, March 13–17, 2011.

Ontiveros, V., Cartillier, A., and Modarres, M., “An Integrated Methodology for Assessing Fire Simulation Codes,” *Nuc. Sci. Eng.,* **166**, November 2010, pp. 179–201.

Ontiveros, V., “An Integrated Methodology for Assessing Fire Simulation Code Uncertainty,” Master Thesis, University of Maryland, College Park, MD, April 2010.

Ontiveros, V., Cartillier, A., Le Gac, C., and Modarres, M., "A Probabilistic Framework for Model Uncertainty in Fire Simulation Codes," *Risk Management for Tomorrow’s Challenges (RM4TC),* Washington, DC, November 15–19, 2009.

Azarkhail, M., Ontiveros, V., and Modarres, M., “A Bayesian Framework for Model Uncertainty Considerations in Fire Simulation Codes,” *International Conference on Nuclear Engineering (ICONE 17)*, Brussels, Belgium, July 12–16, 2008, pp. 639–648.

David Stroup, NRC

EDUCATION

The University of Maryland – College Park, MD
Masters of Science in Mechanical Engineering, 1987
The University of Maryland – College Park, MD
Bachelor of Science in Fire Protection Engineering, 1981
Montgomery College – Rockville, MD
Associate of Arts in Fire Science, 1977

Registered Professional Engineer

Delaware, License No. 7996
Maryland, License No. 20052

EXPERIENCE

U.S. Nuclear Regulatory Commission – Rockville, MD 2/2011-Present
Senior Fire Protection Engineer Office of Nuclear Regulatory Research

- Develop and implement research projects to identify emerging technical issues in fire phenomena, fire modeling, and fire probabilistic risk assessment (PRA)
- Prepare or review fire modeling, fire PRA, and fire research reports
- Participate in the planning, formulation, and implementation of agency programs, policies, and procedures
- Provide oral and written communications on complex technical fire protection subjects to a wide variety of audiences

U.S. Nuclear Regulatory Commission – Rockville, MD 1/2008–1/2011
Fire Protection Engineer Office of Nuclear Regulatory Research

- Implemented research projects to identify emerging technical issues in fire phenomena, fire modeling, and fire probabilistic risk assessment (PRA)
- Prepared or reviewed fire modeling, fire PRA, and fire research reports

National Institute of Standards& Technology – Gaithersburg, MD 12/1995-1/2008
Research Fire Prevention Engineer Building and Fire Research Laboratory

- Conducted research and other investigative work on prediction of fire hazard development, fire risk evaluation, performance design and acceptance, evacuation analysis, performance of materials, and fire model development
- Performed research in the application of the empirical laws of thermodynamics and in heat conduction and mass diffusion in two and three dimensions
- Served as a peer reviewer for several performance-based design projects and technical guidance documents

U.S. General Services Administration – Washington, DC 11/1989–12/1995
Fire Protection Engineer Public Buildings Service

- Developed and evaluated GSA fire protection engineering practices
- Served as official GSA representative to other public and private organizations concerned with fire protection

- Provided guidance to GSA regional personnel, other Services, and Staff Offices regarding the selection, procurement, and use of fire protection equipment and construction techniques

Montgomery College –Rockville, MD 1/1990–6/1990
Instructor, Part-time Department of Engineering, Physical and Computer Sciences

Schirmer Engineering Corporation – Falls Church, VA 7/1989–11/1989
Fire Protection Engineer

- Evaluated proposed and existing buildings and other structures for compliance with various building and fire codes
- Developed alternative strategies for achieving fire safety levels equivalent to those specified in recognized fire and building codes

National Institute of Standards& Technology – Gaithersburg, MD 6/1981–7/1989
Research Fire Prevention Engineer Building and Fire Research Laboratory

- Performed theoretical and experimental research on fire build-up in compartments including planning and interpretation of experiments (bench scale and full scale), translation to usable form, data reduction, analysis, and presentation of results
- Performed experiments and analysis of data to construct computational models of fire growth and suppression

National Institute of Standards& Technology – Gaithersburg, MD 11/1980–6/1981
Fire Prevention Engineering Technician Center for Fire Research

SELECTED PUBLICATIONS

- NUREG-1805, Supplement 1, Volumes 1 and 2, Fire Dynamics Tools (FDTs) Quantitative Fire Hazard Analysis Methods for the Nuclear Regulatory Commission Fire Protection Inspection Program, July 2013.
- NUREG-1824, Supplement 1/EPRI 3002002182, Verification and Validation of Select Fire Models for Nuclear Power Plant Applications, Draft for Public Comment, December 2014.
- NUREG-1934/EPRI 1023259, Nuclear Power Plant Fire Modeling Analysis Guidelines (NPP FIRE MAG), November 2012.
- NUREG-2122, Glossary of Risk-Related Terms in Support of Risk-Informed Decisionmaking, November 2013.
- “Flammability Hazards of Materials”, (Co-author), Fire Protection Handbook, 20th edition, Chapter 2, Section 2.3, National Fire Protection Association, 2008.

ACHIEVEMENTS

Salamander - Fire Protection Engineering Honor Society
General Services Administration Federal Engineer of the Year, 1995
Fellow – Society of Fire Protection Engineers, 2006
U.S. Department of Commerce Bronze Metal, 2007
Nuclear Regulatory Commission Federal Engineer of the Year, 2014
Member, SFPE Standards-Making Committee on Design Fire Scenarios
Society Memberships: Society of Fire Protection Engineers, National Fire Protection Association, American Nuclear Society, and International Association of Fire Safety Science

Mano Subudhi[2], BNL

EDUCATION

1969 - B.S.,	Mechanical Engineering, Banaras Hindu University, India
1970 - M.S.,	Mechanical Engineering, Massachusetts Institute of Technology
1974 - Ph.D.,	Mechanical Engineering, Polytechnic Institute of New York

EXPERIENCE

1976-Present
Brookhaven National Laboratory, Over his career at BNL, Dr. Subudhi developed statistical methods for characterizing degradation within various components (NUREG/CR-6869). He also studied geomagnetic effects on nuclear facilities (NUREG/CR-5990), laboratory testing of electrical components (NUREG/CR-5280), and developed recommendations to improve current maintenance practices (NUREG/CR-5812). He also performed loss of coolant accident (LOCA) testing of Cables used in NPPs (NUREG/CR-6384) and did a configuration management study of radiological facilities. He participated in an International Atomic Energy Agency (IAEA) neutron monitoring experiment and a safeguard assessment of a US DOE facility, Portsmouth Gas Diffusion Plant in Ohio, for down-blending operation of highly-enriched uranium (HEU) from FSU countries to low-enriched uranium (LEU).

Dr. Subudhi is very conversant with all Subsections of the ASME Boiler and Pressure Vessel (B&PV) Code, Section III on Nuclear Power Plant Components; with IEEE Std. 323 on environmental qualification, with IEEE Std. 383 on cable qualification, and with IEEE Std. 344 on seismic qualification. He has served in working groups of these ASME and IEEE standards committees to develop various standards and guidance documents. Recently, he began work on the National Fire Protection Association (NFPA) Standard 805 requirements for fire probabilistic risk assessments (PRAs), using a risk-informed performance-based approach.

1975-1976
Bechtel Power Corp., Mechanical Engineer. Involved in the stress analysis of nuclear power plant components subjected to thermal, dead weight, seismic, thermal transients, pressure and fatigue loads; special problems including water hammer, flow-induced vibrations, and sudden valve closures; and preparation of Nuclear Class I Reports for licensing purpose. Represented Bechtel in interfacing manufacturers, clients and vendors.

SELECTED PUBLICATIONS

"Seismic Analysis of Piping Systems Subjected to Independent Support Excitations by Using Response Spectrum and Time History Methods," *BNL Technical Report No. BNL-NUREG-31296,* April 1982. Also, *Presented at the ASME Summer PVP Conference,* Portland, Oregon, PVP-Vol. 73, June 1983.

"The Assessment of Alternate Procedures for the Seismic Analysis of Multiply Supported Piping Systems," *Proceedings of the 1985 ASME PVP Conference, New Orleans, PVP-Vol. 98.3,* June 1985.

---

[2] Moderator/facilitator for the working group

"Seismic Upgrading of the Brookhaven High Flux Beam Research Reactor," *Proceedings of DOE Natural Phenomena Hazards Mitigation Conference, Las Vegas,* October 1985.

"Improving Motor Reliability in Nuclear Power Plants," *NUREG/CR-4939, BNL-NUREG-52031, Vols. 1, 2, 3,* November 1987.

"Age-Related Degradation of Westinghouse 480-Volt Circuit Breaker," *NUREG/CR-5280, BNL-NUREG-52178, Vols. 1&2,* November 1990.

"Degradation Modeling with Application to Aging and Maintenance Effectiveness Evaluations," (Co-author), *NUREG/CR-5612, BNL-NUREG-52252,* March 1991.

"Life Testing of a Low Voltage Air Circuit Breaker to Assess Age-Related Degradation", *Nuclear Technology, Vol. 97, pp.362-370,* March 1992.

“Managing Aging in Nuclear Power Plants: Insights from NRC’s Maintenance Team Inspection Reports,” *Nuclear Safety, Vol. 35, No. 1,* January-June 1994.

“RAPTOR Gas Gun Testing Experiment,” (Co-author) Proprietary, CRADA BNL-C-96-01, June 1998.

“A Reliability Physics Model for Aging of Cable Insulation Materials,” NUREG/CR-6869, BNL-NUREG-73676-2005, March 2005.

“Application of laser generated ultrasonic pulses in diagnostics of residual stresses in welds,” Proc. of SPIE, 2005.

“Expert Panel Report on Proactive Material Degradation Assessment,” NUREG/CR-6923, BNL-NUREG-77111-2006, February 2007.

“Joint Assessment of Cable Damage and Quantification of Effects from Fire (JACQUE-FIRE): Volume 1 – Phenomena Identification and Ranking Table (PIRT) Exercise for Nuclear Power Plant Fire-Induced Electrical Circuit Failure,” NUREG/CR-7150, Vol. 1, BNL-NUREG-98204-2012, EPRI 1026424, October 2012.

“Joint Assessment of Cable Damage and Quantification of Effects from Fire (JACQUE-FIRE): Volume 2 – Expert Elicitation Exercise for Nuclear Power Plant Fire-Induced Electrical Circuit Failure,” NUREG/CR-7150, Vol. 2, BNL-NUREG-98204-2012, EPRI 3002001989, May 2014.

Gabriel Taylor, NRC

EDUCATION

Masters of Science in Fire Protection Engineering, May 2012
Bachelor of Science in Electrical Engineering, December 2004

Registered Professional Engineer
Maryland, Fire Protection, 2013

EXPERIENCE

U.S. Nuclear Regulatory Commission - Rockville, MD August 2013- Present Senior Fire Protection Engineer

- Evaluated the effectiveness of aspirated smoke detection systems for use in NPP fire PRA applications
- Instructed NUREG/CR-6850 training related to fire-induced circuit failure probability estimation
- Supported Development of Post-Fire Safe Shutdown Training for Regional Inspectors
- Chaired IEEE P1848, Co-chaired IEEE 1202

U.S. Nuclear Regulatory Commission - Rockville, MD October 2007- August 2013
Fire Protection Engineer

- Expert Member of the Probabilistic Risk Assessment (PRA) expert elicitation on fire-induced cable damage spurious operation probability
- Expert Member of the Phenomena Identification and Ranking Table (PIRT) exercise on Nuclear Power Plant Fire-Induced Electrical Circuit Failure
- Instructed NUREG/CR-6850 training related to fire-induced circuit failure probability estimation
- Witnessed fire tests, analyzed results and wrote test reports on Duke Armored cable testing, Navy Digital I&C testing, Progress Penetration Seal Testing.
- International OECD Fire-Events Database and High Energy Arching Fault Task Group
- Managed DOE work on fire-induced failure circuit testing and conducted supplementary data analysis (DESIREE-FIRE, KATE-FIRE)
- Presented research at numerous conferences and to the Advisory Committee on Reactor Safeguards (ACRS)

U.S. Nuclear Regulatory Commission - Rockville, MD April 2005 - October 2007
NSPDP General Engineer

- Graduate of NSPDP Class of 2007
- DORL: Evaluated proposed changes to license amendments in regards to their effect to public safety

- ACRS: Prepared summary report for committee members and assisted with meeting preparations
- RII/Watts Bar Resident Office: Became basic inspector qualified IMC 1245 Appendix A

The Pennsylvania State University - University Park, PA August 2003 - February 2004
Undergraduate Research Assistant, Dr. P. M. Lenahan

- Modified magnet power supply to operate correctly using U.S. power system
- Designed data acquisition system to signal average ESR and SDR signals using LabVIEW 7
- Reviewed, ordered, and installed SDR spectroscopy system

OSRAM Sylvania Inc. - St. Marys, PA January - March 2005 & January- August 2003
Process Engineer & Engineering Co-Op (R&D, Process, EH&S, Electrical Departments)

- Developed and conducted tests to examine customer complaints and analyzed the safety of products
- Developed a recycling program to reduce net residual waste and increase gain from recyclable goods
- PLC programming using VersaPro for GE PLC's (Latter-logic)
- Designed and constructed electrical cabinet using AutoCAD (ergonomic layout for operator and maintenance)

ACHIEVEMENTS

Nuclear Regulatory Commission Federal Engineer of the Year, 2015
Member of NSPE
Member of IEEE, PES, ICC
Member of NFPA
Eagle Scout - Troup #95, Bucktail Council
Eta Kappa Nu (HKN) - Epsilon Chapter - National Electrical/Computer Engineering Honors Society
Dale Carnegie Program Graduate
Penn State Conservation Leadership School Graduate
Rivers Conservation Leadership School Graduate

PUBLICATIONS

Subudhi, M., Martinez-Guridi, G., Taylor, G., et. al., NUREG/CR-7150, Volume 2, "Joint Assessment of Cable Damage and Quantification of Effects from Fire (JACQUE-FIRE), Expert Elicitation Exercise for Nuclear Power Plant Fire-Induced Electrical Circuit Failure," U.S. NRC, Washington, DC, 2014.

Taylor, G., Melly, N.B., Pennywell, T., "Expert Judgment, An Application in Fire-Induced Circuit Analysis," International Workshop on Fire PRA, OECD/NEA Committee on the Safety of Nuclear Installations, Garching, Germany, April 2014.

Melly, N.B., Taylor, G., Stroup, D.W., "U.S. NRC Fire Safety Research Activities," International Workshop on Fire PRA, OECD/NEA Committee on the Safety of Nuclear Installations, Garching, Germany, April 2014.

Taylor, G., Gallucci, R.H.V., Subudhi, M., Martinez-Guiridi, G., "Fire PRA Advancements in Estimating the Likelihood of Fire-Induced Spurious Operations," American Nuclear Society, PSA 2013, International Topical Meeting on Probabilistic Safety Assessment Analysis, Columbia, SC, September 2013.

Taylor, G., Melly, N., Woods, H., Pennywell, T., Olivier, T., Lopez, C., NUREG-2128, "Electrical Cable Test Results and Analysis During Fire Exposure (ELECTRA-FIRE), A Consolidation of Three Major Fire-Induced Circuit and Cable Failure Experiments Performed Between 2001 and 2011," U.S. NRC, Washington, DC, 2013.

Subudhi, M., Higgins, J., Taylor, G.J., et.al., NUREG/CR-7150, Volume 1, "Joint Assessment of Cable Damage and Quantification of Effects from Fire (JACQUE-FIRE), Phenomena Identification and Ranking Table (PIRT) Exercise for Nuclear Power Plant Fire-Induced Electrical Circuit Failure," U.S. NRC, Washington, DC, 2012.

Taylor, G., "Evaluation of Critical Nuclear Power Plant Electrical Cable Response to Severe Thermal Fire Conditions," Masters of Science Thesis, Graduate School of the University of Maryland, College Park, MD 2012.

Taylor, G., Barrett, H., Funk, D., Nowlen, S., "Advances in Understanding the Phenomena of Electrical Cable Fire-Induced Hot Shorting," American Nuclear Society, Annual Meeting, June 2011.

Nowlen, S.P., Brown, J.W., Taylor, G.J., "Electrical Failure Behavior of Kerite® FR Insulated Electrical Cables," American Nuclear Society, Annual Meeting, June 2011.

Taylor, G., Salley, M.H., NUREG-1924, "Electrical Raceway Fire Barrier Systems in U.S. Nuclear Power Plants," U.S. NRC, Washington, DC, 2010.

Taylor, G., McGrattan, K., Nowlen, S.P., "Electrical Circuit and Cable Testing," Interflam 2010, 12th International Fire Science and Engineering Conference, University of Nottingham, UK, July 2010.

Taylor, G., Nowlen, S.P., Brown, J.W., "Direct Current Electrical Shoring in Response to Exposure Fire - The DESIREE-FIRE Project," 20th International Conference on Structural Mechanics in Reactor Technology (SMIRT 20) - 11th International Post-Conference Seminar on Fire Safety in Nuclear Power Plants and Installations," Espoo Finland, August 2009.

Taylor, G., Salley, M.H., "10 Rules of Fire Induced Cable Failure," National Institute of Standards and Technology, Annual Conference on Fire Research, Gaithersburg, MD, 2008.

Justin Williamson[3], Jensen Hughes

EDUCATION

Ph.D., Mechanical Engineering, University of Maryland, 2009
M.S., Fire Protection Engineering, University of Maryland, 2004
B.S., Fire Protection Engineering, University of Maryland, 2001

Justin Williamson, PhD, is a Fire Protection Engineer with six years' experience. He has extensive experience in fire, smoke, heat and mass transfer modeling to identify and solve fire protection problems for the commercial, government, and military sectors. Dr. Williamson's experience includes research, development and analysis of advanced fire modeling. He has worked as a fire modeling software developer and has expertise in the application of model verification, validation, sensitivity and uncertainty analysis required for high level regulatory acceptance of modeling results. He is passionate about applying his scientific expertise to provide effective solutions to complex problems.

PROFESSIONAL HIGHLIGHTS

Fire Protection Engineer, Hughes Associates, Baltimore, MD, 2008–present. Responsibilities include research, development and analysis of advanced fire simulations. Models used include Fire Dynamics Simulator (FDS), Consolidated Fire and Smoke Transport (CFAST), HEATING 7.3, and Fire and Smoke SIMulator (FSSIM). Performs fundamental analysis of dynamic, thermo-physical problems associated with fire, including heat transfer, mass transfer, and fire dynamics. Developed various software tools including FSSIM and customized tools for various applications. Performed complex analyses including fire modeling code compliance evaluations, code equivalence evaluations, Fire Hazard Analyses (FHA), and support for Fire Probabilistic Risk assessment (PRA) in support of commercial, NRC and DOE facilities. Performed engineering inspections in support of fire PRA modeling for Main Control Room abandonment and NFPA 805 transition. Expertise in the application and development of model verification, validation, sensitivity and uncertainty analysis required for high level regulatory acceptance of modeling results.

Internship, Exponent, Thermal Sciences Department, Bowie, MD, 2007–2008. Handled the experimental study of spill characteristics for cryogenic liquids on water and performed CFD simulations of large scale cryogenic liquid spill and dispersion.

Graduate Research Assistant, University of Maryland, Department of Mechanical Engineering, College Park, MD, 2004–2007. Developed local extinction criteria for fire from counterflow flame studies to add more detailed combustion physics for under-ventilated fires in FDS.

Faculty Research Assistant, University of Maryland, Department of Mechanical Engineering, College Park, MD, 2004. Assisted with the Maritime Hazard Assessment Project sponsored by the Department of Defense. Examined hazards of accidental release of cryogenic fuels from cargo ships. Incorporated a partially premixed combustion model in the NIST Fire Dynamics Simulator (FDS) to examine deflagrations.

---

[3] Not a working group member.

Graduate Research Assistant, University of Maryland, Department of Mechanical Engineering, College Park, MD, 2002–2003. Characterized thermal behavior and ignition from cigarette lighter flames. Developed an inherently safe cigarette lighter to reduce the risk of unwanted ignition from juvenile misuse.

NOTABLE PUBLICATIONS AND PRESENTATIONS

Williamson, J., "Measurements and Analysis of Extinction in Vitiated Flame Sheets," University of Maryland, College Park, MD, 2009.

Williamson, J., "Characterizing Cigarette Lighter Flames to Reduce Unwanted Ignition," University of Maryland, College Park, MD, 2003.

Williamson, J., Beyler, C., and Floyd, J., “Validation of Numerical Simulations of Compartments with Forced or Natural Ventilation using the Fire and Smoke Simulator (FSSIM), CFAST and FDS,” *Interflam 2010: Proceedings of the Twelfth International Conference*, University of Nottingham, United Kingdom, July 5–7, 2010, pp. 1043–1052.

Williamson, J. and Marshall, A.W., “Characterizing the ignition hazard from cigarette lighter flames,” *Fire Safety Journal*, **40** (1), February 2005, DOI: 10.1016/j.firesaf.2004.08.004.

Appendix B

Overview of Working Group Activities

This appendix provides a summary of the working group (WG) activities. The members of the WG convened four separate times in 2 to 2½-day meetings from April 2014 through September 2014 at the NRC's RES building in Rockville, Maryland. Specifically, meetings were held on:

1. First meeting: April 1-3, 2014
2. Second meeting: May 21-23, 2014
3. Third meeting: July 22-24, 2014
4. Fourth meeting: September 15-16, 2014

In addition, webinars and conference calls were scheduled throughout this period on an as-needed basis. During the first two meetings, the WG evaluated two major avenues to address the modeling of electrical enclosure fire hazards:

- Re-binning and redefining the peak HRR profiles for electrical enclosures (provided in Table G-1 of NUREG/CR-6850) based on the amount of combustible materials contained within electrical enclosures and the potential for an enclosure fire to grow to its maximum size (peak) when left undetected (i.e., fire severity), and then,

- For each enclosure group or class, developing information in adjusting other effects of the peak HRR profile (or distribution) in the fire analysis.

During the first meeting, the WG members identified and discussed several topics to improve the current methodology for modeling electrical enclosure fire hazards in the fire PRA. Some of the items <u>*considered*</u> are presented in Table B-1.

Table B-1
Identification of Topics for Consideration

Topics or Concepts Identified	Action Taken
Classification (i.e., binning) of electrical enclosure types	A new set of enclosure classifications was developed and described in Chapter 3 of this report.
Characterizing the peak heat release rate for all enclosure types and other equipment (e.g., motors, pumps, dry transformers) with an electrical ignition source	A new set of peak heat release rate probability distributions is described in Chapter 4 of this report. The characterization of peak heat release rates for ignition sources other than electrical enclosures is under review* and therefore, not included in this report.
Effects of obstructed fire plume inside the enclosure on the vertical component of the zone of influence (i.e., fire plume temperatures)	Chapters 5 and 6 of this report describe the recommended approach for incorporating the effects of obstructions in fire plume temperatures in a fire modeling analysis.

Table B-1
Identification of Topics for Consideration

Topics or Concepts Identified	Action Taken
Assessment of heat release rate growth profile based on actual fire test results and fire experience, including the pre-growth, growth, and decay phases.	This topic is under review*
Evaluation of the effect of enclosure counting on the fire ignition frequency including treatment of “well-sealed” electrical enclosures in the counting process	This topic is under review*
Understanding the effects of ventilation-limited conditions associated with electrical enclosure fires	Chapter 4 of this report provides peak heat release rate distributions that are dependent on an electrical enclosure’s ventilation conditions (open or closed door configuration) This report does not cover the modeling heat release rates in ventilation limited conditions. This topic is under review*
Guidelines on treatment of: a. Small electrical enclosures b. Large enclosures, walkthrough enclosures, and main control board c. Fire propagation to adjacent enclosures d. Fire resistance of SIS (manufacturer-wired safety cables), silicon rubber (SR), and Tefzel cable insulation types	a. See Table 4-2 enclosure class 4c for treatment of small electrical enclosures b. See Table 4-2 enclosure class 4 for treatment of large electrical enclosures Treatment of main control board fire modeling and scenario development is under review* c. This topic is under review* d. This topic is under review*
Examples of fire analysis of electrical enclosure fires	Appendix G provides examples of the approach described in the report.

* “Under review” does not imply that the NRC or EPRI intends to address this issue in future efforts. It is intended to recognize issues that were identified but not addressed in the current effort as documented in this report.

During the second meeting, the NRC staff presented the preliminary data of their recent fire testing of electrical enclosures at the CBD facility of the Naval Research Laboratory. In addition, the NRC staff presented a preliminary evaluation of experimental data on electrical enclosure fires from all four sources (i.e., SNL, VTT, IRSN, and CBD).

Also during the second meeting, the WG decided to evaluate the results of a set of Fire Dynamics Simulator (FDS) runs that simulated the fire plume behavior for fires within electrical enclosures. This approach is referred to in this report as the obstructed plume. Preliminary simulations yielded some encouraging results and a test matrix was developed by the group for additional simulations and refinements. The simulation results were later presented and discussed during the third and fourth meetings in order to finalize the approach provided in Chapters 5 and 6 of this report.

Pictures of electrical enclosures typically installed in nuclear power plants and considered in fire PRA analyses were reviewed among the working group, during the second meeting. The pictures illustrated the electrical enclosure size and plant configurations, as well as the internal components that could act as the fire ignition source. Considering the overall size/configuration, the ignition source strength, and the amount of internal combustibles, the WG subsequently reached a consensus in classifying electrical enclosures into two major categories: one based on the electrical function and the other based on the size of an enclosure. After binning the switchgear, load centers, motor control centers (MCCs), battery chargers, and power inverters into three groups within the “electrical function” major group, the WG decided to group all other remaining enclosure types (mostly control and instrument panels) into three specific subgroups based on their volumetric size (e.g., small, medium, and large). Thus, the WG classified all enclosures into six specific classification groups.

In preparation for the third meeting, a webinar was held on June 26, 2014, for the WG to discuss how to correlate peak heat release rate values with a specific amount of combustible materials using the videos from various fire test programs.

The third working group meeting on July 22-24, 2014, fast-tracked the technical work on the heat release rate distributions and the obstructed plume approach. The WG’s focus during the July meeting was concentrated on the HRR distributions for the enclosure classification groups developed in the prior meeting. For each enclosure type, a consensus approach was used to assign the 75th and 98th values based on the individual research, data analysis, and engineering judgment.

During the fourth meeting, the WG finalized the definitions of the volumetric classification of other enclosures, including the subcategories for large and medium categories. The WG also reached a consensus on the final HRR distribution estimates. In addition to finalizing the peak HRR values for all electrical enclosure classes, the WG reviewed the findings of the obstructed plume study. Based on the comments by several WG members, the resulting approach was finalized with additional information for completeness and clarity of all assumptions and limitations addressed in the FDS simulations.

Appendix C

Photographs Supporting Classification of Electrical Enclosures

This appendix provides a collection of photographs for the six classification groups of electrical enclosures defined in Chapter 3 of this report. The intent of the information is to support the classification of electrical enclosures. The photographs represent electrical enclosures typically found in nuclear power facilities. Some of them are taken from non-nuclear sources.

It should be noted that all figures included in this appendix are intended to assist the analyst for selecting and classifying Bin 15[1] cabinets in a typical NPP. The final judgment on assigning a classification group should be based on the information given in Section 3 and adequately documented (with photo illustrating actual internal and fuel configurations).

C.1 Group 1: Switchgear and Load Centers

C.1.1 Switchgear

Switchgear is a general term covering switching and interrupting devices and their combination with associated control, instrumentation, metering, protective, and regulating devices. Common switchgear voltage classifications found in an NPP include medium voltage (4.16 kV, 6.9 kV, 7.2 kV, 12.7 kV, 13.9 kV, etc.), and low voltage (480 V, 600 V). Switchgears are used to direct flow of power to various feeders and to isolate apparatus and circuit from the power system. Figures C-1 through C-4 provide examples of external and internal photographs of medium voltage switchgear equipment.

Figure C-1
Front View of Medium Voltage Switchgear Banks

---

[1] In addition to Bin 15 enclosures, the enclosures here include main control board (Bin 4) and battery charger (Bin 10).

Figure C-2
Front View of 6.9 kV Switchgear Relay and Control Logic Enclosures

Figure C-3
Internal Views of Medium Voltage Switchgear

Figure C-4
Internal Views of Medium Voltage Switchgear, Back Showing Bus Cables (Left), Front Showing Control and Relay Enclosure (Right)

C.1.2 Low Voltage Switchgear and Load Centers

Load centers are low voltage switchgears that are typically used to distribute power to motor control centers (MCCs). Load centers commonly have a medium voltage to low voltage transformer and a lineup of low voltage switchgear. Figures C-5 through C-10 provide example photographs of low voltage switchgear/load centers.

Figure C-5
Front View of Load Center (Disconnect Switch)

Figure C-6
Internal Views of a Load Center (a) Low Voltage Breaker, (b) Empty Breaker Cubicle, and (c) Load Center Control Cubicle

Figure C-7
Load Center (Left) with Oil-Cooled Transformer (Right)

Figure C-8
Front View of Load Center (Right) and Transformer (Left)

Figure C-9
Front View of Load Center (Low Voltage Switchgear)

Figure C-10
Low Voltage Load Center Breaker

C.2 Group 2: Motor Control Centers and Battery Chargers

C.2.1 Motor Control Centers

Low voltage motor control centers (MCCs) contain an externally operable circuit disconnecting means, circuit overprotection, and a magnetic motor controller with auxiliary devices combined in plug-in units in vertical assemblies. Control power transformers may be included to provide a 120 VAC power source for the control portion of the equipment, rather than use in the 480 V or 600 V supply voltage. Vertical and horizontal compartmentalized wire-ways are commonly provided to allow for ease of installation and configuration changes. Figures C-11 and C-12 provide external and internal photographs of MCCs.

Figure C-11
Front View of MCC with Three Vertical Sections

Figure C-12
Internal Views of MCC Cubicle

C.2.2 Battery Chargers

Battery chargers convert alternating current (AC) into a highly regulated direct current (DC) output that is used to charge the station backup batteries and to supply all continuous loads that may be connected to the bus. Battery chargers can be specified to accept any available input voltage, either single- or three-phase. The most common nominal AC input voltages are 120 V, 208 V, and 240 V single-phase voltage, and 120/208 V or 277/480 V for three-phase voltage. Nominal DC output voltages are 12 V, 24 V, 48 V, 125 V, and 250 V. Figures C-13 and C-14 present the external and internal photographs of battery chargers, respectively.

Figure C-13
Front View of a Battery Charger

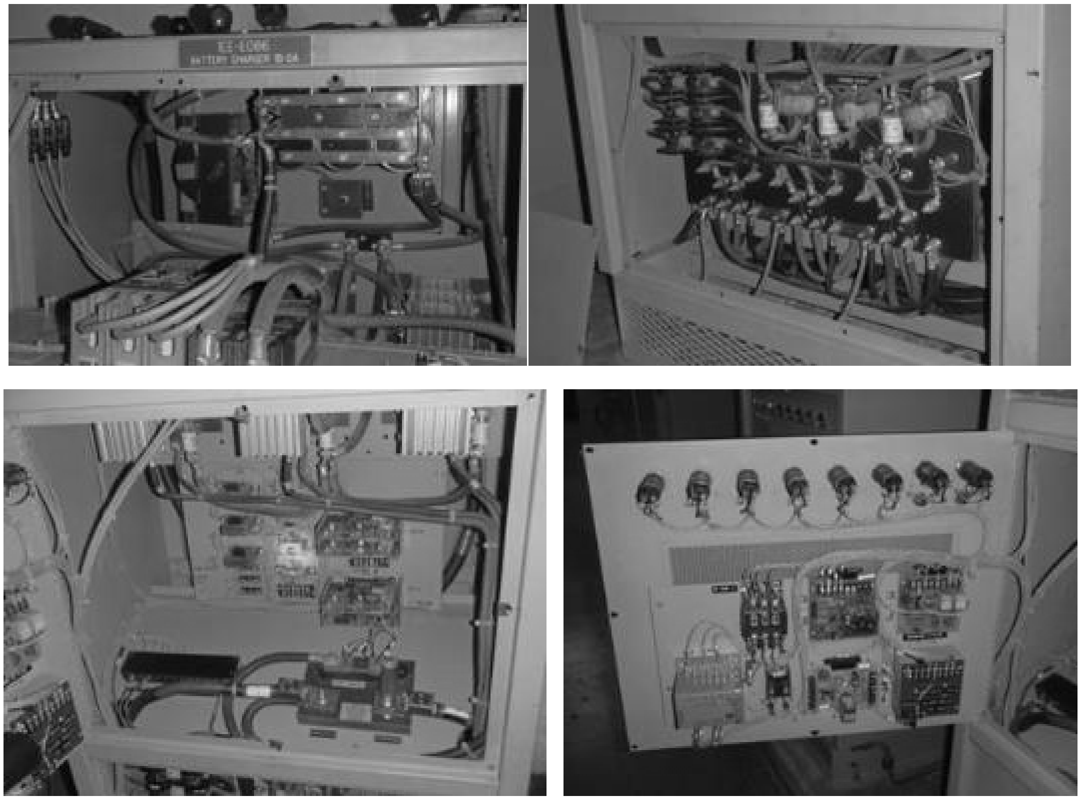

Figure C-14
Internal Views of Battery Chargers

C.3 Group 3: Power Inverters

An inverter changes direct current (DC) power to alternating current (AC) power. Figure C-15 presents external photographs of inverters, while Figure C-16 presents internal photographs of inverters.

Figure C-15
Power Inverters – Front and Back

Figure C-16
Power Inverters – Internal Views

C.4 Group 4a: Large Enclosures

Large enclosures are electrical enclosures of physical volumetric dimensions greater than 50 cubic feet. The large enclosure category does not include power distribution enclosures such as switchgear, load centers, and motor control centers. Figures C-17 through C-20 show large enclosures in the closed and open configurations.

Figure C-17
Auxiliary Shutdown Panels – Large Enclosure (Closed)

Figure C-18
Large Closed Electrical Enclosure

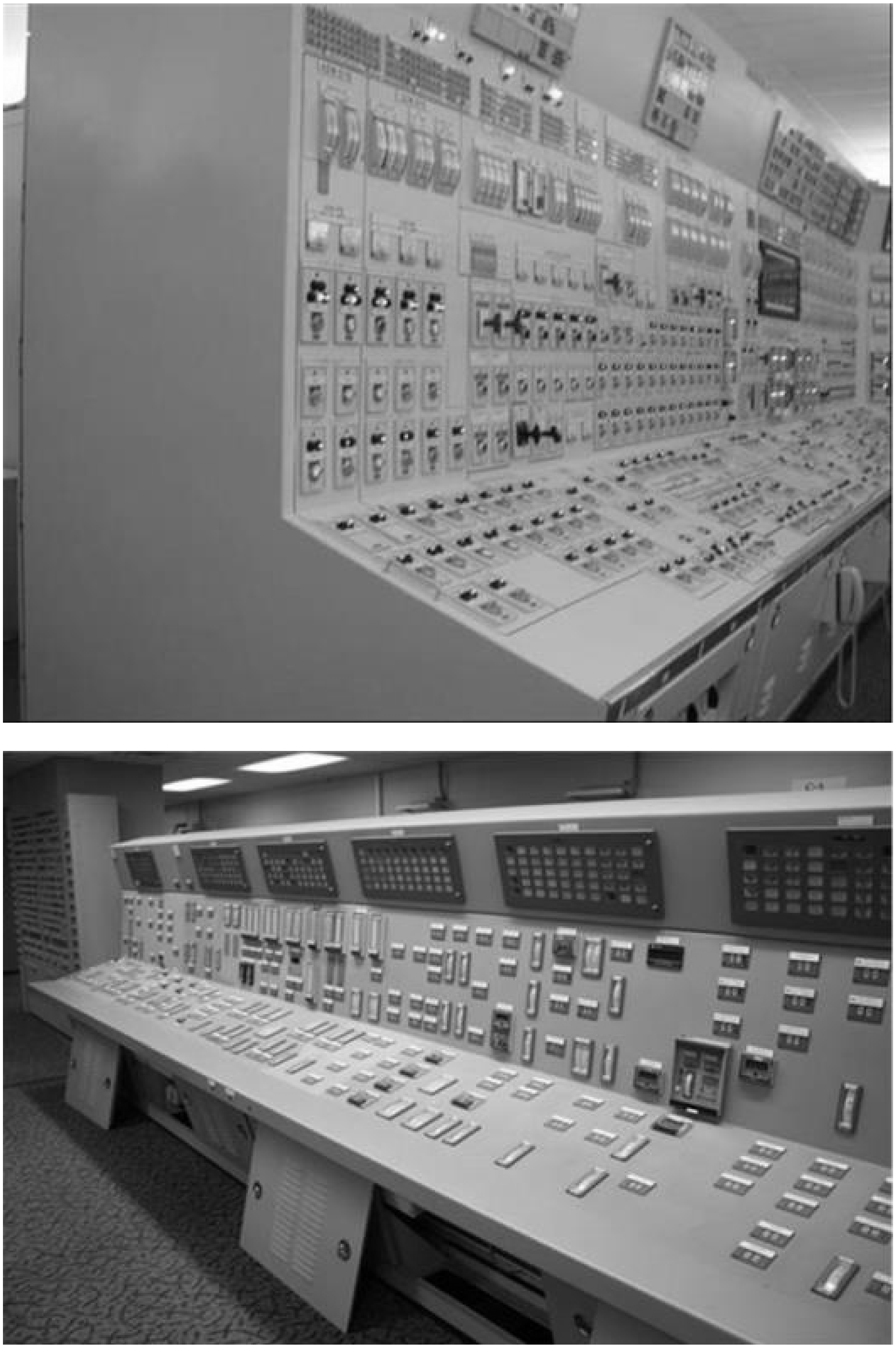

Figure C-19
Large Closed Electrical Enclosure (Main Control Board – MCB)

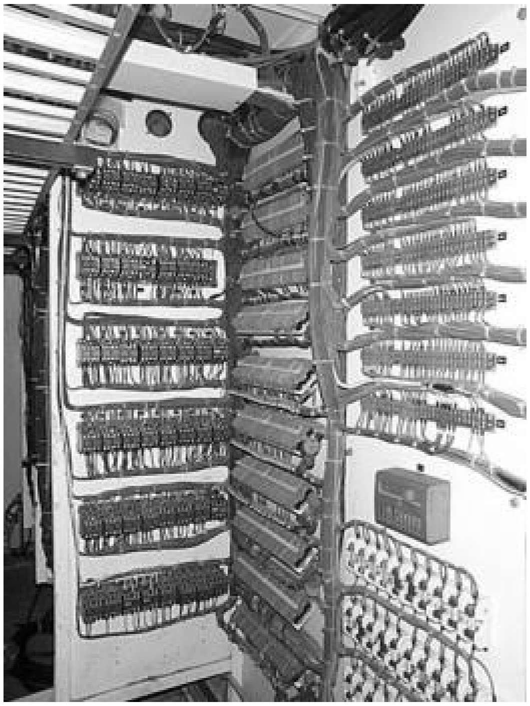

Figure C-20
Large Open Electrical Enclosure (Walkthrough Enclosure)

C.5 Group 4b: Medium Enclosures

Medium enclosures are electrical enclosures of physical volumetric dimensions greater than 12 cubic feet and less than or equal to 50 cubic feet. Figure C-21 presents photographs of electrical enclosures representative of the medium enclosure category.

Figure C-21
Medium Enclosure (Approximately 2 ft. x 2 ft. x 7 ft.)

C.6 Group 4c: Small Enclosures

Small enclosures are small enclosures or panels less than 12 cubic feet in physical dimensions. Small switching enclosures include wall mounted distribution panels (Figures C-22 and C-24), and disconnect switches (Figure C-23).

Figure C-22
Wall Mounted Small Enclosures

Figure C-23
Wall Mounted Low Voltage AC Fused Disconnect Switches

Figure C-24
125 VDC Distribution Panel (Left) and 120 VAC Distribution Panel (Right)

C.7 Large (Group 4a) and Medium (Group 4b) Enclosure Internals

C.7.1 "Default" Loading Configurations [Sub-Category 4a(a) and 4b(a)]

Figures C-25 through C-27 provide examples of internal electrical enclosure combustible mass and loading configurations for which the "Default" HRR values in Table 4-2 are recommended to be used.

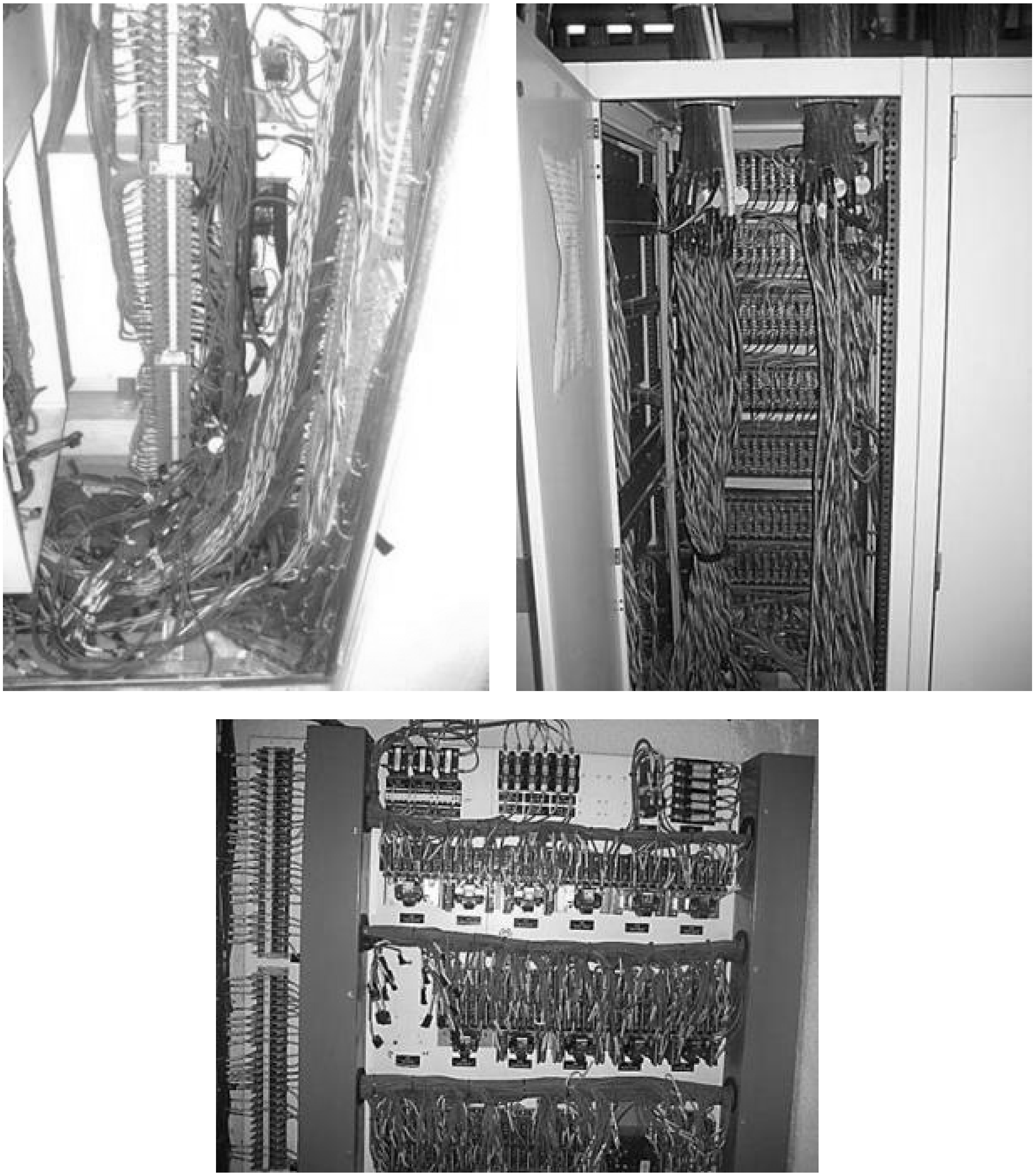

Figure C-25

Internal Enclosure Fuel Loading for Default Sub-Category (1 of 3)

Note in particular the enclosure to the upper left, which has disorderly internal enclosure wiring and loose legacy or extra field wires at the bottom.

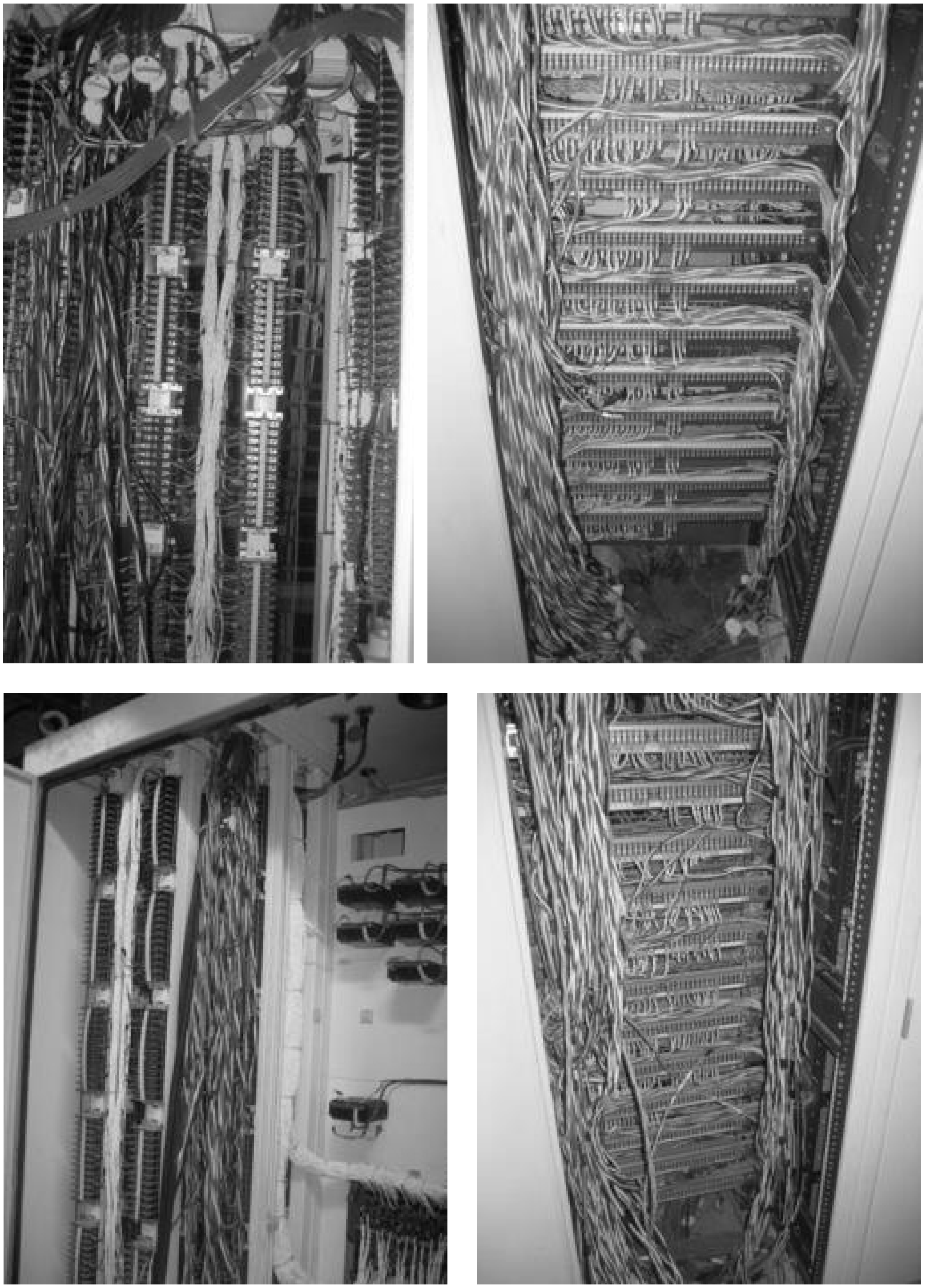

Figure C-26

Internal Enclosure Fuel Loading for Default Sub-Category (2 of 3)

The bottom examples are somewhat extreme in terms of cable loading and loose bundling. Note in particular the enclosure to the lower left, which has a combination of orderly internal enclosure wiring (white wires on the right side of the enclosure) and loose disorderly field wires (center).

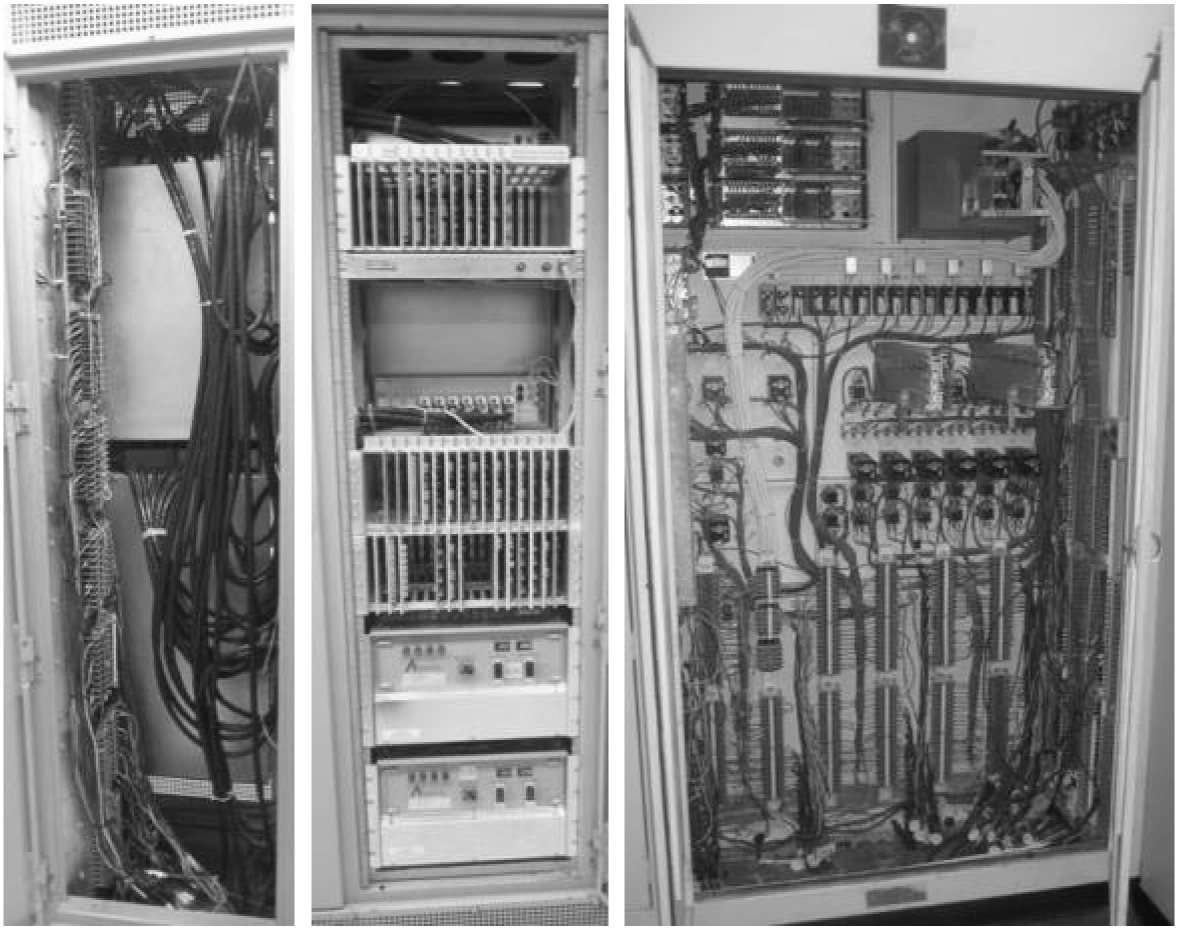

Figure C-27
Internal Enclosure Fuel Loading for Default Sub-Category (3 of 3)
Note that the enclosures on the left and right have many small cables that are not tightly bundled. The enclosure in the center has a significant load of printed circuit cards which are also combustible.

C.7.2 "Low Fuel Loading" Configurations [Sub-Category 4a(b) and 4b(b)]

"Low Fuel Loading" HRR estimates can be used for electrical enclosures whose internal panel wiring is tightly bundled throughout the enclosure. The tight bundling configuration is believed to reduce the surface area of polymeric material being heated from thermal fire conditions and limits to some extent the availability of oxygen to interact with the surface of the combustible. Thus, the tight bundling is believed to reduce the spread rate and heat release rate as shown from experimental testing, and the recommended HRR distributions in Table 4-2 could be used. Figures C-28 and C-29 present internal photographs of electrical enclosures containing panel wiring tightly bundled.

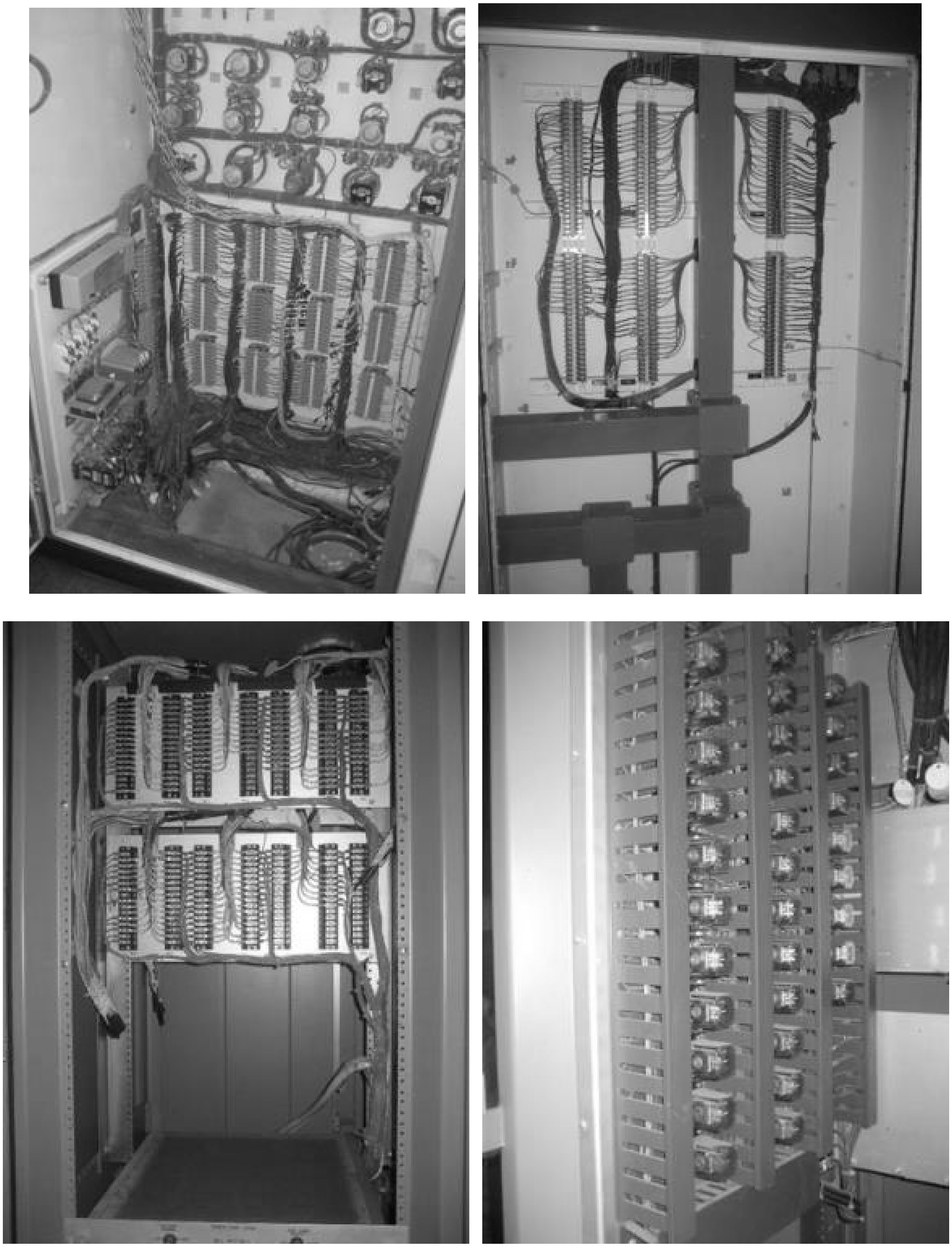

Figure C-28
Examples of “Low Fuel Loading” Sub-Category (1 of 2)
Note that cables are neatly routed and tightly bundled and that there is a relatively low fuel loading given the overall enclosure volume.

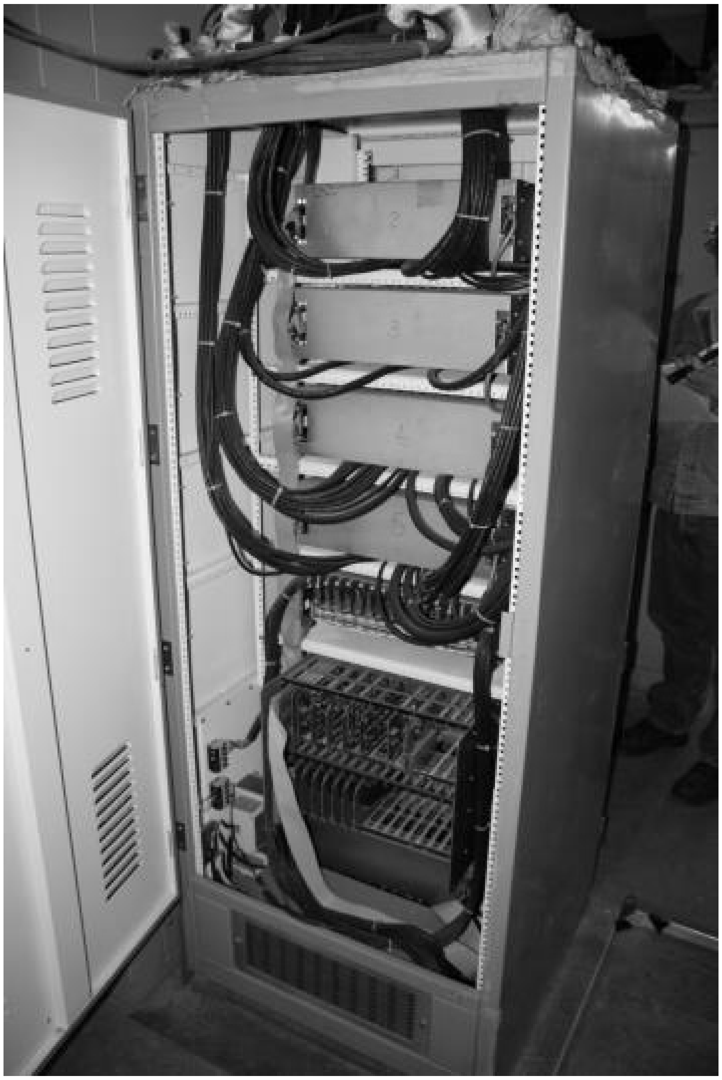

Figure C-29
Examples of "Low Fuel Loading" Sub-Category (2 of 2)
Note that larger size cables are neatly routed and tightly bundled and that there is a relatively low fuel loading given the overall enclosure volume.

C.7.3 "Very Low Fuel Loading" Configurations [Sub-Category 4a(c) and 4b(c)]

"Very Low Fuel Loading" HRR estimates can be used for electrical enclosures that have limited internal panel wiring throughout the enclosure. To classify an electrical enclosure "Very Low Fuel Loading" the internal combustible loading of an electrical enclosure must be minimal (less than 5% combustible volume) and the HRR distributions in Table 4-2 could be used. Figure C-30 presents internal photographs of electrical enclosures with limited panel wiring representative of the "Very Low Fuel Loading" configuration.

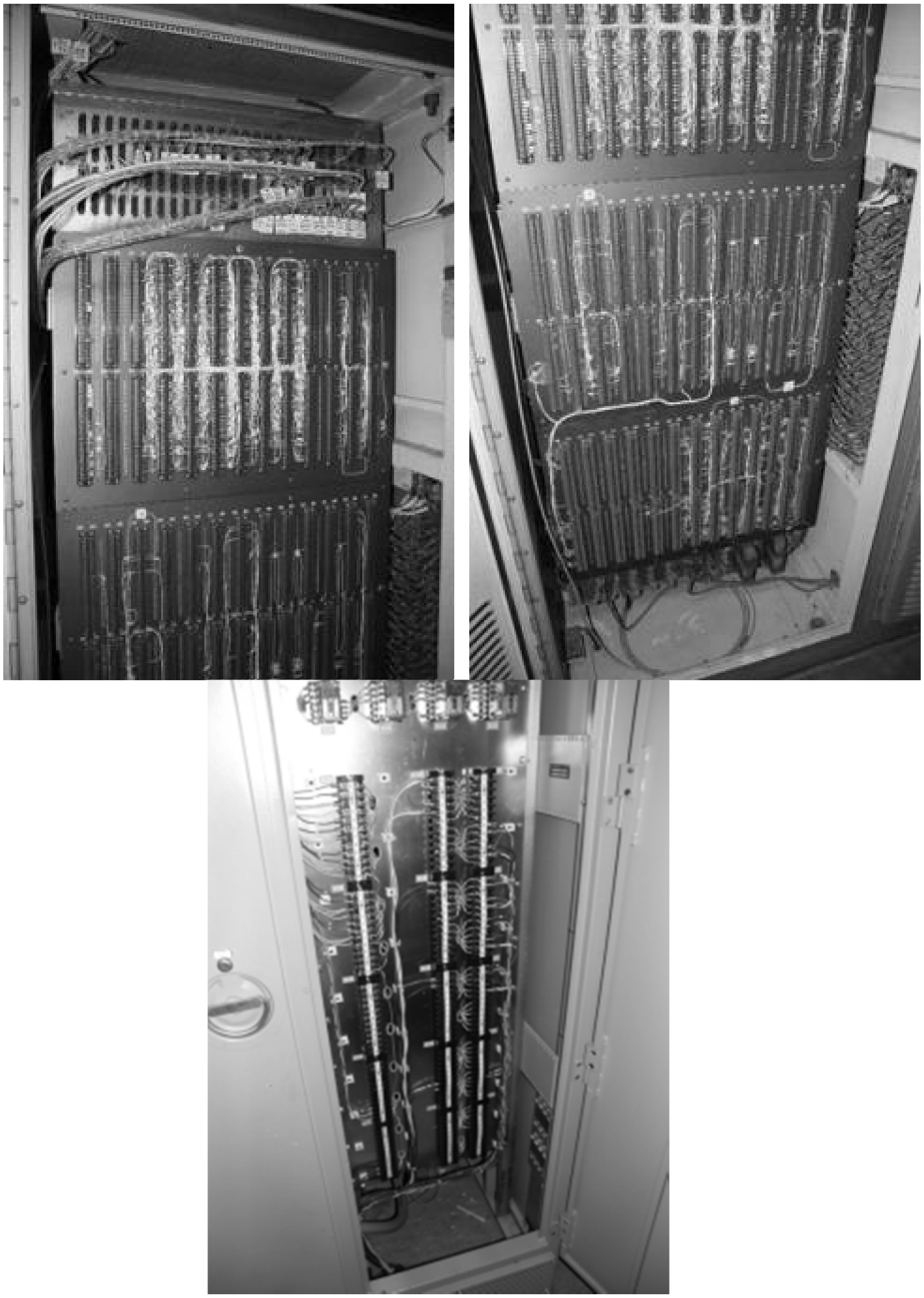

Figure C-30
Examples of "Very Low Fuel Loading" Sub-Category

Appendix D
Electrical Cabinet Heat Release Rate Data Analysis

This appendix provides technical details for determining the alpha and beta parameters for the gamma distributions representing the peak heat release rate (HRR) for electrical enclosures. A total of 25 different electrical enclosure classifications have been assigned gamma probability distributions. The classifications are based on type of cabinets (i.e., cabinet function), size, doors open or closed, thermoset (TS) or thermoplastic (TP) cables, and cable loading. The list of data sources used in the current analysis is provided in Appendix D.1. The data classification for each cabinet fire test is presented in a matrix format in Appendix D.2. The alpha and beta parameters characterizing each gamma distribution are provided in Appendix D.3. Appendix D.3 also describes the methodology for calculating the values within the Microsoft Excel Workbook. Finally, in Appendix D.4, a figure is provided for each cabinet classification, comparing the empirical distribution and the gamma distributions recommended by the working group.

D.1 Data Sources

The following test reports contain the results of fire experiments involving electrical cabinets that are commonly used in nuclear power plants (NPPs). Following each reference, the tests that are included and excluded in the current analysis are identified.

- Chavez, J. (1987), An Experimental Investigation of Internally Ignited Fires in Nuclear Power Plant Control Cabinets: Part I: Cabinet Effects Tests, NUREG/CR-4527 Volume 1, U.S. Nuclear Regulatory Commission, Washington, DC.
    - All tests SNL-ST1 through SNL-ST11 are included in the analysis.
    - Tests SNL-PCT1, SNL-PCT3, SNL-PCT5, and PCT6 are included in the analysis.
        - SNL-PCT2 is excluded because the test involved a large ignition source that is not representative of NPPs.
        - SNL-PCT4A and SNL-PCT4C are excluded because the tests did not involve cables.
- Chavez, J., Nowlen, S. (1988), An Experimental Investigation of Internally Ignited Fires in Nuclear Power Plant Control Cabinets: Part II: Room Effects Tests, NUREG/CR-4527 Volume 2, U.S. Nuclear Regulatory Commission, Washington, DC.
    - Tests 24 and 25 are included in the analysis
        - Test 21 and Test 22 are excluded because the tests did not involve cables.
        - Test 23 is excluded because the test involved a transient ignition source that is not representative of NPPs.
- Mangs, J., Keski-Rahkonen, O. (1994), Full Scale Fire Experiments on Electronic Cabinets, VTT Publications 186, VTT Technical Research Centre of Finland.
    - All VTT186 tests are included.

- Mangs, J., Keski-Rahkonen, O. (1996), Full Scale Fire Experiments on Electronic Cabinets II, VTT Publications 269, VTT Technical Research Centre of Finland.
    - All VTT269 tests are included.
- Mangs, J. (2004), On the Fire Dynamics of Vehicles and Electrical Equipment, VTT Publications 521, VTT Technical Research Centre of Finland.
    - All VTT521 tests are included.
- Plumecocq, W., M. Coutin, S. Melis, L. Rigollet (2011), Characterization of closed-doors electrical cabinet fires in compartments, Fire Safety Journal 46, pp. 243-253.
    - CAA and CAB test series are excluded because the contents of the cabinets were not typical of electrical cabinets in NPPs; i.e., polymethyl methacrylate (PMMA).
    - CAO tests are excluded because the contents of the cabinets are not well characterized.
- McGrattan, K., S. Bareham (2014), Heat Release Rates of Electrical Enclosure Fires (HELEN-FIRE), NUREG/CR-7197, National Institute of Standards and Technology, Gaithersburg, Maryland.
    - All tests CBD-1 through CBD-112 are included.

D.2 Data Classification

The experimental data referenced in Appendix D.1 are classified in Table D-1 below. The categories are based on:

Doors: Open (O) or Closed (C). In addition, closed and open door data for Power SWGR, Power MCC, and Control Small are grouped together.

Thermoset (TS) or **Thermoplastic** (TP). For the purposes of this data classification, experiments using qualified cable are designated as thermoset. Experiments with unqualified cables are designated as thermoplastic.

Enclosure Size: Small (S), <0.3 m^3 (12 ft^3); Medium (M), 0.3 m^3 to 1.7 m^3 (12 ft^3 to 60 ft^3); Large (L), >1.4 m^3 (50 ft^3). Comments in the last column of Table D-1 provide exceptions to these categories, for example medium cabinets with heavy cable loading are put in the Large classification. Notice that cabinets between 1.4 m^3 and 1.7 m^3 (50 ft^3 and 60 ft^3) are classified as both Medium and Large.

Cable Loading: Default (D) or Low (L). This category describes how the cables are configured, based on visual inspection of photographs. Default refers to cables that are hanging loose and not neatly bundled. Low refers to cables that are neatly bundled. Default is also used when the cable loading is unknown.

Fuel Mass: Kilograms of fuel within the cabinet

Types of Cabinets:

Power switchgear and load center (Power SWGR & LC): contains one small bundle within the breaker box; most cables are located at the top; contains three unspliced cables in the back; contains spliced cables for the control/monitoring equipment

Power motor control center and charger (Power MCC): contains one small bundle within the breaker box; most cables are located at the top; contains only three unspliced cables in the back

Control Large: Large Control cabinets (volume >1.4 m^3 (50 ft^3)), see comment column for exceptions

Control Medium and Inverter (Control Medium): Medium Control cabinets and inverters (volume 0.3 m^3 to 1.7 m^3 (12 ft^3 to 60 ft^3)), see comment column for exceptions

Control Small: Small Control cabinets (cabinet volume <0.3 m^3 (12 ft^3) or fuel mass <1 kg)

Low or VLow: The Control cabinets with “Low” or “VLow” in the title refer to the Cable Loading of the cabinet. The experimental data is divided into two classifications—default and low—based on visual inspection. If the Cable Loading is Low, the experimental data is included in the columns marked Low and VLow. The distinction between Low and VLow is used by the expert panel. The panel developed gamma distributions for three classifications—default, low, and very low—which are used for comparison to the experimental data, as shown in Appendix D.3 and Appendix D.4.

Classification: Heat release rate (kW) or FALSE (F). For each test that is included, the peak HRR is provided in kilowatts. If the experiment is not included, FALSE (F) is indicated.

Table D-1
Matrix of Experiments and Cabinet Characteristics

Test ID	Characteristics of the Experiments					Types of Cabinets (Heat Release Rate of Experiment, kW)																									
	Doors	Thermo-set or Thermo-plastic	Enclosure Size	Cable Loading	Fuel Mass (kg)	Power SWGR & LC TS	Power SWGR & LC TP	Power MCC TS	Power MCC TP	Control Large Close TS	Control Large Close TS (Low)	Control Large Close TS (VLow)	Control Large Close TP	Control Large Close TP (Low)	Control Large Close TP (VLow)	Control Large Open TS	Control Large Open TS (Low)	Control Large Open TS (VLow)	Control Large Open TP	Control Large Open TP (Low)	Control Large Open TP (VLow)	Control Medium Close TS	Control Medium Close TS (Low)	Control Medium Close TP	Control Medium Close TP (Low)	Control Medium Open TS	Control Medium Open TS (Low)	Control Medium Open TP	Control Medium Open TP (Low)	Control Small	Comment
SNL-ST1	O	TS	M, L	D	N/A	24	F	24	F	F	F	F	F	F	F	24	F	F	F	F	F	F	F	F	F	24	F	F	F	F	
SNL-ST2	O	TS	M, L	D	N/A	27	F	27	F	F	F	F	F	F	F	27	F	F	F	F	F	F	F	F	F	27	F	F	F	F	
SNL-ST3	O	TS	M, L	D	N/A	77	F	77	F	F	F	F	F	F	F	77	F	F	F	F	F	F	F	F	F	77	F	F	F	F	
SNL-ST4	O	TS	M, L	D	N/A	82	F	82	F	F	F	F	F	F	F	82	F	F	F	F	F	F	F	F	F	82	F	F	F	F	
SNL-ST5	O	TP	M, L	D	N/A	F	F	F	F	F	F	F	F	F	F	F	F	F	132	F	F	F	F	F	F	F	F	132	F	F	
SNL-ST6	O	TS	L	D	N/A	F	F	F	F	F	F	F	F	F	F	82	F	F	F	F	F	F	F	F	F	F	F	F	F	F	
SNL-ST7	C	TS	L	D	N/A	F	F	F	F	95	F	F	F	F	F	F	F	F	F	F	F	F	F	F	F	F	F	F	F	F	
SNL-ST8	C	TS	L	D	N/A	F	F	F	F	93	F	F	F	F	F	F	F	F	F	F	F	F	F	F	F	F	F	F	F	F	
SNL-ST9	O	TS	L	D	N/A	F	F	F	F	F	F	F	F	F	F	74	F	F	F	F	F	F	F	F	F	F	F	F	F	F	
SNL-ST10	C	TP	L	N	N/A	F	F	F	F	F	F	F	280	F	F	F	F	F	F	F	F	F	F	F	F	F	F	F	F	F	
SNL-ST11	O	TP	L	D	N/A	F	F	F	F	F	F	F	F	F	F	F	F	F	506	F	F	F	F	F	F	F	F	F	F	F	
SNL-PCT1	C	TP	L	D	N/A	F	F	F	F	F	F	F	185	F	F	F	F	F	F	F	F	F	F	F	F	F	F	F	F	F	
SNL-PCT3	O	TS	L	D	N/A	F	F	F	F	F	F	F	F	F	F	56	F	F	F	F	F	F	F	F	F	F	F	F	F	F	
SNL-PCT5	O	TP	L	D	N/A	F	F	F	F	F	F	F	F	F	F	F	F	F	791	F	F	F	F	F	F	F	F	F	F	F	
SNL-PCT6	O	TS	L	D	N/A	F	F	F	F	F	F	F	F	F	F	215	F	F	F	F	F	F	F	F	F	F	F	F	F	F	

Table D-1
Matrix of Experiments and Cabinet Characteristics

Test ID	Characteristics of the Experiments					Types of Cabinets (Heat Release Rate of Experiment, kW)																									
	Doors	Thermo-set or Thermo-plastic	Enclosure Size	Cable Loading	Fuel Mass (kg)	Power SWGR & LC TS	Power SWGR & LC TP	Power MCC TS	Power MCC TP	Control Large Close TS	Control Large Close TS (Low)	Control Large Close TS (VLow)	Control Large Close TP	Control Large Close TP (Low)	Control Large Close TP (VLow)	Control Large Open TS	Control Large Open TS (Low)	Control Large Open TS (VLow)	Control Large Open TP	Control Large Open TP (Low)	Control Large Open TP (VLow)	Control Medium Close TS	Control Medium Close TS (Low)	Control Medium Close TP	Control Medium Close TP (Low)	Control Medium Open TS	Control Medium Open TS (Low)	Control Medium Open TP	Control Medium Open TP (Low)	Control Small	Comment
SNL-Test24	O	TP	L	D	N/A	F	F	F	F	F	F	F	F	F	F	F	F	F	1300	F	F	F	F	F	F	F	F	F	F	F	
SNL-Test25	O	TP	L	D	N/A	F	F	F	F	F	F	F	F	F	F	F	F	F	840	F	F	F	F	F	F	F	F	F	F	F	
VTT186-Exp1	C	TP	M	D	N/A	F	F	F	F	F	F	F	400	F	F	F	F	F	F	F	F	F	F	F	F	F	F	F	F	F	1
VTT186-Exp2	C	TP	M	D	N/A	F	F	F	F	F	F	F	50	F	F	F	F	F	F	F	F	F	F	F	F	F	F	F	F	F	1
VTT186-Exp3-1	C	TP	M	D	N/A	F	F	F	F	F	F	F	0	F	F	F	F	F	F	F	F	F	F	F	F	F	F	F	F	F	1
VTT186-Exp3-2	C	TP	M	D	N/A	F	F	F	F	F	F	F	200	F	F	F	F	F	F	F	F	F	F	F	F	F	F	F	F	F	1
VTT269-Exp1	C	TP	M	D	N/A	F	F	F	F	F	F	F	180	F	F	F	F	F	F	F	F	F	F	F	F	F	F	F	F	F	1
VTT269-Exp2A	C	TP	M	D	N/A	F	F	F	F	F	F	F	0	F	F	F	F	F	F	F	F	F	F	F	F	F	F	F	F	F	1
VTT269-Exp2B	C	TP	M	D	N/A	F	F	F	F	F	F	F	0	F	F	F	F	F	F	F	F	F	F	F	F	F	F	F	F	F	1
VTT269-Exp2C	C	TP	M	D	N/A	F	F	F	F	F	F	F	120	F	F	F	F	F	F	F	F	F	F	F	F	F	F	F	F	F	1
VTT269-Exp3	C	TP	M	D	N/A	F	F	F	F	F	F	F	100	F	F	F	F	F	F	F	F	F	F	F	F	F	F	F	F	F	1
VTT521-Exp1	C	TP	M	D	N/A	F	F	F	F	F	F	F	175	F	F	F	F	F	F	F	F	F	F	F	F	F	F	F	F	F	1
VTT521-Exp2A	C	TP	M	D	N/A	F	F	F	F	F	F	F	0	F	F	F	F	F	F	F	F	F	F	F	F	F	F	F	F	F	1
VTT521-Exp2B	C	TP	M	D	N/A	F	F	F	F	F	F	F	0	F	F	F	F	F	F	F	F	F	F	F	F	F	F	F	F	F	1
VTT521-Exp2C	C	TP	M	D	N/A	F	F	F	F	F	F	F	125	F	F	F	F	F	F	F	F	F	F	F	F	F	F	F	F	F	1
VTT521-Exp3	C	TP	M	D	N/A	F	F	F	F	F	F	F	100	F	F	F	F	F	F	F	F	F	F	F	F	F	F	F	F	F	1

Table D-1
Matrix of Experiments and Cabinet Characteristics

Test ID	Characteristics of the Experiments					Types of Cabinets (Heat Release Rate of Experiment, kW)																									
	Doors	Thermo-set or Thermo-plastic	Enclosure Size	Cable Loading	Fuel Mass (kg)	Power SWGR & LC TS	Power SWGR & LC TP	Power MCC TS	Power MCC TP	Control Large Close TS	Control Large Close TS (Low)	Control Large Close TS (VLow)	Control Large Close TP	Control Large Close TP (Low)	Control Large Close TP (VLow)	Control Large Open TS	Control Large Open TS (Low)	Control Large Open TS (VLow)	Control Large Open TP	Control Large Open TP (Low)	Control Large Open TP (VLow)	Control Medium Close TS	Control Medium Close TS (Low)	Control Medium Close TP	Control Medium Close TP (Low)	Control Medium Open TS	Control Medium Open TS (Low)	Control Medium Open TP	Control Medium Open TP (Low)	Control Small	Comment
VTT521-Exp4	C	TP	M	D	N/A	F	F	F	F	F	F	F	400	F	F	F	F	F	F	F	F	F	F	F	F	F	F	F	F	F	1
VTT521-Exp5	C	TP	M	D	N/A	F	F	F	F	F	F	F	50	F	F	F	F	F	F	F	F	F	F	F	F	F	F	F	F	F	1
VTT521-Exp6A	C	TP	M	D	N/A	F	F	F	F	F	F	F	0	F	F	F	F	F	F	F	F	F	F	F	F	F	F	F	F	F	1
VTT521-Exp6B	C	TP	M	D	N/A	F	F	F	F	F	F	F	200	F	F	F	F	F	F	F	F	F	F	F	F	F	F	F	F	F	1
VTT521-Exp7	C	TP	S	D	N/A	F	F	F	F	F	F	F	F	F	F	F	F	F	F	F	F	F	F	F	F	F	F	F	F	35	
VTT521-Exp8	C	TP	S	D	N/A	F	F	F	F	F	F	F	F	F	F	F	F	F	F	F	F	F	F	F	F	F	F	F	F	20	
VTT521-Exp9	C	TP	S	D	N/A	F	F	F	F	F	F	F	F	F	F	F	F	F	F	F	F	F	F	F	F	F	F	F	F	40	
VTT521-Exp10	C	TP	S	D	N/A	F	F	F	F	F	F	F	F	F	F	F	F	F	F	F	F	F	F	F	F	F	F	F	F	20	
CBD-1	O	TS	M	D	0.1	F	F	F	F	F	F	F	F	F	F	F	F	F	F	F	F	F	F	F	F	F	F	F	F	2	2
CBD-2	O	TS	M	L	0.1	F	F	F	F	F	F	F	F	F	F	F	F	F	F	F	F	F	F	F	F	F	F	F	F	2	2
CBD-3	O	TS	M	L	0.1	F	F	F	F	F	F	F	F	F	F	F	F	F	F	F	F	F	F	F	F	F	F	F	F	2	2
CBD-4	O	TS	M	L	0.1	F	F	F	F	F	F	F	F	F	F	F	F	F	F	F	F	F	F	F	F	F	F	F	F	2	2
CBD-5	O	TS	M	L	0.1	F	F	F	F	F	F	F	F	F	F	F	F	F	F	F	F	F	F	F	F	F	F	F	F	1	2
CBD-6	O	TS	M, L	L	0.1	F	F	F	F	F	F	F	F	F	F	F	F	F	F	F	F	F	F	F	F	F	F	F	F	2	2
CBD-7	O	TS	M, L	L	0.1	F	F	F	F	F	F	F	F	F	F	F	F	F	F	F	F	F	F	F	F	F	F	F	F	9	2
CBD-8	O	TS	L	D	0.1	F	F	F	F	F	F	F	F	F	F	F	F	F	F	F	F	F	F	F	F	F	F	F	F	0	2

Table D-1
Matrix of Experiments and Cabinet Characteristics

Test ID	Characteristics of the Experiments					Types of Cabinets (Heat Release Rate of Experiment, kW)																									
	Doors	Thermo-set or Thermo-plastic	Enclosure Size	Cable Loading	Fuel Mass (kg)	Power SWGR & LC TS	Power SWGR & LC TP	Power MCC TS	Power MCC TP	Control Large Close TS	Control Large Close TS (Low)	Control Large Close TS (VLow)	Control Large Close TP	Control Large Close TP (Low)	Control Large Close TP (VLow)	Control Large Open TS	Control Large Open TS (Low)	Control Large Open TS (VLow)	Control Large Open TP	Control Large Open TP (Low)	Control Large Open TP (VLow)	Control Medium Close TS	Control Medium Close TS (Low)	Control Medium Close TP	Control Medium Close TP (Low)	Control Medium Open TS	Control Medium Open TS (Low)	Control Medium Open TP	Control Medium Open TP (Low)	Control Small	Comment
CBD-9	O	TS	L	D	0.1	F	F	F	F	F	F	F	F	F	F	F	F	F	F	F	F	F	F	F	F	F	F	F	F	1	2
CBD-10	O	TS	L	D	0.1	F	F	F	F	F	F	F	F	F	F	F	F	F	F	F	F	F	F	F	F	F	F	F	F	1	2
CBD-11	O	TS	M	D	11	F	F	F	F	F	F	F	F	F	F	F	F	F	F	F	F	F	F	F	F	1	F	F	F	F	
CBD-12	C	TS	M	D	11	F	F	F	F	F	F	F	F	F	F	F	F	F	F	F	F	52	F	F	F	F	F	F	F	F	
CBD-13	C	TS	M	D	0.1	F	F	F	F	F	F	F	F	F	F	F	F	F	F	F	F	F	F	F	F	F	F	F	F	2	2
CBD-14	C	TS	M	D	0.1	F	F	F	F	F	F	F	F	F	F	F	F	F	F	F	F	F	F	F	F	F	F	F	F	4	2
CBD-15	O	TS	M, L	L	3.4	3	F	3	F	F	F	F	F	F	F	F	3	3	F	F	F	F	F	F	F	F	3	F	F	F	
CBD-16	O	TS	M, L	L	1.9	F	F	F	F	F	F	F	F	F	F	F	2	2	F	F	F	F	F	F	F	F	2	F	F	F	
CBD-17	O	TS	M, L	L	2.7	0	F	0	F	F	F	F	F	F	F	F	0	0	F	F	F	F	F	F	F	F	0	F	F	F	
CBD-18	O	TP	M, L	L	1.8	F	F	F	F	F	F	F	F	F	F	F	F	F	F	3	3	F	F	F	F	F	F	F	3	F	
CBD-19	C	TS	M, L	L	3.4	F	F	F	F	F	3	3	F	F	F	F	F	F	F	F	F	F	3	F	F	F	F	F	F	F	
CBD-20	C	TS	M, L	L	1.9	F	F	F	F	F	5	5	F	F	F	F	F	F	F	F	F	F	5	F	F	F	F	F	F	F	
CBD-21	C	TS	M, L	L	1.9	4	F	4	F	F	4	4	F	F	F	F	F	F	F	F	F	F	4	F	F	F	F	F	F	F	
CBD-22	C	TS	M, L	L	1.9	F	F	F	F	F	4	4	F	F	F	F	F	F	F	F	F	F	4	F	F	F	F	F	F	F	
CBD-23	O	TP	M, L	L	1.6	F	F	F	F	F	F	F	F	F	F	F	F	F	F	18	18	F	F	F	F	F	F	F	18	F	
CBD-24	C	TS	M, L	L	0.7	F	F	F	F	F	F	F	F	F	F	F	F	F	F	F	F	F	F	F	F	F	F	F	F	4	2

Table D-1
Matrix of Experiments and Cabinet Characteristics

Test ID	Characteristics of the Experiments					Types of Cabinets (Heat Release Rate of Experiment, kW)																									
	Doors	Thermo-set or Thermo-plastic	Enclosure Size	Cable Loading	Fuel Mass (kg)	Power SWGR & LC TS	Power SWGR & LC TP	Power MCC TS	Power MCC TP	Control Large Close TS	Control Large Close TS (Low)	Control Large Close TS (VLow)	Control Large Close TP	Control Large Close TP (Low)	Control Large Close TP (VLow)	Control Large Open TS	Control Large Open TS (Low)	Control Large Open TS (VLow)	Control Large Open TP	Control Large Open TP (Low)	Control Large Open TP (VLow)	Control Medium Close TS	Control Medium Close TS (Low)	Control Medium Close TP	Control Medium Close TP (Low)	Control Medium Open TS	Control Medium Open TS (Low)	Control Medium Open TP	Control Medium Open TP (Low)	Control Small	Comment
CBD-25	C	TS	M	D	3.1	F	F	F	F	F	F	F	F	F	F	F	F	F	F	F	F	4	F	F	F	F	F	F	F	F	
CBD-26	C	TS	M	D	3.1	F	F	F	F	F	F	F	F	F	F	F	F	F	F	F	F	1	F	F	F	F	F	F	F	F	
CBD-27	C	TS	M	D	3.1	F	F	F	F	F	F	F	F	F	F	F	F	F	F	F	F	1	F	F	F	F	F	F	F	F	
CBD-28	C	TS	M	D	3.1	F	F	F	F	F	F	F	F	F	F	F	F	F	F	F	F	1	F	F	F	F	F	F	F	F	
CBD-28B	O	TS	M	D	3.1	F	F	F	F	F	F	F	F	F	F	F	F	F	F	F	F	F	F	F	F	10	F	F	F	F	
CBD-29	C	TS	M	D	3.1	F	F	F	F	F	F	F	F	F	F	F	F	F	F	F	F	82	F	F	F	F	F	F	F	F	
CBD-30	C	TS	M	D	3.1	F	F	F	F	F	F	F	F	F	F	F	F	F	F	F	F	72	F	F	F	F	F	F	F	F	
CBD-31	C	TS	M, L	D	0.7	F	F	F	F	F	F	F	F	F	F	F	F	F	F	F	F	F	F	F	F	F	F	F	F	28	2
CBD-32	C	TS	M, L	D	0.7	F	F	F	F	F	F	F	F	F	F	F	F	F	F	F	F	F	F	F	F	F	F	F	F	6	2
CBD-33	C	TS	M, L	D	1.5	F	F	F	F	50	F	F	F	F	F	F	F	F	F	F	F	50	F	F	F	F	F	F	F	F	
CBD-34	C	TS	M, L	D	1.5	F	F	F	F	35	F	F	F	F	F	F	F	F	F	F	F	35	F	F	F	F	F	F	F	F	
CBD-35	O	TS	M	D	12	F	F	F	F	F	F	F	F	F	F	F	F	F	F	F	F	F	F	F	F	146	F	F	F	F	
CBD-36	C	TS	M	D	2.8	F	F	F	F	F	F	F	F	F	F	F	F	F	F	F	F	4	F	F	F	F	F	F	F	F	
CBD-37	C	TS	M	D	5.5	F	F	F	F	F	F	F	F	F	F	F	F	F	F	F	F	35	F	F	F	F	F	F	F	F	
CBD-38	C	TS	M	D	5.5	F	F	F	F	F	F	F	F	F	F	F	F	F	F	F	F	169	F	F	F	F	F	F	F	F	
CBD-39	C	TS	M	D	5.8	F	F	F	F	F	F	F	F	F	F	F	F	F	F	F	F	60	F	F	F	F	F	F	F	F	

Table D-1
Matrix of Experiments and Cabinet Characteristics

Test ID	Characteristics of the Experiments					Types of Cabinets (Heat Release Rate of Experiment, kW)																									
	Doors	Thermo-set or Thermo-plastic	Enclosure Size	Cable Loading	Fuel Mass (kg)	Power SWGR & LC TS	Power SWGR & LC TP	Power MCC TS	Power MCC TP	Control Large Close TS	Control Large Close TS (Low)	Control Large Close TS (VLow)	Control Large Close TP	Control Large Close TP (Low)	Control Large Close TP (VLow)	Control Large Open TS	Control Large Open TS (Low)	Control Large Open TS (VLow)	Control Large Open TP	Control Large Open TP (Low)	Control Large Open TP (VLow)	Control Medium Close TS	Control Medium Close TS (Low)	Control Medium Close TP	Control Medium Close TP (Low)	Control Medium Open TS	Control Medium Open TS (Low)	Control Medium Open TP	Control Medium Open TP (Low)	Control Small	Comment
CBD-40	C	TS	L	D	0.1	F	F	F	F	F	F	F	F	F	F	F	F	F	F	F	F	F	F	F	F	F	F	F	F	2	2
CBD-41	C	TS	L	D	5	F	F	F	F	115	F	F	F	F	F	F	F	F	F	F	F	F	F	F	F	F	F	F	F	F	
CBD-41B	O	TS	L	D	5	F	F	F	F	F	F	F	F	F	F	232	F	F	F	F	F	F	F	F	F	F	F	F	F	F	
CBD-42	C	TS	M, L	L	2.9	34	F	34	F	F	34	34	F	F	F	F	F	F	F	F	F	F	34	F	F	F	F	F	F	F	
CBD-43	C	TS	M, L	L	2.9	F	F	F	F	F	18	18	F	F	F	F	F	F	F	F	F	F	18	F	F	F	F	F	F	F	
CBD-44	C	TS	M, L	D	2.9	F	F	F	F	31	F	F	F	F	F	F	F	F	F	F	F	31	F	F	F	F	F	F	F	F	
CBD-45	C	TS	M, L	D	2.9	F	F	F	F	5	F	F	F	F	F	F	F	F	F	F	F	5	F	F	F	F	F	F	F	F	
CBD-46	C	TS	M, L	D	2.8	F	F	F	F	45	F	F	F	F	F	F	F	F	F	F	F	45	F	F	F	F	F	F	F	F	
CBD-47	C	TS	M, L	L	1.4	F	F	F	F	F	40	40	F	F	F	F	F	F	F	F	F	F	40	F	F	F	F	F	F	F	
CBD-48	O	TS	M, L	D	2.8	F	F	F	F	F	F	F	F	F	F	87	F	F	F	F	F	F	F	F	F	87	F	F	F	F	
CBD-49	C	TS	M, L	D	2.8	F	F	F	F	50	F	F	F	F	F	F	F	F	F	F	F	50	F	F	F	F	F	F	F	F	
CBD-50	C	TS	M, L	D	1.4	F	F	F	F	1	F	F	F	F	F	F	F	F	F	F	F	1	F	F	F	F	F	F	F	F	
CBD-51	O	TS	M, L	L	1.4	F	F	F	F	F	F	F	F	F	F	F	31	31	F	F	F	F	F	F	F	F	31	F	F	F	
CBD-52	O	TS	M, L	D	2.8	F	F	F	F	F	F	F	F	F	F	122	F	F	F	F	F	F	F	F	F	122	F	F	F	F	
CBD-53	C	TS	M, L	D	2.8	F	F	F	F	55	F	F	F	F	F	F	F	F	F	F	F	55	F	F	F	F	F	F	F	F	
CBD-53B	O	TS	M, L	D	2.8	F	F	F	F	F	F	F	F	F	F	85	F	F	F	F	F	F	F	F	F	85	F	F	F	F	

Table D-1
Matrix of Experiments and Cabinet Characteristics

Test ID	Characteristics of the Experiments					Types of Cabinets (Heat Release Rate of Experiment, kW)																									
	Doors	Thermo-set or Thermo-plastic	Enclosure Size	Cable Loading	Fuel Mass (kg)	Power SWGR & LC TS	Power SWGR & LC TP	Power MCC TS	Power MCC TP	Control Large Close TS	Control Large Close TS (Low)	Control Large Close TS (VLow)	Control Large Close TP	Control Large Close TP (Low)	Control Large Close TP (VLow)	Control Large Open TS	Control Large Open TS (Low)	Control Large Open TS (VLow)	Control Large Open TP	Control Large Open TP (Low)	Control Large Open TP (VLow)	Control Medium Close TS	Control Medium Close TS (Low)	Control Medium Close TP	Control Medium Close TP (Low)	Control Medium Open TS	Control Medium Open TS (Low)	Control Medium Open TP	Control Medium Open TP (Low)	Control Small	Comment
CBD-54	O	TP	M, L	N	1.6	F	F	F	F	F	F	F	F	F	F	F	F	F	94	F	F	F	F	F	F	F	F	94	F	F	
CBD-55	C	TP	M, L	L	3.1	F	F	F	F	F	F	F	F	21	21	F	F	F	F	F	F	F	F	F	21	F	F	F	F	F	
CBD-56	C	TP	M, L	L	1.7	F	F	F	F	F	F	F	F	8	8	F	F	F	F	F	F	F	F	F	8	F	F	F	F	F	
CBD-57	C	TP	M, L	L	1.7	F	F	F	F	F	F	F	F	5	5	F	F	F	F	F	F	F	F	F	5	F	F	F	F	F	
CBD-58	C	TP	M, L	D	3.4	F	F	F	F	F	F	F	26	F	F	F	F	F	F	F	F	F	F	26	F	F	F	F	F	F	
CBD-59	O	TP	M, L	D	3.4	F	F	F	F	F	F	F	F	F	F	F	F	F	22	F	F	F	F	F	F	F	F	22	F	F	
CBD-60	C	TP	M	D	7.4	F	F	F	F	F	F	F	F	F	F	F	F	F	F	F	F	F	F	88	F	F	F	F	F	F	
CBD-61	C	TS	M	D	12	F	F	F	F	F	F	F	F	F	F	F	F	F	F	F	F	5	F	F	F	F	F	F	F	F	
CBD-62	C	TS	M	D	12	F	F	F	F	F	F	F	F	F	F	F	F	F	F	F	F	3	F	F	F	F	F	F	F	F	
CBD-63	C	TS	M	D	12	F	F	F	F	F	F	F	F	F	F	F	F	F	F	F	F	92	F	F	F	F	F	F	F	F	
CBD-64	C	TS	M	D	6	6	F	F	F	F	F	F	F	F	F	F	F	F	F	F	F	6	F	F	F	F	F	F	F	F	
CBD-65	C	TS	M	D	6	7	F	F	F	F	F	F	F	F	F	F	F	F	F	F	F	7	F	F	F	F	F	F	F	F	
CBD-66	C	TP	M, L	L	3.4	F	F	F	F	F	F	F	F	26	26	F	F	F	F	F	F	F	F	F	26	F	F	F	F	F	
CBD-66B	O	TP	M, L	L	3.4	F	F	F	F	F	F	F	F	F	F	F	F	F	F	26	26	F	F	F	F	F	F	F	26	F	
CBD-67	C	TP	M, L	L	3.4	F	F	F	F	F	F	F	F	25	25	F	F	F	F	F	F	F	F	F	25	F	F	F	F	F	
CBD-67B	C	TP	M, L	L	3.4	F	F	F	F	F	F	F	F	35	35	F	F	F	F	F	F	F	F	F	35	F	F	F	F	F	

Table D-1
Matrix of Experiments and Cabinet Characteristics

Test ID	Characteristics of the Experiments					Types of Cabinets (Heat Release Rate of Experiment, kW)																									
	Doors	Thermo-set or Thermo-plastic	Enclosure Size	Cable Loading	Fuel Mass (kg)	Power SWGR & LC TS	Power SWGR & LC TP	Power MCC TS	Power MCC TP	Control Large Close TS	Control Large Close TS (Low)	Control Large Close TS (VLow)	Control Large Close TP	Control Large Close TP (Low)	Control Large Close TP (VLow)	Control Large Open TS	Control Large Open TS (Low)	Control Large Open TS (VLow)	Control Large Open TP	Control Large Open TP (Low)	Control Large Open TP (VLow)	Control Medium Close TS	Control Medium Close TS (Low)	Control Medium Close TP	Control Medium Close TP (Low)	Control Medium Open TS	Control Medium Open TS (Low)	Control Medium Open TP	Control Medium Open TP (Low)	Control Small	Comment
CBD-68	C	TP	M	D	4.5	F	F	F	F	F	F	F	216	F	F	F	F	F	F	F	F	F	F	F	F	F	F	F	F	F	3
CBD-69	C	TP	M	D	3.5	10	F	F	F	F	F	F	F	F	F	F	F	F	F	F	F	F	F	10	F	F	F	F	F	F	
CBD-70	C	TS	M	D	3.1	F	F	F	F	2	F	F	F	F	F	F	F	F	F	F	F	F	F	F	F	F	F	F	F	F	3
CBD-71	C	TS	M	D	3.1	F	F	F	F	138	F	F	F	F	F	F	F	F	F	F	F	F	F	F	F	F	F	F	F	F	3
CBD-72	C	TS	M, L	L	2.9	5	F	5	F	F	5	5	F	F	F	F	F	F	F	F	F	F	5	F	F	F	F	F	F	F	
CBD-73	C	TS	M, L	D	2.9	4	F	4	F	4	F	F	F	F	F	F	F	F	F	F	F	4	F	F	F	F	F	F	F	F	
CBD-74	C	TS	M, L	L	2.4	5	F	5	F	F	5	5	F	F	F	F	F	F	F	F	F	F	5	F	F	F	F	F	F	F	
CBD-75	C	TS	M, L	L	2.9	15	F	15	F	F	15	15	F	F	F	F	F	F	F	F	F	F	15	F	F	F	F	F	F	F	
CBD-76	C	TS	M, L	L	2.9	9	F	9	F	F	9	9	F	F	F	F	F	F	F	F	F	F	9	F	F	F	F	F	F	F	
CBD-77	C	TS	M, L	D	2.4	11	F	11	F	11	F	F	F	F	F	F	F	F	F	F	F	11	F	F	F	F	F	F	F	F	
CBD-77B	O	TS	M, L	D	2.4	F	F	F	F	F	F	F	F	F	F	17	F	F	F	F	F	F	F	F	F	17	F	F	F	F	
CBD-78	C	TS	M, L	D	2.4	F	F	F	F	54	F	F	F	F	F	F	F	F	F	F	F	54	F	F	F	F	F	F	F	F	
CBD-79	C	TS	M, L	D	6.1	F	F	F	F	40	F	F	F	F	F	F	F	F	F	F	F	F	F	F	F	F	F	F	F	F	3
CBD-79B	O	TS	M, L	D	6.1	F	F	F	F	F	F	F	F	F	F	65	F	F	F	F	F	F	F	F	F	F	F	F	F	F	3
CBD-80	C	TS	M, L	D	2.8	F	F	F	F	20	F	F	F	F	F	F	F	F	F	F	F	20	F	F	F	F	F	F	F	F	
CBD-80B	O	TS	M, L	N	2.8	F	F	F	F	F	F	F	F	F	F	100	F	F	F	F	F	F	F	F	F	100	F	F	F	F	

Table D-1
Matrix of Experiments and Cabinet Characteristics

Test ID	Characteristics of the Experiments					Types of Cabinets (Heat Release Rate of Experiment, kW)																									
	Doors	Thermo-set or Thermo-plastic	Enclosure Size	Cable Loading	Fuel Mass (kg)	Power SWGR & LC TS	Power SWGR & LC TP	Power MCC TS	Power MCC TP	Control Large Close TS	Control Large Close TS (Low)	Control Large Close TS (VLow)	Control Large Close TP	Control Large Close TP (Low)	Control Large Close TP (VLow)	Control Large Open TS	Control Large Open TS (Low)	Control Large Open TS (VLow)	Control Large Open TP	Control Large Open TP (Low)	Control Large Open TP (VLow)	Control Medium Close TS	Control Medium Close TS (Low)	Control Medium Close TP	Control Medium Close TP (Low)	Control Medium Open TS	Control Medium Open TS (Low)	Control Medium Open TP	Control Medium Open TP (Low)	Control Small	Comment
CBD-81	C	TS	M, L	L	2.9	24	F	24	F	F	24	24	F	F	F	F	F	F	F	F	F	F	24	F	F	F	F	F	F	F	
CBD-82	C	TP	M	D	7.4	F	F	F	F	F	F	F	F	F	F	F	F	F	F	F	F	F	F	1	F	F	F	F	F	F	
CBD-82B	O	TP	M	D	7.4	F	F	F	F	F	F	F	F	F	F	F	F	F	F	F	F	F	F	F	F	F	F	63	F	F	
CBD-83	O	TP	M	D	4.5	F	F	F	F	F	F	F	F	F	F	F	F	F	577	F	F	F	F	F	F	F	F	F	F	F	3
CBD-84	O	TS	L	D	3.3	F	F	F	F	F	F	F	F	F	F	37	F	F	F	F	F	F	F	F	F	F	F	F	F	F	
CBD-85	C	TS	L	L	2	F	F	F	F	F	2	2	F	F	F	F	F	F	F	F	F	F	F	F	F	F	F	F	F	F	
CBD-86	O	TS	L	L	2	F	F	F	F	F	F	F	F	F	F	F	19	19	F	F	F	F	F	F	F	F	F	F	F	F	
CBD-87	C	TS	L	D	3.3	F	F	F	F	29	F	F	F	F	F	F	F	F	F	F	F	F	F	F	F	F	F	F	F	F	
CBD-88	C	TP	L	D	1.1	F	F	F	F	F	F	F	147	F	F	F	F	F	F	F	F	F	F	F	F	F	F	F	F	F	
CBD-89	C	TP	L	L	1.1	F	F	F	F	F	F	F	F	25	25	F	F	F	F	F	F	F	F	F	F	F	F	F	F	F	
CBD-90	C	TS	L	L	23	F	F	F	F	F	12	12	F	F	F	F	F	F	F	F	F	F	F	F	F	F	F	F	F	F	
CBD-91	C	TS	L	L	2.1	F	F	F	F	F	3	3	F	F	F	F	F	F	F	F	F	F	F	F	F	F	F	F	F	F	
CBD-92	C	TS	L	L	2.1	F	F	F	F	F	15	15	F	F	F	F	F	F	F	F	F	F	F	F	F	F	F	F	F	F	
CBD-93	C	TP	L	D	3.1	F	F	F	F	F	F	F	59	F	F	F	F	F	F	F	F	F	F	F	F	F	F	F	F	F	
CBD-94	C	TS	L	D	4.9	F	F	F	F	37	F	F	F	F	F	F	F	F	F	F	F	F	F	F	F	F	F	F	F	F	
CBD-95	C	TP	L	L	5.4	F	F	F	F	F	F	F	F	30	30	F	F	F	F	F	F	F	F	F	F	F	F	F	F	F	

Table D-1
Matrix of Experiments and Cabinet Characteristics

Test ID	Characteristics of the Experiments					Types of Cabinets (Heat Release Rate of Experiment, kW)																									
	Doors	Thermo-set or Thermo-plastic	Enclosure Size	Cable Loading	Fuel Mass (kg)	Power SWGR & LC TS	Power SWGR & LC TP	Power MCC TS	Power MCC TP	Control Large Close TS	Control Large Close TS (Low)	Control Large Close TS (VLow)	Control Large Close TP	Control Large Close TP (Low)	Control Large Close TP (VLow)	Control Large Open TS	Control Large Open TS (Low)	Control Large Open TS (VLow)	Control Large Open TP	Control Large Open TP (Low)	Control Large Open TP (VLow)	Control Medium Close TS	Control Medium Close TS (Low)	Control Medium Close TP	Control Medium Close TP (Low)	Control Medium Open TS	Control Medium Open TS (Low)	Control Medium Open TP	Control Medium Open TP (Low)	Control Small	Comment
CBD-96	C	TP	L	L	5.4	F	F	F	F	F	F	F	F	33	33	F	F	F	F	F	F	F	F	F	F	F	F	F	F	F	
CBD-97	C	TP	L	D	4.6	F	F	F	F	F	F	F	5	F	F	F	F	F	F	F	F	F	F	F	F	F	F	F	F	F	
CBD-97B	O	TP	L	D	4.6	F	F	F	F	F	F	F	F	F	F	F	F	F	89	F	F	F	F	F	F	F	F	F	F	F	
CBD-98	C	TS	L	D	7.7	F	F	F	F	121	F	F	F	F	F	F	F	F	F	F	F	F	F	F	F	F	F	F	F	F	
CBD-99	O	TP	L	L	3.3	F	F	F	F	F	F	F	F	F	F	F	F	F	F	3	3	F	F	F	F	F	F	F	F	F	
CBD-100	C	TP	L	D	6.2	F	F	F	F	F	F	F	34	F	F	F	F	F	F	F	F	F	F	F	F	F	F	F	F	F	
CBD-101	C	TP	L	D	6.2	F	F	F	F	F	F	F	66	F	F	F	F	F	F	F	F	F	F	F	F	F	F	F	F	F	
CBD-102	O	TS	L	D	3.6	F	F	F	F	F	F	F	F	F	F	10	F	F	F	F	F	F	F	F	F	F	F	F	F	F	
CBD-103	C	TP	L	D	1.1	F	42	F	42	F	F	F	42	F	F	F	F	F	F	F	F	F	F	F	F	F	F	F	F	F	
CBD-104	O	TP	M	D	4.5	F	F	F	F	F	F	F	F	F	F	F	F	F	F	F	F	F	F	F	F	F	F	250	F	F	
CBD-105	C	TP	M	D	6.1	F	F	F	F	F	F	F	F	F	F	F	F	F	F	F	F	F	F	80	F	F	F	F	F	F	
CBD-106	C	TP	M	D	6.1	F	F	F	F	F	F	F	F	F	F	F	F	F	F	F	F	F	F	10	F	F	F	F	F	F	
CBD-106B	O	TP	M	D	6.1	F	F	F	F	F	F	F	F	F	F	F	F	F	F	F	F	F	F	F	F	F	F	35	F	F	
CBD-107	O	TS	M	D	0.6	F	F	F	F	F	F	F	F	F	F	F	F	F	F	F	F	F	F	F	F	F	F	F	F	55	2
CBD-108	C	TS	M	D	5.5	F	F	F	F	F	F	F	F	F	F	F	F	F	F	F	F	32	F	F	F	F	F	F	F	F	
CBD-109	C	TS	M	L	6.1	F	F	F	F	F	F	F	F	F	F	F	F	F	F	F	F	F	64	F	F	F	F	F	F	F	

Table D-1
Matrix of Experiments and Cabinet Characteristics

Test ID	Characteristics of the Experiments					Types of Cabinets (Heat Release Rate of Experiment, kW)																									
	Doors	Thermo-set or Thermo-plastic	Enclosure Size	Cable Loading	Fuel Mass (kg)	Power SWGR & LC TS	Power SWGR & LC TP	Power MCC TS	Power MCC TP	Control Large Close TS	Control Large Close TS (Low)	Control Large Close TS (VLow)	Control Large Close TP	Control Large Close TP (Low)	Control Large Close TP (VLow)	Control Large Open TS	Control Large Open TS (Low)	Control Large Open TS (VLow)	Control Large Open TP	Control Large Open TP (Low)	Control Large Open TP (VLow)	Control Medium Close TS	Control Medium Close TS (Low)	Control Medium Close TP	Control Medium Close TP (Low)	Control Medium Open TS	Control Medium Open TS (Low)	Control Medium Open TP	Control Medium Open TP (Low)	Control Small	Comment
CBD-110	C	TP	M, L	D	2.2	F	7	F	7	F	F	F	7	F	F	F	F	F	F	F	F	F	F	7	F	F	F	F	F	F	
CBD-111	C	TP	M, L	D	3.1	F	F	F	F	F	F	F	50	F	F	F	F	F	F	F	F	F	F	50	F	F	F	F	F	F	
CBD-111B	O	TP	M, L	D	3.1	F	F	F	F	F	F	F	F	F	F	F	F	F	268	F	F	F	F	F	F	F	F	268	F	F	
CBD-112	O	TP	M, L	D	2.2	F	F	F	F	F	F	F	F	F	F	F	F	F	17	F	F	F	F	F	F	F	F	17	F	F	

Comment 1	Classified as Control Large due to the high cable loading
Comment 2	Categorized as Control Small due to mass <1 kg
Comment 3	Classified as Control Large due to many loose cables that are not neatly bundled

D.3 Determination of Alpha and Beta for the Gamma Distributions

For each electrical enclosure classification listed in Appendix D.2, the working group recommended a probability distribution for the peak heat release rate. The gamma distribution was selected as the parametric function to represent these distributions. In order to calculate the gamma distribution parameters, the working group reached consensus on heat release rate values representing the 75th and the 98th percentile of a gamma distribution. These values are provided in Table D-2 for each electrical enclosure classification. The method for calculating Alpha and Beta from Table D-2 is also provided later in this section.

Table D-2
HRR and Gamma Distribution Parameters

Type of Cabinet	Cabinet Characteristics			HRR (kW), Working Group Suggestion		Gamma distribution parameters, best fit values	
	Doors	TS or TP	Cable Loading	75th	98th	Alpha	Beta
Power SWGR & Load Center	N/A	TS	N/A	30	170	0.32	79
	N/A	TP	N/A	60	170	0.99	44
Power MCC & Charger	N/A	TS	N/A	25	130	0.36	57
	N/A	TP	N/A	50	130	1.21	30
Control LARGE	Closed	TS	Default	50	400	0.23	223
	Closed	TS	Low	25	200	0.23	111
	Closed	TS	Very Low	15	75	0.38	32
	Closed	TP	Default	100	400	0.52	145
	Closed	TP	Low	50	200	0.52	73
	Closed	TP	Very Low	25	75	0.88	21
	Open	TS	Default	100	700	0.26	365
	Open	TS	Low	50	350	0.26	182
	Open	TS	Very Low	15	75	0.38	32
	Open	TP	Default	200	1000	0.38	428
	Open	TP	Low	100	500	0.38	214
	Open	TP	Very Low	25	75	0.88	21
Control MEDIUM & Inverter	Closed	TS	Default	25	200	0.23	111
	Closed	TS	Low	15	100	0.27	51
	Closed	TP	Default	50	200	0.52	73
	Closed	TP	Low	25	100	0.52	36
	Open	TS	Default	40	325	0.23	182
	Open	TS	Low	15	150	0.19	92
	Open	TP	Default	80	325	0.51	119
	Open	TP	Low	25	150	0.30	72
Control SMALL	N/A	N/A	N/A	15	45	0.88	12

The alpha and beta parameters for the gamma distributions were calculated in Microsoft Excel using the “Solver” function. As an example, see the screen capture from Microsoft Excel below, for the case described as “Control Large Closed TS Default”, in which the given values are 50 kW for the 75th percentile and 400 kW for the 98th percentile. For each HRR value listed in the spreadsheet in column L, the cumulative distribution of the gamma function is calculated in column M using the “Gammadist” function. At first, an estimate of alpha=1 and beta=100 is entered into cells M29 and M30.

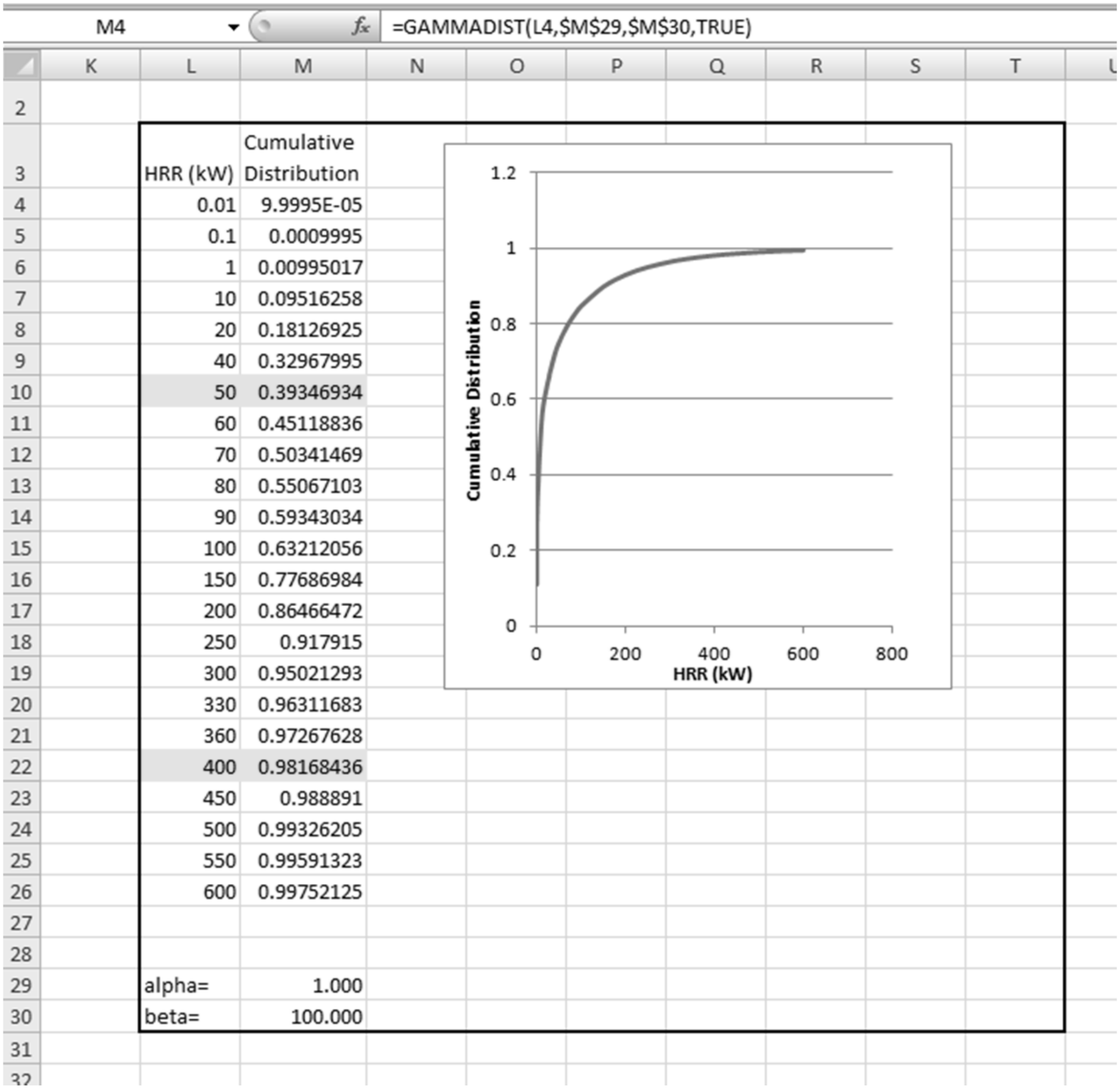

M4 =GAMMADIST(L4,$M$29,$M$30,TRUE)

HRR (kW)	Cumulative Distribution
0.01	9.9995E-05
0.1	0.0009995
1	0.00995017
10	0.09516258
20	0.18126925
40	0.32967995
50	0.39346934
60	0.45118836
70	0.50341469
80	0.55067103
90	0.59343034
100	0.63212056
150	0.77686984
200	0.86466472
250	0.917915
300	0.95021293
330	0.96311683
360	0.97267628
400	0.98168436
450	0.988891
500	0.99326205
550	0.99591323
600	0.99752125
alpha=	1.000
beta=	100.000

Figure D-1
Screen Capture Depicting the Initial Setup in Microsoft Excel for Determining Alpha and Beta Parameters for the Gamma Distribution

The best-fit values of alpha and beta are calculated as follows:

- **Step 1:** Under the “Data” tab, click “Solver” and the following box pops up. Fill in the boxes as shown and click “Solve”.

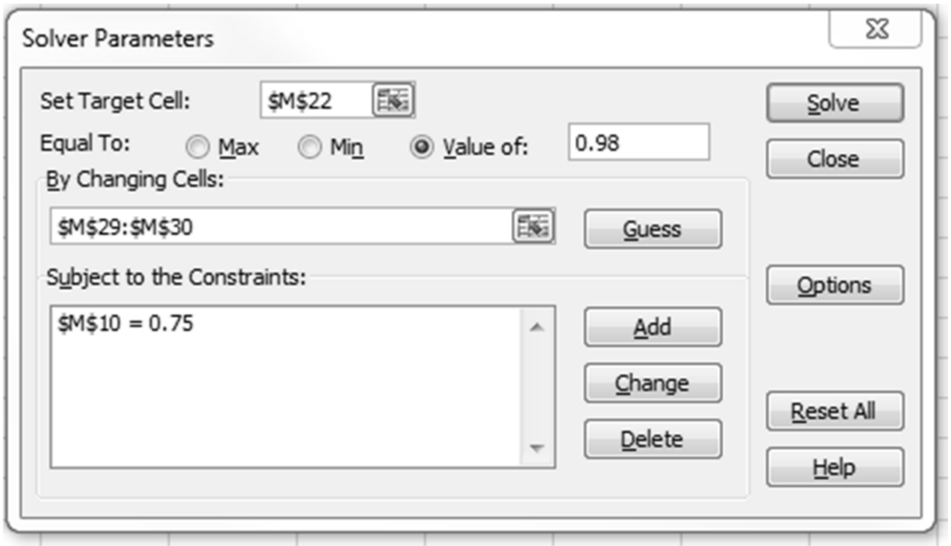

Solver Parameters

Set Target Cell: $M$22

Equal To: ○ Max ○ Min ● Value of: 0.98

By Changing Cells: $M$29:$M$30

Subject to the Constraints:

$M$10 = 0.75

Figure D-2
Step 1 in Calculating Alpha and Beta Parameters for the Gamma Distribution Using Microsoft Excel

- **Step 2:** The following box appears. Click “OK”.

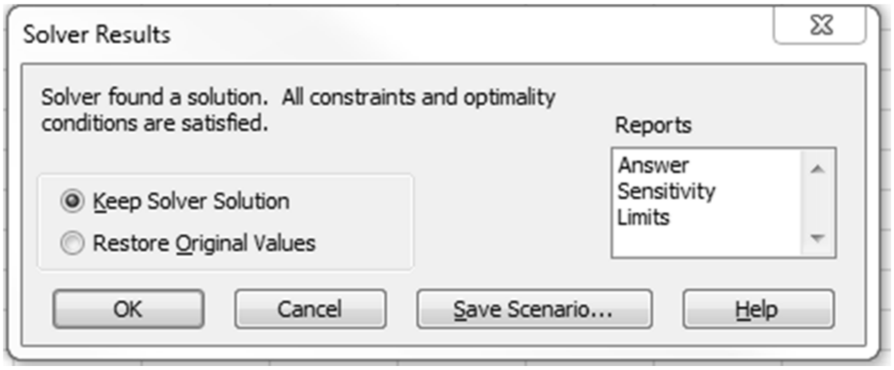

Solver Results

Solver found a solution. All constraints and optimality conditions are satisfied.

● Keep Solver Solution
○ Restore Original Values

Figure D-3
Step 2 in Calculating Alpha and Beta Parameters for the Gamma Distribution Using Microsoft Excel

- **Result:** The best-fit values of alpha and beta appear in cells M29 and M30, as shown below. Checking the results shows that indeed the cumulative distribution of HRR=50 kW is 0.75 and the cumulative distribution of 400 kW is 0.98.

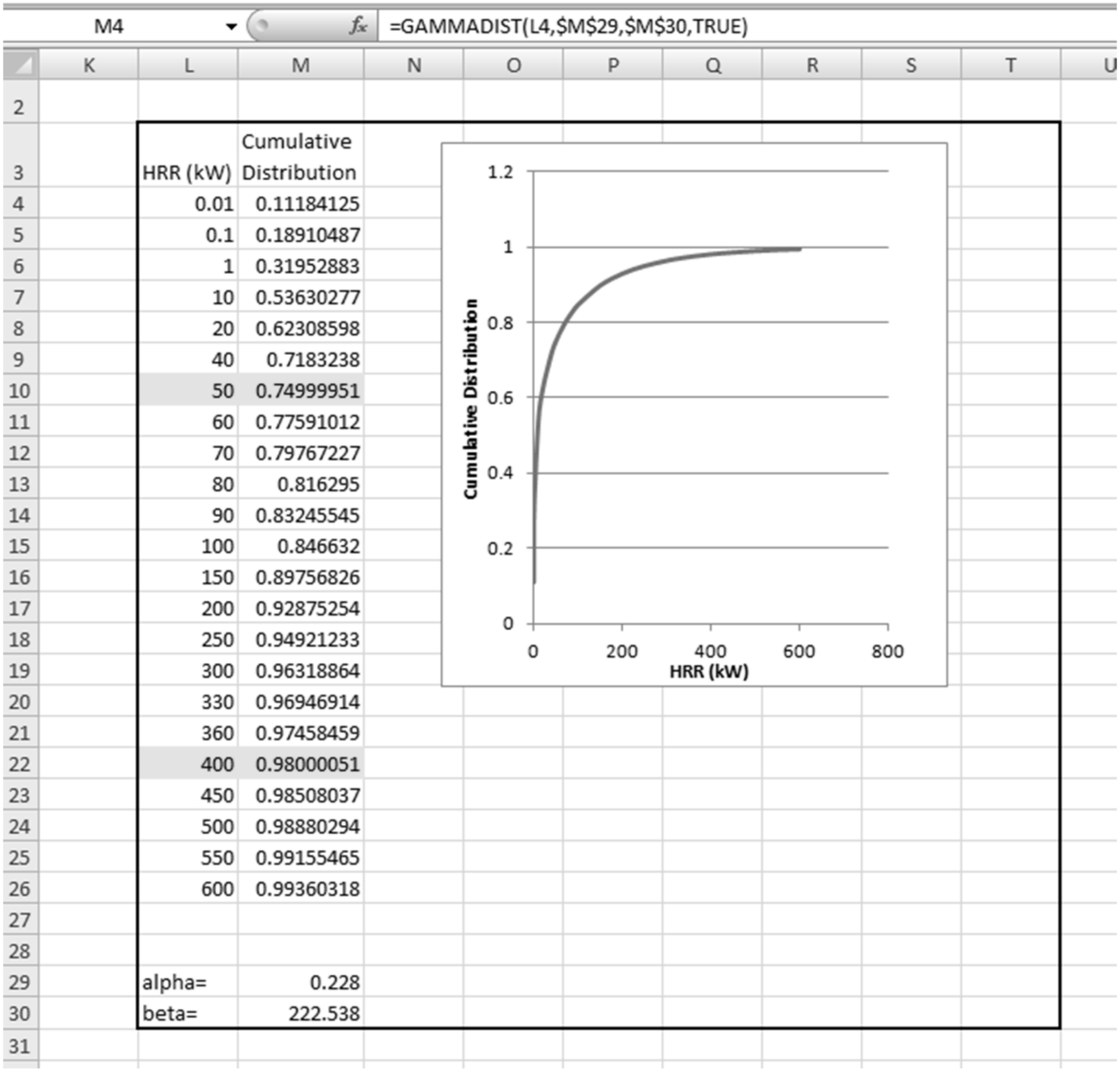

M4 =GAMMADIST(L4,$M$29,$M$30,TRUE)

	L	M
3	HRR (kW)	Cumulative Distribution
4	0.01	0.11184125
5	0.1	0.18910487
6	1	0.31952883
7	10	0.53630277
8	20	0.62308598
9	40	0.7183238
10	50	0.74999951
11	60	0.77591012
12	70	0.79767227
13	80	0.816295
14	90	0.83245545
15	100	0.846632
16	150	0.89756826
17	200	0.92875254
18	250	0.94921233
19	300	0.96318864
20	330	0.96946914
21	360	0.97458459
22	400	0.98000051
23	450	0.98508037
24	500	0.98880294
25	550	0.99155465
26	600	0.99360318
27		
28		
29	alpha=	0.228
30	beta=	222.538

Figure D-4
Final Step in Calculating Alpha and Beta Parameters for the Gamma Distribution Using Microsoft Excel

D.4 Data Analysis

This section provides the following information:

- Plots depicting:
    - The empirical distribution developed using the selected experimental data (red dot-dash line) as assigned to each electrical enclosure classification. The empirical distributions depicted in these plots are considered nominal representations of the applicable data. However, each member of the working group applied their own judgment and may have included (or excluded) additional tests in informing their opinions.
    - The best fit gamma distribution for the experimental data (green dash line). Notice that this best fit is based on the selected experimental data only for the electrical enclosure classification.
    - The gamma distribution recommended by the working group (blue solid line) for each electrical enclosure classification.
- Plots depicting the experimental data selected as representative of each electrical enclosure classification. Values above round markers list the test heat release rate value in units of kW.
- For convenience in reviewing this material, tables are provided that list the parameters for the probability distributions for each of the electrical enclosure classifications discussed in this section (see Tables D-3 through D-9). The Alpha and Beta columns refer to the parameters of the Gamma distribution function, and the 75th and 98th columns refer to the 75th and 98th percentile values of the probability distribution in kW. Each table also specifies whether the distribution applies to open or closed door configuration, thermoset (including qualified thermoplastic) or unqualified thermoplastic cable insulation, and the amount of cable loading within the enclosure.

For some of the enclosure classifications, the assigned data sets are strong (many data points) while others are quite weak (very few data points). Significant differences do exist for certain cases when the empirical and recommended distributions are compared. In some cases the final recommended distributions are somewhat more conservative than the nominal data set while others are less conservative. As suggested earlier, this is because the working group considered the full range of tests and made decisions as to whether or not the data set fully represented each classification group. Specific considerations included in the working group deliberations are described in the sections that follow and include the following general observations:

- In some cases, the working group decided that the selected data set may not have represented worst-case conditions possible for the given enclosure classification. In such cases, the working group gave consideration to other test results that might not be considered fully applicable to the classification group but that could be used to inform the final decisions regarding the worst-case fire potential.
- In other cases, the selected data set may have been found to overstate the fire potential under more realistic conditions. In these cases, the working group may have discounted certain test results and did not attempt to fully bound the assigned data set.
- In some cases, the data sets are very sparse and provide a poor basis for assignment of a final profile. In these cases the working group considered the totality of the available data and consistency with the results for other enclosure classifications.

- The working group's recommended distributions were developed as a cohesive and self-consistent set. In all cases the final recommended distributions were informed, to at least some degree, based on consistency with the other distributions. Hence, the recommended distributions reflect both the absolute behavior of each classification group and the relative behavior anticipated between classification groups.
- The distinctions between the TP and TS cable sub-cases follow a similar pattern for each classification group. The recommended worst-case 98th percentile values are the same for the two sub-cases, but the 75th percentile values for TS cables are half the value assigned to the corresponding TP cable case (meaning large fires are less likely given TS cables). This approach reflects previous studies of cable burning (e.g., the SNL/NRC tests) which have shown that fire spread among cables is a threshold type behavior; that is, cables are generally resistant to fire spread until a minimum threshold of energy is reached, after which fire spread begins. TS cables generally have a higher threshold for fire spread (i.e., it is harder to induce fire spread in TS cables) but tests also show that once a sustained and growing fire is created, TS cables can burn with an intensity equivalent to that of TP cables (e.g., compare SNL tests 23 and 24).
- A final factor considered in establishing the peak HRR distributions was the level of electrical energy available within the enclosure under actual operating conditions. Fire events show that most enclosure ignitions are tied to electrical faults. The working group agreed that, all other factors being equal, the presence of a higher level of electrical energy (i.e., voltage and current) would imply a greater potential for more energetic ignition events, and faster growing fires. While several tests in the available data sets have used electrical ignition sources, none used higher energy electrical ignition sources. As a result, for some of the non-control enclosure classification groups the working group chose to extend the 98th percentile (worst-case) fire conditions somewhat to reflect the higher energy levels present compared to the applicable data sets.

D.4.1 Switchgears and Load Centers

Switchgears and load centers were identified as one classification because of their functionality, which allows for a relatively easy process for identifying the electrical enclosure and assigning a peak heat release rate probability distribution. It should be noted that heat release rate profiles for switchgears and load centers have not been explicitly tested in any of the available experimental programs. The assessment of the probability distributions for the peak heat release rate was based on a comparison between the cable configuration in these types of enclosures, as depicted in numerous pictures inspected by the working group, and the experimental configuration of the different test series. In general terms, the working group agreed that these types of enclosures are characterized by relatively low cable loading dominated by larger diameter power cables. Therefore, the assessment is based mostly on using tests with lower cable loads and vertical electrical enclosures (i.e., no benchboard type enclosures) and with tightly bundled cables, as depicted in Figure D-5 and Figure D-6.

For the case of TS cable, the working group assessment is close to the empirical distribution developed for the selected fire tests (see the solid blue line in Figure D-5). The data sample applicable to this classification includes peak heat release rate values ranging from 0 kW to 82 kW. Specifically, the working group assessment for the 75th percentile is very close to the data sample selected and given the lack of specific testing for these types of cabinets a longer tail for the 98th percentile was selected based on the energy available in these enclosures when energized. In addition, some of the working group members considered tests with higher heat release rates as applicable to this classification. For example, members may have considered tests having tight cable bundle arrangements with a relatively high energy ignition source. This influences the selection of the 98th percentile to ensure a potential fire intensity is captured in the distribution.

In the case of TP cable content, there is a very small set of data given the loading configuration and cable material of the tests. The data sample applicable to this classification includes peak heat release rate values ranging from 7 kW to 42 kW. Therefore the recommended distribution had to be informed by other electrical enclosure classifications. For example, the working group agreed that the 75th percentile should be larger than the equivalent classification for the TS cable (i.e., 30 kW for TS and 60 kW for TP cables). In addition, given the relatively low cable loading of these enclosures in the plant configurations, the working group agreed that the 98th percentile for both TP and TS were equivalent (i.e., 170 kW).

Table D-3
Working Group Recommended Distributions for Switchgears and Load Centers

Classification	Doors	Cable Material	Cable Loading	Alpha	Beta	75th (kW)	98th (kW)
SWGR & Load Center	N/A	TS	N/A	0.32	79	30	170
	N/A	TP	N/A	0.99	44	60	170

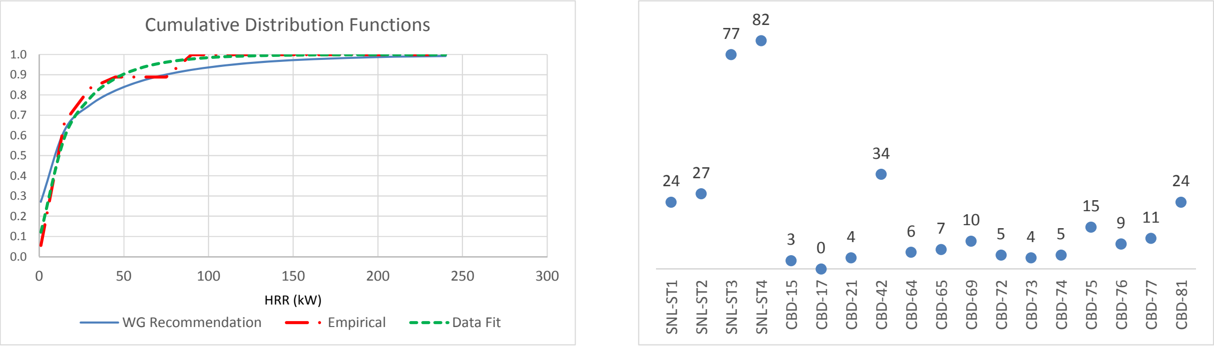

Figure D-5
Power Switchgear and Load Center TS. Values above round markers list the test heat release rate value in units of kW.

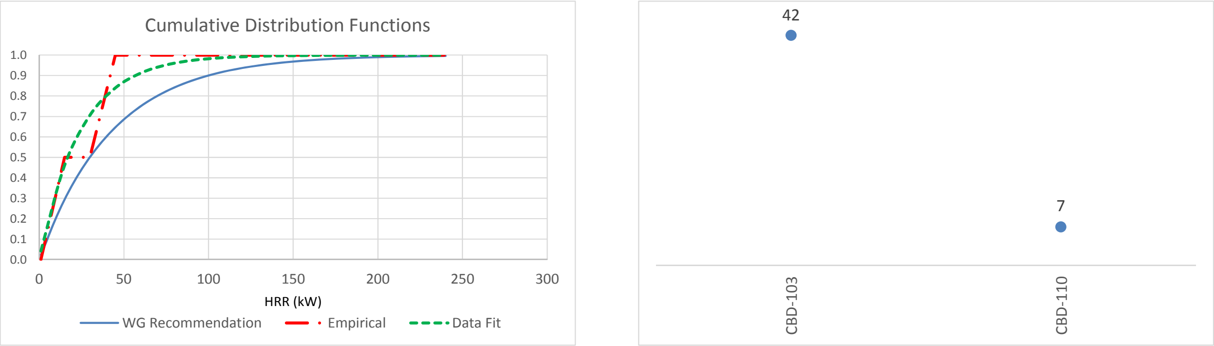

Figure D-6
Power Switchgear and Load Center TP. Values above round markers list the test heat release rate value in units of kW.

D.4.2 Motor Control Centers

As is the case with switchgears and load centers, the heat release rate profiles for motor control centers have not been explicitly tested. A classification for motor control centers was developed due to its characteristic functionality and common usage in NPPs. The assessment of the probability distributions for the peak heat release rate was based on a comparison between the cable configuration in these types of enclosures, as depicted in numerous pictures inspected by the working group, and the experimental configuration of the different test series. In general terms, the working group agreed that these types of enclosures are characterized by relatively low cable loading but also by a cable loading dominated by smaller power and control cables (e.g., as compared to switchgear and load centers). Therefore, the assessment is based mostly on using tests with lower cable loads and vertical electrical enclosures (i.e., no benchboard type enclosures). The working group identified the relatively narrow vertical risers adjacent to the breaker cubicles routing cables along the height of the motor control center as a key factor. This configuration characteristic (i.e., fire spread into the vertical riser) was considered in developing the probability distributions, which are depicted in Figure D-7 and Figure D-8.

For the case of TS cable, the working group assessment is close to the empirical distribution developed for the selected fire events. The data sample applicable to this classification includes peak heat release rate values ranging from 0 kW to 82 kW (see Figure D-7). Specifically, the working group assessment for the 75th percentile is very close to the data sample selected and given the lack of specific testing for these types of cabinets a longer tail for the 98th percentile was selected based on the energy available in these enclosures when energized. In addition, some of the working group members considered tests with higher heat release rates as applicable to this classification (e.g., a given test may have had tight cable bundle arrangements with a relatively high energy ignition source), which influenced the selection of the 98th percentile to ensure a potential fire intensity is captured in the distribution.

In the case of TP cable content, there is a very small set of data given the loading configuration and cable material of the tests. The data sample applicable to this classification includes peak heat release rate values ranging from 7 kW to 42 kW (Figure D-8). Therefore the recommended distribution had to be informed by other electrical enclosure classifications. For example, the working group agreed that the 75th percentile should be larger than the equivalent classification for the TS cable. In addition, given the relatively low cable loading of these enclosures in the plant configurations, the working group agreed that the 98th percentile values for both TP and TS were equivalent.

Table D-4
Working Group Recommended Distributions for Motor Centers

Classification	Doors	Cable Material	Cable Loading	Alpha	Beta	75th (kW)	98th (kW)
MCC & Battery Chargers	N/A	TS	N/A	0.36	57	25	130
	N/A	TP	N/A	1.21	30	50	130

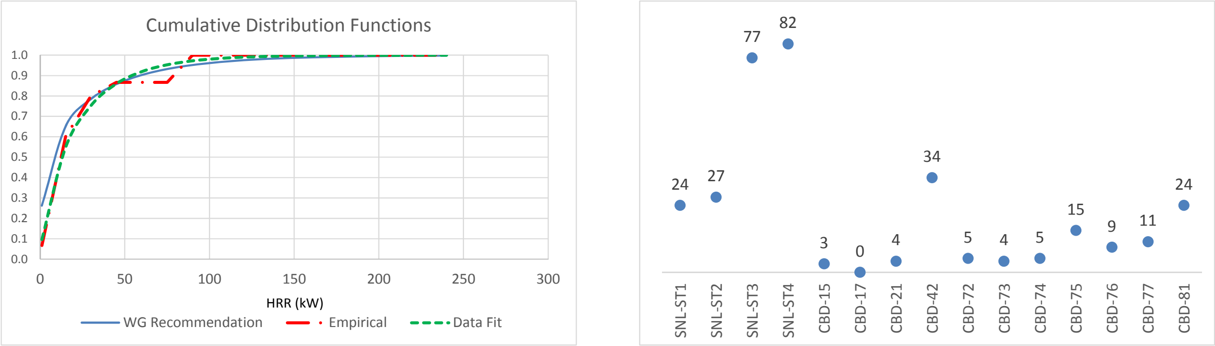

Figure D-7
Power MCC and Charger TS. Values above round markers list the test heat release rate value in units of kW.

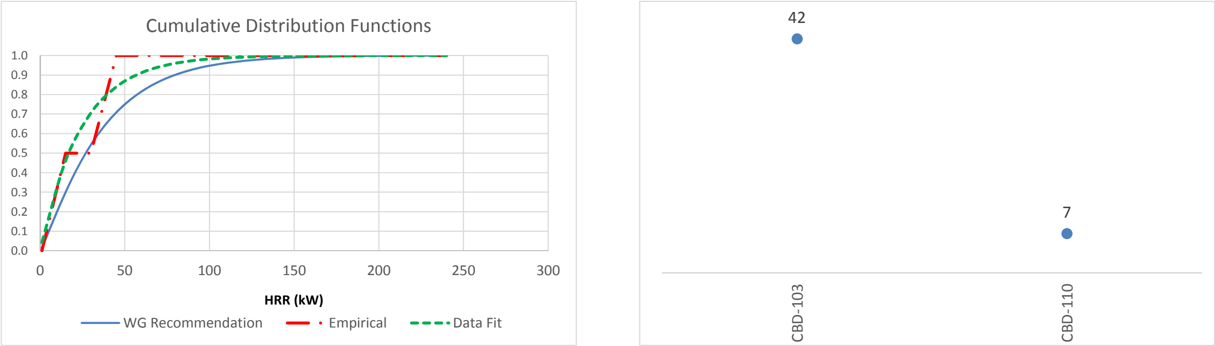

Figure D-8
Power MCC and Charger TP. Values above round markers list the test heat release rate value in units of kW.

D.4.3 Control Large Closed Electrical Enclosures

Due to the wide range of cable configurations associated with control cabinets, this classification includes six probability distributions to account for the total cable/fuel content and the type of cables in the electrical enclosure. For the case of closed large control panels with TS cable, the peak heat release rate in the applicable data ranges from 1 kW to 138 kW as depicted in Figure D-9, Figure D-10, and Figure D-11. The Default, Low, and Very Low fuel loading distributions recommended by the working group are close to the empirical distributions resulting from plotting the applicable data. In addition, the working group extended the 98th percentile in the Default case to 400 kW to account for potential configurations that may include combustible loading other than cables (e.g., circuit cards, etc.) and/or the recognition that once ignited, TS and TP cables could produce similar heat release rate values. Test 1 from VTT test series 186 and Test 4 from VTT test series 521 were used to inform the selection of the 98th percentile value. That test may overstate the fire potential due to the arrangement of fuel near the electrical ignition point. Hence the final distributions for these two classifications represent, to some extent, a blending of the two data sets. That is, the working group agreed that the worst-case potential is similar for TS and TP cables to ignite but that TP cables spread fire more easily. The distributions for Low and Very Low fuel loading include 98th percentiles within the applicable data range.

For the case of TP cable, the peak heat release rate values in the applicable data range from 0 kW to 400 kW as depicted in Figure D-12, Figure D-13, and Figure D-14. Given the “closed cabinet" configuration, the working group agreed to maintain the 98th percentiles assigned earlier to TS cables and to increase the 75th percentiles of the distribution to account for the increased fire hazard associated with TP cable.

Table D-5

Working Group Recommended Distributions for Large Control Enclosures with Closed Doors

Classification	Doors	Cable Material	Cable Loading	Alpha	Beta	75th (kW)	98th (kW)
Control Large	Closed	TS	Default	0.23	223	50	400
	Closed	TS	Low	0.23	111	25	200
	Closed	TS	Very Low	0.38	32	15	75
	Closed	TP	Default	0.52	145	100	400
	Closed	TP	Low	0.52	73	50	200
	Closed	TP	Very Low	0.88	21	25	75

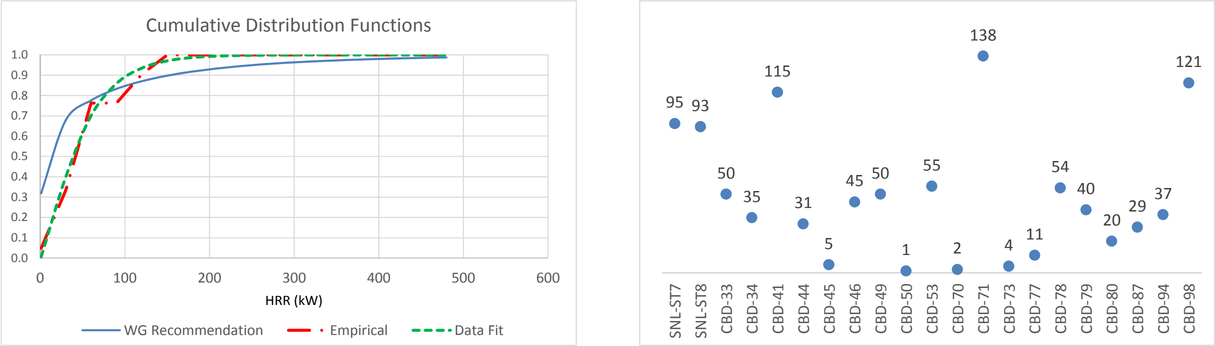

Figure D-9
Control Large Closed TS-Default. Values above round markers list the test heat release rate value in units of kW.

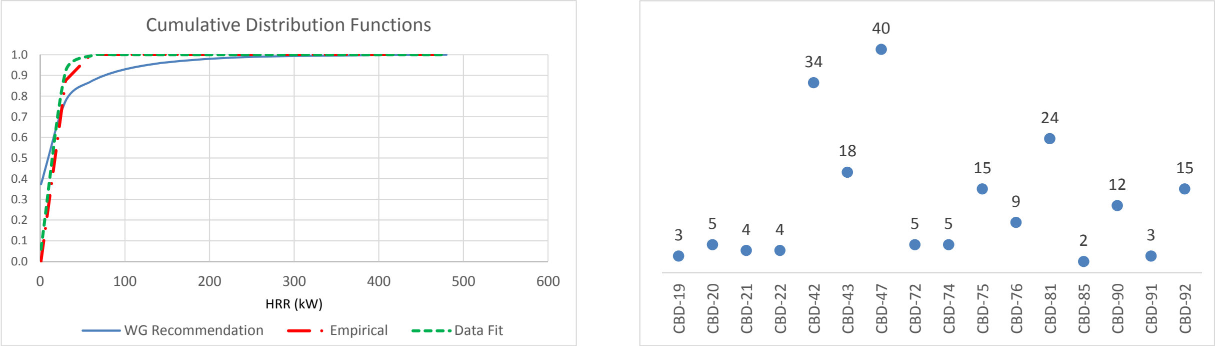

Figure D-10
Control Large Closed TS-Low. Values above round markers list the test heat release rate value in units of kW.

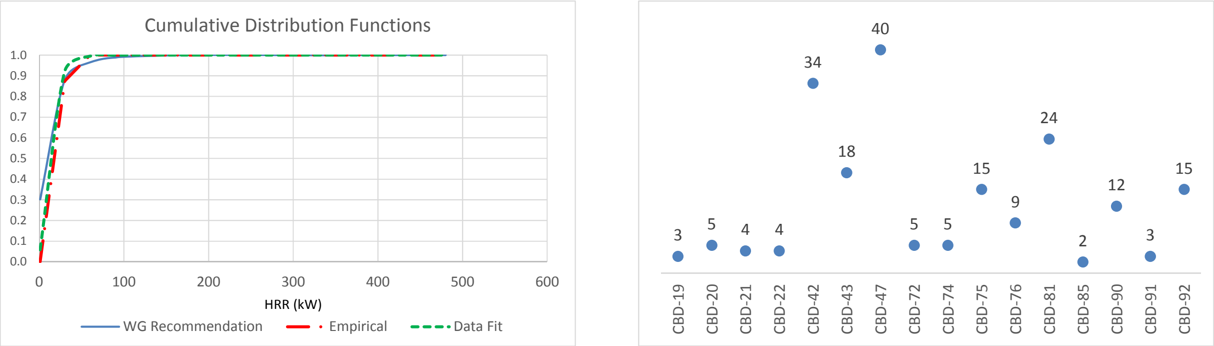

Figure D-11
Control Large Closed TS-Very Low. Values above round markers list the test heat release rate value in units of kW.

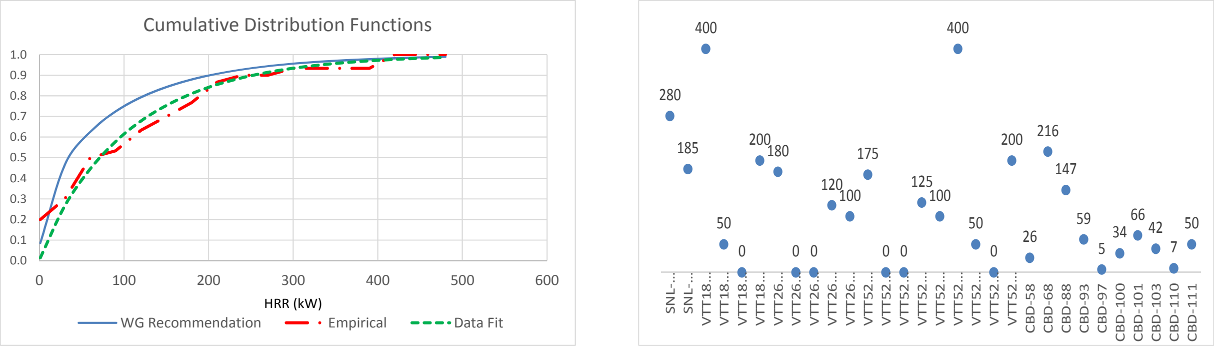

Figure D-12
Control Large Closed TP-Default. Values above round markers list the test heat release rate value in units of kW.

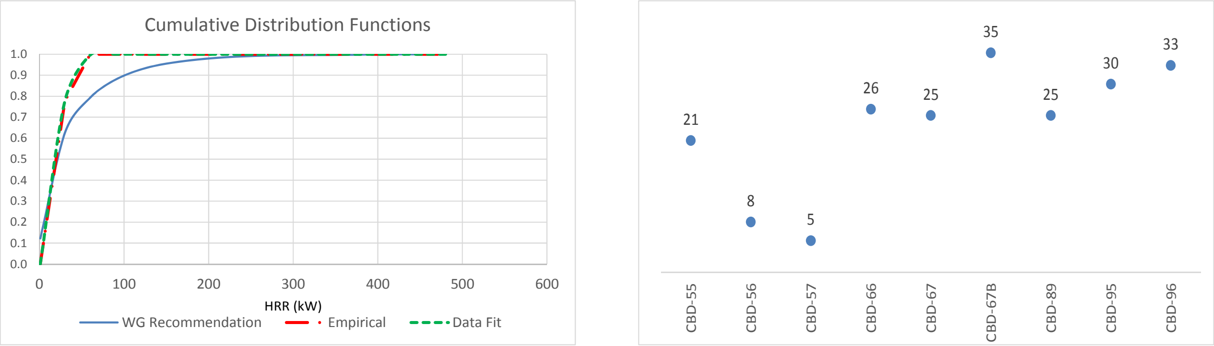

Figure D-13
Control Large Closed TP-Low. Values above round markers list the test heat release rate value in units of kW.

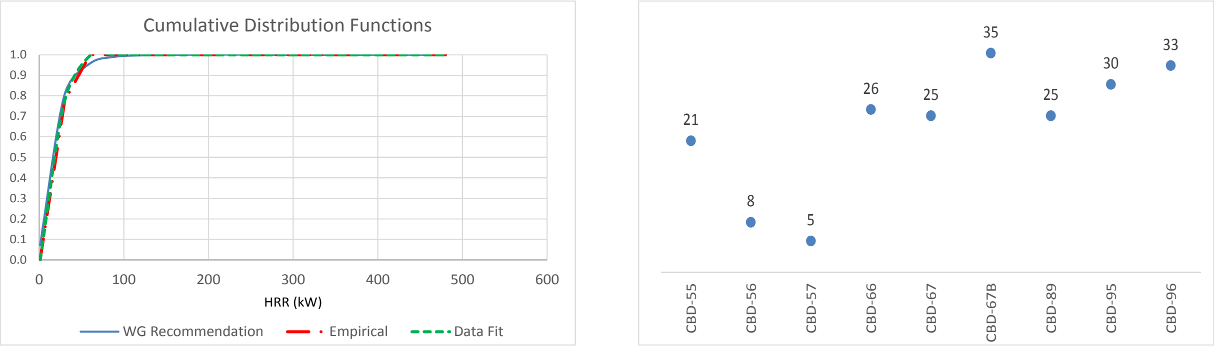

Figure D-14
Control Large Closed TP-Very Low. Values above round markers list the test heat release rate value in units of kW.

D.4.4 Control Large Open Electrical Enclosures

The large open control TS and TP classifications are associated with two of the largest experimental data sets. For the case of TS cable, one of the SNL tests (i.e., Test 23) was removed due to the large ignition source, which is not representative of ignition sources within electrical enclosures in commercial nuclear power plants. The TP data set does include two very large fire tests (SNL Test 24 and SNL Test 25). The TS applicable data ranges from 0 kW to 232 kW, as depicted in Figure D-15, Figure D-16, and Figure D-17. The TP applicable data ranges from 3 kW to 1300 kW, as depicted in Figure D-18, Figure D-19, and Figure D-20. In general, the distributions recommended by the working group are close to the empirical ones. The only exception is the Default distribution for open cabinets with TP cable. Recall the discussion for large cabinets earlier (i.e., the working group discounted the effects of Tests 24 and 25 because of the nature of fuel immediately adjacent to the ignition source). Therefore the empirical data suggests higher heat release rates than what the working group recommended for this classification.

Table D-6
Working Group Recommended Distributions for Large Control Enclosures with Open Doors

Classification	Doors	Cable Material	Cable Loading	Alpha	Beta	75th (kW)	98th (kW)
Control Large	Open	TS	Default	0.26	365	100	700
	Open	TS	Low	0.26	182	50	350
	Open	TS	Very Low	0.38	32	15	75
	Open	TP	Default	0.38	428	200	1000
	Open	TP	Low	0.38	214	100	500
	Open	TP	Very Low	0.88	21	25	75

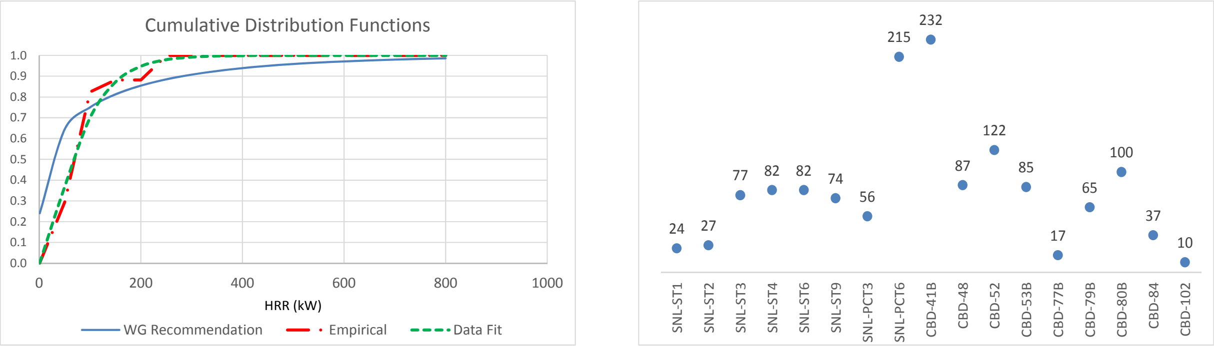

Figure D-15
Control Large Open TS-Default. Values above round markers list the test heat release rate value in units of kW.

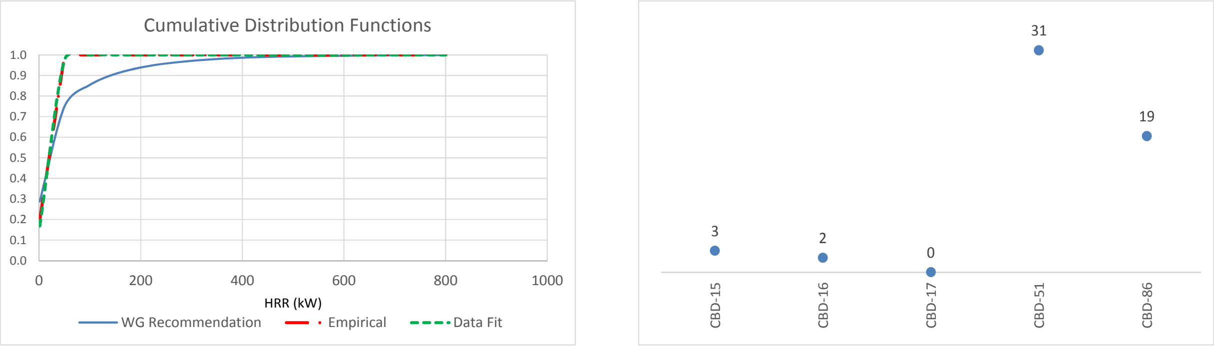

Figure D-16
Control Large Open TS-Low. Values above round markers list the test heat release rate value in units of kW.

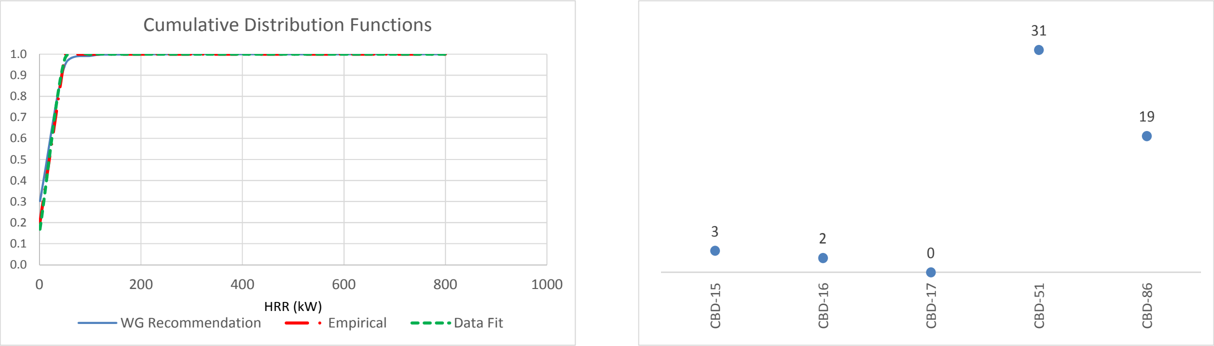

Figure D-17
Control Large Open TS-Very Low. Values above round markers list the test heat release rate value in units of kW.

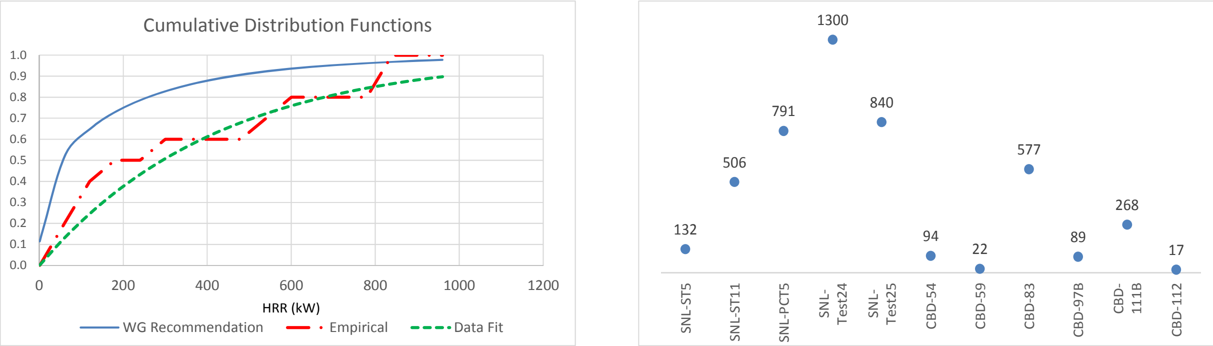

Figure D-18
Control Large Open TP-Default. Values above round markers list the test heat release rate value in units of kW.

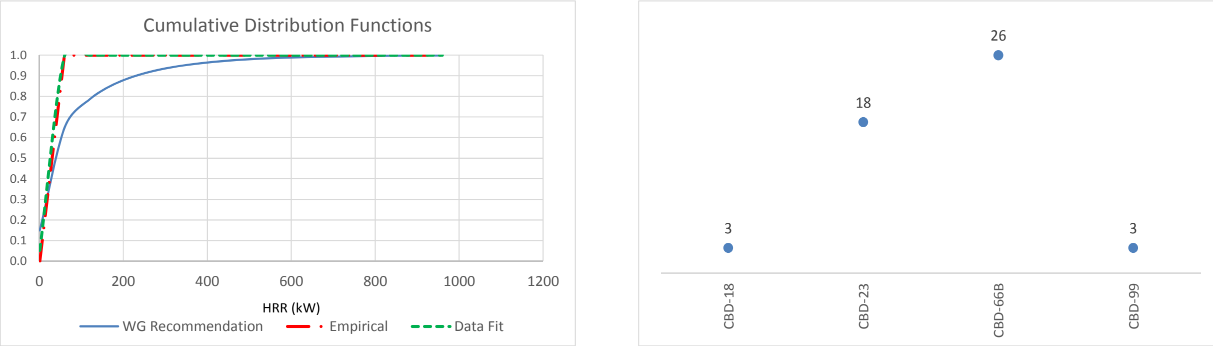

Figure D-19
Control Large Open TP-Low. Values above round markers list the test heat release rate value in units of kW.

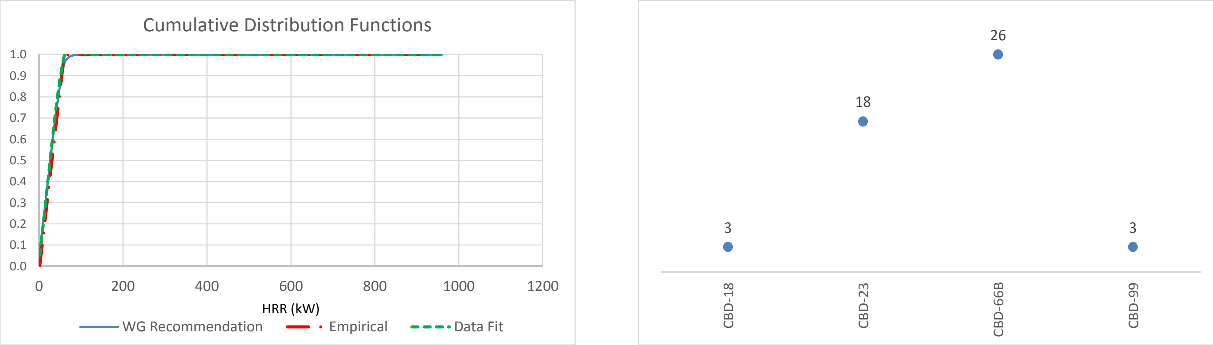

Figure D-20
Control Large Open TP-Very Low. Values above round markers list the test heat release rate value in units of kW.

D.4.5 Control Medium Closed Electrical Enclosures

Due to the wide range of cable configurations associated with control cabinets, this classification includes four probability distributions to account for the cable content, ventilation conditions, and type of cables in the electrical enclosures. For the case of closed medium control panels with TS cable, the peak heat release rates in the applicable data range from 1 kW to 169 kW as depicted in Figure D-21 and Figure D-22. The Default and Low distributions recommended by the working group are close to the empirical distributions resulting from plotting the applicable data. In addition, the working group agreed that the data set might not include potential worst-case conditions and decided to extend the 98th percentile in the Default case to 200 kW to account for potential configurations not included in the experimental programs. CBD Test 38 produced a peak heat release rate of 169 kW, which was used by the working group to inform the selection of the 98th percentile. The distribution for Low include 98th percentiles within the applicable data range.

For the case of TP cable, the peak heat release rate values in the applicable data range from 1 kW to 88 kW as depicted in Figure D-23 and Figure D-24. Given the “closed cabinet” configuration, the working group agreed to maintain the 98th percentiles assigned earlier to TS cables and to increase the 75th percentiles of the distribution to account for the increased fire hazard associated with TP cable. This was based in part on having a limited set of applicable data for medium panels with TP cable.

Table D-7
Working Group Recommended Distributions for Medium Control Enclosures with Closed Doors

Classification	Doors	Cable Material	Cable Loading	Alpha	Beta	75th (kW)	98th (kW)
Control Medium	Closed	TS	Default	0.23	111	25	200
	Closed	TS	Low	0.27	51	15	100
	Closed	TP	Default	0.52	73	50	200
	Closed	TP	Low	0.52	36	25	100

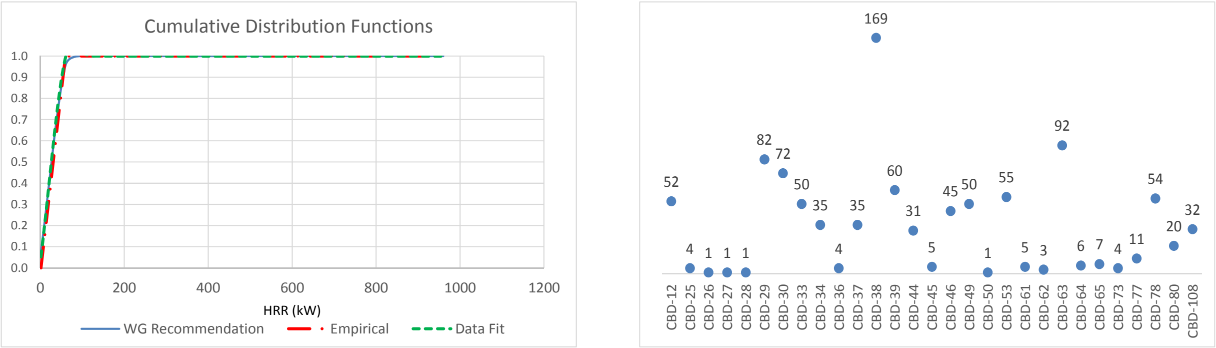

Figure D-21
Medium Closed TS-Default. Values above round markers list the test heat release rate value in units of kW.

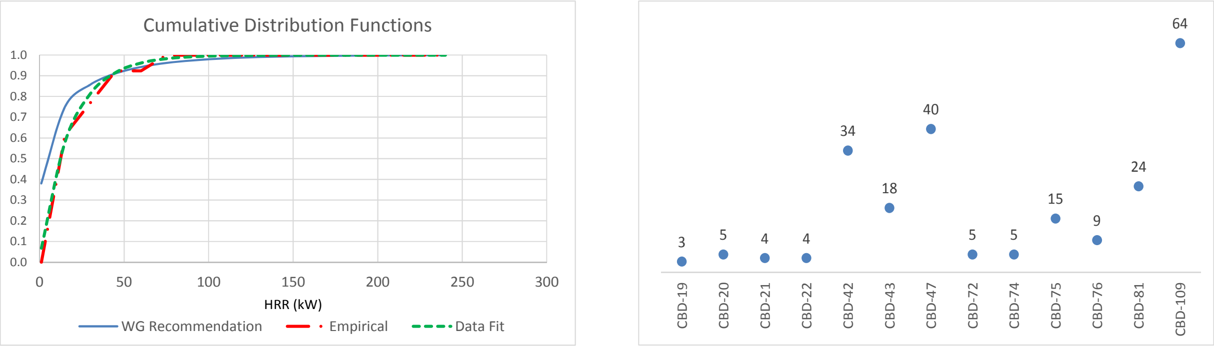

Figure D-22
Control Medium Closed TS-Low. Values above round markers list the test heat release rate value in units of kW.

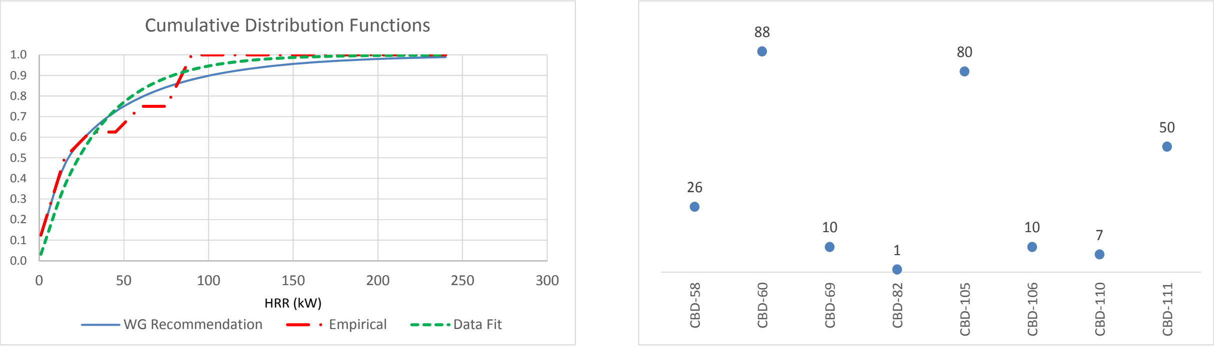

Figure D-23
Control Medium Closed TP-Default. Values above round markers list the test heat release rate value in units of kW.

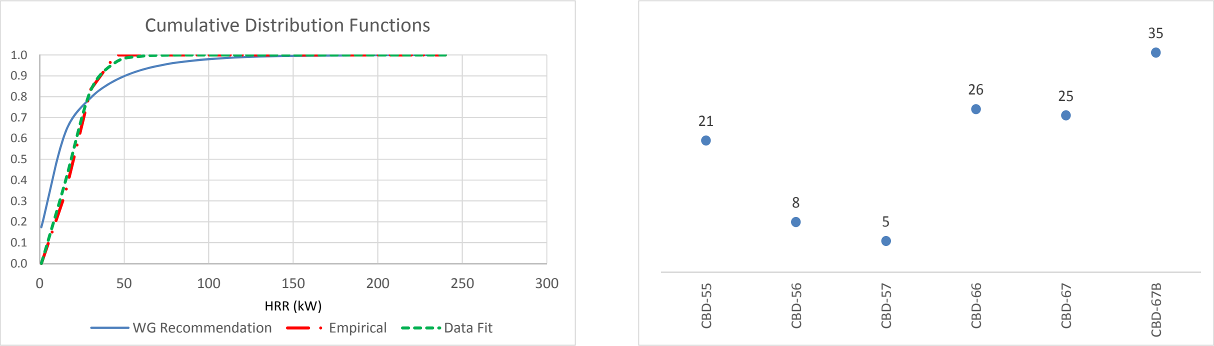

Figure D-24
Control Medium Closed TP-Low. Values above round markers list the test heat release rate value in units of kW.

D.4.6 Control Medium Open Electrical Enclosures

Due to the wide range of cable configurations associated with control cabinets, this classification includes four probability distributions to account for the total cable/fuel content and type of cables in the electrical enclosures. For the case of closed medium control panels with TS cable, the peak heat release rates in the applicable data set range from 0 kW to 146 kW as depicted in Figure D-25 and Figure D-26. The Default and Low distributions recommended by the working group are close to the empirical distributions resulting from plotting the applicable data. In addition, the working group agreed to inform the distribution based on the corresponding TP cable cases and extended the 98th percentile in the Default case to 200 kW to account for potential configurations not included in the experimental programs. In addition, the working group extended the 98th percentile in the Default case to 325 kW to account for potential configurations that may include combustible loading other than cables (e.g., circuit cards, etc.) and/or the recognition that once ignited, TS and TP cables could produce similar heat release rate values. Test CBD 111B, which resulted in a peak heat release rate of 268 kW, was used to inform the selection of the 98th percentile value.

That is, the working group agreed that the worst-case potential cables ignite and spread fire more easily. The distribution for Low include 98th percentiles within the applicable data range. For the case of TP cable, peak heat release rate values in the applicable data range from 3 kW to 268 kW as depicted in Figure D-27 and Figure D-28. Given the “closed cabinet” configuration, the working group agreed to maintain the 98th percentiles assigned earlier to TS cables and to increase the 75th percentiles of the distribution to account for the increased fire hazard associated with TP cable.

Table D-8
Working Group Recommended Distributions for Medium Control Enclosures with Open Doors

Classification	Doors	Cable Material	Cable Loading	Alpha	Beta	75th (kW)	98th (kW)
Control Medium	Open	TS	Default	0.23	182	40	325
	Open	TS	Low	0.19	92	15	150
	Open	TP	Default	0.51	119	80	325
	Open	TP	Low	0.30	72	25	150

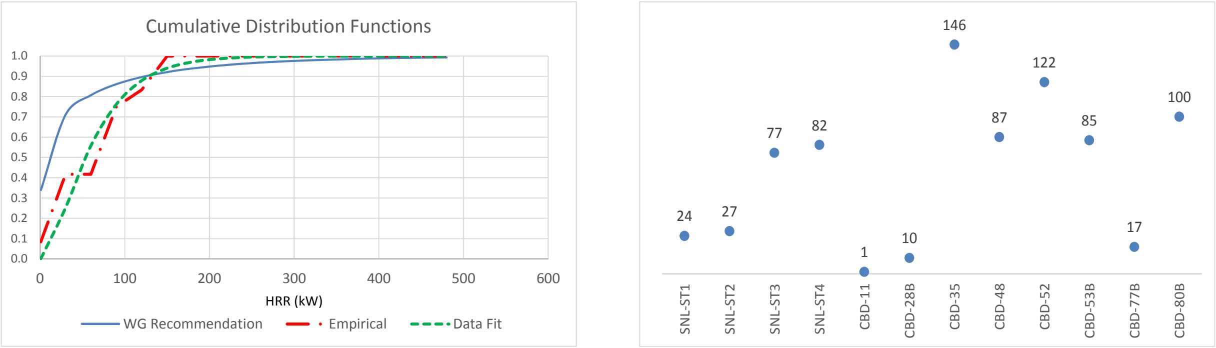

Figure D-25
Medium Open TS-Default. Values above round markers list the test heat release rate value in units of kW.

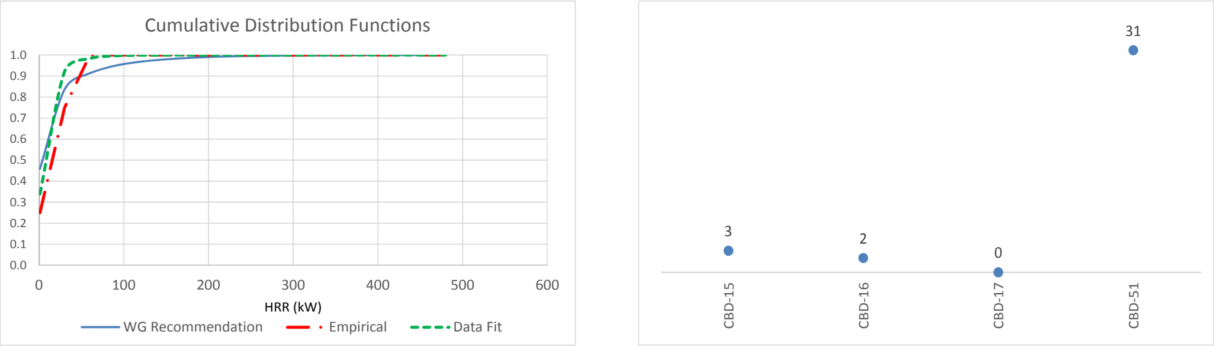

Figure D-26
Control Medium Open TS-Low. Values above round markers list the test heat release rate value in units of kW.

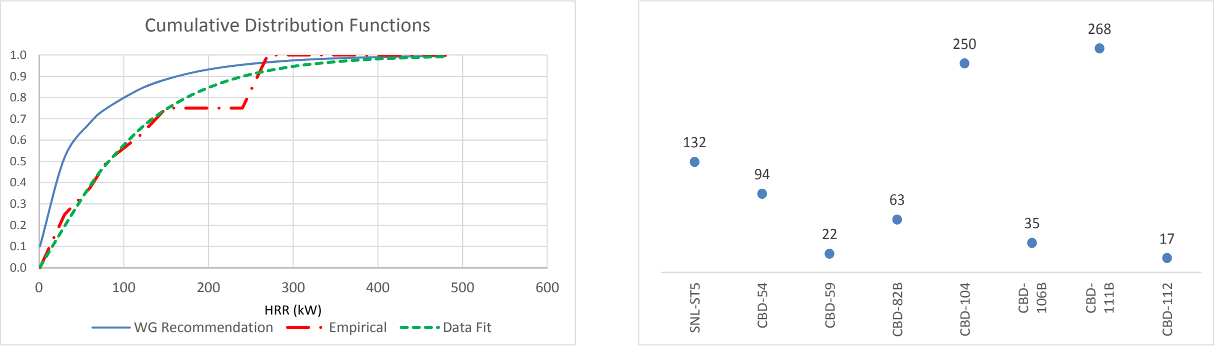

Figure D-27
Control Medium Open TP-Default. Values above round markers list the test heat release rate value in units of kW.

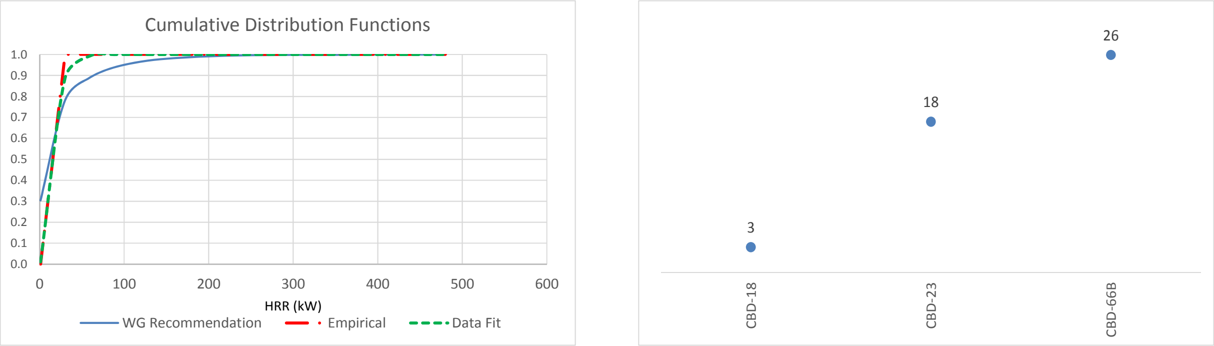

Figure D-28
Control Medium Open TP-Low. Values above round markers list the test heat release rate value in units of kW.

D.4.7 Control Medium/Very Low and Small Electrical Enclosures

Small control electrical enclosures were not specifically tested in the available experimental programs. Consequently, the working group agreed on one peak heat release rate distribution based on available tests consisting of relatively low cable loading and cases of higher fuel loading where little or no fire spread was observed. This data set includes those tests in the NIST/NRC set that used the 1 kW and 5 KW electrical ignition source, which generally failed to induce fire spread. The applicable data, as depicted in Figure D-29, includes peak heat release rate values ranging from 0 kW to 55 kW. The working group agreed that the fire intensities observed from these enclosures should be small, and that the data set likely overstated the fire potential for small electrical enclosures with such limited fuel loads. The working group therefore agreed on a 75th percentile value of 15 kW. The distribution recommended by the working group is close to the empirical one developed directly from the applicable data set.

Table D-9
Working Group Recommended Distributions for Small Control Enclosures

Classification	Doors	Cable Material	Cable Loading	Alpha	Beta	75th (kW)	98th (kW)
Control Small	N/A	N/A	N/A	0.88	12	15	45

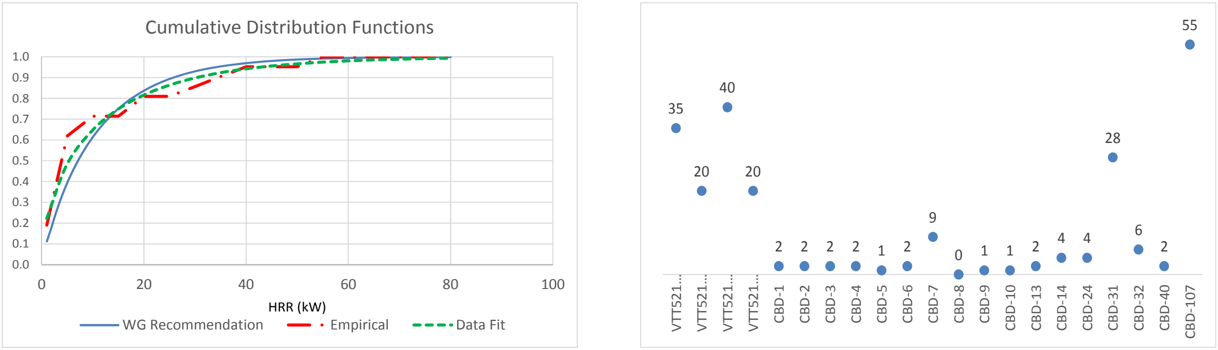

Figure D-29
Control Small. Values above round markers list the test heat release rate value in units of kW.

Appendix E

Obstructed Plume Fire Modeling Results

This appendix presents the results of the FDS computer simulations related to the obstructed plume studies. Table E-1 and Table E-2 list the results of obstructed and unobstructed plume simulations, respectively. Table E-3, Table E-4, Table E-5, Table E-6, Table E-7, Table E-8 and Table E-9 present the results of bias and uncertainty, opening sensitivity, vertical source sensitivity, wall surface sensitivity, soffit sensitivity, steel enclosure thickness, and horizontal plume shift and angle results for the obstructed plume models, respectively. Table E-10 presents a table identifying the FDS run identification numbers associated with the unobstructed (baseline) plume case (in Table E-2) and three obstructed plume cases (in Table E-1) so that one could compare the results of the similar experimental configurations. Finally, Table E-11 presents a matrix of simulation runs in Table E-4 for ease of use on the opening sensitivity study. The fire models used for the simulations, the input data files, and a copy of NUREG-1934 (EPRI 1023259), *Nuclear Power Plant Fire Modeling Analysis Guidelines (NPP FIRE MAG)*, are attached to this report.

Obstructed Simulation Results

Table E-1
Obstructed Simulation Results

Test	HRR (kW)	Diameter (m)	Source Height (m)	Elevation (m)	Maximum Plume Temperature Rise (C)	Baseline Test	Data Filtered	Filtration Criteria
ARCH_1054	1000	0.91	0.30	2.4	402.99	BASE_404	TRUE	Source Located 1 ft. above Ground
ARCH_1054	1000	0.91	0.30	2.7	249.05	BASE_404	TRUE	Source Located 1 ft. above Ground
ARCH_1054	1000	0.91	0.30	3	199.53	BASE_404	TRUE	Source Located 1 ft. above Ground
ARCH_1054	1000	0.91	0.30	3.3	172.57	BASE_404	TRUE	Source Located 1 ft. above Ground
ARCH_1054	1000	0.91	0.30	3.6	153.99	BASE_404	TRUE	Source Located 1 ft. above Ground
ARCH_1054	1000	0.91	0.30	3.9	136.7	BASE_404	TRUE	Source Located 1 ft. above Ground
ARCH_1054	1000	0.91	0.30	4.2	126.62	BASE_404	TRUE	Temperature < 130 C , Source Located 1 ft. above Ground
ARCH_1054	1000	0.91	0.30	4.5	113.14	BASE_404	TRUE	Temperature < 130 C , Source Located 1 ft. above Ground
ARCH_1054	1000	0.91	0.30	4.8	103.21	BASE_404	TRUE	Temperature < 130 C , Source Located 1 ft. above Ground
ARCH_1054	1000	0.91	0.30	5.1	96.109	BASE_404	TRUE	Temperature < 130 C , Source Located 1 ft. above Ground
ARCH_1054	1000	0.91	0.30	5.4	90.815	BASE_404	TRUE	Temperature < 130 C , Source Located 1 ft. above Ground
ARCH_1054	1000	0.91	0.30	5.7	85.55	BASE_404	TRUE	Temperature < 130 C , Source Located 1 ft. above Ground
ARCH_1054	1000	0.91	0.30	6	81.415	BASE_404	TRUE	Temperature < 130 C , Source Located 1 ft. above Ground
ARCH_1055	1000	0.91	1.14	2.4	706.62	BASE_400	FALSE	Not Filtered
ARCH_1055	1000	0.91	1.14	2.7	459.45	BASE_400	FALSE	Not Filtered
ARCH_1055	1000	0.91	1.14	3	337.19	BASE_400	FALSE	Not Filtered

Table E-1
Obstructed Simulation Results

Test	HRR (kW)	Diameter (m)	Source Height (m)	Elevation (m)	Maximum Plume Temperature Rise (C)	Baseline Test	Data Filtered	Filtration Criteria
ARCH_1055	1000	0.91	1.14	3.3	271.35	BASE_400	FALSE	Not Filtered
ARCH_1055	1000	0.91	1.14	3.6	227.5	BASE_400	FALSE	Not Filtered
ARCH_1055	1000	0.91	1.14	3.9	201.32	BASE_400	FALSE	Not Filtered
ARCH_1055	1000	0.91	1.14	4.2	178.36	BASE_400	FALSE	Not Filtered
ARCH_1055	1000	0.91	1.14	4.5	159.08	BASE_400	FALSE	Not Filtered
ARCH_1055	1000	0.91	1.14	4.8	143.06	BASE_400	FALSE	Not Filtered
ARCH_1055	1000	0.91	1.14	5.1	128.93	BASE_400	TRUE	Temperature < 130 C
ARCH_1055	1000	0.91	1.14	5.4	111.59	BASE_400	TRUE	Temperature < 130 C
ARCH_1055	1000	0.91	1.14	5.7	101.23	BASE_400	TRUE	Temperature < 130 C
ARCH_1055	1000	0.91	1.14	6	94.488	BASE_400	TRUE	Temperature < 130 C
ARCH_1056	1000	0.91	1.98	2.4	1071	BASE_401	TRUE	Temperature > 800 C
ARCH_1056	1000	0.91	1.98	2.7	999.09	BASE_401	TRUE	Temperature > 800 C
ARCH_1056	1000	0.91	1.98	3	888.05	BASE_401	TRUE	Temperature > 800 C
ARCH_1056	1000	0.91	1.98	3.3	744.08	BASE_401	FALSE	Not Filtered
ARCH_1056	1000	0.91	1.98	3.6	623.99	BASE_401	FALSE	Not Filtered
ARCH_1056	1000	0.91	1.98	3.9	505.27	BASE_401	FALSE	Not Filtered
ARCH_1056	1000	0.91	1.98	4.2	404.48	BASE_401	FALSE	Not Filtered
ARCH_1056	1000	0.91	1.98	4.5	327.37	BASE_401	FALSE	Not Filtered
ARCH_1056	1000	0.91	1.98	4.8	279.4	BASE_401	FALSE	Not Filtered
ARCH_1056	1000	0.91	1.98	5.1	243.14	BASE_401	FALSE	Not Filtered
ARCH_1056	1000	0.91	1.98	5.4	217.29	BASE_401	FALSE	Not Filtered

Table E-1
Obstructed Simulation Results

Test	HRR (kW)	Diameter (m)	Source Height (m)	Elevation (m)	Maximum Plume Temperature Rise (C)	Baseline Test	Data Filtered	Filtration Criteria
ARCH_1056	1000	0.91	1.98	5.7	197.62	BASE_401	FALSE	Not Filtered
ARCH_1056	1000	0.91	1.98	6	181.65	BASE_401	FALSE	Not Filtered
ARCH_1063	1000	1.22	0.30	2.4	314.81	BASE_405	TRUE	Source Located 1 ft. above Ground
ARCH_1063	1000	1.22	0.30	2.7	200.08	BASE_405	TRUE	Source Located 1 ft. above Ground
ARCH_1063	1000	1.22	0.30	3	161.99	BASE_405	TRUE	Source Located 1 ft. above Ground
ARCH_1063	1000	1.22	0.30	3.3	139.11	BASE_405	TRUE	Source Located 1 ft. above Ground
ARCH_1063	1000	1.22	0.30	3.6	127.87	BASE_405	TRUE	Temperature < 130 C , Source Located 1 ft. above Ground
ARCH_1063	1000	1.22	0.30	3.9	116.51	BASE_405	TRUE	Temperature < 130 C , Source Located 1 ft. above Ground
ARCH_1063	1000	1.22	0.30	4.2	108.46	BASE_405	TRUE	Temperature < 130 C , Source Located 1 ft. above Ground
ARCH_1063	1000	1.22	0.30	4.5	101.39	BASE_405	TRUE	Temperature < 130 C , Source Located 1 ft. above Ground
ARCH_1063	1000	1.22	0.30	4.8	97.629	BASE_405	TRUE	Temperature < 130 C , Source Located 1 ft. above Ground
ARCH_1063	1000	1.22	0.30	5.1	92.41	BASE_405	TRUE	Temperature < 130 C , Source Located 1 ft. above Ground
ARCH_1063	1000	1.22	0.30	5.4	86.168	BASE_405	TRUE	Temperature < 130 C , Source Located 1 ft. above Ground
ARCH_1063	1000	1.22	0.30	5.7	80.069	BASE_405	TRUE	Temperature < 130 C , Source Located 1 ft. above Ground
ARCH_1063	1000	1.22	0.30	6	77.021	BASE_405	TRUE	Temperature < 130 C , Source Located 1 ft. above Ground
ARCH_1064	1000	1.22	1.14	2.4	518.48	BASE_402	FALSE	Not Filtered

Table E-1
Obstructed Simulation Results

Test	HRR (kW)	Diameter (m)	Source Height (m)	Elevation (m)	Maximum Plume Temperature Rise (C)	Baseline Test	Data Filtered	Filtration Criteria
ARCH_1064	1000	1.22	1.14	2.7	310.87	BASE_402	FALSE	Not Filtered
ARCH_1064	1000	1.22	1.14	3	248.02	BASE_402	FALSE	Not Filtered
ARCH_1064	1000	1.22	1.14	3.3	200.07	BASE_402	FALSE	Not Filtered
ARCH_1064	1000	1.22	1.14	3.6	173.69	BASE_402	FALSE	Not Filtered
ARCH_1064	1000	1.22	1.14	3.9	152.29	BASE_402	FALSE	Not Filtered
ARCH_1064	1000	1.22	1.14	4.2	139.64	BASE_402	FALSE	Not Filtered
ARCH_1064	1000	1.22	1.14	4.5	125.97	BASE_402	TRUE	Temperature < 130 C
ARCH_1064	1000	1.22	1.14	4.8	113.42	BASE_402	TRUE	Temperature < 130 C
ARCH_1064	1000	1.22	1.14	5.1	104.74	BASE_402	TRUE	Temperature < 130 C
ARCH_1064	1000	1.22	1.14	5.4	96.844	BASE_402	TRUE	Temperature < 130 C
ARCH_1064	1000	1.22	1.14	5.7	88.525	BASE_402	TRUE	Temperature < 130 C
ARCH_1064	1000	1.22	1.14	6	84.126	BASE_402	TRUE	Temperature < 130 C
ARCH_1065	1000	1.22	1.98	2.4	1017.4	BASE_403	TRUE	Temperature > 800 C
ARCH_1065	1000	1.22	1.98	2.7	912.53	BASE_403	TRUE	Temperature > 800 C
ARCH_1065	1000	1.22	1.98	3	717.19	BASE_403	FALSE	Not Filtered
ARCH_1065	1000	1.22	1.98	3.3	559.48	BASE_403	FALSE	Not Filtered
ARCH_1065	1000	1.22	1.98	3.6	449.2	BASE_403	FALSE	Not Filtered
ARCH_1065	1000	1.22	1.98	3.9	342.39	BASE_403	FALSE	Not Filtered
ARCH_1065	1000	1.22	1.98	4.2	275.39	BASE_403	FALSE	Not Filtered
ARCH_1065	1000	1.22	1.98	4.5	228.68	BASE_403	FALSE	Not Filtered
ARCH_1065	1000	1.22	1.98	4.8	200.89	BASE_403	FALSE	Not Filtered

Table E-1
Obstructed Simulation Results

Test	HRR (kW)	Diameter (m)	Source Height (m)	Elevation (m)	Maximum Plume Temperature Rise (C)	Baseline Test	Data Filtered	Filtration Criteria
ARCH_1065	1000	1.22	1.98	5.1	179.61	BASE_403	FALSE	Not Filtered
ARCH_1065	1000	1.22	1.98	5.4	158.36	BASE_403	FALSE	Not Filtered
ARCH_1065	1000	1.22	1.98	5.7	140.7	BASE_403	FALSE	Not Filtered
ARCH_1065	1000	1.22	1.98	6	132.26	BASE_403	FALSE	Not Filtered
ARCH_822	50	0.30	0.30	2.4	78.421	BASE_300	TRUE	Temperature < 130 C , Source Located 1 ft. above Ground
ARCH_822	50	0.30	0.30	2.7	61.983	BASE_300	TRUE	Temperature < 130 C , Source Located 1 ft. above Ground
ARCH_822	50	0.30	0.30	3	54.471	BASE_300	TRUE	Temperature < 130 C , Source Located 1 ft. above Ground
ARCH_822	50	0.30	0.30	3.3	48.091	BASE_300	TRUE	Temperature < 130 C , Source Located 1 ft. above Ground
ARCH_822	50	0.30	0.30	3.6	44.856	BASE_300	TRUE	Temperature < 130 C , Source Located 1 ft. above Ground
ARCH_822	50	0.30	0.30	3.9	41.157	BASE_300	TRUE	Temperature < 130 C , Source Located 1 ft. above Ground
ARCH_823	100	0.30	0.30	2.4	111.96	BASE_301	TRUE	Temperature < 130 C , Source Located 1 ft. above Ground
ARCH_823	100	0.30	0.30	2.7	85.738	BASE_301	TRUE	Temperature < 130 C , Source Located 1 ft. above Ground
ARCH_823	100	0.30	0.30	3	73.613	BASE_301	TRUE	Temperature < 130 C , Source Located 1 ft. above Ground
ARCH_823	100	0.30	0.30	3.3	63.543	BASE_301	TRUE	Temperature < 130 C , Source Located 1 ft. above Ground
ARCH_823	100	0.30	0.30	3.6	57.189	BASE_301	TRUE	Temperature < 130 C , Source Located 1 ft. above Ground

Table E-1
Obstructed Simulation Results

Test	HRR (kW)	Diameter (m)	Source Height (m)	Elevation (m)	Maximum Plume Temperature Rise (C)	Baseline Test	Data Filtered	Filtration Criteria
ARCH_823	100	0.30	0.30	3.9	51.926	BASE_301	TRUE	Temperature < 130 C , Source Located 1 ft. above Ground
ARCH_823	100	0.30	0.30	4.2	47.036	BASE_301	TRUE	Temperature < 130 C , Source Located 1 ft. above Ground
ARCH_823	100	0.30	0.30	4.5	44.597	BASE_301	TRUE	Temperature < 130 C , Source Located 1 ft. above Ground
ARCH_823	100	0.30	0.30	4.8	42.113	BASE_301	TRUE	Temperature < 130 C , Source Located 1 ft. above Ground
ARCH_829	50	0.30	1.14	2.4	128.48	BASE_311	TRUE	Temperature < 130 C
ARCH_829	50	0.30	1.14	2.7	83.525	BASE_311	TRUE	Temperature < 130 C
ARCH_829	50	0.30	1.14	3	65.94	BASE_311	TRUE	Temperature < 130 C
ARCH_829	50	0.30	1.14	3.3	55.802	BASE_311	TRUE	Temperature < 130 C
ARCH_829	50	0.30	1.14	3.6	50.422	BASE_311	TRUE	Temperature < 130 C
ARCH_829	50	0.30	1.14	3.9	45.23	BASE_311	TRUE	Temperature < 130 C
ARCH_829	50	0.30	1.14	4.2	42.194	BASE_311	TRUE	Temperature < 130 C
ARCH_830	100	0.30	1.14	2.4	218.07	BASE_312	FALSE	Not Filtered
ARCH_830	100	0.30	1.14	2.7	132.16	BASE_312	FALSE	Not Filtered
ARCH_830	100	0.30	1.14	3	104.18	BASE_312	TRUE	Temperature < 130 C
ARCH_830	100	0.30	1.14	3.3	84.312	BASE_312	TRUE	Temperature < 130 C
ARCH_830	100	0.30	1.14	3.6	72.088	BASE_312	TRUE	Temperature < 130 C
ARCH_830	100	0.30	1.14	3.9	64.197	BASE_312	TRUE	Temperature < 130 C
ARCH_830	100	0.30	1.14	4.2	58.619	BASE_312	TRUE	Temperature < 130 C
ARCH_830	100	0.30	1.14	4.5	51.953	BASE_312	TRUE	Temperature < 130 C

Table E-1
Obstructed Simulation Results

Test	HRR (kW)	Diameter (m)	Source Height (m)	Elevation (m)	Maximum Plume Temperature Rise (C)	Baseline Test	Data Filtered	Filtration Criteria
ARCH_830	100	0.30	1.14	4.8	47.76	BASE_312	TRUE	Temperature < 130 C
ARCH_830	100	0.30	1.14	5.1	45.075	BASE_312	TRUE	Temperature < 130 C
ARCH_830	100	0.30	1.14	5.4	42.484	BASE_312	TRUE	Temperature < 130 C
ARCH_836	50	0.30	1.98	2.4	266.03	BASE_322	FALSE	Not Filtered
ARCH_836	50	0.30	1.98	2.7	146.04	BASE_322	FALSE	Not Filtered
ARCH_836	50	0.30	1.98	3	103.12	BASE_322	TRUE	Temperature < 130 C
ARCH_836	50	0.30	1.98	3.3	79.733	BASE_322	TRUE	Temperature < 130 C
ARCH_836	50	0.30	1.98	3.6	68.823	BASE_322	TRUE	Temperature < 130 C
ARCH_836	50	0.30	1.98	3.9	62.17	BASE_322	TRUE	Temperature < 130 C
ARCH_836	50	0.30	1.98	4.2	56.616	BASE_322	TRUE	Temperature < 130 C
ARCH_836	50	0.30	1.98	4.5	50.366	BASE_322	TRUE	Temperature < 130 C
ARCH_836	50	0.30	1.98	4.8	46.16	BASE_322	TRUE	Temperature < 130 C
ARCH_836	50	0.30	1.98	5.1	41.517	BASE_322	TRUE	Temperature < 130 C
ARCH_837	100	0.30	1.98	2.4	531.44	BASE_323	FALSE	Not Filtered
ARCH_837	100	0.30	1.98	2.7	275.75	BASE_323	FALSE	Not Filtered
ARCH_837	100	0.30	1.98	3	191.73	BASE_323	FALSE	Not Filtered
ARCH_837	100	0.30	1.98	3.3	138.23	BASE_323	FALSE	Not Filtered
ARCH_837	100	0.30	1.98	3.6	111.02	BASE_323	TRUE	Temperature < 130 C
ARCH_837	100	0.30	1.98	3.9	90.378	BASE_323	TRUE	Temperature < 130 C
ARCH_837	100	0.30	1.98	4.2	78.574	BASE_323	TRUE	Temperature < 130 C
ARCH_837	100	0.30	1.98	4.5	68.337	BASE_323	TRUE	Temperature < 130 C

Table E-1
Obstructed Simulation Results

Test	HRR (kW)	Diameter (m)	Source Height (m)	Elevation (m)	Maximum Plume Temperature Rise (C)	Baseline Test	Data Filtered	Filtration Criteria
ARCH_837	100	0.30	1.98	4.8	62.439	BASE_323	TRUE	Temperature < 130 C
ARCH_837	100	0.30	1.98	5.1	56.388	BASE_323	TRUE	Temperature < 130 C
ARCH_837	100	0.30	1.98	5.4	50.913	BASE_323	TRUE	Temperature < 130 C
ARCH_837	100	0.30	1.98	5.7	46.702	BASE_323	TRUE	Temperature < 130 C
ARCH_837	100	0.30	1.98	6	43.468	BASE_323	TRUE	Temperature < 130 C
ARCH_887	200	0.61	0.30	2.4	148.43	BASE_302	TRUE	, Source Located 1 ft. above Ground
ARCH_887	200	0.61	0.30	2.7	100.37	BASE_302	TRUE	Temperature < 130 C , Source Located 1 ft. above Ground
ARCH_887	200	0.61	0.30	3	85.081	BASE_302	TRUE	Temperature < 130 C , Source Located 1 ft. above Ground
ARCH_887	200	0.61	0.30	3.3	74.859	BASE_302	TRUE	Temperature < 130 C , Source Located 1 ft. above Ground
ARCH_887	200	0.61	0.30	3.6	69.47	BASE_302	TRUE	Temperature < 130 C , Source Located 1 ft. above Ground
ARCH_887	200	0.61	0.30	3.9	63.212	BASE_302	TRUE	Temperature < 130 C , Source Located 1 ft. above Ground
ARCH_887	200	0.61	0.30	4.2	59.739	BASE_302	TRUE	Temperature < 130 C , Source Located 1 ft. above Ground
ARCH_887	200	0.61	0.30	4.5	57.879	BASE_302	TRUE	Temperature < 130 C , Source Located 1 ft. above Ground
ARCH_887	200	0.61	0.30	4.8	54.59	BASE_302	TRUE	Temperature < 130 C , Source Located 1 ft. above Ground
ARCH_887	200	0.61	0.30	5.1	51.417	BASE_302	TRUE	Temperature < 130 C , Source Located 1 ft. above Ground

Table E-1
Obstructed Simulation Results

Test	HRR (kW)	Diameter (m)	Source Height (m)	Elevation (m)	Maximum Plume Temperature Rise (C)	Baseline Test	Data Filtered	Filtration Criteria
ARCH_887	200	0.61	0.30	5.4	48.415	BASE_302	TRUE	Temperature < 130 C , Source Located 1 ft. above Ground
ARCH_887	200	0.61	0.30	5.7	46.025	BASE_302	TRUE	Temperature < 130 C , Source Located 1 ft. above Ground
ARCH_887	200	0.61	0.30	6	43.88	BASE_302	TRUE	Temperature < 130 C , Source Located 1 ft. above Ground
ARCH_888	300	0.61	0.30	2.4	203.24	BASE_303	TRUE	Source Located 1 ft. above Ground
ARCH_888	300	0.61	0.30	2.7	127.89	BASE_303	TRUE	Temperature < 130 C , Source Located 1 ft. above Ground
ARCH_888	300	0.61	0.30	3	107.9	BASE_303	TRUE	Temperature < 130 C , Source Located 1 ft. above Ground
ARCH_888	300	0.61	0.30	3.3	94.353	BASE_303	TRUE	Temperature < 130 C , Source Located 1 ft. above Ground
ARCH_888	300	0.61	0.30	3.6	84.65	BASE_303	TRUE	Temperature < 130 C , Source Located 1 ft. above Ground
ARCH_888	300	0.61	0.30	3.9	77.241	BASE_303	TRUE	Temperature < 130 C , Source Located 1 ft. above Ground
ARCH_888	300	0.61	0.30	4.2	72.78	BASE_303	TRUE	Temperature < 130 C , Source Located 1 ft. above Ground
ARCH_888	300	0.61	0.30	4.5	67.684	BASE_303	TRUE	Temperature < 130 C , Source Located 1 ft. above Ground
ARCH_888	300	0.61	0.30	4.8	61.735	BASE_303	TRUE	Temperature < 130 C , Source Located 1 ft. above Ground
ARCH_888	300	0.61	0.30	5.1	56.565	BASE_303	TRUE	Temperature < 130 C , Source Located 1 ft. above Ground
ARCH_888	300	0.61	0.30	5.4	51.5	BASE_303	TRUE	Temperature < 130 C , Source

Table E-1
Obstructed Simulation Results

Test	HRR (kW)	Diameter (m)	Source Height (m)	Elevation (m)	Maximum Plume Temperature Rise (C)	Baseline Test	Data Filtered	Filtration Criteria
								Located 1 ft. above Ground
ARCH_888	300	0.61	0.30	5.7	48.936	BASE_303	TRUE	Temperature < 130 C , Source Located 1 ft. above Ground
ARCH_888	300	0.61	0.30	6	46.643	BASE_303	TRUE	Temperature < 130 C , Source Located 1 ft. above Ground
ARCH_889	400	0.61	0.30	2.4	255.22	BASE_304	TRUE	Source Located 1 ft. above Ground
ARCH_889	400	0.61	0.30	2.7	157.96	BASE_304	TRUE	Source Located 1 ft. above Ground
ARCH_889	400	0.61	0.30	3	127.64	BASE_304	TRUE	Temperature < 130 C , Source Located 1 ft. above Ground
ARCH_889	400	0.61	0.30	3.3	109.23	BASE_304	TRUE	Temperature < 130 C , Source Located 1 ft. above Ground
ARCH_889	400	0.61	0.30	3.6	98.671	BASE_304	TRUE	Temperature < 130 C , Source Located 1 ft. above Ground
ARCH_889	400	0.61	0.30	3.9	88.758	BASE_304	TRUE	Temperature < 130 C , Source Located 1 ft. above Ground
ARCH_889	400	0.61	0.30	4.2	80.791	BASE_304	TRUE	Temperature < 130 C , Source Located 1 ft. above Ground
ARCH_889	400	0.61	0.30	4.5	73.599	BASE_304	TRUE	Temperature < 130 C , Source Located 1 ft. above Ground
ARCH_889	400	0.61	0.30	4.8	69.728	BASE_304	TRUE	Temperature < 130 C , Source Located 1 ft. above Ground
ARCH_889	400	0.61	0.30	5.1	66.947	BASE_304	TRUE	Temperature < 130 C , Source Located 1 ft. above Ground
ARCH_889	400	0.61	0.30	5.4	62.583	BASE_304	TRUE	Temperature < 130 C , Source Located 1 ft. above Ground
ARCH_889	400	0.61	0.30	5.7	57.735	BASE_304	TRUE	Temperature < 130 C , Source

Table E-1
Obstructed Simulation Results

Test	HRR (kW)	Diameter (m)	Source Height (m)	Elevation (m)	Maximum Plume Temperature Rise (C)	Baseline Test	Data Filtered	Filtration Criteria
								Located 1 ft. above Ground
ARCH_889	400	0.61	0.30	6	54.117	BASE_304	TRUE	Temperature < 130 C , Source Located 1 ft. above Ground
ARCH_890	500	0.61	0.30	2.4	334.39	BASE_305	TRUE	Source Located 1 ft. above Ground
ARCH_890	500	0.61	0.30	2.7	208.25	BASE_305	TRUE	Source Located 1 ft. above Ground
ARCH_890	500	0.61	0.30	3	163.33	BASE_305	TRUE	Source Located 1 ft. above Ground
ARCH_890	500	0.61	0.30	3.3	136.87	BASE_305	TRUE	Source Located 1 ft. above Ground
ARCH_890	500	0.61	0.30	3.6	120.3	BASE_305	TRUE	Temperature < 130 C , Source Located 1 ft. above Ground
ARCH_890	500	0.61	0.30	3.9	108.92	BASE_305	TRUE	Temperature < 130 C , Source Located 1 ft. above Ground
ARCH_890	500	0.61	0.30	4.2	99.827	BASE_305	TRUE	Temperature < 130 C , Source Located 1 ft. above Ground
ARCH_890	500	0.61	0.30	4.5	89.634	BASE_305	TRUE	Temperature < 130 C , Source Located 1 ft. above Ground
ARCH_890	500	0.61	0.30	4.8	83.218	BASE_305	TRUE	Temperature < 130 C , Source Located 1 ft. above Ground
ARCH_890	500	0.61	0.30	5.1	77.533	BASE_305	TRUE	Temperature < 130 C , Source Located 1 ft. above Ground
ARCH_890	500	0.61	0.30	5.4	72.565	BASE_305	TRUE	Temperature < 130 C , Source Located 1 ft. above Ground
ARCH_890	500	0.61	0.30	5.7	68.466	BASE_305	TRUE	Temperature < 130 C , Source Located 1 ft. above Ground
ARCH_890	500	0.61	0.30	6	65.06	BASE_305	TRUE	Temperature < 130 C , Source Located 1 ft. above Ground

Table E-1
Obstructed Simulation Results

Test	HRR (kW)	Diameter (m)	Source Height (m)	Elevation (m)	Maximum Plume Temperature Rise (C)	Baseline Test	Data Filtered	Filtration Criteria
ARCH_891	600	0.61	0.30	2.4	392.93	BASE_306	TRUE	Source Located 1 ft. above Ground
ARCH_891	600	0.61	0.30	2.7	238.68	BASE_306	TRUE	Source Located 1 ft. above Ground
ARCH_891	600	0.61	0.30	3	182.46	BASE_306	TRUE	Source Located 1 ft. above Ground
ARCH_891	600	0.61	0.30	3.3	151.7	BASE_306	TRUE	Source Located 1 ft. above Ground
ARCH_891	600	0.61	0.30	3.6	132.77	BASE_306	TRUE	Source Located 1 ft. above Ground
ARCH_891	600	0.61	0.30	3.9	117.68	BASE_306	TRUE	Temperature < 130 C , Source Located 1 ft. above Ground
ARCH_891	600	0.61	0.30	4.2	105.86	BASE_306	TRUE	Temperature < 130 C , Source Located 1 ft. above Ground
ARCH_891	600	0.61	0.30	4.5	97.088	BASE_306	TRUE	Temperature < 130 C , Source Located 1 ft. above Ground
ARCH_891	600	0.61	0.30	4.8	89.553	BASE_306	TRUE	Temperature < 130 C , Source Located 1 ft. above Ground
ARCH_891	600	0.61	0.30	5.1	83.845	BASE_306	TRUE	Temperature < 130 C , Source Located 1 ft. above Ground
ARCH_891	600	0.61	0.30	5.4	77.08	BASE_306	TRUE	Temperature < 130 C , Source Located 1 ft. above Ground
ARCH_891	600	0.61	0.30	5.7	70.69	BASE_306	TRUE	Temperature < 130 C , Source Located 1 ft. above Ground
ARCH_891	600	0.61	0.30	6	66.18	BASE_306	TRUE	Temperature < 130 C , Source Located 1 ft. above Ground
ARCH_894	200	0.61	1.14	2.4	259.92	BASE_313	FALSE	Not Filtered
ARCH_894	200	0.61	1.14	2.7	140.83	BASE_313	FALSE	Not Filtered
ARCH_894	200	0.61	1.14	3	107.55	BASE_313	TRUE	Temperature < 130 C

Table E-1
Obstructed Simulation Results

Test	HRR (kW)	Diameter (m)	Source Height (m)	Elevation (m)	Maximum Plume Temperature Rise (C)	Baseline Test	Data Filtered	Filtration Criteria
ARCH_894	200	0.61	1.14	3.3	92.404	BASE_313	TRUE	Temperature < 130 C
ARCH_894	200	0.61	1.14	3.6	80.943	BASE_313	TRUE	Temperature < 130 C
ARCH_894	200	0.61	1.14	3.9	73.928	BASE_313	TRUE	Temperature < 130 C
ARCH_894	200	0.61	1.14	4.2	69.147	BASE_313	TRUE	Temperature < 130 C
ARCH_894	200	0.61	1.14	4.5	60.989	BASE_313	TRUE	Temperature < 130 C
ARCH_894	200	0.61	1.14	4.8	56.486	BASE_313	TRUE	Temperature < 130 C
ARCH_894	200	0.61	1.14	5.1	52.641	BASE_313	TRUE	Temperature < 130 C
ARCH_894	200	0.61	1.14	5.4	49.817	BASE_313	TRUE	Temperature < 130 C
ARCH_894	200	0.61	1.14	5.7	47.225	BASE_313	TRUE	Temperature < 130 C
ARCH_894	200	0.61	1.14	6	45.813	BASE_313	TRUE	Temperature < 130 C
ARCH_895	300	0.61	1.14	2.4	350.38	BASE_314	FALSE	Not Filtered
ARCH_895	300	0.61	1.14	2.7	192.02	BASE_314	FALSE	Not Filtered
ARCH_895	300	0.61	1.14	3	145.64	BASE_314	FALSE	Not Filtered
ARCH_895	300	0.61	1.14	3.3	123.78	BASE_314	TRUE	Temperature < 130 C
ARCH_895	300	0.61	1.14	3.6	107.6	BASE_314	TRUE	Temperature < 130 C
ARCH_895	300	0.61	1.14	3.9	96.495	BASE_314	TRUE	Temperature < 130 C
ARCH_895	300	0.61	1.14	4.2	89.162	BASE_314	TRUE	Temperature < 130 C
ARCH_895	300	0.61	1.14	4.5	82.797	BASE_314	TRUE	Temperature < 130 C
ARCH_895	300	0.61	1.14	4.8	76.094	BASE_314	TRUE	Temperature < 130 C
ARCH_895	300	0.61	1.14	5.1	70.124	BASE_314	TRUE	Temperature < 130 C
ARCH_895	300	0.61	1.14	5.4	65.595	BASE_314	TRUE	Temperature < 130 C

Table E-1
Obstructed Simulation Results

Test	HRR (kW)	Diameter (m)	Source Height (m)	Elevation (m)	Maximum Plume Temperature Rise (C)	Baseline Test	Data Filtered	Filtration Criteria
ARCH_895	300	0.61	1.14	5.7	60.586	BASE_314	TRUE	Temperature < 130 C
ARCH_895	300	0.61	1.14	6	57.174	BASE_314	TRUE	Temperature < 130 C
ARCH_896	400	0.61	1.14	2.4	575.97	BASE_315	FALSE	Not Filtered
ARCH_896	400	0.61	1.14	2.7	273.67	BASE_315	FALSE	Not Filtered
ARCH_896	400	0.61	1.14	3	192.71	BASE_315	FALSE	Not Filtered
ARCH_896	400	0.61	1.14	3.3	155.45	BASE_315	FALSE	Not Filtered
ARCH_896	400	0.61	1.14	3.6	135.42	BASE_315	FALSE	Not Filtered
ARCH_896	400	0.61	1.14	3.9	119.35	BASE_315	TRUE	Temperature < 130 C
ARCH_896	400	0.61	1.14	4.2	105.99	BASE_315	TRUE	Temperature < 130 C
ARCH_896	400	0.61	1.14	4.5	95.01	BASE_315	TRUE	Temperature < 130 C
ARCH_896	400	0.61	1.14	4.8	86.706	BASE_315	TRUE	Temperature < 130 C
ARCH_896	400	0.61	1.14	5.1	79.523	BASE_315	TRUE	Temperature < 130 C
ARCH_896	400	0.61	1.14	5.4	73.124	BASE_315	TRUE	Temperature < 130 C
ARCH_896	400	0.61	1.14	5.7	68.01	BASE_315	TRUE	Temperature < 130 C
ARCH_896	400	0.61	1.14	6	64.528	BASE_315	TRUE	Temperature < 130 C
ARCH_897	500	0.61	1.14	2.4	705.87	BASE_316	FALSE	Not Filtered
ARCH_897	500	0.61	1.14	2.7	405.73	BASE_316	FALSE	Not Filtered
ARCH_897	500	0.61	1.14	3	275.53	BASE_316	FALSE	Not Filtered
ARCH_897	500	0.61	1.14	3.3	207.46	BASE_316	FALSE	Not Filtered
ARCH_897	500	0.61	1.14	3.6	175.04	BASE_316	FALSE	Not Filtered
ARCH_897	500	0.61	1.14	3.9	151.32	BASE_316	FALSE	Not Filtered

Table E-1
Obstructed Simulation Results

Test	HRR (kW)	Diameter (m)	Source Height (m)	Elevation (m)	Maximum Plume Temperature Rise (C)	Baseline Test	Data Filtered	Filtration Criteria
ARCH_897	500	0.61	1.14	4.2	134.1	BASE_316	FALSE	Not Filtered
ARCH_897	500	0.61	1.14	4.5	116.32	BASE_316	TRUE	Temperature < 130 C
ARCH_897	500	0.61	1.14	4.8	105.38	BASE_316	TRUE	Temperature < 130 C
ARCH_897	500	0.61	1.14	5.1	98.169	BASE_316	TRUE	Temperature < 130 C
ARCH_897	500	0.61	1.14	5.4	90.329	BASE_316	TRUE	Temperature < 130 C
ARCH_897	500	0.61	1.14	5.7	83.386	BASE_316	TRUE	Temperature < 130 C
ARCH_897	500	0.61	1.14	6	77.358	BASE_316	TRUE	Temperature < 130 C
ARCH_898	600	0.61	1.14	2.4	777.31	BASE_317	FALSE	Not Filtered
ARCH_898	600	0.61	1.14	2.7	455.11	BASE_317	FALSE	Not Filtered
ARCH_898	600	0.61	1.14	3	337.58	BASE_317	FALSE	Not Filtered
ARCH_898	600	0.61	1.14	3.3	252	BASE_317	FALSE	Not Filtered
ARCH_898	600	0.61	1.14	3.6	213.7	BASE_317	FALSE	Not Filtered
ARCH_898	600	0.61	1.14	3.9	178.56	BASE_317	FALSE	Not Filtered
ARCH_898	600	0.61	1.14	4.2	154.6	BASE_317	FALSE	Not Filtered
ARCH_898	600	0.61	1.14	4.5	133.8	BASE_317	FALSE	Not Filtered
ARCH_898	600	0.61	1.14	4.8	121.31	BASE_317	TRUE	Temperature < 130 C
ARCH_898	600	0.61	1.14	5.1	107.65	BASE_317	TRUE	Temperature < 130 C
ARCH_898	600	0.61	1.14	5.4	97.561	BASE_317	TRUE	Temperature < 130 C
ARCH_898	600	0.61	1.14	5.7	89.094	BASE_317	TRUE	Temperature < 130 C
ARCH_898	600	0.61	1.14	6	82.72	BASE_317	TRUE	Temperature < 130 C
ARCH_901	200	0.61	1.98	2.4	693.58	BASE_324	FALSE	Not Filtered

Table E-1
Obstructed Simulation Results

Test	HRR (kW)	Diameter (m)	Source Height (m)	Elevation (m)	Maximum Plume Temperature Rise (C)	Baseline Test	Data Filtered	Filtration Criteria
ARCH_901	200	0.61	1.98	2.7	369.88	BASE_324	FALSE	Not Filtered
ARCH_901	200	0.61	1.98	3	253.64	BASE_324	FALSE	Not Filtered
ARCH_901	200	0.61	1.98	3.3	194.13	BASE_324	FALSE	Not Filtered
ARCH_901	200	0.61	1.98	3.6	161.03	BASE_324	FALSE	Not Filtered
ARCH_901	200	0.61	1.98	3.9	130.93	BASE_324	FALSE	Not Filtered
ARCH_901	200	0.61	1.98	4.2	111.32	BASE_324	TRUE	Temperature < 130 C
ARCH_901	200	0.61	1.98	4.5	97.46	BASE_324	TRUE	Temperature < 130 C
ARCH_901	200	0.61	1.98	4.8	89.489	BASE_324	TRUE	Temperature < 130 C
ARCH_901	200	0.61	1.98	5.1	82.647	BASE_324	TRUE	Temperature < 130 C
ARCH_901	200	0.61	1.98	5.4	72.712	BASE_324	TRUE	Temperature < 130 C
ARCH_901	200	0.61	1.98	5.7	65.348	BASE_324	TRUE	Temperature < 130 C
ARCH_901	200	0.61	1.98	6	59.505	BASE_324	TRUE	Temperature < 130 C
ARCH_902	300	0.61	1.98	2.4	931.25	BASE_325	TRUE	Temperature > 800 C
ARCH_902	300	0.61	1.98	2.7	657.24	BASE_325	FALSE	Not Filtered
ARCH_902	300	0.61	1.98	3	450.61	BASE_325	FALSE	Not Filtered
ARCH_902	300	0.61	1.98	3.3	345.15	BASE_325	FALSE	Not Filtered
ARCH_902	300	0.61	1.98	3.6	272.2	BASE_325	FALSE	Not Filtered
ARCH_902	300	0.61	1.98	3.9	214.8	BASE_325	FALSE	Not Filtered
ARCH_902	300	0.61	1.98	4.2	178.08	BASE_325	FALSE	Not Filtered
ARCH_902	300	0.61	1.98	4.5	146.34	BASE_325	FALSE	Not Filtered
ARCH_902	300	0.61	1.98	4.8	129.83	BASE_325	TRUE	Temperature < 130 C

Table E-1
Obstructed Simulation Results

Test	HRR (kW)	Diameter (m)	Source Height (m)	Elevation (m)	Maximum Plume Temperature Rise (C)	Baseline Test	Data Filtered	Filtration Criteria
ARCH_902	300	0.61	1.98	5.1	118.19	BASE_325	TRUE	Temperature < 130 C
ARCH_902	300	0.61	1.98	5.4	101.98	BASE_325	TRUE	Temperature < 130 C
ARCH_902	300	0.61	1.98	5.7	92.618	BASE_325	TRUE	Temperature < 130 C
ARCH_902	300	0.61	1.98	6	86.111	BASE_325	TRUE	Temperature < 130 C
ARCH_903	400	0.61	1.98	2.4	1006.2	BASE_326	TRUE	Temperature > 800 C
ARCH_903	400	0.61	1.98	2.7	884.94	BASE_326	TRUE	Temperature > 800 C
ARCH_903	400	0.61	1.98	3	712.12	BASE_326	FALSE	Not Filtered
ARCH_903	400	0.61	1.98	3.3	515.23	BASE_326	FALSE	Not Filtered
ARCH_903	400	0.61	1.98	3.6	387.41	BASE_326	FALSE	Not Filtered
ARCH_903	400	0.61	1.98	3.9	289.44	BASE_326	FALSE	Not Filtered
ARCH_903	400	0.61	1.98	4.2	232.59	BASE_326	FALSE	Not Filtered
ARCH_903	400	0.61	1.98	4.5	183.52	BASE_326	FALSE	Not Filtered
ARCH_903	400	0.61	1.98	4.8	157.37	BASE_326	FALSE	Not Filtered
ARCH_903	400	0.61	1.98	5.1	138.3	BASE_326	FALSE	Not Filtered
ARCH_903	400	0.61	1.98	5.4	121.29	BASE_326	TRUE	Temperature < 130 C
ARCH_903	400	0.61	1.98	5.7	108.2	BASE_326	TRUE	Temperature < 130 C
ARCH_903	400	0.61	1.98	6	99.461	BASE_326	TRUE	Temperature < 130 C
ARCH_904	500	0.61	1.98	2.4	1057.3	BASE_327	TRUE	Temperature > 800 C
ARCH_904	500	0.61	1.98	2.7	1014.7	BASE_327	TRUE	Temperature > 800 C
ARCH_904	500	0.61	1.98	3	921.04	BASE_327	TRUE	Temperature > 800 C
ARCH_904	500	0.61	1.98	3.3	753.53	BASE_327	FALSE	Not Filtered

Table E-1
Obstructed Simulation Results

Test	HRR (kW)	Diameter (m)	Source Height (m)	Elevation (m)	Maximum Plume Temperature Rise (C)	Baseline Test	Data Filtered	Filtration Criteria
ARCH_904	500	0.61	1.98	3.6	594.4	BASE_327	FALSE	Not Filtered
ARCH_904	500	0.61	1.98	3.9	434.66	BASE_327	FALSE	Not Filtered
ARCH_904	500	0.61	1.98	4.2	334.39	BASE_327	FALSE	Not Filtered
ARCH_904	500	0.61	1.98	4.5	256.69	BASE_327	FALSE	Not Filtered
ARCH_904	500	0.61	1.98	4.8	213.59	BASE_327	FALSE	Not Filtered
ARCH_904	500	0.61	1.98	5.1	182.15	BASE_327	FALSE	Not Filtered
ARCH_904	500	0.61	1.98	5.4	158.1	BASE_327	FALSE	Not Filtered
ARCH_904	500	0.61	1.98	5.7	135.49	BASE_327	FALSE	Not Filtered
ARCH_904	500	0.61	1.98	6	119.78	BASE_327	TRUE	Temperature < 130 C
ARCH_905	600	0.61	1.98	2.4	1103.1	BASE_328	TRUE	Temperature > 800 C
ARCH_905	600	0.61	1.98	2.7	1061.1	BASE_328	TRUE	Temperature > 800 C
ARCH_905	600	0.61	1.98	3	1012.7	BASE_328	TRUE	Temperature > 800 C
ARCH_905	600	0.61	1.98	3.3	890.92	BASE_328	TRUE	Temperature > 800 C
ARCH_905	600	0.61	1.98	3.6	734.06	BASE_328	FALSE	Not Filtered
ARCH_905	600	0.61	1.98	3.9	533.68	BASE_328	FALSE	Not Filtered
ARCH_905	600	0.61	1.98	4.2	418.77	BASE_328	FALSE	Not Filtered
ARCH_905	600	0.61	1.98	4.5	319.55	BASE_328	FALSE	Not Filtered
ARCH_905	600	0.61	1.98	4.8	263.95	BASE_328	FALSE	Not Filtered
ARCH_905	600	0.61	1.98	5.1	218.04	BASE_328	FALSE	Not Filtered
ARCH_905	600	0.61	1.98	5.4	182.57	BASE_328	FALSE	Not Filtered
ARCH_905	600	0.61	1.98	5.7	154.08	BASE_328	FALSE	Not Filtered

Table E-1
Obstructed Simulation Results

Test	HRR (kW)	Diameter (m)	Source Height (m)	Elevation (m)	Maximum Plume Temperature Rise (C)	Baseline Test	Data Filtered	Filtration Criteria
ARCH_905	600	0.61	1.98	6	136.82	BASE_328	FALSE	Not Filtered
ARCH_951	300	0.91	0.30	2.4	142.3	BASE_307	TRUE	Source Located 1 ft. above Ground
ARCH_951	300	0.91	0.30	2.7	100.22	BASE_307	TRUE	Temperature < 130 C , Source Located 1 ft. above Ground
ARCH_951	300	0.91	0.30	3	85.336	BASE_307	TRUE	Temperature < 130 C , Source Located 1 ft. above Ground
ARCH_951	300	0.91	0.30	3.3	75.533	BASE_307	TRUE	Temperature < 130 C , Source Located 1 ft. above Ground
ARCH_951	300	0.91	0.30	3.6	71.239	BASE_307	TRUE	Temperature < 130 C , Source Located 1 ft. above Ground
ARCH_951	300	0.91	0.30	3.9	65.25	BASE_307	TRUE	Temperature < 130 C , Source Located 1 ft. above Ground
ARCH_951	300	0.91	0.30	4.2	61.878	BASE_307	TRUE	Temperature < 130 C , Source Located 1 ft. above Ground
ARCH_951	300	0.91	0.30	4.5	57.541	BASE_307	TRUE	Temperature < 130 C , Source Located 1 ft. above Ground
ARCH_951	300	0.91	0.30	4.8	54.979	BASE_307	TRUE	Temperature < 130 C , Source Located 1 ft. above Ground
ARCH_951	300	0.91	0.30	5.1	52.798	BASE_307	TRUE	Temperature < 130 C , Source Located 1 ft. above Ground
ARCH_951	300	0.91	0.30	5.4	51.555	BASE_307	TRUE	Temperature < 130 C , Source Located 1 ft. above Ground
ARCH_951	300	0.91	0.30	5.7	49.802	BASE_307	TRUE	Temperature < 130 C , Source Located 1 ft. above Ground
ARCH_951	300	0.91	0.30	6	47.649	BASE_307	TRUE	Temperature < 130 C , Source Located 1 ft. above Ground

Table E-1
Obstructed Simulation Results

Test	HRR (kW)	Diameter (m)	Source Height (m)	Elevation (m)	Maximum Plume Temperature Rise (C)	Baseline Test	Data Filtered	Filtration Criteria
ARCH_952	400	0.91	0.30	2.4	181.52	BASE_308	TRUE	Source Located 1 ft. above Ground
ARCH_952	400	0.91	0.30	2.7	119.53	BASE_308	TRUE	Temperature < 130 C , Source Located 1 ft. above Ground
ARCH_952	400	0.91	0.30	3	101.81	BASE_308	TRUE	Temperature < 130 C , Source Located 1 ft. above Ground
ARCH_952	400	0.91	0.30	3.3	90.742	BASE_308	TRUE	Temperature < 130 C , Source Located 1 ft. above Ground
ARCH_952	400	0.91	0.30	3.6	82.895	BASE_308	TRUE	Temperature < 130 C , Source Located 1 ft. above Ground
ARCH_952	400	0.91	0.30	3.9	76.825	BASE_308	TRUE	Temperature < 130 C , Source Located 1 ft. above Ground
ARCH_952	400	0.91	0.30	4.2	71.033	BASE_308	TRUE	Temperature < 130 C , Source Located 1 ft. above Ground
ARCH_952	400	0.91	0.30	4.5	66.905	BASE_308	TRUE	Temperature < 130 C , Source Located 1 ft. above Ground
ARCH_952	400	0.91	0.30	4.8	63.285	BASE_308	TRUE	Temperature < 130 C , Source Located 1 ft. above Ground
ARCH_952	400	0.91	0.30	5.1	60.726	BASE_308	TRUE	Temperature < 130 C , Source Located 1 ft. above Ground
ARCH_952	400	0.91	0.30	5.4	58.829	BASE_308	TRUE	Temperature < 130 C , Source Located 1 ft. above Ground
ARCH_952	400	0.91	0.30	5.7	56.644	BASE_308	TRUE	Temperature < 130 C , Source Located 1 ft. above Ground
ARCH_952	400	0.91	0.30	6	54.836	BASE_308	TRUE	Temperature < 130 C , Source Located 1 ft. above Ground
ARCH_953	500	0.91	0.30	2.4	222.62	BASE_309	TRUE	Source Located 1 ft. above Ground

Table E-1
Obstructed Simulation Results

Test	HRR (kW)	Diameter (m)	Source Height (m)	Elevation (m)	Maximum Plume Temperature Rise (C)	Baseline Test	Data Filtered	Filtration Criteria
ARCH_953	500	0.91	0.30	2.7	144.54	BASE_309	TRUE	Source Located 1 ft. above Ground
ARCH_953	500	0.91	0.30	3	119.47	BASE_309	TRUE	Temperature < 130 C , Source Located 1 ft. above Ground
ARCH_953	500	0.91	0.30	3.3	104.67	BASE_309	TRUE	Temperature < 130 C , Source Located 1 ft. above Ground
ARCH_953	500	0.91	0.30	3.6	97.276	BASE_309	TRUE	Temperature < 130 C , Source Located 1 ft. above Ground
ARCH_953	500	0.91	0.30	3.9	88.925	BASE_309	TRUE	Temperature < 130 C , Source Located 1 ft. above Ground
ARCH_953	500	0.91	0.30	4.2	81.512	BASE_309	TRUE	Temperature < 130 C , Source Located 1 ft. above Ground
ARCH_953	500	0.91	0.30	4.5	76.345	BASE_309	TRUE	Temperature < 130 C , Source Located 1 ft. above Ground
ARCH_953	500	0.91	0.30	4.8	72.617	BASE_309	TRUE	Temperature < 130 C , Source Located 1 ft. above Ground
ARCH_953	500	0.91	0.30	5.1	70.106	BASE_309	TRUE	Temperature < 130 C , Source Located 1 ft. above Ground
ARCH_953	500	0.91	0.30	5.4	67.562	BASE_309	TRUE	Temperature < 130 C , Source Located 1 ft. above Ground
ARCH_953	500	0.91	0.30	5.7	65.966	BASE_309	TRUE	Temperature < 130 C , Source Located 1 ft. above Ground
ARCH_953	500	0.91	0.30	6	63.074	BASE_309	TRUE	Temperature < 130 C , Source Located 1 ft. above Ground
ARCH_954	600	0.91	0.30	2.4	249.34	BASE_310	TRUE	Source Located 1 ft. above Ground
ARCH_954	600	0.91	0.30	2.7	160.57	BASE_310	TRUE	Source Located 1 ft. above Ground
ARCH_954	600	0.91	0.30	3	131.61	BASE_310	TRUE	Source Located 1 ft. above Ground

Table E-1
Obstructed Simulation Results

Test	HRR (kW)	Diameter (m)	Source Height (m)	Elevation (m)	Maximum Plume Temperature Rise (C)	Baseline Test	Data Filtered	Filtration Criteria
ARCH_954	600	0.91	0.30	3.3	115.48	BASE_310	TRUE	Temperature < 130 C , Source Located 1 ft. above Ground
ARCH_954	600	0.91	0.30	3.6	105.73	BASE_310	TRUE	Temperature < 130 C , Source Located 1 ft. above Ground
ARCH_954	600	0.91	0.30	3.9	96.502	BASE_310	TRUE	Temperature < 130 C , Source Located 1 ft. above Ground
ARCH_954	600	0.91	0.30	4.2	88.467	BASE_310	TRUE	Temperature < 130 C , Source Located 1 ft. above Ground
ARCH_954	600	0.91	0.30	4.5	81.004	BASE_310	TRUE	Temperature < 130 C , Source Located 1 ft. above Ground
ARCH_954	600	0.91	0.30	4.8	75.232	BASE_310	TRUE	Temperature < 130 C , Source Located 1 ft. above Ground
ARCH_954	600	0.91	0.30	5.1	71.754	BASE_310	TRUE	Temperature < 130 C , Source Located 1 ft. above Ground
ARCH_954	600	0.91	0.30	5.4	68.018	BASE_310	TRUE	Temperature < 130 C , Source Located 1 ft. above Ground
ARCH_954	600	0.91	0.30	5.7	65.049	BASE_310	TRUE	Temperature < 130 C , Source Located 1 ft. above Ground
ARCH_954	600	0.91	0.30	6	63.057	BASE_310	TRUE	Temperature < 130 C , Source Located 1 ft. above Ground
ARCH_958	300	0.91	1.14	2.4	221.52	BASE_318	FALSE	Not Filtered
ARCH_958	300	0.91	1.14	2.7	135.52	BASE_318	FALSE	Not Filtered
ARCH_958	300	0.91	1.14	3	109.65	BASE_318	TRUE	Temperature < 130 C
ARCH_958	300	0.91	1.14	3.3	94	BASE_318	TRUE	Temperature < 130 C
ARCH_958	300	0.91	1.14	3.6	82.876	BASE_318	TRUE	Temperature < 130 C

Table E-1
Obstructed Simulation Results

Test	HRR (kW)	Diameter (m)	Source Height (m)	Elevation (m)	Maximum Plume Temperature Rise (C)	Baseline Test	Data Filtered	Filtration Criteria
ARCH_958	300	0.91	1.14	3.9	74.375	BASE_318	TRUE	Temperature < 130 C
ARCH_958	300	0.91	1.14	4.2	69.917	BASE_318	TRUE	Temperature < 130 C
ARCH_958	300	0.91	1.14	4.5	64.995	BASE_318	TRUE	Temperature < 130 C
ARCH_958	300	0.91	1.14	4.8	60.525	BASE_318	TRUE	Temperature < 130 C
ARCH_958	300	0.91	1.14	5.1	57.31	BASE_318	TRUE	Temperature < 130 C
ARCH_958	300	0.91	1.14	5.4	54.302	BASE_318	TRUE	Temperature < 130 C
ARCH_958	300	0.91	1.14	5.7	51.35	BASE_318	TRUE	Temperature < 130 C
ARCH_958	300	0.91	1.14	6	49.543	BASE_318	TRUE	Temperature < 130 C
ARCH_959	400	0.91	1.14	2.4	274.49	BASE_319	FALSE	Not Filtered
ARCH_959	400	0.91	1.14	2.7	170.19	BASE_319	FALSE	Not Filtered
ARCH_959	400	0.91	1.14	3	135.72	BASE_319	FALSE	Not Filtered
ARCH_959	400	0.91	1.14	3.3	111.31	BASE_319	TRUE	Temperature < 130 C
ARCH_959	400	0.91	1.14	3.6	97.466	BASE_319	TRUE	Temperature < 130 C
ARCH_959	400	0.91	1.14	3.9	88.814	BASE_319	TRUE	Temperature < 130 C
ARCH_959	400	0.91	1.14	4.2	83.577	BASE_319	TRUE	Temperature < 130 C
ARCH_959	400	0.91	1.14	4.5	77.256	BASE_319	TRUE	Temperature < 130 C
ARCH_959	400	0.91	1.14	4.8	72.615	BASE_319	TRUE	Temperature < 130 C
ARCH_959	400	0.91	1.14	5.1	66.86	BASE_319	TRUE	Temperature < 130 C
ARCH_959	400	0.91	1.14	5.4	61.074	BASE_319	TRUE	Temperature < 130 C
ARCH_959	400	0.91	1.14	5.7	56.642	BASE_319	TRUE	Temperature < 130 C
ARCH_959	400	0.91	1.14	6	53.967	BASE_319	TRUE	Temperature < 130 C

Table E-1
Obstructed Simulation Results

Test	HRR (kW)	Diameter (m)	Source Height (m)	Elevation (m)	Maximum Plume Temperature Rise (C)	Baseline Test	Data Filtered	Filtration Criteria
ARCH_960	500	0.91	1.14	2.4	371.76	BASE_320	FALSE	Not Filtered
ARCH_960	500	0.91	1.14	2.7	206.86	BASE_320	FALSE	Not Filtered
ARCH_960	500	0.91	1.14	3	166.01	BASE_320	FALSE	Not Filtered
ARCH_960	500	0.91	1.14	3.3	137.15	BASE_320	FALSE	Not Filtered
ARCH_960	500	0.91	1.14	3.6	120.9	BASE_320	TRUE	Temperature < 130 C
ARCH_960	500	0.91	1.14	3.9	110.17	BASE_320	TRUE	Temperature < 130 C
ARCH_960	500	0.91	1.14	4.2	100.36	BASE_320	TRUE	Temperature < 130 C
ARCH_960	500	0.91	1.14	4.5	91.016	BASE_320	TRUE	Temperature < 130 C
ARCH_960	500	0.91	1.14	4.8	84.619	BASE_320	TRUE	Temperature < 130 C
ARCH_960	500	0.91	1.14	5.1	79.613	BASE_320	TRUE	Temperature < 130 C
ARCH_960	500	0.91	1.14	5.4	72.486	BASE_320	TRUE	Temperature < 130 C
ARCH_960	500	0.91	1.14	5.7	65.353	BASE_320	TRUE	Temperature < 130 C
ARCH_960	500	0.91	1.14	6	61.863	BASE_320	TRUE	Temperature < 130 C
ARCH_961	600	0.91	1.14	2.4	432.98	BASE_321	FALSE	Not Filtered
ARCH_961	600	0.91	1.14	2.7	237.42	BASE_321	FALSE	Not Filtered
ARCH_961	600	0.91	1.14	3	184.16	BASE_321	FALSE	Not Filtered
ARCH_961	600	0.91	1.14	3.3	152.43	BASE_321	FALSE	Not Filtered
ARCH_961	600	0.91	1.14	3.6	133.03	BASE_321	FALSE	Not Filtered
ARCH_961	600	0.91	1.14	3.9	119.15	BASE_321	TRUE	Temperature < 130 C
ARCH_961	600	0.91	1.14	4.2	109.24	BASE_321	TRUE	Temperature < 130 C
ARCH_961	600	0.91	1.14	4.5	100.67	BASE_321	TRUE	Temperature < 130 C

Table E-1
Obstructed Simulation Results

Test	HRR (kW)	Diameter (m)	Source Height (m)	Elevation (m)	Maximum Plume Temperature Rise (C)	Baseline Test	Data Filtered	Filtration Criteria
ARCH_961	600	0.91	1.14	4.8	92.7	BASE_321	TRUE	Temperature < 130 C
ARCH_961	600	0.91	1.14	5.1	86.482	BASE_321	TRUE	Temperature < 130 C
ARCH_961	600	0.91	1.14	5.4	80.763	BASE_321	TRUE	Temperature < 130 C
ARCH_961	600	0.91	1.14	5.7	73.875	BASE_321	TRUE	Temperature < 130 C
ARCH_961	600	0.91	1.14	6	68.907	BASE_321	TRUE	Temperature < 130 C
ARCH_965	300	0.91	1.98	2.4	607.47	BASE_329	FALSE	Not Filtered
ARCH_965	300	0.91	1.98	2.7	331.53	BASE_329	FALSE	Not Filtered
ARCH_965	300	0.91	1.98	3	232.09	BASE_329	FALSE	Not Filtered
ARCH_965	300	0.91	1.98	3.3	177.64	BASE_329	FALSE	Not Filtered
ARCH_965	300	0.91	1.98	3.6	146.25	BASE_329	FALSE	Not Filtered
ARCH_965	300	0.91	1.98	3.9	126.7	BASE_329	TRUE	Temperature < 130 C
ARCH_965	300	0.91	1.98	4.2	112.7	BASE_329	TRUE	Temperature < 130 C
ARCH_965	300	0.91	1.98	4.5	98.797	BASE_329	TRUE	Temperature < 130 C
ARCH_965	300	0.91	1.98	4.8	90.066	BASE_329	TRUE	Temperature < 130 C
ARCH_965	300	0.91	1.98	5.1	83.373	BASE_329	TRUE	Temperature < 130 C
ARCH_965	300	0.91	1.98	5.4	78.82	BASE_329	TRUE	Temperature < 130 C
ARCH_965	300	0.91	1.98	5.7	73.241	BASE_329	TRUE	Temperature < 130 C
ARCH_965	300	0.91	1.98	6	68.812	BASE_329	TRUE	Temperature < 130 C
ARCH_966	400	0.91	1.98	2.4	868.44	BASE_330	TRUE	Temperature > 800 C
ARCH_966	400	0.91	1.98	2.7	552.14	BASE_330	FALSE	Not Filtered
ARCH_966	400	0.91	1.98	3	368	BASE_330	FALSE	Not Filtered

Table E-1
Obstructed Simulation Results

Test	HRR (kW)	Diameter (m)	Source Height (m)	Elevation (m)	Maximum Plume Temperature Rise (C)	Baseline Test	Data Filtered	Filtration Criteria
ARCH_966	400	0.91	1.98	3.3	275.26	BASE_330	FALSE	Not Filtered
ARCH_966	400	0.91	1.98	3.6	219.12	BASE_330	FALSE	Not Filtered
ARCH_966	400	0.91	1.98	3.9	180.14	BASE_330	FALSE	Not Filtered
ARCH_966	400	0.91	1.98	4.2	154.08	BASE_330	FALSE	Not Filtered
ARCH_966	400	0.91	1.98	4.5	130.46	BASE_330	FALSE	Not Filtered
ARCH_966	400	0.91	1.98	4.8	114.68	BASE_330	TRUE	Temperature < 130 C
ARCH_966	400	0.91	1.98	5.1	102.07	BASE_330	TRUE	Temperature < 130 C
ARCH_966	400	0.91	1.98	5.4	92.363	BASE_330	TRUE	Temperature < 130 C
ARCH_966	400	0.91	1.98	5.7	85.204	BASE_330	TRUE	Temperature < 130 C
ARCH_966	400	0.91	1.98	6	80.246	BASE_330	TRUE	Temperature < 130 C
ARCH_967	500	0.91	1.98	2.4	887.06	BASE_331	TRUE	Temperature > 800 C
ARCH_967	500	0.91	1.98	2.7	642.57	BASE_331	FALSE	Not Filtered
ARCH_967	500	0.91	1.98	3	449.19	BASE_331	FALSE	Not Filtered
ARCH_967	500	0.91	1.98	3.3	324.39	BASE_331	FALSE	Not Filtered
ARCH_967	500	0.91	1.98	3.6	252.72	BASE_331	FALSE	Not Filtered
ARCH_967	500	0.91	1.98	3.9	216.54	BASE_331	FALSE	Not Filtered
ARCH_967	500	0.91	1.98	4.2	183.63	BASE_331	FALSE	Not Filtered
ARCH_967	500	0.91	1.98	4.5	153.81	BASE_331	FALSE	Not Filtered
ARCH_967	500	0.91	1.98	4.8	134.52	BASE_331	FALSE	Not Filtered
ARCH_967	500	0.91	1.98	5.1	119.4	BASE_331	TRUE	Temperature < 130 C
ARCH_967	500	0.91	1.98	5.4	107.44	BASE_331	TRUE	Temperature < 130 C

Table E-1
Obstructed Simulation Results

Test	HRR (kW)	Diameter (m)	Source Height (m)	Elevation (m)	Maximum Plume Temperature Rise (C)	Baseline Test	Data Filtered	Filtration Criteria
ARCH_967	500	0.91	1.98	5.7	98.525	BASE_331	TRUE	Temperature < 130 C
ARCH_967	500	0.91	1.98	6	91.036	BASE_331	TRUE	Temperature < 130 C
ARCH_968	600	0.91	1.98	2.4	965.8	BASE_332	TRUE	Temperature > 800 C
ARCH_968	600	0.91	1.98	2.7	717.36	BASE_332	FALSE	Not Filtered
ARCH_968	600	0.91	1.98	3	549.99	BASE_332	FALSE	Not Filtered
ARCH_968	600	0.91	1.98	3.3	412.15	BASE_332	FALSE	Not Filtered
ARCH_968	600	0.91	1.98	3.6	311.81	BASE_332	FALSE	Not Filtered
ARCH_968	600	0.91	1.98	3.9	245.14	BASE_332	FALSE	Not Filtered
ARCH_968	600	0.91	1.98	4.2	209.01	BASE_332	FALSE	Not Filtered
ARCH_968	600	0.91	1.98	4.5	173.48	BASE_332	FALSE	Not Filtered
ARCH_968	600	0.91	1.98	4.8	149.83	BASE_332	FALSE	Not Filtered
ARCH_968	600	0.91	1.98	5.1	131.62	BASE_332	FALSE	Not Filtered
ARCH_968	600	0.91	1.98	5.4	118.34	BASE_332	TRUE	Temperature < 130 C
ARCH_968	600	0.91	1.98	5.7	106.75	BASE_332	TRUE	Temperature < 130 C
ARCH_968	600	0.91	1.98	6	99.896	BASE_332	TRUE	Temperature < 130 C
OBST_1051	1000	0.91	0.30	2.4	533.89	BASE_404	TRUE	Source Located 1 ft. above Ground
OBST_1051	1000	0.91	0.30	2.7	422.39	BASE_404	TRUE	Source Located 1 ft. above Ground
OBST_1051	1000	0.91	0.30	3	340.68	BASE_404	TRUE	Source Located 1 ft. above Ground
OBST_1051	1000	0.91	0.30	3.3	270.01	BASE_404	TRUE	Source Located 1 ft. above Ground
OBST_1051	1000	0.91	0.30	3.6	233.57	BASE_404	TRUE	Source Located 1 ft. above Ground
OBST_1051	1000	0.91	0.30	3.9	215.99	BASE_404	TRUE	Source Located 1 ft. above Ground

Table E-1
Obstructed Simulation Results

Test	HRR (kW)	Diameter (m)	Source Height (m)	Elevation (m)	Maximum Plume Temperature Rise (C)	Baseline Test	Data Filtered	Filtration Criteria
OBST_1051	1000	0.91	0.30	4.2	206.03	BASE_404	TRUE	Source Located 1 ft. above Ground
OBST_1051	1000	0.91	0.30	4.5	193.24	BASE_404	TRUE	Source Located 1 ft. above Ground
OBST_1051	1000	0.91	0.30	4.8	182.06	BASE_404	TRUE	Source Located 1 ft. above Ground
OBST_1051	1000	0.91	0.30	5.1	172.23	BASE_404	TRUE	Source Located 1 ft. above Ground
OBST_1051	1000	0.91	0.30	5.4	163.41	BASE_404	TRUE	Source Located 1 ft. above Ground
OBST_1051	1000	0.91	0.30	5.7	155.42	BASE_404	TRUE	Source Located 1 ft. above Ground
OBST_1051	1000	0.91	0.30	6	147.94	BASE_404	TRUE	Source Located 1 ft. above Ground
OBST_1052	1000	0.91	1.14	2.4	828.59	BASE_400	TRUE	Temperature > 800 C
OBST_1052	1000	0.91	1.14	2.7	639.49	BASE_400	FALSE	Not Filtered
OBST_1052	1000	0.91	1.14	3	485.41	BASE_400	FALSE	Not Filtered
OBST_1052	1000	0.91	1.14	3.3	380.12	BASE_400	FALSE	Not Filtered
OBST_1052	1000	0.91	1.14	3.6	338.6	BASE_400	FALSE	Not Filtered
OBST_1052	1000	0.91	1.14	3.9	319.22	BASE_400	FALSE	Not Filtered
OBST_1052	1000	0.91	1.14	4.2	306.21	BASE_400	FALSE	Not Filtered
OBST_1052	1000	0.91	1.14	4.5	288.02	BASE_400	FALSE	Not Filtered
OBST_1052	1000	0.91	1.14	4.8	270.8	BASE_400	FALSE	Not Filtered
OBST_1052	1000	0.91	1.14	5.1	255.33	BASE_400	FALSE	Not Filtered
OBST_1052	1000	0.91	1.14	5.4	236.32	BASE_400	FALSE	Not Filtered
OBST_1052	1000	0.91	1.14	5.7	219.16	BASE_400	FALSE	Not Filtered
OBST_1052	1000	0.91	1.14	6	204.84	BASE_400	FALSE	Not Filtered
OBST_1053	1000	0.91	1.98	2.4	1086.9	BASE_401	TRUE	Temperature > 800 C

Table E-1
Obstructed Simulation Results

Test	HRR (kW)	Diameter (m)	Source Height (m)	Elevation (m)	Maximum Plume Temperature Rise (C)	Baseline Test	Data Filtered	Filtration Criteria
OBST_1053	1000	0.91	1.98	2.7	883.59	BASE_401	TRUE	Temperature > 800 C
OBST_1053	1000	0.91	1.98	3	823.73	BASE_401	TRUE	Temperature > 800 C
OBST_1053	1000	0.91	1.98	3.3	734.4	BASE_401	FALSE	Not Filtered
OBST_1053	1000	0.91	1.98	3.6	670.23	BASE_401	FALSE	Not Filtered
OBST_1053	1000	0.91	1.98	3.9	596.13	BASE_401	FALSE	Not Filtered
OBST_1053	1000	0.91	1.98	4.2	534.31	BASE_401	FALSE	Not Filtered
OBST_1053	1000	0.91	1.98	4.5	470.83	BASE_401	FALSE	Not Filtered
OBST_1053	1000	0.91	1.98	4.8	424.86	BASE_401	FALSE	Not Filtered
OBST_1053	1000	0.91	1.98	5.1	382.82	BASE_401	FALSE	Not Filtered
OBST_1053	1000	0.91	1.98	5.4	333	BASE_401	FALSE	Not Filtered
OBST_1053	1000	0.91	1.98	5.7	293.13	BASE_401	FALSE	Not Filtered
OBST_1053	1000	0.91	1.98	6	258.54	BASE_401	FALSE	Not Filtered
OBST_1060	1000	1.22	0.30	2.4	397.06	BASE_405	TRUE	Source Located 1 ft. above Ground
OBST_1060	1000	1.22	0.30	2.7	319.73	BASE_405	TRUE	Source Located 1 ft. above Ground
OBST_1060	1000	1.22	0.30	3	250.83	BASE_405	TRUE	Source Located 1 ft. above Ground
OBST_1060	1000	1.22	0.30	3.3	197.52	BASE_405	TRUE	Source Located 1 ft. above Ground
OBST_1060	1000	1.22	0.30	3.6	182.14	BASE_405	TRUE	Source Located 1 ft. above Ground
OBST_1060	1000	1.22	0.30	3.9	171.16	BASE_405	TRUE	Source Located 1 ft. above Ground
OBST_1060	1000	1.22	0.30	4.2	163.99	BASE_405	TRUE	Source Located 1 ft. above Ground
OBST_1060	1000	1.22	0.30	4.5	157.72	BASE_405	TRUE	Source Located 1 ft. above Ground
OBST_1060	1000	1.22	0.30	4.8	152.54	BASE_405	TRUE	Source Located 1 ft. above Ground

Table E-1
Obstructed Simulation Results

Test	HRR (kW)	Diameter (m)	Source Height (m)	Elevation (m)	Maximum Plume Temperature Rise (C)	Baseline Test	Data Filtered	Filtration Criteria
OBST_1060	1000	1.22	0.30	5.1	147.72	BASE_405	TRUE	Source Located 1 ft. above Ground
OBST_1060	1000	1.22	0.30	5.4	141.96	BASE_405	TRUE	Source Located 1 ft. above Ground
OBST_1060	1000	1.22	0.30	5.7	135.56	BASE_405	TRUE	Source Located 1 ft. above Ground
OBST_1060	1000	1.22	0.30	6	131.27	BASE_405	TRUE	Source Located 1 ft. above Ground
OBST_1061	1000	1.22	1.14	2.4	688.56	BASE_402	FALSE	Not Filtered
OBST_1061	1000	1.22	1.14	2.7	513.44	BASE_402	FALSE	Not Filtered
OBST_1061	1000	1.22	1.14	3	396.9	BASE_402	FALSE	Not Filtered
OBST_1061	1000	1.22	1.14	3.3	320.69	BASE_402	FALSE	Not Filtered
OBST_1061	1000	1.22	1.14	3.6	279.7	BASE_402	FALSE	Not Filtered
OBST_1061	1000	1.22	1.14	3.9	255.99	BASE_402	FALSE	Not Filtered
OBST_1061	1000	1.22	1.14	4.2	239.89	BASE_402	FALSE	Not Filtered
OBST_1061	1000	1.22	1.14	4.5	226.26	BASE_402	FALSE	Not Filtered
OBST_1061	1000	1.22	1.14	4.8	216.94	BASE_402	FALSE	Not Filtered
OBST_1061	1000	1.22	1.14	5.1	207.38	BASE_402	FALSE	Not Filtered
OBST_1061	1000	1.22	1.14	5.4	196.74	BASE_402	FALSE	Not Filtered
OBST_1061	1000	1.22	1.14	5.7	184	BASE_402	FALSE	Not Filtered
OBST_1061	1000	1.22	1.14	6	172.26	BASE_402	FALSE	Not Filtered
OBST_1062	1000	1.22	1.98	2.4	1024.3	BASE_403	TRUE	Temperature > 800 C
OBST_1062	1000	1.22	1.98	2.7	743.77	BASE_403	FALSE	Not Filtered
OBST_1062	1000	1.22	1.98	3	668.11	BASE_403	FALSE	Not Filtered
OBST_1062	1000	1.22	1.98	3.3	599.14	BASE_403	FALSE	Not Filtered

Table E-1
Obstructed Simulation Results

Test	HRR (kW)	Diameter (m)	Source Height (m)	Elevation (m)	Maximum Plume Temperature Rise (C)	Baseline Test	Data Filtered	Filtration Criteria
OBST_1062	1000	1.22	1.98	3.6	551	BASE_403	FALSE	Not Filtered
OBST_1062	1000	1.22	1.98	3.9	494.5	BASE_403	FALSE	Not Filtered
OBST_1062	1000	1.22	1.98	4.2	446.72	BASE_403	FALSE	Not Filtered
OBST_1062	1000	1.22	1.98	4.5	405.71	BASE_403	FALSE	Not Filtered
OBST_1062	1000	1.22	1.98	4.8	367.67	BASE_403	FALSE	Not Filtered
OBST_1062	1000	1.22	1.98	5.1	333.88	BASE_403	FALSE	Not Filtered
OBST_1062	1000	1.22	1.98	5.4	295.56	BASE_403	FALSE	Not Filtered
OBST_1062	1000	1.22	1.98	5.7	259.91	BASE_403	FALSE	Not Filtered
OBST_1062	1000	1.22	1.98	6	233	BASE_403	FALSE	Not Filtered
OBST_801	50	0.30	0.30	2.4	87.091	BASE_300	TRUE	Temperature < 130 C , Source Located 1 ft. above Ground
OBST_801	50	0.30	0.30	2.7	74.382	BASE_300	TRUE	Temperature < 130 C , Source Located 1 ft. above Ground
OBST_801	50	0.30	0.30	3	67.295	BASE_300	TRUE	Temperature < 130 C , Source Located 1 ft. above Ground
OBST_801	50	0.30	0.30	3.3	60.832	BASE_300	TRUE	Temperature < 130 C , Source Located 1 ft. above Ground
OBST_801	50	0.30	0.30	3.6	56.846	BASE_300	TRUE	Temperature < 130 C , Source Located 1 ft. above Ground
OBST_801	50	0.30	0.30	3.9	53.889	BASE_300	TRUE	Temperature < 130 C , Source Located 1 ft. above Ground
OBST_801	50	0.30	0.30	4.2	51.386	BASE_300	TRUE	Temperature < 130 C , Source Located 1 ft. above Ground
OBST_801	50	0.30	0.30	4.5	48.698	BASE_300	TRUE	Temperature < 130 C , Source

Table E-1
Obstructed Simulation Results

Test	HRR (kW)	Diameter (m)	Source Height (m)	Elevation (m)	Maximum Plume Temperature Rise (C)	Baseline Test	Data Filtered	Filtration Criteria
								Located 1 ft. above Ground
OBST_801	50	0.30	0.30	4.8	45.556	BASE_300	TRUE	Temperature < 130 C , Source Located 1 ft. above Ground
OBST_801	50	0.30	0.30	5.1	43.585	BASE_300	TRUE	Temperature < 130 C , Source Located 1 ft. above Ground
OBST_801	50	0.30	0.30	5.4	40.939	BASE_300	TRUE	Temperature < 130 C , Source Located 1 ft. above Ground
OBST_802	100	0.30	0.30	2.4	150.06	BASE_301	TRUE	Source Located 1 ft. above Ground
OBST_802	100	0.30	0.30	2.7	115.07	BASE_301	TRUE	Temperature < 130 C , Source Located 1 ft. above Ground
OBST_802	100	0.30	0.30	3	106.42	BASE_301	TRUE	Temperature < 130 C , Source Located 1 ft. above Ground
OBST_802	100	0.30	0.30	3.3	97.657	BASE_301	TRUE	Temperature < 130 C , Source Located 1 ft. above Ground
OBST_802	100	0.30	0.30	3.6	88.334	BASE_301	TRUE	Temperature < 130 C , Source Located 1 ft. above Ground
OBST_802	100	0.30	0.30	3.9	81.554	BASE_301	TRUE	Temperature < 130 C , Source Located 1 ft. above Ground
OBST_802	100	0.30	0.30	4.2	74.802	BASE_301	TRUE	Temperature < 130 C , Source Located 1 ft. above Ground
OBST_802	100	0.30	0.30	4.5	67.73	BASE_301	TRUE	Temperature < 130 C , Source Located 1 ft. above Ground
OBST_802	100	0.30	0.30	4.8	64.039	BASE_301	TRUE	Temperature < 130 C , Source Located 1 ft. above Ground
OBST_802	100	0.30	0.30	5.1	60.336	BASE_301	TRUE	Temperature < 130 C , Source Located 1 ft. above Ground

Table E-1
Obstructed Simulation Results

Test	HRR (kW)	Diameter (m)	Source Height (m)	Elevation (m)	Maximum Plume Temperature Rise (C)	Baseline Test	Data Filtered	Filtration Criteria
OBST_802	100	0.30	0.30	5.4	56.214	BASE_301	TRUE	Temperature < 130 C , Source Located 1 ft. above Ground
OBST_802	100	0.30	0.30	5.7	52.062	BASE_301	TRUE	Temperature < 130 C , Source Located 1 ft. above Ground
OBST_802	100	0.30	0.30	6	49.453	BASE_301	TRUE	Temperature < 130 C , Source Located 1 ft. above Ground
OBST_808	50	0.30	1.14	2.4	138.47	BASE_311	FALSE	Not Filtered
OBST_808	50	0.30	1.14	2.7	100.55	BASE_311	TRUE	Temperature < 130 C
OBST_808	50	0.30	1.14	3	82.454	BASE_311	TRUE	Temperature < 130 C
OBST_808	50	0.30	1.14	3.3	75.188	BASE_311	TRUE	Temperature < 130 C
OBST_808	50	0.30	1.14	3.6	70.849	BASE_311	TRUE	Temperature < 130 C
OBST_808	50	0.30	1.14	3.9	66.382	BASE_311	TRUE	Temperature < 130 C
OBST_808	50	0.30	1.14	4.2	62.626	BASE_311	TRUE	Temperature < 130 C
OBST_808	50	0.30	1.14	4.5	58.6	BASE_311	TRUE	Temperature < 130 C
OBST_808	50	0.30	1.14	4.8	54.769	BASE_311	TRUE	Temperature < 130 C
OBST_808	50	0.30	1.14	5.1	51.378	BASE_311	TRUE	Temperature < 130 C
OBST_808	50	0.30	1.14	5.4	48.644	BASE_311	TRUE	Temperature < 130 C
OBST_808	50	0.30	1.14	5.7	45.892	BASE_311	TRUE	Temperature < 130 C
OBST_808	50	0.30	1.14	6	44.185	BASE_311	TRUE	Temperature < 130 C
OBST_809	100	0.30	1.14	2.4	235.87	BASE_312	FALSE	Not Filtered
OBST_809	100	0.30	1.14	2.7	155.85	BASE_312	FALSE	Not Filtered
OBST_809	100	0.30	1.14	3	121.47	BASE_312	TRUE	Temperature < 130 C

Table E-1
Obstructed Simulation Results

Test	HRR (kW)	Diameter (m)	Source Height (m)	Elevation (m)	Maximum Plume Temperature Rise (C)	Baseline Test	Data Filtered	Filtration Criteria
OBST_809	100	0.30	1.14	3.3	110.1	BASE_312	TRUE	Temperature < 130 C
OBST_809	100	0.30	1.14	3.6	100.82	BASE_312	TRUE	Temperature < 130 C
OBST_809	100	0.30	1.14	3.9	91.194	BASE_312	TRUE	Temperature < 130 C
OBST_809	100	0.30	1.14	4.2	84.456	BASE_312	TRUE	Temperature < 130 C
OBST_809	100	0.30	1.14	4.5	77.93	BASE_312	TRUE	Temperature < 130 C
OBST_809	100	0.30	1.14	4.8	72.592	BASE_312	TRUE	Temperature < 130 C
OBST_809	100	0.30	1.14	5.1	67.397	BASE_312	TRUE	Temperature < 130 C
OBST_809	100	0.30	1.14	5.4	62.75	BASE_312	TRUE	Temperature < 130 C
OBST_809	100	0.30	1.14	5.7	59.553	BASE_312	TRUE	Temperature < 130 C
OBST_809	100	0.30	1.14	6	56.916	BASE_312	TRUE	Temperature < 130 C
OBST_815	50	0.30	1.98	2.4	238.53	BASE_322	FALSE	Not Filtered
OBST_815	50	0.30	1.98	2.7	142.51	BASE_322	FALSE	Not Filtered
OBST_815	50	0.30	1.98	3	107.22	BASE_322	TRUE	Temperature < 130 C
OBST_815	50	0.30	1.98	3.3	93.883	BASE_322	TRUE	Temperature < 130 C
OBST_815	50	0.30	1.98	3.6	86.855	BASE_322	TRUE	Temperature < 130 C
OBST_815	50	0.30	1.98	3.9	78.339	BASE_322	TRUE	Temperature < 130 C
OBST_815	50	0.30	1.98	4.2	71.221	BASE_322	TRUE	Temperature < 130 C
OBST_815	50	0.30	1.98	4.5	63.611	BASE_322	TRUE	Temperature < 130 C
OBST_815	50	0.30	1.98	4.8	58.549	BASE_322	TRUE	Temperature < 130 C
OBST_815	50	0.30	1.98	5.1	55.323	BASE_322	TRUE	Temperature < 130 C
OBST_815	50	0.30	1.98	5.4	51.364	BASE_322	TRUE	Temperature < 130 C

Table E-1
Obstructed Simulation Results

Test	HRR (kW)	Diameter (m)	Source Height (m)	Elevation (m)	Maximum Plume Temperature Rise (C)	Baseline Test	Data Filtered	Filtration Criteria
OBST_815	50	0.30	1.98	5.7	47.838	BASE_322	TRUE	Temperature < 130 C
OBST_815	50	0.30	1.98	6	45.651	BASE_322	TRUE	Temperature < 130 C
OBST_816	100	0.30	1.98	2.4	434.45	BASE_323	FALSE	Not Filtered
OBST_816	100	0.30	1.98	2.7	227.23	BASE_323	FALSE	Not Filtered
OBST_816	100	0.30	1.98	3	170.7	BASE_323	FALSE	Not Filtered
OBST_816	100	0.30	1.98	3.3	145.87	BASE_323	FALSE	Not Filtered
OBST_816	100	0.30	1.98	3.6	130.11	BASE_323	FALSE	Not Filtered
OBST_816	100	0.30	1.98	3.9	116.02	BASE_323	TRUE	Temperature < 130 C
OBST_816	100	0.30	1.98	4.2	104.88	BASE_323	TRUE	Temperature < 130 C
OBST_816	100	0.30	1.98	4.5	91.788	BASE_323	TRUE	Temperature < 130 C
OBST_816	100	0.30	1.98	4.8	84.026	BASE_323	TRUE	Temperature < 130 C
OBST_816	100	0.30	1.98	5.1	78.137	BASE_323	TRUE	Temperature < 130 C
OBST_816	100	0.30	1.98	5.4	71.948	BASE_323	TRUE	Temperature < 130 C
OBST_816	100	0.30	1.98	5.7	66.311	BASE_323	TRUE	Temperature < 130 C
OBST_816	100	0.30	1.98	6	62.282	BASE_323	TRUE	Temperature < 130 C
OBST_866	200	0.61	0.30	2.4	164.84	BASE_302	TRUE	Source Located 1 ft. above Ground
OBST_866	200	0.61	0.30	2.7	132.51	BASE_302	TRUE	Source Located 1 ft. above Ground
OBST_866	200	0.61	0.30	3	107.21	BASE_302	TRUE	Temperature < 130 C , Source Located 1 ft. above Ground
OBST_866	200	0.61	0.30	3.3	95.331	BASE_302	TRUE	Temperature < 130 C , Source Located 1 ft. above Ground
OBST_866	200	0.61	0.30	3.6	91.403	BASE_302	TRUE	Temperature < 130 C , Source

Table E-1
Obstructed Simulation Results

Test	HRR (kW)	Diameter (m)	Source Height (m)	Elevation (m)	Maximum Plume Temperature Rise (C)	Baseline Test	Data Filtered	Filtration Criteria
								Located 1 ft. above Ground
OBST_866	200	0.61	0.30	3.9	87.841	BASE_302	TRUE	Temperature < 130 C , Source Located 1 ft. above Ground
OBST_866	200	0.61	0.30	4.2	85.424	BASE_302	TRUE	Temperature < 130 C , Source Located 1 ft. above Ground
OBST_866	200	0.61	0.30	4.5	81.446	BASE_302	TRUE	Temperature < 130 C , Source Located 1 ft. above Ground
OBST_866	200	0.61	0.30	4.8	77.871	BASE_302	TRUE	Temperature < 130 C , Source Located 1 ft. above Ground
OBST_866	200	0.61	0.30	5.1	74.707	BASE_302	TRUE	Temperature < 130 C , Source Located 1 ft. above Ground
OBST_866	200	0.61	0.30	5.4	70.967	BASE_302	TRUE	Temperature < 130 C , Source Located 1 ft. above Ground
OBST_866	200	0.61	0.30	5.7	67.65	BASE_302	TRUE	Temperature < 130 C , Source Located 1 ft. above Ground
OBST_866	200	0.61	0.30	6	65.534	BASE_302	TRUE	Temperature < 130 C , Source Located 1 ft. above Ground
OBST_867	300	0.61	0.30	2.4	222.46	BASE_303	TRUE	Source Located 1 ft. above Ground
OBST_867	300	0.61	0.30	2.7	180.68	BASE_303	TRUE	Source Located 1 ft. above Ground
OBST_867	300	0.61	0.30	3	140.38	BASE_303	TRUE	Source Located 1 ft. above Ground
OBST_867	300	0.61	0.30	3.3	122.94	BASE_303	TRUE	Temperature < 130 C , Source Located 1 ft. above Ground
OBST_867	300	0.61	0.30	3.6	116.1	BASE_303	TRUE	Temperature < 130 C , Source Located 1 ft. above Ground
OBST_867	300	0.61	0.30	3.9	110.06	BASE_303	TRUE	Temperature < 130 C , Source Located 1 ft. above Ground

Table E-1
Obstructed Simulation Results

Test	HRR (kW)	Diameter (m)	Source Height (m)	Elevation (m)	Maximum Plume Temperature Rise (C)	Baseline Test	Data Filtered	Filtration Criteria
OBST_867	300	0.61	0.30	4.2	105.24	BASE_303	TRUE	Temperature < 130 C , Source Located 1 ft. above Ground
OBST_867	300	0.61	0.30	4.5	99.731	BASE_303	TRUE	Temperature < 130 C , Source Located 1 ft. above Ground
OBST_867	300	0.61	0.30	4.8	95.923	BASE_303	TRUE	Temperature < 130 C , Source Located 1 ft. above Ground
OBST_867	300	0.61	0.30	5.1	91.96	BASE_303	TRUE	Temperature < 130 C , Source Located 1 ft. above Ground
OBST_867	300	0.61	0.30	5.4	86.163	BASE_303	TRUE	Temperature < 130 C , Source Located 1 ft. above Ground
OBST_867	300	0.61	0.30	5.7	81.681	BASE_303	TRUE	Temperature < 130 C , Source Located 1 ft. above Ground
OBST_867	300	0.61	0.30	6	78.494	BASE_303	TRUE	Temperature < 130 C , Source Located 1 ft. above Ground
OBST_868	400	0.61	0.30	2.4	291.34	BASE_304	TRUE	Source Located 1 ft. above Ground
OBST_868	400	0.61	0.30	2.7	240.71	BASE_304	TRUE	Source Located 1 ft. above Ground
OBST_868	400	0.61	0.30	3	182.9	BASE_304	TRUE	Source Located 1 ft. above Ground
OBST_868	400	0.61	0.30	3.3	153	BASE_304	TRUE	Source Located 1 ft. above Ground
OBST_868	400	0.61	0.30	3.6	139.81	BASE_304	TRUE	Source Located 1 ft. above Ground
OBST_868	400	0.61	0.30	3.9	130.81	BASE_304	TRUE	Source Located 1 ft. above Ground
OBST_868	400	0.61	0.30	4.2	123.93	BASE_304	TRUE	Temperature < 130 C , Source Located 1 ft. above Ground
OBST_868	400	0.61	0.30	4.5	117.05	BASE_304	TRUE	Temperature < 130 C , Source Located 1 ft. above Ground
OBST_868	400	0.61	0.30	4.8	111.78	BASE_304	TRUE	Temperature < 130 C , Source

Table E-1
Obstructed Simulation Results

Test	HRR (kW)	Diameter (m)	Source Height (m)	Elevation (m)	Maximum Plume Temperature Rise (C)	Baseline Test	Data Filtered	Filtration Criteria
								Located 1 ft. above Ground
OBST_868	400	0.61	0.30	5.1	107.26	BASE_304	TRUE	Temperature < 130 C , Source Located 1 ft. above Ground
OBST_868	400	0.61	0.30	5.4	101.33	BASE_304	TRUE	Temperature < 130 C , Source Located 1 ft. above Ground
OBST_868	400	0.61	0.30	5.7	97.187	BASE_304	TRUE	Temperature < 130 C , Source Located 1 ft. above Ground
OBST_868	400	0.61	0.30	6	92.575	BASE_304	TRUE	Temperature < 130 C , Source Located 1 ft. above Ground
OBST_869	500	0.61	0.30	2.4	360.38	BASE_305	TRUE	Source Located 1 ft. above Ground
OBST_869	500	0.61	0.30	2.7	296.38	BASE_305	TRUE	Source Located 1 ft. above Ground
OBST_869	500	0.61	0.30	3	226.34	BASE_305	TRUE	Source Located 1 ft. above Ground
OBST_869	500	0.61	0.30	3.3	187.21	BASE_305	TRUE	Source Located 1 ft. above Ground
OBST_869	500	0.61	0.30	3.6	176.3	BASE_305	TRUE	Source Located 1 ft. above Ground
OBST_869	500	0.61	0.30	3.9	161.36	BASE_305	TRUE	Source Located 1 ft. above Ground
OBST_869	500	0.61	0.30	4.2	151.9	BASE_305	TRUE	Source Located 1 ft. above Ground
OBST_869	500	0.61	0.30	4.5	142.66	BASE_305	TRUE	Source Located 1 ft. above Ground
OBST_869	500	0.61	0.30	4.8	135.24	BASE_305	TRUE	Source Located 1 ft. above Ground
OBST_869	500	0.61	0.30	5.1	128.53	BASE_305	TRUE	Temperature < 130 C , Source Located 1 ft. above Ground
OBST_869	500	0.61	0.30	5.4	120.48	BASE_305	TRUE	Temperature < 130 C , Source Located 1 ft. above Ground
OBST_869	500	0.61	0.30	5.7	112.01	BASE_305	TRUE	Temperature < 130 C , Source Located 1 ft. above Ground

Table E-1
Obstructed Simulation Results

Test	HRR (kW)	Diameter (m)	Source Height (m)	Elevation (m)	Maximum Plume Temperature Rise (C)	Baseline Test	Data Filtered	Filtration Criteria
OBST_869	500	0.61	0.30	6	105.22	BASE_305	TRUE	Temperature < 130 C , Source Located 1 ft. above Ground
OBST_870	600	0.61	0.30	2.4	444.1	BASE_306	TRUE	Source Located 1 ft. above Ground
OBST_870	600	0.61	0.30	2.7	366.54	BASE_306	TRUE	Source Located 1 ft. above Ground
OBST_870	600	0.61	0.30	3	267.05	BASE_306	TRUE	Source Located 1 ft. above Ground
OBST_870	600	0.61	0.30	3.3	208.14	BASE_306	TRUE	Source Located 1 ft. above Ground
OBST_870	600	0.61	0.30	3.6	196.87	BASE_306	TRUE	Source Located 1 ft. above Ground
OBST_870	600	0.61	0.30	3.9	187.62	BASE_306	TRUE	Source Located 1 ft. above Ground
OBST_870	600	0.61	0.30	4.2	177.69	BASE_306	TRUE	Source Located 1 ft. above Ground
OBST_870	600	0.61	0.30	4.5	166.61	BASE_306	TRUE	Source Located 1 ft. above Ground
OBST_870	600	0.61	0.30	4.8	156.15	BASE_306	TRUE	Source Located 1 ft. above Ground
OBST_870	600	0.61	0.30	5.1	146.03	BASE_306	TRUE	Source Located 1 ft. above Ground
OBST_870	600	0.61	0.30	5.4	136.86	BASE_306	TRUE	Source Located 1 ft. above Ground
OBST_870	600	0.61	0.30	5.7	127.13	BASE_306	TRUE	Temperature < 130 C , Source Located 1 ft. above Ground
OBST_870	600	0.61	0.30	6	118.31	BASE_306	TRUE	Temperature < 130 C , Source Located 1 ft. above Ground
OBST_873	200	0.61	1.14	2.4	252.79	BASE_313	FALSE	Not Filtered
OBST_873	200	0.61	1.14	2.7	178.78	BASE_313	FALSE	Not Filtered
OBST_873	200	0.61	1.14	3	139.76	BASE_313	FALSE	Not Filtered
OBST_873	200	0.61	1.14	3.3	114.89	BASE_313	TRUE	Temperature < 130 C
OBST_873	200	0.61	1.14	3.6	109.86	BASE_313	TRUE	Temperature < 130 C

Table E-1
Obstructed Simulation Results

Test	HRR (kW)	Diameter (m)	Source Height (m)	Elevation (m)	Maximum Plume Temperature Rise (C)	Baseline Test	Data Filtered	Filtration Criteria
OBST_873	200	0.61	1.14	3.9	105.51	BASE_313	TRUE	Temperature < 130 C
OBST_873	200	0.61	1.14	4.2	98.993	BASE_313	TRUE	Temperature < 130 C
OBST_873	200	0.61	1.14	4.5	92.343	BASE_313	TRUE	Temperature < 130 C
OBST_873	200	0.61	1.14	4.8	91.944	BASE_313	TRUE	Temperature < 130 C
OBST_873	200	0.61	1.14	5.1	88.838	BASE_313	TRUE	Temperature < 130 C
OBST_873	200	0.61	1.14	5.4	79.482	BASE_313	TRUE	Temperature < 130 C
OBST_873	200	0.61	1.14	5.7	75.88	BASE_313	TRUE	Temperature < 130 C
OBST_873	200	0.61	1.14	6	73.076	BASE_313	TRUE	Temperature < 130 C
OBST_874	300	0.61	1.14	2.4	368.65	BASE_314	FALSE	Not Filtered
OBST_874	300	0.61	1.14	2.7	245.86	BASE_314	FALSE	Not Filtered
OBST_874	300	0.61	1.14	3	184.52	BASE_314	FALSE	Not Filtered
OBST_874	300	0.61	1.14	3.3	156.76	BASE_314	FALSE	Not Filtered
OBST_874	300	0.61	1.14	3.6	146.93	BASE_314	FALSE	Not Filtered
OBST_874	300	0.61	1.14	3.9	141.51	BASE_314	FALSE	Not Filtered
OBST_874	300	0.61	1.14	4.2	136.21	BASE_314	FALSE	Not Filtered
OBST_874	300	0.61	1.14	4.5	128.41	BASE_314	TRUE	Temperature < 130 C
OBST_874	300	0.61	1.14	4.8	121.42	BASE_314	TRUE	Temperature < 130 C
OBST_874	300	0.61	1.14	5.1	113.6	BASE_314	TRUE	Temperature < 130 C
OBST_874	300	0.61	1.14	5.4	105.07	BASE_314	TRUE	Temperature < 130 C
OBST_874	300	0.61	1.14	5.7	97.706	BASE_314	TRUE	Temperature < 130 C
OBST_874	300	0.61	1.14	6	93.251	BASE_314	TRUE	Temperature < 130 C

Table E-1
Obstructed Simulation Results

Test	HRR (kW)	Diameter (m)	Source Height (m)	Elevation (m)	Maximum Plume Temperature Rise (C)	Baseline Test	Data Filtered	Filtration Criteria
OBST_875	400	0.61	1.14	2.4	527.19	BASE_315	FALSE	Not Filtered
OBST_875	400	0.61	1.14	2.7	351.26	BASE_315	FALSE	Not Filtered
OBST_875	400	0.61	1.14	3	254.18	BASE_315	FALSE	Not Filtered
OBST_875	400	0.61	1.14	3.3	201.11	BASE_315	FALSE	Not Filtered
OBST_875	400	0.61	1.14	3.6	188.81	BASE_315	FALSE	Not Filtered
OBST_875	400	0.61	1.14	3.9	177.84	BASE_315	FALSE	Not Filtered
OBST_875	400	0.61	1.14	4.2	169.98	BASE_315	FALSE	Not Filtered
OBST_875	400	0.61	1.14	4.5	162.77	BASE_315	FALSE	Not Filtered
OBST_875	400	0.61	1.14	4.8	154.43	BASE_315	FALSE	Not Filtered
OBST_875	400	0.61	1.14	5.1	146.06	BASE_315	FALSE	Not Filtered
OBST_875	400	0.61	1.14	5.4	135.51	BASE_315	FALSE	Not Filtered
OBST_875	400	0.61	1.14	5.7	124.66	BASE_315	TRUE	Temperature < 130 C
OBST_875	400	0.61	1.14	6	117.1	BASE_315	TRUE	Temperature < 130 C
OBST_876	500	0.61	1.14	2.4	670.82	BASE_316	FALSE	Not Filtered
OBST_876	500	0.61	1.14	2.7	454.57	BASE_316	FALSE	Not Filtered
OBST_876	500	0.61	1.14	3	325.36	BASE_316	FALSE	Not Filtered
OBST_876	500	0.61	1.14	3.3	246.23	BASE_316	FALSE	Not Filtered
OBST_876	500	0.61	1.14	3.6	230.64	BASE_316	FALSE	Not Filtered
OBST_876	500	0.61	1.14	3.9	220.37	BASE_316	FALSE	Not Filtered
OBST_876	500	0.61	1.14	4.2	209.08	BASE_316	FALSE	Not Filtered
OBST_876	500	0.61	1.14	4.5	196.49	BASE_316	FALSE	Not Filtered

Table E-1
Obstructed Simulation Results

Test	HRR (kW)	Diameter (m)	Source Height (m)	Elevation (m)	Maximum Plume Temperature Rise (C)	Baseline Test	Data Filtered	Filtration Criteria
OBST_876	500	0.61	1.14	4.8	185.18	BASE_316	FALSE	Not Filtered
OBST_876	500	0.61	1.14	5.1	174.3	BASE_316	FALSE	Not Filtered
OBST_876	500	0.61	1.14	5.4	162.71	BASE_316	FALSE	Not Filtered
OBST_876	500	0.61	1.14	5.7	150.55	BASE_316	FALSE	Not Filtered
OBST_876	500	0.61	1.14	6	140.12	BASE_316	FALSE	Not Filtered
OBST_877	600	0.61	1.14	2.4	805.93	BASE_317	TRUE	Temperature > 800 C
OBST_877	600	0.61	1.14	2.7	574.34	BASE_317	FALSE	Not Filtered
OBST_877	600	0.61	1.14	3	403.91	BASE_317	FALSE	Not Filtered
OBST_877	600	0.61	1.14	3.3	299.89	BASE_317	FALSE	Not Filtered
OBST_877	600	0.61	1.14	3.6	267.2	BASE_317	FALSE	Not Filtered
OBST_877	600	0.61	1.14	3.9	252.02	BASE_317	FALSE	Not Filtered
OBST_877	600	0.61	1.14	4.2	238.02	BASE_317	FALSE	Not Filtered
OBST_877	600	0.61	1.14	4.5	220.1	BASE_317	FALSE	Not Filtered
OBST_877	600	0.61	1.14	4.8	206.1	BASE_317	FALSE	Not Filtered
OBST_877	600	0.61	1.14	5.1	194.77	BASE_317	FALSE	Not Filtered
OBST_877	600	0.61	1.14	5.4	183.24	BASE_317	FALSE	Not Filtered
OBST_877	600	0.61	1.14	5.7	170.25	BASE_317	FALSE	Not Filtered
OBST_877	600	0.61	1.14	6	157.23	BASE_317	FALSE	Not Filtered
OBST_880	200	0.61	1.98	2.4	604.85	BASE_324	FALSE	Not Filtered
OBST_880	200	0.61	1.98	2.7	379.73	BASE_324	FALSE	Not Filtered
OBST_880	200	0.61	1.98	3	281.92	BASE_324	FALSE	Not Filtered

Table E-1
Obstructed Simulation Results

Test	HRR (kW)	Diameter (m)	Source Height (m)	Elevation (m)	Maximum Plume Temperature Rise (C)	Baseline Test	Data Filtered	Filtration Criteria
OBST_880	200	0.61	1.98	3.3	206.03	BASE_324	FALSE	Not Filtered
OBST_880	200	0.61	1.98	3.6	163.97	BASE_324	FALSE	Not Filtered
OBST_880	200	0.61	1.98	3.9	135.19	BASE_324	FALSE	Not Filtered
OBST_880	200	0.61	1.98	4.2	120.13	BASE_324	TRUE	Temperature < 130 C
OBST_880	200	0.61	1.98	4.5	114.48	BASE_324	TRUE	Temperature < 130 C
OBST_880	200	0.61	1.98	4.8	108.02	BASE_324	TRUE	Temperature < 130 C
OBST_880	200	0.61	1.98	5.1	101.9	BASE_324	TRUE	Temperature < 130 C
OBST_880	200	0.61	1.98	5.4	92.323	BASE_324	TRUE	Temperature < 130 C
OBST_880	200	0.61	1.98	5.7	84.71	BASE_324	TRUE	Temperature < 130 C
OBST_880	200	0.61	1.98	6	79.047	BASE_324	TRUE	Temperature < 130 C
OBST_881	300	0.61	1.98	2.4	756.24	BASE_325	FALSE	Not Filtered
OBST_881	300	0.61	1.98	2.7	518.35	BASE_325	FALSE	Not Filtered
OBST_881	300	0.61	1.98	3	352.98	BASE_325	FALSE	Not Filtered
OBST_881	300	0.61	1.98	3.3	273.32	BASE_325	FALSE	Not Filtered
OBST_881	300	0.61	1.98	3.6	234.24	BASE_325	FALSE	Not Filtered
OBST_881	300	0.61	1.98	3.9	213.54	BASE_325	FALSE	Not Filtered
OBST_881	300	0.61	1.98	4.2	199.06	BASE_325	FALSE	Not Filtered
OBST_881	300	0.61	1.98	4.5	179.94	BASE_325	FALSE	Not Filtered
OBST_881	300	0.61	1.98	4.8	165.89	BASE_325	FALSE	Not Filtered
OBST_881	300	0.61	1.98	5.1	153.19	BASE_325	FALSE	Not Filtered
OBST_881	300	0.61	1.98	5.4	138.07	BASE_325	FALSE	Not Filtered

Table E-1
Obstructed Simulation Results

Test	HRR (kW)	Diameter (m)	Source Height (m)	Elevation (m)	Maximum Plume Temperature Rise (C)	Baseline Test	Data Filtered	Filtration Criteria
OBST_881	300	0.61	1.98	5.7	124.6	BASE_325	TRUE	Temperature < 130 C
OBST_881	300	0.61	1.98	6	114.21	BASE_325	TRUE	Temperature < 130 C
OBST_882	400	0.61	1.98	2.4	894.05	BASE_326	TRUE	Temperature > 800 C
OBST_882	400	0.61	1.98	2.7	596.62	BASE_326	FALSE	Not Filtered
OBST_882	400	0.61	1.98	3	471.3	BASE_326	FALSE	Not Filtered
OBST_882	400	0.61	1.98	3.3	398.26	BASE_326	FALSE	Not Filtered
OBST_882	400	0.61	1.98	3.6	356	BASE_326	FALSE	Not Filtered
OBST_882	400	0.61	1.98	3.9	315.04	BASE_326	FALSE	Not Filtered
OBST_882	400	0.61	1.98	4.2	285.76	BASE_326	FALSE	Not Filtered
OBST_882	400	0.61	1.98	4.5	253.9	BASE_326	FALSE	Not Filtered
OBST_882	400	0.61	1.98	4.8	223.38	BASE_326	FALSE	Not Filtered
OBST_882	400	0.61	1.98	5.1	200.05	BASE_326	FALSE	Not Filtered
OBST_882	400	0.61	1.98	5.4	175.4	BASE_326	FALSE	Not Filtered
OBST_882	400	0.61	1.98	5.7	154.3	BASE_326	FALSE	Not Filtered
OBST_882	400	0.61	1.98	6	139.3	BASE_326	FALSE	Not Filtered
OBST_883	500	0.61	1.98	2.4	1025	BASE_327	TRUE	Temperature > 800 C
OBST_883	500	0.61	1.98	2.7	767.26	BASE_327	FALSE	Not Filtered
OBST_883	500	0.61	1.98	3	593.89	BASE_327	FALSE	Not Filtered
OBST_883	500	0.61	1.98	3.3	517.17	BASE_327	FALSE	Not Filtered
OBST_883	500	0.61	1.98	3.6	457.04	BASE_327	FALSE	Not Filtered
OBST_883	500	0.61	1.98	3.9	396.41	BASE_327	FALSE	Not Filtered

Table E-1
Obstructed Simulation Results

Test	HRR (kW)	Diameter (m)	Source Height (m)	Elevation (m)	Maximum Plume Temperature Rise (C)	Baseline Test	Data Filtered	Filtration Criteria
OBST_883	500	0.61	1.98	4.2	349.43	BASE_327	FALSE	Not Filtered
OBST_883	500	0.61	1.98	4.5	305.67	BASE_327	FALSE	Not Filtered
OBST_883	500	0.61	1.98	4.8	272.27	BASE_327	FALSE	Not Filtered
OBST_883	500	0.61	1.98	5.1	247.61	BASE_327	FALSE	Not Filtered
OBST_883	500	0.61	1.98	5.4	220	BASE_327	FALSE	Not Filtered
OBST_883	500	0.61	1.98	5.7	194.5	BASE_327	FALSE	Not Filtered
OBST_883	500	0.61	1.98	6	175.45	BASE_327	FALSE	Not Filtered
OBST_884	600	0.61	1.98	2.4	1097.7	BASE_328	TRUE	Temperature > 800 C
OBST_884	600	0.61	1.98	2.7	859.9	BASE_328	TRUE	Temperature > 800 C
OBST_884	600	0.61	1.98	3	742.72	BASE_328	FALSE	Not Filtered
OBST_884	600	0.61	1.98	3.3	652.09	BASE_328	FALSE	Not Filtered
OBST_884	600	0.61	1.98	3.6	576.72	BASE_328	FALSE	Not Filtered
OBST_884	600	0.61	1.98	3.9	500.69	BASE_328	FALSE	Not Filtered
OBST_884	600	0.61	1.98	4.2	448.14	BASE_328	FALSE	Not Filtered
OBST_884	600	0.61	1.98	4.5	394.23	BASE_328	FALSE	Not Filtered
OBST_884	600	0.61	1.98	4.8	347.72	BASE_328	FALSE	Not Filtered
OBST_884	600	0.61	1.98	5.1	304.84	BASE_328	FALSE	Not Filtered
OBST_884	600	0.61	1.98	5.4	262.25	BASE_328	FALSE	Not Filtered
OBST_884	600	0.61	1.98	5.7	230.22	BASE_328	FALSE	Not Filtered
OBST_884	600	0.61	1.98	6	206.23	BASE_328	FALSE	Not Filtered
OBST_930	300	0.91	0.30	2.4	160.04	BASE_307	TRUE	Source Located 1 ft. above Ground

Table E-1
Obstructed Simulation Results

Test	HRR (kW)	Diameter (m)	Source Height (m)	Elevation (m)	Maximum Plume Temperature Rise (C)	Baseline Test	Data Filtered	Filtration Criteria
OBST_930	300	0.91	0.30	2.7	128.35	BASE_307	TRUE	Temperature < 130 C , Source Located 1 ft. above Ground
OBST_930	300	0.91	0.30	3	99.968	BASE_307	TRUE	Temperature < 130 C , Source Located 1 ft. above Ground
OBST_930	300	0.91	0.30	3.3	87.329	BASE_307	TRUE	Temperature < 130 C , Source Located 1 ft. above Ground
OBST_930	300	0.91	0.30	3.6	84.8	BASE_307	TRUE	Temperature < 130 C , Source Located 1 ft. above Ground
OBST_930	300	0.91	0.30	3.9	81.026	BASE_307	TRUE	Temperature < 130 C , Source Located 1 ft. above Ground
OBST_930	300	0.91	0.30	4.2	79.399	BASE_307	TRUE	Temperature < 130 C , Source Located 1 ft. above Ground
OBST_930	300	0.91	0.30	4.5	77.372	BASE_307	TRUE	Temperature < 130 C , Source Located 1 ft. above Ground
OBST_930	300	0.91	0.30	4.8	75.677	BASE_307	TRUE	Temperature < 130 C , Source Located 1 ft. above Ground
OBST_930	300	0.91	0.30	5.1	73.803	BASE_307	TRUE	Temperature < 130 C , Source Located 1 ft. above Ground
OBST_930	300	0.91	0.30	5.4	71.873	BASE_307	TRUE	Temperature < 130 C , Source Located 1 ft. above Ground
OBST_930	300	0.91	0.30	5.7	69.841	BASE_307	TRUE	Temperature < 130 C , Source Located 1 ft. above Ground
OBST_930	300	0.91	0.30	6	67.783	BASE_307	TRUE	Temperature < 130 C , Source Located 1 ft. above Ground
OBST_931	400	0.91	0.30	2.4	200.28	BASE_308	TRUE	Source Located 1 ft. above Ground
OBST_931	400	0.91	0.30	2.7	159.04	BASE_308	TRUE	Source Located 1 ft. above Ground

Table E-1
Obstructed Simulation Results

Test	HRR (kW)	Diameter (m)	Source Height (m)	Elevation (m)	Maximum Plume Temperature Rise (C)	Baseline Test	Data Filtered	Filtration Criteria
OBST_931	400	0.91	0.30	3	127.39	BASE_308	TRUE	Temperature < 130 C , Source Located 1 ft. above Ground
OBST_931	400	0.91	0.30	3.3	109.61	BASE_308	TRUE	Temperature < 130 C , Source Located 1 ft. above Ground
OBST_931	400	0.91	0.30	3.6	104.4	BASE_308	TRUE	Temperature < 130 C , Source Located 1 ft. above Ground
OBST_931	400	0.91	0.30	3.9	100.86	BASE_308	TRUE	Temperature < 130 C , Source Located 1 ft. above Ground
OBST_931	400	0.91	0.30	4.2	97.017	BASE_308	TRUE	Temperature < 130 C , Source Located 1 ft. above Ground
OBST_931	400	0.91	0.30	4.5	93.238	BASE_308	TRUE	Temperature < 130 C , Source Located 1 ft. above Ground
OBST_931	400	0.91	0.30	4.8	90.169	BASE_308	TRUE	Temperature < 130 C , Source Located 1 ft. above Ground
OBST_931	400	0.91	0.30	5.1	86.888	BASE_308	TRUE	Temperature < 130 C , Source Located 1 ft. above Ground
OBST_931	400	0.91	0.30	5.4	83.318	BASE_308	TRUE	Temperature < 130 C , Source Located 1 ft. above Ground
OBST_931	400	0.91	0.30	5.7	80.717	BASE_308	TRUE	Temperature < 130 C , Source Located 1 ft. above Ground
OBST_931	400	0.91	0.30	6	77.924	BASE_308	TRUE	Temperature < 130 C , Source Located 1 ft. above Ground
OBST_932	500	0.91	0.30	2.4	252.84	BASE_309	TRUE	Source Located 1 ft. above Ground
OBST_932	500	0.91	0.30	2.7	197.23	BASE_309	TRUE	Source Located 1 ft. above Ground
OBST_932	500	0.91	0.30	3	155.39	BASE_309	TRUE	Source Located 1 ft. above Ground
OBST_932	500	0.91	0.30	3.3	133.65	BASE_309	TRUE	Source Located 1 ft. above Ground

Table E-1
Obstructed Simulation Results

Test	HRR (kW)	Diameter (m)	Source Height (m)	Elevation (m)	Maximum Plume Temperature Rise (C)	Baseline Test	Data Filtered	Filtration Criteria
OBST_932	500	0.91	0.30	3.6	125.14	BASE_309	TRUE	Temperature < 130 C , Source Located 1 ft. above Ground
OBST_932	500	0.91	0.30	3.9	120.05	BASE_309	TRUE	Temperature < 130 C , Source Located 1 ft. above Ground
OBST_932	500	0.91	0.30	4.2	115.56	BASE_309	TRUE	Temperature < 130 C , Source Located 1 ft. above Ground
OBST_932	500	0.91	0.30	4.5	111.08	BASE_309	TRUE	Temperature < 130 C , Source Located 1 ft. above Ground
OBST_932	500	0.91	0.30	4.8	108.49	BASE_309	TRUE	Temperature < 130 C , Source Located 1 ft. above Ground
OBST_932	500	0.91	0.30	5.1	106.33	BASE_309	TRUE	Temperature < 130 C , Source Located 1 ft. above Ground
OBST_932	500	0.91	0.30	5.4	103.09	BASE_309	TRUE	Temperature < 130 C , Source Located 1 ft. above Ground
OBST_932	500	0.91	0.30	5.7	99.274	BASE_309	TRUE	Temperature < 130 C , Source Located 1 ft. above Ground
OBST_932	500	0.91	0.30	6	95.942	BASE_309	TRUE	Temperature < 130 C , Source Located 1 ft. above Ground
OBST_933	600	0.91	0.30	2.4	305.13	BASE_310	TRUE	Source Located 1 ft. above Ground
OBST_933	600	0.91	0.30	2.7	237.66	BASE_310	TRUE	Source Located 1 ft. above Ground
OBST_933	600	0.91	0.30	3	189.79	BASE_310	TRUE	Source Located 1 ft. above Ground
OBST_933	600	0.91	0.30	3.3	160.75	BASE_310	TRUE	Source Located 1 ft. above Ground
OBST_933	600	0.91	0.30	3.6	148.5	BASE_310	TRUE	Source Located 1 ft. above Ground
OBST_933	600	0.91	0.30	3.9	139.86	BASE_310	TRUE	Source Located 1 ft. above Ground
OBST_933	600	0.91	0.30	4.2	135	BASE_310	TRUE	Source Located 1 ft. above Ground

Table E-1
Obstructed Simulation Results

Test	HRR (kW)	Diameter (m)	Source Height (m)	Elevation (m)	Maximum Plume Temperature Rise (C)	Baseline Test	Data Filtered	Filtration Criteria
OBST_933	600	0.91	0.30	4.5	130.94	BASE_310	TRUE	Source Located 1 ft. above Ground
OBST_933	600	0.91	0.30	4.8	126.3	BASE_310	TRUE	Temperature < 130 C , Source Located 1 ft. above Ground
OBST_933	600	0.91	0.30	5.1	121.48	BASE_310	TRUE	Temperature < 130 C , Source Located 1 ft. above Ground
OBST_933	600	0.91	0.30	5.4	116.38	BASE_310	TRUE	Temperature < 130 C , Source Located 1 ft. above Ground
OBST_933	600	0.91	0.30	5.7	112.08	BASE_310	TRUE	Temperature < 130 C , Source Located 1 ft. above Ground
OBST_933	600	0.91	0.30	6	108.23	BASE_310	TRUE	Temperature < 130 C , Source Located 1 ft. above Ground
OBST_937	300	0.91	1.14	2.4	256.44	BASE_318	FALSE	Not Filtered
OBST_937	300	0.91	1.14	2.7	190.78	BASE_318	FALSE	Not Filtered
OBST_937	300	0.91	1.14	3	146.6	BASE_318	FALSE	Not Filtered
OBST_937	300	0.91	1.14	3.3	128.92	BASE_318	TRUE	Temperature < 130 C
OBST_937	300	0.91	1.14	3.6	122.18	BASE_318	TRUE	Temperature < 130 C
OBST_937	300	0.91	1.14	3.9	115.48	BASE_318	TRUE	Temperature < 130 C
OBST_937	300	0.91	1.14	4.2	110.78	BASE_318	TRUE	Temperature < 130 C
OBST_937	300	0.91	1.14	4.5	105.77	BASE_318	TRUE	Temperature < 130 C
OBST_937	300	0.91	1.14	4.8	101.51	BASE_318	TRUE	Temperature < 130 C
OBST_937	300	0.91	1.14	5.1	97.445	BASE_318	TRUE	Temperature < 130 C
OBST_937	300	0.91	1.14	5.4	93.173	BASE_318	TRUE	Temperature < 130 C
OBST_937	300	0.91	1.14	5.7	88.159	BASE_318	TRUE	Temperature < 130 C

Table E-1
Obstructed Simulation Results

Test	HRR (kW)	Diameter (m)	Source Height (m)	Elevation (m)	Maximum Plume Temperature Rise (C)	Baseline Test	Data Filtered	Filtration Criteria
OBST_937	300	0.91	1.14	6	84.368	BASE_318	TRUE	Temperature < 130 C
OBST_938	400	0.91	1.14	2.4	345.72	BASE_319	FALSE	Not Filtered
OBST_938	400	0.91	1.14	2.7	232.8	BASE_319	FALSE	Not Filtered
OBST_938	400	0.91	1.14	3	182.85	BASE_319	FALSE	Not Filtered
OBST_938	400	0.91	1.14	3.3	156.65	BASE_319	FALSE	Not Filtered
OBST_938	400	0.91	1.14	3.6	147.22	BASE_319	FALSE	Not Filtered
OBST_938	400	0.91	1.14	3.9	141.22	BASE_319	FALSE	Not Filtered
OBST_938	400	0.91	1.14	4.2	136.82	BASE_319	FALSE	Not Filtered
OBST_938	400	0.91	1.14	4.5	130.48	BASE_319	FALSE	Not Filtered
OBST_938	400	0.91	1.14	4.8	124.77	BASE_319	TRUE	Temperature < 130 C
OBST_938	400	0.91	1.14	5.1	119.2	BASE_319	TRUE	Temperature < 130 C
OBST_938	400	0.91	1.14	5.4	112.58	BASE_319	TRUE	Temperature < 130 C
OBST_938	400	0.91	1.14	5.7	106.5	BASE_319	TRUE	Temperature < 130 C
OBST_938	400	0.91	1.14	6	100.49	BASE_319	TRUE	Temperature < 130 C
OBST_939	500	0.91	1.14	2.4	440.75	BASE_320	FALSE	Not Filtered
OBST_939	500	0.91	1.14	2.7	305.96	BASE_320	FALSE	Not Filtered
OBST_939	500	0.91	1.14	3	224.42	BASE_320	FALSE	Not Filtered
OBST_939	500	0.91	1.14	3.3	186.46	BASE_320	FALSE	Not Filtered
OBST_939	500	0.91	1.14	3.6	176.39	BASE_320	FALSE	Not Filtered
OBST_939	500	0.91	1.14	3.9	169.66	BASE_320	FALSE	Not Filtered
OBST_939	500	0.91	1.14	4.2	164.02	BASE_320	FALSE	Not Filtered

Table E-1
Obstructed Simulation Results

Test	HRR (kW)	Diameter (m)	Source Height (m)	Elevation (m)	Maximum Plume Temperature Rise (C)	Baseline Test	Data Filtered	Filtration Criteria
OBST_939	500	0.91	1.14	4.5	156.28	BASE_320	FALSE	Not Filtered
OBST_939	500	0.91	1.14	4.8	149.36	BASE_320	FALSE	Not Filtered
OBST_939	500	0.91	1.14	5.1	141.6	BASE_320	FALSE	Not Filtered
OBST_939	500	0.91	1.14	5.4	132.1	BASE_320	FALSE	Not Filtered
OBST_939	500	0.91	1.14	5.7	122.61	BASE_320	TRUE	Temperature < 130 C
OBST_939	500	0.91	1.14	6	114.99	BASE_320	TRUE	Temperature < 130 C
OBST_940	600	0.91	1.14	2.4	562.49	BASE_321	FALSE	Not Filtered
OBST_940	600	0.91	1.14	2.7	385.62	BASE_321	FALSE	Not Filtered
OBST_940	600	0.91	1.14	3	292.81	BASE_321	FALSE	Not Filtered
OBST_940	600	0.91	1.14	3.3	240.08	BASE_321	FALSE	Not Filtered
OBST_940	600	0.91	1.14	3.6	214.75	BASE_321	FALSE	Not Filtered
OBST_940	600	0.91	1.14	3.9	196.25	BASE_321	FALSE	Not Filtered
OBST_940	600	0.91	1.14	4.2	187.07	BASE_321	FALSE	Not Filtered
OBST_940	600	0.91	1.14	4.5	179.33	BASE_321	FALSE	Not Filtered
OBST_940	600	0.91	1.14	4.8	172.41	BASE_321	FALSE	Not Filtered
OBST_940	600	0.91	1.14	5.1	165.68	BASE_321	FALSE	Not Filtered
OBST_940	600	0.91	1.14	5.4	156.24	BASE_321	FALSE	Not Filtered
OBST_940	600	0.91	1.14	5.7	145.56	BASE_321	FALSE	Not Filtered
OBST_940	600	0.91	1.14	6	136.35	BASE_321	FALSE	Not Filtered
OBST_944	300	0.91	1.98	2.4	448.28	BASE_329	FALSE	Not Filtered
OBST_944	300	0.91	1.98	2.7	294.2	BASE_329	FALSE	Not Filtered

Table E-1
Obstructed Simulation Results

Test	HRR (kW)	Diameter (m)	Source Height (m)	Elevation (m)	Maximum Plume Temperature Rise (C)	Baseline Test	Data Filtered	Filtration Criteria
OBST_944	300	0.91	1.98	3	230.14	BASE_329	FALSE	Not Filtered
OBST_944	300	0.91	1.98	3.3	198.17	BASE_329	FALSE	Not Filtered
OBST_944	300	0.91	1.98	3.6	190.23	BASE_329	FALSE	Not Filtered
OBST_944	300	0.91	1.98	3.9	182.18	BASE_329	FALSE	Not Filtered
OBST_944	300	0.91	1.98	4.2	172.71	BASE_329	FALSE	Not Filtered
OBST_944	300	0.91	1.98	4.5	161.02	BASE_329	FALSE	Not Filtered
OBST_944	300	0.91	1.98	4.8	150.26	BASE_329	FALSE	Not Filtered
OBST_944	300	0.91	1.98	5.1	139.52	BASE_329	FALSE	Not Filtered
OBST_944	300	0.91	1.98	5.4	127.37	BASE_329	TRUE	Temperature < 130 C
OBST_944	300	0.91	1.98	5.7	116.2	BASE_329	TRUE	Temperature < 130 C
OBST_944	300	0.91	1.98	6	106.93	BASE_329	TRUE	Temperature < 130 C
OBST_945	400	0.91	1.98	2.4	634.19	BASE_330	FALSE	Not Filtered
OBST_945	400	0.91	1.98	2.7	393.3	BASE_330	FALSE	Not Filtered
OBST_945	400	0.91	1.98	3	320.01	BASE_330	FALSE	Not Filtered
OBST_945	400	0.91	1.98	3.3	271.01	BASE_330	FALSE	Not Filtered
OBST_945	400	0.91	1.98	3.6	256.39	BASE_330	FALSE	Not Filtered
OBST_945	400	0.91	1.98	3.9	242.45	BASE_330	FALSE	Not Filtered
OBST_945	400	0.91	1.98	4.2	224.26	BASE_330	FALSE	Not Filtered
OBST_945	400	0.91	1.98	4.5	202.73	BASE_330	FALSE	Not Filtered
OBST_945	400	0.91	1.98	4.8	185.73	BASE_330	FALSE	Not Filtered
OBST_945	400	0.91	1.98	5.1	169.17	BASE_330	FALSE	Not Filtered

Table E-1
Obstructed Simulation Results

Test	HRR (kW)	Diameter (m)	Source Height (m)	Elevation (m)	Maximum Plume Temperature Rise (C)	Baseline Test	Data Filtered	Filtration Criteria
OBST_945	400	0.91	1.98	5.4	151.88	BASE_330	FALSE	Not Filtered
OBST_945	400	0.91	1.98	5.7	135.11	BASE_330	FALSE	Not Filtered
OBST_945	400	0.91	1.98	6	123.31	BASE_330	TRUE	Temperature < 130 C
OBST_946	500	0.91	1.98	2.4	766.89	BASE_331	FALSE	Not Filtered
OBST_946	500	0.91	1.98	2.7	474.78	BASE_331	FALSE	Not Filtered
OBST_946	500	0.91	1.98	3	395.78	BASE_331	FALSE	Not Filtered
OBST_946	500	0.91	1.98	3.3	350.79	BASE_331	FALSE	Not Filtered
OBST_946	500	0.91	1.98	3.6	323.72	BASE_331	FALSE	Not Filtered
OBST_946	500	0.91	1.98	3.9	302.66	BASE_331	FALSE	Not Filtered
OBST_946	500	0.91	1.98	4.2	280.58	BASE_331	FALSE	Not Filtered
OBST_946	500	0.91	1.98	4.5	255.83	BASE_331	FALSE	Not Filtered
OBST_946	500	0.91	1.98	4.8	233.31	BASE_331	FALSE	Not Filtered
OBST_946	500	0.91	1.98	5.1	210.86	BASE_331	FALSE	Not Filtered
OBST_946	500	0.91	1.98	5.4	188.4	BASE_331	FALSE	Not Filtered
OBST_946	500	0.91	1.98	5.7	165.77	BASE_331	FALSE	Not Filtered
OBST_946	500	0.91	1.98	6	150.43	BASE_331	FALSE	Not Filtered
OBST_947	600	0.91	1.98	2.4	908.27	BASE_332	TRUE	Temperature > 800 C
OBST_947	600	0.91	1.98	2.7	586.87	BASE_332	FALSE	Not Filtered
OBST_947	600	0.91	1.98	3	489.56	BASE_332	FALSE	Not Filtered
OBST_947	600	0.91	1.98	3.3	448.06	BASE_332	FALSE	Not Filtered
OBST_947	600	0.91	1.98	3.6	410.02	BASE_332	FALSE	Not Filtered

Table E-1
Obstructed Simulation Results

Test	HRR (kW)	Diameter (m)	Source Height (m)	Elevation (m)	Maximum Plume Temperature Rise (C)	Baseline Test	Data Filtered	Filtration Criteria
OBST_947	600	0.91	1.98	3.9	371.04	BASE_332	FALSE	Not Filtered
OBST_947	600	0.91	1.98	4.2	338.75	BASE_332	FALSE	Not Filtered
OBST_947	600	0.91	1.98	4.5	299.61	BASE_332	FALSE	Not Filtered
OBST_947	600	0.91	1.98	4.8	266.02	BASE_332	FALSE	Not Filtered
OBST_947	600	0.91	1.98	5.1	237.54	BASE_332	FALSE	Not Filtered
OBST_947	600	0.91	1.98	5.4	209.53	BASE_332	FALSE	Not Filtered
OBST_947	600	0.91	1.98	5.7	184.54	BASE_332	FALSE	Not Filtered
OBST_947	600	0.91	1.98	6	167.13	BASE_332	FALSE	Not Filtered
THREEWALL_1057	1000	0.91	0.30	2.4	621.54	BASE_404	TRUE	Source Located 1 ft. above Ground
THREEWALL_1057	1000	0.91	0.30	2.7	405.17	BASE_404	TRUE	Source Located 1 ft. above Ground
THREEWALL_1057	1000	0.91	0.30	3	294.64	BASE_404	TRUE	Source Located 1 ft. above Ground
THREEWALL_1057	1000	0.91	0.30	3.3	232.75	BASE_404	TRUE	Source Located 1 ft. above Ground
THREEWALL_1057	1000	0.91	0.30	3.6	196.9	BASE_404	TRUE	Source Located 1 ft. above Ground
THREEWALL_1057	1000	0.91	0.30	3.9	169.25	BASE_404	TRUE	Source Located 1 ft. above Ground
THREEWALL_1057	1000	0.91	0.30	4.2	152.11	BASE_404	TRUE	Source Located 1 ft. above Ground
THREEWALL_1057	1000	0.91	0.30	4.5	138.74	BASE_404	TRUE	Source Located 1 ft. above Ground
THREEWALL_1057	1000	0.91	0.30	4.8	131.68	BASE_404	TRUE	Source Located 1 ft. above Ground
THREEWALL_1057	1000	0.91	0.30	5.1	121.29	BASE_404	TRUE	Temperature < 130 C , Source Located 1 ft. above Ground
THREEWALL_1057	1000	0.91	0.30	5.4	109.71	BASE_404	TRUE	Temperature < 130 C , Source Located 1 ft. above Ground
THREEWALL_1057	1000	0.91	0.30	5.7	103.98	BASE_404	TRUE	Temperature < 130 C , Source

Table E-1
Obstructed Simulation Results

Test	HRR (kW)	Diameter (m)	Source Height (m)	Elevation (m)	Maximum Plume Temperature Rise (C)	Baseline Test	Data Filtered	Filtration Criteria
								Located 1 ft. above Ground
THREEWALL_1057	1000	0.91	0.30	6	99.867	BASE_404	TRUE	Temperature < 130 C , Source Located 1 ft. above Ground
THREEWALL_1058	1000	0.91	1.14	2.4	889.87	BASE_400	TRUE	Temperature > 800 C
THREEWALL_1058	1000	0.91	1.14	2.7	640.76	BASE_400	FALSE	Not Filtered
THREEWALL_1058	1000	0.91	1.14	3	504.86	BASE_400	FALSE	Not Filtered
THREEWALL_1058	1000	0.91	1.14	3.3	401.71	BASE_400	FALSE	Not Filtered
THREEWALL_1058	1000	0.91	1.14	3.6	339.8	BASE_400	FALSE	Not Filtered
THREEWALL_1058	1000	0.91	1.14	3.9	284.72	BASE_400	FALSE	Not Filtered
THREEWALL_1058	1000	0.91	1.14	4.2	250.82	BASE_400	FALSE	Not Filtered
THREEWALL_1058	1000	0.91	1.14	4.5	215.58	BASE_400	FALSE	Not Filtered
THREEWALL_1058	1000	0.91	1.14	4.8	188.42	BASE_400	FALSE	Not Filtered
THREEWALL_1058	1000	0.91	1.14	5.1	166.49	BASE_400	FALSE	Not Filtered
THREEWALL_1058	1000	0.91	1.14	5.4	146.15	BASE_400	FALSE	Not Filtered
THREEWALL_1058	1000	0.91	1.14	5.7	135.05	BASE_400	FALSE	Not Filtered
THREEWALL_1058	1000	0.91	1.14	6	126.88	BASE_400	TRUE	Temperature < 130 C
THREEWALL_1059	1000	0.91	1.98	2.4	1062.2	BASE_401	TRUE	Temperature > 800 C
THREEWALL_1059	1000	0.91	1.98	2.7	1070.8	BASE_401	TRUE	Temperature > 800 C
THREEWALL_1059	1000	0.91	1.98	3	1025.2	BASE_401	TRUE	Temperature > 800 C
THREEWALL_1059	1000	0.91	1.98	3.3	921.05	BASE_401	TRUE	Temperature > 800 C
THREEWALL_1059	1000	0.91	1.98	3.6	827.48	BASE_401	TRUE	Temperature > 800 C
THREEWALL_1059	1000	0.91	1.98	3.9	666.54	BASE_401	FALSE	Not Filtered

Table E-1
Obstructed Simulation Results

Test	HRR (kW)	Diameter (m)	Source Height (m)	Elevation (m)	Maximum Plume Temperature Rise (C)	Baseline Test	Data Filtered	Filtration Criteria
THREEWALL_1059	1000	0.91	1.98	4.2	547.72	BASE_401	FALSE	Not Filtered
THREEWALL_1059	1000	0.91	1.98	4.5	431.6	BASE_401	FALSE	Not Filtered
THREEWALL_1059	1000	0.91	1.98	4.8	354.89	BASE_401	FALSE	Not Filtered
THREEWALL_1059	1000	0.91	1.98	5.1	306.67	BASE_401	FALSE	Not Filtered
THREEWALL_1059	1000	0.91	1.98	5.4	264.2	BASE_401	FALSE	Not Filtered
THREEWALL_1059	1000	0.91	1.98	5.7	227.16	BASE_401	FALSE	Not Filtered
THREEWALL_1059	1000	0.91	1.98	6	206.73	BASE_401	FALSE	Not Filtered
THREEWALL_1066	1000	1.22	0.30	2.4	429.91	BASE_405	TRUE	Source Located 1 ft. above Ground
THREEWALL_1066	1000	1.22	0.30	2.7	269.44	BASE_405	TRUE	Source Located 1 ft. above Ground
THREEWALL_1066	1000	1.22	0.30	3	211.98	BASE_405	TRUE	Source Located 1 ft. above Ground
THREEWALL_1066	1000	1.22	0.30	3.3	185.78	BASE_405	TRUE	Source Located 1 ft. above Ground
THREEWALL_1066	1000	1.22	0.30	3.6	165.07	BASE_405	TRUE	Source Located 1 ft. above Ground
THREEWALL_1066	1000	1.22	0.30	3.9	141.74	BASE_405	TRUE	Source Located 1 ft. above Ground
THREEWALL_1066	1000	1.22	0.30	4.2	133.48	BASE_405	TRUE	Source Located 1 ft. above Ground
THREEWALL_1066	1000	1.22	0.30	4.5	125.97	BASE_405	TRUE	Temperature < 130 C , Source Located 1 ft. above Ground
THREEWALL_1066	1000	1.22	0.30	4.8	115.34	BASE_405	TRUE	Temperature < 130 C , Source Located 1 ft. above Ground
THREEWALL_1066	1000	1.22	0.30	5.1	107.39	BASE_405	TRUE	Temperature < 130 C , Source Located 1 ft. above Ground
THREEWALL_1066	1000	1.22	0.30	5.4	99.885	BASE_405	TRUE	Temperature < 130 C , Source Located 1 ft. above Ground
THREEWALL_1066	1000	1.22	0.30	5.7	93.595	BASE_405	TRUE	Temperature < 130 C , Source

Table E-1
Obstructed Simulation Results

Test	HRR (kW)	Diameter (m)	Source Height (m)	Elevation (m)	Maximum Plume Temperature Rise (C)	Baseline Test	Data Filtered	Filtration Criteria
								Located 1 ft. above Ground
THREEWALL_1066	1000	1.22	0.30	6	89.031	BASE_405	TRUE	Temperature < 130 C , Source Located 1 ft. above Ground
THREEWALL_1067	1000	1.22	1.14	2.4	683.06	BASE_402	FALSE	Not Filtered
THREEWALL_1067	1000	1.22	1.14	2.7	460.84	BASE_402	FALSE	Not Filtered
THREEWALL_1067	1000	1.22	1.14	3	363.31	BASE_402	FALSE	Not Filtered
THREEWALL_1067	1000	1.22	1.14	3.3	299.81	BASE_402	FALSE	Not Filtered
THREEWALL_1067	1000	1.22	1.14	3.6	255.01	BASE_402	FALSE	Not Filtered
THREEWALL_1067	1000	1.22	1.14	3.9	210.95	BASE_402	FALSE	Not Filtered
THREEWALL_1067	1000	1.22	1.14	4.2	187.89	BASE_402	FALSE	Not Filtered
THREEWALL_1067	1000	1.22	1.14	4.5	161.24	BASE_402	FALSE	Not Filtered
THREEWALL_1067	1000	1.22	1.14	4.8	145.62	BASE_402	FALSE	Not Filtered
THREEWALL_1067	1000	1.22	1.14	5.1	132.94	BASE_402	FALSE	Not Filtered
THREEWALL_1067	1000	1.22	1.14	5.4	122.79	BASE_402	TRUE	Temperature < 130 C
THREEWALL_1067	1000	1.22	1.14	5.7	114.24	BASE_402	TRUE	Temperature < 130 C
THREEWALL_1067	1000	1.22	1.14	6	108.6	BASE_402	TRUE	Temperature < 130 C
THREEWALL_1068	1000	1.22	1.98	2.4	1071.1	BASE_403	TRUE	Temperature > 800 C
THREEWALL_1068	1000	1.22	1.98	2.7	1067.8	BASE_403	TRUE	Temperature > 800 C
THREEWALL_1068	1000	1.22	1.98	3	1011.9	BASE_403	TRUE	Temperature > 800 C
THREEWALL_1068	1000	1.22	1.98	3.3	858.81	BASE_403	TRUE	Temperature > 800 C
THREEWALL_1068	1000	1.22	1.98	3.6	679.45	BASE_403	FALSE	Not Filtered
THREEWALL_1068	1000	1.22	1.98	3.9	516.14	BASE_403	FALSE	Not Filtered

Table E-1
Obstructed Simulation Results

Test	HRR (kW)	Diameter (m)	Source Height (m)	Elevation (m)	Maximum Plume Temperature Rise (C)	Baseline Test	Data Filtered	Filtration Criteria
THREEWALL_1068	1000	1.22	1.98	4.2	417.07	BASE_403	FALSE	Not Filtered
THREEWALL_1068	1000	1.22	1.98	4.5	338.85	BASE_403	FALSE	Not Filtered
THREEWALL_1068	1000	1.22	1.98	4.8	292.29	BASE_403	FALSE	Not Filtered
THREEWALL_1068	1000	1.22	1.98	5.1	254.15	BASE_403	FALSE	Not Filtered
THREEWALL_1068	1000	1.22	1.98	5.4	224.04	BASE_403	FALSE	Not Filtered
THREEWALL_1068	1000	1.22	1.98	5.7	199.74	BASE_403	FALSE	Not Filtered
THREEWALL_1068	1000	1.22	1.98	6	181.86	BASE_403	FALSE	Not Filtered
THREEWALL_843	50	0.30	0.30	2.4	106.22	BASE_300	TRUE	Temperature < 130 C , Source Located 1 ft. above Ground
THREEWALL_843	50	0.30	0.30	2.7	69.818	BASE_300	TRUE	Temperature < 130 C , Source Located 1 ft. above Ground
THREEWALL_843	50	0.30	0.30	3	58.899	BASE_300	TRUE	Temperature < 130 C , Source Located 1 ft. above Ground
THREEWALL_843	50	0.30	0.30	3.3	50.866	BASE_300	TRUE	Temperature < 130 C , Source Located 1 ft. above Ground
THREEWALL_843	50	0.30	0.30	3.6	46.842	BASE_300	TRUE	Temperature < 130 C , Source Located 1 ft. above Ground
THREEWALL_843	50	0.30	0.30	3.9	43.306	BASE_300	TRUE	Temperature < 130 C , Source Located 1 ft. above Ground
THREEWALL_843	50	0.30	0.30	4.2	40.867	BASE_300	TRUE	Temperature < 130 C , Source Located 1 ft. above Ground
THREEWALL_844	100	0.30	0.30	2.4	151.65	BASE_301	TRUE	Source Located 1 ft. above Ground
THREEWALL_844	100	0.30	0.30	2.7	99.551	BASE_301	TRUE	Temperature < 130 C , Source Located 1 ft. above Ground

Table E-1
Obstructed Simulation Results

Test	HRR (kW)	Diameter (m)	Source Height (m)	Elevation (m)	Maximum Plume Temperature Rise (C)	Baseline Test	Data Filtered	Filtration Criteria
THREEWALL_844	100	0.30	0.30	3	85.142	BASE_301	TRUE	Temperature < 130 C , Source Located 1 ft. above Ground
THREEWALL_844	100	0.30	0.30	3.3	73.312	BASE_301	TRUE	Temperature < 130 C , Source Located 1 ft. above Ground
THREEWALL_844	100	0.30	0.30	3.6	64.692	BASE_301	TRUE	Temperature < 130 C , Source Located 1 ft. above Ground
THREEWALL_844	100	0.30	0.30	3.9	59.171	BASE_301	TRUE	Temperature < 130 C , Source Located 1 ft. above Ground
THREEWALL_844	100	0.30	0.30	4.2	54.595	BASE_301	TRUE	Temperature < 130 C , Source Located 1 ft. above Ground
THREEWALL_844	100	0.30	0.30	4.5	51.396	BASE_301	TRUE	Temperature < 130 C , Source Located 1 ft. above Ground
THREEWALL_844	100	0.30	0.30	4.8	47.861	BASE_301	TRUE	Temperature < 130 C , Source Located 1 ft. above Ground
THREEWALL_844	100	0.30	0.30	5.1	45.037	BASE_301	TRUE	Temperature < 130 C , Source Located 1 ft. above Ground
THREEWALL_844	100	0.30	0.30	5.4	42.201	BASE_301	TRUE	Temperature < 130 C , Source Located 1 ft. above Ground
THREEWALL_844	100	0.30	0.30	5.7	40.709	BASE_301	TRUE	Temperature < 130 C , Source Located 1 ft. above Ground
THREEWALL_850	50	0.30	1.14	2.4	175.3	BASE_311	FALSE	Not Filtered
THREEWALL_850	50	0.30	1.14	2.7	107.81	BASE_311	TRUE	Temperature < 130 C
THREEWALL_850	50	0.30	1.14	3	89.936	BASE_311	TRUE	Temperature < 130 C
THREEWALL_850	50	0.30	1.14	3.3	75.701	BASE_311	TRUE	Temperature < 130 C
THREEWALL_850	50	0.30	1.14	3.6	66.33	BASE_311	TRUE	Temperature < 130 C

Table E-1
Obstructed Simulation Results

Test	HRR (kW)	Diameter (m)	Source Height (m)	Elevation (m)	Maximum Plume Temperature Rise (C)	Baseline Test	Data Filtered	Filtration Criteria
THREEWALL_850	50	0.30	1.14	3.9	58.179	BASE_311	TRUE	Temperature < 130 C
THREEWALL_850	50	0.30	1.14	4.2	52.582	BASE_311	TRUE	Temperature < 130 C
THREEWALL_850	50	0.30	1.14	4.5	47.396	BASE_311	TRUE	Temperature < 130 C
THREEWALL_850	50	0.30	1.14	4.8	43.576	BASE_311	TRUE	Temperature < 130 C
THREEWALL_850	50	0.30	1.14	5.1	42.094	BASE_311	TRUE	Temperature < 130 C
THREEWALL_851	100	0.30	1.14	2.4	275.53	BASE_312	FALSE	Not Filtered
THREEWALL_851	100	0.30	1.14	2.7	159.25	BASE_312	FALSE	Not Filtered
THREEWALL_851	100	0.30	1.14	3	127.63	BASE_312	TRUE	Temperature < 130 C
THREEWALL_851	100	0.30	1.14	3.3	105.49	BASE_312	TRUE	Temperature < 130 C
THREEWALL_851	100	0.30	1.14	3.6	91.185	BASE_312	TRUE	Temperature < 130 C
THREEWALL_851	100	0.30	1.14	3.9	80.914	BASE_312	TRUE	Temperature < 130 C
THREEWALL_851	100	0.30	1.14	4.2	74.131	BASE_312	TRUE	Temperature < 130 C
THREEWALL_851	100	0.30	1.14	4.5	66.294	BASE_312	TRUE	Temperature < 130 C
THREEWALL_851	100	0.30	1.14	4.8	61.449	BASE_312	TRUE	Temperature < 130 C
THREEWALL_851	100	0.30	1.14	5.1	57.622	BASE_312	TRUE	Temperature < 130 C
THREEWALL_851	100	0.30	1.14	5.4	53.854	BASE_312	TRUE	Temperature < 130 C
THREEWALL_851	100	0.30	1.14	5.7	49.889	BASE_312	TRUE	Temperature < 130 C
THREEWALL_851	100	0.30	1.14	6	47.38	BASE_312	TRUE	Temperature < 130 C
THREEWALL_857	50	0.30	1.98	2.4	435.6	BASE_322	FALSE	Not Filtered
THREEWALL_857	50	0.30	1.98	2.7	255.48	BASE_322	FALSE	Not Filtered
THREEWALL_857	50	0.30	1.98	3	177.34	BASE_322	FALSE	Not Filtered

Table E-1
Obstructed Simulation Results

Test	HRR (kW)	Diameter (m)	Source Height (m)	Elevation (m)	Maximum Plume Temperature Rise (C)	Baseline Test	Data Filtered	Filtration Criteria
THREEWALL_857	50	0.30	1.98	3.3	131.29	BASE_322	FALSE	Not Filtered
THREEWALL_857	50	0.30	1.98	3.6	103.33	BASE_322	TRUE	Temperature < 130 C
THREEWALL_857	50	0.30	1.98	3.9	86.596	BASE_322	TRUE	Temperature < 130 C
THREEWALL_857	50	0.30	1.98	4.2	75.4	BASE_322	TRUE	Temperature < 130 C
THREEWALL_857	50	0.30	1.98	4.5	64.238	BASE_322	TRUE	Temperature < 130 C
THREEWALL_857	50	0.30	1.98	4.8	57.548	BASE_322	TRUE	Temperature < 130 C
THREEWALL_857	50	0.30	1.98	5.1	52.801	BASE_322	TRUE	Temperature < 130 C
THREEWALL_857	50	0.30	1.98	5.4	49.598	BASE_322	TRUE	Temperature < 130 C
THREEWALL_857	50	0.30	1.98	5.7	45.826	BASE_322	TRUE	Temperature < 130 C
THREEWALL_857	50	0.30	1.98	6	43.713	BASE_322	TRUE	Temperature < 130 C
THREEWALL_858	100	0.30	1.98	2.4	820.14	BASE_323	TRUE	Temperature > 800 C
THREEWALL_858	100	0.30	1.98	2.7	530.25	BASE_323	FALSE	Not Filtered
THREEWALL_858	100	0.30	1.98	3	347.37	BASE_323	FALSE	Not Filtered
THREEWALL_858	100	0.30	1.98	3.3	238.83	BASE_323	FALSE	Not Filtered
THREEWALL_858	100	0.30	1.98	3.6	189.87	BASE_323	FALSE	Not Filtered
THREEWALL_858	100	0.30	1.98	3.9	155.33	BASE_323	FALSE	Not Filtered
THREEWALL_858	100	0.30	1.98	4.2	129.01	BASE_323	TRUE	Temperature < 130 C
THREEWALL_858	100	0.30	1.98	4.5	106.66	BASE_323	TRUE	Temperature < 130 C
THREEWALL_858	100	0.30	1.98	4.8	92.817	BASE_323	TRUE	Temperature < 130 C
THREEWALL_858	100	0.30	1.98	5.1	82.359	BASE_323	TRUE	Temperature < 130 C
THREEWALL_858	100	0.30	1.98	5.4	72.31	BASE_323	TRUE	Temperature < 130 C

Table E-1
Obstructed Simulation Results

Test	HRR (kW)	Diameter (m)	Source Height (m)	Elevation (m)	Maximum Plume Temperature Rise (C)	Baseline Test	Data Filtered	Filtration Criteria
THREEWALL_858	100	0.30	1.98	5.7	65.47	BASE_323	TRUE	Temperature < 130 C
THREEWALL_858	100	0.30	1.98	6	59.874	BASE_323	TRUE	Temperature < 130 C
THREEWALL_908	200	0.61	0.30	2.4	209.07	BASE_302	TRUE	Source Located 1 ft. above Ground
THREEWALL_908	200	0.61	0.30	2.7	138.48	BASE_302	TRUE	Source Located 1 ft. above Ground
THREEWALL_908	200	0.61	0.30	3	110.24	BASE_302	TRUE	Temperature < 130 C , Source Located 1 ft. above Ground
THREEWALL_908	200	0.61	0.30	3.3	92.241	BASE_302	TRUE	Temperature < 130 C , Source Located 1 ft. above Ground
THREEWALL_908	200	0.61	0.30	3.6	86.418	BASE_302	TRUE	Temperature < 130 C , Source Located 1 ft. above Ground
THREEWALL_908	200	0.61	0.30	3.9	79.258	BASE_302	TRUE	Temperature < 130 C , Source Located 1 ft. above Ground
THREEWALL_908	200	0.61	0.30	4.2	72.942	BASE_302	TRUE	Temperature < 130 C , Source Located 1 ft. above Ground
THREEWALL_908	200	0.61	0.30	4.5	68.566	BASE_302	TRUE	Temperature < 130 C , Source Located 1 ft. above Ground
THREEWALL_908	200	0.61	0.30	4.8	64.97	BASE_302	TRUE	Temperature < 130 C , Source Located 1 ft. above Ground
THREEWALL_908	200	0.61	0.30	5.1	61.531	BASE_302	TRUE	Temperature < 130 C , Source Located 1 ft. above Ground
THREEWALL_908	200	0.61	0.30	5.4	57.966	BASE_302	TRUE	Temperature < 130 C , Source Located 1 ft. above Ground
THREEWALL_908	200	0.61	0.30	5.7	55.271	BASE_302	TRUE	Temperature < 130 C , Source Located 1 ft. above Ground
THREEWALL_908	200	0.61	0.30	6	53.819	BASE_302	TRUE	Temperature < 130 C , Source Located 1 ft. above Ground

Table E-1
Obstructed Simulation Results

Test	HRR (kW)	Diameter (m)	Source Height (m)	Elevation (m)	Maximum Plume Temperature Rise (C)	Baseline Test	Data Filtered	Filtration Criteria
THREEWALL_909	300	0.61	0.30	2.4	294.83	BASE_303	TRUE	Source Located 1 ft. above Ground
THREEWALL_909	300	0.61	0.30	2.7	191.52	BASE_303	TRUE	Source Located 1 ft. above Ground
THREEWALL_909	300	0.61	0.30	3	149.7	BASE_303	TRUE	Source Located 1 ft. above Ground
THREEWALL_909	300	0.61	0.30	3.3	122.65	BASE_303	TRUE	Temperature < 130 C , Source Located 1 ft. above Ground
THREEWALL_909	300	0.61	0.30	3.6	109.56	BASE_303	TRUE	Temperature < 130 C , Source Located 1 ft. above Ground
THREEWALL_909	300	0.61	0.30	3.9	100.78	BASE_303	TRUE	Temperature < 130 C , Source Located 1 ft. above Ground
THREEWALL_909	300	0.61	0.30	4.2	93.85	BASE_303	TRUE	Temperature < 130 C , Source Located 1 ft. above Ground
THREEWALL_909	300	0.61	0.30	4.5	84.794	BASE_303	TRUE	Temperature < 130 C , Source Located 1 ft. above Ground
THREEWALL_909	300	0.61	0.30	4.8	78.946	BASE_303	TRUE	Temperature < 130 C , Source Located 1 ft. above Ground
THREEWALL_909	300	0.61	0.30	5.1	73.842	BASE_303	TRUE	Temperature < 130 C , Source Located 1 ft. above Ground
THREEWALL_909	300	0.61	0.30	5.4	69.304	BASE_303	TRUE	Temperature < 130 C , Source Located 1 ft. above Ground
THREEWALL_909	300	0.61	0.30	5.7	66.545	BASE_303	TRUE	Temperature < 130 C , Source Located 1 ft. above Ground
THREEWALL_909	300	0.61	0.30	6	63.528	BASE_303	TRUE	Temperature < 130 C , Source Located 1 ft. above Ground
THREEWALL_910	400	0.61	0.30	2.4	383.52	BASE_304	TRUE	Source Located 1 ft. above Ground
THREEWALL_910	400	0.61	0.30	2.7	228.97	BASE_304	TRUE	Source Located 1 ft. above Ground

Table E-1
Obstructed Simulation Results

Test	HRR (kW)	Diameter (m)	Source Height (m)	Elevation (m)	Maximum Plume Temperature Rise (C)	Baseline Test	Data Filtered	Filtration Criteria
THREEWALL_910	400	0.61	0.30	3	183.34	BASE_304	TRUE	Source Located 1 ft. above Ground
THREEWALL_910	400	0.61	0.30	3.3	151.37	BASE_304	TRUE	Source Located 1 ft. above Ground
THREEWALL_910	400	0.61	0.30	3.6	133.13	BASE_304	TRUE	Source Located 1 ft. above Ground
THREEWALL_910	400	0.61	0.30	3.9	117.64	BASE_304	TRUE	Temperature < 130 C , Source Located 1 ft. above Ground
THREEWALL_910	400	0.61	0.30	4.2	104.51	BASE_304	TRUE	Temperature < 130 C , Source Located 1 ft. above Ground
THREEWALL_910	400	0.61	0.30	4.5	94.862	BASE_304	TRUE	Temperature < 130 C , Source Located 1 ft. above Ground
THREEWALL_910	400	0.61	0.30	4.8	88.761	BASE_304	TRUE	Temperature < 130 C , Source Located 1 ft. above Ground
THREEWALL_910	400	0.61	0.30	5.1	84.237	BASE_304	TRUE	Temperature < 130 C , Source Located 1 ft. above Ground
THREEWALL_910	400	0.61	0.30	5.4	78.224	BASE_304	TRUE	Temperature < 130 C , Source Located 1 ft. above Ground
THREEWALL_910	400	0.61	0.30	5.7	72.443	BASE_304	TRUE	Temperature < 130 C , Source Located 1 ft. above Ground
THREEWALL_910	400	0.61	0.30	6	68.486	BASE_304	TRUE	Temperature < 130 C , Source Located 1 ft. above Ground
THREEWALL_911	500	0.61	0.30	2.4	540.81	BASE_305	TRUE	Source Located 1 ft. above Ground
THREEWALL_911	500	0.61	0.30	2.7	328	BASE_305	TRUE	Source Located 1 ft. above Ground
THREEWALL_911	500	0.61	0.30	3	244.14	BASE_305	TRUE	Source Located 1 ft. above Ground
THREEWALL_911	500	0.61	0.30	3.3	192.58	BASE_305	TRUE	Source Located 1 ft. above Ground
THREEWALL_911	500	0.61	0.30	3.6	164.65	BASE_305	TRUE	Source Located 1 ft. above Ground

Table E-1
Obstructed Simulation Results

Test	HRR (kW)	Diameter (m)	Source Height (m)	Elevation (m)	Maximum Plume Temperature Rise (C)	Baseline Test	Data Filtered	Filtration Criteria
THREEWALL_911	500	0.61	0.30	3.9	141.73	BASE_305	TRUE	Source Located 1 ft. above Ground
THREEWALL_911	500	0.61	0.30	4.2	127.64	BASE_305	TRUE	Temperature < 130 C , Source Located 1 ft. above Ground
THREEWALL_911	500	0.61	0.30	4.5	114.66	BASE_305	TRUE	Temperature < 130 C , Source Located 1 ft. above Ground
THREEWALL_911	500	0.61	0.30	4.8	105.09	BASE_305	TRUE	Temperature < 130 C , Source Located 1 ft. above Ground
THREEWALL_911	500	0.61	0.30	5.1	98.004	BASE_305	TRUE	Temperature < 130 C , Source Located 1 ft. above Ground
THREEWALL_911	500	0.61	0.30	5.4	90.971	BASE_305	TRUE	Temperature < 130 C , Source Located 1 ft. above Ground
THREEWALL_911	500	0.61	0.30	5.7	83.486	BASE_305	TRUE	Temperature < 130 C , Source Located 1 ft. above Ground
THREEWALL_911	500	0.61	0.30	6	78.099	BASE_305	TRUE	Temperature < 130 C , Source Located 1 ft. above Ground
THREEWALL_912	600	0.61	0.30	2.4	627.21	BASE_306	TRUE	Source Located 1 ft. above Ground
THREEWALL_912	600	0.61	0.30	2.7	383.78	BASE_306	TRUE	Source Located 1 ft. above Ground
THREEWALL_912	600	0.61	0.30	3	277.38	BASE_306	TRUE	Source Located 1 ft. above Ground
THREEWALL_912	600	0.61	0.30	3.3	220.14	BASE_306	TRUE	Source Located 1 ft. above Ground
THREEWALL_912	600	0.61	0.30	3.6	186.98	BASE_306	TRUE	Source Located 1 ft. above Ground
THREEWALL_912	600	0.61	0.30	3.9	160.79	BASE_306	TRUE	Source Located 1 ft. above Ground
THREEWALL_912	600	0.61	0.30	4.2	139.96	BASE_306	TRUE	Source Located 1 ft. above Ground
THREEWALL_912	600	0.61	0.30	4.5	120.03	BASE_306	TRUE	Temperature < 130 C , Source Located 1 ft. above Ground

Table E-1
Obstructed Simulation Results

Test	HRR (kW)	Diameter (m)	Source Height (m)	Elevation (m)	Maximum Plume Temperature Rise (C)	Baseline Test	Data Filtered	Filtration Criteria
THREEWALL_912	600	0.61	0.30	4.8	108.42	BASE_306	TRUE	Temperature < 130 C , Source Located 1 ft. above Ground
THREEWALL_912	600	0.61	0.30	5.1	99.334	BASE_306	TRUE	Temperature < 130 C , Source Located 1 ft. above Ground
THREEWALL_912	600	0.61	0.30	5.4	91.383	BASE_306	TRUE	Temperature < 130 C , Source Located 1 ft. above Ground
THREEWALL_912	600	0.61	0.30	5.7	84.312	BASE_306	TRUE	Temperature < 130 C , Source Located 1 ft. above Ground
THREEWALL_912	600	0.61	0.30	6	81.252	BASE_306	TRUE	Temperature < 130 C , Source Located 1 ft. above Ground
THREEWALL_915	200	0.61	1.14	2.4	320.06	BASE_313	FALSE	Not Filtered
THREEWALL_915	200	0.61	1.14	2.7	179.86	BASE_313	FALSE	Not Filtered
THREEWALL_915	200	0.61	1.14	3	154.36	BASE_313	FALSE	Not Filtered
THREEWALL_915	200	0.61	1.14	3.3	128.98	BASE_313	TRUE	Temperature < 130 C
THREEWALL_915	200	0.61	1.14	3.6	113.2	BASE_313	TRUE	Temperature < 130 C
THREEWALL_915	200	0.61	1.14	3.9	106.12	BASE_313	TRUE	Temperature < 130 C
THREEWALL_915	200	0.61	1.14	4.2	94.481	BASE_313	TRUE	Temperature < 130 C
THREEWALL_915	200	0.61	1.14	4.5	87.577	BASE_313	TRUE	Temperature < 130 C
THREEWALL_915	200	0.61	1.14	4.8	85.132	BASE_313	TRUE	Temperature < 130 C
THREEWALL_915	200	0.61	1.14	5.1	71.536	BASE_313	TRUE	Temperature < 130 C
THREEWALL_915	200	0.61	1.14	5.4	66.804	BASE_313	TRUE	Temperature < 130 C
THREEWALL_915	200	0.61	1.14	5.7	62.677	BASE_313	TRUE	Temperature < 130 C
THREEWALL_915	200	0.61	1.14	6	58.233	BASE_313	TRUE	Temperature < 130 C

Table E-1
Obstructed Simulation Results

Test	HRR (kW)	Diameter (m)	Source Height (m)	Elevation (m)	Maximum Plume Temperature Rise (C)	Baseline Test	Data Filtered	Filtration Criteria
THREEWALL_916	300	0.61	1.14	2.4	508.54	BASE_314	FALSE	Not Filtered
THREEWALL_916	300	0.61	1.14	2.7	270.02	BASE_314	FALSE	Not Filtered
THREEWALL_916	300	0.61	1.14	3	194.28	BASE_314	FALSE	Not Filtered
THREEWALL_916	300	0.61	1.14	3.3	161.38	BASE_314	FALSE	Not Filtered
THREEWALL_916	300	0.61	1.14	3.6	143.99	BASE_314	FALSE	Not Filtered
THREEWALL_916	300	0.61	1.14	3.9	130.29	BASE_314	FALSE	Not Filtered
THREEWALL_916	300	0.61	1.14	4.2	116.98	BASE_314	TRUE	Temperature < 130 C
THREEWALL_916	300	0.61	1.14	4.5	103.62	BASE_314	TRUE	Temperature < 130 C
THREEWALL_916	300	0.61	1.14	4.8	93.72	BASE_314	TRUE	Temperature < 130 C
THREEWALL_916	300	0.61	1.14	5.1	85.707	BASE_314	TRUE	Temperature < 130 C
THREEWALL_916	300	0.61	1.14	5.4	77.268	BASE_314	TRUE	Temperature < 130 C
THREEWALL_916	300	0.61	1.14	5.7	69.468	BASE_314	TRUE	Temperature < 130 C
THREEWALL_916	300	0.61	1.14	6	66.588	BASE_314	TRUE	Temperature < 130 C
THREEWALL_917	400	0.61	1.14	2.4	683.59	BASE_315	FALSE	Not Filtered
THREEWALL_917	400	0.61	1.14	2.7	390.31	BASE_315	FALSE	Not Filtered
THREEWALL_917	400	0.61	1.14	3	270.68	BASE_315	FALSE	Not Filtered
THREEWALL_917	400	0.61	1.14	3.3	203.21	BASE_315	FALSE	Not Filtered
THREEWALL_917	400	0.61	1.14	3.6	172.33	BASE_315	FALSE	Not Filtered
THREEWALL_917	400	0.61	1.14	3.9	152.92	BASE_315	FALSE	Not Filtered
THREEWALL_917	400	0.61	1.14	4.2	138.8	BASE_315	FALSE	Not Filtered
THREEWALL_917	400	0.61	1.14	4.5	121.89	BASE_315	TRUE	Temperature < 130 C

Table E-1
Obstructed Simulation Results

Test	HRR (kW)	Diameter (m)	Source Height (m)	Elevation (m)	Maximum Plume Temperature Rise (C)	Baseline Test	Data Filtered	Filtration Criteria
THREEWALL_917	400	0.61	1.14	4.8	110.66	BASE_315	TRUE	Temperature < 130 C
THREEWALL_917	400	0.61	1.14	5.1	101.05	BASE_315	TRUE	Temperature < 130 C
THREEWALL_917	400	0.61	1.14	5.4	91.643	BASE_315	TRUE	Temperature < 130 C
THREEWALL_917	400	0.61	1.14	5.7	84.816	BASE_315	TRUE	Temperature < 130 C
THREEWALL_917	400	0.61	1.14	6	80.483	BASE_315	TRUE	Temperature < 130 C
THREEWALL_918	500	0.61	1.14	2.4	826.87	BASE_316	TRUE	Temperature > 800 C
THREEWALL_918	500	0.61	1.14	2.7	486.61	BASE_316	FALSE	Not Filtered
THREEWALL_918	500	0.61	1.14	3	333.59	BASE_316	FALSE	Not Filtered
THREEWALL_918	500	0.61	1.14	3.3	242.06	BASE_316	FALSE	Not Filtered
THREEWALL_918	500	0.61	1.14	3.6	204.52	BASE_316	FALSE	Not Filtered
THREEWALL_918	500	0.61	1.14	3.9	175.58	BASE_316	FALSE	Not Filtered
THREEWALL_918	500	0.61	1.14	4.2	154.38	BASE_316	FALSE	Not Filtered
THREEWALL_918	500	0.61	1.14	4.5	130.96	BASE_316	FALSE	Not Filtered
THREEWALL_918	500	0.61	1.14	4.8	118.68	BASE_316	TRUE	Temperature < 130 C
THREEWALL_918	500	0.61	1.14	5.1	108.22	BASE_316	TRUE	Temperature < 130 C
THREEWALL_918	500	0.61	1.14	5.4	99.367	BASE_316	TRUE	Temperature < 130 C
THREEWALL_918	500	0.61	1.14	5.7	89.439	BASE_316	TRUE	Temperature < 130 C
THREEWALL_918	500	0.61	1.14	6	83.231	BASE_316	TRUE	Temperature < 130 C
THREEWALL_919	600	0.61	1.14	2.4	846.23	BASE_317	TRUE	Temperature > 800 C
THREEWALL_919	600	0.61	1.14	2.7	582.28	BASE_317	FALSE	Not Filtered
THREEWALL_919	600	0.61	1.14	3	436.03	BASE_317	FALSE	Not Filtered

Table E-1
Obstructed Simulation Results

Test	HRR (kW)	Diameter (m)	Source Height (m)	Elevation (m)	Maximum Plume Temperature Rise (C)	Baseline Test	Data Filtered	Filtration Criteria
THREEWALL_919	600	0.61	1.14	3.3	325.81	BASE_317	FALSE	Not Filtered
THREEWALL_919	600	0.61	1.14	3.6	268	BASE_317	FALSE	Not Filtered
THREEWALL_919	600	0.61	1.14	3.9	223.92	BASE_317	FALSE	Not Filtered
THREEWALL_919	600	0.61	1.14	4.2	196.1	BASE_317	FALSE	Not Filtered
THREEWALL_919	600	0.61	1.14	4.5	172.14	BASE_317	FALSE	Not Filtered
THREEWALL_919	600	0.61	1.14	4.8	158.53	BASE_317	FALSE	Not Filtered
THREEWALL_919	600	0.61	1.14	5.1	143.64	BASE_317	FALSE	Not Filtered
THREEWALL_919	600	0.61	1.14	5.4	129.78	BASE_317	TRUE	Temperature < 130 C
THREEWALL_919	600	0.61	1.14	5.7	118.04	BASE_317	TRUE	Temperature < 130 C
THREEWALL_919	600	0.61	1.14	6	110.28	BASE_317	TRUE	Temperature < 130 C
THREEWALL_922	200	0.61	1.98	2.4	894.59	BASE_324	TRUE	Temperature > 800 C
THREEWALL_922	200	0.61	1.98	2.7	607.45	BASE_324	FALSE	Not Filtered
THREEWALL_922	200	0.61	1.98	3	438.25	BASE_324	FALSE	Not Filtered
THREEWALL_922	200	0.61	1.98	3.3	329.14	BASE_324	FALSE	Not Filtered
THREEWALL_922	200	0.61	1.98	3.6	256.87	BASE_324	FALSE	Not Filtered
THREEWALL_922	200	0.61	1.98	3.9	203.85	BASE_324	FALSE	Not Filtered
THREEWALL_922	200	0.61	1.98	4.2	168.83	BASE_324	FALSE	Not Filtered
THREEWALL_922	200	0.61	1.98	4.5	145.65	BASE_324	FALSE	Not Filtered
THREEWALL_922	200	0.61	1.98	4.8	129.93	BASE_324	TRUE	Temperature < 130 C
THREEWALL_922	200	0.61	1.98	5.1	115.64	BASE_324	TRUE	Temperature < 130 C
THREEWALL_922	200	0.61	1.98	5.4	103.08	BASE_324	TRUE	Temperature < 130 C

Table E-1
Obstructed Simulation Results

Test	HRR (kW)	Diameter (m)	Source Height (m)	Elevation (m)	Maximum Plume Temperature Rise (C)	Baseline Test	Data Filtered	Filtration Criteria
THREEWALL_922	200	0.61	1.98	5.7	91.731	BASE_324	TRUE	Temperature < 130 C
THREEWALL_922	200	0.61	1.98	6	84.103	BASE_324	TRUE	Temperature < 130 C
THREEWALL_923	300	0.61	1.98	2.4	983.87	BASE_325	TRUE	Temperature > 800 C
THREEWALL_923	300	0.61	1.98	2.7	922.29	BASE_325	TRUE	Temperature > 800 C
THREEWALL_923	300	0.61	1.98	3	726.09	BASE_325	FALSE	Not Filtered
THREEWALL_923	300	0.61	1.98	3.3	510.62	BASE_325	FALSE	Not Filtered
THREEWALL_923	300	0.61	1.98	3.6	388.3	BASE_325	FALSE	Not Filtered
THREEWALL_923	300	0.61	1.98	3.9	290.83	BASE_325	FALSE	Not Filtered
THREEWALL_923	300	0.61	1.98	4.2	230.29	BASE_325	FALSE	Not Filtered
THREEWALL_923	300	0.61	1.98	4.5	182.55	BASE_325	FALSE	Not Filtered
THREEWALL_923	300	0.61	1.98	4.8	157.83	BASE_325	FALSE	Not Filtered
THREEWALL_923	300	0.61	1.98	5.1	140.83	BASE_325	FALSE	Not Filtered
THREEWALL_923	300	0.61	1.98	5.4	122.74	BASE_325	TRUE	Temperature < 130 C
THREEWALL_923	300	0.61	1.98	5.7	110.35	BASE_325	TRUE	Temperature < 130 C
THREEWALL_923	300	0.61	1.98	6	101.38	BASE_325	TRUE	Temperature < 130 C
THREEWALL_924	400	0.61	1.98	2.4	1014.1	BASE_326	TRUE	Temperature > 800 C
THREEWALL_924	400	0.61	1.98	2.7	978.89	BASE_326	TRUE	Temperature > 800 C
THREEWALL_924	400	0.61	1.98	3	883.71	BASE_326	TRUE	Temperature > 800 C
THREEWALL_924	400	0.61	1.98	3.3	681.79	BASE_326	FALSE	Not Filtered
THREEWALL_924	400	0.61	1.98	3.6	519.42	BASE_326	FALSE	Not Filtered
THREEWALL_924	400	0.61	1.98	3.9	388.24	BASE_326	FALSE	Not Filtered

Table E-1
Obstructed Simulation Results

Test	HRR (kW)	Diameter (m)	Source Height (m)	Elevation (m)	Maximum Plume Temperature Rise (C)	Baseline Test	Data Filtered	Filtration Criteria
THREEWALL_924	400	0.61	1.98	4.2	306.26	BASE_326	FALSE	Not Filtered
THREEWALL_924	400	0.61	1.98	4.5	246.33	BASE_326	FALSE	Not Filtered
THREEWALL_924	400	0.61	1.98	4.8	213.8	BASE_326	FALSE	Not Filtered
THREEWALL_924	400	0.61	1.98	5.1	183.16	BASE_326	FALSE	Not Filtered
THREEWALL_924	400	0.61	1.98	5.4	157.27	BASE_326	FALSE	Not Filtered
THREEWALL_924	400	0.61	1.98	5.7	137.47	BASE_326	FALSE	Not Filtered
THREEWALL_924	400	0.61	1.98	6	126.19	BASE_326	TRUE	Temperature < 130 C
THREEWALL_925	500	0.61	1.98	2.4	1106.3	BASE_327	TRUE	Temperature > 800 C
THREEWALL_925	500	0.61	1.98	2.7	1011.3	BASE_327	TRUE	Temperature > 800 C
THREEWALL_925	500	0.61	1.98	3	928.71	BASE_327	TRUE	Temperature > 800 C
THREEWALL_925	500	0.61	1.98	3.3	799.73	BASE_327	FALSE	Not Filtered
THREEWALL_925	500	0.61	1.98	3.6	664.76	BASE_327	FALSE	Not Filtered
THREEWALL_925	500	0.61	1.98	3.9	518.6	BASE_327	FALSE	Not Filtered
THREEWALL_925	500	0.61	1.98	4.2	405.1	BASE_327	FALSE	Not Filtered
THREEWALL_925	500	0.61	1.98	4.5	310.44	BASE_327	FALSE	Not Filtered
THREEWALL_925	500	0.61	1.98	4.8	262.34	BASE_327	FALSE	Not Filtered
THREEWALL_925	500	0.61	1.98	5.1	221.57	BASE_327	FALSE	Not Filtered
THREEWALL_925	500	0.61	1.98	5.4	192.52	BASE_327	FALSE	Not Filtered
THREEWALL_925	500	0.61	1.98	5.7	166.57	BASE_327	FALSE	Not Filtered
THREEWALL_925	500	0.61	1.98	6	146.18	BASE_327	FALSE	Not Filtered
THREEWALL_926	600	0.61	1.98	2.4	1089.8	BASE_328	TRUE	Temperature > 800 C

Table E-1
Obstructed Simulation Results

Test	HRR (kW)	Diameter (m)	Source Height (m)	Elevation (m)	Maximum Plume Temperature Rise (C)	Baseline Test	Data Filtered	Filtration Criteria
THREEWALL_926	600	0.61	1.98	2.7	1070.9	BASE_328	TRUE	Temperature > 800 C
THREEWALL_926	600	0.61	1.98	3	984.08	BASE_328	TRUE	Temperature > 800 C
THREEWALL_926	600	0.61	1.98	3.3	844.18	BASE_328	TRUE	Temperature > 800 C
THREEWALL_926	600	0.61	1.98	3.6	706.97	BASE_328	FALSE	Not Filtered
THREEWALL_926	600	0.61	1.98	3.9	561.53	BASE_328	FALSE	Not Filtered
THREEWALL_926	600	0.61	1.98	4.2	440.71	BASE_328	FALSE	Not Filtered
THREEWALL_926	600	0.61	1.98	4.5	340.56	BASE_328	FALSE	Not Filtered
THREEWALL_926	600	0.61	1.98	4.8	284.69	BASE_328	FALSE	Not Filtered
THREEWALL_926	600	0.61	1.98	5.1	244.92	BASE_328	FALSE	Not Filtered
THREEWALL_926	600	0.61	1.98	5.4	208.27	BASE_328	FALSE	Not Filtered
THREEWALL_926	600	0.61	1.98	5.7	183.19	BASE_328	FALSE	Not Filtered
THREEWALL_926	600	0.61	1.98	6	166.48	BASE_328	FALSE	Not Filtered
THREEWALL_972	300	0.91	0.30	2.4	184.56	BASE_307	TRUE	Source Located 1 ft. above Ground
THREEWALL_972	300	0.91	0.30	2.7	118.56	BASE_307	TRUE	Temperature < 130 C , Source Located 1 ft. above Ground
THREEWALL_972	300	0.91	0.30	3	97.066	BASE_307	TRUE	Temperature < 130 C , Source Located 1 ft. above Ground
THREEWALL_972	300	0.91	0.30	3.3	83.193	BASE_307	TRUE	Temperature < 130 C , Source Located 1 ft. above Ground
THREEWALL_972	300	0.91	0.30	3.6	76.028	BASE_307	TRUE	Temperature < 130 C , Source Located 1 ft. above Ground
THREEWALL_972	300	0.91	0.30	3.9	70.479	BASE_307	TRUE	Temperature < 130 C , Source Located 1 ft. above Ground

Table E-1
Obstructed Simulation Results

Test	HRR (kW)	Diameter (m)	Source Height (m)	Elevation (m)	Maximum Plume Temperature Rise (C)	Baseline Test	Data Filtered	Filtration Criteria
THREEWALL_972	300	0.91	0.30	4.2	66.231	BASE_307	TRUE	Temperature < 130 C , Source Located 1 ft. above Ground
THREEWALL_972	300	0.91	0.30	4.5	64.326	BASE_307	TRUE	Temperature < 130 C , Source Located 1 ft. above Ground
THREEWALL_972	300	0.91	0.30	4.8	62.587	BASE_307	TRUE	Temperature < 130 C , Source Located 1 ft. above Ground
THREEWALL_972	300	0.91	0.30	5.1	60.063	BASE_307	TRUE	Temperature < 130 C , Source Located 1 ft. above Ground
THREEWALL_972	300	0.91	0.30	5.4	56.428	BASE_307	TRUE	Temperature < 130 C , Source Located 1 ft. above Ground
THREEWALL_972	300	0.91	0.30	5.7	52.662	BASE_307	TRUE	Temperature < 130 C , Source Located 1 ft. above Ground
THREEWALL_972	300	0.91	0.30	6	50.738	BASE_307	TRUE	Temperature < 130 C , Source Located 1 ft. above Ground
THREEWALL_973	400	0.91	0.30	2.4	240.59	BASE_308	TRUE	Source Located 1 ft. above Ground
THREEWALL_973	400	0.91	0.30	2.7	144.47	BASE_308	TRUE	Source Located 1 ft. above Ground
THREEWALL_973	400	0.91	0.30	3	115.08	BASE_308	TRUE	Temperature < 130 C , Source Located 1 ft. above Ground
THREEWALL_973	400	0.91	0.30	3.3	102.6	BASE_308	TRUE	Temperature < 130 C , Source Located 1 ft. above Ground
THREEWALL_973	400	0.91	0.30	3.6	92.14	BASE_308	TRUE	Temperature < 130 C , Source Located 1 ft. above Ground
THREEWALL_973	400	0.91	0.30	3.9	82.221	BASE_308	TRUE	Temperature < 130 C , Source Located 1 ft. above Ground
THREEWALL_973	400	0.91	0.30	4.2	76.611	BASE_308	TRUE	Temperature < 130 C , Source Located 1 ft. above Ground

Table E-1
Obstructed Simulation Results

Test	HRR (kW)	Diameter (m)	Source Height (m)	Elevation (m)	Maximum Plume Temperature Rise (C)	Baseline Test	Data Filtered	Filtration Criteria
THREEWALL_973	400	0.91	0.30	4.5	72.131	BASE_308	TRUE	Temperature < 130 C , Source Located 1 ft. above Ground
THREEWALL_973	400	0.91	0.30	4.8	69.414	BASE_308	TRUE	Temperature < 130 C , Source Located 1 ft. above Ground
THREEWALL_973	400	0.91	0.30	5.1	66.911	BASE_308	TRUE	Temperature < 130 C , Source Located 1 ft. above Ground
THREEWALL_973	400	0.91	0.30	5.4	63.254	BASE_308	TRUE	Temperature < 130 C , Source Located 1 ft. above Ground
THREEWALL_973	400	0.91	0.30	5.7	58.782	BASE_308	TRUE	Temperature < 130 C , Source Located 1 ft. above Ground
THREEWALL_973	400	0.91	0.30	6	56.053	BASE_308	TRUE	Temperature < 130 C , Source Located 1 ft. above Ground
THREEWALL_974	500	0.91	0.30	2.4	303.21	BASE_309	TRUE	Source Located 1 ft. above Ground
THREEWALL_974	500	0.91	0.30	2.7	185.97	BASE_309	TRUE	Source Located 1 ft. above Ground
THREEWALL_974	500	0.91	0.30	3	144.03	BASE_309	TRUE	Source Located 1 ft. above Ground
THREEWALL_974	500	0.91	0.30	3.3	120.84	BASE_309	TRUE	Temperature < 130 C , Source Located 1 ft. above Ground
THREEWALL_974	500	0.91	0.30	3.6	110.2	BASE_309	TRUE	Temperature < 130 C , Source Located 1 ft. above Ground
THREEWALL_974	500	0.91	0.30	3.9	101.09	BASE_309	TRUE	Temperature < 130 C , Source Located 1 ft. above Ground
THREEWALL_974	500	0.91	0.30	4.2	92.989	BASE_309	TRUE	Temperature < 130 C , Source Located 1 ft. above Ground
THREEWALL_974	500	0.91	0.30	4.5	85.945	BASE_309	TRUE	Temperature < 130 C , Source Located 1 ft. above Ground
THREEWALL_974	500	0.91	0.30	4.8	82.585	BASE_309	TRUE	Temperature < 130 C , Source

Table E-1
Obstructed Simulation Results

Test	HRR (kW)	Diameter (m)	Source Height (m)	Elevation (m)	Maximum Plume Temperature Rise (C)	Baseline Test	Data Filtered	Filtration Criteria
								Located 1 ft. above Ground
THREEWALL_974	500	0.91	0.30	5.1	78.139	BASE_309	TRUE	Temperature < 130 C , Source Located 1 ft. above Ground
THREEWALL_974	500	0.91	0.30	5.4	72.292	BASE_309	TRUE	Temperature < 130 C , Source Located 1 ft. above Ground
THREEWALL_974	500	0.91	0.30	5.7	65.906	BASE_309	TRUE	Temperature < 130 C , Source Located 1 ft. above Ground
THREEWALL_974	500	0.91	0.30	6	61.784	BASE_309	TRUE	Temperature < 130 C , Source Located 1 ft. above Ground
THREEWALL_975	600	0.91	0.30	2.4	351.27	BASE_310	TRUE	Source Located 1 ft. above Ground
THREEWALL_975	600	0.91	0.30	2.7	208.86	BASE_310	TRUE	Source Located 1 ft. above Ground
THREEWALL_975	600	0.91	0.30	3	165.74	BASE_310	TRUE	Source Located 1 ft. above Ground
THREEWALL_975	600	0.91	0.30	3.3	142	BASE_310	TRUE	Source Located 1 ft. above Ground
THREEWALL_975	600	0.91	0.30	3.6	128.21	BASE_310	TRUE	Temperature < 130 C , Source Located 1 ft. above Ground
THREEWALL_975	600	0.91	0.30	3.9	116.86	BASE_310	TRUE	Temperature < 130 C , Source Located 1 ft. above Ground
THREEWALL_975	600	0.91	0.30	4.2	106	BASE_310	TRUE	Temperature < 130 C , Source Located 1 ft. above Ground
THREEWALL_975	600	0.91	0.30	4.5	95.935	BASE_310	TRUE	Temperature < 130 C , Source Located 1 ft. above Ground
THREEWALL_975	600	0.91	0.30	4.8	89.561	BASE_310	TRUE	Temperature < 130 C , Source Located 1 ft. above Ground
THREEWALL_975	600	0.91	0.30	5.1	85.5	BASE_310	TRUE	Temperature < 130 C , Source Located 1 ft. above Ground

Table E-1
Obstructed Simulation Results

Test	HRR (kW)	Diameter (m)	Source Height (m)	Elevation (m)	Maximum Plume Temperature Rise (C)	Baseline Test	Data Filtered	Filtration Criteria
THREEWALL_975	600	0.91	0.30	5.4	81.763	BASE_310	TRUE	Temperature < 130 C , Source Located 1 ft. above Ground
THREEWALL_975	600	0.91	0.30	5.7	77.857	BASE_310	TRUE	Temperature < 130 C , Source Located 1 ft. above Ground
THREEWALL_975	600	0.91	0.30	6	74.923	BASE_310	TRUE	Temperature < 130 C , Source Located 1 ft. above Ground
THREEWALL_979	300	0.91	1.14	2.4	310.52	BASE_318	FALSE	Not Filtered
THREEWALL_979	300	0.91	1.14	2.7	184.64	BASE_318	FALSE	Not Filtered
THREEWALL_979	300	0.91	1.14	3	146.48	BASE_318	FALSE	Not Filtered
THREEWALL_979	300	0.91	1.14	3.3	124.98	BASE_318	TRUE	Temperature < 130 C
THREEWALL_979	300	0.91	1.14	3.6	112.59	BASE_318	TRUE	Temperature < 130 C
THREEWALL_979	300	0.91	1.14	3.9	100.44	BASE_318	TRUE	Temperature < 130 C
THREEWALL_979	300	0.91	1.14	4.2	91.793	BASE_318	TRUE	Temperature < 130 C
THREEWALL_979	300	0.91	1.14	4.5	84.386	BASE_318	TRUE	Temperature < 130 C
THREEWALL_979	300	0.91	1.14	4.8	78.823	BASE_318	TRUE	Temperature < 130 C
THREEWALL_979	300	0.91	1.14	5.1	74.82	BASE_318	TRUE	Temperature < 130 C
THREEWALL_979	300	0.91	1.14	5.4	69.589	BASE_318	TRUE	Temperature < 130 C
THREEWALL_979	300	0.91	1.14	5.7	65.922	BASE_318	TRUE	Temperature < 130 C
THREEWALL_979	300	0.91	1.14	6	63.23	BASE_318	TRUE	Temperature < 130 C
THREEWALL_980	400	0.91	1.14	2.4	380.97	BASE_319	FALSE	Not Filtered
THREEWALL_980	400	0.91	1.14	2.7	231.62	BASE_319	FALSE	Not Filtered
THREEWALL_980	400	0.91	1.14	3	184.42	BASE_319	FALSE	Not Filtered

Table E-1
Obstructed Simulation Results

Test	HRR (kW)	Diameter (m)	Source Height (m)	Elevation (m)	Maximum Plume Temperature Rise (C)	Baseline Test	Data Filtered	Filtration Criteria
THREEWALL_980	400	0.91	1.14	3.3	151.59	BASE_319	FALSE	Not Filtered
THREEWALL_980	400	0.91	1.14	3.6	134.53	BASE_319	FALSE	Not Filtered
THREEWALL_980	400	0.91	1.14	3.9	121.09	BASE_319	TRUE	Temperature < 130 C
THREEWALL_980	400	0.91	1.14	4.2	111.18	BASE_319	TRUE	Temperature < 130 C
THREEWALL_980	400	0.91	1.14	4.5	103.03	BASE_319	TRUE	Temperature < 130 C
THREEWALL_980	400	0.91	1.14	4.8	97.236	BASE_319	TRUE	Temperature < 130 C
THREEWALL_980	400	0.91	1.14	5.1	91.365	BASE_319	TRUE	Temperature < 130 C
THREEWALL_980	400	0.91	1.14	5.4	84.422	BASE_319	TRUE	Temperature < 130 C
THREEWALL_980	400	0.91	1.14	5.7	79.351	BASE_319	TRUE	Temperature < 130 C
THREEWALL_980	400	0.91	1.14	6	75.216	BASE_319	TRUE	Temperature < 130 C
THREEWALL_981	500	0.91	1.14	2.4	522.3	BASE_320	FALSE	Not Filtered
THREEWALL_981	500	0.91	1.14	2.7	283.14	BASE_320	FALSE	Not Filtered
THREEWALL_981	500	0.91	1.14	3	223.96	BASE_320	FALSE	Not Filtered
THREEWALL_981	500	0.91	1.14	3.3	187.48	BASE_320	FALSE	Not Filtered
THREEWALL_981	500	0.91	1.14	3.6	163.06	BASE_320	FALSE	Not Filtered
THREEWALL_981	500	0.91	1.14	3.9	146.31	BASE_320	FALSE	Not Filtered
THREEWALL_981	500	0.91	1.14	4.2	133.8	BASE_320	FALSE	Not Filtered
THREEWALL_981	500	0.91	1.14	4.5	122.56	BASE_320	TRUE	Temperature < 130 C
THREEWALL_981	500	0.91	1.14	4.8	112.15	BASE_320	TRUE	Temperature < 130 C
THREEWALL_981	500	0.91	1.14	5.1	104.23	BASE_320	TRUE	Temperature < 130 C
THREEWALL_981	500	0.91	1.14	5.4	96.185	BASE_320	TRUE	Temperature < 130 C

Table E-1
Obstructed Simulation Results

Test	HRR (kW)	Diameter (m)	Source Height (m)	Elevation (m)	Maximum Plume Temperature Rise (C)	Baseline Test	Data Filtered	Filtration Criteria
THREEWALL_981	500	0.91	1.14	5.7	90.141	BASE_320	TRUE	Temperature < 130 C
THREEWALL_981	500	0.91	1.14	6	84.866	BASE_320	TRUE	Temperature < 130 C
THREEWALL_982	600	0.91	1.14	2.4	604.51	BASE_321	FALSE	Not Filtered
THREEWALL_982	600	0.91	1.14	2.7	350.93	BASE_321	FALSE	Not Filtered
THREEWALL_982	600	0.91	1.14	3	268.81	BASE_321	FALSE	Not Filtered
THREEWALL_982	600	0.91	1.14	3.3	221.1	BASE_321	FALSE	Not Filtered
THREEWALL_982	600	0.91	1.14	3.6	193.38	BASE_321	FALSE	Not Filtered
THREEWALL_982	600	0.91	1.14	3.9	171.54	BASE_321	FALSE	Not Filtered
THREEWALL_982	600	0.91	1.14	4.2	153.52	BASE_321	FALSE	Not Filtered
THREEWALL_982	600	0.91	1.14	4.5	138.27	BASE_321	FALSE	Not Filtered
THREEWALL_982	600	0.91	1.14	4.8	126.36	BASE_321	TRUE	Temperature < 130 C
THREEWALL_982	600	0.91	1.14	5.1	116.64	BASE_321	TRUE	Temperature < 130 C
THREEWALL_982	600	0.91	1.14	5.4	108.26	BASE_321	TRUE	Temperature < 130 C
THREEWALL_982	600	0.91	1.14	5.7	100.09	BASE_321	TRUE	Temperature < 130 C
THREEWALL_982	600	0.91	1.14	6	94.122	BASE_321	TRUE	Temperature < 130 C
THREEWALL_986	300	0.91	1.98	2.4	844.4	BASE_329	TRUE	Temperature > 800 C
THREEWALL_986	300	0.91	1.98	2.7	681.25	BASE_329	FALSE	Not Filtered
THREEWALL_986	300	0.91	1.98	3	490.11	BASE_329	FALSE	Not Filtered
THREEWALL_986	300	0.91	1.98	3.3	353.3	BASE_329	FALSE	Not Filtered
THREEWALL_986	300	0.91	1.98	3.6	278.73	BASE_329	FALSE	Not Filtered
THREEWALL_986	300	0.91	1.98	3.9	227.21	BASE_329	FALSE	Not Filtered

Table E-1
Obstructed Simulation Results

Test	HRR (kW)	Diameter (m)	Source Height (m)	Elevation (m)	Maximum Plume Temperature Rise (C)	Baseline Test	Data Filtered	Filtration Criteria
THREEWALL_986	300	0.91	1.98	4.2	182.1	BASE_329	FALSE	Not Filtered
THREEWALL_986	300	0.91	1.98	4.5	148.46	BASE_329	FALSE	Not Filtered
THREEWALL_986	300	0.91	1.98	4.8	126.79	BASE_329	TRUE	Temperature < 130 C
THREEWALL_986	300	0.91	1.98	5.1	112.9	BASE_329	TRUE	Temperature < 130 C
THREEWALL_986	300	0.91	1.98	5.4	99.758	BASE_329	TRUE	Temperature < 130 C
THREEWALL_986	300	0.91	1.98	5.7	88.638	BASE_329	TRUE	Temperature < 130 C
THREEWALL_986	300	0.91	1.98	6	81.318	BASE_329	TRUE	Temperature < 130 C
THREEWALL_987	400	0.91	1.98	2.4	909.89	BASE_330	TRUE	Temperature > 800 C
THREEWALL_987	400	0.91	1.98	2.7	857.59	BASE_330	TRUE	Temperature > 800 C
THREEWALL_987	400	0.91	1.98	3	676.43	BASE_330	FALSE	Not Filtered
THREEWALL_987	400	0.91	1.98	3.3	441.27	BASE_330	FALSE	Not Filtered
THREEWALL_987	400	0.91	1.98	3.6	339.87	BASE_330	FALSE	Not Filtered
THREEWALL_987	400	0.91	1.98	3.9	266.42	BASE_330	FALSE	Not Filtered
THREEWALL_987	400	0.91	1.98	4.2	220.39	BASE_330	FALSE	Not Filtered
THREEWALL_987	400	0.91	1.98	4.5	182.32	BASE_330	FALSE	Not Filtered
THREEWALL_987	400	0.91	1.98	4.8	164.19	BASE_330	FALSE	Not Filtered
THREEWALL_987	400	0.91	1.98	5.1	148.53	BASE_330	FALSE	Not Filtered
THREEWALL_987	400	0.91	1.98	5.4	135.35	BASE_330	FALSE	Not Filtered
THREEWALL_987	400	0.91	1.98	5.7	121.94	BASE_330	TRUE	Temperature < 130 C
THREEWALL_987	400	0.91	1.98	6	113.94	BASE_330	TRUE	Temperature < 130 C
THREEWALL_988	500	0.91	1.98	2.4	973.68	BASE_331	TRUE	Temperature > 800 C

Table E-1
Obstructed Simulation Results

Test	HRR (kW)	Diameter (m)	Source Height (m)	Elevation (m)	Maximum Plume Temperature Rise (C)	Baseline Test	Data Filtered	Filtration Criteria
THREEWALL_988	500	0.91	1.98	2.7	891.03	BASE_331	TRUE	Temperature > 800 C
THREEWALL_988	500	0.91	1.98	3	799.43	BASE_331	FALSE	Not Filtered
THREEWALL_988	500	0.91	1.98	3.3	606.92	BASE_331	FALSE	Not Filtered
THREEWALL_988	500	0.91	1.98	3.6	454.55	BASE_331	FALSE	Not Filtered
THREEWALL_988	500	0.91	1.98	3.9	343.91	BASE_331	FALSE	Not Filtered
THREEWALL_988	500	0.91	1.98	4.2	282.91	BASE_331	FALSE	Not Filtered
THREEWALL_988	500	0.91	1.98	4.5	229.44	BASE_331	FALSE	Not Filtered
THREEWALL_988	500	0.91	1.98	4.8	198.62	BASE_331	FALSE	Not Filtered
THREEWALL_988	500	0.91	1.98	5.1	177.02	BASE_331	FALSE	Not Filtered
THREEWALL_988	500	0.91	1.98	5.4	157.24	BASE_331	FALSE	Not Filtered
THREEWALL_988	500	0.91	1.98	5.7	137.4	BASE_331	FALSE	Not Filtered
THREEWALL_988	500	0.91	1.98	6	125.87	BASE_331	TRUE	Temperature < 130 C
THREEWALL_989	600	0.91	1.98	2.4	1027.7	BASE_332	TRUE	Temperature > 800 C
THREEWALL_989	600	0.91	1.98	2.7	965.5	BASE_332	TRUE	Temperature > 800 C
THREEWALL_989	600	0.91	1.98	3	918.36	BASE_332	TRUE	Temperature > 800 C
THREEWALL_989	600	0.91	1.98	3.3	752.38	BASE_332	FALSE	Not Filtered
THREEWALL_989	600	0.91	1.98	3.6	582.49	BASE_332	FALSE	Not Filtered
THREEWALL_989	600	0.91	1.98	3.9	431.65	BASE_332	FALSE	Not Filtered
THREEWALL_989	600	0.91	1.98	4.2	349.02	BASE_332	FALSE	Not Filtered
THREEWALL_989	600	0.91	1.98	4.5	270.92	BASE_332	FALSE	Not Filtered
THREEWALL_989	600	0.91	1.98	4.8	233.27	BASE_332	FALSE	Not Filtered

Table E-1
Obstructed Simulation Results

Test	HRR (kW)	Diameter (m)	Source Height (m)	Elevation (m)	Maximum Plume Temperature Rise (C)	Baseline Test	Data Filtered	Filtration Criteria
THREEWALL_989	600	0.91	1.98	5.1	202.93	BASE_332	FALSE	Not Filtered
THREEWALL_989	600	0.91	1.98	5.4	176.71	BASE_332	FALSE	Not Filtered
THREEWALL_989	600	0.91	1.98	5.7	151.1	BASE_332	FALSE	Not Filtered
THREEWALL_989	600	0.91	1.98	6	137.61	BASE_332	FALSE	Not Filtered

Unobstructed Simulation Results

Table E-2
Unobstructed Simulation Results

Test	HRR (kW)	Diameter (m)	Source Height (m)	Elevation (m)	Maximum Plume Temperature Rise (C)	Heskestad Plume Temperature (Equation 4-3)	Data Filtered	Filtration Criteria
BASE_404	1000	0.91	0.30	2.4	795.4	819.38	TRUE	Source Located 1 ft. above Ground , Heskestad > 800 C
BASE_404	1000	0.91	0.30	2.7	698.73	626.09	TRUE	Source Located 1 ft. above Ground
BASE_404	1000	0.91	0.30	3	605.33	496.65	TRUE	Source Located 1 ft. above Ground
BASE_404	1000	0.91	0.30	3.3	507.53	405.28	TRUE	Source Located 1 ft. above Ground
BASE_404	1000	0.91	0.30	3.6	423.26	338.12	TRUE	Source Located 1 ft. above Ground
BASE_404	1000	0.91	0.30	3.9	338.41	287.15	TRUE	Source Located 1 ft. above Ground
BASE_404	1000	0.91	0.30	4.2	282.38	247.45	TRUE	Source Located 1 ft. above Ground
BASE_404	1000	0.91	0.30	4.5	235.94	215.85	TRUE	Source Located 1 ft. above Ground
BASE_404	1000	0.91	0.30	4.8	211.9	190.25	TRUE	Source Located 1 ft. above Ground
BASE_404	1000	0.91	0.30	5.1	189.94	169.19	TRUE	Source Located 1 ft. above Ground
BASE_404	1000	0.91	0.30	5.4	166.35	151.62	TRUE	Source Located 1 ft. above Ground
BASE_404	1000	0.91	0.30	5.7	146.53	136.80	TRUE	Source Located 1 ft. above Ground
BASE_404	1000	0.91	0.30	6	133.59	124.17	TRUE	Heskestad < 130 C , Source Located 1 ft. above Ground
BASE_400	1000	0.91	1.14	2.4	883.35	1000.00	TRUE	Heskestad > 800 C
BASE_400	1000	0.91	1.14	2.7	869.76	1000.00	TRUE	Heskestad > 800 C
BASE_400	1000	0.91	1.14	3	821.26	1000.00	TRUE	Heskestad > 800 C
BASE_400	1000	0.91	1.14	3.3	737.09	772.37	FALSE	Not Filtered
BASE_400	1000	0.91	1.14	3.6	641.71	595.31	FALSE	Not Filtered
BASE_400	1000	0.91	1.14	3.9	540.23	475.29	FALSE	Not Filtered

Table E-2
Unobstructed Simulation Results

Test	HRR (kW)	Diameter (m)	Source Height (m)	Elevation (m)	Maximum Plume Temperature Rise (C)	Heskestad Plume Temperature (Equation 4-3)	Data Filtered	Filtration Criteria
BASE_400	1000	0.91	1.14	4.2	442.68	389.79	FALSE	Not Filtered
BASE_400	1000	0.91	1.14	4.5	364.05	326.49	FALSE	Not Filtered
BASE_400	1000	0.91	1.14	4.8	309.85	278.17	FALSE	Not Filtered
BASE_400	1000	0.91	1.14	5.1	266.48	240.36	FALSE	Not Filtered
BASE_400	1000	0.91	1.14	5.4	227.22	210.14	FALSE	Not Filtered
BASE_400	1000	0.91	1.14	5.7	187.04	185.58	FALSE	Not Filtered
BASE_400	1000	0.91	1.14	6	162.96	165.31	FALSE	Not Filtered
BASE_401	1000	0.91	1.98	2.4	867.85	1000.00	TRUE	Heskestad > 800 C
BASE_401	1000	0.91	1.98	2.7	821.69	1000.00	TRUE	Heskestad > 800 C
BASE_401	1000	0.91	1.98	3	843.29	1000.00	TRUE	Heskestad > 800 C
BASE_401	1000	0.91	1.98	3.3	863.68	1000.00	TRUE	Heskestad > 800 C
BASE_401	1000	0.91	1.98	3.6	847.71	1000.00	TRUE	Heskestad > 800 C
BASE_401	1000	0.91	1.98	3.9	778.57	982.15	TRUE	Heskestad > 800 C
BASE_401	1000	0.91	1.98	4.2	712.61	729.52	FALSE	Not Filtered
BASE_401	1000	0.91	1.98	4.5	619.77	566.88	FALSE	Not Filtered
BASE_401	1000	0.91	1.98	4.8	546.09	455.37	FALSE	Not Filtered
BASE_401	1000	0.91	1.98	5.1	448.48	375.23	FALSE	Not Filtered
BASE_401	1000	0.91	1.98	5.4	362.78	315.49	FALSE	Not Filtered
BASE_401	1000	0.91	1.98	5.7	297.95	269.64	FALSE	Not Filtered
BASE_401	1000	0.91	1.98	6	255.43	233.59	FALSE	Not Filtered
BASE_405	1000	1.22	0.30	2.4	781.27	819.38	TRUE	Source Located 1 ft. above Ground , Heskestad > 800 C

Table E-2
Unobstructed Simulation Results

Test	HRR (kW)	Diameter (m)	Source Height (m)	Elevation (m)	Maximum Plume Temperature Rise (C)	Heskestad Plume Temperature (Equation 4-3)	Data Filtered	Filtration Criteria
BASE_405	1000	1.22	0.30	2.7	709.22	626.09	TRUE	Source Located 1 ft. above Ground
BASE_405	1000	1.22	0.30	3	615.79	496.65	TRUE	Source Located 1 ft. above Ground
BASE_405	1000	1.22	0.30	3.3	498.02	405.28	TRUE	Source Located 1 ft. above Ground
BASE_405	1000	1.22	0.30	3.6	410.4	338.12	TRUE	Source Located 1 ft. above Ground
BASE_405	1000	1.22	0.30	3.9	327.49	287.15	TRUE	Source Located 1 ft. above Ground
BASE_405	1000	1.22	0.30	4.2	278.55	247.45	TRUE	Source Located 1 ft. above Ground
BASE_405	1000	1.22	0.30	4.5	237.14	215.85	TRUE	Source Located 1 ft. above Ground
BASE_405	1000	1.22	0.30	4.8	206.01	190.25	TRUE	Source Located 1 ft. above Ground
BASE_405	1000	1.22	0.30	5.1	182.4	169.19	TRUE	Source Located 1 ft. above Ground
BASE_405	1000	1.22	0.30	5.4	160.44	151.62	TRUE	Source Located 1 ft. above Ground
BASE_405	1000	1.22	0.30	5.7	142.62	136.80	TRUE	Source Located 1 ft. above Ground
BASE_405	1000	1.22	0.30	6	129.63	124.17	TRUE	Heskestad < 130 C , Source Located 1 ft. above Ground
BASE_402	1000	1.22	1.14	2.4	884.72	1000.00	TRUE	Heskestad > 800 C
BASE_402	1000	1.22	1.14	2.7	872.06	1000.00	TRUE	Heskestad > 800 C
BASE_402	1000	1.22	1.14	3	844.23	764.70	FALSE	Not Filtered
BASE_402	1000	1.22	1.14	3.3	780	590.25	FALSE	Not Filtered
BASE_402	1000	1.22	1.14	3.6	703.37	471.76	FALSE	Not Filtered
BASE_402	1000	1.22	1.14	3.9	609.22	387.22	FALSE	Not Filtered
BASE_402	1000	1.22	1.14	4.2	536.91	324.55	FALSE	Not Filtered
BASE_402	1000	1.22	1.14	4.5	442.2	276.67	FALSE	Not Filtered
BASE_402	1000	1.22	1.14	4.8	371.59	239.17	FALSE	Not Filtered

Table E-2
Unobstructed Simulation Results

Test	HRR (kW)	Diameter (m)	Source Height (m)	Elevation (m)	Maximum Plume Temperature Rise (C)	Heskestad Plume Temperature (Equation 4-3)	Data Filtered	Filtration Criteria
BASE_402	1000	1.22	1.14	5.1	319.12	209.19	FALSE	Not Filtered
BASE_402	1000	1.22	1.14	5.4	270.59	184.79	FALSE	Not Filtered
BASE_402	1000	1.22	1.14	5.7	231.36	164.65	FALSE	Not Filtered
BASE_402	1000	1.22	1.14	6	203.95	147.81	FALSE	Not Filtered
BASE_403	1000	1.22	1.98	2.4	832.64	1000.00	TRUE	Heskestad > 800 C
BASE_403	1000	1.22	1.98	2.7	849.5	1000.00	TRUE	Heskestad > 800 C
BASE_403	1000	1.22	1.98	3	881.01	1000.00	TRUE	Heskestad > 800 C
BASE_403	1000	1.22	1.98	3.3	897.01	1000.00	TRUE	Heskestad > 800 C
BASE_403	1000	1.22	1.98	3.6	882.44	970.90	TRUE	Heskestad > 800 C
BASE_403	1000	1.22	1.98	3.9	843.66	722.52	FALSE	Not Filtered
BASE_403	1000	1.22	1.98	4.2	798.56	562.20	FALSE	Not Filtered
BASE_403	1000	1.22	1.98	4.5	714.56	452.07	FALSE	Not Filtered
BASE_403	1000	1.22	1.98	4.8	619.77	372.81	FALSE	Not Filtered
BASE_403	1000	1.22	1.98	5.1	524.43	313.65	FALSE	Not Filtered
BASE_403	1000	1.22	1.98	5.4	430.81	268.21	FALSE	Not Filtered
BASE_403	1000	1.22	1.98	5.7	350.83	232.45	FALSE	Not Filtered
BASE_403	1000	1.22	1.98	6	294.37	203.75	FALSE	Not Filtered
BASE_300	50	0.30	0.30	2.4	78.578	85.19	TRUE	Heskestad < 130 C , Source Located 1 ft. above Ground
BASE_300	50	0.30	0.30	2.7	62.259	67.56	TRUE	Heskestad < 130 C , Source Located 1 ft. above Ground
BASE_300	50	0.30	0.30	3	51.393	55.11	TRUE	Heskestad < 130 C , Source

Table E-2
Unobstructed Simulation Results

Test	HRR (kW)	Diameter (m)	Source Height (m)	Elevation (m)	Maximum Plume Temperature Rise (C)	Heskestad Plume Temperature (Equation 4-3)	Data Filtered	Filtration Criteria
								Located 1 ft. above Ground
BASE_300	50	0.30	0.30	3.3	42.918	45.97	TRUE	Heskestad < 130 C , Source Located 1 ft. above Ground
BASE_300	50	0.30	0.30	3.6	38.301	39.03	TRUE	Heskestad < 130 C , Source Located 1 ft. above Ground
BASE_300	50	0.30	0.30	3.9	33.654	33.63	TRUE	Heskestad < 130 C , Source Located 1 ft. above Ground
BASE_301	100	0.30	0.30	2.4	144.68	150.77	TRUE	Source Located 1 ft. above Ground
BASE_301	100	0.30	0.30	2.7	115.38	117.84	TRUE	Heskestad < 130 C , Source Located 1 ft. above Ground
BASE_301	100	0.30	0.30	3	94.51	95.07	TRUE	Heskestad < 130 C , Source Located 1 ft. above Ground
BASE_301	100	0.30	0.30	3.3	78.22	78.61	TRUE	Heskestad < 130 C , Source Located 1 ft. above Ground
BASE_301	100	0.30	0.30	3.6	66.281	66.27	TRUE	Heskestad < 130 C , Source Located 1 ft. above Ground
BASE_301	100	0.30	0.30	3.9	54.636	56.77	TRUE	Heskestad < 130 C , Source Located 1 ft. above Ground
BASE_301	100	0.30	0.30	4.2	48.663	49.27	TRUE	Heskestad < 130 C , Source Located 1 ft. above Ground
BASE_301	100	0.30	0.30	4.5	44.269	43.24	TRUE	Heskestad < 130 C , Source Located 1 ft. above Ground
BASE_301	100	0.30	0.30	4.8	41.438	38.31	TRUE	Heskestad < 130 C , Source Located 1 ft. above Ground
BASE_311	50	0.30	1.14	2.4	191.73	209.49	FALSE	Not Filtered
BASE_311	50	0.30	1.14	2.7	132.04	143.24	FALSE	Not Filtered

Table E-2
Unobstructed Simulation Results

Test	HRR (kW)	Diameter (m)	Source Height (m)	Elevation (m)	Maximum Plume Temperature Rise (C)	Heskestad Plume Temperature (Equation 4-3)	Data Filtered	Filtration Criteria
BASE_311	50	0.30	1.14	3	103.75	105.13	TRUE	Heskestad < 130 C
BASE_311	50	0.30	1.14	3.3	80.93	81.00	TRUE	Heskestad < 130 C
BASE_311	50	0.30	1.14	3.6	66.604	64.65	TRUE	Heskestad < 130 C
BASE_311	50	0.30	1.14	3.9	54.69	53.01	TRUE	Heskestad < 130 C
BASE_311	50	0.30	1.14	4.2	47.827	44.39	TRUE	Heskestad < 130 C
BASE_312	100	0.30	1.14	2.4	362.7	402.61	FALSE	Not Filtered
BASE_312	100	0.30	1.14	2.7	221.13	264.28	FALSE	Not Filtered
BASE_312	100	0.30	1.14	3	162.78	188.91	FALSE	Not Filtered
BASE_312	100	0.30	1.14	3.3	123.92	142.87	FALSE	Not Filtered
BASE_312	100	0.30	1.14	3.6	99.71	112.48	TRUE	Heskestad < 130 C
BASE_312	100	0.30	1.14	3.9	82.29	91.25	TRUE	Heskestad < 130 C
BASE_312	100	0.30	1.14	4.2	70.911	75.78	TRUE	Heskestad < 130 C
BASE_312	100	0.30	1.14	4.5	58.39	64.12	TRUE	Heskestad < 130 C
BASE_312	100	0.30	1.14	4.8	51.09	55.08	TRUE	Heskestad < 130 C
BASE_312	100	0.30	1.14	5.1	44.749	47.92	TRUE	Heskestad < 130 C
BASE_312	100	0.30	1.14	5.4	39.094	42.15	TRUE	Heskestad < 130 C
BASE_322	50	0.30	1.98	2.4	790.05	1000.00	TRUE	Heskestad > 800 C
BASE_322	50	0.30	1.98	2.7	434.88	584.26	FALSE	Not Filtered
BASE_322	50	0.30	1.98	3	242.82	306.03	FALSE	Not Filtered
BASE_322	50	0.30	1.98	3.3	154.53	192.28	FALSE	Not Filtered
BASE_322	50	0.30	1.98	3.6	115.32	133.75	FALSE	Not Filtered

Table E-2
Unobstructed Simulation Results

Test	HRR (kW)	Diameter (m)	Source Height (m)	Elevation (m)	Maximum Plume Temperature Rise (C)	Heskestad Plume Temperature (Equation 4-3)	Data Filtered	Filtration Criteria
BASE_322	50	0.30	1.98	3.9	89.33	99.29	TRUE	Heskestad < 130 C
BASE_322	50	0.30	1.98	4.2	71.831	77.12	TRUE	Heskestad < 130 C
BASE_322	50	0.30	1.98	4.5	56.449	61.93	TRUE	Heskestad < 130 C
BASE_322	50	0.30	1.98	4.8	46.519	51.02	TRUE	Heskestad < 130 C
BASE_322	50	0.30	1.98	5.1	40.578	42.89	TRUE	Heskestad < 130 C
BASE_323	100	0.30	1.98	2.4	1020.6	1000.00	TRUE	Heskestad > 800 C
BASE_323	100	0.30	1.98	2.7	908.31	1000.00	TRUE	Heskestad > 800 C
BASE_323	100	0.30	1.98	3	614.44	619.87	FALSE	Not Filtered
BASE_323	100	0.30	1.98	3.3	348.63	365.81	FALSE	Not Filtered
BASE_323	100	0.30	1.98	3.6	238.38	245.21	FALSE	Not Filtered
BASE_323	100	0.30	1.98	3.9	165.26	177.64	FALSE	Not Filtered
BASE_323	100	0.30	1.98	4.2	127.9	135.61	FALSE	Not Filtered
BASE_323	100	0.30	1.98	4.5	99.95	107.50	TRUE	Heskestad < 130 C
BASE_323	100	0.30	1.98	4.8	84.38	87.67	TRUE	Heskestad < 130 C
BASE_323	100	0.30	1.98	5.1	70.453	73.11	TRUE	Heskestad < 130 C
BASE_323	100	0.30	1.98	5.4	58.577	62.07	TRUE	Heskestad < 130 C
BASE_323	100	0.30	1.98	5.7	50.134	53.47	TRUE	Heskestad < 130 C
BASE_323	100	0.30	1.98	6	43.943	46.64	TRUE	Heskestad < 130 C
BASE_302	200	0.61	0.30	2.4	213.45	211.71	TRUE	Source Located 1 ft. above Ground
BASE_302	200	0.61	0.30	2.7	170.01	168.19	TRUE	Source Located 1 ft. above Ground
BASE_302	200	0.61	0.30	3	142.96	137.40	TRUE	Source Located 1 ft. above Ground

Table E-2
Unobstructed Simulation Results

Test	HRR (kW)	Diameter (m)	Source Height (m)	Elevation (m)	Maximum Plume Temperature Rise (C)	Heskestad Plume Temperature (Equation 4-3)	Data Filtered	Filtration Criteria
BASE_302	200	0.61	0.30	3.3	121.27	114.73	TRUE	Heskestad < 130 C , Source Located 1 ft. above Ground
BASE_302	200	0.61	0.30	3.6	105.52	97.51	TRUE	Heskestad < 130 C , Source Located 1 ft. above Ground
BASE_302	200	0.61	0.30	3.9	88.62	84.08	TRUE	Heskestad < 130 C , Source Located 1 ft. above Ground
BASE_302	200	0.61	0.30	4.2	76.736	73.38	TRUE	Heskestad < 130 C , Source Located 1 ft. above Ground
BASE_302	200	0.61	0.30	4.5	67.501	64.71	TRUE	Heskestad < 130 C , Source Located 1 ft. above Ground
BASE_302	200	0.61	0.30	4.8	61.141	57.56	TRUE	Heskestad < 130 C , Source Located 1 ft. above Ground
BASE_302	200	0.61	0.30	5.1	56.723	51.60	TRUE	Heskestad < 130 C , Source Located 1 ft. above Ground
BASE_302	200	0.61	0.30	5.4	51.975	46.57	TRUE	Heskestad < 130 C , Source Located 1 ft. above Ground
BASE_302	200	0.61	0.30	5.7	45.998	42.28	TRUE	Heskestad < 130 C , Source Located 1 ft. above Ground
BASE_302	200	0.61	0.30	6	43.08	38.59	TRUE	Heskestad < 130 C , Source Located 1 ft. above Ground
BASE_303	300	0.61	0.30	2.4	296.14	307.62	TRUE	Source Located 1 ft. above Ground
BASE_303	300	0.61	0.30	2.7	220.38	241.06	TRUE	Source Located 1 ft. above Ground
BASE_303	300	0.61	0.30	3	183.17	194.88	TRUE	Source Located 1 ft. above Ground
BASE_303	300	0.61	0.30	3.3	148.23	161.39	TRUE	Source Located 1 ft. above Ground
BASE_303	300	0.61	0.30	3.6	128.16	136.24	TRUE	Source Located 1 ft. above Ground

Table E-2
Unobstructed Simulation Results

Test	HRR (kW)	Diameter (m)	Source Height (m)	Elevation (m)	Maximum Plume Temperature Rise (C)	Heskestad Plume Temperature (Equation 4-3)	Data Filtered	Filtration Criteria
BASE_303	300	0.61	0.30	3.9	108.27	116.82	TRUE	Heskestad < 130 C , Source Located 1 ft. above Ground
BASE_303	300	0.61	0.30	4.2	93.85	101.48	TRUE	Heskestad < 130 C , Source Located 1 ft. above Ground
BASE_303	300	0.61	0.30	4.5	81.84	89.13	TRUE	Heskestad < 130 C , Source Located 1 ft. above Ground
BASE_303	300	0.61	0.30	4.8	74.599	79.02	TRUE	Heskestad < 130 C , Source Located 1 ft. above Ground
BASE_303	300	0.61	0.30	5.1	67.063	70.63	TRUE	Heskestad < 130 C , Source Located 1 ft. above Ground
BASE_303	300	0.61	0.30	5.4	60.342	63.57	TRUE	Heskestad < 130 C , Source Located 1 ft. above Ground
BASE_303	300	0.61	0.30	5.7	53.847	57.58	TRUE	Heskestad < 130 C , Source Located 1 ft. above Ground
BASE_303	300	0.61	0.30	6	50.33	52.45	TRUE	Heskestad < 130 C , Source Located 1 ft. above Ground
BASE_304	400	0.61	0.30	2.4	411.81	407.41	TRUE	Source Located 1 ft. above Ground
BASE_304	400	0.61	0.30	2.7	304.43	315.31	TRUE	Source Located 1 ft. above Ground
BASE_304	400	0.61	0.30	3	247.49	252.53	TRUE	Source Located 1 ft. above Ground
BASE_304	400	0.61	0.30	3.3	200.37	207.60	TRUE	Source Located 1 ft. above Ground
BASE_304	400	0.61	0.30	3.6	162.17	174.22	TRUE	Source Located 1 ft. above Ground
BASE_304	400	0.61	0.30	3.9	133.24	148.67	TRUE	Source Located 1 ft. above Ground
BASE_304	400	0.61	0.30	4.2	115.82	128.63	TRUE	Heskestad < 130 C , Source Located 1 ft. above Ground
BASE_304	400	0.61	0.30	4.5	101.45	112.58	TRUE	Heskestad < 130 C , Source

Table E-2
Unobstructed Simulation Results

Test	HRR (kW)	Diameter (m)	Source Height (m)	Elevation (m)	Maximum Plume Temperature Rise (C)	Heskestad Plume Temperature (Equation 4-3)	Data Filtered	Filtration Criteria
								Located 1 ft. above Ground
BASE_304	400	0.61	0.30	4.8	90.29	99.52	TRUE	Heskestad < 130 C , Source Located 1 ft. above Ground
BASE_304	400	0.61	0.30	5.1	82.61	88.72	TRUE	Heskestad < 130 C , Source Located 1 ft. above Ground
BASE_304	400	0.61	0.30	5.4	75.416	79.68	TRUE	Heskestad < 130 C , Source Located 1 ft. above Ground
BASE_304	400	0.61	0.30	5.7	69.567	72.03	TRUE	Heskestad < 130 C , Source Located 1 ft. above Ground
BASE_304	400	0.61	0.30	6	64.731	65.49	TRUE	Heskestad < 130 C , Source Located 1 ft. above Ground
BASE_305	500	0.61	0.30	2.4	521.63	512.32	TRUE	Source Located 1 ft. above Ground
BASE_305	500	0.61	0.30	2.7	399.1	391.90	TRUE	Source Located 1 ft. above Ground
BASE_305	500	0.61	0.30	3	316.2	311.14	TRUE	Source Located 1 ft. above Ground
BASE_305	500	0.61	0.30	3.3	246.46	254.06	TRUE	Source Located 1 ft. above Ground
BASE_305	500	0.61	0.30	3.6	196.89	212.07	TRUE	Source Located 1 ft. above Ground
BASE_305	500	0.61	0.30	3.9	156	180.17	TRUE	Source Located 1 ft. above Ground
BASE_305	500	0.61	0.30	4.2	135.57	155.31	TRUE	Source Located 1 ft. above Ground
BASE_305	500	0.61	0.30	4.5	118.31	135.52	TRUE	Source Located 1 ft. above Ground
BASE_305	500	0.61	0.30	4.8	101.09	119.48	TRUE	Heskestad < 130 C , Source Located 1 ft. above Ground
BASE_305	500	0.61	0.30	5.1	90.49	106.27	TRUE	Heskestad < 130 C , Source Located 1 ft. above Ground
BASE_305	500	0.61	0.30	5.4	82.81	95.25	TRUE	Heskestad < 130 C , Source Located 1 ft. above Ground

Table E-2
Unobstructed Simulation Results

Test	HRR (kW)	Diameter (m)	Source Height (m)	Elevation (m)	Maximum Plume Temperature Rise (C)	Heskestad Plume Temperature (Equation 4-3)	Data Filtered	Filtration Criteria
BASE_305	500	0.61	0.30	5.7	77.621	85.96	TRUE	Heskestad < 130 C , Source Located 1 ft. above Ground
BASE_305	500	0.61	0.30	6	72.416	78.03	TRUE	Heskestad < 130 C , Source Located 1 ft. above Ground
BASE_306	600	0.61	0.30	2.4	621.32	623.47	TRUE	Source Located 1 ft. above Ground
BASE_306	600	0.61	0.30	2.7	493.05	471.55	TRUE	Source Located 1 ft. above Ground
BASE_306	600	0.61	0.30	3	392.91	371.26	TRUE	Source Located 1 ft. above Ground
BASE_306	600	0.61	0.30	3.3	300.99	301.22	TRUE	Source Located 1 ft. above Ground
BASE_306	600	0.61	0.30	3.6	239.8	250.16	TRUE	Source Located 1 ft. above Ground
BASE_306	600	0.61	0.30	3.9	196.28	211.66	TRUE	Source Located 1 ft. above Ground
BASE_306	600	0.61	0.30	4.2	168.47	181.84	TRUE	Source Located 1 ft. above Ground
BASE_306	600	0.61	0.30	4.5	143.2	158.21	TRUE	Source Located 1 ft. above Ground
BASE_306	600	0.61	0.30	4.8	127.89	139.14	TRUE	Source Located 1 ft. above Ground
BASE_306	600	0.61	0.30	5.1	116.33	123.50	TRUE	Heskestad < 130 C , Source Located 1 ft. above Ground
BASE_306	600	0.61	0.30	5.4	106.77	110.49	TRUE	Heskestad < 130 C , Source Located 1 ft. above Ground
BASE_306	600	0.61	0.30	5.7	95.54	99.55	TRUE	Heskestad < 130 C , Source Located 1 ft. above Ground
BASE_306	600	0.61	0.30	6	87.35	90.24	TRUE	Heskestad < 130 C , Source Located 1 ft. above Ground
BASE_313	200	0.61	1.14	2.4	600.42	515.47	FALSE	Not Filtered
BASE_313	200	0.61	1.14	2.7	414.5	354.17	FALSE	Not Filtered
BASE_313	200	0.61	1.14	3	309.8	260.78	FALSE	Not Filtered

Table E-2
Unobstructed Simulation Results

Test	HRR (kW)	Diameter (m)	Source Height (m)	Elevation (m)	Maximum Plume Temperature Rise (C)	Heskestad Plume Temperature (Equation 4-3)	Data Filtered	Filtration Criteria
BASE_313	200	0.61	1.14	3.3	229.95	201.37	FALSE	Not Filtered
BASE_313	200	0.61	1.14	3.6	175.92	160.99	FALSE	Not Filtered
BASE_313	200	0.61	1.14	3.9	133.61	132.18	FALSE	Not Filtered
BASE_313	200	0.61	1.14	4.2	112.07	110.81	TRUE	Heskestad < 130 C
BASE_313	200	0.61	1.14	4.5	97.7	94.47	TRUE	Heskestad < 130 C
BASE_313	200	0.61	1.14	4.8	86.66	81.68	TRUE	Heskestad < 130 C
BASE_313	200	0.61	1.14	5.1	76.924	71.45	TRUE	Heskestad < 130 C
BASE_313	200	0.61	1.14	5.4	69.128	63.12	TRUE	Heskestad < 130 C
BASE_313	200	0.61	1.14	5.7	62.155	56.25	TRUE	Heskestad < 130 C
BASE_313	200	0.61	1.14	6	57.725	50.50	TRUE	Heskestad < 130 C
BASE_314	300	0.61	1.14	2.4	794.04	808.95	TRUE	Heskestad > 800 C
BASE_314	300	0.61	1.14	2.7	633.17	535.11	FALSE	Not Filtered
BASE_314	300	0.61	1.14	3	494.2	384.36	FALSE	Not Filtered
BASE_314	300	0.61	1.14	3.3	355.45	291.68	FALSE	Not Filtered
BASE_314	300	0.61	1.14	3.6	273.81	230.20	FALSE	Not Filtered
BASE_314	300	0.61	1.14	3.9	207.36	187.12	FALSE	Not Filtered
BASE_314	300	0.61	1.14	4.2	174.38	155.63	FALSE	Not Filtered
BASE_314	300	0.61	1.14	4.5	143.36	131.83	FALSE	Not Filtered
BASE_314	300	0.61	1.14	4.8	125.13	113.37	TRUE	Heskestad < 130 C
BASE_314	300	0.61	1.14	5.1	106.46	98.72	TRUE	Heskestad < 130 C
BASE_314	300	0.61	1.14	5.4	91.29	86.88	TRUE	Heskestad < 130 C

Table E-2
Unobstructed Simulation Results

Test	HRR (kW)	Diameter (m)	Source Height (m)	Elevation (m)	Maximum Plume Temperature Rise (C)	Heskestad Plume Temperature (Equation 4-3)	Data Filtered	Filtration Criteria
BASE_314	300	0.61	1.14	5.7	81.09	77.16	TRUE	Heskestad < 130 C
BASE_314	300	0.61	1.14	6	73.481	69.07	TRUE	Heskestad < 130 C
BASE_315	400	0.61	1.14	2.4	894.49	1000.00	TRUE	Heskestad > 800 C
BASE_315	400	0.61	1.14	2.7	791.96	735.01	FALSE	Not Filtered
BASE_315	400	0.61	1.14	3	664.52	515.78	FALSE	Not Filtered
BASE_315	400	0.61	1.14	3.3	488.44	385.18	FALSE	Not Filtered
BASE_315	400	0.61	1.14	3.6	370.93	300.47	FALSE	Not Filtered
BASE_315	400	0.61	1.14	3.9	277.21	242.07	FALSE	Not Filtered
BASE_315	400	0.61	1.14	4.2	223.36	199.93	FALSE	Not Filtered
BASE_315	400	0.61	1.14	4.5	175.71	168.41	FALSE	Not Filtered
BASE_315	400	0.61	1.14	4.8	149.38	144.15	FALSE	Not Filtered
BASE_315	400	0.61	1.14	5.1	132.48	125.03	TRUE	Heskestad < 130 C
BASE_315	400	0.61	1.14	5.4	116.77	109.68	TRUE	Heskestad < 130 C
BASE_315	400	0.61	1.14	5.7	102.83	97.13	TRUE	Heskestad < 130 C
BASE_315	400	0.61	1.14	6	93.62	86.73	TRUE	Heskestad < 130 C
BASE_316	500	0.61	1.14	2.4	879.86	1000.00	TRUE	Heskestad > 800 C
BASE_316	500	0.61	1.14	2.7	792.75	957.56	TRUE	Heskestad > 800 C
BASE_316	500	0.61	1.14	3	694.1	656.81	FALSE	Not Filtered
BASE_316	500	0.61	1.14	3.3	573.87	483.05	FALSE	Not Filtered
BASE_316	500	0.61	1.14	3.6	456.09	372.71	FALSE	Not Filtered
BASE_316	500	0.61	1.14	3.9	339.35	297.80	FALSE	Not Filtered

Table E-2
Unobstructed Simulation Results

Test	HRR (kW)	Diameter (m)	Source Height (m)	Elevation (m)	Maximum Plume Temperature Rise (C)	Heskestad Plume Temperature (Equation 4-3)	Data Filtered	Filtration Criteria
BASE_316	500	0.61	1.14	4.2	277.73	244.38	FALSE	Not Filtered
BASE_316	500	0.61	1.14	4.5	223.54	204.79	FALSE	Not Filtered
BASE_316	500	0.61	1.14	4.8	182.29	174.55	FALSE	Not Filtered
BASE_316	500	0.61	1.14	5.1	155.41	150.87	FALSE	Not Filtered
BASE_316	500	0.61	1.14	5.4	133.98	131.94	FALSE	Not Filtered
BASE_316	500	0.61	1.14	5.7	119.94	116.55	TRUE	Heskestad < 130 C
BASE_316	500	0.61	1.14	6	108.39	103.84	TRUE	Heskestad < 130 C
BASE_317	600	0.61	1.14	2.4	908.01	1000.00	TRUE	Heskestad > 800 C
BASE_317	600	0.61	1.14	2.7	864.94	1000.00	TRUE	Heskestad > 800 C
BASE_317	600	0.61	1.14	3	781.95	809.22	TRUE	Heskestad > 800 C
BASE_317	600	0.61	1.14	3.3	647.71	586.29	FALSE	Not Filtered
BASE_317	600	0.61	1.14	3.6	534.14	447.60	FALSE	Not Filtered
BASE_317	600	0.61	1.14	3.9	416.5	354.83	FALSE	Not Filtered
BASE_317	600	0.61	1.14	4.2	328.89	289.41	FALSE	Not Filtered
BASE_317	600	0.61	1.14	4.5	264.69	241.36	FALSE	Not Filtered
BASE_317	600	0.61	1.14	4.8	222.42	204.91	FALSE	Not Filtered
BASE_317	600	0.61	1.14	5.1	186.54	176.53	FALSE	Not Filtered
BASE_317	600	0.61	1.14	5.4	158.69	153.95	FALSE	Not Filtered
BASE_317	600	0.61	1.14	5.7	136.29	135.67	FALSE	Not Filtered
BASE_317	600	0.61	1.14	6	123.49	120.63	TRUE	Heskestad < 130 C
BASE_324	200	0.61	1.98	2.4	802.19	1000.00	TRUE	Heskestad > 800 C

Table E-2
Unobstructed Simulation Results

Test	HRR (kW)	Diameter (m)	Source Height (m)	Elevation (m)	Maximum Plume Temperature Rise (C)	Heskestad Plume Temperature (Equation 4-3)	Data Filtered	Filtration Criteria
BASE_324	200	0.61	1.98	2.7	812.66	1000.00	TRUE	Heskestad > 800 C
BASE_324	200	0.61	1.98	3	680.91	748.51	FALSE	Not Filtered
BASE_324	200	0.61	1.98	3.3	486.99	473.69	FALSE	Not Filtered
BASE_324	200	0.61	1.98	3.6	354.53	330.95	FALSE	Not Filtered
BASE_324	200	0.61	1.98	3.9	255.02	246.42	FALSE	Not Filtered
BASE_324	200	0.61	1.98	4.2	205.62	191.81	FALSE	Not Filtered
BASE_324	200	0.61	1.98	4.5	166.23	154.28	FALSE	Not Filtered
BASE_324	200	0.61	1.98	4.8	136.56	127.26	TRUE	Heskestad < 130 C
BASE_324	200	0.61	1.98	5.1	115.36	107.09	TRUE	Heskestad < 130 C
BASE_324	200	0.61	1.98	5.4	98.47	91.59	TRUE	Heskestad < 130 C
BASE_324	200	0.61	1.98	5.7	83.73	79.39	TRUE	Heskestad < 130 C
BASE_324	200	0.61	1.98	6	73.846	69.59	TRUE	Heskestad < 130 C
BASE_325	300	0.61	1.98	2.4	834.33	1000.00	TRUE	Heskestad > 800 C
BASE_325	300	0.61	1.98	2.7	924.98	1000.00	TRUE	Heskestad > 800 C
BASE_325	300	0.61	1.98	3	881.51	1000.00	TRUE	Heskestad > 800 C
BASE_325	300	0.61	1.98	3.3	729.09	736.43	FALSE	Not Filtered
BASE_325	300	0.61	1.98	3.6	570.95	497.07	FALSE	Not Filtered
BASE_325	300	0.61	1.98	3.9	413.79	361.73	FALSE	Not Filtered
BASE_325	300	0.61	1.98	4.2	313.04	277.01	FALSE	Not Filtered
BASE_325	300	0.61	1.98	4.5	224.91	220.11	FALSE	Not Filtered
BASE_325	300	0.61	1.98	4.8	177.16	179.84	FALSE	Not Filtered

Table E-2
Unobstructed Simulation Results

Test	HRR (kW)	Diameter (m)	Source Height (m)	Elevation (m)	Maximum Plume Temperature Rise (C)	Heskestad Plume Temperature (Equation 4-3)	Data Filtered	Filtration Criteria
BASE_325	300	0.61	1.98	5.1	150.9	150.19	FALSE	Not Filtered
BASE_325	300	0.61	1.98	5.4	129.86	127.65	TRUE	Heskestad < 130 C
BASE_325	300	0.61	1.98	5.7	107.49	110.08	TRUE	Heskestad < 130 C
BASE_325	300	0.61	1.98	6	94.42	96.08	TRUE	Heskestad < 130 C
BASE_326	400	0.61	1.98	2.4	847.41	1000.00	TRUE	Heskestad > 800 C
BASE_326	400	0.61	1.98	2.7	909.47	1000.00	TRUE	Heskestad > 800 C
BASE_326	400	0.61	1.98	3	917.03	1000.00	TRUE	Heskestad > 800 C
BASE_326	400	0.61	1.98	3.3	850.04	1000.00	TRUE	Heskestad > 800 C
BASE_326	400	0.61	1.98	3.6	715.9	678.92	FALSE	Not Filtered
BASE_326	400	0.61	1.98	3.9	558.26	483.57	FALSE	Not Filtered
BASE_326	400	0.61	1.98	4.2	402.99	364.83	FALSE	Not Filtered
BASE_326	400	0.61	1.98	4.5	294.05	286.71	FALSE	Not Filtered
BASE_326	400	0.61	1.98	4.8	235.69	232.29	FALSE	Not Filtered
BASE_326	400	0.61	1.98	5.1	201.69	192.70	FALSE	Not Filtered
BASE_326	400	0.61	1.98	5.4	168.14	162.90	FALSE	Not Filtered
BASE_326	400	0.61	1.98	5.7	139.4	139.84	FALSE	Not Filtered
BASE_326	400	0.61	1.98	6	119.04	121.60	TRUE	Heskestad < 130 C
BASE_327	500	0.61	1.98	2.4	869.39	1000.00	TRUE	Heskestad > 800 C
BASE_327	500	0.61	1.98	2.7	904.4	1000.00	TRUE	Heskestad > 800 C
BASE_327	500	0.61	1.98	3	946.1	1000.00	TRUE	Heskestad > 800 C
BASE_327	500	0.61	1.98	3.3	913.68	1000.00	TRUE	Heskestad > 800 C

Table E-2
Unobstructed Simulation Results

Test	HRR (kW)	Diameter (m)	Source Height (m)	Elevation (m)	Maximum Plume Temperature Rise (C)	Heskestad Plume Temperature (Equation 4-3)	Data Filtered	Filtration Criteria
BASE_327	500	0.61	1.98	3.6	812.4	879.58	TRUE	Heskestad > 800 C
BASE_327	500	0.61	1.98	3.9	650.44	613.57	FALSE	Not Filtered
BASE_327	500	0.61	1.98	4.2	526.14	456.37	FALSE	Not Filtered
BASE_327	500	0.61	1.98	4.5	415.12	354.97	FALSE	Not Filtered
BASE_327	500	0.61	1.98	4.8	327.36	285.36	FALSE	Not Filtered
BASE_327	500	0.61	1.98	5.1	261.93	235.27	FALSE	Not Filtered
BASE_327	500	0.61	1.98	5.4	213.41	197.91	FALSE	Not Filtered
BASE_327	500	0.61	1.98	5.7	181.16	169.21	FALSE	Not Filtered
BASE_327	500	0.61	1.98	6	158.89	146.63	FALSE	Not Filtered
BASE_328	600	0.61	1.98	2.4	896.1	-20.00	TRUE	Heskestad < 130 C
BASE_328	600	0.61	1.98	2.7	892.48	1000.00	TRUE	Heskestad > 800 C
BASE_328	600	0.61	1.98	3	908.94	1000.00	TRUE	Heskestad > 800 C
BASE_328	600	0.61	1.98	3.3	936.98	1000.00	TRUE	Heskestad > 800 C
BASE_328	600	0.61	1.98	3.6	907.68	1000.00	TRUE	Heskestad > 800 C
BASE_328	600	0.61	1.98	3.9	782.46	753.25	FALSE	Not Filtered
BASE_328	600	0.61	1.98	4.2	650.93	552.54	FALSE	Not Filtered
BASE_328	600	0.61	1.98	4.5	501.29	425.53	FALSE	Not Filtered
BASE_328	600	0.61	1.98	4.8	397.92	339.54	FALSE	Not Filtered
BASE_328	600	0.61	1.98	5.1	314.02	278.32	FALSE	Not Filtered
BASE_328	600	0.61	1.98	5.4	250.3	233.04	FALSE	Not Filtered
BASE_328	600	0.61	1.98	5.7	213.26	198.49	FALSE	Not Filtered

Table E-2
Unobstructed Simulation Results

Test	HRR (kW)	Diameter (m)	Source Height (m)	Elevation (m)	Maximum Plume Temperature Rise (C)	Heskestad Plume Temperature (Equation 4-3)	Data Filtered	Filtration Criteria
BASE_328	600	0.61	1.98	6	176.59	171.46	FALSE	Not Filtered
BASE_307	300	0.91	0.30	2.4	294.61	239.11	TRUE	Source Located 1 ft. above Ground
BASE_307	300	0.91	0.30	2.7	233.57	193.49	TRUE	Source Located 1 ft. above Ground
BASE_307	300	0.91	0.30	3	194.58	160.36	TRUE	Source Located 1 ft. above Ground
BASE_307	300	0.91	0.30	3.3	158.8	135.45	TRUE	Source Located 1 ft. above Ground
BASE_307	300	0.91	0.30	3.6	133.72	116.21	TRUE	Heskestad < 130 C , Source Located 1 ft. above Ground
BASE_307	300	0.91	0.30	3.9	110.18	100.99	TRUE	Heskestad < 130 C , Source Located 1 ft. above Ground
BASE_307	300	0.91	0.30	4.2	97.21	88.73	TRUE	Heskestad < 130 C , Source Located 1 ft. above Ground
BASE_307	300	0.91	0.30	4.5	84.82	78.69	TRUE	Heskestad < 130 C , Source Located 1 ft. above Ground
BASE_307	300	0.91	0.30	4.8	76.364	70.35	TRUE	Heskestad < 130 C , Source Located 1 ft. above Ground
BASE_307	300	0.91	0.30	5.1	68.72	63.34	TRUE	Heskestad < 130 C , Source Located 1 ft. above Ground
BASE_307	300	0.91	0.30	5.4	61.382	57.39	TRUE	Heskestad < 130 C , Source Located 1 ft. above Ground
BASE_307	300	0.91	0.30	5.7	56.444	52.28	TRUE	Heskestad < 130 C , Source Located 1 ft. above Ground
BASE_307	300	0.91	0.30	6	52.33	47.86	TRUE	Heskestad < 130 C , Source Located 1 ft. above Ground
BASE_308	400	0.91	0.30	2.4	378.29	312.56	TRUE	Source Located 1 ft. above Ground
BASE_308	400	0.91	0.30	2.7	287.23	250.60	TRUE	Source Located 1 ft. above Ground

Table E-2
Unobstructed Simulation Results

Test	HRR (kW)	Diameter (m)	Source Height (m)	Elevation (m)	Maximum Plume Temperature Rise (C)	Heskestad Plume Temperature (Equation 4-3)	Data Filtered	Filtration Criteria
BASE_308	400	0.91	0.30	3	227.12	206.19	TRUE	Source Located 1 ft. above Ground
BASE_308	400	0.91	0.30	3.3	180.15	173.15	TRUE	Source Located 1 ft. above Ground
BASE_308	400	0.91	0.30	3.6	154.74	147.84	TRUE	Source Located 1 ft. above Ground
BASE_308	400	0.91	0.30	3.9	130.12	127.97	TRUE	Heskestad < 130 C , Source Located 1 ft. above Ground
BASE_308	400	0.91	0.30	4.2	112.85	112.05	TRUE	Heskestad < 130 C , Source Located 1 ft. above Ground
BASE_308	400	0.91	0.30	4.5	99.44	99.08	TRUE	Heskestad < 130 C , Source Located 1 ft. above Ground
BASE_308	400	0.91	0.30	4.8	89.37	88.36	TRUE	Heskestad < 130 C , Source Located 1 ft. above Ground
BASE_308	400	0.91	0.30	5.1	80.38	79.38	TRUE	Heskestad < 130 C , Source Located 1 ft. above Ground
BASE_308	400	0.91	0.30	5.4	72.991	71.77	TRUE	Heskestad < 130 C , Source Located 1 ft. above Ground
BASE_308	400	0.91	0.30	5.7	66.197	65.27	TRUE	Heskestad < 130 C , Source Located 1 ft. above Ground
BASE_308	400	0.91	0.30	6	62.1	59.66	TRUE	Heskestad < 130 C , Source Located 1 ft. above Ground
BASE_309	500	0.91	0.30	2.4	530.61	388.34	TRUE	Source Located 1 ft. above Ground
BASE_309	500	0.91	0.30	2.7	399.64	308.67	TRUE	Source Located 1 ft. above Ground
BASE_309	500	0.91	0.30	3	316.36	252.27	TRUE	Source Located 1 ft. above Ground
BASE_309	500	0.91	0.30	3.3	253.48	210.73	TRUE	Source Located 1 ft. above Ground
BASE_309	500	0.91	0.30	3.6	211.54	179.14	TRUE	Source Located 1 ft. above Ground

Table E-2
Unobstructed Simulation Results

Test	HRR (kW)	Diameter (m)	Source Height (m)	Elevation (m)	Maximum Plume Temperature Rise (C)	Heskestad Plume Temperature (Equation 4-3)	Data Filtered	Filtration Criteria
BASE_309	500	0.91	0.30	3.9	173.13	154.50	TRUE	Source Located 1 ft. above Ground
BASE_309	500	0.91	0.30	4.2	149.53	134.87	TRUE	Source Located 1 ft. above Ground
BASE_309	500	0.91	0.30	4.5	131.51	118.94	TRUE	Heskestad < 130 C , Source Located 1 ft. above Ground
BASE_309	500	0.91	0.30	4.8	116.85	105.83	TRUE	Heskestad < 130 C , Source Located 1 ft. above Ground
BASE_309	500	0.91	0.30	5.1	100.39	94.88	TRUE	Heskestad < 130 C , Source Located 1 ft. above Ground
BASE_309	500	0.91	0.30	5.4	89.79	85.64	TRUE	Heskestad < 130 C , Source Located 1 ft. above Ground
BASE_309	500	0.91	0.30	5.7	81.01	77.76	TRUE	Heskestad < 130 C , Source Located 1 ft. above Ground
BASE_309	500	0.91	0.30	6	75.255	70.98	TRUE	Heskestad < 130 C , Source Located 1 ft. above Ground
BASE_310	600	0.91	0.30	2.4	596.83	467.23	TRUE	Source Located 1 ft. above Ground
BASE_310	600	0.91	0.30	2.7	462.19	368.31	TRUE	Source Located 1 ft. above Ground
BASE_310	600	0.91	0.30	3	379.52	299.11	TRUE	Source Located 1 ft. above Ground
BASE_310	600	0.91	0.30	3.3	298.51	248.59	TRUE	Source Located 1 ft. above Ground
BASE_310	600	0.91	0.30	3.6	243.35	210.46	TRUE	Source Located 1 ft. above Ground
BASE_310	600	0.91	0.30	3.9	196.5	180.89	TRUE	Source Located 1 ft. above Ground
BASE_310	600	0.91	0.30	4.2	172.41	157.46	TRUE	Source Located 1 ft. above Ground
BASE_310	600	0.91	0.30	4.5	150.21	138.53	TRUE	Source Located 1 ft. above Ground
BASE_310	600	0.91	0.30	4.8	136	122.99	TRUE	Heskestad < 130 C , Source Located 1 ft. above Ground

Table E-2
Unobstructed Simulation Results

Test	HRR (kW)	Diameter (m)	Source Height (m)	Elevation (m)	Maximum Plume Temperature Rise (C)	Heskestad Plume Temperature (Equation 4-3)	Data Filtered	Filtration Criteria
BASE_310	600	0.91	0.30	5.1	121.42	110.07	TRUE	Heskestad < 130 C , Source Located 1 ft. above Ground
BASE_310	600	0.91	0.30	5.4	106.73	99.19	TRUE	Heskestad < 130 C , Source Located 1 ft. above Ground
BASE_310	600	0.91	0.30	5.7	96.21	89.93	TRUE	Heskestad < 130 C , Source Located 1 ft. above Ground
BASE_310	600	0.91	0.30	6	87.94	81.98	TRUE	Heskestad < 130 C , Source Located 1 ft. above Ground
BASE_318	300	0.91	1.14	2.4	692.22	528.15	FALSE	Not Filtered
BASE_318	300	0.91	1.14	2.7	538.13	380.26	FALSE	Not Filtered
BASE_318	300	0.91	1.14	3	417.48	289.03	FALSE	Not Filtered
BASE_318	300	0.91	1.14	3.3	314.68	228.39	FALSE	Not Filtered
BASE_318	300	0.91	1.14	3.6	259.57	185.82	FALSE	Not Filtered
BASE_318	300	0.91	1.14	3.9	205.38	154.66	FALSE	Not Filtered
BASE_318	300	0.91	1.14	4.2	170.6	131.09	FALSE	Not Filtered
BASE_318	300	0.91	1.14	4.5	142.25	112.79	TRUE	Heskestad < 130 C
BASE_318	300	0.91	1.14	4.8	125.76	98.25	TRUE	Heskestad < 130 C
BASE_318	300	0.91	1.14	5.1	109.41	86.50	TRUE	Heskestad < 130 C
BASE_318	300	0.91	1.14	5.4	97.66	76.85	TRUE	Heskestad < 130 C
BASE_318	300	0.91	1.14	5.7	88.61	68.81	TRUE	Heskestad < 130 C
BASE_318	300	0.91	1.14	6	79.48	62.04	TRUE	Heskestad < 130 C
BASE_319	400	0.91	1.14	2.4	776.45	724.41	FALSE	Not Filtered
BASE_319	400	0.91	1.14	2.7	661.63	509.75	FALSE	Not Filtered

Table E-2
Unobstructed Simulation Results

Test	HRR (kW)	Diameter (m)	Source Height (m)	Elevation (m)	Maximum Plume Temperature Rise (C)	Heskestad Plume Temperature (Equation 4-3)	Data Filtered	Filtration Criteria
BASE_319	400	0.91	1.14	3	527.06	381.39	FALSE	Not Filtered
BASE_319	400	0.91	1.14	3.3	401.4	297.92	FALSE	Not Filtered
BASE_319	400	0.91	1.14	3.6	320.13	240.27	FALSE	Not Filtered
BASE_319	400	0.91	1.14	3.9	245.06	198.60	FALSE	Not Filtered
BASE_319	400	0.91	1.14	4.2	201.27	167.40	FALSE	Not Filtered
BASE_319	400	0.91	1.14	4.5	164.98	143.36	FALSE	Not Filtered
BASE_319	400	0.91	1.14	4.8	140.84	124.41	TRUE	Heskestad < 130 C
BASE_319	400	0.91	1.14	5.1	123.14	109.17	TRUE	Heskestad < 130 C
BASE_319	400	0.91	1.14	5.4	104.51	96.71	TRUE	Heskestad < 130 C
BASE_319	400	0.91	1.14	5.7	91.71	86.38	TRUE	Heskestad < 130 C
BASE_319	400	0.91	1.14	6	81.9	77.71	TRUE	Heskestad < 130 C
BASE_320	500	0.91	1.14	2.4	840.34	942.74	TRUE	Heskestad > 800 C
BASE_320	500	0.91	1.14	2.7	756.11	648.67	FALSE	Not Filtered
BASE_320	500	0.91	1.14	3	644.4	478.07	FALSE	Not Filtered
BASE_320	500	0.91	1.14	3.3	513.15	369.41	FALSE	Not Filtered
BASE_320	500	0.91	1.14	3.6	405.57	295.50	FALSE	Not Filtered
BASE_320	500	0.91	1.14	3.9	313.67	242.70	FALSE	Not Filtered
BASE_320	500	0.91	1.14	4.2	259.89	203.52	FALSE	Not Filtered
BASE_320	500	0.91	1.14	4.5	213.94	173.57	FALSE	Not Filtered
BASE_320	500	0.91	1.14	4.8	176.05	150.10	FALSE	Not Filtered
BASE_320	500	0.91	1.14	5.1	151.54	131.32	FALSE	Not Filtered

Table E-2
Unobstructed Simulation Results

Test	HRR (kW)	Diameter (m)	Source Height (m)	Elevation (m)	Maximum Plume Temperature Rise (C)	Heskestad Plume Temperature (Equation 4-3)	Data Filtered	Filtration Criteria
BASE_320	500	0.91	1.14	5.4	128.29	116.03	TRUE	Heskestad < 130 C
BASE_320	500	0.91	1.14	5.7	109.45	103.41	TRUE	Heskestad < 130 C
BASE_320	500	0.91	1.14	6	96.93	92.85	TRUE	Heskestad < 130 C
BASE_321	600	0.91	1.14	2.4	889.62	1000.00	TRUE	Heskestad > 800 C
BASE_321	600	0.91	1.14	2.7	821.75	799.00	FALSE	Not Filtered
BASE_321	600	0.91	1.14	3	702.23	580.18	FALSE	Not Filtered
BASE_321	600	0.91	1.14	3.3	572.03	443.62	FALSE	Not Filtered
BASE_321	600	0.91	1.14	3.6	458.85	352.09	FALSE	Not Filtered
BASE_321	600	0.91	1.14	3.9	366.35	287.43	FALSE	Not Filtered
BASE_321	600	0.91	1.14	4.2	299.58	239.87	FALSE	Not Filtered
BASE_321	600	0.91	1.14	4.5	246.77	203.76	FALSE	Not Filtered
BASE_321	600	0.91	1.14	4.8	205.76	175.63	FALSE	Not Filtered
BASE_321	600	0.91	1.14	5.1	181.11	153.23	FALSE	Not Filtered
BASE_321	600	0.91	1.14	5.4	153.17	135.08	FALSE	Not Filtered
BASE_321	600	0.91	1.14	5.7	130.5	120.14	TRUE	Heskestad < 130 C
BASE_321	600	0.91	1.14	6	116.01	107.67	TRUE	Heskestad < 130 C
BASE_329	300	0.91	1.98	2.4	786.08	1000.00	TRUE	Heskestad > 800 C
BASE_329	300	0.91	1.98	2.7	833.93	1000.00	TRUE	Heskestad > 800 C
BASE_329	300	0.91	1.98	3	779.18	724.86	FALSE	Not Filtered
BASE_329	300	0.91	1.98	3.3	642.61	490.88	FALSE	Not Filtered
BASE_329	300	0.91	1.98	3.6	503.08	358.00	FALSE	Not Filtered

Table E-2
Unobstructed Simulation Results

Test	HRR (kW)	Diameter (m)	Source Height (m)	Elevation (m)	Maximum Plume Temperature Rise (C)	Heskestad Plume Temperature (Equation 4-3)	Data Filtered	Filtration Criteria
BASE_329	300	0.91	1.98	3.9	371.31	274.58	FALSE	Not Filtered
BASE_329	300	0.91	1.98	4.2	288.47	218.42	FALSE	Not Filtered
BASE_329	300	0.91	1.98	4.5	214	178.62	FALSE	Not Filtered
BASE_329	300	0.91	1.98	4.8	173.05	149.28	FALSE	Not Filtered
BASE_329	300	0.91	1.98	5.1	148.51	126.95	TRUE	Heskestad < 130 C
BASE_329	300	0.91	1.98	5.4	127.52	109.52	TRUE	Heskestad < 130 C
BASE_329	300	0.91	1.98	5.7	112.57	95.63	TRUE	Heskestad < 130 C
BASE_329	300	0.91	1.98	6	97.15	84.36	TRUE	Heskestad < 130 C
BASE_330	400	0.91	1.98	2.4	774.29	1000.00	TRUE	Heskestad > 800 C
BASE_330	400	0.91	1.98	2.7	859.64	1000.00	TRUE	Heskestad > 800 C
BASE_330	400	0.91	1.98	3	856.89	1000.00	TRUE	Heskestad > 800 C
BASE_330	400	0.91	1.98	3.3	771.36	669.58	FALSE	Not Filtered
BASE_330	400	0.91	1.98	3.6	659.28	478.13	FALSE	Not Filtered
BASE_330	400	0.91	1.98	3.9	496.43	361.36	FALSE	Not Filtered
BASE_330	400	0.91	1.98	4.2	394.1	284.35	FALSE	Not Filtered
BASE_330	400	0.91	1.98	4.5	308.32	230.60	FALSE	Not Filtered
BASE_330	400	0.91	1.98	4.8	249.53	191.45	FALSE	Not Filtered
BASE_330	400	0.91	1.98	5.1	198.13	161.94	FALSE	Not Filtered
BASE_330	400	0.91	1.98	5.4	160.84	139.09	FALSE	Not Filtered
BASE_330	400	0.91	1.98	5.7	138.31	121.00	TRUE	Heskestad < 130 C
BASE_330	400	0.91	1.98	6	120.88	106.40	TRUE	Heskestad < 130 C

Table E-2
Unobstructed Simulation Results

Test	HRR (kW)	Diameter (m)	Source Height (m)	Elevation (m)	Maximum Plume Temperature Rise (C)	Heskestad Plume Temperature (Equation 4-3)	Data Filtered	Filtration Criteria
BASE_331	500	0.91	1.98	2.4	788.64	1000.00	TRUE	Heskestad > 800 C
BASE_331	500	0.91	1.98	2.7	857.78	1000.00	TRUE	Heskestad > 800 C
BASE_331	500	0.91	1.98	3	859.73	1000.00	TRUE	Heskestad > 800 C
BASE_331	500	0.91	1.98	3.3	814.29	866.63	TRUE	Heskestad > 800 C
BASE_331	500	0.91	1.98	3.6	722.21	606.27	FALSE	Not Filtered
BASE_331	500	0.91	1.98	3.9	590.36	451.82	FALSE	Not Filtered
BASE_331	500	0.91	1.98	4.2	478.39	351.92	FALSE	Not Filtered
BASE_331	500	0.91	1.98	4.5	385.71	283.21	FALSE	Not Filtered
BASE_331	500	0.91	1.98	4.8	308.82	233.69	FALSE	Not Filtered
BASE_331	500	0.91	1.98	5.1	257.61	196.71	FALSE	Not Filtered
BASE_331	500	0.91	1.98	5.4	203.98	168.27	FALSE	Not Filtered
BASE_331	500	0.91	1.98	5.7	161.05	145.89	FALSE	Not Filtered
BASE_331	500	0.91	1.98	6	135.64	127.92	TRUE	Heskestad < 130 C
BASE_332	600	0.91	1.98	2.4	805.72	1000.00	TRUE	Heskestad > 800 C
BASE_332	600	0.91	1.98	2.7	850.96	1000.00	TRUE	Heskestad > 800 C
BASE_332	600	0.91	1.98	3	885.48	1000.00	TRUE	Heskestad > 800 C
BASE_332	600	0.91	1.98	3.3	870.38	1000.00	TRUE	Heskestad > 800 C
BASE_332	600	0.91	1.98	3.6	811.98	744.13	FALSE	Not Filtered
BASE_332	600	0.91	1.98	3.9	691.37	546.97	FALSE	Not Filtered
BASE_332	600	0.91	1.98	4.2	589.37	421.86	FALSE	Not Filtered
BASE_332	600	0.91	1.98	4.5	462.96	336.98	FALSE	Not Filtered

Table E-2
Unobstructed Simulation Results

Test	HRR (kW)	Diameter (m)	Source Height (m)	Elevation (m)	Maximum Plume Temperature Rise (C)	Heskestad Plume Temperature (Equation 4-3)	Data Filtered	Filtration Criteria
BASE_332	600	0.91	1.98	4.8	366.56	276.46	FALSE	Not Filtered
BASE_332	600	0.91	1.98	5.1	290.06	231.64	FALSE	Not Filtered
BASE_332	600	0.91	1.98	5.4	232.74	197.40	FALSE	Not Filtered
BASE_332	600	0.91	1.98	5.7	198.21	170.60	FALSE	Not Filtered
BASE_332	600	0.91	1.98	6	174.61	149.18	FALSE	Not Filtered

Determination of Bias and Uncertainty

Table E-3
Determination of Bias and Uncertainty

Test	Obstructed FDS Temperature (C)	Heskestad Temperature (C)	Ln(∆FDS/∆Heskestad)
ARCH_1055	251.35	772.37	-1.12
ARCH_1055	207.5	595.31	-1.05
ARCH_1055	181.32	475.29	-0.96
ARCH_1055	158.36	389.79	-0.90
ARCH_1055	139.08	326.49	-0.85
ARCH_1055	123.06	278.17	-0.82
ARCH_1056	384.48	729.52	-0.64
ARCH_1056	307.37	566.88	-0.61
ARCH_1056	259.4	455.37	-0.56
ARCH_1056	223.14	375.23	-0.52
ARCH_1056	197.29	315.49	-0.47
ARCH_1056	177.62	269.64	-0.42
ARCH_1056	161.65	233.59	-0.37
ARCH_1064	228.02	764.70	-1.21
ARCH_1064	180.07	590.25	-1.19
ARCH_1064	153.69	471.76	-1.12
ARCH_1064	132.29	387.22	-1.07
ARCH_1064	119.64	324.55	-1.00
ARCH_1065	322.39	722.52	-0.81
ARCH_1065	255.39	562.20	-0.79
ARCH_1065	208.68	452.07	-0.77
ARCH_1065	180.89	372.81	-0.72
ARCH_1065	159.61	313.65	-0.68
ARCH_1065	138.36	268.21	-0.66
ARCH_1065	120.7	232.45	-0.66
ARCH_1065	112.26	203.75	-0.60
ARCH_830	198.07	402.61	-0.71
ARCH_830	112.16	264.28	-0.86
ARCH_836	126.04	584.26	-1.53
ARCH_837	171.73	619.87	-1.28

Table E-3
Determination of Bias and Uncertainty

Test	Obstructed FDS Temperature (C)	Heskestad Temperature (C)	Ln(∆FDS/∆Heskestad)
ARCH_837	118.23	365.81	-1.13
ARCH_894	239.92	515.47	-0.76
ARCH_894	120.83	354.17	-1.08
ARCH_895	172.02	535.11	-1.13
ARCH_895	125.64	384.36	-1.12
ARCH_896	253.67	735.01	-1.06
ARCH_896	172.71	515.78	-1.09
ARCH_896	135.45	385.18	-1.05
ARCH_896	115.42	300.47	-0.96
ARCH_897	255.53	656.81	-0.94
ARCH_897	187.46	483.05	-0.95
ARCH_897	155.04	372.71	-0.88
ARCH_897	131.32	297.80	-0.82
ARCH_897	114.1	244.38	-0.76
ARCH_898	232	586.29	-0.93
ARCH_898	193.7	447.60	-0.84
ARCH_898	158.56	354.83	-0.81
ARCH_898	134.6	289.41	-0.77
ARCH_898	113.8	241.36	-0.75
ARCH_901	233.64	748.51	-1.16
ARCH_901	174.13	473.69	-1.00
ARCH_901	141.03	330.95	-0.85
ARCH_901	110.93	246.42	-0.80
ARCH_902	325.15	736.43	-0.82
ARCH_902	252.2	497.07	-0.68
ARCH_902	194.8	361.73	-0.62
ARCH_902	158.08	277.01	-0.56
ARCH_902	126.34	220.11	-0.56
ARCH_903	367.41	678.92	-0.61
ARCH_903	269.44	483.57	-0.58
ARCH_903	212.59	364.83	-0.54

Table E-3
Determination of Bias and Uncertainty

Test	Obstructed FDS Temperature (C)	Heskestad Temperature (C)	Ln(∆FDS/∆Heskestad)
ARCH_903	163.52	286.71	-0.56
ARCH_903	137.37	232.29	-0.53
ARCH_903	118.3	192.70	-0.49
ARCH_904	414.66	613.57	-0.39
ARCH_904	314.39	456.37	-0.37
ARCH_904	236.69	354.97	-0.41
ARCH_904	193.59	285.36	-0.39
ARCH_904	162.15	235.27	-0.37
ARCH_904	138.1	197.91	-0.36
ARCH_904	115.49	169.21	-0.38
ARCH_905	513.68	753.25	-0.38
ARCH_905	398.77	552.54	-0.33
ARCH_905	299.55	425.53	-0.35
ARCH_905	243.95	339.54	-0.33
ARCH_905	198.04	278.32	-0.34
ARCH_905	162.57	233.04	-0.36
ARCH_905	134.08	198.49	-0.39
ARCH_905	116.82	171.46	-0.38
ARCH_958	201.52	528.15	-0.96
ARCH_958	115.52	380.26	-1.19
ARCH_959	254.49	724.41	-1.05
ARCH_959	150.19	509.75	-1.22
ARCH_959	115.72	381.39	-1.19
ARCH_960	186.86	648.67	-1.24
ARCH_960	146.01	478.07	-1.19
ARCH_960	117.15	369.41	-1.15
ARCH_961	164.16	580.18	-1.26
ARCH_961	132.43	443.62	-1.21
ARCH_961	113.03	352.09	-1.14
ARCH_965	212.09	724.86	-1.23
ARCH_965	157.64	490.88	-1.14

Table E-3
Determination of Bias and Uncertainty

Test	Obstructed FDS Temperature (C)	Heskestad Temperature (C)	Ln(∆FDS/∆Heskestad)
ARCH_965	126.25	358.00	-1.04
ARCH_966	255.26	669.58	-0.96
ARCH_966	199.12	478.13	-0.88
ARCH_966	160.14	361.36	-0.81
ARCH_966	134.08	284.35	-0.75
ARCH_966	110.46	230.60	-0.74
ARCH_967	232.72	606.27	-0.96
ARCH_967	196.54	451.82	-0.83
ARCH_967	163.63	351.92	-0.77
ARCH_967	133.81	283.21	-0.75
ARCH_967	114.52	233.69	-0.71
ARCH_968	291.81	744.13	-0.94
ARCH_968	225.14	546.97	-0.89
ARCH_968	189.01	421.86	-0.80
ARCH_968	153.48	336.98	-0.79
ARCH_968	129.83	276.46	-0.76
ARCH_968	111.62	231.64	-0.73
OBST_1052	360.12	772.37	-0.76
OBST_1052	318.6	595.31	-0.63
OBST_1052	299.22	475.29	-0.46
OBST_1052	286.21	389.79	-0.31
OBST_1052	268.02	326.49	-0.20
OBST_1052	250.8	278.17	-0.10
OBST_1052	235.33	240.36	-0.02
OBST_1052	216.32	210.14	0.03
OBST_1052	199.16	185.58	0.07
OBST_1052	184.84	165.31	0.11
OBST_1053	514.31	729.52	-0.35
OBST_1053	450.83	566.88	-0.23
OBST_1053	404.86	455.37	-0.12
OBST_1053	362.82	375.23	-0.03

Table E-3
Determination of Bias and Uncertainty

Test	Obstructed FDS Temperature (C)	Heskestad Temperature (C)	Ln(∆FDS/∆Heskestad)
OBST_1053	313	315.49	-0.01
OBST_1053	273.13	269.64	0.01
OBST_1053	238.54	233.59	0.02
OBST_1061	376.9	764.70	-0.71
OBST_1061	300.69	590.25	-0.67
OBST_1061	259.7	471.76	-0.60
OBST_1061	235.99	387.22	-0.50
OBST_1061	219.89	324.55	-0.39
OBST_1061	206.26	276.67	-0.29
OBST_1061	196.94	239.17	-0.19
OBST_1061	187.38	209.19	-0.11
OBST_1061	176.74	184.79	-0.04
OBST_1061	164	164.65	0.00
OBST_1061	152.26	147.81	0.03
OBST_1062	474.5	722.52	-0.42
OBST_1062	426.72	562.20	-0.28
OBST_1062	385.71	452.07	-0.16
OBST_1062	347.67	372.81	-0.07
OBST_1062	313.88	313.65	0.00
OBST_1062	275.56	268.21	0.03
OBST_1062	239.91	232.45	0.03
OBST_1062	213	203.75	0.04
OBST_808	118.47	209.49	-0.57
OBST_809	215.87	402.61	-0.62
OBST_809	135.85	264.28	-0.67
OBST_815	122.51	584.26	-1.56
OBST_816	150.7	619.87	-1.41
OBST_816	125.87	365.81	-1.07
OBST_816	110.11	245.21	-0.80
OBST_873	232.79	515.47	-0.79
OBST_873	158.78	354.17	-0.80

Table E-3
Determination of Bias and Uncertainty

Test	Obstructed FDS Temperature (C)	Heskestad Temperature (C)	Ln(∆FDS/∆Heskestad)
OBST_873	119.76	260.78	-0.78
OBST_874	225.86	535.11	-0.86
OBST_874	164.52	384.36	-0.85
OBST_874	136.76	291.68	-0.76
OBST_874	126.93	230.20	-0.60
OBST_874	121.51	187.12	-0.43
OBST_874	116.21	155.63	-0.29
OBST_875	331.26	735.01	-0.80
OBST_875	234.18	515.78	-0.79
OBST_875	181.11	385.18	-0.75
OBST_875	168.81	300.47	-0.58
OBST_875	157.84	242.07	-0.43
OBST_875	149.98	199.93	-0.29
OBST_875	142.77	168.41	-0.17
OBST_875	134.43	144.15	-0.07
OBST_875	126.06	125.03	0.01
OBST_876	305.36	656.81	-0.77
OBST_876	226.23	483.05	-0.76
OBST_876	210.64	372.71	-0.57
OBST_876	200.37	297.80	-0.40
OBST_876	189.08	244.38	-0.26
OBST_876	176.49	204.79	-0.15
OBST_876	165.18	174.55	-0.06
OBST_876	154.3	150.87	0.02
OBST_876	142.71	131.94	0.08
OBST_876	130.55	116.55	0.11
OBST_877	279.89	586.29	-0.74
OBST_877	247.2	447.60	-0.59
OBST_877	232.02	354.83	-0.42
OBST_877	218.02	289.41	-0.28
OBST_877	200.1	241.36	-0.19

Table E-3
Determination of Bias and Uncertainty

Test	Obstructed FDS Temperature (C)	Heskestad Temperature (C)	Ln(∆FDS/∆Heskestad)
OBST_877	186.1	204.91	-0.10
OBST_877	174.77	176.53	-0.01
OBST_877	163.24	153.95	0.06
OBST_877	150.25	135.67	0.10
OBST_877	137.23	120.63	0.13
OBST_880	261.92	748.51	-1.05
OBST_880	186.03	473.69	-0.93
OBST_880	143.97	330.95	-0.83
OBST_880	115.19	246.42	-0.76
OBST_881	253.32	736.43	-1.07
OBST_881	214.24	497.07	-0.84
OBST_881	193.54	361.73	-0.63
OBST_881	179.06	277.01	-0.44
OBST_881	159.94	220.11	-0.32
OBST_881	145.89	179.84	-0.21
OBST_881	133.19	150.19	-0.12
OBST_881	118.07	127.65	-0.08
OBST_882	336	678.92	-0.70
OBST_882	295.04	483.57	-0.49
OBST_882	265.76	364.83	-0.32
OBST_882	233.9	286.71	-0.20
OBST_882	203.38	232.29	-0.13
OBST_882	180.05	192.70	-0.07
OBST_882	155.4	162.90	-0.05
OBST_882	134.3	139.84	-0.04
OBST_882	119.3	121.60	-0.02
OBST_883	376.41	613.57	-0.49
OBST_883	329.43	456.37	-0.33
OBST_883	285.67	354.97	-0.22
OBST_883	252.27	285.36	-0.12
OBST_883	227.61	235.27	-0.03

Table E-3
Determination of Bias and Uncertainty

Test	Obstructed FDS Temperature (C)	Heskestad Temperature (C)	Ln(∆FDS/∆Heskestad)
OBST_883	200	197.91	0.01
OBST_883	174.5	169.21	0.03
OBST_883	155.45	146.63	0.06
OBST_884	480.69	753.25	-0.45
OBST_884	428.14	552.54	-0.26
OBST_884	374.23	425.53	-0.13
OBST_884	327.72	339.54	-0.04
OBST_884	284.84	278.32	0.02
OBST_884	242.25	233.04	0.04
OBST_884	210.22	198.49	0.06
OBST_884	186.23	171.46	0.08
OBST_937	236.44	528.15	-0.80
OBST_937	170.78	380.26	-0.80
OBST_937	126.6	289.03	-0.83
OBST_938	325.72	724.41	-0.80
OBST_938	212.8	509.75	-0.87
OBST_938	162.85	381.39	-0.85
OBST_938	136.65	297.92	-0.78
OBST_938	127.22	240.27	-0.64
OBST_938	121.22	198.60	-0.49
OBST_938	116.82	167.40	-0.36
OBST_938	110.48	143.36	-0.26
OBST_939	285.96	648.67	-0.82
OBST_939	204.42	478.07	-0.85
OBST_939	166.46	369.41	-0.80
OBST_939	156.39	295.50	-0.64
OBST_939	149.66	242.70	-0.48
OBST_939	144.02	203.52	-0.35
OBST_939	136.28	173.57	-0.24
OBST_939	129.36	150.10	-0.15
OBST_939	121.6	131.32	-0.08

Table E-3
Determination of Bias and Uncertainty

Test	Obstructed FDS Temperature (C)	Heskestad Temperature (C)	Ln(∆FDS/∆Heskestad)
OBST_939	112.1	116.03	-0.03
OBST_940	272.81	580.18	-0.75
OBST_940	220.08	443.62	-0.70
OBST_940	194.75	352.09	-0.59
OBST_940	176.25	287.43	-0.49
OBST_940	167.07	239.87	-0.36
OBST_940	159.33	203.76	-0.25
OBST_940	152.41	175.63	-0.14
OBST_940	145.68	153.23	-0.05
OBST_940	136.24	135.08	0.01
OBST_940	125.56	120.14	0.04
OBST_944	210.14	724.86	-1.24
OBST_944	178.17	490.88	-1.01
OBST_944	170.23	358.00	-0.74
OBST_944	162.18	274.58	-0.53
OBST_944	152.71	218.42	-0.36
OBST_944	141.02	178.62	-0.24
OBST_944	130.26	149.28	-0.14
OBST_944	119.52	126.95	-0.06
OBST_945	251.01	669.58	-0.98
OBST_945	236.39	478.13	-0.70
OBST_945	222.45	361.36	-0.49
OBST_945	204.26	284.35	-0.33
OBST_945	182.73	230.60	-0.23
OBST_945	165.73	191.45	-0.14
OBST_945	149.17	161.94	-0.08
OBST_945	131.88	139.09	-0.05
OBST_945	115.11	121.00	-0.05
OBST_946	303.72	606.27	-0.69
OBST_946	282.66	451.82	-0.47
OBST_946	260.58	351.92	-0.30

Table E-3
Determination of Bias and Uncertainty

Test	Obstructed FDS Temperature (C)	Heskestad Temperature (C)	Ln(∆FDS/∆Heskestad)
OBST_946	235.83	283.21	-0.18
OBST_946	213.31	233.69	-0.09
OBST_946	190.86	196.71	-0.03
OBST_946	168.4	168.27	0.00
OBST_946	145.77	145.89	0.00
OBST_946	130.43	127.92	0.02
OBST_947	390.02	744.13	-0.65
OBST_947	351.04	546.97	-0.44
OBST_947	318.75	421.86	-0.28
OBST_947	279.61	336.98	-0.19
OBST_947	246.02	276.46	-0.12
OBST_947	217.54	231.64	-0.06
OBST_947	189.53	197.40	-0.04
OBST_947	164.54	170.60	-0.04
OBST_947	147.13	149.18	-0.01
THREEWALL_1058	381.71	772.37	-0.70
THREEWALL_1058	319.8	595.31	-0.62
THREEWALL_1058	264.72	475.29	-0.59
THREEWALL_1058	230.82	389.79	-0.52
THREEWALL_1058	195.58	326.49	-0.51
THREEWALL_1058	168.42	278.17	-0.50
THREEWALL_1058	146.49	240.36	-0.50
THREEWALL_1058	126.15	210.14	-0.51
THREEWALL_1058	115.05	185.58	-0.48
THREEWALL_1059	527.72	729.52	-0.32
THREEWALL_1059	411.6	566.88	-0.32
THREEWALL_1059	334.89	455.37	-0.31
THREEWALL_1059	286.67	375.23	-0.27
THREEWALL_1059	244.2	315.49	-0.26
THREEWALL_1059	207.16	269.64	-0.26
THREEWALL_1059	186.73	233.59	-0.22

Table E-3
Determination of Bias and Uncertainty

Test	Obstructed FDS Temperature (C)	Heskestad Temperature (C)	Ln(∆FDS/∆Heskestad)
THREEWALL_1067	343.31	764.70	-0.80
THREEWALL_1067	279.81	590.25	-0.75
THREEWALL_1067	235.01	471.76	-0.70
THREEWALL_1067	190.95	387.22	-0.71
THREEWALL_1067	167.89	324.55	-0.66
THREEWALL_1067	141.24	276.67	-0.67
THREEWALL_1067	125.62	239.17	-0.64
THREEWALL_1067	112.94	209.19	-0.62
THREEWALL_1068	496.14	722.52	-0.38
THREEWALL_1068	397.07	562.20	-0.35
THREEWALL_1068	318.85	452.07	-0.35
THREEWALL_1068	272.29	372.81	-0.31
THREEWALL_1068	234.15	313.65	-0.29
THREEWALL_1068	204.04	268.21	-0.27
THREEWALL_1068	179.74	232.45	-0.26
THREEWALL_1068	161.86	203.75	-0.23
THREEWALL_850	155.3	209.49	-0.30
THREEWALL_851	255.53	402.61	-0.45
THREEWALL_851	139.25	264.28	-0.64
THREEWALL_857	235.48	584.26	-0.91
THREEWALL_857	157.34	306.03	-0.67
THREEWALL_857	111.29	192.28	-0.55
THREEWALL_858	327.37	619.87	-0.64
THREEWALL_858	218.83	365.81	-0.51
THREEWALL_858	169.87	245.21	-0.37
THREEWALL_858	135.33	177.64	-0.27
THREEWALL_915	300.06	515.47	-0.54
THREEWALL_915	159.86	354.17	-0.80
THREEWALL_915	134.36	260.78	-0.66
THREEWALL_916	250.02	535.11	-0.76
THREEWALL_916	174.28	384.36	-0.79

Table E-3
Determination of Bias and Uncertainty

Test	Obstructed FDS Temperature (C)	Heskestad Temperature (C)	Ln(∆FDS/∆Heskestad)
THREEWALL_916	141.38	291.68	-0.72
THREEWALL_916	123.99	230.20	-0.62
THREEWALL_916	110.29	187.12	-0.53
THREEWALL_917	370.31	735.01	-0.69
THREEWALL_917	250.68	515.78	-0.72
THREEWALL_917	183.21	385.18	-0.74
THREEWALL_917	152.33	300.47	-0.68
THREEWALL_917	132.92	242.07	-0.60
THREEWALL_917	118.8	199.93	-0.52
THREEWALL_918	313.59	656.81	-0.74
THREEWALL_918	222.06	483.05	-0.78
THREEWALL_918	184.52	372.71	-0.70
THREEWALL_918	155.58	297.80	-0.65
THREEWALL_918	134.38	244.38	-0.60
THREEWALL_918	110.96	204.79	-0.61
THREEWALL_919	305.81	586.29	-0.65
THREEWALL_919	248	447.60	-0.59
THREEWALL_919	203.92	354.83	-0.55
THREEWALL_919	176.1	289.41	-0.50
THREEWALL_919	152.14	241.36	-0.46
THREEWALL_919	138.53	204.91	-0.39
THREEWALL_919	123.64	176.53	-0.36
THREEWALL_922	418.25	748.51	-0.58
THREEWALL_922	309.14	473.69	-0.43
THREEWALL_922	236.87	330.95	-0.33
THREEWALL_922	183.85	246.42	-0.29
THREEWALL_922	148.83	191.81	-0.25
THREEWALL_922	125.65	154.28	-0.21
THREEWALL_923	490.62	736.43	-0.41
THREEWALL_923	368.3	497.07	-0.30
THREEWALL_923	270.83	361.73	-0.29

Table E-3
Determination of Bias and Uncertainty

Test	Obstructed FDS Temperature (C)	Heskestad Temperature (C)	Ln(∆FDS/∆Heskestad)
THREEWALL_923	210.29	277.01	-0.28
THREEWALL_923	162.55	220.11	-0.30
THREEWALL_923	137.83	179.84	-0.27
THREEWALL_923	120.83	150.19	-0.22
THREEWALL_924	499.42	678.92	-0.31
THREEWALL_924	368.24	483.57	-0.27
THREEWALL_924	286.26	364.83	-0.24
THREEWALL_924	226.33	286.71	-0.24
THREEWALL_924	193.8	232.29	-0.18
THREEWALL_924	163.16	192.70	-0.17
THREEWALL_924	137.27	162.90	-0.17
THREEWALL_924	117.47	139.84	-0.17
THREEWALL_925	498.6	613.57	-0.21
THREEWALL_925	385.1	456.37	-0.17
THREEWALL_925	290.44	354.97	-0.20
THREEWALL_925	242.34	285.36	-0.16
THREEWALL_925	201.57	235.27	-0.15
THREEWALL_925	172.52	197.91	-0.14
THREEWALL_925	146.57	169.21	-0.14
THREEWALL_925	126.18	146.63	-0.15
THREEWALL_926	541.53	753.25	-0.33
THREEWALL_926	420.71	552.54	-0.27
THREEWALL_926	320.56	425.53	-0.28
THREEWALL_926	264.69	339.54	-0.25
THREEWALL_926	224.92	278.32	-0.21
THREEWALL_926	188.27	233.04	-0.21
THREEWALL_926	163.19	198.49	-0.20
THREEWALL_926	146.48	171.46	-0.16
THREEWALL_979	290.52	528.15	-0.60
THREEWALL_979	164.64	380.26	-0.84
THREEWALL_979	126.48	289.03	-0.83

Table E-3
Determination of Bias and Uncertainty

Test	Obstructed FDS Temperature (C)	Heskestad Temperature (C)	Ln(∆FDS/∆Heskestad)
THREEWALL_980	360.97	724.41	-0.70
THREEWALL_980	211.62	509.75	-0.88
THREEWALL_980	164.42	381.39	-0.84
THREEWALL_980	131.59	297.92	-0.82
THREEWALL_980	114.53	240.27	-0.74
THREEWALL_981	263.14	648.67	-0.90
THREEWALL_981	203.96	478.07	-0.85
THREEWALL_981	167.48	369.41	-0.79
THREEWALL_981	143.06	295.50	-0.73
THREEWALL_981	126.31	242.70	-0.65
THREEWALL_981	113.8	203.52	-0.58
THREEWALL_982	248.81	580.18	-0.85
THREEWALL_982	201.1	443.62	-0.79
THREEWALL_982	173.38	352.09	-0.71
THREEWALL_982	151.54	287.43	-0.64
THREEWALL_982	133.52	239.87	-0.59
THREEWALL_982	118.27	203.76	-0.54
THREEWALL_986	470.11	724.86	-0.43
THREEWALL_986	333.3	490.88	-0.39
THREEWALL_986	258.73	358.00	-0.32
THREEWALL_986	207.21	274.58	-0.28
THREEWALL_986	162.1	218.42	-0.30
THREEWALL_986	128.46	178.62	-0.33
THREEWALL_987	421.27	669.58	-0.46
THREEWALL_987	319.87	478.13	-0.40
THREEWALL_987	246.42	361.36	-0.38
THREEWALL_987	200.39	284.35	-0.35
THREEWALL_987	162.32	230.60	-0.35
THREEWALL_987	144.19	191.45	-0.28
THREEWALL_987	128.53	161.94	-0.23
THREEWALL_987	115.35	139.09	-0.19

Table E-3
Determination of Bias and Uncertainty

Test	Obstructed FDS Temperature (C)	Heskestad Temperature (C)	Ln(∆FDS/∆Heskestad)
THREEWALL_988	434.55	606.27	-0.33
THREEWALL_988	323.91	451.82	-0.33
THREEWALL_988	262.91	351.92	-0.29
THREEWALL_988	209.44	283.21	-0.30
THREEWALL_988	178.62	233.69	-0.27
THREEWALL_988	157.02	196.71	-0.23
THREEWALL_988	137.24	168.27	-0.20
THREEWALL_988	117.4	145.89	-0.22
THREEWALL_989	562.49	744.13	-0.28
THREEWALL_989	411.65	546.97	-0.28
THREEWALL_989	329.02	421.86	-0.25
THREEWALL_989	250.92	336.98	-0.29
THREEWALL_989	213.27	276.46	-0.26
THREEWALL_989	182.93	231.64	-0.24
THREEWALL_989	156.71	197.40	-0.23
THREEWALL_989	131.1	170.60	-0.26
THREEWALL_989	117.61	149.18	-0.24

USING EQUATIONS FROM SECTION 5.2.4.5

$$\overline{\ln\left(\frac{M}{E}\right)} = \frac{1}{n}\sum_{i=1}^{n} \ln\left(\frac{M_i}{E_i}\right) = -0.50 \qquad (5\text{-}11)$$

$$\tilde{\sigma}_M^2 + \tilde{\sigma}_E^2 = \frac{1}{1-n}\sum_{i=1}^{n}\left[\ln\left(\frac{M_i}{E_i}\right) - \overline{\ln\left(\frac{M}{E}\right)}\right]^2 = 0.11 \qquad (5\text{-}12)$$

$$\tilde{\sigma}_E = 0.20$$

$$\tilde{\sigma}_M = 0.28$$

$$\delta = \exp\left(\overline{\ln\left(\frac{M}{E}\right)} + \frac{\tilde{\sigma}_M^2}{2} - \frac{\tilde{\sigma}_E^2}{2}\right) = 0.62 \qquad (5\text{-}13)$$

Opening Sensitivity Cases

Table E-4
Opening Sensitivity Results

Test	HRR (kW)	Diameter (m)	Source Height (m)	Elevation (m)	Maximum Plume Temperature Rise (C)	Opening Percentage
ARCH_1101	200	0.61	1.98	2.4	937.56	6
ARCH_1101	200	0.61	1.98	2.7	804.3	6
ARCH_1101	200	0.61	1.98	3	530.41	6
ARCH_1101	200	0.61	1.98	3.3	327	6
ARCH_1101	200	0.61	1.98	3.6	228.87	6
ARCH_1101	200	0.61	1.98	3.9	164.39	6
ARCH_1101	200	0.61	1.98	4.2	128.92	6
ARCH_1101	200	0.61	1.98	4.5	103.83	6
ARCH_1101	200	0.61	1.98	4.8	89.37	6
ARCH_1101	200	0.61	1.98	5.1	79.014	6
ARCH_1101	200	0.61	1.98	5.4	70.186	6
ARCH_1101	200	0.61	1.98	5.7	63.806	6
ARCH_1101	200	0.61	1.98	6	57.845	6
ARCH_1104	200	0.61	1.98	2.4	938.78	10
ARCH_1104	200	0.61	1.98	2.7	797.27	10
ARCH_1104	200	0.61	1.98	3	538.71	10
ARCH_1104	200	0.61	1.98	3.3	306.25	10
ARCH_1104	200	0.61	1.98	3.6	219.26	10
ARCH_1104	200	0.61	1.98	3.9	172.2	10
ARCH_1104	200	0.61	1.98	4.2	143.44	10
ARCH_1104	200	0.61	1.98	4.5	117.38	10

Table E-4
Opening Sensitivity Results

Test	HRR (kW)	Diameter (m)	Source Height (m)	Elevation (m)	Maximum Plume Temperature Rise (C)	Opening Percentage
ARCH_1104	200	0.61	1.98	4.8	103.22	10
ARCH_1104	200	0.61	1.98	5.1	91.39	10
ARCH_1104	200	0.61	1.98	5.4	78.053	10
ARCH_1104	200	0.61	1.98	5.7	69.999	10
ARCH_1104	200	0.61	1.98	6	66.112	10
ARCH_1107	200	0.61	1.98	2.4	936.64	14
ARCH_1107	200	0.61	1.98	2.7	809.41	14
ARCH_1107	200	0.61	1.98	3	558.92	14
ARCH_1107	200	0.61	1.98	3.3	338.16	14
ARCH_1107	200	0.61	1.98	3.6	250.38	14
ARCH_1107	200	0.61	1.98	3.9	186.33	14
ARCH_1107	200	0.61	1.98	4.2	148.42	14
ARCH_1107	200	0.61	1.98	4.5	124.24	14
ARCH_1107	200	0.61	1.98	4.8	107.65	14
ARCH_1107	200	0.61	1.98	5.1	93.37	14
ARCH_1107	200	0.61	1.98	5.4	80.35	14
ARCH_1107	200	0.61	1.98	5.7	69.691	14
ARCH_1107	200	0.61	1.98	6	60.263	14
ARCH_1110	600	0.91	1.98	2.4	864.32	7
ARCH_1110	600	0.91	1.98	2.7	811.89	7
ARCH_1110	600	0.91	1.98	3	712.42	7
ARCH_1110	600	0.91	1.98	3.3	619.63	7

Table E-4
Opening Sensitivity Results

Test	HRR (kW)	Diameter (m)	Source Height (m)	Elevation (m)	Maximum Plume Temperature Rise (C)	Opening Percentage
ARCH_1110	600	0.91	1.98	3.6	537.1	7
ARCH_1110	600	0.91	1.98	3.9	410.59	7
ARCH_1110	600	0.91	1.98	4.2	313.78	7
ARCH_1110	600	0.91	1.98	4.5	239.77	7
ARCH_1110	600	0.91	1.98	4.8	192.91	7
ARCH_1110	600	0.91	1.98	5.1	170.72	7
ARCH_1110	600	0.91	1.98	5.4	149.15	7
ARCH_1110	600	0.91	1.98	5.7	135.01	7
ARCH_1110	600	0.91	1.98	6	121.85	7
ARCH_1113	600	0.91	1.98	2.4	935.11	10
ARCH_1113	600	0.91	1.98	2.7	879.75	10
ARCH_1113	600	0.91	1.98	3	808.18	10
ARCH_1113	600	0.91	1.98	3.3	684.08	10
ARCH_1113	600	0.91	1.98	3.6	597.73	10
ARCH_1113	600	0.91	1.98	3.9	456.27	10
ARCH_1113	600	0.91	1.98	4.2	367.47	10
ARCH_1113	600	0.91	1.98	4.5	297.95	10
ARCH_1113	600	0.91	1.98	4.8	245.22	10
ARCH_1113	600	0.91	1.98	5.1	199.07	10
ARCH_1113	600	0.91	1.98	5.4	168.48	10
ARCH_1113	600	0.91	1.98	5.7	146.04	10
ARCH_1113	600	0.91	1.98	6	128.03	10

Table E-4
Opening Sensitivity Results

Test	HRR (kW)	Diameter (m)	Source Height (m)	Elevation (m)	Maximum Plume Temperature Rise (C)	Opening Percentage
ARCH_1116	600	0.91	1.98	2.4	938.2	12
ARCH_1116	600	0.91	1.98	2.7	893.53	12
ARCH_1116	600	0.91	1.98	3	792.6	12
ARCH_1116	600	0.91	1.98	3.3	662.2	12
ARCH_1116	600	0.91	1.98	3.6	551	12
ARCH_1116	600	0.91	1.98	3.9	440.94	12
ARCH_1116	600	0.91	1.98	4.2	332.47	12
ARCH_1116	600	0.91	1.98	4.5	261.76	12
ARCH_1116	600	0.91	1.98	4.8	232.45	12
ARCH_1116	600	0.91	1.98	5.1	190.96	12
ARCH_1116	600	0.91	1.98	5.4	158.47	12
ARCH_1116	600	0.91	1.98	5.7	141.04	12
ARCH_1116	600	0.91	1.98	6	123.93	12
OBST_1100	200	0.61	1.98	2.4	901.43	6
OBST_1100	200	0.61	1.98	2.7	602.1	6
OBST_1100	200	0.61	1.98	3	389.92	6
OBST_1100	200	0.61	1.98	3.3	270.13	6
OBST_1100	200	0.61	1.98	3.6	216.79	6
OBST_1100	200	0.61	1.98	3.9	177.04	6
OBST_1100	200	0.61	1.98	4.2	151.64	6
OBST_1100	200	0.61	1.98	4.5	127.06	6
OBST_1100	200	0.61	1.98	4.8	109.56	6

Table E-4
Opening Sensitivity Results

Test	HRR (kW)	Diameter (m)	Source Height (m)	Elevation (m)	Maximum Plume Temperature Rise (C)	Opening Percentage
OBST_1100	200	0.61	1.98	5.1	96.42	6
OBST_1100	200	0.61	1.98	5.4	85.68	6
OBST_1100	200	0.61	1.98	5.7	76.722	6
OBST_1100	200	0.61	1.98	6	69.612	6
OBST_1103	200	0.61	1.98	2.4	965.45	10
OBST_1103	200	0.61	1.98	2.7	768.83	10
OBST_1103	200	0.61	1.98	3	559.68	10
OBST_1103	200	0.61	1.98	3.3	391	10
OBST_1103	200	0.61	1.98	3.6	297.69	10
OBST_1103	200	0.61	1.98	3.9	228.19	10
OBST_1103	200	0.61	1.98	4.2	187.49	10
OBST_1103	200	0.61	1.98	4.5	152.8	10
OBST_1103	200	0.61	1.98	4.8	133.98	10
OBST_1103	200	0.61	1.98	5.1	115.76	10
OBST_1103	200	0.61	1.98	5.4	98.46	10
OBST_1103	200	0.61	1.98	5.7	85.02	10
OBST_1103	200	0.61	1.98	6	75.158	10
OBST_1106	200	0.61	1.98	2.4	918.35	14
OBST_1106	200	0.61	1.98	2.7	728.72	14
OBST_1106	200	0.61	1.98	3	533.61	14
OBST_1106	200	0.61	1.98	3.3	370.73	14
OBST_1106	200	0.61	1.98	3.6	286.68	14

Table E-4
Opening Sensitivity Results

Test	HRR (kW)	Diameter (m)	Source Height (m)	Elevation (m)	Maximum Plume Temperature Rise (C)	Opening Percentage
OBST_1106	200	0.61	1.98	3.9	217.32	14
OBST_1106	200	0.61	1.98	4.2	172.61	14
OBST_1106	200	0.61	1.98	4.5	136.16	14
OBST_1106	200	0.61	1.98	4.8	111.35	14
OBST_1106	200	0.61	1.98	5.1	95.45	14
OBST_1106	200	0.61	1.98	5.4	82.94	14
OBST_1106	200	0.61	1.98	5.7	73.083	14
OBST_1106	200	0.61	1.98	6	67.295	14
OBST_1109	600	0.91	1.98	2.4	854.62	7
OBST_1109	600	0.91	1.98	2.7	849.81	7
OBST_1109	600	0.91	1.98	3	785.25	7
OBST_1109	600	0.91	1.98	3.3	695.57	7
OBST_1109	600	0.91	1.98	3.6	592.45	7
OBST_1109	600	0.91	1.98	3.9	473.33	7
OBST_1109	600	0.91	1.98	4.2	390.05	7
OBST_1109	600	0.91	1.98	4.5	318.33	7
OBST_1109	600	0.91	1.98	4.8	274	7
OBST_1109	600	0.91	1.98	5.1	239.74	7
OBST_1109	600	0.91	1.98	5.4	204.37	7
OBST_1109	600	0.91	1.98	5.7	175.5	7
OBST_1109	600	0.91	1.98	6	151.72	7
OBST_1112	600	0.91	1.98	2.4	923.28	10

Table E-4
Opening Sensitivity Results

Test	HRR (kW)	Diameter (m)	Source Height (m)	Elevation (m)	Maximum Plume Temperature Rise (C)	Opening Percentage
OBST_1112	600	0.91	1.98	2.7	915.92	10
OBST_1112	600	0.91	1.98	3	864.74	10
OBST_1112	600	0.91	1.98	3.3	774.66	10
OBST_1112	600	0.91	1.98	3.6	662.67	10
OBST_1112	600	0.91	1.98	3.9	565.45	10
OBST_1112	600	0.91	1.98	4.2	481.41	10
OBST_1112	600	0.91	1.98	4.5	382.74	10
OBST_1112	600	0.91	1.98	4.8	316	10
OBST_1112	600	0.91	1.98	5.1	262.73	10
OBST_1112	600	0.91	1.98	5.4	216.83	10
OBST_1112	600	0.91	1.98	5.7	183.67	10
OBST_1112	600	0.91	1.98	6	160.17	10
OBST_1115	600	0.91	1.98	2.4	951.08	12
OBST_1115	600	0.91	1.98	2.7	897.98	12
OBST_1115	600	0.91	1.98	3	892.86	12
OBST_1115	600	0.91	1.98	3.3	794.16	12
OBST_1115	600	0.91	1.98	3.6	690.03	12
OBST_1115	600	0.91	1.98	3.9	577.49	12
OBST_1115	600	0.91	1.98	4.2	458.86	12
OBST_1115	600	0.91	1.98	4.5	368.8	12
OBST_1115	600	0.91	1.98	4.8	307.16	12
OBST_1115	600	0.91	1.98	5.1	253.02	12

Table E-4
Opening Sensitivity Results

Test	HRR (kW)	Diameter (m)	Source Height (m)	Elevation (m)	Maximum Plume Temperature Rise (C)	Opening Percentage
OBST_1115	600	0.91	1.98	5.4	212.6	12
OBST_1115	600	0.91	1.98	5.7	177.64	12
OBST_1115	600	0.91	1.98	6	157.52	12
THREEWALL_1102	200	0.61	1.98	2.4	948.99	6
THREEWALL_1102	200	0.61	1.98	2.7	824.5	6
THREEWALL_1102	200	0.61	1.98	3	625.36	6
THREEWALL_1102	200	0.61	1.98	3.3	381.42	6
THREEWALL_1102	200	0.61	1.98	3.6	255.08	6
THREEWALL_1102	200	0.61	1.98	3.9	178.07	6
THREEWALL_1102	200	0.61	1.98	4.2	135.23	6
THREEWALL_1102	200	0.61	1.98	4.5	106.91	6
THREEWALL_1102	200	0.61	1.98	4.8	90.78	6
THREEWALL_1102	200	0.61	1.98	5.1	78.946	6
THREEWALL_1102	200	0.61	1.98	5.4	70.587	6
THREEWALL_1102	200	0.61	1.98	5.7	60.087	6
THREEWALL_1102	200	0.61	1.98	6	53.403	6
THREEWALL_1105	200	0.61	1.98	2.4	955.95	10
THREEWALL_1105	200	0.61	1.98	2.7	780.37	10
THREEWALL_1105	200	0.61	1.98	3	569.42	10
THREEWALL_1105	200	0.61	1.98	3.3	358.73	10
THREEWALL_1105	200	0.61	1.98	3.6	252.27	10
THREEWALL_1105	200	0.61	1.98	3.9	177.91	10

Table E-4
Opening Sensitivity Results

Test	HRR (kW)	Diameter (m)	Source Height (m)	Elevation (m)	Maximum Plume Temperature Rise (C)	Opening Percentage
THREEWALL_1105	200	0.61	1.98	4.2	136.88	10
THREEWALL_1105	200	0.61	1.98	4.5	113.62	10
THREEWALL_1105	200	0.61	1.98	4.8	94.94	10
THREEWALL_1105	200	0.61	1.98	5.1	81.84	10
THREEWALL_1105	200	0.61	1.98	5.4	71.209	10
THREEWALL_1105	200	0.61	1.98	5.7	63.762	10
THREEWALL_1105	200	0.61	1.98	6	57.409	10
THREEWALL_1108	200	0.61	1.98	2.4	928.8	14
THREEWALL_1108	200	0.61	1.98	2.7	751.6	14
THREEWALL_1108	200	0.61	1.98	3	583.09	14
THREEWALL_1108	200	0.61	1.98	3.3	395.52	14
THREEWALL_1108	200	0.61	1.98	3.6	280.94	14
THREEWALL_1108	200	0.61	1.98	3.9	203.94	14
THREEWALL_1108	200	0.61	1.98	4.2	160.04	14
THREEWALL_1108	200	0.61	1.98	4.5	128.85	14
THREEWALL_1108	200	0.61	1.98	4.8	112.91	14
THREEWALL_1108	200	0.61	1.98	5.1	97.66	14
THREEWALL_1108	200	0.61	1.98	5.4	85.96	14
THREEWALL_1108	200	0.61	1.98	5.7	71.963	14
THREEWALL_1108	200	0.61	1.98	6	64.651	14
THREEWALL_1111	600	0.91	1.98	2.4	792.68	7
THREEWALL_1111	600	0.91	1.98	2.7	782.33	7

Table E-4
Opening Sensitivity Results

Test	HRR (kW)	Diameter (m)	Source Height (m)	Elevation (m)	Maximum Plume Temperature Rise (C)	Opening Percentage
THREEWALL_1111	600	0.91	1.98	3	806.99	7
THREEWALL_1111	600	0.91	1.98	3.3	686.87	7
THREEWALL_1111	600	0.91	1.98	3.6	597.97	7
THREEWALL_1111	600	0.91	1.98	3.9	461.87	7
THREEWALL_1111	600	0.91	1.98	4.2	344.28	7
THREEWALL_1111	600	0.91	1.98	4.5	260.38	7
THREEWALL_1111	600	0.91	1.98	4.8	221.84	7
THREEWALL_1111	600	0.91	1.98	5.1	188.45	7
THREEWALL_1111	600	0.91	1.98	5.4	164.6	7
THREEWALL_1111	600	0.91	1.98	5.7	144.27	7
THREEWALL_1111	600	0.91	1.98	6	129.47	7
THREEWALL_1114	600	0.91	1.98	2.4	911.41	10
THREEWALL_1114	600	0.91	1.98	2.7	869.36	10
THREEWALL_1114	600	0.91	1.98	3	834.75	10
THREEWALL_1114	600	0.91	1.98	3.3	702.84	10
THREEWALL_1114	600	0.91	1.98	3.6	591.34	10
THREEWALL_1114	600	0.91	1.98	3.9	464.06	10
THREEWALL_1114	600	0.91	1.98	4.2	370.37	10
THREEWALL_1114	600	0.91	1.98	4.5	300.22	10
THREEWALL_1114	600	0.91	1.98	4.8	243.72	10
THREEWALL_1114	600	0.91	1.98	5.1	206.52	10
THREEWALL_1114	600	0.91	1.98	5.4	172.52	10

Table E-4
Opening Sensitivity Results

Test	HRR (kW)	Diameter (m)	Source Height (m)	Elevation (m)	Maximum Plume Temperature Rise (C)	Opening Percentage
THREEWALL_1114	600	0.91	1.98	5.7	151.32	10
THREEWALL_1114	600	0.91	1.98	6	136.66	10
THREEWALL_1117	600	0.91	1.98	2.4	905	12
THREEWALL_1117	600	0.91	1.98	2.7	892.38	12
THREEWALL_1117	600	0.91	1.98	3	865.65	12
THREEWALL_1117	600	0.91	1.98	3.3	722.89	12
THREEWALL_1117	600	0.91	1.98	3.6	603.73	12
THREEWALL_1117	600	0.91	1.98	3.9	511.39	12
THREEWALL_1117	600	0.91	1.98	4.2	406.63	12
THREEWALL_1117	600	0.91	1.98	4.5	321.86	12
THREEWALL_1117	600	0.91	1.98	4.8	259.92	12
THREEWALL_1117	600	0.91	1.98	5.1	212.13	12
THREEWALL_1117	600	0.91	1.98	5.4	179.44	12
THREEWALL_1117	600	0.91	1.98	5.7	154.98	12
THREEWALL_1117	600	0.91	1.98	6	139.12	12

Vertical Source Sensitivity Results

Table E-5
Vertical Fire Source Sensitivity Results

Test	HRR (kW)	Source Height (m)	Elevation (m)	Maximum Plume Temperature Rise (C)
ARCH_1201	200	1.96	2.4	268.98
ARCH_1201	200	1.96	2.7	144.1
ARCH_1201	200	1.96	3	113.12
ARCH_1201	200	1.96	3.3	96.37
ARCH_1201	200	1.96	3.6	78.483
ARCH_1201	200	1.96	3.9	71.331
ARCH_1201	200	1.96	4.2	65.5
ARCH_1201	200	1.96	4.5	53.038
ARCH_1201	200	1.96	4.8	46.024
ARCH_1201	200	1.96	5.1	42.5
ARCH_1201	200	1.96	5.4	37.767
ARCH_1201	200	1.96	5.7	33.437
ARCH_1201	200	1.96	6	31.546
ARCH_1204	600	1.96	2.4	373.37
ARCH_1204	600	1.96	2.7	208.88
ARCH_1204	600	1.96	3	159.73
ARCH_1204	600	1.96	3.3	127.46
ARCH_1204	600	1.96	3.6	111.86
ARCH_1204	600	1.96	3.9	93.95
ARCH_1204	600	1.96	4.2	81.8
ARCH_1204	600	1.96	4.5	70.262
ARCH_1204	600	1.96	4.8	61.122
ARCH_1204	600	1.96	5.1	55.523
ARCH_1204	600	1.96	5.4	49.187
ARCH_1204	600	1.96	5.7	45.015
ARCH_1204	600	1.96	6	41.931
ARCH_1207	1000	1.96	2.4	548.76
ARCH_1207	1000	1.96	2.7	333.12
ARCH_1207	1000	1.96	3	244.24
ARCH_1207	1000	1.96	3.3	193.98
ARCH_1207	1000	1.96	3.6	165.92

Table E-5
Vertical Fire Source Sensitivity Results

Test	HRR (kW)	Source Height (m)	Elevation (m)	Maximum Plume Temperature Rise (C)
ARCH_1207	1000	1.96	3.9	134.32
ARCH_1207	1000	1.96	4.2	116.62
ARCH_1207	1000	1.96	4.5	102.34
ARCH_1207	1000	1.96	4.8	93.31
ARCH_1207	1000	1.96	5.1	84.96
ARCH_1207	1000	1.96	5.4	76.94
ARCH_1207	1000	1.96	5.7	71.158
ARCH_1207	1000	1.96	6	67.532
OBST_1200	200	1.96	2.4	278.25
OBST_1200	200	1.96	2.7	191.68
OBST_1200	200	1.96	3	137.65
OBST_1200	200	1.96	3.3	116.8
OBST_1200	200	1.96	3.6	106.52
OBST_1200	200	1.96	3.9	103.48
OBST_1200	200	1.96	4.2	96.76
OBST_1200	200	1.96	4.5	93.14
OBST_1200	200	1.96	4.8	85.47
OBST_1200	200	1.96	5.1	82.24
OBST_1200	200	1.96	5.4	77.125
OBST_1200	200	1.96	5.7	68.407
OBST_1200	200	1.96	6	67.908
OBST_1203	600	1.96	2.4	395.28
OBST_1203	600	1.96	2.7	269.3
OBST_1203	600	1.96	3	200.42
OBST_1203	600	1.96	3.3	168.84
OBST_1203	600	1.96	3.6	162.48
OBST_1203	600	1.96	3.9	152.5
OBST_1203	600	1.96	4.2	142.48
OBST_1203	600	1.96	4.5	132.94
OBST_1203	600	1.96	4.8	124.94
OBST_1203	600	1.96	5.1	118.76
OBST_1203	600	1.96	5.4	112.77

Table E-5
Vertical Fire Source Sensitivity Results

Test	HRR (kW)	Source Height (m)	Elevation (m)	Maximum Plume Temperature Rise (C)
OBST_1203	600	1.96	5.7	105.93
OBST_1203	600	1.96	6	99.98
OBST_1206	1000	1.96	2.4	571.45
OBST_1206	1000	1.96	2.7	426.7
OBST_1206	1000	1.96	3	324.5
OBST_1206	1000	1.96	3.3	250.95
OBST_1206	1000	1.96	3.6	218.76
OBST_1206	1000	1.96	3.9	203.03
OBST_1206	1000	1.96	4.2	194.93
OBST_1206	1000	1.96	4.5	184.31
OBST_1206	1000	1.96	4.8	176.19
OBST_1206	1000	1.96	5.1	167.67
OBST_1206	1000	1.96	5.4	157.48
OBST_1206	1000	1.96	5.7	147.61
OBST_1206	1000	1.96	6	138.06
THREEWALL_1202	200	1.96	2.4	389.57
THREEWALL_1202	200	1.96	2.7	196.97
THREEWALL_1202	200	1.96	3	166.17
THREEWALL_1202	200	1.96	3.3	127.37
THREEWALL_1202	200	1.96	3.6	108.9
THREEWALL_1202	200	1.96	3.9	100.05
THREEWALL_1202	200	1.96	4.2	87.32
THREEWALL_1202	200	1.96	4.5	75.058
THREEWALL_1202	200	1.96	4.8	66.517
THREEWALL_1202	200	1.96	5.1	61.544
THREEWALL_1202	200	1.96	5.4	61.094
THREEWALL_1202	200	1.96	5.7	53.701
THREEWALL_1202	200	1.96	6	49.642
THREEWALL_1205	600	1.96	2.4	656.67
THREEWALL_1205	600	1.96	2.7	324.79
THREEWALL_1205	600	1.96	3	246.83
THREEWALL_1205	600	1.96	3.3	193.16

Table E-5
Vertical Fire Source Sensitivity Results

Test	HRR (kW)	Source Height (m)	Elevation (m)	Maximum Plume Temperature Rise (C)
THREEWALL_1205	600	1.96	3.6	166.46
THREEWALL_1205	600	1.96	3.9	144.38
THREEWALL_1205	600	1.96	4.2	127.18
THREEWALL_1205	600	1.96	4.5	114.05
THREEWALL_1205	600	1.96	4.8	104.54
THREEWALL_1205	600	1.96	5.1	95.21
THREEWALL_1205	600	1.96	5.4	84.74
THREEWALL_1205	600	1.96	5.7	78.468
THREEWALL_1205	600	1.96	6	74.278
THREEWALL_1208	1000	1.96	2.4	851.7
THREEWALL_1208	1000	1.96	2.7	522.48
THREEWALL_1208	1000	1.96	3	381.06
THREEWALL_1208	1000	1.96	3.3	293.78
THREEWALL_1208	1000	1.96	3.6	241
THREEWALL_1208	1000	1.96	3.9	203.84
THREEWALL_1208	1000	1.96	4.2	176.73
THREEWALL_1208	1000	1.96	4.5	151.32
THREEWALL_1208	1000	1.96	4.8	136.85
THREEWALL_1208	1000	1.96	5.1	123.86
THREEWALL_1208	1000	1.96	5.4	113.06
THREEWALL_1208	1000	1.96	5.7	106.48
THREEWALL_1208	1000	1.96	6	102.17

Wall Surface Source Sensitivity Results

Table E-6
Wall Surface Fire Source Sensitivity Results

Test	HRR (kW)	Source Height (m)	Elevation (m)	Maximum Plume Temperature Rise (C)
ARCH_1300	200	N/A	2.4	217.1
ARCH_1300	200	N/A	2.7	138.23
ARCH_1300	200	N/A	3	112.58
ARCH_1300	200	N/A	3.3	86.48
ARCH_1300	200	N/A	3.6	70.548
ARCH_1300	200	N/A	3.9	59.215
ARCH_1300	200	N/A	4.2	50.1
ARCH_1300	200	N/A	4.5	40.591
ARCH_1300	200	N/A	4.8	38.02
ARCH_1300	200	N/A	5.1	32.326
ARCH_1300	200	N/A	5.4	30.396
ARCH_1300	200	N/A	5.7	26.979
ARCH_1300	200	N/A	6	25.194
ARCH_1301	600	N/A	2.4	393.79
ARCH_1301	600	N/A	2.7	209.47
ARCH_1301	600	N/A	3	151.92
ARCH_1301	600	N/A	3.3	116.88
ARCH_1301	600	N/A	3.6	103.04
ARCH_1301	600	N/A	3.9	94.12
ARCH_1301	600	N/A	4.2	86.7
ARCH_1301	600	N/A	4.5	77.009
ARCH_1301	600	N/A	4.8	69.681
ARCH_1301	600	N/A	5.1	63.48
ARCH_1301	600	N/A	5.4	57.863
ARCH_1301	600	N/A	5.7	53.021
ARCH_1301	600	N/A	6	48.236
ARCH_1302	1000	N/A	2.4	536.82
ARCH_1302	1000	N/A	2.7	273.11
ARCH_1302	1000	N/A	3	195.72
ARCH_1302	1000	N/A	3.3	151.17
ARCH_1302	1000	N/A	3.6	130.34
ARCH_1302	1000	N/A	3.9	119.55
ARCH_1302	1000	N/A	4.2	109.61
ARCH_1302	1000	N/A	4.5	99.71
ARCH_1302	1000	N/A	4.8	92.99

Table E-6
Wall Surface Fire Source Sensitivity Results

Test	HRR (kW)	Source Height (m)	Elevation (m)	Maximum Plume Temperature Rise (C)
ARCH_1302	1000	N/A	5.1	86.59
ARCH_1302	1000	N/A	5.4	79.901
ARCH_1302	1000	N/A	5.7	74.873
ARCH_1302	1000	N/A	6	69.845
THREEWALL_1303	200	N/A	2.4	194.03
THREEWALL_1303	200	N/A	2.7	111.49
THREEWALL_1303	200	N/A	3	86.47
THREEWALL_1303	200	N/A	3.3	72.89
THREEWALL_1303	200	N/A	3.6	58.965
THREEWALL_1303	200	N/A	3.9	53.597
THREEWALL_1303	200	N/A	4.2	48.005
THREEWALL_1303	200	N/A	4.5	41.282
THREEWALL_1303	200	N/A	4.8	37.605
THREEWALL_1303	200	N/A	5.1	34.67
THREEWALL_1303	200	N/A	5.4	34.316
THREEWALL_1303	200	N/A	5.7	29.146
THREEWALL_1303	200	N/A	6	28.554
THREEWALL_1304	600	N/A	2.4	351.26
THREEWALL_1304	600	N/A	2.7	202.93
THREEWALL_1304	600	N/A	3	160.17
THREEWALL_1304	600	N/A	3.3	124.65
THREEWALL_1304	600	N/A	3.6	108.96
THREEWALL_1304	600	N/A	3.9	94.17
THREEWALL_1304	600	N/A	4.2	86.77
THREEWALL_1304	600	N/A	4.5	79.251
THREEWALL_1304	600	N/A	4.8	70.232
THREEWALL_1304	600	N/A	5.1	63.272
THREEWALL_1304	600	N/A	5.4	56.567
THREEWALL_1304	600	N/A	5.7	50.222
THREEWALL_1304	600	N/A	6	48.415
THREEWALL_1306	1000	N/A	2.4	462.11
THREEWALL_1306	1000	N/A	2.7	283.33
THREEWALL_1306	1000	N/A	3	229.63
THREEWALL_1306	1000	N/A	3.3	185.73
THREEWALL_1306	1000	N/A	3.6	159.07
THREEWALL_1306	1000	N/A	3.9	133.87

Table E-6
Wall Surface Fire Source Sensitivity Results

Test	HRR (kW)	Source Height (m)	Elevation (m)	Maximum Plume Temperature Rise (C)
THREEWALL_1306	1000	N/A	4.2	119.87
THREEWALL_1306	1000	N/A	4.5	103.54
THREEWALL_1306	1000	N/A	4.8	94.86
THREEWALL_1306	1000	N/A	5.1	86.99
THREEWALL_1306	1000	N/A	5.4	80.12
THREEWALL_1306	1000	N/A	5.7	73.768
THREEWALL_1306	1000	N/A	6	68.647

Soffit Sensitivity Results

Table E-7
Soffit Sensitivity Results

Test	HRR (kW)	Source Height (m)	Elevation (m)	Maximum Plume Temperature Rise (C)
ARCH_1401	200	1.14	2.4	171.43
ARCH_1401	200	1.14	2.7	107.11
ARCH_1401	200	1.14	3	92.4
ARCH_1401	200	1.14	3.3	74.129
ARCH_1401	200	1.14	3.6	68.538
ARCH_1401	200	1.14	3.9	53.736
ARCH_1401	200	1.14	4.2	49.268
ARCH_1401	200	1.14	4.5	43.278
ARCH_1401	200	1.14	4.8	38.74
ARCH_1401	200	1.14	5.1	35.033
ARCH_1401	200	1.14	5.4	30.479
ARCH_1401	200	1.14	5.7	29.695
ARCH_1401	200	1.14	6	26.62
ARCH_1404	600	1.14	2.4	271.05
ARCH_1404	600	1.14	2.7	177.17
ARCH_1404	600	1.14	3	143.77
ARCH_1404	600	1.14	3.3	115.75
ARCH_1404	600	1.14	3.6	102.35
ARCH_1404	600	1.14	3.9	90.26
ARCH_1404	600	1.14	4.2	79.924
ARCH_1404	600	1.14	4.5	71.303
ARCH_1404	600	1.14	4.8	66.625
ARCH_1404	600	1.14	5.1	60.925
ARCH_1404	600	1.14	5.4	53.258
ARCH_1404	600	1.14	5.7	46.84
ARCH_1404	600	1.14	6	44.228
ARCH_1407	1000	1.14	2.4	411.81
ARCH_1407	1000	1.14	2.7	257.94
ARCH_1407	1000	1.14	3	204.41
ARCH_1407	1000	1.14	3.3	171.02
ARCH_1407	1000	1.14	3.6	146.92
ARCH_1407	1000	1.14	3.9	124.11
ARCH_1407	1000	1.14	4.2	110.35
ARCH_1407	1000	1.14	4.5	95.13
ARCH_1407	1000	1.14	4.8	85.1

Table E-7
Soffit Sensitivity Results

Test	HRR (kW)	Source Height (m)	Elevation (m)	Maximum Plume Temperature Rise (C)
ARCH_1407	1000	1.14	5.1	78.778
ARCH_1407	1000	1.14	5.4	70.232
ARCH_1407	1000	1.14	5.7	65.497
ARCH_1410	200	1.98	2.4	738.18
ARCH_1410	200	1.98	2.7	531.25
ARCH_1410	200	1.98	3	321.95
ARCH_1410	200	1.98	3.3	231.67
ARCH_1410	200	1.98	3.6	200.36
ARCH_1410	200	1.98	3.9	165.42
ARCH_1410	200	1.98	4.2	132.76
ARCH_1410	200	1.98	4.5	96.17
ARCH_1410	200	1.98	4.8	86.44
ARCH_1410	200	1.98	5.1	85.38
ARCH_1410	200	1.98	5.4	70.331
ARCH_1410	200	1.98	5.7	57.028
ARCH_1410	200	1.98	6	53.461
ARCH_1413	600	1.98	2.4	954.42
ARCH_1413	600	1.98	2.7	789.76
ARCH_1413	600	1.98	3	604.22
ARCH_1413	600	1.98	3.3	423.99
ARCH_1413	600	1.98	3.6	326.94
ARCH_1413	600	1.98	3.9	257.85
ARCH_1413	600	1.98	4.2	212.79
ARCH_1413	600	1.98	4.5	172.49
ARCH_1413	600	1.98	4.8	146.63
ARCH_1413	600	1.98	5.1	127.04
ARCH_1413	600	1.98	5.4	111.77
ARCH_1413	600	1.98	5.7	99.91
ARCH_1413	600	1.98	6	91.55
ARCH_1416	1000	1.98	2.4	994.8
ARCH_1416	1000	1.98	2.7	962.81
ARCH_1416	1000	1.98	3	785.87
ARCH_1416	1000	1.98	3.3	592.31
ARCH_1416	1000	1.98	3.6	444.35
ARCH_1416	1000	1.98	3.9	331.3
ARCH_1416	1000	1.98	4.2	266.22

Table E-7
Soffit Sensitivity Results

Test	HRR (kW)	Source Height (m)	Elevation (m)	Maximum Plume Temperature Rise (C)
ARCH_1416	1000	1.98	4.5	223.96
ARCH_1416	1000	1.98	4.8	197.1
ARCH_1416	1000	1.98	5.1	175.42
ARCH_1416	1000	1.98	5.4	151.29
ARCH_1416	1000	1.98	5.7	130.44
ARCH_1416	1000	1.98	6	121.45
OBST_1400	200	1.14	2.4	184.04
OBST_1400	200	1.14	2.7	118.62
OBST_1400	200	1.14	3	91.06
OBST_1400	200	1.14	3.3	85.89
OBST_1400	200	1.14	3.6	79.421
OBST_1400	200	1.14	3.9	72.139
OBST_1400	200	1.14	4.2	71.684
OBST_1400	200	1.14	4.5	62.392
OBST_1400	200	1.14	4.8	58.739
OBST_1400	200	1.14	5.1	60.088
OBST_1400	200	1.14	5.4	50.108
OBST_1400	200	1.14	5.7	47.747
OBST_1400	200	1.14	6	41.442
OBST_1403	600	1.14	2.4	158.1
OBST_1403	600	1.14	2.7	95.82
OBST_1403	600	1.14	3	80.94
OBST_1403	600	1.14	3.3	75.894
OBST_1403	600	1.14	3.6	72.973
OBST_1403	600	1.14	3.9	68.895
OBST_1403	600	1.14	4.2	65.861
OBST_1403	600	1.14	4.5	60.361
OBST_1403	600	1.14	4.8	55.75
OBST_1403	600	1.14	5.1	52.542
OBST_1403	600	1.14	5.4	49.347
OBST_1403	600	1.14	5.7	46.011
OBST_1403	600	1.14	6	43.146
OBST_1406	1000	1.14	2.4	556.48
OBST_1406	1000	1.14	2.7	305.76
OBST_1406	1000	1.14	3	234.27
OBST_1406	1000	1.14	3.3	209.24

Table E-7
Soffit Sensitivity Results

Test	HRR (kW)	Source Height (m)	Elevation (m)	Maximum Plume Temperature Rise (C)
OBST_1406	1000	1.14	3.6	194.4
OBST_1406	1000	1.14	3.9	182.5
OBST_1406	1000	1.14	4.2	173.52
OBST_1406	1000	1.14	4.5	164.84
OBST_1406	1000	1.14	4.8	156.91
OBST_1406	1000	1.14	5.1	148.39
OBST_1406	1000	1.14	5.4	138.98
OBST_1406	1000	1.14	5.7	128.8
OBST_1409	200	1.98	2.4	402.02
OBST_1409	200	1.98	2.7	256.32
OBST_1409	200	1.98	3	190.56
OBST_1409	200	1.98	3.3	147.92
OBST_1409	200	1.98	3.6	132.96
OBST_1409	200	1.98	3.9	126.64
OBST_1409	200	1.98	4.2	114.66
OBST_1409	200	1.98	4.5	109.51
OBST_1409	200	1.98	4.8	96.45
OBST_1409	200	1.98	5.1	86.48
OBST_1409	200	1.98	5.4	80.21
OBST_1409	200	1.98	5.7	76.865
OBST_1409	200	1.98	6	58.705
OBST_1412	600	1.98	2.4	370.99
OBST_1412	600	1.98	2.7	223.24
OBST_1412	600	1.98	3	176.23
OBST_1412	600	1.98	3.3	147.97
OBST_1412	600	1.98	3.6	143.57
OBST_1412	600	1.98	3.9	135.99
OBST_1412	600	1.98	4.2	125.67
OBST_1412	600	1.98	4.5	113.93
OBST_1412	600	1.98	4.8	104.76
OBST_1412	600	1.98	5.1	97.8
OBST_1412	600	1.98	5.4	88.74
OBST_1412	600	1.98	5.7	77.893
OBST_1412	600	1.98	6	69.543
OBST_1415	1000	1.98	2.4	905.23
OBST_1415	1000	1.98	2.7	642.45

Table E-7
Soffit Sensitivity Results

Test	HRR (kW)	Source Height (m)	Elevation (m)	Maximum Plume Temperature Rise (C)
OBST_1415	1000	1.98	3	470.26
OBST_1415	1000	1.98	3.3	424.23
OBST_1415	1000	1.98	3.6	397.15
OBST_1415	1000	1.98	3.9	357.09
OBST_1415	1000	1.98	4.2	327.61
OBST_1415	1000	1.98	4.5	301.04
OBST_1415	1000	1.98	4.8	275.26
OBST_1415	1000	1.98	5.1	249.89
OBST_1415	1000	1.98	5.4	222.05
OBST_1415	1000	1.98	5.7	192.79
OBST_1415	1000	1.98	6	169.22
THREEWALL_1402	200	1.14	2.4	193.98
THREEWALL_1402	200	1.14	2.7	145.26
THREEWALL_1402	200	1.14	3	125.38
THREEWALL_1402	200	1.14	3.3	101.96
THREEWALL_1402	200	1.14	3.6	84.66
THREEWALL_1402	200	1.14	3.9	72.809
THREEWALL_1402	200	1.14	4.2	60.607
THREEWALL_1402	200	1.14	4.5	54.012
THREEWALL_1402	200	1.14	4.8	51.346
THREEWALL_1402	200	1.14	5.1	41.729
THREEWALL_1402	200	1.14	5.4	36.629
THREEWALL_1402	200	1.14	5.7	35.579
THREEWALL_1402	200	1.14	6	32.219
THREEWALL_1405	600	1.14	2.4	476.72
THREEWALL_1405	600	1.14	2.7	316.14
THREEWALL_1405	600	1.14	3	233.69
THREEWALL_1405	600	1.14	3.3	189.15
THREEWALL_1405	600	1.14	3.6	163.93
THREEWALL_1405	600	1.14	3.9	138.63
THREEWALL_1405	600	1.14	4.2	121.14
THREEWALL_1405	600	1.14	4.5	105.84
THREEWALL_1405	600	1.14	4.8	94.26
THREEWALL_1405	600	1.14	5.1	87.32
THREEWALL_1405	600	1.14	5.4	80.06
THREEWALL_1405	600	1.14	5.7	72.691

Table E-7
Soffit Sensitivity Results

Test	HRR (kW)	Source Height (m)	Elevation (m)	Maximum Plume Temperature Rise (C)
THREEWALL_1405	600	1.14	6	67.461
THREEWALL_1408	1000	1.14	2.4	625.88
THREEWALL_1408	1000	1.14	3	379.77
THREEWALL_1408	1000	1.14	3.3	307.8
THREEWALL_1408	1000	1.14	3.6	254.14
THREEWALL_1408	1000	1.14	3.9	206.26
THREEWALL_1408	1000	1.14	4.2	177.04
THREEWALL_1408	1000	1.14	4.5	147.71
THREEWALL_1408	1000	1.14	4.8	132.24
THREEWALL_1408	1000	1.14	5.1	115.84
THREEWALL_1408	1000	1.14	5.4	102.15
THREEWALL_1408	1000	1.14	5.7	95.34
THREEWALL_1408	1000	1.14	6	91.38
THREEWALL_1411	200	1.98	2.4	878.98
THREEWALL_1411	200	1.98	2.7	769.44
THREEWALL_1411	200	1.98	3	459.87
THREEWALL_1411	200	1.98	3.3	320.98
THREEWALL_1411	200	1.98	3.6	277.11
THREEWALL_1411	200	1.98	3.9	225.03
THREEWALL_1411	200	1.98	4.2	158.3
THREEWALL_1411	200	1.98	4.5	136.72
THREEWALL_1411	200	1.98	4.8	105.45
THREEWALL_1411	200	1.98	5.1	91.15
THREEWALL_1411	200	1.98	5.4	89.57
THREEWALL_1411	200	1.98	5.7	67.042
THREEWALL_1411	200	1.98	6	65.321
THREEWALL_1414	600	1.98	2.4	1004.1
THREEWALL_1414	600	1.98	2.7	1018.4
THREEWALL_1414	600	1.98	3	889.06
THREEWALL_1414	600	1.98	3.3	677.2
THREEWALL_1414	600	1.98	3.6	549.32
THREEWALL_1414	600	1.98	3.9	393.67
THREEWALL_1414	600	1.98	4.2	311.25
THREEWALL_1414	600	1.98	4.5	250.77
THREEWALL_1414	600	1.98	4.8	208.71
THREEWALL_1414	600	1.98	5.1	176.82

Table E-7
Soffit Sensitivity Results

Test	HRR (kW)	Source Height (m)	Elevation (m)	Maximum Plume Temperature Rise (C)
THREEWALL_1414	600	1.98	5.4	151.71
THREEWALL_1414	600	1.98	5.7	129
THREEWALL_1414	600	1.98	6	117.24
THREEWALL_1417	1000	1.98	2.4	985.6
THREEWALL_1417	1000	1.98	3	1016.6
THREEWALL_1417	1000	1.98	3.3	878.92
THREEWALL_1417	1000	1.98	3.6	749.52
THREEWALL_1417	1000	1.98	3.9	564.62
THREEWALL_1417	1000	1.98	4.2	441.37
THREEWALL_1417	1000	1.98	4.5	331.07
THREEWALL_1417	1000	1.98	4.8	264.23
THREEWALL_1417	1000	1.98	5.1	231.36
THREEWALL_1417	1000	1.98	5.4	198.27
THREEWALL_1417	1000	1.98	5.7	175.81
THREEWALL_1417	1000	1.98	6	160.01

Thickness of Steel Enclosure Sensitivity Results

Table E-8
Thickness of Steel Enclosure Sensitivity Results

Test	HRR (kW)	Source Height (m)	Elevation (m)	Maximum Plume Temperature Rise (C)	Thickness (m)
ARCH_1501	200	1.14	2.4	250.82	0.001
ARCH_1501	200	1.14	2.7	122.91	0.001
ARCH_1501	200	1.14	3	91.45	0.001
ARCH_1501	200	1.14	3.3	73.979	0.001
ARCH_1501	200	1.14	3.6	65.335	0.001
ARCH_1501	200	1.14	3.9	57.142	0.001
ARCH_1501	200	1.14	4.2	51.134	0.001
ARCH_1501	200	1.14	4.5	44.485	0.001
ARCH_1501	200	1.14	4.8	40.524	0.001
ARCH_1501	200	1.14	5.1	35.815	0.001
ARCH_1501	200	1.14	5.4	30.292	0.001
ARCH_1501	200	1.14	5.7	26.372	0.001
ARCH_1501	200	1.14	6	23.782	0.001
ARCH_1504	600	1.14	2.4	435.35	0.001
ARCH_1504	600	1.14	2.7	224.49	0.001
ARCH_1504	600	1.14	3	170.42	0.001
ARCH_1504	600	1.14	3.3	138.38	0.001
ARCH_1504	600	1.14	3.6	118.28	0.001
ARCH_1504	600	1.14	3.9	101.34	0.001
ARCH_1504	600	1.14	4.2	88.47	0.001
ARCH_1504	600	1.14	4.5	77.319	0.001
ARCH_1504	600	1.14	4.8	70.064	0.001
ARCH_1504	600	1.14	5.1	63.279	0.001
ARCH_1504	600	1.14	5.4	55.88	0.001
ARCH_1504	600	1.14	5.7	49.069	0.001
ARCH_1504	600	1.14	6	46.318	0.001
ARCH_1507	1000	1.14	2.4	492.48	0.001
ARCH_1507	1000	1.14	2.7	277.71	0.001
ARCH_1507	1000	1.14	3	204.56	0.001
ARCH_1507	1000	1.14	3.3	167.04	0.001
ARCH_1507	1000	1.14	3.6	141.3	0.001
ARCH_1507	1000	1.14	3.9	122.79	0.001
ARCH_1507	1000	1.14	4.2	108.05	0.001
ARCH_1507	1000	1.14	4.5	96.97	0.001
ARCH_1507	1000	1.14	4.8	87.07	0.001

Table E-8
Thickness of Steel Enclosure Sensitivity Results

Test	HRR (kW)	Source Height (m)	Elevation (m)	Maximum Plume Temperature Rise (C)	Thickness (m)
ARCH_1507	1000	1.14	5.1	80.05	0.001
ARCH_1507	1000	1.14	5.4	72.417	0.001
ARCH_1507	1000	1.14	5.7	66.252	0.001
OBST_1500	200	1.14	2.4	221.43	0.001
OBST_1500	200	1.14	2.7	142.99	0.001
OBST_1500	200	1.14	3	111.06	0.001
OBST_1500	200	1.14	3.3	96.39	0.001
OBST_1500	200	1.14	3.6	91.29	0.001
OBST_1500	200	1.14	3.9	86.53	0.001
OBST_1500	200	1.14	4.2	82.34	0.001
OBST_1500	200	1.14	4.5	76.998	0.001
OBST_1500	200	1.14	4.8	72.526	0.001
OBST_1500	200	1.14	5.1	68.481	0.001
OBST_1500	200	1.14	5.4	63.629	0.001
OBST_1500	200	1.14	5.7	59.183	0.001
OBST_1500	200	1.14	6	55.542	0.001
OBST_1503	600	1.14	2.4	527.39	0.001
OBST_1503	600	1.14	2.7	357.75	0.001
OBST_1503	600	1.14	3	259.18	0.001
OBST_1503	600	1.14	3.3	207.71	0.001
OBST_1503	600	1.14	3.6	192.77	0.001
OBST_1503	600	1.14	3.9	185.88	0.001
OBST_1503	600	1.14	4.2	178.84	0.001
OBST_1503	600	1.14	4.5	167.41	0.001
OBST_1503	600	1.14	4.8	156.9	0.001
OBST_1503	600	1.14	5.1	147.64	0.001
OBST_1503	600	1.14	5.4	136.39	0.001
OBST_1503	600	1.14	5.7	127.67	0.001
OBST_1503	600	1.14	6	119.2	0.001
OBST_1506	1000	1.14	2.4	644.94	0.001
OBST_1506	1000	1.14	2.7	476.7	0.001
OBST_1506	1000	1.14	3	361.87	0.001
OBST_1506	1000	1.14	3.3	282.67	0.001
OBST_1506	1000	1.14	3.6	247.17	0.001
OBST_1506	1000	1.14	3.9	232.76	0.001
OBST_1506	1000	1.14	4.2	222.02	0.001

Table E-8
Thickness of Steel Enclosure Sensitivity Results

Test	HRR (kW)	Source Height (m)	Elevation (m)	Maximum Plume Temperature Rise (C)	Thickness (m)
OBST_1506	1000	1.14	4.5	209.18	0.001
OBST_1506	1000	1.14	4.8	200.17	0.001
OBST_1506	1000	1.14	5.1	189.85	0.001
OBST_1506	1000	1.14	5.4	178.66	0.001
OBST_1506	1000	1.14	5.7	168.58	0.001
THREEWALL_1502	200	1.14	2.4	303.37	0.001
THREEWALL_1502	200	1.14	2.7	165.48	0.001
THREEWALL_1502	200	1.14	3	121.14	0.001
THREEWALL_1502	200	1.14	3.3	98	0.001
THREEWALL_1502	200	1.14	3.6	88.09	0.001
THREEWALL_1502	200	1.14	3.9	79.77	0.001
THREEWALL_1502	200	1.14	4.2	72.972	0.001
THREEWALL_1502	200	1.14	4.5	64.726	0.001
THREEWALL_1502	200	1.14	4.8	59.19	0.001
THREEWALL_1502	200	1.14	5.1	54.454	0.001
THREEWALL_1502	200	1.14	5.4	47.665	0.001
THREEWALL_1502	200	1.14	5.7	42.54	0.001
THREEWALL_1502	200	1.14	6	39.323	0.001
THREEWALL_1505	600	1.14	2.4	623.89	0.001
THREEWALL_1505	600	1.14	2.7	350.4	0.001
THREEWALL_1505	600	1.14	3	267.62	0.001
THREEWALL_1505	600	1.14	3.3	212.45	0.001
THREEWALL_1505	600	1.14	3.6	185.57	0.001
THREEWALL_1505	600	1.14	3.9	155.18	0.001
THREEWALL_1505	600	1.14	4.2	131.07	0.001
THREEWALL_1505	600	1.14	4.5	113.77	0.001
THREEWALL_1505	600	1.14	4.8	100.05	0.001
THREEWALL_1505	600	1.14	5.1	86.74	0.001
THREEWALL_1505	600	1.14	5.4	75.044	0.001
THREEWALL_1505	600	1.14	5.7	67.165	0.001
THREEWALL_1505	600	1.14	6	63.244	0.001
THREEWALL_1508	1000	1.14	2.4	715.92	0.001
THREEWALL_1508	1000	1.14	2.7	476.43	0.001
THREEWALL_1508	1000	1.14	3	360.41	0.001
THREEWALL_1508	1000	1.14	3.3	278.18	0.001
THREEWALL_1508	1000	1.14	3.6	231.1	0.001

Table E-8
Thickness of Steel Enclosure Sensitivity Results

Test	HRR (kW)	Source Height (m)	Elevation (m)	Maximum Plume Temperature Rise (C)	Thickness (m)
THREEWALL_1508	1000	1.14	3.9	195.64	0.001
THREEWALL_1508	1000	1.14	4.2	166.35	0.001
THREEWALL_1508	1000	1.14	4.5	147.25	0.001
THREEWALL_1508	1000	1.14	4.8	134.56	0.001
THREEWALL_1508	1000	1.14	5.1	123.22	0.001
THREEWALL_1508	1000	1.14	5.4	110.95	0.001
THREEWALL_1508	1000	1.14	5.7	104.12	0.001
THREEWALL_1511	200	1.14	2.4	304.79	0.01
THREEWALL_1511	200	1.14	2.7	160.73	0.01
THREEWALL_1511	200	1.14	3	119.09	0.01
THREEWALL_1511	200	1.14	3.3	97.25	0.01
THREEWALL_1511	200	1.14	3.6	85.38	0.01
THREEWALL_1511	200	1.14	3.9	74.484	0.01
THREEWALL_1511	200	1.14	4.2	66.641	0.01
THREEWALL_1511	200	1.14	4.5	60.376	0.01
THREEWALL_1511	200	1.14	4.8	52.668	0.01
THREEWALL_1511	200	1.14	5.1	47.908	0.01
THREEWALL_1511	200	1.14	5.4	43.55	0.01
THREEWALL_1511	200	1.14	5.7	39.752	0.01
THREEWALL_1511	200	1.14	6	35.703	0.01
THREEWALL_1514	600	1.14	2.4	595.67	0.01
THREEWALL_1514	600	1.14	2.7	324.91	0.01
THREEWALL_1514	600	1.14	3	240.21	0.01
THREEWALL_1514	600	1.14	3.3	187.97	0.01
THREEWALL_1514	600	1.14	3.6	163.55	0.01
THREEWALL_1514	600	1.14	3.9	139.83	0.01
THREEWALL_1514	600	1.14	4.2	120.71	0.01
THREEWALL_1514	600	1.14	4.5	104.05	0.01
THREEWALL_1514	600	1.14	4.8	92.7	0.01
THREEWALL_1514	600	1.14	5.1	85.08	0.01
THREEWALL_1514	600	1.14	5.4	76.946	0.01
THREEWALL_1514	600	1.14	5.7	70.893	0.01
THREEWALL_1514	600	1.14	6	67.715	0.01
THREEWALL_1517	1000	1.14	2.4	701.19	0.01
THREEWALL_1517	1000	1.14	2.7	470.49	0.01
THREEWALL_1517	1000	1.14	3	346.27	0.01

Table E-8
Thickness of Steel Enclosure Sensitivity Results

Test	HRR (kW)	Source Height (m)	Elevation (m)	Maximum Plume Temperature Rise (C)	Thickness (m)
THREEWALL_1517	1000	1.14	3.3	262.03	0.01
THREEWALL_1517	1000	1.14	3.6	220.57	0.01
THREEWALL_1517	1000	1.14	3.9	185.24	0.01
THREEWALL_1517	1000	1.14	4.2	163.31	0.01
THREEWALL_1517	1000	1.14	4.5	140.66	0.01
THREEWALL_1517	1000	1.14	4.8	125.6	0.01
THREEWALL_1517	1000	1.14	5.1	116.23	0.01
THREEWALL_1517	1000	1.14	5.4	104.95	0.01
THREEWALL_1517	1000	1.14	5.7	93.75	0.01
ARCH_1510	200	1.14	2.4	228.86	0.01
ARCH_1510	200	1.14	2.7	116.86	0.01
ARCH_1510	200	1.14	3	86.34	0.01
ARCH_1510	200	1.14	3.3	69.641	0.01
ARCH_1510	200	1.14	3.6	61.122	0.01
ARCH_1510	200	1.14	3.9	52.889	0.01
ARCH_1510	200	1.14	4.2	46.881	0.01
ARCH_1510	200	1.14	4.5	41.449	0.01
ARCH_1510	200	1.14	4.8	37.267	0.01
ARCH_1510	200	1.14	5.1	33.707	0.01
ARCH_1510	200	1.14	5.4	30.218	0.01
ARCH_1510	200	1.14	5.7	26.702	0.01
ARCH_1510	200	1.14	6	24.662	0.01
ARCH_1513	600	1.14	2.4	377.92	0.01
ARCH_1513	600	1.14	2.7	209.24	0.01
ARCH_1513	600	1.14	3	155.21	0.01
ARCH_1513	600	1.14	3.3	124.19	0.01
ARCH_1513	600	1.14	3.6	107.66	0.01
ARCH_1513	600	1.14	3.9	95.51	0.01
ARCH_1513	600	1.14	4.2	85.55	0.01
ARCH_1513	600	1.14	4.5	74.663	0.01
ARCH_1513	600	1.14	4.8	67.36	0.01
ARCH_1513	600	1.14	5.1	60.475	0.01
ARCH_1513	600	1.14	5.4	53.375	0.01
ARCH_1513	600	1.14	5.7	48.259	0.01
ARCH_1513	600	1.14	6	43.989	0.01
ARCH_1516	1000	1.14	2.4	474.54	0.01

Table E-8
Thickness of Steel Enclosure Sensitivity Results

Test	HRR (kW)	Source Height (m)	Elevation (m)	Maximum Plume Temperature Rise (C)	Thickness (m)
ARCH_1516	1000	1.14	2.7	274.81	0.01
ARCH_1516	1000	1.14	3	198.87	0.01
ARCH_1516	1000	1.14	3.3	153.78	0.01
ARCH_1516	1000	1.14	3.6	132.35	0.01
ARCH_1516	1000	1.14	3.9	112.46	0.01
ARCH_1516	1000	1.14	4.2	100.01	0.01
ARCH_1516	1000	1.14	4.5	89.47	0.01
ARCH_1516	1000	1.14	4.8	78.582	0.01
ARCH_1516	1000	1.14	5.1	73.207	0.01
ARCH_1516	1000	1.14	5.4	65.564	0.01
ARCH_1516	1000	1.14	5.7	61.595	0.01
OBST_1509	200	1.14	2.4	220.64	0.01
OBST_1509	200	1.14	2.7	143.53	0.01
OBST_1509	200	1.14	3	108.73	0.01
OBST_1509	200	1.14	3.3	93.59	0.01
OBST_1509	200	1.14	3.6	87.24	0.01
OBST_1509	200	1.14	3.9	81.81	0.01
OBST_1509	200	1.14	4.2	77.448	0.01
OBST_1509	200	1.14	4.5	71.911	0.01
OBST_1509	200	1.14	4.8	66.742	0.01
OBST_1509	200	1.14	5.1	61.984	0.01
OBST_1509	200	1.14	5.4	56.47	0.01
OBST_1509	200	1.14	5.7	52.427	0.01
OBST_1509	200	1.14	6	48.606	0.01
OBST_1512	600	1.14	2.4	500.81	0.01
OBST_1512	600	1.14	2.7	344.7	0.01
OBST_1512	600	1.14	3	248.73	0.01
OBST_1512	600	1.14	3.3	212.99	0.01
OBST_1512	600	1.14	3.6	191.17	0.01
OBST_1512	600	1.14	3.9	177.62	0.01
OBST_1512	600	1.14	4.2	171.53	0.01
OBST_1512	600	1.14	4.5	162.67	0.01
OBST_1512	600	1.14	4.8	155.08	0.01
OBST_1512	600	1.14	5.1	147.56	0.01
OBST_1512	600	1.14	5.4	136.28	0.01
OBST_1512	600	1.14	5.7	124.2	0.01

Table E-8
Thickness of Steel Enclosure Sensitivity Results

Test	HRR (kW)	Source Height (m)	Elevation (m)	Maximum Plume Temperature Rise (C)	Thickness (m)
OBST_1512	600	1.14	6	114.51	0.01
OBST_1515	1000	1.14	2.4	639.31	0.01
OBST_1515	1000	1.14	2.7	488.85	0.01
OBST_1515	1000	1.14	3	345.77	0.01
OBST_1515	1000	1.14	3.3	278.41	0.01
OBST_1515	1000	1.14	3.6	247.68	0.01
OBST_1515	1000	1.14	3.9	238.16	0.01
OBST_1515	1000	1.14	4.2	226.04	0.01
OBST_1515	1000	1.14	4.5	211.45	0.01
OBST_1515	1000	1.14	4.8	201.03	0.01
OBST_1515	1000	1.14	5.1	190.12	0.01
OBST_1515	1000	1.14	5.4	178.62	0.01

Horizontal Plume Shift and Angle Sensitivity Results

Table E-9
Horizontal Plume Shift and Angle Sensitivity Results

Test	HRR (kW)	Source Height (m)	Elevation (m)	Maximum Plume Temperature Rise (C)	Diameter (m)	R_{PO} (m)	R_{rad}Thermoplastic (m)	R_{rad}Thermoset (m)	Angle
ARCH_1055	1000	1.14	2.4	686.62	0.91	0.7	2.40	1.88	13
ARCH_1055	1000	1.14	2.7	439.45	0.91	0.9	2.40	1.88	18
ARCH_1055	1000	1.14	3	317.19	0.91	1.02	2.40	1.88	18
ARCH_1055	1000	1.14	3.3	251.35	0.91	1.1	2.40	1.88	18
ARCH_1055	1000	1.14	3.6	207.5	0.91	1.22	2.40	1.88	18
ARCH_1055	1000	1.14	3.9	181.32	0.91	1.26	2.40	1.88	17
ARCH_1055	1000	1.14	4.2	158.36	0.91	1.3	2.40	1.88	16
ARCH_1055	1000	1.14	4.5	139.08	0.91	1.34	2.40	1.88	16
ARCH_1055	1000	1.14	4.8	123.06	0.91	1.38	2.40	1.88	15
ARCH_1056	1000	1.98	3.3	724.08	0.91	0.42	2.40	1.88	1
ARCH_1056	1000	1.98	3.6	603.99	0.91	0.42	2.40	1.88	1
ARCH_1064	1000	1.14	2.4	498.48	1.22	0.9	2.53	2.01	16
ARCH_1064	1000	1.14	2.7	290.87	1.22	1.1	2.53	2.01	20
ARCH_1064	1000	1.14	3	228.02	1.22	1.22	2.53	2.01	20
ARCH_1064	1000	1.14	3.3	180.07	1.22	1.38	2.53	2.01	21
ARCH_1064	1000	1.14	3.6	153.69	1.22	1.46	2.53	2.01	21
ARCH_1064	1000	1.14	3.9	132.29	1.22	1.54	2.53	2.01	20
ARCH_1064	1000	1.14	4.2	119.64	1.22	1.62	2.53	2.01	19
ARCH_1065	1000	1.98	3	697.19	1.22	0.62	2.53	2.01	4
ARCH_1065	1000	1.98	3.3	539.48	1.22	0.62	2.53	2.01	3
ARCH_1065	1000	1.98	3.6	429.2	1.22	0.58	2.53	2.01	1
ARCH_1065	1000	1.98	3.9	322.39	1.22	0.58	2.53	2.01	1

Table E-9
Horizontal Plume Shift and Angle Sensitivity Results

Test	HRR (kW)	Source Height (m)	Elevation (m)	Maximum Plume Temperature Rise (C)	Diameter (m)	R_{PO} (m)	R_{rad}Thermoplastic (m)	R_{rad}Thermoset (m)	Angle
ARCH_830	100	1.14	2.4	198.07	0.30	0.34	0.77	0.60	9
ARCH_830	100	1.14	2.7	112.16	0.30	0.5	0.77	0.60	13
ARCH_836	50	1.98	2.4	246.03	0.30	0.3	0.58	0.46	22
ARCH_836	50	1.98	2.7	126.04	0.30	0.38	0.58	0.46	19
ARCH_837	100	1.98	2.4	511.44	0.30	0.22	0.77	0.60	11
ARCH_837	100	1.98	2.7	255.75	0.30	0.38	0.77	0.60	19
ARCH_837	100	1.98	3	171.73	0.30	0.42	0.77	0.60	16
ARCH_837	100	1.98	3.3	118.23	0.30	0.46	0.77	0.60	14
ARCH_894	200	1.14	2.4	239.92	0.61	0.54	1.16	0.93	12
ARCH_894	200	1.14	2.7	120.83	0.61	0.82	1.16	0.93	19
ARCH_895	300	1.14	2.4	330.38	0.61	0.5	1.36	1.08	10
ARCH_895	300	1.14	2.7	172.02	0.61	0.78	1.36	1.08	18
ARCH_895	300	1.14	3	125.64	0.61	0.9	1.36	1.08	19
ARCH_896	400	1.14	2.4	555.97	0.61	0.5	1.53	1.20	10
ARCH_896	400	1.14	2.7	253.67	0.61	0.7	1.53	1.20	15
ARCH_896	400	1.14	3	172.71	0.61	0.86	1.53	1.20	18
ARCH_896	400	1.14	3.3	135.45	0.61	0.94	1.53	1.20	17
ARCH_896	400	1.14	3.6	115.42	0.61	1.1	1.53	1.20	19
ARCH_897	500	1.14	2.4	685.87	0.61	0.46	1.68	1.31	9
ARCH_897	500	1.14	2.7	385.73	0.61	0.62	1.68	1.31	13
ARCH_897	500	1.14	3	255.53	0.61	0.7	1.68	1.31	13
ARCH_897	500	1.14	3.3	187.46	0.61	0.82	1.68	1.31	14
ARCH_897	500	1.14	3.6	155.04	0.61	0.98	1.68	1.31	16
ARCH_897	500	1.14	3.9	131.32	0.61	1.02	1.68	1.31	15
ARCH_897	500	1.14	4.2	114.1	0.61	1.06	1.68	1.31	14

Table E-9
Horizontal Plume Shift and Angle Sensitivity Results

Test	HRR (kW)	Source Height (m)	Elevation (m)	Maximum Plume Temperature Rise (C)	Diameter (m)	R_{PO} (m)	R_{rad}Thermoplastic (m)	R_{rad}Thermoset (m)	Angle
ARCH_898	600	1.14	2.4	757.31	0.61	0.5	1.82	1.41	10
ARCH_898	600	1.14	2.7	435.11	0.61	0.66	1.82	1.41	14
ARCH_898	600	1.14	3	317.58	0.61	0.74	1.82	1.41	14
ARCH_898	600	1.14	3.3	232	0.61	0.86	1.82	1.41	15
ARCH_898	600	1.14	3.6	193.7	0.61	0.9	1.82	1.41	14
ARCH_898	600	1.14	3.9	158.56	0.61	0.94	1.82	1.41	14
ARCH_898	600	1.14	4.2	134.6	0.61	0.98	1.82	1.41	13
ARCH_898	600	1.14	4.5	113.8	0.61	1.02	1.82	1.41	13
ARCH_901	200	1.98	2.4	673.58	0.61	0.38	1.16	0.93	15
ARCH_901	200	1.98	2.7	349.88	0.61	0.46	1.16	0.93	15
ARCH_901	200	1.98	3	233.64	0.61	0.5	1.16	0.93	13
ARCH_901	200	1.98	3.3	174.13	0.61	0.5	1.16	0.93	10
ARCH_901	200	1.98	3.6	141.03	0.61	0.54	1.16	0.93	9
ARCH_901	200	1.98	3.9	110.93	0.61	0.54	1.16	0.93	8
ARCH_902	300	1.98	2.7	637.24	0.61	0.42	1.36	1.08	12
ARCH_902	300	1.98	3	430.61	0.61	0.42	1.36	1.08	8
ARCH_902	300	1.98	3.3	325.15	0.61	0.42	1.36	1.08	6
ARCH_902	300	1.98	3.6	252.2	0.61	0.42	1.36	1.08	5
ARCH_902	300	1.98	3.9	194.8	0.61	0.42	1.36	1.08	4
ARCH_902	300	1.98	4.2	158.08	0.61	0.42	1.36	1.08	4
ARCH_902	300	1.98	4.5	126.34	0.61	0.42	1.36	1.08	3
ARCH_903	400	1.98	3	692.12	0.61	0.42	1.53	1.20	8
ARCH_903	400	1.98	3.3	495.23	0.61	0.42	1.53	1.20	6
ARCH_903	400	1.98	3.6	367.41	0.61	0.42	1.53	1.20	5
ARCH_903	400	1.98	3.9	269.44	0.61	0.42	1.53	1.20	4

Table E-9
Horizontal Plume Shift and Angle Sensitivity Results

Test	HRR (kW)	Source Height (m)	Elevation (m)	Maximum Plume Temperature Rise (C)	Diameter (m)	R_{PO} (m)	R_{rad}Thermoplastic (m)	R_{rad}Thermoset (m)	Angle
ARCH_903	400	1.98	4.2	212.59	0.61	0.38	1.53	1.20	3
ARCH_903	400	1.98	4.5	163.52	0.61	0.38	1.53	1.20	3
ARCH_903	400	1.98	4.8	137.37	0.61	0.38	1.53	1.20	2
ARCH_903	400	1.98	5.1	118.3	0.61	0.38	1.53	1.20	2
ARCH_904	500	1.98	3.3	733.53	0.61	0.38	1.68	1.31	5
ARCH_904	500	1.98	3.6	574.4	0.61	0.42	1.68	1.31	5
ARCH_904	500	1.98	3.9	414.66	0.61	0.42	1.68	1.31	4
ARCH_904	500	1.98	4.2	314.39	0.61	0.38	1.68	1.31	3
ARCH_904	500	1.98	4.5	236.69	0.61	0.38	1.68	1.31	3
ARCH_904	500	1.98	4.8	193.59	0.61	0.34	1.68	1.31	1
ARCH_904	500	1.98	5.1	162.15	0.61	0.34	1.68	1.31	1
ARCH_904	500	1.98	5.4	138.1	0.61	0.3	1.68	1.31	1
ARCH_904	500	1.98	5.7	115.49	0.61	0.3	1.68	1.31	0
ARCH_905	600	1.98	3.6	714.06	0.61	0.42	1.82	1.41	5
ARCH_905	600	1.98	3.9	513.68	0.61	0.42	1.82	1.41	4
ARCH_905	600	1.98	4.2	398.77	0.61	0.42	1.82	1.41	4
ARCH_905	600	1.98	4.5	299.55	0.61	0.42	1.82	1.41	3
ARCH_905	600	1.98	4.8	243.95	0.61	0.38	1.82	1.41	2
ARCH_905	600	1.98	5.1	198.04	0.61	0.38	1.82	1.41	2
ARCH_905	600	1.98	5.4	162.57	0.61	0.34	1.82	1.41	1
ARCH_905	600	1.98	5.7	134.08	0.61	0.34	1.82	1.41	1
ARCH_905	600	1.98	6	116.82	0.61	0.34	1.82	1.41	1
ARCH_958	300	1.14	2.4	201.52	0.91	0.78	1.50	1.21	17
ARCH_958	300	1.14	2.7	115.52	0.91	1.1	1.50	1.21	24
ARCH_959	400	1.14	2.4	254.49	0.91	0.74	1.67	1.34	15

Table E-9
Horizontal Plume Shift and Angle Sensitivity Results

Test	HRR (kW)	Source Height (m)	Elevation (m)	Maximum Plume Temperature Rise (C)	Diameter (m)	R_{PO} (m)	R_{rad}Thermoplastic (m)	R_{rad}Thermoset (m)	Angle
ARCH_959	400	1.14	2.7	150.19	0.91	1.06	1.67	1.34	23
ARCH_959	400	1.14	3	115.72	0.91	1.22	1.67	1.34	24
ARCH_960	500	1.14	2.4	351.76	0.91	0.7	1.82	1.45	13
ARCH_960	500	1.14	2.7	186.86	0.91	0.98	1.82	1.45	20
ARCH_960	500	1.14	3	146.01	0.91	1.18	1.82	1.45	23
ARCH_960	500	1.14	3.3	117.15	0.91	1.3	1.82	1.45	23
ARCH_961	600	1.14	2.4	412.98	0.91	0.7	1.95	1.55	13
ARCH_961	600	1.14	2.7	217.42	0.91	0.98	1.95	1.55	20
ARCH_961	600	1.14	3	164.16	0.91	1.14	1.95	1.55	22
ARCH_961	600	1.14	3.3	132.43	0.91	1.26	1.95	1.55	22
ARCH_961	600	1.14	3.6	113.03	0.91	1.38	1.95	1.55	22
ARCH_965	300	1.98	2.4	587.47	0.91	0.54	1.50	1.21	18
ARCH_965	300	1.98	2.7	311.53	0.91	0.58	1.50	1.21	14
ARCH_965	300	1.98	3	212.09	0.91	0.58	1.50	1.21	10
ARCH_965	300	1.98	3.3	157.64	0.91	0.62	1.50	1.21	9
ARCH_965	300	1.98	3.6	126.25	0.91	0.66	1.50	1.21	9
ARCH_966	400	1.98	2.7	532.14	0.91	0.62	1.67	1.34	17
ARCH_966	400	1.98	3	348	0.91	0.58	1.67	1.34	10
ARCH_966	400	1.98	3.3	255.26	0.91	0.58	1.67	1.34	8
ARCH_966	400	1.98	3.6	199.12	0.91	0.62	1.67	1.34	8
ARCH_966	400	1.98	3.9	160.14	0.91	0.62	1.67	1.34	6
ARCH_966	400	1.98	4.2	134.08	0.91	0.62	1.67	1.34	6
ARCH_966	400	1.98	4.5	110.46	0.91	0.62	1.67	1.34	5
ARCH_967	500	1.98	2.7	622.57	0.91	0.62	1.82	1.45	17
ARCH_967	500	1.98	3	429.19	0.91	0.54	1.82	1.45	8

Table E-9
Horizontal Plume Shift and Angle Sensitivity Results

Test	HRR (kW)	Source Height (m)	Elevation (m)	Maximum Plume Temperature Rise (C)	Diameter (m)	R_{PO} (m)	R_{rad}Thermoplastic (m)	R_{rad}Thermoset (m)	Angle
ARCH_967	500	1.98	3.3	304.39	0.91	0.54	1.82	1.45	6
ARCH_967	500	1.98	3.6	232.72	0.91	0.58	1.82	1.45	6
ARCH_967	500	1.98	3.9	196.54	0.91	0.58	1.82	1.45	5
ARCH_967	500	1.98	4.2	163.63	0.91	0.58	1.82	1.45	5
ARCH_967	500	1.98	4.5	133.81	0.91	0.58	1.82	1.45	4
ARCH_967	500	1.98	4.5	133.81	0.91	0.58	1.82	1.45	4
ARCH_967	500	1.98	4.8	114.52	0.91	0.58	1.82	1.45	4
ARCH_968	600	1.98	2.7	697.36	0.91	0.5	1.95	1.55	8
ARCH_968	600	1.98	3	529.99	0.91	0.54	1.95	1.55	8
ARCH_968	600	1.98	3.3	392.15	0.91	0.54	1.95	1.55	6
ARCH_968	600	1.98	3.6	291.81	0.91	0.54	1.95	1.55	5
ARCH_968	600	1.98	3.9	225.14	0.91	0.5	1.95	1.55	3
ARCH_968	600	1.98	4.2	189.01	0.91	0.5	1.95	1.55	2
ARCH_968	600	1.98	4.5	153.48	0.91	0.46	1.95	1.55	1
ARCH_968	600	1.98	4.8	129.83	0.91	0.42	1.95	1.55	0
ARCH_968	600	1.98	5.1	111.62	0.91	0.42	1.95	1.55	0
THREEWALL_1058	1000	1.14	2.7	620.76	0.91	1.06	2.40	1.88	23
THREEWALL_1058	1000	1.14	3	484.86	0.91	1.22	2.40	1.88	24
THREEWALL_1058	1000	1.14	3.3	381.71	0.91	1.34	2.40	1.88	23
THREEWALL_1058	1000	1.14	3.6	319.8	0.91	1.42	2.40	1.88	22
THREEWALL_1058	1000	1.14	3.9	264.72	0.91	1.46	2.40	1.88	21
THREEWALL_1058	1000	1.14	4.2	230.82	0.91	1.54	2.40	1.88	20
THREEWALL_1058	1000	1.14	4.5	195.58	0.91	1.58	2.40	1.88	19
THREEWALL_1058	1000	1.14	4.8	168.42	0.91	1.62	2.40	1.88	18
THREEWALL_1058	1000	1.14	5.1	146.49	0.91	1.66	2.40	1.88	18

Table E-9
Horizontal Plume Shift and Angle Sensitivity Results

Test	HRR (kW)	Source Height (m)	Elevation (m)	Maximum Plume Temperature Rise (C)	Diameter (m)	R_{PO} (m)	R_{rad}Thermoplastic (m)	R_{rad}Thermoset (m)	Angle
THREEWALL_1058	1000	1.14	5.4	126.15	0.91	1.7	2.40	1.88	17
THREEWALL_1058	1000	1.14	5.7	115.05	0.91	1.58	2.40	1.88	14
THREEWALL_1059	1000	1.98	3.9	646.54	0.91	0.58	2.40	1.88	5
THREEWALL_1059	1000	1.98	4.2	527.72	0.91	0.58	2.40	1.88	5
THREEWALL_1059	1000	1.98	4.5	411.6	0.91	0.58	2.40	1.88	4
THREEWALL_1059	1000	1.98	4.8	334.89	0.91	0.58	2.40	1.88	4
THREEWALL_1059	1000	1.98	5.1	286.67	0.91	0.58	2.40	1.88	3
THREEWALL_1059	1000	1.98	5.4	244.2	0.91	0.58	2.40	1.88	3
THREEWALL_1059	1000	1.98	5.7	207.16	0.91	0.58	2.40	1.88	3
THREEWALL_1059	1000	1.98	6	186.73	0.91	0.58	2.40	1.88	2
THREEWALL_1067	1000	1.14	2.4	663.06	1.22	0.94	2.53	2.01	18
THREEWALL_1067	1000	1.14	2.7	440.84	1.22	1.22	2.53	2.01	24
THREEWALL_1067	1000	1.14	3	343.31	1.22	1.38	2.53	2.01	24
THREEWALL_1067	1000	1.14	3.3	279.81	1.22	1.5	2.53	2.01	24
THREEWALL_1067	1000	1.14	3.6	235.01	1.22	1.66	2.53	2.01	25
THREEWALL_1067	1000	1.14	3.9	190.95	1.22	1.74	2.53	2.01	24
THREEWALL_1067	1000	1.14	4.2	167.89	1.22	1.82	2.53	2.01	23
THREEWALL_1067	1000	1.14	4.5	141.24	1.22	1.82	2.53	2.01	21
THREEWALL_1067	1000	1.14	4.8	125.62	1.22	1.98	2.53	2.01	21
THREEWALL_1067	1000	1.14	5.1	112.94	1.22	1.86	2.53	2.01	18
THREEWALL_1068	1000	1.98	3.6	659.45	1.22	0.7	2.53	2.01	6
THREEWALL_1068	1000	1.98	3.9	496.14	1.22	0.78	2.53	2.01	7
THREEWALL_1068	1000	1.98	4.2	397.07	1.22	0.82	2.53	2.01	7
THREEWALL_1068	1000	1.98	4.5	318.85	1.22	0.78	2.53	2.01	5
THREEWALL_1068	1000	1.98	4.8	272.29	1.22	0.74	2.53	2.01	4

Table E-9
Horizontal Plume Shift and Angle Sensitivity Results

Test	HRR (kW)	Source Height (m)	Elevation (m)	Maximum Plume Temperature Rise (C)	Diameter (m)	R_{PO} (m)	R_{rad}Thermoplastic (m)	R_{rad}Thermoset (m)	Angle
THREEWALL_1068	1000	1.98	5.1	234.15	1.22	0.78	2.53	2.01	4
THREEWALL_1068	1000	1.98	5.4	204.04	1.22	0.7	2.53	2.01	3
THREEWALL_1068	1000	1.98	5.7	179.74	1.22	0.7	2.53	2.01	2
THREEWALL_1068	1000	1.98	6	161.86	1.22	0.7	2.53	2.01	2
THREEWALL_850	50	1.14	2.4	155.3	0.30	0.46	0.58	0.46	14
THREEWALL_851	100	1.14	2.4	255.53	0.30	0.46	0.77	0.60	14
THREEWALL_851	100	1.14	2.7	139.25	0.30	0.7	0.77	0.60	20
THREEWALL_857	50	1.98	2.4	415.6	0.30	0.26	0.58	0.46	17
THREEWALL_857	50	1.98	2.7	235.48	0.30	0.34	0.58	0.46	16
THREEWALL_857	50	1.98	3	157.34	0.30	0.38	0.58	0.46	14
THREEWALL_857	50	1.98	3.3	111.29	0.30	0.46	0.58	0.46	14
THREEWALL_858	100	1.98	2.7	510.25	0.30	0.34	0.77	0.60	16
THREEWALL_858	100	1.98	3	327.37	0.30	0.38	0.77	0.60	14
THREEWALL_858	100	1.98	3.3	218.83	0.30	0.38	0.77	0.60	11
THREEWALL_858	100	1.98	3.6	169.87	0.30	0.42	0.77	0.60	10
THREEWALL_858	100	1.98	3.9	135.33	0.30	0.42	0.77	0.60	8
THREEWALL_915	200	1.14	2.4	300.06	0.61	0.7	1.16	0.93	19
THREEWALL_915	200	1.14	2.7	159.86	0.61	0.94	1.16	0.93	23
THREEWALL_915	200	1.14	3	134.36	0.61	1.1	1.16	0.93	24
THREEWALL_916	300	1.14	2.4	488.54	0.61	0.66	1.36	1.08	17
THREEWALL_916	300	1.14	2.7	250.02	0.61	0.9	1.36	1.08	22
THREEWALL_916	300	1.14	3	174.28	0.61	1.02	1.36	1.08	22
THREEWALL_916	300	1.14	3.3	141.38	0.61	1.14	1.36	1.08	22
THREEWALL_916	300	1.14	3.6	123.99	0.61	1.26	1.36	1.08	22
THREEWALL_916	300	1.14	3.9	110.29	0.61	1.34	1.36	1.08	21

Table E-9
Horizontal Plume Shift and Angle Sensitivity Results

Test	HRR (kW)	Source Height (m)	Elevation (m)	Maximum Plume Temperature Rise (C)	Diameter (m)	R_{PO} (m)	R_{rad}Thermoplastic (m)	R_{rad}Thermoset (m)	Angle
THREEWALL_917	400	1.14	2.4	663.59	0.61	0.62	1.53	1.20	16
THREEWALL_917	400	1.14	2.7	370.31	0.61	0.86	1.53	1.20	21
THREEWALL_917	400	1.14	3	250.68	0.61	0.98	1.53	1.20	21
THREEWALL_917	400	1.14	3.3	183.21	0.61	1.1	1.53	1.20	21
THREEWALL_917	400	1.14	3.6	152.33	0.61	1.18	1.53	1.20	20
THREEWALL_917	400	1.14	3.9	132.92	0.61	1.3	1.53	1.20	20
THREEWALL_917	400	1.14	4.2	118.8	0.61	1.34	1.53	1.20	19
THREEWALL_918	500	1.14	2.7	466.61	0.61	0.78	1.68	1.31	18
THREEWALL_918	500	1.14	3	313.59	0.61	0.86	1.68	1.31	18
THREEWALL_918	500	1.14	3.3	222.06	0.61	1.02	1.68	1.31	19
THREEWALL_918	500	1.14	3.6	184.52	0.61	1.14	1.68	1.31	19
THREEWALL_918	500	1.14	3.9	155.58	0.61	1.22	1.68	1.31	19
THREEWALL_918	500	1.14	4.2	134.38	0.61	1.3	1.68	1.31	19
THREEWALL_918	500	1.14	4.5	110.96	0.61	1.34	1.68	1.31	18
THREEWALL_919	600	1.14	2.7	562.28	0.61	0.78	1.82	1.41	18
THREEWALL_919	600	1.14	3	416.03	0.61	0.9	1.82	1.41	19
THREEWALL_919	600	1.14	3.3	305.81	0.61	1.02	1.82	1.41	19
THREEWALL_919	600	1.14	3.6	248	0.61	1.14	1.82	1.41	19
THREEWALL_919	600	1.14	3.9	203.92	0.61	1.18	1.82	1.41	18
THREEWALL_919	600	1.14	4.2	176.1	0.61	1.22	1.82	1.41	17
THREEWALL_919	600	1.14	4.5	152.14	0.61	1.26	1.82	1.41	16
THREEWALL_919	600	1.14	4.8	138.53	0.61	1.26	1.82	1.41	15
THREEWALL_919	600	1.14	5.1	123.64	0.61	1.3	1.82	1.41	15
THREEWALL_922	200	1.98	2.7	587.45	0.61	0.5	1.16	0.93	18
THREEWALL_922	200	1.98	3	418.25	0.61	0.54	1.16	0.93	15

Table E-9
Horizontal Plume Shift and Angle Sensitivity Results

Test	HRR (kW)	Source Height (m)	Elevation (m)	Maximum Plume Temperature Rise (C)	Diameter (m)	R_{PO} (m)	R_{rad}Thermoplastic (m)	R_{rad}Thermoset (m)	Angle
THREEWALL_922	200	1.98	3.3	309.14	0.61	0.58	1.16	0.93	13
THREEWALL_922	200	1.98	3.6	236.87	0.61	0.62	1.16	0.93	12
THREEWALL_922	200	1.98	3.9	183.85	0.61	0.62	1.16	0.93	10
THREEWALL_922	200	1.98	4.2	148.83	0.61	0.62	1.16	0.93	9
THREEWALL_922	200	1.98	4.5	125.65	0.61	0.62	1.16	0.93	8
THREEWALL_923	300	1.98	3	706.09	0.61	0.54	1.36	1.08	15
THREEWALL_923	300	1.98	3.3	490.62	0.61	0.58	1.36	1.08	13
THREEWALL_923	300	1.98	3.6	368.3	0.61	0.58	1.36	1.08	11
THREEWALL_923	300	1.98	3.9	270.83	0.61	0.62	1.36	1.08	10
THREEWALL_923	300	1.98	4.2	210.29	0.61	0.62	1.36	1.08	9
THREEWALL_923	300	1.98	4.5	162.55	0.61	0.62	1.36	1.08	8
THREEWALL_923	300	1.98	4.8	137.83	0.61	0.62	1.36	1.08	7
THREEWALL_923	300	1.98	5.1	120.83	0.61	0.62	1.36	1.08	6
THREEWALL_924	400	1.98	3.3	661.79	0.61	0.58	1.53	1.20	13
THREEWALL_924	400	1.98	3.6	499.42	0.61	0.58	1.53	1.20	11
THREEWALL_924	400	1.98	3.9	368.24	0.61	0.58	1.53	1.20	9
THREEWALL_924	400	1.98	4.2	286.26	0.61	0.58	1.53	1.20	8
THREEWALL_924	400	1.98	4.5	226.33	0.61	0.58	1.53	1.20	7
THREEWALL_924	400	1.98	4.8	193.8	0.61	0.58	1.53	1.20	6
THREEWALL_924	400	1.98	5.1	163.16	0.61	0.58	1.53	1.20	6
THREEWALL_924	400	1.98	5.4	137.27	0.61	0.58	1.53	1.20	5
THREEWALL_924	400	1.98	5.7	117.47	0.61	0.62	1.53	1.20	5
THREEWALL_925	500	1.98	3.3	779.73	0.61	0.54	1.68	1.31	12
THREEWALL_925	500	1.98	3.6	644.76	0.61	0.54	1.68	1.31	9
THREEWALL_925	500	1.98	3.9	498.6	0.61	0.54	1.68	1.31	8

Table E-9
Horizontal Plume Shift and Angle Sensitivity Results

Test	HRR (kW)	Source Height (m)	Elevation (m)	Maximum Plume Temperature Rise (C)	Diameter (m)	R_{PO} (m)	R_{rad}Thermoplastic (m)	R_{rad}Thermoset (m)	Angle
THREEWALL_925	500	1.98	4.2	385.1	0.61	0.58	1.68	1.31	8
THREEWALL_925	500	1.98	4.5	290.44	0.61	0.54	1.68	1.31	6
THREEWALL_925	500	1.98	4.8	242.34	0.61	0.54	1.68	1.31	5
THREEWALL_925	500	1.98	5.1	201.57	0.61	0.54	1.68	1.31	5
THREEWALL_925	500	1.98	5.4	172.52	0.61	0.58	1.68	1.31	5
THREEWALL_925	500	1.98	5.7	146.57	0.61	0.58	1.68	1.31	5
THREEWALL_925	500	1.98	6	126.18	0.61	0.58	1.68	1.31	4
THREEWALL_926	600	1.98	3.6	686.97	0.61	0.54	1.82	1.41	9
THREEWALL_926	600	1.98	3.9	541.53	0.61	0.54	1.82	1.41	8
THREEWALL_926	600	1.98	4.2	420.71	0.61	0.54	1.82	1.41	7
THREEWALL_926	600	1.98	4.5	320.56	0.61	0.54	1.82	1.41	6
THREEWALL_926	600	1.98	4.8	264.69	0.61	0.54	1.82	1.41	5
THREEWALL_926	600	1.98	5.1	224.92	0.61	0.54	1.82	1.41	5
THREEWALL_926	600	1.98	5.4	188.27	0.61	0.54	1.82	1.41	5
THREEWALL_926	600	1.98	5.7	163.19	0.61	0.5	1.82	1.41	4
THREEWALL_926	600	1.98	6	146.48	0.61	0.5	1.82	1.41	3
THREEWALL_979	300	1.14	2.4	290.52	0.91	0.9	1.50	1.21	21
THREEWALL_979	300	1.14	2.7	164.64	0.91	1.18	1.50	1.21	26
THREEWALL_979	300	1.14	3	126.48	0.91	1.34	1.50	1.21	27
THREEWALL_980	400	1.14	2.4	360.97	0.91	0.86	1.67	1.34	20
THREEWALL_980	400	1.14	2.7	211.62	0.91	1.18	1.67	1.34	26
THREEWALL_980	400	1.14	3	164.42	0.91	1.34	1.67	1.34	27
THREEWALL_980	400	1.14	3.3	131.59	0.91	1.5	1.67	1.34	27
THREEWALL_980	400	1.14	3.6	114.53	0.91	1.62	1.67	1.34	26
THREEWALL_981	500	1.14	2.4	502.3	0.91	0.86	1.82	1.45	20

Table E-9
Horizontal Plume Shift and Angle Sensitivity Results

Test	HRR (kW)	Source Height (m)	Elevation (m)	Maximum Plume Temperature Rise (C)	Diameter (m)	R_{PO} (m)	R_{rad}Thermoplastic (m)	R_{rad}Thermoset (m)	Angle
THREEWALL_981	500	1.14	2.7	263.14	0.91	1.14	1.82	1.45	25
THREEWALL_981	500	1.14	3	203.96	0.91	1.34	1.82	1.45	27
THREEWALL_981	500	1.14	3.3	167.48	0.91	1.46	1.82	1.45	26
THREEWALL_981	500	1.14	3.6	143.06	0.91	1.54	1.82	1.45	25
THREEWALL_981	500	1.14	3.9	126.31	0.91	1.62	1.82	1.45	24
THREEWALL_981	500	1.14	4.2	113.8	0.91	1.66	1.82	1.45	22
THREEWALL_982	600	1.14	2.4	584.51	0.91	0.86	1.95	1.55	20
THREEWALL_982	600	1.14	2.7	330.93	0.91	1.14	1.95	1.55	25
THREEWALL_982	600	1.14	3	248.81	0.91	1.3	1.95	1.55	26
THREEWALL_982	600	1.14	3.3	201.1	0.91	1.42	1.95	1.55	25
THREEWALL_982	600	1.14	3.6	173.38	0.91	1.54	1.95	1.55	25
THREEWALL_982	600	1.14	3.9	151.54	0.91	1.62	1.95	1.55	24
THREEWALL_982	600	1.14	4.2	133.52	0.91	1.7	1.95	1.55	23
THREEWALL_982	600	1.14	4.5	118.27	0.91	1.78	1.95	1.55	22
THREEWALL_986	300	1.98	2.7	661.25	0.91	0.66	1.50	1.21	20
THREEWALL_986	300	1.98	3	470.11	0.91	0.66	1.50	1.21	14
THREEWALL_986	300	1.98	3.3	333.3	0.91	0.7	1.50	1.21	13
THREEWALL_986	300	1.98	3.6	258.73	0.91	0.7	1.50	1.21	10
THREEWALL_986	300	1.98	3.9	207.21	0.91	0.74	1.50	1.21	10
THREEWALL_986	300	1.98	4.2	162.1	0.91	0.74	1.50	1.21	9
THREEWALL_986	300	1.98	4.5	128.46	0.91	0.74	1.50	1.21	8
THREEWALL_987	400	1.98	3	656.43	0.91	0.7	1.67	1.34	16
THREEWALL_987	400	1.98	3.3	421.27	0.91	0.7	1.67	1.34	13
THREEWALL_987	400	1.98	3.6	319.87	0.91	0.74	1.67	1.34	12
THREEWALL_987	400	1.98	3.9	246.42	0.91	0.7	1.67	1.34	9

Table E-9
Horizontal Plume Shift and Angle Sensitivity Results

Test	HRR (kW)	Source Height (m)	Elevation (m)	Maximum Plume Temperature Rise (C)	Diameter (m)	R_{PO} (m)	R_{rad}Thermoplastic (m)	R_{rad}Thermoset (m)	Angle
THREEWALL_987	400	1.98	4.2	200.39	0.91	0.74	1.67	1.34	9
THREEWALL_987	400	1.98	4.5	162.32	0.91	0.66	1.67	1.34	6
THREEWALL_987	400	1.98	4.8	144.19	0.91	0.7	1.67	1.34	6
THREEWALL_987	400	1.98	5.1	128.53	0.91	0.7	1.67	1.34	5
THREEWALL_987	400	1.98	5.4	115.35	0.91	0.7	1.67	1.34	5
THREEWALL_988	500	1.98	3	779.43	0.91	0.7	1.82	1.45	16
THREEWALL_988	500	1.98	3.3	586.92	0.91	0.7	1.82	1.45	13
THREEWALL_988	500	1.98	3.6	434.55	0.91	0.7	1.82	1.45	10
THREEWALL_988	500	1.98	3.9	323.91	0.91	0.7	1.82	1.45	9
THREEWALL_988	500	1.98	4.2	262.91	0.91	0.7	1.82	1.45	8
THREEWALL_988	500	1.98	4.5	209.44	0.91	0.66	1.82	1.45	6
THREEWALL_988	500	1.98	4.8	178.62	0.91	0.7	1.82	1.45	6
THREEWALL_988	500	1.98	5.1	157.02	0.91	0.7	1.82	1.45	5
THREEWALL_988	500	1.98	5.4	137.24	0.91	0.66	1.82	1.45	4
THREEWALL_988	500	1.98	5.7	117.4	0.91	0.7	1.82	1.45	5
THREEWALL_989	600	1.98	3.3	732.38	0.91	0.7	1.95	1.55	13
THREEWALL_989	600	1.98	3.6	562.49	0.91	0.74	1.95	1.55	12
THREEWALL_989	600	1.98	3.9	411.65	0.91	0.7	1.95	1.55	9
THREEWALL_989	600	1.98	4.2	329.02	0.91	0.7	1.95	1.55	8
THREEWALL_989	600	1.98	4.5	250.92	0.91	0.7	1.95	1.55	7
THREEWALL_989	600	1.98	4.8	213.27	0.91	0.7	1.95	1.55	6
THREEWALL_989	600	1.98	5.1	182.93	0.91	0.7	1.95	1.55	5
THREEWALL_989	600	1.98	5.4	156.71	0.91	0.7	1.95	1.55	5
THREEWALL_989	600	1.98	5.7	131.1	0.91	0.7	1.95	1.55	5
THREEWALL_989	600	1.98	6	117.61	0.91	0.62	1.95	1.55	3

Table E-9
Horizontal Plume Shift and Angle Sensitivity Results

Test	HRR (kW)	Source Height (m)	Elevation (m)	Maximum Plume Temperature Rise (C)	Diameter (m)	R_{PO} (m)	R_{rad}Thermoplastic (m)	R_{rad}Thermoset (m)	Angle
OBST_1052	1000	1.14	2.7	619.49	0.91	0.46	2.40	1.88	2
OBST_1061	1000	1.14	2.4	668.56	1.22	0.66	2.53	2.01	5
OBST_1061	1000	1.14	2.7	493.44	1.22	0.58	2.53	2.01	1
OBST_808	50	1.14	2.4	118.47	0.30	0.22	0.58	0.46	4
OBST_815	50	1.98	2.4	218.53	0.30	0.22	0.58	0.46	11
OBST_816	100	1.98	2.4	414.45	0.30	0.22	0.77	0.60	11
OBST_874	300	1.14	2.4	348.65	0.61	0.42	1.36	1.08	7
OBST_874	300	1.14	2.7	225.86	0.61	0.38	1.36	1.08	4
OBST_876	500	1.14	2.4	650.82	0.61	0.38	1.68	1.31	5
OBST_876	500	1.14	3	305.36	0.61	0.3	1.68	1.31	1
OBST_938	400	1.14	2.4	325.72	0.91	0.58	1.67	1.34	8
OBST_938	400	1.14	2.7	212.8	0.91	0.46	1.67	1.34	2
OBST_940	600	1.14	3	272.81	0.91	0.42	1.95	1.55	0
OBST_944	300	1.98	2.4	428.28	0.91	0.46	1.50	1.21	7
OBST_945	400	1.98	2.4	614.19	0.91	0.46	1.67	1.34	7

Index to Obstructed and Unobstructed Simulation Numbers

Table E-10
Index to Obstructed and Unobstructed Simulation Numbers

HRR (kW)	Source Height (m)	Source Diameter (m)	BASE_# (Unobstructed Plume)	OBST_# (Top Plate Only)	ARCH_# (Top Plate + 2 Walls)	THREEWALL_# (Top Plate + 3 Walls)
50	0.3048	0.3048	300	801	822	843
50	1.1430	0.3048	311	808	829	850
50	1.9812	0.3048	322	815	836	857
100	0.3048	0.3048	301	802	823	844
100	1.1430	0.3048	312	809	830	851
100	1.9812	0.3048	323	816	837	858
200	0.3048	0.6096	302	866	887	908
200	1.1430	0.6096	313	873	894	915
200	1.9812	0.6096	324	880	901	922
300	0.3048	0.6096	303	867	888	909
300	1.1430	0.6096	314	874	895	916
300	1.9812	0.6096	325	881	902	923
300	0.3048	0.9144	307	930	951	972
300	1.1430	0.9144	318	937	958	979
300	1.9812	0.9144	329	944	965	986
400	0.3048	0.6096	304	868	889	910
400	1.1430	0.6096	315	875	896	917
400	1.9812	0.6096	326	882	903	924
400	0.3048	0.9144	308	931	952	973
400	1.1430	0.9144	319	938	959	980
400	1.9812	0.9144	330	945	966	987
500	0.3048	0.6096	305	869	890	911
500	1.1430	0.6096	316	876	897	918
500	1.9812	0.6096	327	883	904	925
500	0.3048	0.9144	309	932	953	974
500	1.1430	0.9144	320	939	960	981
500	1.9812	0.9144	331	946	967	988
600	0.3048	0.6096	306	870	891	912
600	1.1430	0.6096	317	877	898	919
600	1.9812	0.6096	328	884	905	926
600	0.3048	0.9144	310	933	954	975
600	1.1430	0.9144	321	940	961	982
600	1.9812	0.9144	332	947	968	989
1000	0.3048	0.9144	404	1051	1054	1057
1000	1.1430	0.9144	400	1052	1055	1058

Table E-10
Index to Obstructed and Unobstructed Simulation Numbers

HRR (kW)	Source Height (m)	Source Diameter (m)	BASE_# (Unobstructed Plume)	OBST_# (Top Plate Only)	ARCH_# (Top Plate + 2 Walls)	THREEWALL_# (Top Plate + 3 Walls)
1000	1.9812	0.9144	401	1053	1056	1059
1000	0.3048	1.2192	405	1060	1063	1066
1000	1.1430	1.2192	402	1061	1064	1067
1000	1.9812	1.2192	403	1062	1065	1068

Index to Opening Sensitivity Simulation Numbers

Table E-11
Index to Opening Sensitivity Simulation Numbers

HRR (KW)	OPENING (%)	OBST_#	ARCH_#	THREEWALL_#
200	14	1106	1107	1108
600	12	1115	1116	1117
200	10	1103	1104	1105
600	10	1112	1113	1114
200	6.5	1100	1101	1102
600	7	1109	1110	1111

Appendix F
Examples of Enclosure Fire Analysis

This appendix includes two examples illustrating the process of applying guidance documented in this report. The examples cover the recommended process for classifying electrical enclosures that are selected as ignition sources for Fire PRA applications, assigning peak heat release rate probability distributions to such enclosures, and determining their corresponding zones of influence.

F.1 Example 1: Load Center Fire with Targets in the Fire Plume

This example describes the process of assigning a peak heat release rate probability distribution to an electrical enclosure, determining the resulting severity factor, and defining the corresponding zone of influence. The example consists of the following steps:

1. Scenario definition
2. Classification of the electrical enclosure
3. Determination of the peak heat release rate distribution
4. Determination of the corresponding zone of influence
5. Determination of the severity factor

The following sections describe each of the above listed steps in detail.

F.1.1 Description of the Scenario

A fire is postulated in a load center cubicle (i.e., vertical section) located in a typical electrical room in a commercial nuclear power plant. The load center vertical section is 3 feet wide and 2 feet deep. The height of the enclosure is 7 feet. The scenario is depicted in Figure F-1.

There are two cable trays in the room, and each of them contains target cables that are within the scope of the Fire PRA. The cables in trays T-1 and T-2 have thermoplastic jackets and insulation. Table H-1 in NUREG/CR-6850 recommends a value of 205°C (400°F) for temperature damage criteria and 6 kW/m^2 (0.5 BTU/ft^2s) for radiant heat damage criteria.

Cables of interest are in trays T-1 and T-2, which are located at 3 feet and 5 feet above the load center, respectively. These cable trays are exposed to fire plume conditions. Through inspection of the ignition source and cable tray layout during walkdowns and using plant drawings, the following scenario progression and target sets are evaluated:

- Target Set 0: This scenario consists of a fire damaging only the load center.
- Target Set 1: This scenario consists of damage propagating outside the load center and damage the cable tray, T-1, above the electrical enclosure—that is, damage in the fire plume less than 5 feet above the electrical enclosure. In this scenario, T-2 also fails due to the fire propagating from cable tray T-1.

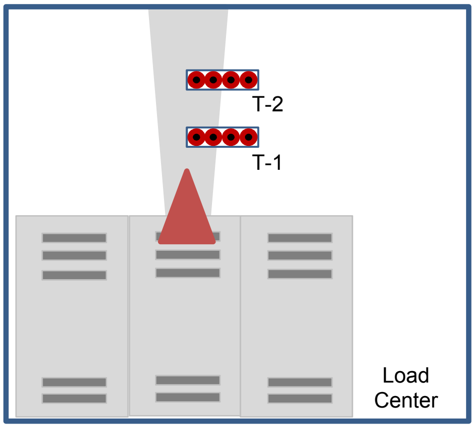

Figure F-1
Pictorial Representation of the Load Center Example

F.1.2 Classification of the Electrical Enclosure

The scenario consists of a load center. Since the load center is an electrical enclosure that has been primarily classified by its function, the classification of this electrical enclosure for the purposes of assigning a peak heat release rate probability distribution is straightforward. The load center is classified as “Switchgears and Load Centers” in Table 4-1 of this report. Figure F-1 depicts the load center as three cabinets. Cabinet to cabinet propagation is not considered in this example.

F.1.3 Determination of Peak Heat Release Rate Probability Distributions

Given the classification described in the previous section, the peak heat release rate probability distribution assigned to the load center is a Gamma with parameters Alpha = 0.99 and Beta = 44. This is the distribution listed for load centers with thermoplastic cables in Table 4-1. This probability distribution has a 98th percentile of 170 kW. Recall that the guidance in Chapter 8 of NUREG/CR-6850 recommends the use of the 98th percentile as the value to use for screening purposes.

F.1.4 Determination of the Zone of Influence

The zone of influence generated by a fire in the load center is calculated using the 98th percentile of the peak heat release rate probability distribution as recommended in Chapter 8 and Appendix F of NUREG/CR-6850. As indicated earlier in this example, the 98th percentile value is 170 kW.

Use the Heskestad plume temperature correlation for determining the vertical component of the zone of influence. Fire modeling analysts routinely use the Heskestad fire plume temperature correlation in support of Fire PRAs and other performance-based applications. Consequently, there are various practical implementations currently available for solving the correlation. Since this correlation is available within the NUREG 1805 library of programmed fire models (Chapter 9 of NUREG-1805), perform the calculation using this available tool.

The zone of influence resulting from an unobstructed plume is calculated to be 6.25 feet. That is, using the following input parameters in the NUREG 1805 Chapter 9 spreadsheet:

- Heat release rate: 170 kW;
- Elevation above the fuel source: 6.25 feet;
- Area of the combustible fuel: 2 feet by 3 feet = 6 ft^2; and
- Ambient temperature: 77^oF.

results in a plume temperature of 201 ^oC, which is conservative and sufficiently close to the damage criteria for thermoplastic cable. It should be noted that the following ambient and default values are also used throughout this example:

- Ambient air specific heat: 1.0 kJ/kg-K;
- Ambient air density: 1.18 kg/m^3;
- Acceleration of gravity: 9.81 m/sec^2; and
- Convective heat release rate fraction: 0.7.

Figure F-2 depicts the input block of the NUREG 1805 Chapter 9 spreadsheet model:

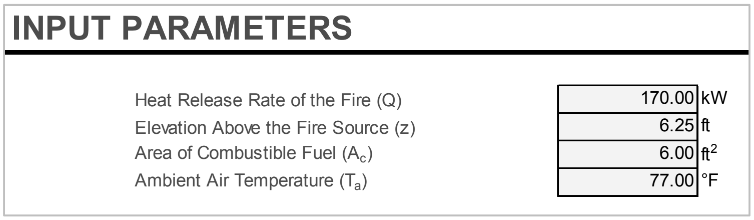

INPUT PARAMETERS

Heat Release Rate of the Fire (Q)	170.00	kW
Elevation Above the Fire Source (z)	6.25	ft
Area of Combustible Fuel (A_c)	6.00	ft^2
Ambient Air Temperature (T_a)	77.00	°F

Figure F-2
Input Parameters for Fire Plume Correlation in NUREG 1805, Chapter 9 Spreadsheet

Based on the guidance documented in Chapter 6 of this report, the vertical component of the zone of influence generated by obstructed plumes is reduced by 24%. In this example, the resulting vertical distance is 6.25 feet x 0.76 = 4.75 feet. Notice that the cable tray T-1 is 4 feet above the base of the fire, and therefore, cannot be screened. In this scenario, cable tray T-1 is both a target, as it contains “target cables”, and an intervening combustible.

F.1.5 Determination of Severity Factors

The severity factor is calculated following the process described in Chapter 8 and Appendices E and F of NUREG/CR-6850, but using the probability distributions and the obstructed plume modeling described in this report. Specifically:

- The Heskestad fire plume correlation is used for determining the heat release rate necessary to generate a temperature of 205^oC at the location of the cable tray T-1. Refer to the resulting heat release rate as the “critical heat release rate”. Recall that the separation between the top of the load center and the bottom of the cable tray T-1 is 3 feet. The guidance in Chapter 12 of Supplement 1 of NUREG/CR-6850 suggests treating the base of the fire as 1 foot below the top of the cabinet; therefore the total separation is 4 feet. Cable tray T-2 will be subjected to a fire involving the electrical enclosure (i.e., the ignition source) and cable tray T-1.

- Using the probability distribution specified in the previous section, the severity factor is the area under the distribution to the right of the resulting critical heat release rate. In other words, the severity factor is the probability that the heat release rate of the electrical enclosure fire will exceed the critical heat release rate, given its probability distribution.

The input parameters, which are listed in Figure F-3, are used in the NUREG 1805 Chapter 9 spreadsheet as follows:

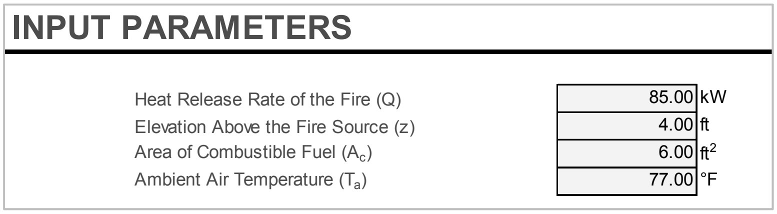

INPUT PARAMETERS

Heat Release Rate of the Fire (Q)	85.00	kW
Elevation Above the Fire Source (z)	4.00	ft
Area of Combustible Fuel (A_c)	6.00	ft^2
Ambient Air Temperature (T_a)	77.00	°F

Figure F-3
Input Parameters for Fire Plume Correlation in NUREG 1805, Chapter 9 Spreadsheet

That elevation above the fire input parameter is entered as 4 feet, which accounts for the distance of 3 feet between the top of the electrical enclosure and the cable tray T-1 and the guidance in Chapter 12 of Supplement 1 of NUREG/CR-6850, which recommends postulating the fire 1 foot below the top of the enclosure. The area of the combustible fuel results from the multiplication of the width and depth of the cabinet, i.e., 3 feet x 2 feet = 6 ft^2. The ambient temperature is assumed to be 77 ^{o}F for this example.

The heat release rate input parameter is varied in the spreadsheet until the resulting plume temperature is approximately 205 $^{\circ}$C, which is the damage criterion for thermoplastic cables. Alternatively the “goal seek” data tool, under the “What if Analysis” tab in Microsoft Excel, can be used to solve for the HRR directly, which will lead to a resulting value of 205 $^{\circ}$C. In this case, a heat release rate value of 85kW results in a plume temperature 4 feet above the base of the fire of 204 $^{\circ}$C. Therefore, the critical heat release rate is 85 kW.

The severity factor resulting from a critical heat release rate of 85 kW can be readily obtained using the gamma distribution function in Microsoft Excel as follows:
SF = 1-GAMMADIST(85,0.99,44,TRUE) = 0.14.

Notice that the above analysis assumes an unobstructed fire plume generated by a fire postulated outside the electrical enclosure. At this point we can incorporate the “obstructed fire plume” approach described in Chapters 5 and 6 of this report. Recall from Chapters 5 and 6 that the obstructed plume is expected to have a temperature 38% lower than the equivalent unobstructed one. The NUREG 1805 calculation can then be altered using the obstructed plume method which is illustrated below to clearly illustrate the process. We will use the same terms as the above example but add an additional factor to account for the 38% reduction in temperature. The effective fire diameter D is calculated as 2.76 ft (0.84 m) for a burning area of 6 sq-ft. The distance above the base of the fire z remains as 4 ft (1.22 m). All default values listed earlier in the example remain constant but an additional term, “β”, is added to account for the 38% reduction in temperature as follows:

$$\Delta T = \beta\left(9.1\left[\frac{T_0}{\left(g c_p^2 \rho_0^2\right)}\right]^{1/3}\right)\dot{Q}_c^{2/3}(z - z_0)^{-5/3}$$

$$z_0 = -1.02D + 0.083\dot{Q}^{2/5} = -1.02(0.84) + 0.083(145)^{2/5} = -0.25$$

$$T = 0.62\left[\left(9.1\left[\frac{298.15}{\left(9.81\,(1.0^2)(1.18^2)\right)}\right]^{1/3}\right)\left(145(0.7)\right)^{2/3}\left(1.22 - (-0.25)\right)^{-5/3} + 25\right]$$

$$T \approx 0.62(291.5) + 25 \approx 205\ ^{\circ}\mathrm{C}$$

The resulting critical heat release rate is calculated to be approximately 145 kW by solving the above equation. That is, a 145 kW fire generates plume temperatures of approximately 205 °C 4 ft above the base of the fire, which is the damage criterion for thermoplastic cables. With a heat release rate of 145 kW, the resulting severity factor is
SF = 1-GAMMADIST(145,0.99,44,TRUE) = 0.04.

The severity factor is only applied to the cable tray closest to the ignition source. Since cable tray T2 could be exposed to a fire involving the ignition source and cable tray T1, given this configuration, the analysts would need to determine if the resulting fire plume exposure from the ignition source and cable tray T1 can damage cable tray T2. If it is determined that the cable tray can be damaged, the fire propagation guidance in Appendix R of NUREG/CR-6850 can be used for determining the time to damage.

F.1.6 Summary of Results

This section summarizes the example results and provides a comparison between the methods and inputs recommended in NUREG/CR-6850 and the guidance provided in this report. The numerical results using inputs in NUREG/CR-6850 were calculated using the same process described earlier in this example. The gamma distribution for vertical cabinets with unqualified cables and fires limited to one cable bundle was selected for the load center (alpha = 1.6, beta = 41.5). The results are summarized and compared in Table F-1.

Table F-1
Summary of Results from Example 1

NUREG/CR-6850			RACHELLE-FIRE (Unobstructed Plume)			RACHELLE-FIRE (Obstructed Plume)	
Peak HRR Probability Distribution 98th Percentiles (kW)	Vertical ZOI (ft)	Resulting Severity Factor	Peak HRR Probability Distribution 98th Percentiles (kW)	Vertical ZOI (ft)	Resulting Severity Factor	Vertical ZOI (ft)	Resulting Severity Factor
211 kW	7.0	0.28	170	6.25	0.14	4.75	0.04

F.2 Example 2 – Application of RACHELLE_FIRE to Realistic Plant Analysis Units

This example is a limited pilot application of the results presented in RACHELLE_FIRE to realistic plant configurations from actual Plant Analysis Units (PAU) and addresses impacts and issues that may arise when evaluating fire scenarios. The steps for this example include:

1) Selection of compartments to analyze
2) Identification of applicable ignition sources
3) Identification of applicable heat release rates (HRR)
4) Determination of appropriate zones of influence (ZOI)
5) Selection of targets
6) Determination of severity factors
7) Determination of CDF*

Steps 3 through 7 will be repeated for several cases in order to allow for review and comparison of results for insights on the effectiveness and potential limitations of the guidance. Each case will include the evaluation of all of the selected scenarios in each PAU. The methodology to perform the fire modeling steps follows that described in Example 1. The cases being analyzed are:

Case	Description
1	NUREG/CR-6850 guidance without significant refinement
2	NUREG/CR-6850 guidance (including supplemental guidance) with refinement of fire size and refined target selection
3	Same as Case 2 except RACHELLE_FIRE HRRs applied
4	Same as Case 2 except RACHELLE_FIRE HRRs applied with vertical ZOI adjusted to account for obstructed plume
5	Same as Case 4 except some RACHELLE_FIRE HRRs revised based on cabinet internals inspection

An additional case was also included to compare the benefits of RACHELLE_FIRE to benefits of potential modifications.

Case	Description
2a	Same as Case 2 with automatic suppression credited in the compartment

* Scenario ignition frequencies, manual non-suppression probabilities and CCDPs are calculated using common practice; however, the details of that analysis are not included as a part of this example. The exact same methods are used for all cases. CDF is presented for evaluation of risk insights and is based on the generic equation where:

$$CDF = IGF * NSP * CCDP$$

It is noted that the purpose of this example is not to illustrate the fire modeling calculations, but to show the potential impacts of applying the new guidance given in this report to realistic plant configurations. Example 1 provides a general demonstration for the specific fire modeling calculations.

F.2.1 Selection of Compartments for Analysis

For this example, three locations (PAUs) have been selected at a plant based on the type of cabinets present and overall risk significance, to demonstrate the application and potential risk impact by applying the new guidance presented in this report. The three locations selected are shown in Figures F-4, F-5, and F-6 as fire compartments A, B, and C, respectively. All of the fire compartments can be assumed to have 3-hour fire rated walls and full room ionizing fire detection installed. None of the compartments are occupied or have automatic suppression systems. A general description for each location is as follows:

Compartment	Description
A	The compartment contains equipment primarily associated with rod control. It has a floor area of approximately 850 square feet and a ceiling height of 11 feet. The targets in this room consist of both conduits and cable trays.
B	The compartment is adjacent to the main control room and contains primarily process control cabinets. It has a floor area of approximately 600 square feet and a ceiling height of 11 feet. There are a significant number of cable trays in this location.
C	This compartment is a battery room containing both trains of station batteries and related electrical cabinets. It has a floor area of approximately 500 square feet and a ceiling height of 12 feet. There are several cable tray stacks primarily located on the back and side walls in addition to conduit targets.

F.2.2 Selection of Sources for Analysis

Only the unscreened (unscreened cabinets include those which are not considered small and well sealed) electrical cabinet sources (reference NUREG/CR-6850 Bin 15) are included in this example. Each selected source is assigned a source number. The source locations are identified in each compartment in Figures F-4, F-5, and F-6. The sources are also listed in Table F-2. A source description and basic source dimensions are also included. Compartments A and B contain primarily control cabinets whereas compartment C is power cabinets.

F.2.3 Evaluation of Individual Cases

Each case is evaluated using the same process. The process consists of selecting the applicable HRR(s) for the ignition sources, developing the scenarios, and quantifying the risk. The scenario development in this example is based on calculating the ZOI for the selected HRR and selecting targets within the ZOI. A severity factor is also calculated based on the distance to the nearest target (see Example 1 for details of determining severity factors and ZOI). If the target set includes secondary combustibles, such as exposed cables, propagation is assumed and additional targets are included in the set.

Table F-2 Source List

Source ID	Description	Source Dimens. (in)			Area	Volume
		Length	Width	Height	ft^2	ft^3
A_0312	CABINET #312	32	48	96	10.67	85.3
A_0314	DC HOLD CABINET	50	45	98	15.63	127.6
A_0315	LOGIC CABINET	50	45	98	15.63	127.6
A_0316	POWER CABINET – 2BD	24	83	98	13.83	113.0
A_0317	POWER CABINET – 2AC	24	83	98	13.83	113.0
A_0318	POWER CABINET – 1BD	24	83	78	13.83	89.9
A_0319	POWER CABINET – 1AC	24	83	98	13.83	113.0
A_0320	CORE EXIT THERMOCOUPLE CABINET	30	30	96	6.25	50.0
A_0321	IMPACT MONITORING SYSTEM CABINET	30	26	90	5.42	40.6
B_0337	CABINET #14	32	22	84	4.89	34.2
B_0338	CABINET #15	32	22	84	4.89	34.2
B_0339	CABINET #16	32	22	84	4.89	34.2
B_0340	CABINET #17	32	22	84	4.89	34.2
B_0341	CABINET #18	32	22	84	4.89	34.2
B_0343	CABINET #19	32	22	84	4.89	34.2
B_0344	CABINET #20	32	22	84	4.89	34.2
B_0345	CABINET #21	32	22	84	4.89	34.2
B_0346	CABINET #22	32	22	84	4.89	34.2
B_0347	CABINET #28	32	22	84	4.89	34.2
B_0348	CABINET #23	32	22	84	4.89	34.2
B_0349	CABINET #24	32	22	84	4.89	34.2
B_0350	CABINET #25	32	22	84	4.89	34.2
B_0352	CABINET #1	32	22	84	4.89	34.2
B_0353	CABINET #2	32	22	84	4.89	34.2
B_0354	CABINET #3	32	22	84	4.89	34.2
B_0356	CABINET #4	32	22	84	4.89	34.2
B_0357	CABINET #5	32	22	84	4.89	34.2
B_0358	CABINET #6	32	22	84	4.89	34.2
B_0359	CABINET #7	32	22	84	4.89	34.2
B_0360	CABINET #8	32	22	84	4.89	34.2
B_0361	CABINET #9	32	22	84	4.89	34.2
B_0362	CABINET #10	32	22	84	4.89	34.2
B_0363	CABINET #11	32	22	84	4.89	34.2
B_0364	CABINET #12	32	22	84	4.89	34.2
C_0183	BATTERY CHARGER – A	36	46	68	11.50	65.2
C_0184	BATTERY CHARGER – A-1	36	46	68	11.50	65.2
C_0185	MCC-A	20	40	90	5.56	41.7
C_0186	MCC-B	57	19	90	7.52	56.4
C_0188	BATTERY CHARGER – B-1	46	36	68	11.50	65.2
C_0189	BATTERY CHARGER – B	46	36	68	11.50	65.2

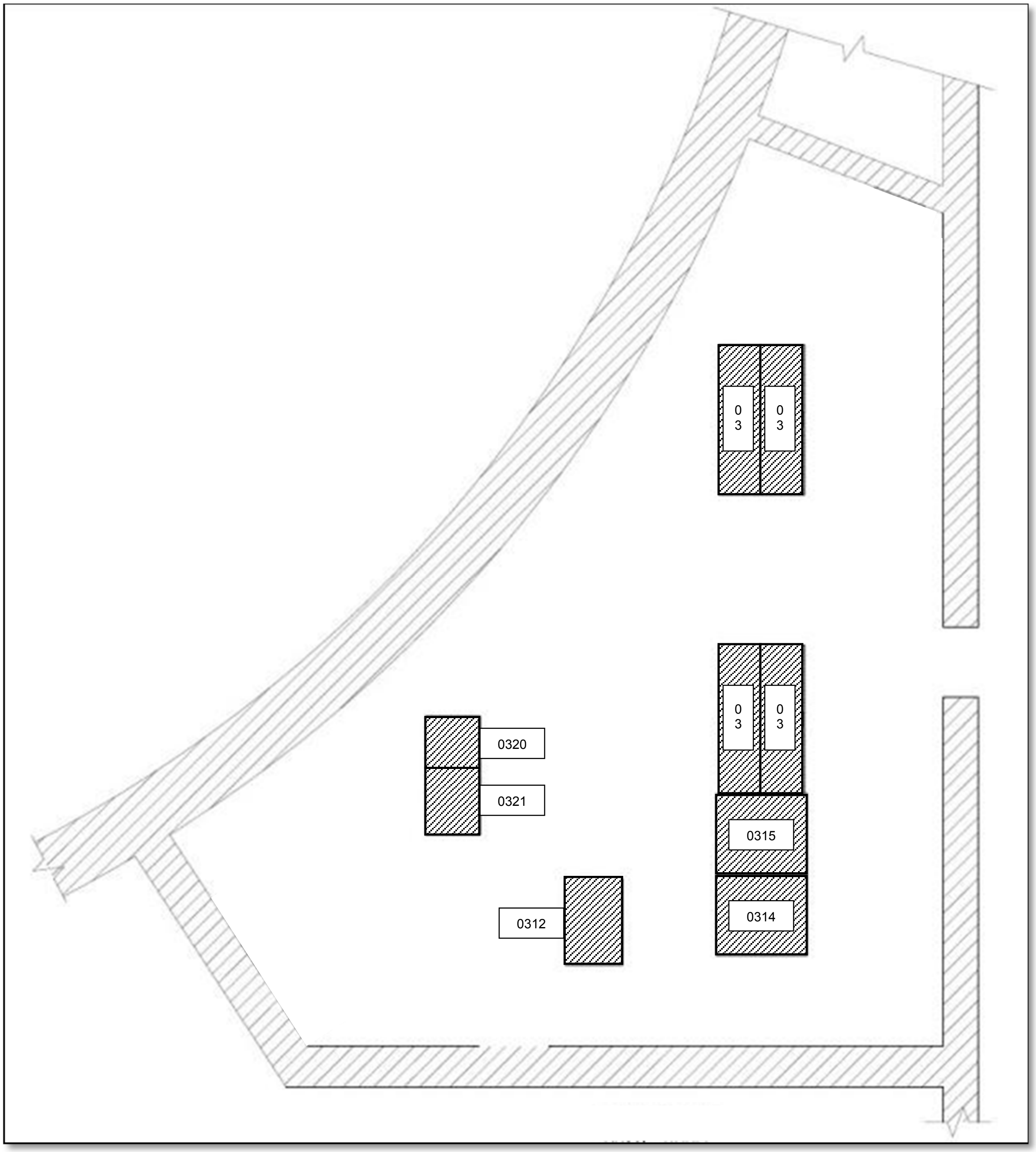

Figure F-4
Fire Compartment A

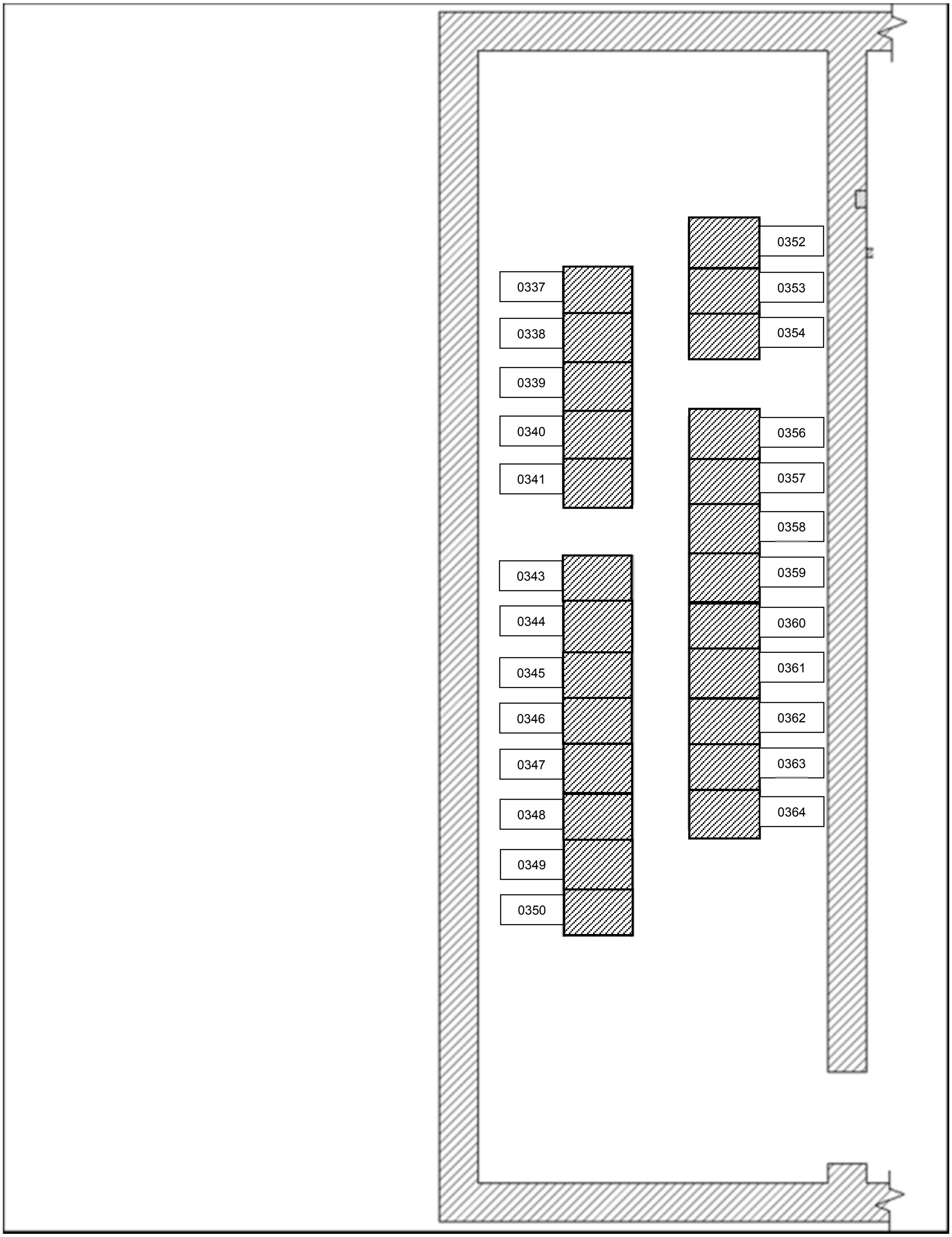

Figure F-5
Fire Compartment B

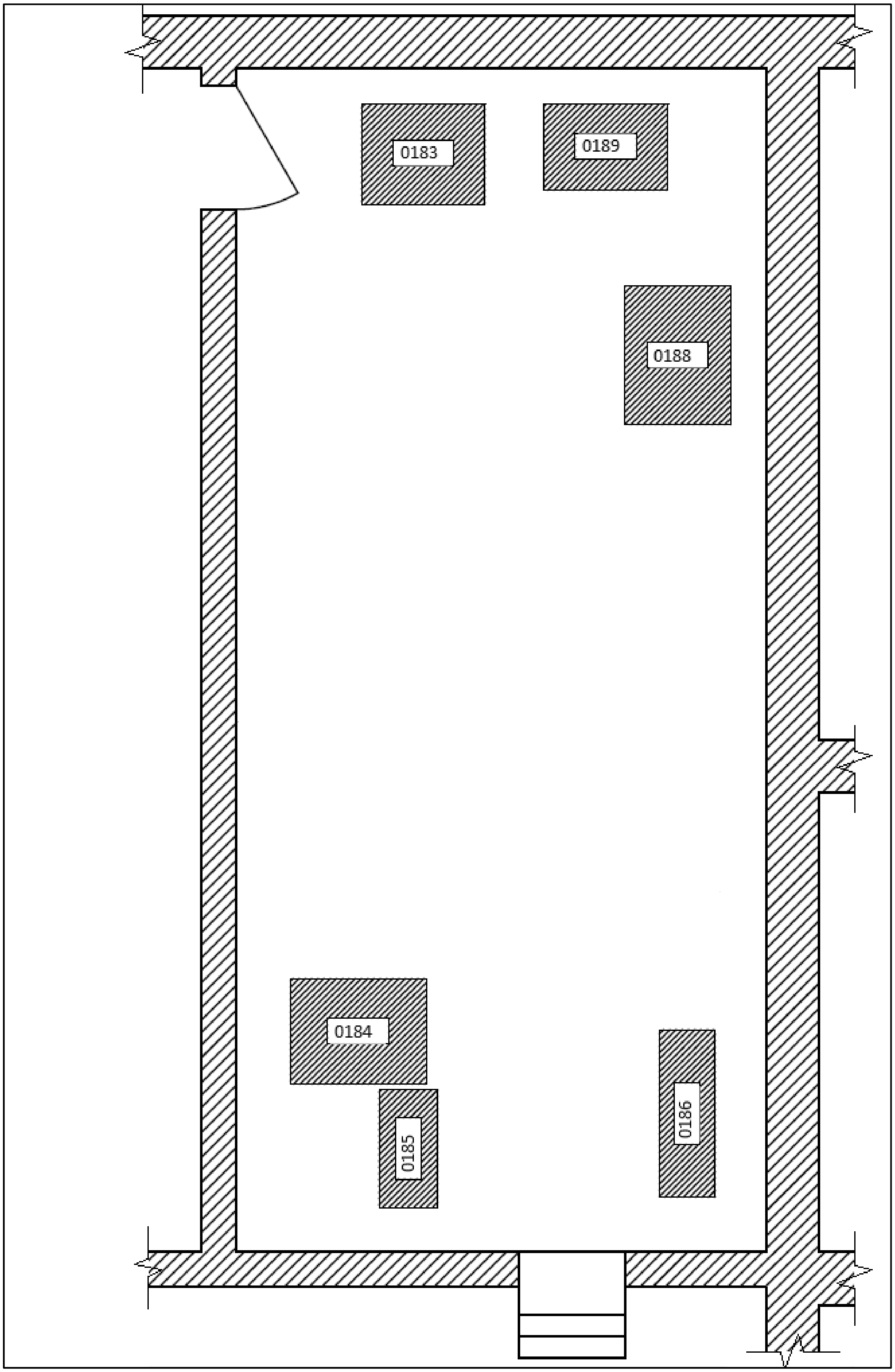

Figure F-6
Fire Compartment C

Each scenario also evaluates fire growth and potential hot gas layer (HGL) development based on the room configuration. If suppression is unsuccessful when HGL conditions are met, all targets in the compartment are assumed failed. The details of this analysis are not part of this example, however the methods are consistent with common practice. It should also be noted that the 98th percentile HRR should always be used for screening, however selection of scenarios and additional points from the HRR distribution to evaluate is based on the judgment of the analyst as needed to achieve more realistic results.

The results for each case include the HRRs selected, severity factors, HRR ZOIs, the number of targets in the ZOIs, the total CDF for the source, and the percentage of the CDF due to HGL conditions. The total CDF includes contribution from all evaluated scenarios for the source.

The following notes provide specific information to assist in assessing the data provided in Tables F-3 through F-7.

1. The cabling within the cabinets is IEEE-383 qualified or equivalent.
2. The plant is comprised primarily of thermoplastic cables. Thermoplastic damage criteria are used; radiant heating damage criterion is 6 kW/m^2 (0.5 BTU/ft^{2}s); temperature damage criterion is 205°C (400°F).
3. Source to target distances were initially measured from the top and sides of the cabinet. The radial distance was used to determine the nearest target.
4. A distance to first target of “NA” is an indicator that there were no external targets in the calculated ZOI.

F.2.3.1 Case 1

Case 1 defines an ignition source level analysis using methods based on NUREG/CR-6850. Each electrical cabinet is fire modeled using the 98th percentile HRR as a screening value, and the ZOIs are based on a bounding fire size located at the top of the cabinet as determined for initial source walkdowns to identify target sets. The target sets include all potential combustibles (e.g., cables, trays, raceways, conduits, etc.) observed in the ZOIs.

The electrical cabinet sources in each compartment are listed in Table F-2. Table F-3 includes additional information specific to Case 1. This includes the assigned HRR, SF, number of targets (raceways) in the zone of influence (ZOI), core damage frequency (CDF) and the percentage of the CDF that is due to HGL conditions.

1. HRRs were determined using NUREG/CR-6850, Table G-1:
    a. Case 1: Vertical cabinets with qualified cable, fire limited to one cable bundle; 75th is 69 kW, 98th is 211 kW
    b. Case 2: Vertical cabinets with qualified cable, fire in more than one cable bundle; 75th is 211 kW, 98th is 702 kW

2. Vertical ZOI (Elevation Above the Fire Source (z)) was calculated using NUREG-1805, Fire Dynamics Tools (FDT^s), Chapter 9, Estimating Centerline Temperature of a Buoyant Fire Plume, with the following input parameters:

Heat Release Rate of the Fire (Q):	Varies, see item 1
Ambient Air Temperature (T_a):	77°F
Specific Heat of Air (c_p):	1.00 kJ/kg-K
Ambient Air Density (ρ_a):	1.18 kg/m^3
Acceleration of Gravity (g):	9.81 m/sec^2
Convective Heat Release Fraction (χ_c):	0.70
Area of Combustible Fuel (Ac):	1.0 ft^2

The inputs described above need to be evaluated to ensure that the methods used were applied within the verification and validation (V&V) range of applicability as defined in NUREG-1824.

Froude Number: The 1.0 ft^2 value for the area of the fuel was selected to bound all larger fuel packages. This yields an effective diameter (D) of 1.1 ft (0.34 m). The Froude Number, $\dot{Q}^*$, is used to determine if the heat release rate relative to the diameter of the fire scenario is within the range of HRR that is within the scope of NUREG-1824 (acceptable range 0.4-2.4). It is calculated using the following equation (NUREG-1934, Equation 2-4):

$$\dot{Q}^* = \frac{\dot{Q}}{\rho_a c_p T_a D^2 \sqrt{gD}}$$

Flame Height Ratio: The flame length ratio, L_f/H_f, is used to determine if the flame height relative to the upper horizontal boundary of the fire scenario is within the range of HRR that is within the scope of NUREG-1824 (acceptable range 0.2-1.0). The equation for the calculation of this parameter is the following (NUREG-1934, Equation 2-6):

$$l_f = D\left(3.7 \times \dot{Q}^{*\frac{2}{5}} - 1.02\right)$$

HRR	Froude	Height of Target		Flame Height	Flame Length Ratio
	Q*	H_t (ft)	H_t (m)	L_f (m)	L_f/H_f
69	0.90	5.11	1.56	0.87	0.56
211	2.76	8.56	2.61	1.56	0.60
702	9.19	14.70	4.48	2.74	0.61

The vertical ZOI calculations for the Fire Froude number present an “out of range” result. The “out of range” case is due to the calculation exceeding the upper limit of the range, suggesting a high intensity fire for the selected fire diameter. One reason for exceeding the upper limit is the use of the 98th percentile heat release rates for the corresponding fire diameters. Based on the guidance in Chapter 8 of NUREG/CR-6850, 98th percentile heat release rate values are used for screening and can be considered on the high end of the values assigned to ignition sources. In addition, setting the Froude number calculation to the upper range limit of 2.4 for the 98th percentile heat release rate values would result in a larger diameter. With a larger diameter, the flame height calculation would result in shorter flame lengths, and plume temperature calculations would suggest lower temperatures. The “out of range” results are based on conservative ZOI calculations for the Fire PRA.

3. Horizontal ZOI (Distance between Fire and Target (L)) was calculated using NUREG-1805, Fire Dynamics Tools (FDT^s), Chapter 5.1, Estimating Radiant Heat Flux from Fire to a Target Fuel at Ground Level Under Wind-Free Conditions, Solid Flame Radiation Model 2, with the following input parameters:

Heat Release Rate of the Fire (Q):	Varies, see item 1
Fuel Area or Dike Area (A_{dike}):	6.0 ft^2 (reference ML12146A439)
Vertical Distance of Target from Ground (H_1):	User defined increments for each HRR such that the mid-height level of the flame, where radiation effects are maximized, was used.

Once again, the inputs described above need to be evaluated to ensure that the methods used were applied within the verification and validation (V&V) range of applicability as defined in NUREG-1824.

Froude Number: The 6.0 ft^2 value for the area of the fuel was selected to bound all larger fuel packages. This yields an effective diameter (D) of 2.8 ft (0.84 m). The Froude Number, $\dot{Q}^*$, (acceptable range 0.4-2.4) again is used to determine if the heat release rate relative to the diameter of the fire scenario is within the range of HRR that is within the scope of NUREG-1824. It is calculated using the equation presented above.

Radial Distance Ratio: The Radial Distance Ratio, r/D, is used to determine if the horizontal radial distance from the fire to the target is within the range of distances included in NUREG-1824 (acceptable range 2.2-5.7). The Horizontal Distance between Target and Center of Fire, r, is defined as:

$$r = L + \frac{D}{2}$$

HRR	Froude	Distance between Fire and Target		Horizontal Distance between Target and Center of Fire	Radial Distance Ratio
	Q*	L (ft)	L (m)	r (m)	r/D
69	0.10	2.59	0.79	1.21	1.44
211	0.29	4.56	1.39	1.81	2.15
702	0.98	6.57	2.00	2.42	2.88

The horizontal component refers mostly to flame radiation for targets located near the flames. Consequently, ZOI calculations for the Fire Froude number are mostly “out of range” as they are based on experiments where the radiation was measured at some longer distance from the flames. The “out of range” results for the Fire Froude number are therefore expected given that the ZOI calculations define a region close to the flames. However, it should be noted that the Fire Froude Number is not the key parameter recommended for flame radiation scenarios. Table 2-5 of NUREG-1934 recommends the use of the radial distance ratio dimensionless parameter for radiation heat flux applications.

For the radial distance ratio dimensionless parameter, all the calculations that are “out of range” are on the low side of the range, suggesting again that the ZOI is characterized by distances close to the flames. These calculations were conducted with the solid flame radiation model described in Chapter 5.2 of NUREG-1805. A review of Figure 6-8 in Volume 3 of NUREG-1824 suggests that the majority of the validation results (with a few exceptions for Cable G in radiation ranges larger than the 6 kW/m^2 for ZOI calculations) suggest over-predictions of the flame radiation, which would result in longer horizontal distances for the ZOI. Table 4-1 in NUREG-1934 suggests an average prediction of 2.02 times greater than experimental values for radiant heat flux calculations using FDTs.

In summary, the reason for the number of ZOI results that are “out of range” is because the ZOI distances are close to the flames, and the experiments selected for validation purposes measured radiation at longer distances from the flames. This is a limitation on the available data for validation and not necessarily a limitation on the use of the solid flame radiation model for calculating horizontal components of the ZOI for Fire PRA applications. To account for this limitation, it is noted that validation results from Figure 6-8 in Volume 3 of NUREG-1824 indicate significant heat flux over-predictions over the intensity levels used for ZOI calculations (i.e., between 6 and 11 kW/m^2) that would result in longer, and therefore conservative, horizontal distances.

4. Severity factor is developed using the same methods as discussed in Appendix F.1.5 of Example 1.

5. Based on the results provided in Table F-3 there is a varying degree of risk associated with the electrical cabinets in each compartment. There is also a significant potential for HGL conditions to develop. The initial results indicate that additional refinements should be investigated.

Table F-3
Cabinet List with NUREG/CR-6850 Based HRR (Case 1)

Source ID	Description	Source Dimens. (in)			Area	Volume	6850 HRR	98th ZOI (in)		To First Target	SF	98th # Targets	98th # Trays	CDF	% HGL
		Length	Width	Height	ft^2	ft^3	98th	Horizontal	Vertical	inches					
A_0312	CABINET #312	32	48	96	10.7	85.3	211	55	104	32	0.648	3	0	0.00E+00	0.0%
A_0314	DC HOLD CABINET	50	45	98	15.6	127.6	702	79	176	29	0.828	20	5	9.26E-07	98.2%
A_0315	LOGIC CABINET	50	45	98	15.6	127.6	702	79	176	29	0.828	20	5	1.02E-06	98.4%
A_0316	POWER CABINET – 2BD	24	83	98	13.8	113.0	702	79	176	35	0.786	5	0	0.00E+00	0.0%
A_0317	POWER CABINET – 2AC	24	83	98	13.8	113.0	702	79	176	29	0.828	30	8	4.12E-06	32.5%
A_0318	POWER CABINET – 1BD	24	83	78	13.8	89.9	702	79	176	32	0.807	10	0	1.12E-08	0.0%
A_0319	POWER CABINET – 1AC	24	83	98	13.8	113.0	702	79	176	30	0.821	34	8	2.10E-06	31.7%
A_0320	CORE EXIT THERMOCOUPLE CABINET	30	30	96	6.3	50.0	702	79	176	N/A	0.000	4	0	0.00E+00	0.0%
A_0321	IMPACT MONITORING SYSTEM CABINET	30	26	90	5.4	40.6	211	55	104	8	0.917	3	0	0.00E+00	0.0%
B_0337	CABINET #14	32	22	84	4.9	34.2	702	79	176	5	0.958	37	12	7.93E-07	4.3%
B_0338	CABINET #15	32	22	84	4.9	34.2	702	79	176	5	0.958	34	12	7.93E-07	4.3%
B_0339	CABINET #16	32	22	84	4.9	34.2	702	79	176	5	0.958	33	12	1.05E-07	32.4%
B_0340	CABINET #17	32	22	84	4.9	34.2	702	79	176	5	0.958	29	12	3.53E-08	96.3%
B_0341	CABINET #18	32	22	84	4.9	34.2	702	79	176	5	0.958	25	12	3.53E-08	96.3%
B_0343	CABINET #19	32	22	84	4.9	34.2	702	79	176	5	0.958	24	12	3.55E-08	95.7%
B_0344	CABINET #20	32	22	84	4.9	34.2	702	79	176	5	0.958	22	12	3.59E-08	94.7%
B_0345	CABINET #21	32	22	84	4.9	34.2	702	79	176	5	0.958	21	11	3.43E-08	99.3%
B_0346	CABINET #22	32	22	84	4.9	34.2	702	79	176	5	0.958	21	11	3.40E-08	99.9%
B_0347	CABINET #28	32	22	84	4.9	34.2	702	79	176	5	0.958	19	11	3.40E-08	99.9%
B_0348	CABINET #23	32	22	84	4.9	34.2	702	79	176	5	0.958	19	11	3.53E-08	96.3%
B_0349	CABINET #24	32	22	84	4.9	34.2	702	79	176	5	0.958	15	11	3.53E-08	96.3%
B_0350	CABINET #25	32	22	84	4.9	34.2	702	79	176	5	0.958	13	11	3.53E-08	96.3%
B_0352	CABINET #1	32	22	84	4.9	34.2	702	79	176	5	0.958	26	5	1.82E-08	92.6%
B_0353	CABINET #2	32	22	84	4.9	34.2	702	79	176	5	0.958	22	5	1.82E-08	92.6%
B_0354	CABINET #3	32	22	84	4.9	34.2	702	79	176	5	0.958	21	5	1.82E-08	92.8%
B_0356	CABINET #4	32	22	84	4.9	34.2	702	79	176	5	0.958	15	5	1.84E-08	91.6%
B_0357	CABINET #5	32	22	84	4.9	34.2	702	79	176	5	0.958	12	5	1.84E-08	91.6%
B_0358	CABINET #6	32	22	84	4.9	34.2	702	79	176	5	0.958	14	5	1.95E-08	86.4%
B_0359	CABINET #7	32	22	84	4.9	34.2	702	79	176	5	0.958	19	7	2.79E-08	94.5%
B_0360	CABINET #8	32	22	84	4.9	34.2	702	79	176	5	0.958	18	5	1.88E-08	89.8%
B_0361	CABINET #9	32	22	84	4.9	34.2	702	79	176	5	0.958	17	5	1.84E-08	91.6%
B_0362	CABINET #10	32	22	84	4.9	34.2	702	79	176	5	0.958	17	5	1.71E-08	98.5%
B_0363	CABINET #11	32	22	84	4.9	34.2	702	79	176	5	0.958	17	5	1.84E-08	91.5%
B_0364	CABINET #12	32	22	84	4.9	34.2	702	79	176	5	0.958	15	5	1.82E-08	92.6%
C_0183	BATTERY CHARGER – A	36	46	68	11.5	65.2	211	55	104	15	0.854	11	4	7.16E-07	77.5%
C_0184	BATTERY CHARGER – A-1	36	46	68	11.5	65.2	211	55	104	7	0.924	20	5	1.06E-06	83.5%
C_0185	MCC-A	20	40	90	5.6	41.7	211	55	104	N/A	0.000	3	0	1.18E-07	0.0%
C_0186	MCC-B	57	19	90	7.5	56.4	211	55	104	N/A	0.000	4	1	1.99E-08	0.0%
C_0188	BATTERY CHARGER – B-1	46	36	68	11.5	65.2	211	55	104	10	0.900	7	3	1.91E-07	97.4%
C_0189	BATTERY CHARGER – B	46	36	68	11.5	65.2	211	55	104	40	0.538	3	2	1.82E-09	0.0%

F.2.3.2 Case 2

For Case 2 the scenarios were refined in several ways. First, a second HRR was selected at the 75th percentile from the distribution. For quantification, a two point model was used where 10% of the ignition frequency was applied to the 98th percentile HRR and 90% was applied to the 75th percentile HRR. Also, a more realistic fire size using actual cabinet dimensions was applied, and the fire was placed at one foot below the top of the cabinet in accordance with FAQ 08-0043, “Location of Fires Within Electrical Cabinets”. Finally, the cable tray targets were reviewed to more realistically address propagation and fire growth. Table F-4 provides the updated data and results. This case represents a baseline to compare the impacts of applying revised HRRs from RACHELLE_FIRE (Cases 3, 4, and 5)

1. The 98th percentile HRRs for each cabinet are the same as in Case 1.
2. Vertical ZOI (z) is calculated using NUREG-1805, Fire Dynamics Tools (FDT^s), Chapter 9, Estimating Centerline Temperature of a Buoyant Fire Plume, with the same input parameters as Case 1, with the exception of the Area of Combustible Fuel (Ac).

   The Froude Number is evaluated for each cabinet to ensure that the value for the area of the fuel is within its V&V range of applicability (acceptable range 0.4-2.4). For cabinets where the Fire Froude number is “out of range” on the upper bound, the area of the fuel was adjusted (diameter decreased) to correspond to the maximum acceptable Froude Number. For “out of range” cases below the acceptable range, the actual cabinet dimension was used. This ensures that the results for each vertical ZOI case remain applicable and conservative.
3. Horizontal ZOI (L) was calculated using NUREG-1805, Fire Dynamics Tools (FDT^s), Chapter 5.1, “Estimating Radiant Heat Flux from Fire to a Target Fuel at Ground Level Under Wind-Free Conditions, Solid Flame Radiation Model 2”, with the same input parameters as Case 1, with the exception of the Area of Combustible Fuel (Ac).

   Once again, the Froude Number is evaluated for each cabinet to ensure that the value for the area of the fuel is within its V&V range of applicability (acceptable range 0.4-2.4). For cabinets where the Fire Froude number is “out of range” on the upper bound, the area of the fuel was adjusted (diameter decreased) to correspond to the maximum acceptable Froude Number. For “out of range” cases below the acceptable range, the actual cabinet dimension was used. This ensures that the results for each vertical ZOI case remain applicable and conservative.
4. Severity factor is developed using the same methods as discussed in Appendix F.1.5 of Example 1.

Table F-4 Cabinet List with NUREG/CR-6850 Based HRR and Scenario Refinements

Source ID	Description	6850 HRR		75th ZOI (in)		98th ZOI (in)		To First Target	SF	75th # Targets	98th # Targets	75th # Trays	98th # Trays	CDF	% HGL
		75th	98th	Horizontal	Vertical	Horizontal	Vertical	inches							
A_0312	CABINET #312	69	211	34	56	54	88	44	0.299	3	3	0	0	0.00E+00	0.0%
A_0314	DC HOLD CABINET	211	702	54	88	86	142	41	0.478	13	20	3	5	1.58E-07	96.5%
A_0315	LOGIC CABINET	211	702	54	88	86	142	41	0.478	20	20	5	5	3.09E-07	97.4%
A_0316	POWER CABINET – 2BD	211	702	54	88	86	142	46	0.440	4	5	0	0	0.00E+00	0.0%
A_0317	POWER CABINET – 2AC	211	702	54	88	86	142	41	0.478	25	30	7	8	1.74E-06	25.6%
A_0318	POWER CABINET – 1BD	211	702	54	88	86	142	42	0.471	10	10	0	0	4.87E-09	0.0%
A_0319	POWER CABINET – 1AC	211	702	54	88	86	142	40	0.486	25	34	5	8	9.11E-07	19.0%
A_0320	CORE EXIT THERMOCOUPLE CABINET	211	702	54	88	80	156	N/A	0.000	4	4	0	0	0.00E+00	0.0%
A_0321	IMPACT MONITORING SYSTEM CABINET	69	211	34	56	54	88	19	0.620	3	3	0	0	0.00E+00	0.0%
B_0337	CABINET #14	211	702	54	88	76	160	17	0.802	24	37	4	4	6.74E-08	11.0%
B_0338	CABINET #15	211	702	54	88	76	160	17	0.802	29	34	4	4	6.74E-08	11.0%
B_0339	CABINET #16	211	702	54	88	76	160	17	0.802	26	33	4	4	1.41E-08	52.5%
B_0340	CABINET #17	211	702	54	88	76	160	17	0.802	23	29	4	4	8.70E-09	85.0%
B_0341	CABINET #18	211	702	54	88	76	160	17	0.802	20	25	4	4	8.70E-09	85.0%
B_0343	CABINET #19	211	702	54	88	76	160	17	0.802	18	24	4	4	8.72E-09	84.9%
B_0344	CABINET #20	211	702	54	88	76	160	17	0.802	14	22	4	4	9.19E-09	80.5%
B_0345	CABINET #21	211	702	54	88	76	160	17	0.802	13	21	4	4	7.43E-09	99.6%
B_0346	CABINET #22	211	702	54	88	76	160	17	0.802	14	21	4	4	7.41E-09	99.8%
B_0347	CABINET #28	211	702	54	88	76	160	17	0.802	12	19	4	4	7.41E-09	99.8%
B_0348	CABINET #23	211	702	54	88	76	160	17	0.802	12	19	4	4	8.70E-09	85.0%
B_0349	CABINET #24	211	702	54	88	76	160	17	0.802	12	15	4	4	8.70E-09	85.0%
B_0350	CABINET #25	211	702	54	88	76	160	17	0.802	12	13	4	4	8.70E-09	85.0%
B_0352	CABINET #1	211	702	54	88	76	160	17	0.802	17	26	2	2	8.16E-09	83.7%
B_0353	CABINET #2	211	702	54	88	76	160	17	0.802	18	22	2	2	8.16E-09	83.7%
B_0354	CABINET #3	211	702	54	88	76	160	17	0.802	14	21	2	2	8.13E-09	84.0%
B_0356	CABINET #4	211	702	54	88	76	160	17	0.802	10	15	2	2	8.24E-09	82.8%
B_0357	CABINET #5	211	702	54	88	76	160	17	0.802	9	12	2	2	8.24E-09	82.8%
B_0358	CABINET #6	211	702	54	88	76	160	17	0.802	10	14	2	2	8.81E-09	77.5%
B_0359	CABINET #7	211	702	54	88	76	160	17	0.802	12	19	2	2	8.24E-09	82.8%
B_0360	CABINET #8	211	702	54	88	76	160	17	0.802	15	18	2	2	8.62E-09	79.2%
B_0361	CABINET #9	211	702	54	88	76	160	17	0.802	15	17	2	2	8.24E-09	82.8%
B_0362	CABINET #10	211	702	54	88	76	160	17	0.802	16	17	2	2	6.96E-09	98.2%
B_0363	CABINET #11	211	702	54	88	76	160	17	0.802	15	17	2	2	8.18E-09	83.5%
B_0364	CABINET #12	211	702	54	88	76	160	17	0.802	14	15	2	2	8.16E-09	83.7%
C_0183	BATTERY CHARGER – A	69	211	34	56	54	88	19	0.620	10	11	4	4	3.48E-07	79.7%
C_0184	BATTERY CHARGER – A-1	69	211	34	56	54	88	19	0.620	19	20	5	5	4.71E-07	83.6%
C_0185	MCC-A	69	211	34	56	54	88	N/A	0.000	3	3	0	0	1.18E-07	0.0%
C_0186	MCC-B	69	211	34	56	54	88	N/A	0.000	4	4	1	1	1.99E-08	0.0%
C_0188	BATTERY CHARGER – B-1	69	211	34	56	54	88	16	0.660	7	7	2	2	3.08E-09	0.0%
C_0189	BATTERY CHARGER – B	69	211	34	56	54	88	42	0.322	0	3	0	1	3.11E-10	0.0%

F.2.3.3 Case 3

For Case 3 revised HRRs were applied using the guidance described in RACHELLE_FIRE Table 4-1 and Table 4-2 as described below:

- Group 2: MCCs and Battery Chargers; 75th is 25 kW, 98th is 130 kW
- Group 4a(a): Large Enclosures, Closed; 75th is 50 kW, 98th is 400 kW
- Group 4b(a): Medium Enclosures, Closed; 75th is 25 kW, 98th is 200 kW

Other scenario parameters are consistent with Case 2. Table F-5 provides the updated data and results.

Table F-5
Cabinet List with RACHELLE_FIRE HRRs (Case 3)

Source ID	Description	Binning Group	HRR		75th ZOI (in)		98th ZOI (in)		To First Target	SF	75th # Targets	98th # Targets	75th # Trays	98th # Trays	CDF	% HGL
		Table 4.1 and 4.2	75th	98th	Horizontal	Vertical	Horizontal	Vertical	inches							
A_0312	CABINET #312	4a(a), Closed, TP	50	400	30	49	69	113	44	0.189	3	3	0	0	0.00E+00	0.0%
A_0314	DC HOLD CABINET	4a(a), Closed, TP	50	400	30	49	69	113	41	0.202	3	16	0	4	4.83E-08	98.7%
A_0315	LOGIC CABINET	4a(a), Closed, TP	50	400	30	49	69	113	41	0.202	3	20	0	5	8.45E-08	97.7%
A_0316	POWER CABINET – 2BD	4a(a), Closed, TP	50	400	30	49	69	113	46	0.180	1	5	0	0	0.00E+00	0.0%
A_0317	POWER CABINET – 2AC	4a(a), Closed, TP	50	400	30	49	69	113	41	0.202	1	26	0	7	4.46E-07	27.1%
A_0318	POWER CABINET – 1BD	4a(a), Closed, TP	50	400	30	49	69	113	42	0.197	3	10	0	0	1.29E-09	0.0%
A_0319	POWER CABINET – 1AC	4a(a), Closed, TP	50	400	30	49	69	113	40	0.206	5	32	0	7	2.37E-07	25.5%
A_0320	CORE EXIT THERMOCOUPLE CABINET	4b(a), Closed, TP	25	200	22	37	53	86	N/A	0.000	4	4	0	0	0.00E+00	0.0%
A_0321	IMPACT MONITORING SYSTEM CABINET	4b(a), Closed, TP	25	200	22	37	53	86	19	0.281	3	3	0	0	0.00E+00	0.0%
B_0337	CABINET #14	4b(a), Closed, TP	25	200	22	37	53	86	17	0.296	16	23	4	4	3.84E-09	65.7%
B_0338	CABINET #15	4b(a), Closed, TP	25	200	22	37	53	86	17	0.296	11	22	4	4	3.84E-09	65.7%
B_0339	CABINET #16	4b(a), Closed, TP	25	200	22	37	53	86	17	0.296	12	23	4	4	3.82E-09	66.2%
B_0340	CABINET #17	4b(a), Closed, TP	25	200	22	37	53	86	17	0.296	16	19	4	4	3.82E-09	66.2%
B_0341	CABINET #18	4b(a), Closed, TP	25	200	22	37	53	86	17	0.296	15	20	4	4	3.82E-09	66.2%
B_0343	CABINET #19	4b(a), Closed, TP	25	200	22	37	53	86	17	0.296	12	17	4	4	3.82E-09	66.2%
B_0344	CABINET #20	4b(a), Closed, TP	25	200	22	37	53	86	17	0.296	11	14	4	4	4.23E-09	59.8%
B_0345	CABINET #21	4b(a), Closed, TP	25	200	22	37	53	86	17	0.296	9	12	4	4	2.53E-09	99.8%
B_0346	CABINET #22	4b(a), Closed, TP	25	200	22	37	53	86	17	0.296	8	9	4	4	2.53E-09	99.8%
B_0347	CABINET #28	4b(a), Closed, TP	25	200	22	37	53	86	17	0.296	8	12	4	4	2.53E-09	99.8%
B_0348	CABINET #23	4b(a), Closed, TP	25	200	22	37	53	86	17	0.296	11	12	4	4	3.82E-09	66.2%
B_0349	CABINET #24	4b(a), Closed, TP	25	200	22	37	53	86	17	0.296	11	12	4	4	3.82E-09	66.2%
B_0350	CABINET #25	4b(a), Closed, TP	25	200	22	37	53	86	17	0.296	7	12	3	4	3.82E-09	66.2%
B_0352	CABINET #1	4b(a), Closed, TP	25	200	22	37	53	86	17	0.296	6	17	2	2	2.16E-09	39.1%
B_0353	CABINET #2	4b(a), Closed, TP	25	200	22	37	53	86	17	0.296	8	13	2	2	2.16E-09	39.0%
B_0354	CABINET #3	4b(a), Closed, TP	25	200	22	37	53	86	17	0.296	4	12	2	2	2.13E-09	39.6%
B_0356	CABINET #4	4b(a), Closed, TP	25	200	22	37	53	86	17	0.296	6	8	2	2	2.13E-09	39.6%
B_0357	CABINET #5	4b(a), Closed, TP	25	200	22	37	53	86	17	0.296	4	8	2	2	2.15E-09	39.3%
B_0358	CABINET #6	4b(a), Closed, TP	25	200	22	37	53	86	17	0.296	4	10	2	2	2.31E-09	36.6%
B_0359	CABINET #7	4b(a), Closed, TP	25	200	22	37	53	86	17	0.296	5	9	2	2	2.16E-09	39.0%
B_0360	CABINET #8	4b(a), Closed, TP	25	200	22	37	53	86	17	0.296	6	11	2	2	2.55E-09	33.2%
B_0361	CABINET #9	4b(a), Closed, TP	25	200	22	37	53	86	17	0.296	4	14	2	2	2.15E-09	39.3%
B_0362	CABINET #10	4b(a), Closed, TP	25	200	22	37	53	86	17	0.296	9	16	2	2	8.62E-10	98.0%
B_0363	CABINET #11	4b(a), Closed, TP	25	200	22	37	53	86	17	0.296	9	14	2	2	2.16E-09	39.0%
B_0364	CABINET #12	4b(a), Closed, TP	25	200	22	37	53	86	17	0.296	5	14	2	2	2.16E-09	39.0%
C_0183	BATTERY CHARGER – A	2, TP	25	130	22	37	44	72	19	0.340	5	10	2	4	8.74E-08	56.2%
C_0184	BATTERY CHARGER – A-1	2, TP	25	130	22	37	44	72	19	0.340	19	19	5	5	2.43E-07	82.7%
C_0185	MCC-A	2, TP	25	130	22	37	44	72	N/A	0.000	0	0	0	0	1.18E-07	0.0%
C_0186	MCC-B	2, TP	25	130	22	37	44	72	N/A	0.000	0	0	0	0	1.99E-08	0.0%
C_0188	BATTERY CHARGER – B-1	2, TP	25	130	22	37	44	72	16	0.374	7	7	2	2	1.76E-09	0.0%
C_0189	BATTERY CHARGER – B	2, TP	25	130	22	37	44	72	42	0.140	0	1	0	0	0.00E+00	0.0%

F.2.3.4 Case 4

In addition to updated HRRs, Case 4 accounts for the obstructed plume due to the cabinet enclosure. Based on the guidance presented in this report, the plume temperature will exhibit a 38% temperature reduction (Chapter 6) resulting in a vertical ZOI reduction of 24% (Chapter 6). These reductions were applied and the CDFs calculated using the same process as for cases 1 and 2. The results are presented in Table F-6.

Table F-6
Cabinet List with RACHELLE_FIRE HRRs and Obstructed Plume (Case 4)

Source ID	Description	Binning Group	HRR		75th ZOI (in)		98th ZOI (in)		To First Target	SF	75th # Targets	98th # Targets	75th # Trays	98th # Trays	CDF	% HGL
		Table 4.1 and 4.2	75th	98th	Horizontal	Vertical	Horizontal	Vertical	inches							
A_0312	CABINET #312	4a(a), Closed, TP	50	400	30	37	69	84	44	0.118	0	3	0	0	0.00E+00	0.0%
A_0314	DC HOLD CABINET	4a(a), Closed, TP	50	400	30	37	69	84	41	0.129	0	16	0	4	4.83E-08	98.7%
A_0315	LOGIC CABINET	4a(a), Closed, TP	50	400	30	37	69	84	41	0.129	0	20	0	5	8.45E-08	97.7%
A_0316	POWER CABINET – 2BD	4a(a), Closed, TP	50	400	30	37	69	84	46	0.110	0	5	0	0	0.00E+00	0.0%
A_0317	POWER CABINET – 2AC	4a(a), Closed, TP	50	400	30	37	69	84	41	0.129	0	26	0	7	4.46E-07	27.1%
A_0318	POWER CABINET – 1BD	4a(a), Closed, TP	50	400	30	37	69	84	42	0.125	0	10	0	0	1.29E-09	0.0%
A_0319	POWER CABINET – 1AC	4a(a), Closed, TP	50	400	30	37	69	84	40	0.133	0	32	0	7	2.37E-07	25.5%
A_0320	CORE EXIT THERMOCOUPLE CABINET	4b(a), Closed, TP	25	200	22	28	53	64	N/A	0.000	4	4	0	0	0.00E+00	0.0%
A_0321	IMPACT MONITORING SYSTEM CABINET	4b(a), Closed, TP	25	200	22	28	53	64	19	0.204	3	3	0	0	0.00E+00	0.0%
B_0337	CABINET #14	4b(a), Closed, TP	25	200	22	28	53	64	17	0.219	17	23	4	4	3.19E-09	58.7%
B_0338	CABINET #15	4b(a), Closed, TP	25	200	22	28	53	64	17	0.219	12	22	4	4	3.19E-09	58.7%
B_0339	CABINET #16	4b(a), Closed, TP	25	200	22	28	53	64	17	0.219	13	23	4	4	3.16E-09	59.2%
B_0340	CABINET #17	4b(a), Closed, TP	25	200	22	28	53	64	17	0.219	17	19	4	4	3.16E-09	59.3%
B_0341	CABINET #18	4b(a), Closed, TP	25	200	22	28	53	64	17	0.219	16	20	4	4	3.16E-09	59.3%
B_0343	CABINET #19	4b(a), Closed, TP	25	200	22	28	53	64	17	0.219	12	17	4	4	3.16E-09	59.3%
B_0344	CABINET #20	4b(a), Closed, TP	25	200	22	28	53	64	17	0.219	11	14	4	4	3.57E-09	52.5%
B_0345	CABINET #21	4b(a), Closed, TP	25	200	22	28	53	64	17	0.219	9	12	4	4	1.88E-09	99.8%
B_0346	CABINET #22	4b(a), Closed, TP	25	200	22	28	53	64	17	0.219	8	9	4	4	1.88E-09	99.8%
B_0347	CABINET #28	4b(a), Closed, TP	25	200	22	28	53	64	17	0.219	8	12	4	4	1.88E-09	99.8%
B_0348	CABINET #23	4b(a), Closed, TP	25	200	22	28	53	64	17	0.219	11	12	4	4	3.16E-09	59.3%
B_0349	CABINET #24	4b(a), Closed, TP	25	200	22	28	53	64	17	0.219	11	12	4	4	3.16E-09	59.3%
B_0350	CABINET #25	4b(a), Closed, TP	25	200	22	28	53	64	17	0.219	7	12	3	4	3.16E-09	59.3%
B_0352	CABINET #1	4b(a), Closed, TP	25	200	22	28	53	64	17	0.219	6	17	2	2	2.16E-09	39.1%
B_0353	CABINET #2	4b(a), Closed, TP	25	200	22	28	53	64	17	0.219	8	13	2	2	2.16E-09	39.0%
B_0354	CABINET #3	4b(a), Closed, TP	25	200	22	28	53	64	17	0.219	4	12	2	2	2.13E-09	39.6%
B_0356	CABINET #4	4b(a), Closed, TP	25	200	22	28	53	64	17	0.219	6	8	2	2	2.13E-09	39.6%
B_0357	CABINET #5	4b(a), Closed, TP	25	200	22	28	53	64	17	0.219	4	8	2	2	2.15E-09	39.3%
B_0358	CABINET #6	4b(a), Closed, TP	25	200	22	28	53	64	17	0.219	4	10	2	2	2.28E-09	37.1%
B_0359	CABINET #7	4b(a), Closed, TP	25	200	22	28	53	64	17	0.219	5	9	2	2	2.16E-09	39.1%
B_0360	CABINET #8	4b(a), Closed, TP	25	200	22	28	53	64	17	0.219	6	11	2	2	2.54E-09	33.3%
B_0361	CABINET #9	4b(a), Closed, TP	25	200	22	28	53	64	17	0.219	4	14	2	2	2.15E-09	39.3%
B_0362	CABINET #10	4b(a), Closed, TP	25	200	22	28	53	64	17	0.219	9	16	2	2	8.61E-10	98.1%
B_0363	CABINET #11	4b(a), Closed, TP	25	200	22	28	53	64	17	0.219	9	14	2	2	2.16E-09	39.0%
B_0364	CABINET #12	4b(a), Closed, TP	25	200	22	28	53	64	17	0.219	5	14	2	2	2.16E-09	39.0%
C_0183	BATTERY CHARGER – A	2, TP	25	130	22	28	44	54	19	0.235	2	10	0	4	6.12E-08	80.2%
C_0184	BATTERY CHARGER – A-1	2, TP	25	130	22	28	44	54	19	0.235	19	19	5	5	1.74E-07	82.9%
C_0185	MCC-A	2, TP	25	130	22	28	44	54	N/A	0.000	0	0	0	0	1.18E-07	0.0%
C_0186	MCC-B	2, TP	25	130	22	28	44	54	N/A	0.000	0	0	0	0	1.99E-08	0.0%
C_0188	BATTERY CHARGER – B-1	2, TP	25	130	22	28	44	54	16	0.270	7	7	2	2	1.29E-09	0.0%
C_0189	BATTERY CHARGER – B	2, TP	25	130	22	28	44	54	42	0.063	0	1	0	0	0.00E+00	0.0%

F.2.3.5 Case 5

For cabinets contributing significantly to risk, additional internal inspections were made to evaluate the fuel loading level, fuel type, and cable bundling arrangement to see if further reduction to the cabinet's HRR was possible. The following photos show cabinets for which the HRR could be further reduced.

<u>Fire Compartment A</u>

<u>Source 0315</u>

Figure F-7
Photos of Source 0315 Outside (right cabinet in photo) and Inside

The fuel load for Source 0315 (Figure F-7) is a single cable bundle that is tightly bound and does not hang loosely. However the circuit cards present are in moderate quantities.

Based on the guidance provided in Table 4-1, re-binning the cabinet from Default (Table 4-2, Group 4a(a)) to Low (Table 4-2, Group 4a(b)) is not justified. The amount of circuit cards precludes re-grouping to a lower combustible load.

Source 0319

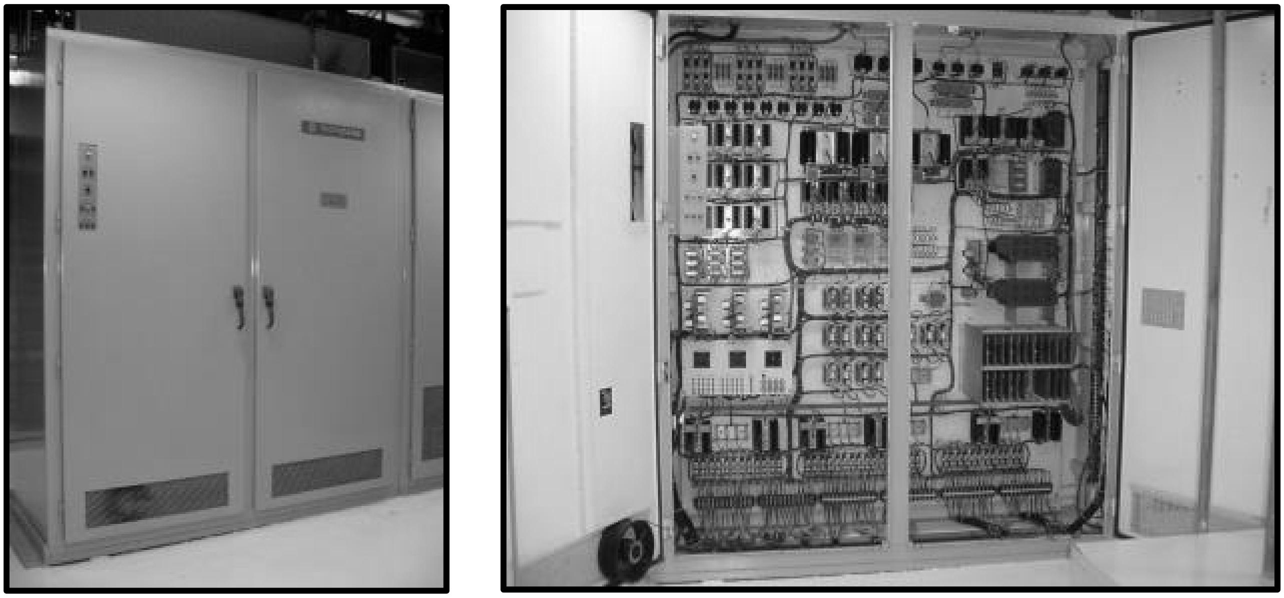

Figure F-8
Photos of Source 0319 Outside and Inside

Sources 0317 and 0319 (Figure F-8) are both power cabinets with similar combustible loading. The fuel load is at most moderate and the cable bundle arrangement is comprised of tightly bundled cables and arranged in an orderly manner. There are only a handful of exposed printed circuit cards present.

Based on the guidance provided in Table 4-1, re-binning the cabinet from Default (Table 4-2, Group 4a(a)) to Low (Table 4-2, Group 4a(b)) is acceptable.

Fire Compartment B

Source 0362

Figure F-9
Photo of Source 0362 Outside

Figure F-10
Photo of Source 0362 Inside Front

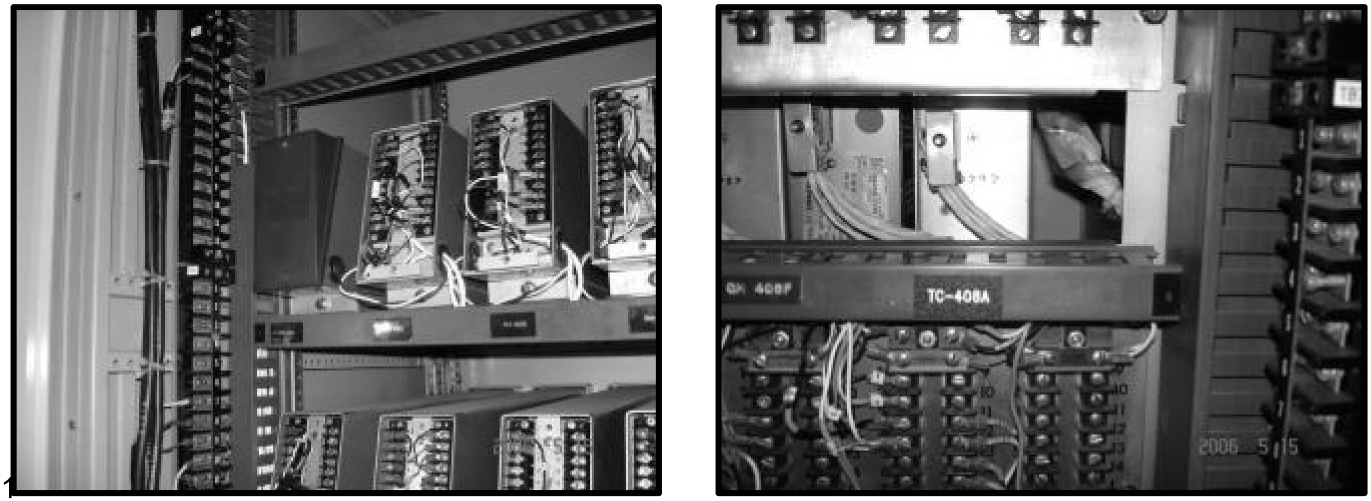

Figure F-11
Photos of Source 0362 Inside Rear

Source 0362 (Figures F-9, F-10, and F-11) is indicative of all other power cabinets within this compartment. The fuel load is at most moderate, with very few cables. Most of the cabinet is comprised of non-combustible material.

Based on the guidance provided in Table 4-1, re-binning the cabinet from Default (Table 4-2, Group 4b(a)) to Low (Table 4-2, Group 4b(b)) is acceptable. HRRs were applied as follows:

- Group 2: Battery Chargers; 75th is 25 kW, 98th is 130 kW
- Group 4a(a): Large Enclosures, Closed; 75th is 50 kW, 98th is 400 kW
- Group 4a(b): Large Enclosures, Closed; 75th is 25 kW, 98th is 200 kW
- Group 4b(a): Medium Enclosures, Closed; 75th is 25 kW, 98th is 200 kW
- Group 4b(b): Medium Enclosures, Closed; 75th is 15 kW, 98th is 100 kW

Table F-7
Credit for Inspecting Cabinet Internals (Case 5)

Source ID	Description	Binning Group	HRR		75th ZOI (in)		98th ZOI (in)		To First Target	SF	75th # Targets	98th # Targets	75th # Trays	98th # Trays	CDF	% HGL
		Table 4.1 and 4.2	75th	98th	Horizontal	Vertical	Horizontal	Vertical	inches							
A_0312	CABINET #312	4a(a), Closed, TP	50	400	30	37	69	84	44	0.118	0	3	0	0	0.00E+00	0.0%
A_0314	DC HOLD CABINET	4a(a), Closed, TP	50	400	30	37	69	84	41	0.129	0	16	0	4	4.83E-08	98.7%
A_0315	LOGIC CABINET	4a(a), Closed, TP	50	400	30	37	69	84	41	0.129	0	20	0	5	8.45E-08	97.7%
A_0316	POWER CABINET – 2BD	4a(a), Closed, TP	50	400	30	37	69	84	46	0.110	0	5	0	0	0.00E+00	0.0%
A_0317	POWER CABINET – 2AC	4a(b), Closed, TP	25	200	22	28	53	64	41	0.084	0	14	0	4	2.08E-08	99.7%
A_0318	POWER CABINET – 1BD	4a(a), Closed, TP	50	400	30	37	69	84	42	0.125	0	10	0	0	1.29E-09	0.0%
A_0319	POWER CABINET – 1AC	4a(b), Closed, TP	25	200	22	28	53	64	40	0.087	0	16	0	2	1.31E-10	0.0%
A_0320	CORE EXIT THERMOCOUPLE CABINET	4b(a), Closed, TP	25	200	22	28	53	64	N/A	0.000	4	4	0	0	0.00E+00	0.0%
A_0321	IMPACT MONITORING SYSTEM CABINET	4b(a), Closed, TP	25	200	22	28	53	64	19	0.204	3	3	0	0	0.00E+00	0.0%
B_0337	CABINET #14	4b(b), Closed, TP	15	100	18	23	40	48	17	0.199	16	21	4	4	3.00E-09	56.1%
B_0338	CABINET #15	4b(b), Closed, TP	15	100	18	23	40	48	17	0.199	11	20	4	4	3.00E-09	56.1%
B_0339	CABINET #16	4b(b), Closed, TP	15	100	18	23	40	48	17	0.199	12	20	4	4	2.98E-09	56.7%
B_0340	CABINET #17	4b(b), Closed, TP	15	100	18	23	40	48	17	0.199	16	18	4	4	2.97E-09	56.7%
B_0341	CABINET #18	4b(b), Closed, TP	15	100	18	23	40	48	17	0.199	14	19	4	4	2.97E-09	56.7%
B_0343	CABINET #19	4b(b), Closed, TP	15	100	18	23	40	48	17	0.199	12	13	4	4	2.97E-09	56.7%
B_0344	CABINET #20	4b(b), Closed, TP	15	100	18	23	40	48	17	0.199	11	14	4	4	3.38E-09	49.9%
B_0345	CABINET #21	4b(b), Closed, TP	15	100	18	23	40	48	17	0.199	9	11	4	4	1.69E-09	99.8%
B_0346	CABINET #22	4b(b), Closed, TP	15	100	18	23	40	48	17	0.199	8	9	4	4	1.69E-09	99.8%
B_0347	CABINET #28	4b(b), Closed, TP	15	100	18	23	40	48	17	0.199	8	11	4	4	1.69E-09	99.8%
B_0348	CABINET #23	4b(b), Closed, TP	15	100	18	23	40	48	17	0.199	11	11	4	4	2.97E-09	56.7%
B_0349	CABINET #24	4b(b), Closed, TP	15	100	18	23	40	48	17	0.199	11	12	4	4	2.97E-09	56.7%
B_0350	CABINET #25	4b(b), Closed, TP	15	100	18	23	40	48	17	0.199	7	12	3	4	2.97E-09	56.7%
B_0352	CABINET #1	4b(b), Closed, TP	15	100	18	23	40	48	17	0.199	5	16	2	2	1.32E-09	0.0%
B_0353	CABINET #2	4b(b), Closed, TP	15	100	18	23	40	48	17	0.199	7	12	2	2	1.32E-09	0.0%
B_0354	CABINET #3	4b(b), Closed, TP	15	100	18	23	40	48	17	0.199	4	11	2	2	1.29E-09	0.0%
B_0356	CABINET #4	4b(b), Closed, TP	15	100	18	23	40	48	17	0.199	6	7	2	2	1.29E-09	0.0%
B_0357	CABINET #5	4b(b), Closed, TP	15	100	18	23	40	48	17	0.199	4	7	2	2	1.29E-09	0.0%
B_0358	CABINET #6	4b(b), Closed, TP	15	100	18	23	40	48	17	0.199	4	6	2	2	1.41E-09	0.0%
B_0359	CABINET #7	4b(b), Closed, TP	15	100	18	23	40	48	17	0.199	4	7	2	2	1.30E-09	0.0%
B_0360	CABINET #8	4b(b), Closed, TP	15	100	18	23	40	48	17	0.199	5	10	2	2	1.69E-09	0.0%
B_0361	CABINET #9	4b(b), Closed, TP	15	100	18	23	40	48	17	0.199	4	14	2	2	1.30E-09	0.0%
B_0362	CABINET #10	4b(b), Closed, TP	15	100	18	23	40	48	17	0.199	9	13	2	2	2.76E-12	0.0%
B_0363	CABINET #11	4b(b), Closed, TP	15	100	18	23	40	48	17	0.199	8	13	2	2	1.32E-09	0.0%
B_0364	CABINET #12	4b(b), Closed, TP	15	100	18	23	40	48	17	0.199	5	13	2	2	1.32E-09	0.0%
C_0183	BATTERY CHARGER – A	2, TP	25	130	22	28	44	54	19	0.235	2	10	0	4	6.12E-08	80.2%
C_0184	BATTERY CHARGER – A-1	2, TP	25	130	22	28	44	54	19	0.235	19	19	5	5	1.74E-07	82.9%
C_0185	MCC-A	2, TP	25	130	22	28	44	54	N/A	0.000	0	0	0	0	1.18E-07	0.0%
C_0186	MCC-B	2, TP	25	130	22	28	44	54	N/A	0.000	0	0	0	0	1.99E-08	0.0%
C_0188	BATTERY CHARGER – B-1	2, TP	25	130	22	28	44	54	16	0.270	7	7	2	2	1.29E-09	0.0%
C_0189	BATTERY CHARGER – B	2, TP	25	130	22	28	44	54	42	0.063	0	1	0	0	0.00E+00	0.0%

F.2.3.6 Additional Case 2a

In many plants modifications are required to reduce risk. In this example, Case 2 represents an analysis that has applied a significant amount of fire modeling refinement; however, the risk may still be higher than required to meet the application. Because a high percentage of the risk is due to HGL development, the addition of an automatic suppression system may be an option.

Case 2a was added to compare the benefits of applying the RACHELLE_FIRE guidance compared to installing a modification to provide automatic suppression. The automatic suppression is assumed to be 95% effective at preventing fire spread beyond the local damage set (i.e., preventing HGL). The results for Case 2a are presented in Table F-8. Note that manual suppression is included in both Case 2 and 2a and also has some impact on HGL development.

Table F-8
Case 2 with Automatic Suppression Credit (Case 2a)

Source ID	Description	CDF	% HGL
A_0312	CABINET #312	0.00E+00	0.0%
A_0314	DC HOLD CABINET	4.26E-08	86.6%
A_0315	LOGIC CABINET	5.29E-08	83.8%
A_0316	POWER CABINET – 2BD	0.00E+00	0.0%
A_0317	POWER CABINET – 2AC	1.49E-06	3.5%
A_0318	POWER CABINET – 1BD	4.87E-09	0.0%
A_0319	POWER CABINET – 1AC	8.19E-07	2.9%
A_0320	CORE EXIT THERMOCOUPLE CABINET	0.00E+00	0.0%
A_0321	IMPACT MONITORING SYSTEM CABINET	0.00E+00	0.0%
B_0337	CABINET #14	6.61E-08	8.7%
B_0338	CABINET #15	6.61E-08	8.7%
B_0339	CABINET #16	1.25E-08	46.0%
B_0340	CABINET #17	7.04E-09	81.5%
B_0341	CABINET #18	7.04E-09	81.5%
B_0343	CABINET #19	7.05E-09	81.3%
B_0344	CABINET #20	7.53E-09	76.2%
B_0345	CABINET #21	5.77E-09	99.4%
B_0346	CABINET #22	5.75E-09	99.7%
B_0347	CABINET #28	5.75E-09	99.7%
B_0348	CABINET #23	7.04E-09	81.5%
B_0349	CABINET #24	7.04E-09	81.5%
B_0350	CABINET #25	7.04E-09	81.5%
B_0352	CABINET #1	7.04E-09	81.1%
B_0353	CABINET #2	7.04E-09	81.1%
B_0354	CABINET #3	7.01E-09	81.4%
B_0356	CABINET #4	7.12E-09	80.1%
B_0357	CABINET #5	7.12E-09	80.1%
B_0358	CABINET #6	7.69E-09	74.2%
B_0359	CABINET #7	7.12E-09	80.1%
B_0360	CABINET #8	7.50E-09	76.1%
B_0361	CABINET #9	7.12E-09	80.1%
B_0362	CABINET #10	5.83E-09	97.8%
B_0363	CABINET #11	7.05E-09	80.9%
B_0364	CABINET #12	7.04E-09	81.1%
C_0183	BATTERY CHARGER – A	1.17E-07	35.1%
C_0184	BATTERY CHARGER – A-1	1.32E-07	35.4%
C_0185	MCC-A	1.18E-07	0.0%
C_0186	MCC-B	1.99E-08	0.0%
C_0188	BATTERY CHARGER – B-1	3.08E-09	0.0%
C_0189	BATTERY CHARGER – B	3.11E-10	0.0%

F.2.4 Results Review

Table F-9 provides a summary of the CDF results by compartment for each of the cases evaluated. The CDFs for Case 1 indicate relatively high risk numbers prior to applying more refined fire modeling. Before evaluating the RACHELLE_FIRE HRRs it is desired to apply currently available guidance as described in Appendix F.2.3.2 in order to get a realistic measure of the potential CDF impacts using the revised guidance. From Table F-10 it can be seen that there was about 64% reduction in CDF due to the refinements applied. These results are used as the baseline to evaluate the RACHELLE_FIRE impacts.

Table F-9
Compartment CDF Comparison

Compartment	Case 1	Case 2	Case 3	Case 4	Case 5
A	8.18E-06	3.13E-06	8.18E-07	8.18E-07	1.55E-07
B	2.27E-06	3.31E-07	7.13E-08	6.28E-08	5.02E-08
C	2.10E-06	9.61E-07	4.69E-07	3.74E-07	4.01E-07
all	1.26E-05	4.42E-06	1.36E-06	1.25E-06	6.06E-07

Table F-10
CDF Reduction Percentages Between Cases

Compartment	Case 1to2	Case 2to3	Case 3to4	Case 4to5	Case 2to4	Case 2to5
A	61.8%	73.8%	0.0%	81.0%	73.8%	95.0%
B	85.4%	78.4%	12.0%	20.2%	81.0%	84.8%
C	54.3%	51.1%	20.4%	0.0%	61.1%	61.1%
all	64.8%	69.3%	7.7%	53.8%	71.6%	86.9%

Applying the revised guidance presented in RACHELLE_FIRE resulted in an overall calculated CDF reduction of nearly 87% for the locations evaluated. However, the benefits varied based on the room configurations. Tables F-11 through F-14 provide a comparison of specific parameters, and results for the various cases.

The most obvious contribution to the CDF reduction is due to the reduction of the severity factors (Table F-13). Overall severity factors were reduced by about 74% on average. This reduction represents the fraction of the HRR distribution that can cause damage to targets. Figure F-12 provides a comparison of the possible change in severity factors based on MCC HRRs between NUREG/CR-6850 guidance and RACHELLE_FIRE guidance assuming qualified cables, thermoplastic targets, and other parameters used for this example.

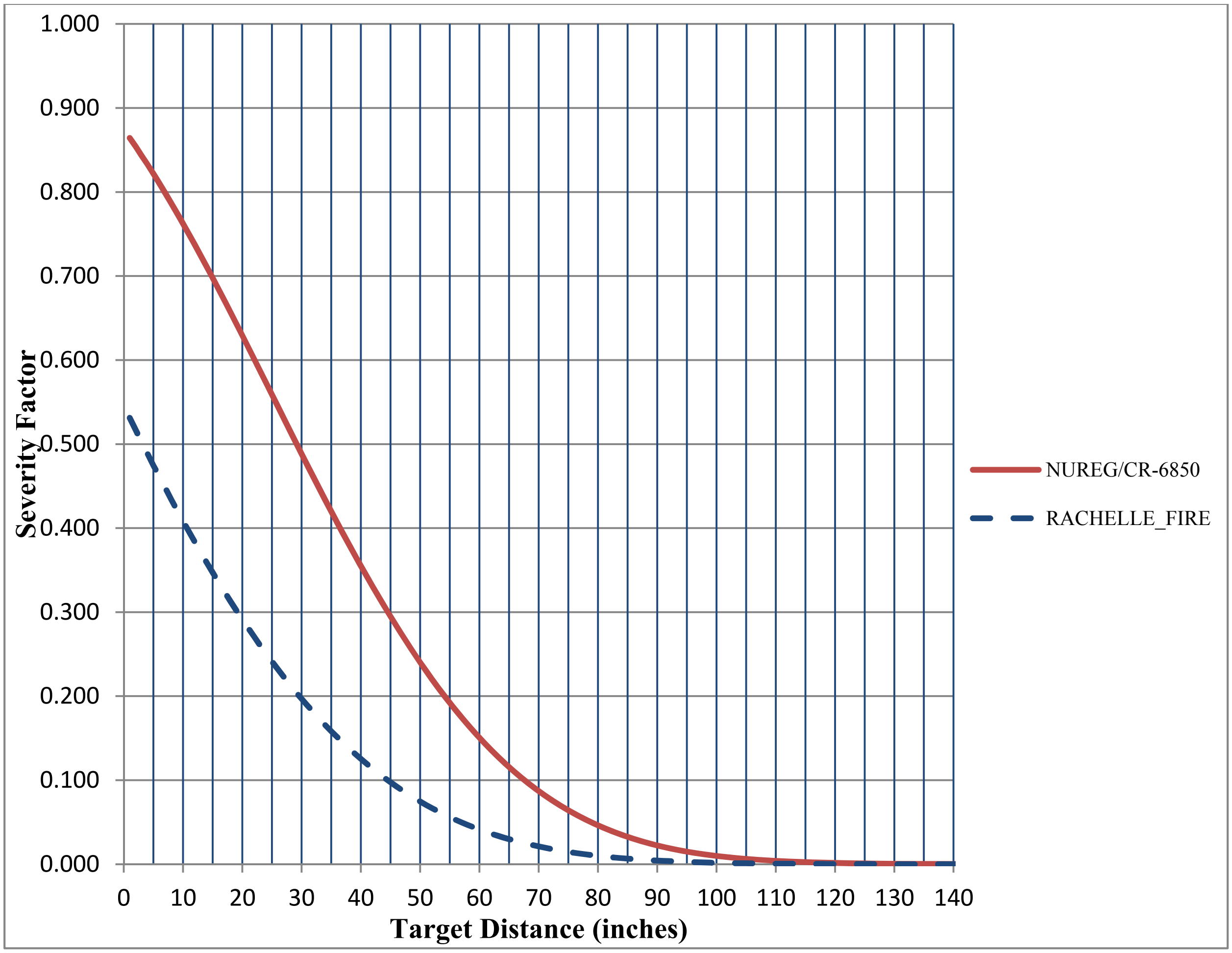

Figure F-12
Severity Factor Comparison

The CDF is also reduced based on a smaller ZOI for the RACHELLE_FIRE HRRs. The smaller ZOIs allow some targets to be excluded from the analysis. The total number of targets was reduced by 36% for the 98th percentile fires, and 54% for the 75th percentile fires (Ref. Table F-12). The largest impact was due to the reduction in horizontal ZOI because most of these targets were not involved in fire propagation. The vertical ZOI showed less impact due to the propagation of secondary combustibles (i.e., cable trays). It follows that there can still be a significant potential to develop HGL even with the updated HRRs applied. This is mainly a function of the amount of secondary combustibles and nearness to the ignition source. In some scenarios, the percentage of CDF due to HGL increased because the number of targets in the local target set was reduced but the probability of developing HGL did not change if the nearest cable tray was still within the ZOI.

The impacts vary by compartment based on the source target configurations and the room parameters. Compartment A had the greatest CDF reduction at 95%. Compartment A is an average room with most targets at least 24 inches from the source. Compartment B also had a significant CDF reduction of about 84%. A substantial benefit was realized in these compartments based on the HRR refinements in Case 5. Compartment C had less impact but still saw a 61% reduction in CDF by applying the guidance. The impacts from treatment of obstructed plumes varied from less than 1% up to 20% reduction in CDF for compartments A and C respectively.

A comparison was also made based on adding suppression versus applying the RACHELLE_FIRE guidance. The results presented in Table F-11 show that the CDF reduction of the modification was not as much as from applying the RACHELLE_FIRE guidance.

Table F-11
Modification Impact Comparison

Compartment	Case 2 (no supp)	Case 2a (w/supp)	Case 5 (no supp)	Case 2to2a	Case 2to5
A	3.13E-06	2.41E-06	1.55E-07	23.0%	95.0%
B	3.31E-07	2.96E-07	5.02E-08	10.4%	84.8%
C	9.61E-07	3.90E-07	4.01E-07	59.4%	61.1%
all	4.42E-06	3.10E-06	6.06E-07	29.9%	86.9%

Table F-12
Comparison of Number of Targets

Source ID	# of Targets (98th)					# of Targets (75th)				
	Case 1	Case 2	Case 3	Case 4	Case 5	Case 1	Case 2	Case 3	Case 4	Case 5
A_0312	3	3	3	3	3	N/A	3	3	0	0
A_0314	20	20	16	16	16	N/A	13	3	0	0
A_0315	20	20	20	20	20	N/A	20	3	0	0
A_0316	5	5	5	5	5	N/A	4	1	0	0
A_0317	30	30	26	26	14	N/A	25	1	0	0
A_0318	10	10	10	10	10	N/A	10	3	0	0
A_0319	34	34	32	32	16	N/A	25	5	0	0
A_0320	4	4	4	4	4	N/A	4	4	4	4
A_0321	3	3	3	3	3	N/A	3	3	3	3
B_0337	37	37	23	23	21	N/A	24	16	17	16
B_0338	34	34	22	22	20	N/A	29	11	12	11
B_0339	33	33	23	23	20	N/A	26	12	13	12
B_0340	29	29	19	19	18	N/A	23	16	17	16
B_0341	25	25	20	20	19	N/A	20	15	16	14
B_0343	24	24	17	17	13	N/A	18	12	12	12
B_0344	22	22	14	14	14	N/A	14	11	11	11
B_0345	21	21	12	12	11	N/A	13	9	9	9
B_0346	21	21	9	9	9	N/A	14	8	8	8
B_0347	19	19	12	12	11	N/A	12	8	8	8
B_0348	19	19	12	12	11	N/A	12	11	11	11
B_0349	15	15	12	12	12	N/A	12	11	11	11
B_0350	13	13	12	12	12	N/A	12	7	7	7
B_0352	26	26	17	17	16	N/A	17	6	6	5
B_0353	22	22	13	13	12	N/A	18	8	8	7
B_0354	21	21	12	12	11	N/A	14	4	4	4
B_0356	15	15	8	8	7	N/A	10	6	6	6
B_0357	12	12	8	8	7	N/A	9	4	4	4
B_0358	14	14	10	10	6	N/A	10	4	4	4
B_0359	19	19	9	9	7	N/A	12	5	5	4
B_0360	18	18	11	11	10	N/A	15	6	6	5
B_0361	17	17	14	14	14	N/A	15	4	4	4
B_0362	17	17	16	16	13	N/A	16	9	9	9
B_0363	17	17	14	14	13	N/A	15	9	9	8
B_0364	15	15	14	14	13	N/A	14	5	5	5
C_0183	11	11	10	10	10	N/A	10	5	2	2
C_0184	20	20	19	19	19	N/A	19	19	19	19
C_0185	3	3	0	0	0	N/A	3	0	0	0
C_0186	4	4	0	0	0	N/A	4	0	0	0
C_0188	7	7	7	7	7	N/A	7	7	7	7
C_0189	3	3	1	1	1	N/A	0	0	0	0
Total	702	702	509	509	448	0	544	274	257	246

Table F-13
Severity Factor Comparison

Source ID	Severity Factor				
	Case 1	Case 2	Case 3	Case 4	Case 5
A_0312	0.648	0.299	0.189	0.118	0.118
A_0314	0.828	0.478	0.202	0.129	0.129
A_0315	0.828	0.478	0.202	0.129	0.129
A_0316	0.786	0.440	0.180	0.110	0.110
A_0317	0.828	0.478	0.202	0.129	0.084
A_0318	0.807	0.471	0.197	0.125	0.125
A_0319	0.821	0.486	0.206	0.133	0.087
A_0320	0.000	0.000	0.000	0.000	0.000
A_0321	0.917	0.620	0.281	0.204	0.204
B_0337	0.958	0.802	0.296	0.219	0.199
B_0338	0.958	0.802	0.296	0.219	0.199
B_0339	0.958	0.802	0.296	0.219	0.199
B_0340	0.958	0.802	0.296	0.219	0.199
B_0341	0.958	0.802	0.296	0.219	0.199
B_0343	0.958	0.802	0.296	0.219	0.199
B_0344	0.958	0.802	0.296	0.219	0.199
B_0345	0.958	0.802	0.296	0.219	0.199
B_0346	0.958	0.802	0.296	0.219	0.199
B_0347	0.958	0.802	0.296	0.219	0.199
B_0348	0.958	0.802	0.296	0.219	0.199
B_0349	0.958	0.802	0.296	0.219	0.199
B_0350	0.958	0.802	0.296	0.219	0.199
B_0352	0.958	0.802	0.296	0.219	0.199
B_0353	0.958	0.802	0.296	0.219	0.199
B_0354	0.958	0.802	0.296	0.219	0.199
B_0356	0.958	0.802	0.296	0.219	0.199
B_0357	0.958	0.802	0.296	0.219	0.199
B_0358	0.958	0.802	0.296	0.219	0.199
B_0359	0.958	0.802	0.296	0.219	0.199
B_0360	0.958	0.802	0.296	0.219	0.199
B_0361	0.958	0.802	0.296	0.219	0.199
B_0362	0.958	0.802	0.296	0.219	0.199
B_0363	0.958	0.802	0.296	0.219	0.199
B_0364	0.958	0.802	0.296	0.219	0.199
C_0183	0.854	0.620	0.340	0.235	0.235
C_0184	0.924	0.620	0.340	0.235	0.235
C_0185	0.000	0.000	0.000	0.000	0.000
C_0186	0.000	0.000	0.000	0.000	0.000
C_0188	0.900	0.660	0.374	0.270	0.270
C_0189	0.538	0.322	0.140	0.063	0.063
Avg.	0.841	0.651	0.256	0.184	0.169

Table F-14
Comparison of HGL Fraction

Source ID	CDF					HGL				
	Case 1	Case 2	Case 3	Case 4	Case 5	Case 1	Case 2	Case 3	Case 4	Case 5
A_0312	0.00E+00	0.00E+00	0.00E+00	0.00E+00	0.00E+00	0.0%	0.0%	0.0%	0.0%	0.0%
A_0314	9.26E-07	1.58E-07	4.83E-08	4.83E-08	4.83E-08	98.2%	96.5%	98.7%	98.7%	98.7%
A_0315	1.02E-06	3.09E-07	8.45E-08	8.45E-08	8.45E-08	98.4%	97.4%	97.7%	97.7%	97.7%
A_0316	0.00E+00	0.00E+00	0.00E+00	0.00E+00	0.00E+00	0.0%	0.0%	0.0%	0.0%	0.0%
A_0317	4.12E-06	1.74E-06	4.46E-07	4.46E-07	2.08E-08	32.5%	25.6%	27.1%	27.1%	99.7%
A_0318	1.12E-08	4.87E-09	1.29E-09	1.29E-09	1.29E-09	0.0%	0.0%	0.0%	0.0%	0.0%
A_0319	2.10E-06	9.11E-07	2.37E-07	2.37E-07	1.31E-10	31.7%	19.0%	25.5%	25.5%	0.0%
A_0320	0.00E+00	0.00E+00	0.00E+00	0.00E+00	0.00E+00	0.0%	0.0%	0.0%	0.0%	0.0%
A_0321	0.00E+00	0.00E+00	0.00E+00	0.00E+00	0.00E+00	0.0%	0.0%	0.0%	0.0%	0.0%
B_0337	7.93E-07	6.74E-08	3.84E-09	3.19E-09	3.00E-09	4.3%	11.0%	65.7%	58.7%	56.1%
B_0338	7.93E-07	6.74E-08	3.84E-09	3.19E-09	3.00E-09	4.3%	11.0%	65.7%	58.7%	56.1%
B_0339	1.05E-07	1.41E-08	3.82E-09	3.16E-09	2.98E-09	32.4%	52.5%	66.2%	59.2%	56.7%
B_0340	3.53E-08	8.70E-09	3.82E-09	3.16E-09	2.97E-09	96.3%	85.0%	66.2%	59.3%	56.7%
B_0341	3.53E-08	8.70E-09	3.82E-09	3.16E-09	2.97E-09	96.3%	85.0%	66.2%	59.3%	56.7%
B_0343	3.55E-08	8.72E-09	3.82E-09	3.16E-09	2.97E-09	95.7%	84.9%	66.2%	59.3%	56.7%
B_0344	3.59E-08	9.19E-09	4.23E-09	3.57E-09	3.38E-09	94.7%	80.5%	59.8%	52.5%	49.9%
B_0345	3.43E-08	7.43E-09	2.53E-09	1.88E-09	1.69E-09	99.3%	99.6%	99.8%	99.8%	99.8%
B_0346	3.40E-08	7.41E-09	2.53E-09	1.88E-09	1.69E-09	99.9%	99.8%	99.8%	99.8%	99.8%
B_0347	3.40E-08	7.41E-09	2.53E-09	1.88E-09	1.69E-09	99.9%	99.8%	99.8%	99.8%	99.8%
B_0348	3.53E-08	8.70E-09	3.82E-09	3.16E-09	2.97E-09	96.3%	85.0%	66.2%	59.3%	56.7%
B_0349	3.53E-08	8.70E-09	3.82E-09	3.16E-09	2.97E-09	96.3%	85.0%	66.2%	59.3%	56.7%
B_0350	3.53E-08	8.70E-09	3.82E-09	3.16E-09	2.97E-09	96.3%	85.0%	66.2%	59.3%	56.7%
B_0352	1.82E-08	8.16E-09	2.16E-09	2.16E-09	1.32E-09	92.6%	83.7%	39.1%	39.1%	0.0%
B_0353	1.82E-08	8.16E-09	2.16E-09	2.16E-09	1.32E-09	92.6%	83.7%	39.0%	39.0%	0.0%
B_0354	1.82E-08	8.13E-09	2.13E-09	2.13E-09	1.29E-09	92.8%	84.0%	39.6%	39.6%	0.0%
B_0356	1.84E-08	8.24E-09	2.13E-09	2.13E-09	1.29E-09	91.6%	82.8%	39.6%	39.6%	0.0%
B_0357	1.84E-08	8.24E-09	2.15E-09	2.15E-09	1.29E-09	91.6%	82.8%	39.3%	39.3%	0.0%
B_0358	1.95E-08	8.81E-09	2.31E-09	2.28E-09	1.41E-09	86.4%	77.5%	36.6%	37.1%	0.0%
B_0359	2.79E-08	8.24E-09	2.16E-09	2.16E-09	1.30E-09	94.5%	82.8%	39.0%	39.1%	0.0%
B_0360	1.88E-08	8.62E-09	2.55E-09	2.54E-09	1.69E-09	89.8%	79.2%	33.2%	33.3%	0.0%
B_0361	1.84E-08	8.24E-09	2.15E-09	2.15E-09	1.30E-09	91.6%	82.8%	39.3%	39.3%	0.0%
B_0362	1.71E-08	6.96E-09	8.62E-10	8.61E-10	2.76E-12	98.5%	98.2%	98.0%	98.1%	0.0%
B_0363	1.84E-08	8.18E-09	2.16E-09	2.16E-09	1.32E-09	91.5%	83.5%	39.0%	39.0%	0.0%
B_0364	1.82E-08	8.16E-09	2.16E-09	2.16E-09	1.32E-09	92.6%	83.7%	39.0%	39.0%	0.0%
C_0183	7.16E-07	3.48E-07	8.74E-08	6.12E-08	6.12E-08	77.5%	79.7%	56.2%	80.2%	80.2%
C_0184	1.06E-06	4.71E-07	2.43E-07	1.74E-07	1.74E-07	83.5%	83.6%	82.7%	82.9%	82.9%
C_0185	1.18E-07	1.18E-07	1.18E-07	1.18E-07	1.18E-07	0.0%	0.0%	0.0%	0.0%	0.0%
C_0186	1.99E-08	1.99E-08	1.99E-08	1.99E-08	1.99E-08	0.0%	0.0%	0.0%	0.0%	0.0%
C_0188	1.91E-07	3.08E-09	1.76E-09	1.29E-09	1.29E-09	97.4%	0.0%	0.0%	0.0%	0.0%
C_0189	1.82E-09	3.11E-10	0.00E+00	0.00E+00	0.00E+00	0.0%	0.0%	0.0%	0.0%	0.0%
Total/Avg.	1.26E-05	4.42E-06	1.36E-06	1.25E-06	5.79E-07	65.9%	59.3%	46.6%	45.4%	32.9%

F.2.5 Conclusions

The revised guidance provided in RACHELLE_FIRE can be implemented effectively and can provide significant improvement in the fire risk of actual plant configurations. The amount of reduction from using the previous guidance will vary based on specific compartment and scenario parameters. Some specific insights are listed below.

- The new guidance can result in significantly reduced severity factors. This reduction is a direct result of reduced HRRs. This effect is pronounced for the non-power oriented functional classification groups (4a-4c), as most of the distributions are weighted more toward the lower end than in the previous guidance.
- Accounting for cabinet effects such as the obstructed plume nature of fires in closed cabinets provides significant reduction in the calculated vertical ZOI, and SF. Previous guidance treated the source fires as open fires. The new guidance addresses cases where the fire is inside of an enclosure.
- Reduction of the horizontal ZOI had the most impact in screening additional targets. This is primarily due to fire growth considerations involving secondary combustibles that have a greater impact on targets above the source rather than to the sides.
- Fire growth due to propagation of secondary combustibles may still drive results, especially if HGL is possible. The reduced HRRs and revised guidance had very little impact on fire propagation in cable trays.
- Inspection of cabinet internals can result in significant benefits for risk reduction. Control cabinets vary greatly. By opening the cabinets and inspecting the internal configuration, reduced HRRs can be justified in many instances.
- This example also provided some insights into the significance of applying refined fire modeling methods including a source specific fire size. Although bounding fire sizes may be more efficient to use for initial walkdowns and target selection, significant benefits can be obtained in many scenarios by applying source specific fire sizes.
- Applying the RACHELLE_FIRE guidance can provide useful insights for decisions regarding the need or justification of installing modifications.

NRC FORM 335
(12-2010)
NRCMD 3.7

U.S. NUCLEAR REGULATORY COMMISSION

BIBLIOGRAPHIC DATA SHEET

(See instructions on the reverse)

1. REPORT NUMBER
(Assigned by NRC, Add Vol., Supp., Rev., and Addendum Numbers, if any.)
NUREG-2178 Vol. 1
DRAFT

2. TITLE AND SUBTITLE
Refining and Characterizing Heat Release Rates from Electrical Enclosures during Fire (RACHELLE-FIRE)
Volume 1
Draft Report for Comment

3. DATE REPORT PUBLISHED

MONTH	YEAR
April	2015

4. FIN OR GRANT NUMBER

5. AUTHOR(S)
N. Melly (NRC), D. Stroup (NRC), G. Taylor (NRC), M. Subudhi (BNL), S. Nowlen (Consultant), A. Lindeman (EPRI), J. DeJoseph (Duke Energy), F. Joglar (Jensen Hughes), V. Ontiveros (Jensen Hughes), J. Williamson (Jensen Hughes), D. Miskiewicz (EPM)

6. TYPE OF REPORT
Technical

7. PERIOD COVERED (Inclusive Dates)

8. PERFORMING ORGANIZATION - NAME AND ADDRESS (If NRC, provide Division, Office or Region, U. S. Nuclear Regulatory Commission, and mailing address; if contractor, provide name and mailing address.)

9. SPONSORING ORGANIZATION - NAME AND ADDRESS (If NRC, type "Same as above", if contractor, provide NRC Division, Office or Region, U. S. Nuclear Regulatory Commission, and mailing address.)

Division of Risk Analysis
Office of Nuclear Regulatory Research
U.S. Nuclear regulatory Commission
Washington, DC 20555-0001

Electric Power Research Institute
3420 Hillview Avenue
Palo Alto, CA 94304

10. SUPPLEMENTARY NOTES
M.H. Salley, NRC Project Manager

11. ABSTRACT (200 words or less)

The Refining And Characterizing Heat Release Rates From Electrical Enclosures During Fire (RACHELLE-FIRE) program involves a working group of experienced fire protection and fire probabilistic risk assessment researchers and practitioners focused on enhancing the methodology used to model electrical enclosure fires in nuclear power plants (NPPs). This report documents the results from the working group's efforts to develop technical information in three areas: (1) classification of electrical enclosures in terms of function, size, contents, and ventilation, (2) determination of peak heat release rate (HRR) probability distributions considering specific electrical enclosure characteristics, and (3) development of a method to account for the impact of the enclosure on the vertical thermal zone of influence (ZOI) above the enclosure during fire. Electrical enclosures have been classified in groups based on their electrical function, contents and size. Peak HRR distributions for the different classification groups have been developed. These distributions are based on the results of different experimental programs intended to measure the HRR associated with fires in electrical enclosures. Peak HRR values can be refined based on visual inspection of the interior of the enclosures. In order to provide a comprehensive characterization of electrical enclosure fires, the working group evaluated the temperature characteristics of fire plumes associated with these events using the Fire Dynamics Simulator (FDS) program. Computer simulations of various enclosure configurations were developed for evaluating the fire burning inside electrical enclosures and the fire plume temperature characteristics that would be generated. Based on this research, new fire plume temperature profiles reflecting the obstructed nature of fire plumes generated from fires inside electrical enclosures are provided.

12. KEY WORDS/DESCRIPTORS (List words or phrases that will assist researchers in locating the report.)
Electrical Enclosure, Fire Hazard Analysis (FHA), Fire Modeling, Fire Probabilistic Risk Assessment (PRA), Fire Probabilistic Safety Assessment (PSA), Fire Protection, Fire Safety, Heat Release Rate, Nuclear Power Plant, Risk-informed Performance-based (RI/PB) Regulation,

13 AVAILABILITY STATEMENT
unlimited

14. SECURITY CLASSIFICATION
(This Page)
unclassified
(This Report)
unclassified

15. NUMBER OF PAGES

16. PRICE

UNITED STATES
NUCLEAR REGULATORY COMMISSION
WASHINGTON, DC 20555-0001

OFFICIAL BUSINESS

@NRCgov

NUREG-2178, Vol. 1
Draft

Refining And Characterizing Heat Release Rates From Electrical
Enclosures During Fire (RACHELLE-FIRE)

April 2015